Canadian Journal of
Fisheries and Aquatic Sciences

Journal canadien des
sciences halieutiques et aquatiques

Volume 68
Number 9 / Numéro 9
September / Septembre
2011

An NRC Research Press Journal
Un journal de NRC Research Press

www.nrcresearchpress.com

NRC
Research Press

ISSN 0706-652X / CJFSDX 68(9) 1511–1694 (2011)

The *Canadian Journal of Fisheries and Aquatic Sciences*, previously published as *Contributions to Canadian Biology* 1901–1925, *Contributions to Canadian Biology and Fisheries* 1926–1934, *Journal of the Biological Board of Canada* 1934–1937, and *Journal of the Fisheries Research Board of Canada* 1938–1979, is issued monthly to form annual volumes of 12 numbers plus supplements.

Editorial policy. The Journal publishes original research articles, perspectives (syntheses, critiques, reevaluations), discussions (comment and reply), and rapid communications. Manuscripts may concern cells, organisms, populations, communities, ecosystems, or processes that affect aquatic systems. They may cover a range of disciplines including biology and ecology of marine and freshwater organisms, limnology, oceanography, physiology, toxicology, genetics, economics, disease, and management. Preference will be given to manuscripts that emphasize understanding of observed phenomena and interpretation of experimental results. The Journal encourages papers that lead from clearly stated purpose or rationale and from testable hypotheses, concepts, or questions to identifiable conclusions or syntheses. Such papers may amplify, modify, question, or redirect accumulated knowledge embodied in contemporary perceptions of a particular state of aquatic sciences. The Journal discourages papers that are essentially descriptive, except in emerging disciplines; have only site-specific or local applications (a certain year, place, taxon, chemical compound, etc.); only confirm previously established principles; or apply standard techniques without breaking new methodological ground.

Manuscripts for publication should be submitted to the Editorial Office via NRC Research Press' online submission and peer review system (**ScholarOne**) at mc.manuscriptcentral.com/cjfas-pubs.

Submissions in either English or French are acceptable. The information must be original, that is, not copyrighted, published, or submitted elsewhere except in abstract form or unless by written consent of the Editors.

Correspondence concerning accepted manuscripts and corrected proofs should be sent to NRC Research Press, Ottawa, ON K1A 0R6, Canada (fax: 613-952-7656; e-mail: pubs@nrcresearchpress.com).

Instructions to Authors are published at nrcresearchpress.com/page/cjfas/authors. The **Publishing Policy** of NRC Research Press is available at nrcresearchpress.com/page/about/policies/pub.

The ***Canadian Journal of Fisheries and Aquatic Sciences*, ISSN 0706-652X**, is published **Monthly, 12 times per year**, by **NRC Research Press, c/o USACAN Media Dist. Srv. Corp.** at 26 Power Dam Way, Suite S1-S3, Plattsburgh, NY 12901, USA. Periodicals postage paid at Plattsburgh, NY. POSTMASTER: Send address changes to ***Canadian Journal of Fisheries and Aquatic Sciences***, c/o NRC Research Press, P.O. Box 2888, Plattsburgh, NY 12901, USA.

Publié sans interruption depuis 1901, le *Journal canadien des sciences halieutiques et aquatiques* a paru sous plusieurs titres : *Contributions to Canadian Biology* 1901–1925, *Contributions to Canadian Biology and Fisheries* 1926–1934, *Journal of the Biological Board of Canada* 1934–1937, et *Journal of the Fisheries Research Board of Canada* 1938–1979. Le Journal paraît tous les mois, formant ainsi un volume de 12 numéros, et offre en plus jusqu'à deux suppléments par année.

Politique éditoriale. On publie, dans le Journal, des articles rendant compte de recherche originale, des perspectives (synthèses, critiques et réévaluations), des discussions (commentaires et réponses) et des communications rapides. Les documents peuvent porter sur les cellules, organismes, populations, communautés, écosystèmes ou processus qui affectent les systèmes aquatiques. Ils peuvent relever de divers domaines y compris la biologie et l'écologie des organismes marins et d'eau douce, la limnologie, l'océanographie, la physiologie, la toxicologie, la génétique, l'économie, la pathologie et la gestion. On accorde la préséance aux articles qui contribuent à la compréhension de phénomènes observés et à l'interprétation de résultats expérimentaux. On invite les auteurs à soumettre des articles ayant des objectifs précis ou relevant d'hypothèses, de concepts ou de questions vérifiables et se terminant par de solides conclusions ou d'utiles synthèses. Ces articles enrichissent, changent, mettent en question ou réorientent les connaissances acquises sur divers aspects des sciences aquatiques. On décourage toutefois la soumission d'articles simplement descriptifs (à moins qu'il ne s'agisse de nouvelles disciplines), d'application très limitée (applicables à une seule année, une seule région ou un seul taxon, portant sur un unique composé chimique, etc.); d'articles qui ne font que reprendre les principes énoncés dans des articles précédents; et d'articles rendant compte de l'application de normes sans gain de méthodologie.

Les auteurs sont invités à soumettre leur **manuscrit** au Bureau de la rédaction par le truchement du Système de soumission et d'examen en direct des articles (**ScholarOne**) de NRC Research Press au mc.manuscriptcentral.com/cjfas-pubs.

Les contributions peuvent être en anglais ou en français. Elles doivent être originales, c.-à.-d. qu'elles ne doivent pas avoir fait l'objet d'un copyright, avoir été publiées ou soumises ailleurs, sauf sous forme abrégée ou avec le consentement des rédacteurs en chef.

La correspondance ayant trait aux manuscrits acceptés et les épreuves corrigés doivent être envoyées à NRC Research Press, Ottawa, ON K1A 0R6, Canada (télécopieur : 613-952-7656; courriel : pubs@nrcresearchpress.com).

Les **Recommandations aux auteurs** sont publiées au nrcresearchpress.com/page/cjfas/authors. La **Politique éditoriale** est disponible auprès de NRC Research Press au nrcresearchpress.com/page/about/policies/pub.

This Journal is indexed or abstracted in / Cette revue est signalée ou résumée dans
Aqualine; Aquatic Sciences and Fisheries Abstracts; BIOBASE; Biological and Agricultural Index; BIOSIS; CAB Abstracts; Canadian Fisheries Abstracts; Chemical Abstracts; Current Awareness in Biological Sciences; Current Abstracts; Current Contents; General Science Index; GeoRef; Oceanic Abstracts; PASCAL; Pollution Abstracts; Referativnyi Zhurnal; Science Citation Index; Water Resources Abstracts

Volume 68, Number 9, September 2011

Canadian Journal of Fisheries and Aquatic Sciences

Published by the NRC Research Press

Volume 68, numéro 9, septembre 2011

Journal canadien des sciences halieutiques et aquatiques

Publié par NRC Research Press

Editors / Rédacteurs en chef   Don Jackson and Rolf Vinebrooke

Assistant to the Editors / Adjointe au rédacteur en chef **Holly Foster**

Associate Editors / Comité de rédaction

M.J. Bradford, *Simon Fraser University*
D. Brickman, *Fisheries and Oceans Canada, Dartmouth*
S.E. Campana, *Fisheries and Oceans Canada, Dartmouth*
Y. Chen, *University of Maine*
I. Fleming, *Memorial University of Newfoundland*
D. Fraser, *Concordia University*
B.M. Gillanders, *University of Adelaide*
J.W.A. Grant, *Concordia University*
M.M. Hansen, *Aarhus University*
R. Hilborn, *University of Washington*
J.M. Jech, *National Marine Fisheries Service, NOAA, Woods Hole, Mass.*
B. Jonsson, *Norwegian Institute for Nature Research*
J. Karlsson, *Umeå University*
K.A. Kidd, *University of New Brunswick*
C.E. Kraft, *Cornell University*
D.L. MacLatchy, *Wilfrid Laurier University*
P. Magnan, *Université du Québec à Trois Rivières*
C.T. Marshall, *University of Aberdeen*
P. Moran, *Universidad de Vigo*
J. Post, *University of Calgary*
Y.T. Prairie, *Université du Québec à Montréal*
T.J. Quinn II, *University of Alaska – Fairbanks*
C.W. Ramcharan, *Laurentian University*
J.S. Richardson, *The University of British Columbia*
M.-J. Rochet, *French Research Institute for Exploitation of the Sea, Nantes*
K. Rose, *Louisiana State University*
J. Rosenfeld, *British Columbia Ministry of Fisheries*
B. Sainte-Marie, *Fisheries and Oceans Canada, Mont-Joli*
R.E.H. Smith, *University of Waterloo*
S.J. Smith, *Fisheries and Oceans Canada, Dartmouth*
W.G. Sprules, *University of Toronto*
E.B. Taylor, *The University of British Columbia*
W. Tonn, *University of Alberta*
M. Trudel, *Fisheries and Oceans Canada, Nanaimo*
A. Vasemägi, *University of Turku*
C.J. Walters, *The University of British Columbia*
G. Weyhenmeyer, *Uppsala University*

NRC Research Press / NRC Research Press

Fax / télécopieur : 613-952-7656; e-mail / courriel : pubs@nrcresearchpress.com; URL / URL : nrcresearchpress.com

Editor-in-Chief / Directeur de la publication **Bruce P. Dancik**
Deputy Editor-in-Chief / Sous-directrice de la publication **Cindy E. Prescott**
Executive Director / Directeur général **Cameron D. Macdonald**

Director, Business Strategy and Development / Directeur, Stratégie et développement des affaires **Mike Boroczki**
Manager, Business Development / Gestionnaire du développement **Peter D'Amico**
Marketing and Sales Coordinator / Coordonnatrice des ventes et du marketing **Judy Letourneau** (613-993-0151)
Client Services Representative / Représentante des services à la clientèle **Eileen Evans-Nantais** (613-990-7873)

Director, Publishing Operations / Directrice, Services d'édition **Suzanne Kettley**
Managing Editor / Directrice de la rédaction **Cecily M. Pearson** (613-993-9099)
Scientific Publishing Editors / Réviseurs de publications scientifiques **Thad Costigan, Tina Wilston**
Publishing Assistant / Adjointe à l'édition **Diana Leck**

Acting Production Manager / Gestionnaire de la production par intérim **Cory Klinkenberg**
e-Publishing Technician / Technicien à l'édition électronique **Jeffrey Wisking**
Graphics Technician / Technicien en graphisme **Leslie Cameron**
Web Technician / Technicien Web **Dennis Cafferty**

NRC Research Press accepts no responsibility for statements or opinions expressed by a contributor. Acceptance of an advertisement, announcement, or other material does not imply endorsement by either the Journal's Editors or NRC Research Press.

© 2011 Canadian Science Publishing or its licensors
As of 2009, copyright in all articles in NRC Research Press journals remains with the authors. All articles published previously are copyright Canadian Science Publishing (which operates as NRC Research Press) or its licensors.

No part of the NRC Research Press journals may be reproduced, stored, or transmitted in any form or by any means, without the written permission of the publisher, except as stated below.

Under the Canadian *Copyright Act*, individuals may download or print single copies of articles for personal research or study. Any person may reproduce short excerpts from articles in the journals for any purpose that respects the moral rights of authors, provided that the source is fully acknowledged. As a courtesy, the consent of authors of such material should be obtained directly from the author.

Authorization to reproduce items for other than personal research or study, as stated above, may be obtained by clicking on the "Reprints and Permissions" link in the table of contents of the electronic article in question or via Access Copyright (www.accesscopyright.ca).

NRC Research Press also extends certain additional rights to authors.

The above rights do not extend to copying or reproduction for general distribution, for advertising or promotional purposes, for creating new collective works, or for resale. For such copying or reproduction, arrangements must be made with NRC Research Press, Ottawa, ON K1A 0R6, Canada.

Subscription information

The *Canadian Journal of Fisheries and Aquatic Sciences* (ISSN 0706-652X) is published monthly by NRC Research Press. The 2011 subscription rates are as follows. Institutional: electronic $1240; print, $1490; electronic + print, $1865. Personal: electronic, $320, print + electronic, $430. For all orders outside Canada, rates are in U.S. dollars. Print subscriptions include second class postage. For air mail add US$204 to the foreign rate. Canadian customers please include GST (business no. 81942 4656 RT0001). Subscriptions are entered for the calendar year. Remittances should be made payable to Canadian Science Publishing. Price for regular single issues: institutional, $150.00; personal, $50.00. Supplements will be priced separately. Special rates apply to members of Canadian scientific and engineering societies if they subscribe through their respective societies.

Issues of the *Canadian Journal of Fisheries and Aquatic Sciences* are available on the Web. Pricing information can be found at nrcresearchpress.com/page/librarians/subscriptions/pricing.

There are no refunds on cancelled subscriptions once delivery has begun. All claims must be submitted within 12 months of the publication date. The publisher expects to supply missing issues only when losses have occurred in transit and when the reserve stock will permit. Subscriptions, renewals, requests for single or back issues, and all remittances should be sent to Canadian Science Publishing, NRC Research Press, Subscription Office, P.O. Box 830399, Birmingham, AL 35283-0399, USA (telephone: 1-800-633-4931 in North America or 1-800-852-7404 outside North America; fax: 205-995-1588).

Microform backfiles are available from NA Publishing Inc., P.O. Box 998, Ann Arbor, MI 48106-0998, U.S.A., (734) 302-6500. www.napublishing.com.

NRC Research Press ne se tient en aucune façon responsable des opinions exprimées par un collaborateur ou des déclarations que pourrait faire ce dernier. La publication d'annonces publicitaires, d'avis et autres n'implique pas l'endossement de leur contenu par les rédacteurs en chef de la Revue ou NRC Research Press.

© 2011 Éditions Sciences Canada ou ses concédants de licence
Depuis 2009, les auteurs conservent le droit d'auteur de tout article qu'ils publient dans les revues de NRC Research Press. Éditions Sciences Canada (qui œuvre sous la dénomination commerciale NRC Research Press) ou leurs concédants de licence, quant à eux, se réservent les droits d'auteur sur tous les articles précédemment publiés à NRC Research Press.

Il est interdit de reproduire, de sauvegarder ou de transmettre toute partie des revues de NRC Research Press dans quelque format ou de quelque façon que ce soit sans le consentement écrit de l'éditeur, sauf dans les cas énoncés ci-après.

Aux termes de la *Loi sur le droit d'auteur* du Canada, les particuliers peuvent télécharger ou imprimer des copies individuelles d'articles pour leurs études ou leurs recherches personnelles. Toute personne peut reproduire de courts extraits des articles d'une revue pourvu que les droits moraux de l'auteur soient respectés et que la source soit clairement indiquée. Il convient de demander directement à l'auteur son consentement.

On peut obtenir l'autorisation de reproduire du contenu à d'autres fins que l'usage personnel (tel que décrit ci-dessus), en cliquant sur le lien « Réimpressions et autorisations » dans la table des matières de l'article électronique en question ou par l'intermédiaire d'Access Copyright (www.accesscopyright.ca).

NRC Research Press accorde aussi des privilèges supplémentaires aux auteurs.

Les droits ci-dessus ne s'appliquent pas à la reproduction à grande échelle aux fins de distribution générale, de publicité ou de promotion, de compilation de nouveaux ouvrages collectifs ou de revente, par exemple. Les droits de reproduction de ce genre doivent faire l'objet d'une entente particulière avec NRC Research Press, Ottawa, ON K1A 0R6, Canada.

Renseignements sur l'abonnement

Journal canadien des sciences halieutiques et aquatiques (ISSN 0706-652X) est une publication mensuelle de NRC Research Press. En 2011, les tarifs d'abonnement pour les organismes sont les suivants : 1240 $ pour la version électronique; 1490 $ pour l'imprimé; 1865 $ pour les deux versions. Pour leur part, les particuliers paient les tarifs suivants : 320 $ pour la version électronique; 430 $ pour la version électronique et l'imprimé. Les tarifs des commandes provenant de l'extérieur du Canada sont en dollars des États-Unis. L'abonnement à l'imprimé comprend le tarif du courrier de deuxième classe. L'expédition par avion exige des frais de 204 $US en sus du prix d'abonnement à l'étranger. Les clients du Canada doivent ajouter la TPS (numéro d'entreprise 81942 4656 RT0001). Les abonnements sont pour l'année civile. Tout paiement doit être adressé aux Éditions sciences Canada. Le prix par numéro régulier est de 150,00 $ pour les organismes et de 50,00 $ pour les particuliers. Le prix des hors-série varie. Les membres des sociétés canadiennes de sciences et de génie bénéficient de taux préférentiels en s'abonnant via leurs sociétés respectives.

Tous les numéros de Journal canadien des sciences halieutiques et aquatiques sont accessibles sur le Web. On trouvera des renseignements sur les tarifs au nrcresearchpress.com/page/librarians/subscriptions/pricing.

Aucun remboursement ne sera accordé, ni aucune annulation acceptée, une fois que les livraisons auront commencé. Toute réclamation doit être présentée dans les 12 mois suivant la date de publication. L'éditeur ne fournira de numéros manquants que si le document a été perdu pendant l'expédition et que si les réserves le permettent. Pour un abonnement ou un renouvellement, pour une demande de numéro (actuel ou ancien), ainsi que pour une réclamation, adressez-vous au Bureau des abonnements, Éditions Sciences Canada, NRC Research Press, P.O. Box 830399, Birmingham, AL 35283-0399, É.-U. (téléphone : 1-800-633-4931, en Amérique du Nord, ou 1-800-852-7404, ailleurs; télécopieur : 205-995-1588).

On peut obtenir les archives sur microforme auprès de NA Publishing, Inc., P.O. Box 998, Ann Arbor, MI 48106-0998, U.S.A., (734) 302-6500, www.napublishing.com.

The distribution of the Chironomidae (Insecta: Diptera) along multiple environmental gradients in lakes and ponds of the eastern Canadian Arctic

Andrew S. Medeiros and Roberto Quinlan

Abstract: An examination of the Chironomidae, the dominant aquatic invertebrate taxa found in Arctic lakes and ponds, was conducted to determine the environmental gradients that may limit their geographical distribution in the eastern Canadian Arctic. Subfossil chironomid head capsules, comprising 86 taxa, were sampled from surficial sediments of 63 lakes that spanned from tree line (northern Manitoba) across multiple regions within the eastern Canadian Arctic. Water chemistry and environmental data were then compared with chironomid assemblages using multivariate analysis. The distribution of chironomids was found to primarily follow a temperature gradient, but additional significant relationships were also found along a nutrient–productivity gradient. Several species of the Tribe Chironomini, which generally represent warm-water adapted taxa, were also found far beyond tree line in the southern Kivalliq region of Nunavut, indicating a more northerly range than previously known. While temperature and trophic status were found to strongly influence the distribution of some taxa, partially constrained gradient analysis indicates that specific chironomid taxa could be used to indicate a primary response to climate regardless of trophic status. This may allow for more holistic inferences of how aquatic communities may respond to climate change as the range of temperature dependant species expand into Arctic systems.

Résumé : Nous examinons les Chironomidae, les taxons dominants d'invertébrés aquatiques habitant les lacs et étangs arctiques, afin de déterminer les gradients environnementaux qui peuvent restreindre leur répartition géographique dans l'est de l'Arctique canadien. Nous avons prélevé des capsules céphaliques subfossiles de chironomidés, appartenant à 86 taxons, dans les sédiments de surface de 63 lacs qui se répartissent de la ligne des arbres (nord du Manitoba) jusque dans de nombreuses régions de l'intérieur de l'est de l'Arctique canadien. Une analyse multidimensionnelle a servi ensuite à comparer les données sur l'environnement et la chimie des eaux aux peuplements de chironomidés. La répartition des chironomidés suit principalement un gradient de température, mais il existe aussi des relations additionnelles significatives avec un gradient de nutriments/productivité. Plusieurs espèces de la tribu des Chironomini, qui contient généralement des taxons adaptés aux eaux chaudes, se retrouvent aussi loin au-delà de la ligne des arbres dans la région sud de Kivalliq dans le Nunavut, ce qui indique une répartition plus nordique que signalé antérieurement. Alors que la température et le statut trophique influencent fortement la répartition de quelques taxons, une analyse de gradient partiellement contrainte indique que certains taxons particuliers de chironomnidés peuvent être utilisés pour indiquer une réaction primaire au climat indépendamment du statut trophique. Cela peut permettre des déductions plus holistiques sur la manière dont les communautés aquatiques peuvent réagir au changement climatique à mesure que l'aire de répartition des espèces dépendantes de la température s'étend vers les systèmes arctiques.

[Traduit par la Rédaction]

Introduction

Changes in climate are expected to have cascading effects on aquatic invertebrate communities as aquatic food web structure is altered, owing to a reduction of ice cover and subsequent expansion of the localized growing season for algal communities (Rouse et al. 1997). Bio-indicators that respond to major limnological changes, such as temperature, dissolved oxygen, and nutrients, can be used to generate relationships between localized environmental conditions and subsequent biotic community structure. However, the use of these indicators to make interpretations about the ecological response of aquatic systems to long-term changes in climate requires baseline knowledge of the relationship between aquatic communities and their limnological environment.

The family Chironomidae (Insecta: Diptera) is one of the most dominant and most diverse groups in Arctic aquatic systems (Oliver and Dillon 1997). There are four basic stages in the life cycle of chironomids: egg, larva, pupa, and adult. While the adult terrestrial stage of the chironomid life cycle is short, the four-stage aquatic larval phase can persist for years until conditions are favourable for pupation and emer-

Received 15 September 2010. Accepted 9 May 2011. Published at www.nrcresearchpress.com/cjfas on 31 August 2011.
J2011-0144

Paper handled by Associate Editor Gary Sprules.

A.S. Medeiros and R. Quinlan. York University, Department of Biology, 4700 Keele Street, Toronto, ON M3J 1P3, Canada.

Corresponding author: Andrew S. Medeiros (e-mail: fraggle@yorku.ca).

Can. J. Fish. Aquat. Sci. **68**: 1511–1527 (2011) doi:10.1139/F2011-076 Published by NRC Research Press

Fig. 1. Locations of all recent (>1980 AD) published examinations of subfossil Chironomidae assemblages within the territory of Nunavut, Canada.

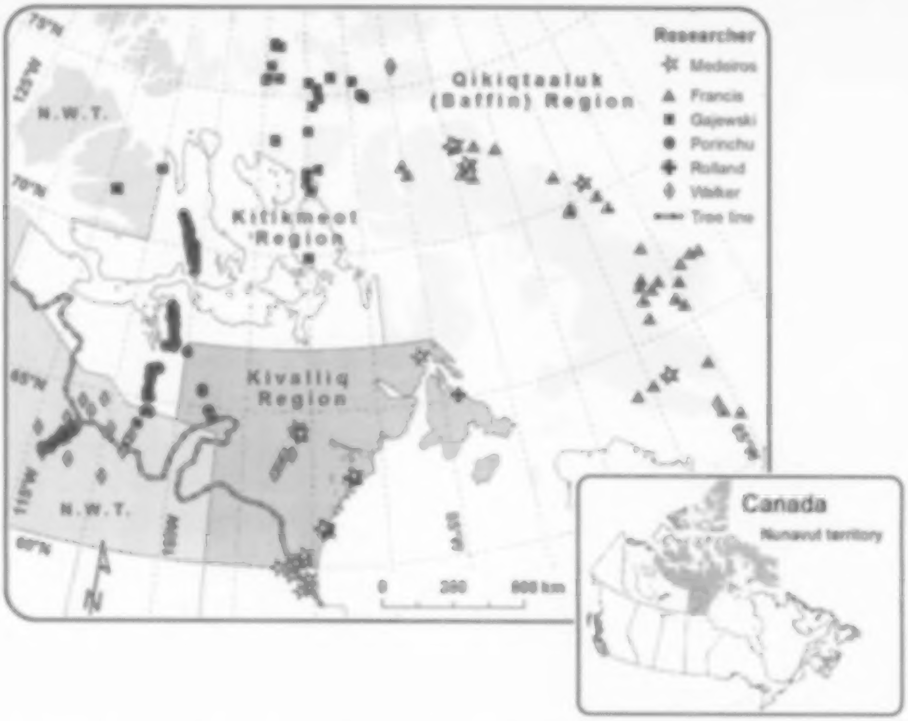

gence (Butler 1982). The emergence period depends on the conditions of the environment, including particular heat–sun thresholds, oxygen concentrations of the water, water levels, food resources, and temperature (Danks 1971; Pinder 1995). Many species of chironomids are specially adapted for specific habitats and environmental conditions (Pinder 1995), and have been used as indicators of climatic conditions (Walker et al. 1991), trophic status (Brooks et al. 2001), dissolved oxygen (Quinlan and Smol 2001*a*), biomonitoring (Medeiros et al. 2011), and productivity (Brodersen and Lindegaard 1999*a*). The chitinized remains of the four larval stages are well preserved in lake sediments (Walker 2003), and the examination of the diversity and abundance of their subfossil remains in surficial (0–1.0 cm) lake sediments allows for an interpretation of the environmental conditions conducive to their survival and persistence in a given system.

Substantial portions of the eastern Canadian Arctic are under sampled for Chironomidae distributions. For example, the Kivalliq region of Nunavut, formerly the district of Keewatin, encompasses 445 109 km^2 (Statistics Canada 2006), roughly the size of Sweden (Fig. 1). Several lakes were sampled by Porinchu et al. (2009) along a transect from the mainland Kitikmeot region, and far northwestern area of the Kivalliq (Fig. 1). In addition, there have been a few faunal surveys of aquatic invertebrates (e.g., Giberson et al. 2007). However, Walker's (1990) examination of four lakes for subfossil chironomid assemblages may represent the single instance of this type of lake study within this large mainland area. The lack of recent research on the Chironomidae within the eastern Canadian Arctic represents a gap in knowledge of community composition in an area where climate warming may result in range extensions of several southern warm-water adapted taxa. A warming climate would allow for the establishment and proliferation of these taxa, and the ecological range of several species defined by warm-water temperature thresholds for survival, to extend into tundra environments. Thus, the recent appearance of warm-water adapted species should be reflected in lakes just north of their previous historical northern limits. However, the limited baseline knowledge of Arctic chironomid communities challenges our ability to understand the ecological gradients that may define the range of many species, especially when the taxonomy of morphotypes is limited. Recent work with DNA barcoding has made progress in identifying specific species and improving taxonomic keys. For example, Stur and Ekrem (2011) noted several species of Tanytarsini that have long been grouped together or misidentified owing to similar larval traits.

As the topography, geologic history, landscape characteristics, and climate can differ greatly across regions within the Arctic, the limnology and invertebrate diversity of aquatic systems likely also differ. The relationships between ecological interactions (e.g., competition and predation) and chironomid distributions in Arctic systems are mostly unknown. For example, the influence of bird populations on the limnology of lakes and ponds in nesting areas may significantly alter local nutrient regimes (Côté et al. 2010), and cause shifts in the abundance and diversity of local chironomid assemblages (Frisch et al. 2007; Michelutti et al. 2011). As Brodersen and Anderson (2002) indicated that the temperature optima

Table 1. Descriptive statistics of environmental variables for the 63 sampled lakes and ponds.

Variable	Mean	SD	Min.	Max.	Transformation
SA (ha)	204.8*	413.9*	0.8	2214*	log
Depth (m)	4.5	4.3	0.5	20.6	log
MSSWT (°C)	12.7	3.2	4.9	18.3	—
pH (–log[H$^+$])	7.7	0.6	6.3	8.9	—
CHLA (μg·L^{-1})	1.1	0.8	0.1	3.7	√
Cl (mg·L^{-1})	12.1	31.0	0.2	235.0	log(x+1)
SO_4 (mg·L^{-1})	2.8	3.2	0.0	21.2	log(x+1)
DOC (mg·L^{-1})	5.2	5.5	0.6	42.1	log
DIC (mg·L^{-1})	4.9	3.8	0.6	19.4	∛
SiO_2 (mg·L^{-1})	0.6	0.8	0.0	3.5	√
ORP (mV)	169.7	123.1	38.0	512.3	log
NH_3 (μg·L^{-1})	43.0	38.5	2.5	189.0	∛
TP (μg·L^{-1})	7.1	5.6	1.7	41.7	log
TN (μg·L^{-1})	349.2	161.2	89.0	840.0	√

Note: Abbreviations: surface area (SA), mid-summer surface water temperature (MSSWT), chlorophyll *a* (CHLA), dissolved organic carbon (DOC), dissolved inorganic carbon (DIC), oxygen reduction potential (ORP), total nitrogen (TN), total phosphorus (TP).

*Excludes Baker Lake.

for chironomid taxa and trophic variables were strongly correlated, it may be difficult to separate the influence of productivity from the influence of temperature on chironomids. Kernan et al. (2009) also found that regional differences in a pan-European study of several indicators, including midge distributions, could not solely be explained by environmental variables, suggesting that biogeographic influences (e.g., dispersion and colonization) may also be important. In addition, while a gradient of richness and diversity in invertebrate community structure is well documented as one moves along a transect from lakes and ponds within areas defined by lower mean July temperature to those characterized by a higher mean July temperature (Walker et al. 1997; Barley et al. 2006; Porinchu et al. 2009), there have been fewer studies examining possible gradients in available nutrients and localized environmental conditions that may influence the community structure within the same geographic area (Brodersen and Anderson 2002).

To address these issues we sought to answer the following questions: What is the community composition of the Chironomidae in lakes and ponds of the eastern Canadian Arctic? What environmental factors govern the distribution of these species in a particular environment? Could localized differences in temperature, nutrient availability, depth, or other environmental characteristics influence the chironomid community structure in lakes and ponds within the same geographical area? Can common environmental influences on chironomid distributions be found across multiple regions?

Therefore, to achieve a better understanding of the community structure of Chironomidae populations within lakes and ponds across several communities in Nunavut, an examination of lakes and ponds was conducted within several under-sampled areas in the eastern Canadian Arctic. This analysis focused on the environmental factors that may influence the diversity and abundance of chironomid assemblages across several regions within Nunavut, as well as the localized environmental conditions that govern the range of chironomid taxa in the eastern Canadian Arctic.

Materials and methods

Study areas

Lakes and ponds near settlements were sampled across a span of several regions, along a transect beginning at tree line (Northern Manitoba), extending through the Kivalliq region towards the northeastern islands within the Baffin region of Nunavut (Fig. 1; Table 1). These lakes were also sampled in groups of varying landscape and environmental characteristics, concentrated in the vicinity of several towns within the Kivalliq region (Arviat, Baker Lake, Rankin Inlet, and Repulse bay).

The position of the southernmost town of Arviat (central-west Hudson's Bay, 61°7′0″N, 94°3′0″W), ~260 km north of Churchill, Manitoba (58°46′0″N, 94°10′0″W), makes it an ideal location to determine if the ranges of several species of the Tribe Chironomini extend into the lakes and ponds north of tree line within southern Nunavut. Several Chironomini species have been documented in the vicinity of the Town of Churchill, Manitoba (R. Quinlan, unpublished data), but there are no records further north. The landscape of Arivat is relatively flat (mean elevation of 12 m above sea level), and dominated by matted compact cushions of prickly saxifraga (*Saxifraga tricuspidata*) and moss campion (*Silene acaulis*). These cushions were intermixed with clumps of dwarf fireweed (*Chamerion latifolium*). Large stands of *Salix* sp. shrubs, approximately 1.0–1.5 m in height, were also frequently present in catchment areas. Dominant shrubs found throughout the vicinity of Arviat contrasted with other areas sampled in the Kivalliq region, where the number and height of shrubs observed were less prominent.

The town of Rankin Inlet (62°48′41″N, 92°6′57″W), 200 km northeast of Arviat, has extensive all-terrain vehicle trails allowing for the examination of several lakes across a large gradient of landscape characteristics (e.g., varying depth, elevation, catchment vegetation, and underlying hydrology). While lakes and ponds sampled within the vicinity of Arviat and Rankin Inlet were in valleys of low elevation (<50 m), lakes in other regions were generally found isolated at higher

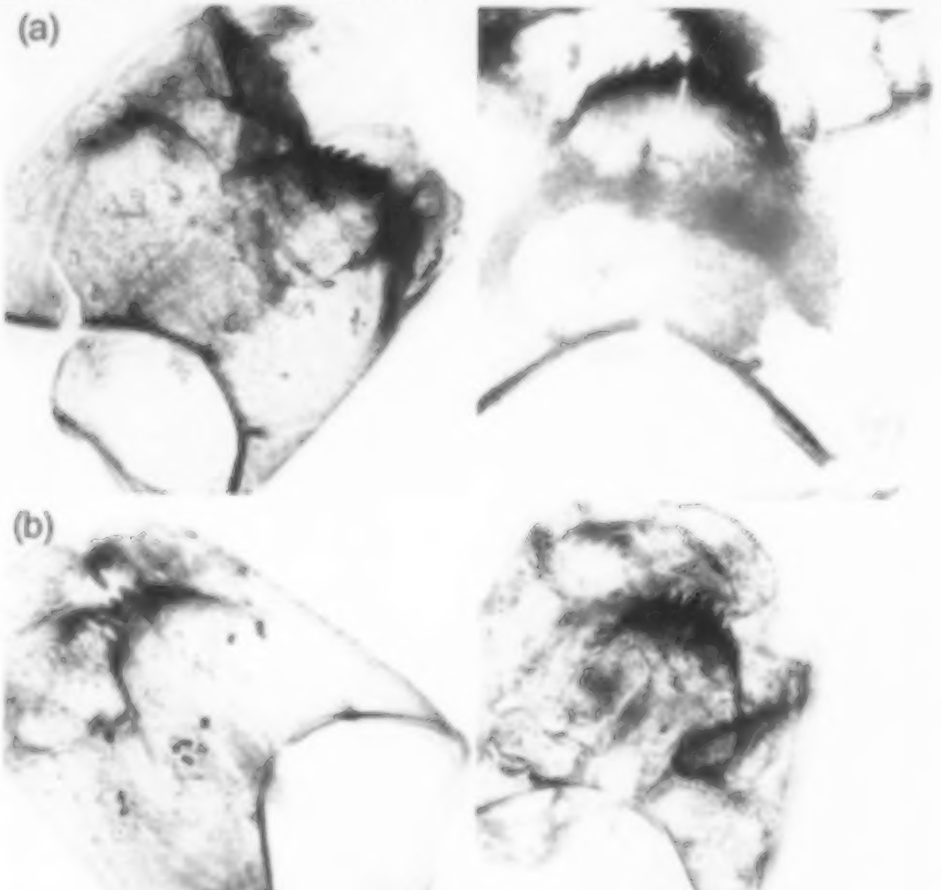

Fig. 2. Diagnostic images for *Zalutschia* types found: (*a*) *Zalutschia* sp. C. (Barley et al. 2006 as type B); (*b*) *Zalutschia* nr. *lingulata pauca* (Wiederholm, 1983); (*c*) *Zalutschia zalutschicola* (Sæther, 1976).

elevations (100–200 m). These included Iqaluit (63°45′8″N, 68°33′50″W), Clyde River (70°27′0″N, 68°34′0″W), and Repulse Bay (66°31′17″N, 86°13′29″W). Catchment vegetation for these areas were primarily represented by dwarf shrubs of alpine bearberry (*Arctostaphylos alpina*), mountain cranberry (*Vaccinium vitis-idaea* ssp. *minus*), and Arctic white heather (*Cassiope tetragona*). Poaceae commonly found throughout catchment areas included species of wildrye (*Elymus* sp.), bluegrass (*Poa* sp.), and fescue (*Festuca* sp.). Dwarf fireweed (*Chamerion latifolium*) was also common in disturbed areas along all-terrain vehicle trails and roads.

Field sampling

Sediment and water samples for 57 lakes were collected during the ice-free seasons between June and August in each of the years from 2006 to 2009. Samples consisted of 16 lakes from the vicinity of Rankin Inlet, 10 from Arviat, 9 from the Churchill vicinity, 7 from Baker Lake, 6 from Iqaluit, 6 from Repulse Bay, and 3 from Clyde River. Of these 57 lakes, replicate cores were recovered from the approximate center and (or) deepest portion of lakes using a Glew (1991) mini-corer (3.8 cm inner diameter) and (or) Uwitec (http://www.uwitec.at) gravity corer (8.4 cm inner diameter) deployed from a collapsible PakCanoe, inflatable Zodiac boat, or float-plane. Sediment cores were extruded in the field at 0.5 cm resolution, stored in Whirl-Pak bags, and kept cool (4 °C) and dark until processed in the laboratory. Sediment and water samples for 11 lakes were also collected by S. Finkelstein (University of Toronto, Department of Geography, Toronto, Ontario) between 27 July 2008 and 31 July 2008 within Sirmilik National Park (4 northern Sirmilik Baffin Lakes from the Qorbignaluk headlands, 7 south–southwestern Bylot Island Lakes) and included in our data set.

During sediment core collection, physicochemical variables were measured using an YSI 600QS multi-parameter probe, including mid-summer surface water temperature (MSSWT, measured at 0.5–1.0 m below surface of water), bottom water temperature (measured 1.0 m above sediments at a mid-basin location), specific conductance, pH, and dissolved oxygen. Depth was measured with a depth sounder and the global positioning system (GPS) location of each mid-basin coring location was taken with a Garmin 1200XL GPS device. Epilimnetic water samples were collected at 0.5 m below the water surface in precleaned polyethylene bottles and immediately treated in the field following the protocols outlined in the Analytical Methods Manual of Environment Canada (Environment Canada 1994). Water samples for each lake were analysed by the National Laboratory for Environmental Testing at the Canadian Centre for Inland Waters, Burlington, Canada (Table 1).

While air temperature has been found to be a significant environmental variable for directing Chironomidae community distributions (e.g., Walker et al. 1997; Barley et al. 2006; Porinchu et al. 2009), if lakes are within a relatively close geographical proximity then the use of air temperature (or a reconstructed air temperature estimate) derived from interpolations amongst meteorological stations in the region is problematic. This problem is particularly acute if there is a lack of a substantive altitudinal gradient amongst sites from the same regional locale. Likewise, using air temperature, as opposed to water temperature, does not incorporate catchment-specific characteristics that may influence the water temperature of lakes and ponds, such as water clarity and light penetration (e.g., catchment vegetation influencing allochthonous dissolved organic carbon (DOC) inputs), water source (e.g., glacially derived), basin morphometry (e.g., surface area (SA) and depth), and local topography. These localized parameters can determine the total volume of a water body and exposure to wind and solar insolation, which may influence waterbody response to climate change. For example, neighbouring water bodies with different local topography may have substantively different responses to climate change (Keatley et al. 2008). To provide a control for spot measurements of temperature and environmental variables, several lakes were sampled multiple times over the 4-year study (June–August 2006 to 2009). These duplicate samples, in both water chemistry and chironomids from surficial sediments, were plotted passively into the ordination analysis as a control, but removed from ordination diagrams owing to the repetitive nature of these samples obscuring data-points.

Laboratory analysis

Surface sediments (1–4 g wet mass) were subsampled and washed through nested 212 and 106 µm mesh sieves with DH_20. Retained residues were then washed with 95% ethanol in preparation for sifting. Residues were sifted using a stereomicroscope at 30–40× magnification, and subfossil chironomid headcapsules extracted with the use of fine forceps. Specimens were permanently mounted on glass microscope slides in Entellan mounting medium for identification.

For each lake, a minimum of 50 head capsules were enumerated. If the total number of head capsules found was fewer than 50, more sediment was subsampled until the total identified remains were greater than 50 (Quinlan and Smol 2001*b*). Surficial sediments from each lake represented the surface–water interval (0–0.5 cm sediment depth), with the exception of A3, where 0–1 cm of sediment was extracted because of low numbers within the first 0–0.5 cm interval.

Specimen identifications were made at 400–1000× magnification to the lowest taxonomic resolution possible based on Sæther (1976), Oliver and Roussel (1983), Wiederholm (1983), Walker (1988), Uutala (1990), Epler (2001), Rieradevall and Brooks (2001), Brooks et al. (2007), and Walker (2007). The genus *Heterotrissocladius* and *Psectrocladius* (*Psectrocladius*) were identified to species (e.g., *H. maeaeri*-type 1, *H. maeaeri*-type 2, *H. grimshawi*, *H. marcidus*, *H. subpilosus*; *Psectrocladius* (*Psectrocladius*) *sordidellus*, *P.* (*P.*) *barbimanus*, *P.* (*P.*) *psilopterus*, and *P.* (*P.*) *limbatellus* gr.) but conservatively grouped for analysis because of a lack of clear demarcations in different character states of diagnostic taxonomic features.

There were three distinct types of *Zalutschia* found in our data set (Fig. 2). We feel that, from visual inspection, *Zalutschia* sp. B as described by Brooks et al. (2007) is a different species than the *Zalutschia* type B identified by Barley et al. (2006). Therefore we have referred to *Zalutschia* type B in Barley et al. (2006) as Zalutschia sp. C in our study. The diagnosis of this specimen is based on the wider asymmetrical median teeth, which have two outwardly pointing peaks. The first lateral tooth is distinctly separate from the median tooth, and half the size of the second lateral tooth. The second to sixth lateral teeth are of comparable size and progressively subequal. The ventromental plates curve upwards at the apex, but do not obstruct any of the lateral teeth. We did not find any specimens of *Zalutschia* sp. B as described by Brooks et al. (2007). The diagnosis for *Zalutschia lingulata pauca* is sometimes designated *Zalutschia* sp. A, however, we feel that this taxon has marked differences in diagnostic features from Brooks et al. (2007) and Barley et al. (2006) that are available in Sæther (1976) and pictured in Wiederholm (1983). As the description of *Zalutschia lingulata pauca* is a European type, we have designated our specimen as *Zalutschia* nr. *lingulata pauca*. The first lateral tooth of *Zalutschia lingulata pauca* could be described as an accessory tooth as it is attached to the median teeth at the base, is much thinner and less pronounced than the other laterals, and can vary from equal in height to the second lateral to slightly subequal. The second to sixth lateral teeth gradually diminish in size. The ventromental plates are elongated compared with *Zalutschia* sp. C, can partially obscure the fourth to sixth laterals, and markedly curve upwards at the apex.

Data screening

Five lakes from the northern Baffin region, missing primary environmental variables (due to lack of processed water samples), were removed from analysis. Further variables that had concentrations below the detection limit in a majority of sites sampled (e.g., NO_3, NO_2, and soluble reactive phosphorus) were deleted from the data set. If variables were below the detection limit in fewer than half the study lakes, half the detection limit was substituted for use in numerical analysis.

Environmental and water chemistry variables were normalized (Table 1) and checked with a Kolmogorov–Smirnov test of normality. Testing for outliers was also conducted for both species and environmental data, where the 95% confidence limits were calculated for the sample scores on the first two axes of a principal components analysis (PCA) of environmental data and a detrended correspondence analysis (DCA) of species data (Gauch 1982). No sites within our data set were considered outliers as no sites had sample scores that exceeded the 95% confidence limit for both the PCA and the DCA. Taxa are presented as square root transformed percent abundances, calculated as the percentage of total identifiable midges.

Numerical analyses

Relationships between environmental variables and chironomid community composition were examined with the use of ordinations performed using CANOCO v4.53 (ter Braak and Šmilauer 1998). A DCA, a variation of reciprocal averaging (correspondence analysis), was conducted (with detrending by segments, square-root transformation of species abundance, and down-weighting of rare taxa) to observe the relationship between species and environmental data in ordinal space. The DCA was also used to determine the gradient lengths of species composition along the first two axes to select between linear- or unimodal-based ordinations.

Environmental variables that explained a significant ($P < 0.05$) direction of variation in species data were determined through direct gradient analyses. The significance of each environmental variable was then tested in an ordination singly constrained to each variable, using both redundancy analysis (RDA; linear model) and canonical correspondence analysis (CCA; unimodal model), performed with CANOCO using 999 unrestricted Monte Carlo permutations (reduced model). The selection of environmental variables was conducted with a backwards selection process for both RDA and CCA techniques and included only environmental variables that were found to be significant ($P < 0.05$) in singly constrained ordinations. The collinearity of environmental variables was minimized during this process, where variables with the highest variance inflation factor (VIF) were removed sequentially. The backwards selection procedure was repeated until all remaining environmental variables had VIFs < 10.

To examine whether there were significant differences between site locations based on the relative abundances of chironomid species, a two-way indicator species analysis (TWINSPAN; Hill 1979) was conducted. This analysis ordinates the site locations using reciprocal averaging, and creates a dichotomy using a calculated centroid line to make binomial divisions and create a hierarchical classification of sites (Hill 1979). Pseudo-species cut levels were defined as 0%, 2%, 5%, 10%, and 20% on the relative abundance data of chironomid species.

Each TWINSPAN division delineated sample locations into groups based on the chironomid community composition at each site. Tests for significant ($P < 0.05$) differences between groups was carried out with the use of parametric analyses of variance (ANOVAs) that compared the means of DCA axis scores for samples within each TWINSPAN group. Significant differences in environmental variables amongst the TWINSPAN groups were then tested with subsequent parametric ANOVAs, or Kruskal–Wallis one-way ANOVA for those variables that violated statistical assumptions of normality. This elucidated the environmental preferences of taxa based on the placement of a location within a particular TWINSPAN division.

The relationship between selected taxa and site location was visualized using C2 software (Juggins 2003). The relative abundance of species was arranged in rank order, where RDA axis 1 species scores were singly constrained to MSSWT, with lakes ordered in terms of latitude from south to north. Attribute plots were created using CanoDraw 4.12 (ter Braak and Šmilauer 1998), where relationships between specific taxa and environmental variables were based on significant ($P < 0.05$) correlations when examined by a Spearman's rank correlation matrix with Bonferroni-corrected P values. In addition, a series of partially constrained ordinations were run to examine relationships between primary gradients independently of each other. The RDA ordination was run in CANOCO with MSSWT as the primary explanatory variable for chironomid distributions, with TN set as a covariable (and vice versa). Species that were significant to either constrained gradient were retained.

Results

Over 6500 head capsules were extracted and identified from the surface-sediment intervals (0–0.5 cm), with an average of 102 head capsules per lake (median = 79.5; range 50–373). Eighty-six taxa were represented within the 63-lake data set (Fig. 3). The range in surface temperature for all lakes

Fig. 3. Relative abundances of selected taxa recovered from surface samples of Nunavut lakes and ponds from June 2006 to August 2009. Taxa are arranged according to the sample scores of the redundancy analysis (RDA) constrained to mid-summer surface water temperature, with cold-water taxa on the left of the diagram. Sites are arranged by latitude; south (top) to north (bottom).

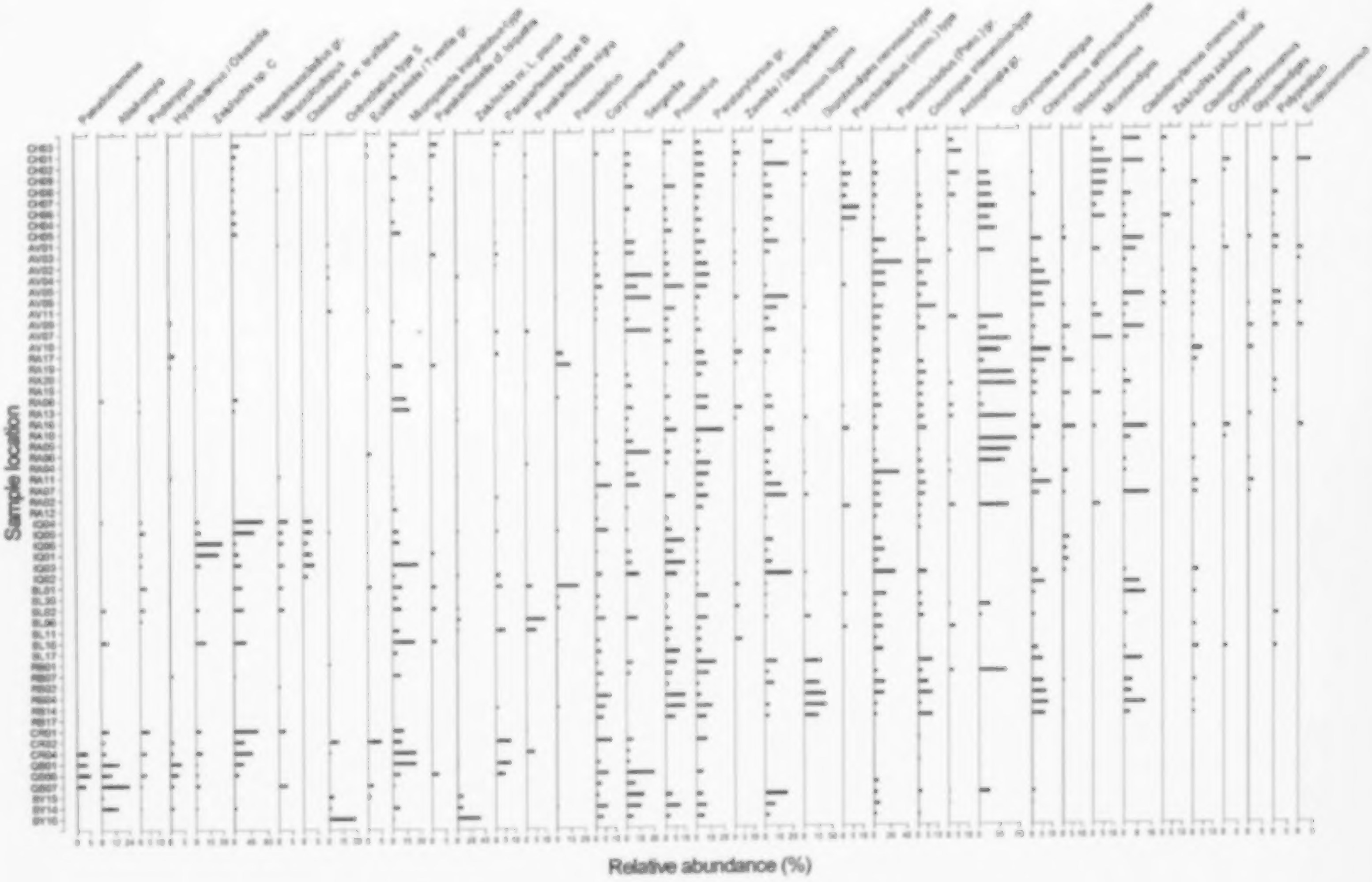

sampled was from 4.9 to 18.3 °C (a gradient of 13.4 °C) and the range in mid-basin depth was 0.30–20.6 m (a gradient of 20.3 m). All lakes were observed to be polymictic at the time of sampling (difference in surface temperature and bottom temperature < 1.0 °C).

Ordination analyses

The gradient length of species data, determined from DCA, were 2.6 and 2.1 SD units for axis 1 and 2, respectively. These are representative of axes of intermediate lengths, therefore both linear- and unimodal-based ordination techniques were used. Ordinations constrained to each environmental variable identified the following significant ($P <$ 0.05) environmental variables: MSSWT, bottom water temperature, depth, pH, total phosphorus (TP), TN, DOC, dissolved inorganic carbon (DIC), SiO_2, K, Na, Cl, Mg, Ca, SO_4, NH_3, and conductivity (COND) at 25 °C. The backwards selection process eliminated Ca, Mg, K, Na, COND, and bottom water temperature.

The species–environment correlation between species axis 1 and canonical axis 1 was similar in the CCA (0.919) as in the RDA (0.929); however, total species variance explained was higher in the RDA (48.3% in RDA, 36.6% in CCA). Thus, further analysis was based on linear RDA ordinations rather than unimodal-based ordinations (CCA). The first two RDA axes accounted for 30.0% of the species variance (Table 2), 61.4% of the species–environment relation, and each axis explained a significant amount of species variation ($P < 0.001$). Relationships between these environmental variables and the species data set were examined through canonical correlation coefficients of variables to the first two axes, their associated *t* test value to each axis, and the interset correlations of the environmental variables (Table 3). Depth, MSSWT, Cl, DIC, DOC, SA, and SiO_2 were significantly correlated ($P < 0.01$) with the first RDA axis. Depth, TN, Cl, and SiO_2 were significantly correlated ($P < 0.01$) with the second RDA axis.

Environmental distributions

A TWINSPAN analysis was conducted to examine relationships that may describe the environmental preferences of several taxa. The TWINSPAN analysis of the chironomid communities in the lake data set indicated a significant division between lakes in colder regions from those in warmer regions (group C, Fig. 4). This was characterized by a significant ($P < 0.05$) separation based on cold-water (*Heterotrissocladius* gr., *Zalutschia* sp. C) and warm-water adapted taxa (*Dicrotendipes*, *Cladotanytarsus mancus* gr.), lower TP, TN, CHLA, temperature, and higher depth (Fig. 5). The second TWINSPAN division was also significant, and separated sites based on area, TN, CHLA, DIC, COND, and depth (group B, Fig. 5). This was characterized by shallow sites in warmer regions represented by *Chironomus anthracinus*-type, and productive, deeper, larger lakes in warmer regions represented by *Corynocera ambigua*, *Arctopelopia* gr., and *Zavrelia/Stempellinella* gr. (group A, Fig. 4). Sites grouped according to these TWINSPAN divisions had significant differences (*t* tests, $P < 0.05$) in either DCA axis 1 or axis 2 sample scores.

A RDA biplot of sites (Fig. 6) shows that RDA axis 1 separates colder, deeper sites, with lower TN (e.g., CR04 and IQ05), from warmer, shallow sites with higher TN (e.g., AV02 and RB01). Cold-water adapted species (e.g., *Pseudodiamesa*, *Hydrobaenus/Oliveridia* gr., *Abiskomyia*, and *Micropsectra* type R) are found opposite of high MSSWT at the bottom right quadrant of the ordination, whereas warm-water adapted species (e.g., *Polypedilum*, *Cryptochironomus*, *Endochironomus*, *Cladopelma*, and *Glyptotendipes*) are found clustered towards the top left quadrant (Fig. 7). Thus, for numerous subfossil chironomid taxa, distributions along a climate gradient agree with previous studies from the Arctic (e.g., Walker et al. 1997; Gajewski et al. 2005; Porinchu et al. 2009).

Redundancy analysis axis 2 primarily separated areas with warm, shallow (2–5 m), large lakes with higher available nutrients (e.g., Churchill locations), higher productivity, and higher DIC from those that are colder, deeper, with lower available nutrients, lower productivity, lower DIC, and a smaller SA (e.g., RB02 and RB17; Fig. 6). The separation of lakes and ponds by RDA axis 2 were represented by the second TWINSPAN division that separated warmer, shallow lakes and ponds with higher available nutrients (Fig. 4, group A) from larger lakes with higher productivity (Fig. 4, group B). Species that followed this pattern oriented along RDA axis 2 were *Microtendipes*, *Zavrelia/Stempellinella* gr., *Corynocera ambigua*, *Psectrocladius* (*Monopsectrocladius*) gr. (warmer, deeper, and larger lakes with higher productivity), and *Limnophyes*, *Dicrotendipes*, *Procladius*, *Corynoneura arctica* (colder, shallow, smaller lakes with lower productivity).

While specific taxa were found to have distinct relationships with both MSSWT and TN, partially constrained ordinations revealed that several taxa may have relationships with one variable that were independent of the other. In a partially constrained ordination with MSSWT as the sole explanatory gradient and TN as a covariable, strong correlations were found with MSSWT independent of TN (Fig. 8*a*). In time-series data sets, as either monitoring data or using paleoecological data in a biostratigraphic analysis, changes in these taxa may be indicative of changes that are tightly linked to climate (e.g., water temperature, ice-cover phenology, etc.) regardless of a particular trophic status. These included cold-water indicator taxa such as *Hydrobaenus*, *Micropsectra* type R, and *Zalutschia* nr. *lingulata pauca*, and warm-water indicator taxa such as *Parachironomus* and *Polypedilum*. In a partially constrained ordination with TN as the sole explanatory gradient and MSSWT as a covariable, there were several taxa that still had a strong correlation with a TN gradient (Fig. 8*b*). These included *Cricotopus bicintus*, *Dicrotendipes*, *Eukiefferiella/Tventia* gr., *Micropsectra contracta*, *Mesocricotopus*, *Micropsectra insignilobus*, *Micropsectra padulla*, and *Parakiefferiella* sp. B.

Discussion

Influences of temperature and depth on Chironomidae

Chironomids are able to survive and persist across long gradients of environmental conditions, such as temperature, oxygen, productivity, and salinity, which has allowed for a global distribution (Porinchu and MacDonald 2003). While the composition of the chironomid assemblages in a particular habitat depends on both the terrestrial and aquatic envi-

Table 2. Eigenvalues of first four redundancy analysis axes, species environment correlation for each canonical axis, and cumulative percentage variance of species data and species.

	Axis 1	Axis 2	
Eigenvalues	0.194	0.106	
Species–environment correlations	0.929	0.780	
Cumulative percentage variance of species data	19.4	30.0	
Cumulative percentage variance of species–environment relation	40.2	62.1	
Sum of all eigenvalues			1.000
Sum of all canonical eigenvalues			0.483

Table 3. Regression coefficients of the first two redundancy analysis (RDA) axes (AX1 and AX2), their associated *t* test values, and interset correlations for backwards-selected environmental variables.

	Regression coefficients		Interset correlations		*t* values	
Environmental variables	AX1	AX2	AX1	AX2	AX1	AX2
Depth	0.388	0.475	0.724	0.366	**4.18**	**2.54**
TN	–0.142	–0.579	–0.752	0.035	–0.90	**–1.83**
MSSWT	–0.322	0.229	–0.717	0.160	**–3.03**	1.07
TP	–0.129	0.225	–0.545	0.149	–1.17	1.02
Cl	0.313	–0.787	–0.522	0.080	**2.15**	**–2.68**
DIC	–0.288	0.196	–0.537	–0.112	**–2.83**	0.95
SiO2	0.438	–0.917	0.398	–0.468	**4.03**	**–4.17**
SO_4	–0.139	0.332	–0.487	–0.018	–1.01	1.19
NH_3	0.014	0.138	–0.420	0.098	0.16	0.78
SA	0.208	0.049	0.157	0.456	**2.38**	0.28
CHLA	0.021	0.257	–0.283	0.311	0.25	1.52
pH	0.109	–0.171	–0.278	–0.237	1.41	–1.10
DOC	–0.179	0.269	–0.398	0.106	**–2.42**	1.80
ORP	–0.123	–0.198	0.448	–0.167	–1.17	–0.94

Note: Abbreviations: total nitrogen (TN), mid-summer surface water temperature (MSSWT), total phosphorus (TP), dissolved inorganic carbon (DIC), surface area (SA), chlorophyll-*a* (CHLA), dissolved organic carbon (DOC), and oxygen reduction potential (ORP). Bolded *t* values are statistically significant ($P < 0.05$).

ronment (Pinder 1995), the relatively short duration of the adult stage compared with the larval stage, along with a general lack of feeding in the adult stage, suggests that environmental controls on the larval stage are more important in determining range and distributions. Initial qualitative descriptions of chironomid species and the presence–absence and (or) abundance of larvae in different lake types (Thienemann 1915; Brundin 1951; Sæther 1979; Wiederholm 1980) were used to develop lake-typology classification schemes, and have been used to relate assemblages to trophic status and to detect environmental stress (Johnson 1995; Wiederholm 1984; Clements et al. 2000).

Within Arctic aquatic systems, chironomid assemblages have been identified to be especially sensitive to perturbations in environmental and landscape conditions (Walker 2001). Walker et al. (1991) found that several warm-adapted taxa are primarily found in southern, temperate habitats; whereas, cold-adapted taxa are found in northern, cold environments. Thus, the distribution and range of many Arctic chironomid taxa were thought to be primarily temperature dependent (Walker et al. 1991). This study's collection of surface sediment samples from across the eastern Canadian Arctic allowed for the representation of chironomid community structure across several regions, and across several environmental gradients within those regions. As expected, deep lakes in colder regions of higher latitude were found to be primarily represented by chironomid communities of the cold-water adapted Diamesinae and Orthocladiinae subfamilies (e.g *Abiskoymia* sp., *Pseudodiamesa*, *Heterotrissocladius* gr., and *Hydrobaenus*/*Oliveridia* gr.). Lakes within these colder regions had taxa that primarily clustered in TWINSPAN group C, and represented colder and deeper lakes. For example, lakes sampled within the Iqaluit area (south-central Baffin Island), were predominantly represented by the cold-water adapted taxon *Heterotrissocladius* gr. This is consistent with Walker and MacDonald (1995), where *Heterotrissocladius*, *Parakiefferiella* cf. *triquetra*, and *Protanypus* were associated with the largest and deepest lakes in the western Canadian Arctic. The association of these cold-water adapted taxa (e.g., *Abiskoymia*) and temperature (Fig. 9*a*) are often used as a proxy indicator of periods of cold climate in paleolimnological studies (Francis et al. 2006).

In contrast, lakes and ponds within the warmer and more productive areas of Arviat, Rankin Inlet (with the exception of RA08), Repulse Bay, and Bylot Island contained species that are considered warm-water adapted taxa of the Tribe Chironomini (Oliver and Roussel 1983; Brooks et al. 2007) such as: *Microtendipes*, *Dictotendipes*, *Cladopelma*, *Polype-*

Fig. 4. The classification of the 63 sampling locations across the eastern Canadian Arctic with the use of two-way indicator species analysis (TWINSPAN). Significant differences ($P < 0.05$) between TWINSPAN divisions via ANOVA of detrended correspondence analysis (DCA) axis 1 sample scores (solid-line boxes) and DCA axis 2 sample scores (dashed-line boxes) are indicated. Taxon names are reflective of the TWINSPAN indicator taxa.

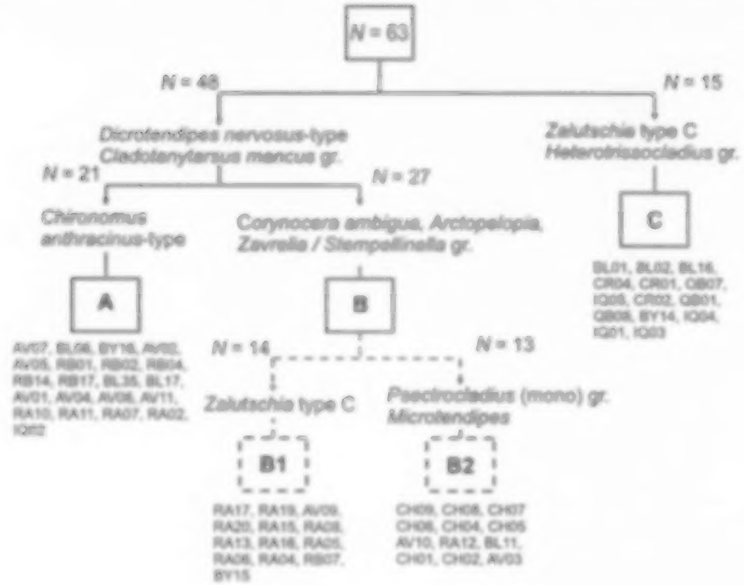
N = 63
N = 48
N = 15
Dicrotendipes nervosus-type
Cladotanytarsus mancus gr.
Zalutschia type C
Heterotrissocladius gr.
N = 21
N = 27
Chironomus anthracinus-type
Corynocera ambigua, Arctopelopia, Zavrelia / Stempellinella gr.
C
BL01, BL02, BL16, CR04, CR01, QB07, IQ05, CR02, QB01, QB09, BY14, IQ04, IQ01, IQ03
A
AV07, BL08, BY16, AV02, AV05, RB01, RB02, RB04, RB14, RB17, BL35, BL17, AV01, AV04, AV08, AV11, RA10, RA11, RA07, RA02, IQ02
B
N = 14
N = 13
Zalutschia type C
Psectrocladius (mono) gr.
Microtendipes
B1
B2
RA17, RA19, AV09, RA20, RA15, RA08, RA13, RA16, RA05, RA06, RA04, RB07, BY15
CH09, CH08, CH07, CH06, CH04, CH05, AV10, RA12, BL11, CH01, CH02, AV03

dilum, *Cryptochironomus*, *Parachironomus*, *Endochironomus*, and *Glyptotendipes*. These sites also had an absence of *Heterotrissocladius* remains. Occurrences of warm-water adapted taxa in Arctic lakes have been documented in a few cases (e.g., Iceland, Langdon et al. 2008; Kiktitmeot tree line region, Porinchu et al. 2009), but have not previously been found in lakes within colder regions of the eastern Canadian Arctic north of tree line (e.g., Kivalliq, Baffin regions). For example, *Cladopelma* sp. were found in nine lakes in our data set, and ranged in abundance from 0% to 5% in lakes that were from 0.5 to 7 m deep. This is noteworthy as *Cladopelma*, a warm-stenotherm, has a Holarctic distribution in warm, low-latitude lakes (Walker et al. 1991; Brooks et al. 2007), and in temperate systems is found primarily in shallow polymictic lakes, with very rare occurrences in deeper, stratified lakes (R. Quinlan, unpublished data). *Cladopelma* was also found in shallow ponds within the vicinity of Iqaluit (IQ02), along with *Dicrotendipes*, *Chironomus anthracinus*-type, and a high abundance of *Tanytarsus lugens* compared to other lakes sampled within the Baffin region. In addition, six lakes sampled within the vicinity of Iqaluit also contained *Chaoborus* mandibles, which were not found in sediments from any other region sampled. The presence of adult *Chaoborus* in the southern Baffin region was noted in Lamontagne et al. (1994), but *Chaoborus* are traditionally strongly associated with temperate systems, and were thought to be limited by tree line (Walker et al. 1997).

Although several lakes that were represented by cold-water adapted taxa were observed to separate primarily based on MSSWT (e.g., TWINSPAN group C), several lakes did not follow a simple latitude–temperature–depth relationship. For example, lakes in the tree line region were relatively shallow (2–5 m), but colder than similar lakes ~100 km north in the Arviat area. Lakes clustered around this tree line area within the vicinity of Churchill had higher abundances of cold-water adapted taxa, such as *Heterotrissocladius* gr. and *Micropsectra insignilobus*-type. Likewise, shallow ponds in the colder northern and central areas of Repulse Bay and Baker Lake contained several taxa of the Tribe Chironomini that are traditionally thought of as warm-water adapted (e.g., *Dicrotendipes* and *Cladopelma*). The variation in the distribution of chironomid taxa dependant on localized conditions within a particular bioregion was also noted by Kernan et al. (2009) who found that the inter-regional differences among lakes in Europe accounted for a large portion of the biotic response to large-scale variations in environmental conditions. Thus, our analysis suggests that, while temperature is a primary factor governing the distribution of midges in Arctic lakes when conducting large spatial gradient analyses of the entire data set, there is within-region variability with several lakes and ponds containing taxa that fall outside of a "traditional" paradigm that invokes the presence of warm-water adapted Chironomidae taxa in lakes at southern latitudes, with shallow depth and high temperatures.

Nutrients and productivity

The role of nutrients and productivity in governing the distribution of chironomids has been alluded to in several recent studies (Brodersen and Anderson 2002; Langdon et al. 2010). The difficulty of interpreting the influence of nutrients on the abundances of several taxa is complicated by the latitudinal transect-sampling approach of several Arctic surveys (Walker et al. 1991; Porinchu et al. 2009) that rely on the environmental conditions of relatively few lakes sampled along transects that cross large geographical areas (Telford and Birks 2009). While temperature gradients are maximized through

Fig. 5. Boxplots of selected environmental variables by two-way indicator species analysis (TWINSPAN) group: (*a*) mid-summer surface water temperature (MSSWT); (*b*) surface area (SA); (*c*) depth; (*d*) conductivity (COND); (*e*) dissolved inorganic carbon (DIC); (*f*) chlorophyll *a* (CHLA); (*g*) total nitrogen (TN); (*h*) total phosphorus (TP).

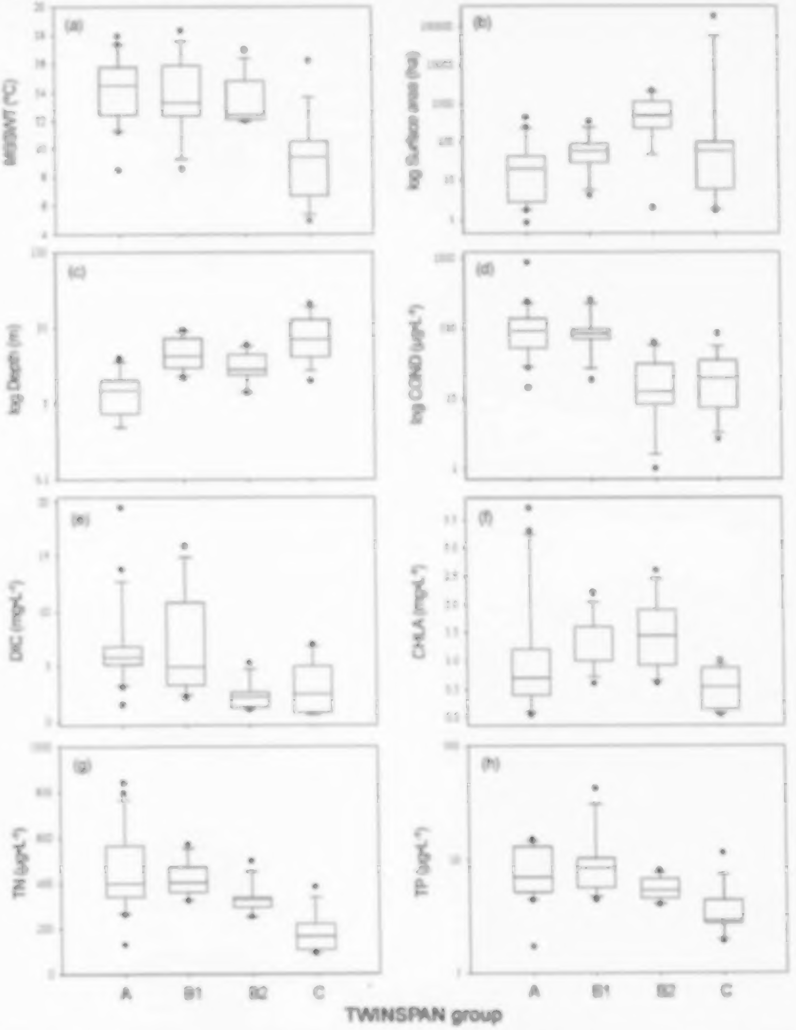

latitudinal transect-sampling, other environmental factors may not be realized owing to short gradients of parameters responsive to local factors. This may result in results that may be scale dependent, with only long environmental gradients generating statistically significant responses from assemblages (Walker et al. 1992; Velle et al. 2010). Our approach of sampling lakes and ponds from multiple regions of varying latitude and mean July temperature, as well as multiple lakes from within the same geographical area, was to examine both the "pure" and interactive influences of nutrients–productivity and temperature on Chironomidae communities.

The significant influence of DIC and DOC on the first RDA axis is representative of larger, deeper lakes in colder regions that have lower nutrient inputs from catchment areas. Lakes and ponds ordinated in the upper-left quadrant of the RDA, reflective of higher MSSWT, higher inputs of DIC and DOC, and higher TN, had higher abundances of warm-water adapted Chironomini. The role of DIC and DOC in particular may be important in the distribution of several species (e.g., *Cricotopus intersectus*-type, *Endochironomus*, *Cladopelma*, and *Tanytarsus lugens/Corynocera oliveri* gr.), based on their placement in RDA ordinations. In particular, *Tanytarsus lugens/Corynocera oliveri* were found to be positively associated to lakes with higher DOC concentrations, and were absent from lakes with low DOC (<1.0 mg·L^{-1}) in the Clyde River vicinity. Gajewski et al. (2005) also found that *Tanytarsus lugens/Corynocera oliveri* were found at higher DOC concentrations, but absent from the central Arctic Archipelago where watershed DOC inputs were limited. Likewise, Langdon et al. (2008) suggest a positive relationship between *Tanytarsus lugens* and total organic carbon. The restriction of zooplankton and benthic invertebrates due to high UVB penetration in Arctic ultra-oligotrophic systems with low DOC–DIC (Molot et al. 2004) could also be limit-

Fig. 6. Redundancy analysis (RDA) of sampled locations and significant environmental indicators. Two-way indicator species analysis (TWINSPAN) divisions significant to detrended correspondence analysis (DCA) axis 1 are indicated: ●, division A; ▲, division B; ■, division C. Environmental abbreviations are as in Table 1.

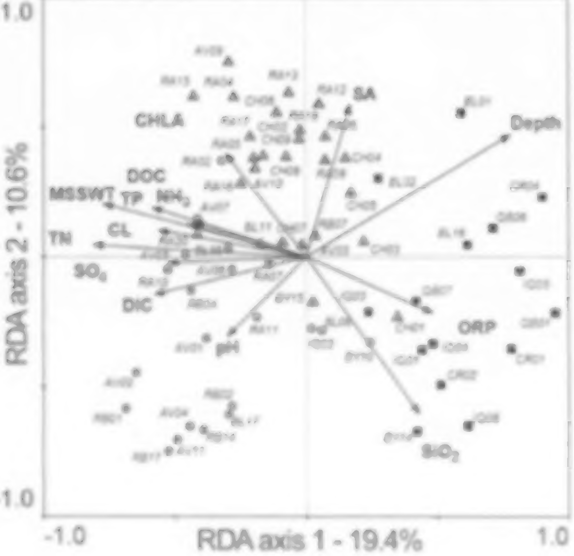

Fig. 7. Redundancy analysis (RDA) of species and significant environmental indicators. Environmental abbreviations are as in Table 1. Selected species are indicated, and abbreviated as follows: Abisk, *Abiskomyia*; Hydrob, *Hydrobaenus/Oliveridia* gr.; Psecp, *Psectrocladius psectrocladius* gr.; ParakN, *Parakiefferiella nigra*; Pseudo, *Pseudodiamesa*; Psecp, *Psectrocladius psectrocladius* gr.; ZalutC; *Zalutschia* sp. C; ZalutL, *Zalutchia* nr. *lingulata pauca*; ZalutZ, *Zalutchia zalutschicola*; Htotal, *Heterotrissocladius* gr.; Mesoc, *Mesocricotopus*; Cinter, *Cricotopus intersectus*-type; CoryO, *Corynocera Oliveri-type*; Paracl, *Paracladius*; CoryArc, *Coryononuera arctica*; Eukif, *Eukiefferiella/Tvetenia* gr.; Limno, *Limnophyes*; OrthoS, *Orthocladius* type S; Metro, *Metrocnemus* gr.; Cladman, *Cladotanytarsus mancus* gr.; Minsigs, *Micropsectra insignilobus*-type; Cambig, *Corynocera ambigua*; ZavStemp, *Zavrelia/Stempellinella* gr.; Protany, *Protanypus*; ParaT, *Paratanytarsus* gr.; Dicrot, *Dicrotendipes nervosus*-type; Microten, *Microtendipes pedellus*-type; Crypto, *Cryptochironomus*; Cpelma, *Cladopelma*; Chiron, *Chironomus anthracinus*-type; Polyp, *Polypedilum*; Harnesh, *Harnischia/Paracladopelma* gr.; Proclad, *Procladius*; and Sticto, *Strictochironomus* gr.

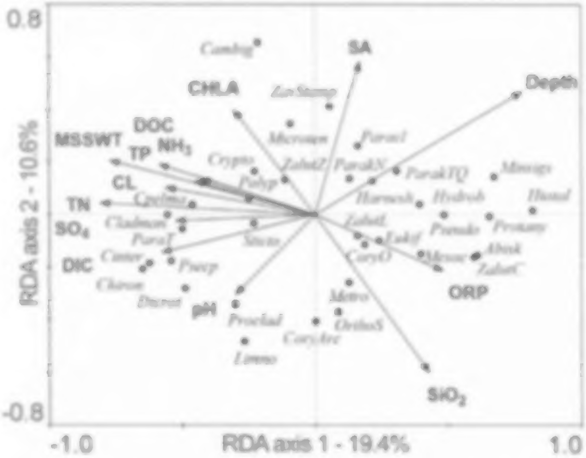

ing Arctic aquatic food webs, subsequently influencing these taxa.

Several specific taxa were found to have higher abundances in lakes and ponds with both high MSSWT and TN (e.g., *Cricotopus intersectus*-type, *Chironomus anthracinus*, and *Cladotanytarsus mancus* gr.). In contrast, *Micropsectra insignolobus*-type was primarily found in colder lakes and ponds with lower TN, and was generally absent in lakes that were classified by TWINSPAN group C (productive, larger lakes). *Cricotopus intersectus*-type in particular was found in lakes and ponds with higher available nutrients and higher MSSWT, which contrasts with most other species of *Cricotopus* that are usually associated with cold-water conditions (Oliver and Roussel 1983). This relationship was also identified by Langdon et al. (2008), who found *Cricotopus intersectus*-type in lakes with higher mean-July temperature in northwest Iceland. Heiri and Lotter (2010) found that the coarse taxonomic resolution of several commonly grouped taxa reduces the effectiveness of chironomids as environmental indicators. Thus, the relationships of indicator taxa such as *Cricotopus intersectus*-type and *Micropsectra insignolobus*-type are of particular interest, as these chironomids are often grouped to a lower taxonomic resolution in other chironomid examinations in the Arctic (Walker and MacDonald 1995; Gajewski et al. 2005; Francis et al. 2006).

Several relationships were also observed with the association with environmental variables significantly correlated to RDA axis 2, which is reflective of lakes and ponds in areas of higher depth and higher productivity. *Dicrotendipes nervosus*-type and *Microtendipes pedellus*-type represented the highest relative abundance of warm-water adapted (Tribe Chironomini) species in several lakes. Walker and MacDonald (1995) related *Microtendipes* to the proximity of tree line. While lakes sampled along our tree-line gradient did indicate higher relative abundances of *Microtendipes pedellus*-type, they were also present several hundred kilometres north of tree line in warmer, larger, moderately deep (2–8 m) lakes with higher productivity (Fig. 9*b*).

In contrast, *Dicrotendipes nervosus*-type was primarily found in shallow ponds in colder regions with higher total nitrogen (Fig. 9*d*). *Dicrotendipes* is traditionally considered a warm-water adapted taxon associated with tree line (Oliver and Roussel 1983; Walker and MacDonald 1995). However, *Dicrotendipes* were found at particularly high relative abundances farther north in shallow, buffered lakes around the town of Repulse Bay (15%–23%). In addition, *Dicrotendipes* were abundant (30%–40%) in well-buffered lakes with higher nutrients on Victoria Island (Porinchu et al. 2009), and in warmer Icelandic lakes (Langdon et al. 2008). Three shallow lakes sampled on the south–south-western side of Bylot Island also contained small numbers of *Dicrotendipes*. It is therefore likely that the combination of depth, nutrients, and temperature are the primary determinants of this species in Arctic systems, as they are primarily found in smaller, shallow lakes and ponds with higher available nutrients (repre-

Fig. 8. Species arrows in a singly constrained partial redundancy analysis (RDA) of: (*a*) midsummer surface water temperature (MSSWT) with total nitrogen (TN) as a covariable; and (*b*) TN with MSSWT as a covariable. Only species arrows with a strong correlation (|*r*| > 0.5) are shown.

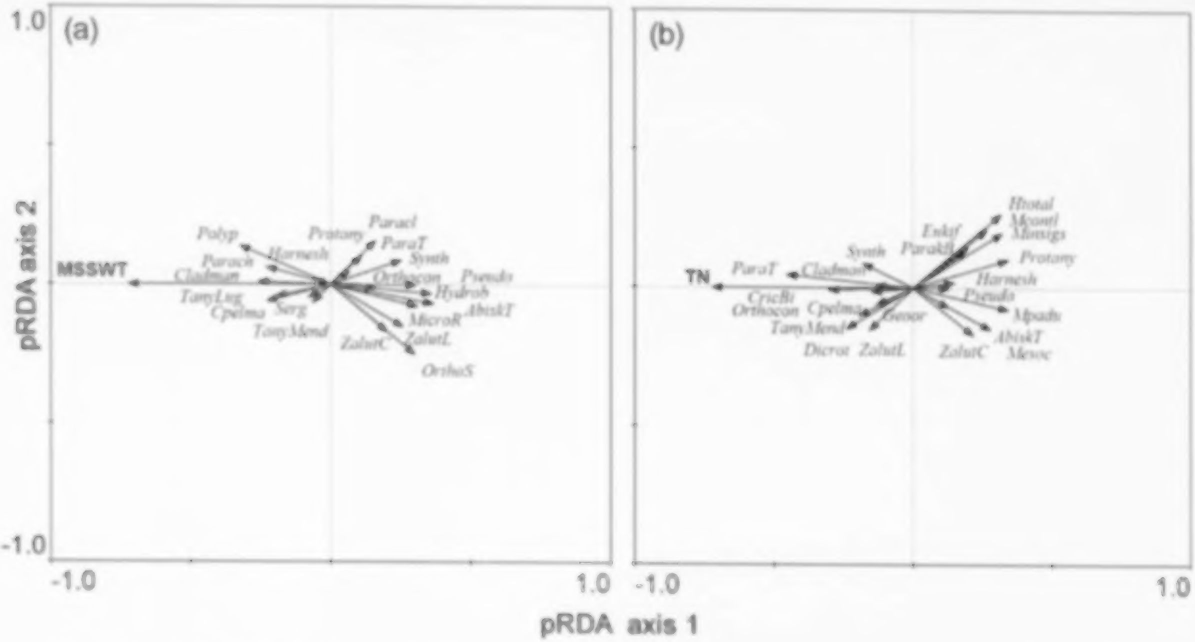

sented by RDA axis 2, TWINSPAN group A). The pattern of either lake temperature and (or) trophic status in strongly influencing the distribution of some taxa is similar to Brodersen and Anderson (2002) and Langdon et al. (2010), who found that the temperature optima and trophic optima of chironomid taxa were strongly correlated.

Regionality

Unique regional patterns in the distribution of specific chironomid taxa were also observed. Lakes within the southern Kivalliq region were often dominated by several species of Tanytarsini (e.g., *Cladotanytarsus mancus* gr., *Tanytarsus lugens*, and *Corynocera ambigua*). For example, *Corynocera ambigua* represented the most dominant species found in the Kivalliq region, and was found to comprise 20%–80% of the chironomid community in warmer, deeper sites with higher productivity (Fig. 9*c*). This aptly named taxon has a perplexing environmental preference as it has been found to be highly abundant in a variety of environments. Brodersen and Lindegaard (1999*b*) found *Corynocera ambigua* at high abundances in shallow, warm, eutrophic lakes in Denmark. In contrast, Larocque-Tobler et al. (2010) found that *Corynocera ambigua* dominated a time period of inferred cold climate (8200 years BP) in a Switzerland lake, and was presently absent from any lake sampled within the same area. Our results indicate that *Corynocera ambigua* is less abundant, or absent altogether, in shallow (<3 m) lakes and (or) ponds compared with deeper sites within the same geographical area. The relative abundances of other Tanytarsini were also higher in these shallow lakes.

Corynocera ambigua were not found in any of our northern surface samples from Baffin Island, or extensive Baffin surveys by Francis et al. (2006). While this taxon's distribution suggests that its brachypterous adult stage is limiting its geographic distribution and dispersal from mainland regions of central Nunavut to Baffin Island, recent surveys by Porinchu et al. (2009) found high abundances of *C. ambigua* in several lakes on Victoria Island. Likewise, *C. ambigua* also occurs in several of the lakes sampled on Bylot Island (2.8–4.8 m depth), and comprised more than 18% of the chironomid community in Lake BY15. Walker and Cwynar (2006) and Barley et al. (2006) have suggested that the distribution of this flightless chironomid species may be reflective of a Beringian refugium, as it has been previously found in very limited areas across the Arctic Archipelago. In contrast, Velle et al. (2005) found that high abundances of *C. ambigua* occurred at species-rich periods following deglaciation in Scandinavian lakes, suggesting that environmental factors, and not mobility, were the primary factor for early colonization. Our results reveal a pattern of *C. ambigua* dominance in larger productive lakes, and absence in shallow unproductive lakes and ponds within the same geographical area. This suggests its distribution is influenced by environmental variables (e.g., food availability and competition). *Corynocera ambigua*'s absence from island sites in eastern Nunavut also suggests its distribution is influenced by biogeographical patterns (dispersion and (or) colonization).

The chironomid communities of the Bylot Island lakes sampled were significantly different in each of the lakes sampled. Each lake was reflective of a different TWINSPAN division, but were represented by taxa not commonly found at high abundances in any other region examined (*Orthocladius* type S, *Tanytarsus lugens/Corynocera oliveri*, and *Zalutschia* nr. *lingulata pauca*). These taxa contrasted with those

Fig. 9. Abundances of environmental indicator taxa plotted on the redundancy analysis (RDA) with significant environmental indicators indicated for *a*, *Abiskomyia* sp.; *b*, *Microtendipes pedellus*-type.; *c*, *Corynoceru ambigua* gr.; *d*, *Dicrotendipes nervosus*-type. Two-way indicator species analysis (TWINSPAN) divisions significant to detrended correspondence analysis (DCA) axis 1 are shown; ●, division A; ▲, division B; ■, division C. Larger symbols represent higher relative abundances as in the Fig. 7*a* inset legend.

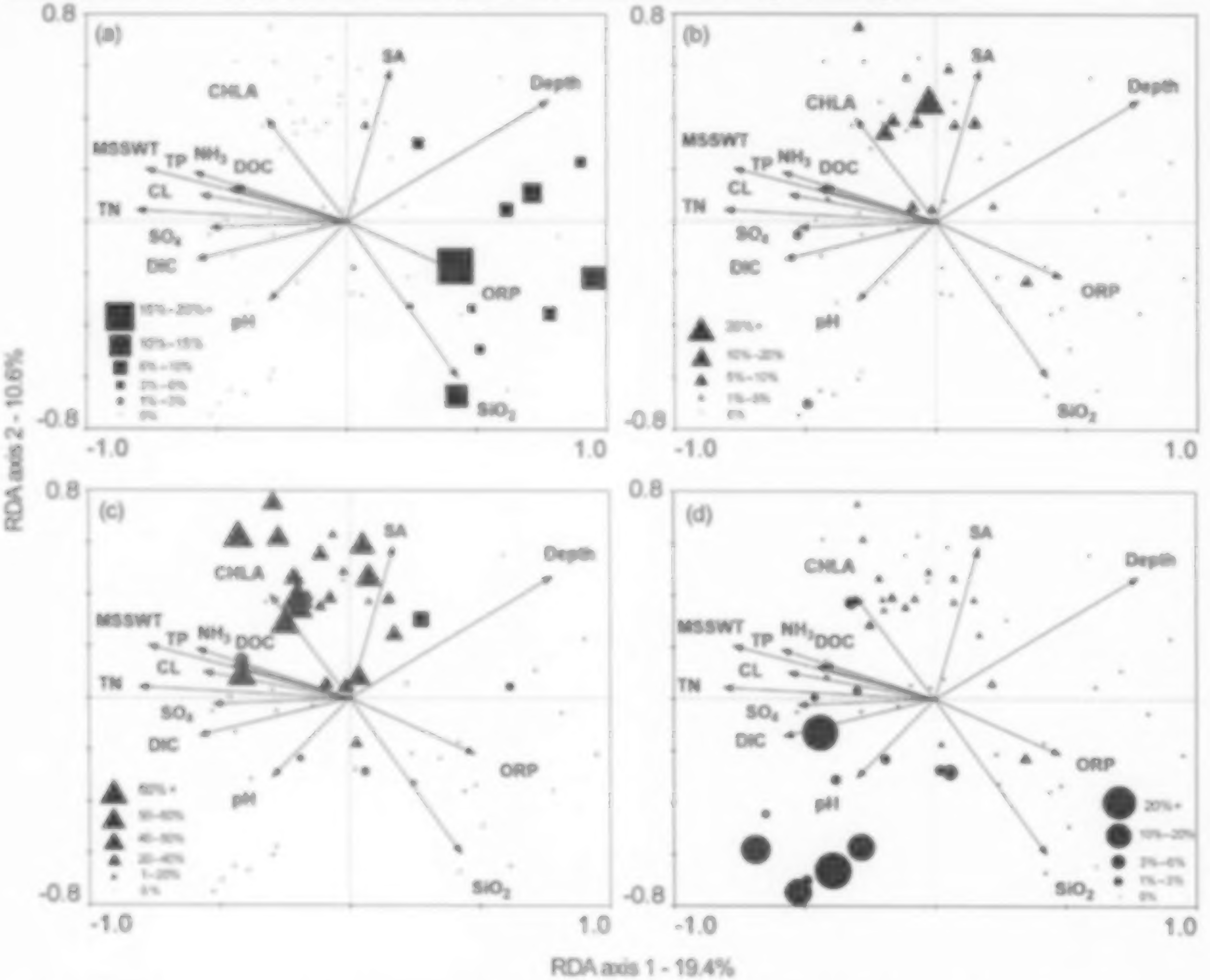

found in lakes directly south in the Qorbignaluk headlands (72°14′37″N, 78°42′49″W) of Baffin Island, which contained mostly cold-water adapted Orthocladiinae taxa. For example, all three Bylot Island lakes contained small numbers of *Dicrotendipes* and *C. ambigua*, but very low numbers of *Heterotrissocladius* gr. that dominated the northern Baffin lakes. Likewise, the chironomid assemblages differ from other archipelago locales that were previously surveyed (Gajewski et al. 2005; Francis et al. 2006). The difference in the chironomid community found in each of the three Bylot Island lakes was pronounced, and resulted in the placement of each lake in a different TWINSPAN division. While each Bylot Island lake contained similar taxa, the composition of the most dominant taxa differed greatly between each lake. This may be explained by the alteration of nutrient regimes in Bylot Island lakes affected by high geese populations within the area (Côté et al. 2010). These highly seasonal localized inputs may be influencing the direction of benthic invertebrate communities in specific lakes towards those more commonly found at higher temperatures owing to nutrient enrichment (Brodersen and Anderson 2002; Michelutti et al. 2011). The significant differences found in the chironomid assemblage composition of these Bylot Island lakes, which are in a similar geographic and climatic area as the northern Baffin samples, highlight the influence of nutrients and productivity on the chironomid community composition of Arctic lakes. Thus, differences in nutrients and productivity at a local scale can be reflected in significant differences in chironomid assemblages.

Future community change

Increases in temperature, reduced ice-cover, and increased thermal stratification as a result of climate warming have shifted the structure of biological communities in Arctic lakes (Walker et al. 1991; Douglas et al. 1994; Rühland et al. 2003). The distribution of chironomid taxa within the eastern Canadian Arctic primarily follow a temperature gradient, however, our results indicate additional relationships along a nutrient–productivity gradient. In addition, while several species common in temperate systems are also cold-tolerant (Danks 2004) and have been found to have successful multi-cohort extended aquatic life-cycles in Arctic environments (Butler 1982), factors such as competition, predation, ice dynamics, and resource availability may be limiting the success of several warm-water taxa within Arctic systems beyond simple cold-tolerance. This is evident in the strong north–south gradient observed in the assemblage composition of several Chironomidae taxa.

From a perspective of using chironomid assemblages to examine climate warming within Arctic lakes and ponds, the presence of several genera of traditionally warm-water adapted taxa of the Tribe Chironomini (e.g., *Cladopelma*, *Dicrotendipes*, *Microtendipes*, and *Polypedilum*) could be an indicator of increased temperatures within these systems. However, the response of this invertebrate community to future climate warming will also be dependent on localized climate-mediated changes to lake and catchment properties including food–web dynamics and catchment vegetation influence on allochthonous inputs of nutrients.

Partially constrained gradient analysis showed that some chironomid taxa could be responding to temperature and nitrogen independently. Those taxa that are strongly correlated to MSSWT, irrespective of the variation in the nitrogen gradient, could be used to differentiate between regional climatic gradients and local controls on nutrient levels. Likewise, those specific taxa found to primarily follow a nitrogen gradient irrespective of the variation in MSSWT could be strong indicators of responses to changes in localized gradients. Thus, changes in specific indicator taxa may be able to separate the two gradients. These relationships could then be applied to biostratigraphic analyses to reconstruct past changes in lake environments, where paleolimnologists may be able to differentiate between climate effects and trophic status effects in influencing long-term changes in subfossil assemblage composition. Likewise, the biostratigraphic examination of taxa that are likely influenced by coincident changes in both temperature and nutrients–productivity (e.g., *Cladotanytarsus mancus*), may offer new insights into the ecological response of aquatic communities to changes in both these variables as a result of possible future climate change. This study also suggests that, for more holistic inferences of how aquatic communities may respond to climate change (e.g., via quantitative inference models), sample selection should also be based on a nutrient–productivity gradient in addition to a large temperature gradient. This can be generated by sampling a number of lakes from within similar areas of varying landscape position and trophic status.

Acknowledgements

This project was funded by a Natural Sciences and Engineering Research Council of Canada (NSERC) Discovery Grant and NSERC Northern Research Supplement held by R.Q., a NSERC Northern Research Internship held by A.S.M., the Northern Scientific Training Program, and additional York University, Toronto, Ontario, funding for graduate student research. We are grateful to Stephen Brooks and Joshua Kurek for assistance with the diagnosis of our *Zalutschia* specimens, Sarah Finkelstein and Jane Devlin (University of Toronto) for sediment samples and water chemistry data for lakes and ponds within Sirmilik National Park, and Derek Muir, Xiaowa Wang, and colleagues at the National Laboratory for Environmental Testing water quality laboratory for water chemistry analysis. Fieldwork assistance and support was provided by Mary Ellen Thomas, Jamal Shirley, Dorothy Tootoo, and the staff at the Nunavut Research Institute and Nunavut Arctic College. We also thank Andy Aliyak, Raymond Biastoch, Andrew Dunford, Milissa Elliott, and Christopher Luszczek for field sampling assistance.

References

Barley, E.M., Walker, I.R., Kurek, J., Cwynar, L.C., Mathewes, R.W., Gajewski, K., and Finney, B.P. 2006. A northwest North American training set: distribution of freshwater midges in relation to air temperature and lake depth. J. Paleolimnol. **36**(3): 295–314. doi:10.1007/s10933-006-0014-6.

Brodersen, K.P., and Anderson, J.N. 2002. Distribution of chironomids (Diptera) in low arctic West Greenland lakes: trophic conditions, temperature and environmental reconstruction. Freshw. Biol. **47**(6): 1137–1157. doi:10.1046/j.1365-2427.2002.00831.x.

Brodersen, K.P., and Lindegaard, C. 1999*a*. Classification, assessment and trophic reconstruction of Danish lakes using chironomids. Freshw. Biol. **42**(1): 143–157. doi:10.1046/j.1365-2427.1999.00457.x.

Brodersen, K.P., and Lindegaard, C. 1999*b*. Mass occurance and sporadic distribution of *Corynocera ambigua* Zetterstedt (Diptera, Chironomidae) in Danish lakes. Neo- and palaeolimnological records. J. Paleolimnol. **22**(1): 41–52. doi:10.1023/A:1008032619776.

Brooks, S.J., Bennion, H., and Birks, J.P. 2001. Tracing lake trophic history with a chironomid total phosphorus inference model. Freshw. Biol. **46**(4): 513–532. doi:10.1046/j.1365-2427.2001.00684.x.

Brooks, S.J., Langdon, P.G., and Heiri, O. 2007. The identification and use of Palaearctic Chironomidae larvae in palaeoecology. QRA Technical Guide No. 10, Quaternary Research Association, London, UK.

Brundin, L. 1951. The relation of O_2-microstratification at the mud surface to the ecology of the profundal bottom fauna. Report of the Institute for Freshwater Research, Drottningholm, Denmark. **32**: 32–42.

Butler, M.G. 1982. A 7-year life-cycle for 2 Chironomus species in Arctic Alaskan tundra ponds (Diptera, Chironomidae). Can. J. Zool. **60**(1): 58–70. doi:10.1139/z82-008.

Clements, W.H., Carlisle, D.M., Lazorchak, J.M., and Johnson, P.C. 2000. Heavy metals structure benthic communities in Colorado mountain streams. Ecol. Appl. **10**(2): 626–638. doi:10.1890/1051-0761(2000)010[0626:HMSBCI]2.0.CO;2.

Côté, G., Pienitz, R., Velle, G., and Wang, X.A. 2010. Impact of geese on the limnology of lakes and ponds from Bylot Island (Nunavut, Canada). Int. Rev. Hydrobiol. **95**(2): 105–129. doi:10.1002/iroh.200911151.

Danks, H.V. 1971. Overwintering of some north temperate and arctic chironomidae. II. Chironomid Biology. Can. Entomol. **103**(12): 1875–1910. doi:10.4039/Ent1031875-12.

Danks, H.V. 2004. Seasonal adaptations in arctic insects. Integr. Comp. Biol. **44**(2): 85–94. doi:10.1093/icb/44.2.85.

Douglas, M.S.V., Smol, J.P., and Blake, W., Jr. 1994. Marked post-18th century environmental change in high-Arctic ecosystems. Science, **266**(5184): 416–419. doi:10.1126/science.266.5184.416. PMID:17816685.

Environment Canada. 1994. Manual of analytical methods. National Laboratory for Environmental Testing, Canadian Centre for Inland Waters, Burlington, Ont.

Epler, J.H. 2001. Identification Manual for the larval Chironomidae (Diptera) of North and South Carolina. A guide to the taxonomy of the midges of the southeastern United States, including Florida. Special Publication SJ2001–SP13. North Carolina Department of Environment and Natural Resources, Raleigh, N.C., and St. Johns River Water Management District, Palatka, Fla.

Francis, D.R., Wolfe, A.P., Walker, I.R., and Miller, G.H. 2006. Interglacial and Holocene temperature reconstructions based on midge remains in sediments of two lakes from Baffin Island, Nunavut, Arctic Canada. Palaeogeogr. Palaeoclimatol. Palaeoecol. **236**(1–2): 107–124. doi:10.1016/j.palaeo.2006.01.005.

Frisch, D., Green, A.J., and Figuerola, J. 2007. High dispersal capacity of a broad spectrum of aquatic invertebrates via waterbirds. Aquat. Sci. **69**(4): 568–574. doi:10.1007/s00027-007-0915-0.

Gajewski, K., Bouchard, G., Wilson, S.E., Kurek, J., and Cwynar, L.C. 2005. Distribution of Chironomidae (Insecta: Diptera) head capsules in recent sediments of Canadian Arctic lakes. Hydrobiologia, **549**(1): 131–143. doi:10.1007/s10750-005-5444-z.

Gauch, H.G., Jr. 1982. Noise reduction by eigenvector ordinations. Ecology, **63**(6): 1643–1649. doi:10.2307/1940105.

Giberson, D.J., Burian, S.K., and Shouldice, M. 2007. Life history of the northern mayfly *Baetis bundyae* in Rankin Inlet, Nunavut, Canada, with updates to the list of mayflies of Nunavut. Can. Entomol. **139**(5): 628–642. doi:10.4039/n06-089.

Glew, J. 1991. Miniature gravity corer for recovering short sediment cores. J. Paleolimnol. **5**(3): 285–287. doi:10.1007/BF00200351.

Heiri, O., and Lotter, A.F. 2010. How does taxonomic resolution affect chironomid-based temperature reconstruction? J. Paleolimnol. **44**(2): 589–601. doi:10.1007/s10933-010-9439-z.

Hill, M.O. 1979. TWINSPAN. A Fortran program for arranging multivariate data in an ordered two-way table by classification of the individuals and attributes. Cornell University, Ithaca, N.Y.

Johnson, R.K. 1995. The indicator concept in freshwater biomonitoring. Thienemann Lecture. *In* Chironomids — from genes to ecosystems. *Edited by* P.S. Cranston. CSIRO, Melbourne, Australia. pp. 11–27.

Juggins, S. 2003. C2 user guide. Software for Ecological and Palaeoecological Data Analysis and Visualisation, University of Newcastle, Newcastle upon Tyne, U.K.

Keatley, B.E., Douglas, M.S.V., and Smol, J.P. 2008. Prolonged ice cover dampens diatom community responses to recent climatic change in High Arctic lakes. Arct. Antarct. Alp. Res. **40**(2): 364–372. doi:10.1657/1523-0430(06-068)[KEATLEY]2.0.CO;2.

Kernan, M., Ventura, M., Bitušík, P., Brancelj, A., Clarke, G., Velle, G., Raddum, G.G., Stuchlík, E., and Catalan, J. 2009. Regionalisation of remote European mountain lake ecosystems according to their biota: environmental versus geographical patterns. Freshw. Biol. **54**(12): 2470–2493. doi:10.1111/j.1365-2427.2009.02284.x.

Lamontagne, S., Donald, D.B., and Schindler, D.W. 1994. The distribution of four *Chaoborus* species (Diptera: Chaoboridae) along an elevation gradient in Canadian Rocky Mountain lakes. Can. J. Zool. **72**(9): 1531–1537. doi:10.1139/z94-203.

Langdon, P.G., Ruiz, Z., Wynne, S., Sayer, C.D., and Davidson, T.A. 2010. Ecological influences on larval chironomid communities in shallow lakes: implications for palaeolimnological interpretations. Freshw. Biol. **55**(3): 531–545. doi:10.1111/j.1365-2427.2009.02345.x.

Langdon, P.G., Holmes, N., and Caseldine, C.J. 2008. Environmental controls on modern chironomid faunas from NW Iceland and implications for reconstructing climate change. J. Paleolimnol. **40**(1): 273–293. doi:10.1007/s10933-007-9157-3.

Larocque-Tobler, I., Heiri, O., and Wehrli, M. 2010. Late Glacial and Holocene temperature changes at Egelsee, Switzerland, reconstructed using subfossil chironomids. J. Paleolimnol. **43**(4): 649–666. doi:10.1007/s10933-009-9358-z.

Medeiros, A.S., Luszczek, C.E., Shirley, J., and Quinlan, R. 2011. Benthic biomonitoring in arctic tundra streams: a community-based approach in Iqaluit, Nunavut, Canada. Arctic, **64**(1): 59–72.

Michelutti, N., Mallory, M.L., Blais, J.M., Douglas, M.S.V., and Smol, J.P. 2011. Chironomid assemblages from seabird-affected high arctic ponds. Polar Biol. **34**(6): 799–812. doi:10.1007/s00300-010-0934-5.

Molot, L.A., Keller, W., Leavitt, P.R., Robarts, R.D., Waiser, M.J., Arts, M.T., Clair, T.A., Pienitz, R., Yan, N.D., McNicol, D.K., Prairie, Y.T., Dillon, P.J., Macrae, M., Bello, R., Nordin, R.N., Curtis, P.J., Smol, J.P., and Douglas, M.S.V. 2004. Risk analysis of dissolved organic matter-mediated ultraviolet B exposure in Canadian inland waters. Can. J. Fish. Aquat. Sci. **61**(12): 2511–2521. doi:10.1139/f04-165.

Oliver, D.R., and Dillon, M.E. 1997. Chironomids (Diptera: Chironomidae) of the Yukon Arctic North Slope and Hershel Island. *In* Insects of the Yukon. *Edited by* H.V. Danks and J.A. Downes. Biological Survey of Canada (Terrestrial Arthropods), Ottawa. pp. 615–635.

Oliver, D.R., and Roussel, M.E. 1983. The insects and arachnids of Canada, Part 11: The genera of larval midges of Canada – Diptera: Chironomidae. Publication 1746, Agriculture Canada, Ottawa, Ont.

Pinder, L.C.V. 1995. The habitats of Chironomidae larvae. *In* The Chironomidae: biology and ecology of non-biting midges. *Edited by* P.D. Armitage, P.S. Cranston, and L.C.V. Pinder. Chapman and Hall, London, UK. pp. 107–133.

Porinchu, D., Rolland, N., and Moser, K. 2009. Development of a chironomid-based air temperature inference model for the central Canadian Arctic. J. Paleolimnol. **41**(2): 349–368. doi:10.1007/s10933-008-9233-3.

Porinchu, D.F., and MacDonald, G.M. 2003. The use and application of freshwater midges (Chironomidae: Insecta: Diptera) in geographical research. Prog. Phys. Geogr. **27**(3): 378–422. doi:10.1191/0309133303767888491.

Quinlan, R., and Smol, J.P. 2001*a*. Chironomid-based inference models for estimating end-of-summer hypolimnetic oxygen from south-central Ontario shield lakes. Freshw. Biol. **46**(11): 1529–1551. doi:10.1046/j.1365-2427.2001.00763.x.

Quinlan, R., and Smol, J.P. 2001*b*. Setting minimum head capsule abundance and taxa deletion criteria in chironomid-based inference models. J. Paleolimnol. **26**(3): 327–342. doi:10.1023/A:1017546821591.

Rieradevall, M., and Brooks, S.J. 2001. An identification guide to subfossil Tanypodinae larvae (Insecta: Diptera: Chironomidae) based on cephalic setation. J. Paleolimnol. **25**(1): 81–99. doi:10.1023/A:1008185517959.

Rouse, W., Douglas, M., Hecky, R., Hershey A., Kling, G., Lesack, L., Marsh, P., McDonald, M., Nicholson, B., Roulet, N., and Smol, J.P. 1997. Effects of climate change on the freshwaters of Arctic and sub Arctic North America. Hydrol. Process. **11**(8): 873–902. doi:10.1002/(SICI)1099-1085(19970630)11:8<873::AID-HYP510>3.0.CO;2-6.

Rühland, K., Priesnitz, A., and Smol, J.P. 2003. Paleolimnological evidence from diatoms for recent environmental changes in 50 lakes across Canadian Arctic treeline. Arct. Antarct. Alp. Res. **35**(1): 110–123. doi:10.1657/1523-0430(2003)035[0110:PEFDFR]2.0.CO;2.

Sæther, O.A. 1976. Revision of *Hydrobaenus*, *Trissocladius*, *Zalutschia*, *Paratrissocladius*, and some related genera (Diptera: Chironomidae). Bull. Fish. Res. Board Can. **195**: 1–287.

Sæther, O.A. 1979. Chironomid communities as water quality indicators [online]. Holarct. Ecol. **2**(2):65–74. Available from: http://www.jstor.org/stable/3682659 [accessed 22 Dec 2010].

Statistics Canada. 2006. 2006 Census of Canada. Government of Canada, Ottawa, Ontario.

Stur, E., and Ekrem, T. 2011. Exploring unknown life stages of Arctic Tanytarsini (Diptera: Chironomidae) with DNA barcoding. Zootaxa, **2743**(18): 27–39.

Telford, R.J., and Birks, H.J.B. 2009. Evaluation of transfer functions in spatially structured environments. Quat. Sci. Rev. **28**(13–14): 1309–1316. doi:10.1016/j.quascirev.2008.12.020.

ter Braak, C.J.F., and Šmilauer, P. 1998. CANOCO reference manual and user's guide to CANOCO for windows: Software for canonical community ordination. Version 4. Microcomputer Power, New York.

Thienemann, A. 1915. Die Chironomidenfauna der Eifelmaare. Verhandlungen des Naturhistischer Verein der Rheinlande und Westfalens, **72**: 1–58.

Uutala, A.F. 1990. *Chaoborus* (Diptera:Chaoboridae) mandibles — paleolimnological indicators of the historic status of fish populations in acid-sensitive lakes. J. Paleolimnol. **4**(2): 139-151. doi:10.1007/BF00226321.

Velle, G., Brodersen, K.P., Birks, H.J.B., and Willassen, E. 2010. Midges as quantitative temperature indicator species: Lessons for palaeoecology. Holocene, **20**(6): 989–1002. doi:10.1177/0959683610365933.

Velle, G., Brooks, S.J., Birks, H.J.B., and Willassen, E. 2005. Chironomids as a tool for inferring Holocene climate: an assessment based on six sites in southern Scandinavia. Quat. Sci. Rev. **24**(12–13): 1429–1462. doi:10.1016/j.quascirev.2004.10.010.

Walker, I.R. 2007. The WWW field guide to fossil midges [online]. Available from http://www.paleolab.ca/wwwguide [accessed 5 May 2010].

Walker, I.R., and Cwynar, L.C. 2006. Midges and paleotemperature reconstruction – the North American experience. Quat. Sci. Rev. **25**(15–16): 1911–1925. doi:10.1016/j.quascirev.2006.01.014.

Walker, I.R. 2003. Chironomid overview. *In* Encyclopaedia of Quaternary Science, Vol. 1. *Edited by* S.A. Elias. Elsevier, Amsterdam, the Netherlands. pp. 360–366.

Walker, I.R. 2001. Midges: Chironomidae and related Diptera. *In* Tracking environmental change using lake sediments, vol. 4. Zoological indicators. *Edited by* J.P. Smol, H.J.B. Birks, and W.M. Last. Kluwer Academic Publishers, Dordrecht, the Netherlands. pp. 43–66.

Walker, I.R., Levesque, A.J., Cwynar, L.C., and Lotter, A.F. 1997. An expanded surface-water paleotemperature inference model for use with fossil-midges from eastern Canada. J. Paleolimnol. **18**(2): 165–178. doi:10.1023/A:1007997602935.

Walker, I.R., and MacDonald, G.M. 1995. Distributions of Chironomidae (Insecta:Diptera) and other freshwater midges with respect to treeline, Northwest Territories, Canada. Arct. Alp. Res. **27**(3): 258–263. doi:10.2307/1551956.

Walker, I.R., Smol, J.P., Engstrom, D.R., and Birks, H.J.B. 1992. Aquatic invertebrates, climate, scale, and statistical hypothesis testing: a response to Hann, Warner, and Warwick. Can. J. Fish. Aquat. Sci. **49**(6): 1276–1280.

Walker, I.R., Smol, J.P., Engstrom, D.R., and Birks, H.J.B. 1991. An Assessment of Chironomidae as quantitative indicators of past climate change. Can. J. Fish. Aquat. Sci. **48**(6): 975–987. doi:10.1139/f91-114.

Walker, I.R. 1990. Modern assemblages of Arctic and alpine Chironomidae as analogues for late-glacial communities. Hydrobiologia, **214**(1): 223–227.

Walker, I.R. 1988. Late-quaternary palaeoecology of Chironomidae (Diptera:Insecta) from lake sediments in British Columbia. Ph.D. thesis, Simon Fraser University, Burnaby, B.C.

Wiederholm, T. 1984. Incidence of deformed chironomid larvae (Diptera: Chironomidae) in Swedish lakes. Hydrobiologia, **109**(3): 243–249. doi:10.1007/BF00007742.

Wiederholm, T. (*Editor*). 1983. Chironomidae of the Holarctic region. Keys and diagnosis. Part 1. Larvae. Entomologica Scandinavica Suppl. No. 19.

Wiederholm, T. 1980. Use of benthos in lake monitoring. J. Water Pollut. Control Fed. **52**(3): 537–547.

A computational model for asynchronous oocyte growth dynamics in a batch-spawning fish

Zhenhong Li, Daniel L. Villeneuve, Kathleen M. Jensen, Gerald T. Ankley, and Karen H. Watanabe

Abstract: A computational model of oocyte growth dynamics (i.e., oocyte recruitment, growth, and spawning) in a batch-spawning fish, fathead minnow (FHM, *Pimephales promelas*), has been developed. The model provides a quantitative link between oocyte growth dynamics and biochemical processes in FHMs through the absorption of vitellogenin (a lipoprotein precursor of egg yolk proteins) into oocytes, which contributes significantly to oocyte growth in fish. The model simulates the number and volume of oocytes in different batches within a FHM ovary. Model-predicted clutch sizes and spawning intervals matched the experimental data well for both unexposed FHMs and FHMs exposed to 17β-trenbolone (a relatively stable metabolite of trenbolone acetate, a synthetic androgen used as a growth promoter in livestock). Overall, the model presents a novel approach to simulating oocyte growth dynamics in a batch-spawning fish and meets an urgent need in ecotoxicological studies to link the effects of endocrine disrupting chemicals at a biochemical level to adverse effects upon reproduction.

Résumé : Nous mettons au point un modèle informatique de la dynamique de la croissance des oocytes (c'est-à-dire, du recrutement des oocytes, de leur croissance et de leur ponte) chez un poisson qui pond par masses, la tête-de-boule (FHM, *Pimephales promelas*). Le modèle fournit un lien quantitatif entre la dynamique de la croissance des oocytes et les processus biochimiques chez la FHM par l'absorption dans les oocytes de la vitellogénine (un précurseur lipoprotéinique des protéines du vitellus), qui contribue significativement à la croissance des oocytes chez les poissons. Le modèle simule le nombre et le volume des oocytes dans les différentes masses dans un ovaire de FHM. Les tailles des pontes et les intervalles entre les pontes prédits par le modèle correspondent bien aux données expérimentales, tant chez les FHM non exposés que chez les FHM exposés au 17β-trenbolone (un métabolite relativement stable de l'acétate de trenbolone, un androgène de synthèse utilisé pour promouvoir la croissance chez le bétail). Globalement, le modèle représente une approche nouvelle pour simuler la dynamique de la croissance des oocytes chez un poisson qui pond ses œufs par masses et répond à un besoin pressant dans les études écotoxicologiques de pouvoir relier au niveau biochimique les effets des produits chimiques disruptifs du système endocrinien aux conséquences négatives sur la reproduction.

[Traduit par la Rédaction]

Introduction

At least two distinct modes of spawning, total and batch, have been characterized in oviparous fish. During a breeding season, total-spawning females spawn all of their eggs at one time (e.g., Atlantic salmon, *Salmo salar*); in contrast, batch-spawning females spawn many times. Examples of batch-spawning fish include several species used for laboratory experimentation such as the fathead minnow (FHM, *Pimephales promelas*), zebrafish (*Danio rerio*), and Japanese medaka (*Oryzias latipes*) (Nagahama et al. 1995; Wallace and Selman 1981; Yaron et al. 2003). To date, most of the research on oocyte development and regulation has been conducted with total-spawning fish species (Nagahama et al. 1995; Tyler et al. 1996; Tyler and Sumpter 1996), with comparatively few studies having been conducted with batch-spawning fish species. Further, most of the studies done with batch-spawning fish have been from the perspective of basic reproduction (Jensen et al. 2001; Leino et al. 2005; Wolf et al. 2004).

It is important to understand mechanisms of oocyte development and regulation in batch-spawning fish because many of them are used as ecotoxicological research models worldwide and effects upon reproduction are a major concern. For example, the FHM is arguably the most widely used small fish model for regulatory ecotoxicology in the USA (Ankley and Villeneuve 2006). In the 1990s, the U.S. Environmental Protection Agency (USEPA) initiated a program using FHMs

Received 9 June 2010. Accepted 15 April 2011. Published at www.nrcresearchpress.com/cjfas on 29 August 2011.
J21869

Paper handled by Associate Editor Karen Kidd.

Z. Li and K.H. Watanabe. Division of Environmental and Biomolecular Systems, Department of Science and Engineering, Oregon Health & Science University, West Campus, Beaverton, OR 97006, USA.
D.L. Villeneuve, K.M. Jensen, and G.T. Ankley. US Environmental Protection Agency, Office of Research and Development, National Health and Environmental Effects Research Laboratory, Mid-Continent Ecology Division, Duluth, MN 55804, USA.

Corresponding author: K.H. Watanabe (e-mail: watanabe@ebs.ogi.edu).

Can. J. Fish. Aquat. Sci. **68**: 1528–1538 (2011) doi:10.1139/F2011-066 **Published by NRC Research Press**

Table 1. Summary of data used in model parameterization, calibration test, and model evaluation.

Data	EDC	Dose ($\mu g \cdot L^{-1}$)	EL (days)	No. of female FHM	No. of groups	Endpoints	Application
Paired-spawning design							
I	None	0	0	50	50	CS, SI, AF, [plasma VTG]	Parameterize (Table 2) and evaluate (Fig. 4) the model
I	None	0	0	10	10	CS, SI, AF	Parameterize the model (Table 2)
Group-spawning design							
II	None	0	0	77	20	AF, [plasma VTG]	Model evaluation (Fig. 5)
III	TB	0.005, 0.05, 0.5, 5, and 50	21	71	18	AF, [plasma VTG]	Model evaluation (Fig. 6)

Note: EDC, endocrine disrupting chemicals; TB, 17β-trenbolone; EL, exposure length; FHM, fathead minnows; CS, clutch size; SI, spawning interval; AF, average fecundity; [plasma VTG], plasma vitellogenin concentration.

to screen and test endocrine-disrupting chemicals (EDCs) that affect the hypothalamic–pituitary–gonadal (HPG) axis (http://www.epa.gov/scipoly/oscpendo/index.htm) (Ankley et al. 2009*a*). In these studies, traditional endpoints (e.g., fecundity, number of eggs per female spawns per day) and molecular endpoints (e.g., plasma vitellogenin (VTG) concentration) are used to evaluate the toxic effects of EDCs (Ankley et al. 2009*a*).

To link chemical effects at the molecular level (e.g., plasma VTG concentration) to effects on the individual (e.g., fecundity) and ultimately the population, it is important to understand the mechanisms regulating oocyte development both qualitatively and quantitatively. To explore these mechanisms, a traditional approach is a whole-fish test. However, the cost of this approach is high, and testing the reproductive effects of all chemicals or chemical mixtures is impractical. Therefore, other methods are needed to inform scientists and regulators. Computational modeling is a method that is less expensive than experiments, is useful for combining knowledge from multiple experimental studies, and enables testing of possible biological mechanisms.

A statistical model developed by Miller et al. (2007) provides a linear relationship between relative fecundity and relative plasma VTG concentration (expressed as a proportion of the baseline measurements for each endpoint) for female FHMs exposed to five EDCs that reduce VTG synthesis. Other than Miller et al. (2007), we are not aware of any reports in the open literature of a computational model for oocyte growth and spawning in fishes. In this study, to simulate oocyte growth dynamics in FHMs, we developed a computational model that incorporates more biological processes than the statistical model by Miller et al. (2007). As a first-order approximation in model building, we simplified the mechanisms controlling oocyte growth, leaving hormonal regulation to future work. The model simulates oocyte growth and spawning in both unexposed FHMs and FHMs exposed to 17β-trenbolone, one of the five EDCs used by Miller et al. (2007).

17β-trenbolone is a relatively stable metabolic product of trenbolone acetate, a synthetic androgen used as a growth promoter in livestock (e.g., cattle). 17β-trenbolone enters the environment mainly as runoff from livestock feedlots. Durhan et al. (2006) studied a cattle feedlot located in southwestern central Ohio and reported that the 17β-trenbolone concentration in feedlot discharge was between 10 and 20 $ng \cdot L^{-1}$. 17β-trenbolone is a strong androgen receptor agonist that depresses VTG production. Exposure to 17β-trenbolone at concentrations similar to those found in the environment decreases egg production in female FHMs and produces changes in plasma concentrations of 17β-estradiol, testosterone, and VTG (Ankley et al. 2003). Increasing 17β-trenbolone exposure concentrations results in "U-shaped" responses for plasma 17β-estradiol, testosterone, and VTG concentrations (Ankley et al. 2003).

Materials and methods

Experimental data

Fathead minnow fecundity data (Table 1) were obtained from 13 studies conducted at the USEPA Mid-Continent Ecology Division Laboratory in Duluth, Minnesota, from 1999 to 2006. The experimental designs and corresponding data summaries were described by Watanabe et al. (2007). Among the 13 studies, one was a baseline reproduction study in unexposed (baseline) FHMs (Jensen et al. 2001), and the rest were reproduction studies in which FHMs were exposed to 12 EDCs, including methoxychlor and methyltestosterone (Ankley et al. 2001), fadrozole (Ankley et al. 2002), 17β-trenbolone (Ankley et al. 2003), flutamide (Jensen et al. 2004), prochloraz and fenarimol (Ankley et al. 2005*a*), perfluorooctane sulfonate (Ankley et al. 2005*b*), 17α-trenbolone (Jensen et al. 2006), prometon (Villeneuve et al. 2006), ketoconazole (Ankley et al. 2007), and haloperidol (Villeneuve et al. 2010). For modeling purposes, we used fecundity data from the baseline reproduction study (data I), the control FHMs from the 12 EDC exposure experiments (data II), and FHMs exposed to 17β-trenbolone (data III) (Ankley et al. 2003). The 13 studies were classified into two groups based on experimental design: paired-spawning-design (PSD) studies with one male and one female per tank and group-spawning-design (GSD) studies with two males and four females per tank. The PSD studies were performed in unexposed FHMs (Jensen et al. 2001) and FHMs exposed to prochloraz and fenarimol (Ankley et al. 2005*a*), perfluorooctane sulfonate (Ankley et al. 2005*b*), 17α-trenbolone (Jensen et al. 2006), prometon (Villeneuve et al. 2006), and haloperidol (Villeneuve et al. 2010). The GSD studies were performed in FHMs exposed to methoxychlor and methyltestosterone (Ankley et al. 2001), fadrozole (Ankley et al. 2002), 17β-trenbolone (Ankley et al. 2003), flutamide (Jensen et al. 2004), and ketoconazole (Ankley et al. 2007).

We created a scheme to show how data were used in the model parameterization and evaluation (Fig. 1). From PSD studies, we had records of clutch sizes (eggs per spawn), spawning intervals (days), and average fecundity (eggs per fe-

Fig. 1. A scheme for data usage in model parameterization and evaluation. The solid arrows represent parameter generation and model output. The broken arrows represent comparisons between model predictions and experimental data. VTG, plasma vitellogenin.

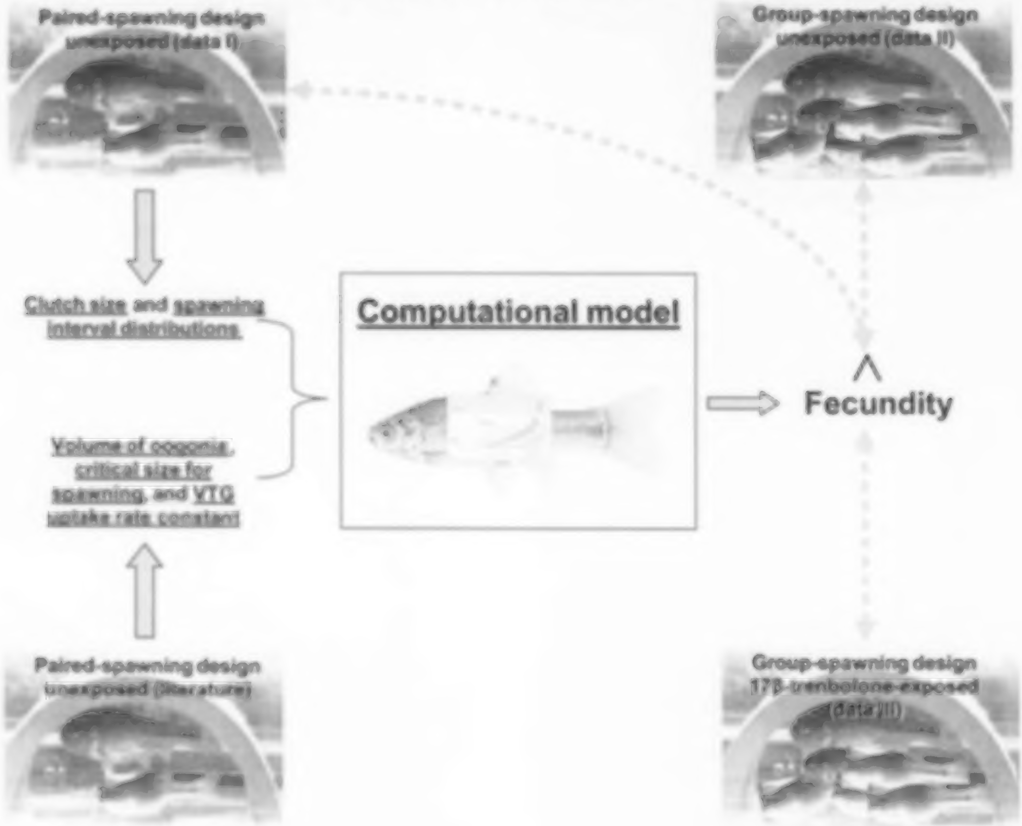
Paired-spawning design
unexposed (data I)
Group-spawning design
unexposed (data II)
Clutch size and spawning interval distributions
Volume of oogonia, critical size for spawning, and VTG uptake rate constant
Computational model
Fecundity
Paired-spawning design
unexposed (literature)
Group-spawning design
17β-trenbolone-exposed
(data III)

male per day) for 60 female FHMs. In total, there were 391 records for clutch sizes and 331 records for spawning intervals; both data sets were used to fit probability distributions (Table 2). The fitted distributions were used in our oocyte growth dynamics model to represent the distributions of oocyte recruitment size and oocyte recruitment interval, respectively. For 50 of the 60 female FHMs, we had records of plasma VTG concentrations, which were determined when the adult female fish were sacrificed in each study. At the time of sacrifice, the point in the spawning cycle of each female FHM was not determined. The plasma VTG concentration was used as a model input to simulate clutch size, spawning interval, and average fecundity in each of the 50 females. The simulation results were then used to evaluate how well the model predictions matched the experimental data.

For control FHMs from GSD studies, we used records for 77 female FHMs comprising 20 experimental groups (in most cases, there were four female FHMs per group). For each FHM, we had a measurement of plasma VTG concentration, and for each group, we had a record of average fecundity, which was calculated as number of eggs per female per day based on the number of FHM females in the group. Data from these studies were used in model evaluation.

In the 17β-trenbolone exposure study, 71 female FHMs were from 18 experimental groups (i.e., four female FHMs per group, with data missing for one fish). Fish were exposed to one of six 17β-trenbolone concentrations (i.e., 0, 0.005, 0.05, 0.5, 5, 50 $\mu g \cdot L^{-1}$) for 21 days (three groups per concentration). Data from this study were used to evaluate our model predictions.

Model development

A conceptual model (Fig. 2) depicts how we simplified the processes of oocyte recruitment, growth, and spawning in FHM. Following the conceptual model, the computational model simulates oocyte recruitment, growth, and subsequent batch spawning. MCSim, a free software package (Bois and Maszle 1997; http://www.gnu.org/software/mcsim/), was used to develop the computational model, and the ordinary differential equations describing oocyte growth dynamics were integrated using Euler's method. The MCSim model specification file and an example of the model input file can be found in the Supplementary data.[1]

In our model, oogonia are periodically recruited into oocyte growth starting when FHMs are three months old (2160 h after hatch) (Villeneuve et al. 2007). An oogonium,

---

[1] Supplementary data are available with the article through the journal Web site (http://nrcresearchpress.com/cjfas).

Table 2. Summary statistics of fecundity data from unexposed female fathead minnows (FHMs, $n = 60$) with a paired-spawning experimental design. The studies were performed in unexposed FHMs (Jensen et al. 2001) and FHMs exposed to prochloraz and fenarimol (Ankley et al. 2005*a*), perfluorooctane sulfonate (Ankley et al. 2005*b*), 17α-trenbolone (Jensen et al. 2006), prometon (Villeneuve et al. 2006), and haloperidol (Villeneuve et al. 2010). Data were used to obtain probability distributions for clutch size and spawning interval.

	No. of records	Mean	Median	SD	Min	Max	Distribution fitting	Distribution used in model simulations
Clutch size	391	88	75	68	1	317	Lognormal (4.11, 0.96)	Truncated lognormal (4.11, 0.96, 1, 317)
Spawning interval	331	3.9	3.0	2.5	1.0	25.0	Lognormal (1.21, 0.57)	Truncated lognormal (1.21, 0.57, 1, 25)

Note: SD, standard deviation; Min, minimum; Max, maximum.

prior to being recruited into the growth phase, was defined as having a volume of 5.2×10^{-7} μL, a value calculated from the diameter of an oogonium in FHM (Leino et al. 2005). Because we do not know the detailed mechanisms controlling oocyte recruitment or fecundity in FHM, we assumed that the number of oogonia recruited into the growth phase and the recruitment interval between two consecutive batches followed the fitted distributions of clutch size and spawning interval, with upper and lower bounds set at the maximum and minimum recorded values, respectively. In addition, although we know that atresia (i.e., oocyte degeneration) plays an important role in regulating the number of oocytes in many vertebrates, limited quantitative studies concerning this process have been done in teleosts (Tyler and Sumpter 1996; Wallace and Selman 1981). Hence, we assumed that once oocytes were recruited into the growth phase, their number would not change, and all oocytes would be spawned.

In MCSim, we used a vector function to track oocyte batches (Supplementary data).[1] The clutch size distribution was sampled randomly to determine the number of oocytes recruited into each batch. Similarly, the spawning interval distribution was sampled randomly to determine oocyte recruitment intervals between two successive batches of oocytes.

After being recruited into the growth phase, oocyte growth depends on the uptake of VTG. This relationship is consistent with previous knowledge that the majority of oocyte growth is associated with the accumulation of yolk proteins in the cytoplasm (Specker and Sullivan 1994). The rate of VTG uptake was formulated to be proportional to the plasma VTG concentration and the oocyte volume (eq. 1) for two reasons: (*i*) it was observed in rainbow trout that the rate of VTG uptake increased with oocyte diameter even when it was normalized to oocyte surface area (Tyler et al. 1988; Specker and Sullivan 1994); and (*ii*) an increase in VTG or VTG degradation products in oocytes was associated with an increase in plasma VTG concentrations (Perazzolo et al. 1999). Because we did not have data specific for FHMs, we assumed that the process of VTG uptake into FHM oocytes utilized a mechanism similar to that of trout:

$$(1) \qquad \frac{\mathrm{d}(M_{\mathrm{VTG}})}{\mathrm{d}t} = \rho_{\mathrm{VTG\_Ooc}} \times C_{\mathrm{VTG}} \times V_{\mathrm{Ooc}}$$

where M_{VTG} (nmol) is the amount of VTG absorbed into each oocyte in each batch, $\rho_{\mathrm{VTG\_Ooc}}$ (h^{-1}) is the VTG absorption rate constant, C_{VTG} (nmol·μL^{-1}) is the plasma VTG concentration, and V_{Ooc} (μL) is the volume of each oocyte in each batch. For each batch of oocytes, we assumed that all oocytes grew equally and that their volumes were the same.

In an optimized laboratory setting, the spawning interval of reproductively active unexposed FHMs ranges from 1 to 15 days, with most values falling in the range of 3 to 4 days (Jensen et al. 2001). In addition, at least four stages of oocytes (primary growth, cortical alveolus, early vitellogenic, and late vitellogenic stages) have been observed in a FHM ovary at one time (Jensen et al. 2001; Leino et al. 2005; Villeneuve et al. 2007). As a result, we assumed that there are at least four batches of oocytes developing simultaneously. Given that there are four batches of oocytes inside a FHM ovary and that the spawning intervals are typically 3 to 4 days, the oocyte growth period in FHMs should be on the order of 12 to 16 days. In our model, we set $\rho_{\mathrm{VTG\_Ooc}}$ at $1 \cdot \mathrm{h}^{-1}$, which resulted in an average oocyte growth period of approximately 13 days. This pattern agrees with oocyte growth mechanisms in many mammals, amphibians, and other fish species (Coward and Bromage 1998; Gilbert 2000; Hirao and Miyano 2008).

Along with VTG, other molecules (e.g., water and minerals) enter oocytes (Specker and Sullivan 1994; Tyler et al. 1990) and also contribute to the increase in oocyte volume. In our model, the volume of an oocyte is equal to its initial volume (volume of oogonia) plus the oocyte growth volume. We assumed that there was a proportional relationship between the uptake of VTG and other molecules during vitellogenesis, and therefore the oocyte growth volume was formulated to be proportional to the amount of VTG absorbed into the oocyte:

$$(2) \qquad V_{\mathrm{Ooc}} = V_{\mathrm{Oog}} + 0.156 \times M_{\mathrm{VTG}} \times r_{\mathrm{VTG\_Water}}$$

where V_{Oog} (μL) is the initial volume of an oocyte, 0.156 (mg·nmol^{-1}) is the molecular mass of VTG, and $r_{\mathrm{VTG\_Water}}$ (μL·mg^{-1}) is the ratio of the volume of oocyte growth to the amount of VTG absorbed. In this study, we set the value of $r_{\mathrm{VTG\_Water}}$ to 3, an empirical value that accounts for water and the absorption of other molecules into oocytes. This value is based on the observation that trout eggs are about two-thirds water (Milla et al. 2006), the moisture content in FHM oocytes is approximately three-fourths, and the density of FHM ovary is approximately 1 mg·μL^{-1} (D.L. Villeneuve, unpublished data).

In our model, we used oocyte size as a criterion to determine when spawning will occur. The critical oocyte size was set to 0.52 μL, a value calculated from the diameter of mature oocytes reported in FHM (Leino et al. 2005). When oo-

Fig. 2. A conceptual model of oocyte growth dynamics in female fathead minnows. The *x* axis represents time in days. The shaded rectangle at the bottom represents a pool of oogonia. The squares with different fill patterns in the middle represent different batches of oocytes. The squares at the top represent oocytes spawned on a specific day. The number in each square represents the number of oocytes in the batch. VTG, plasma vitellogenin.

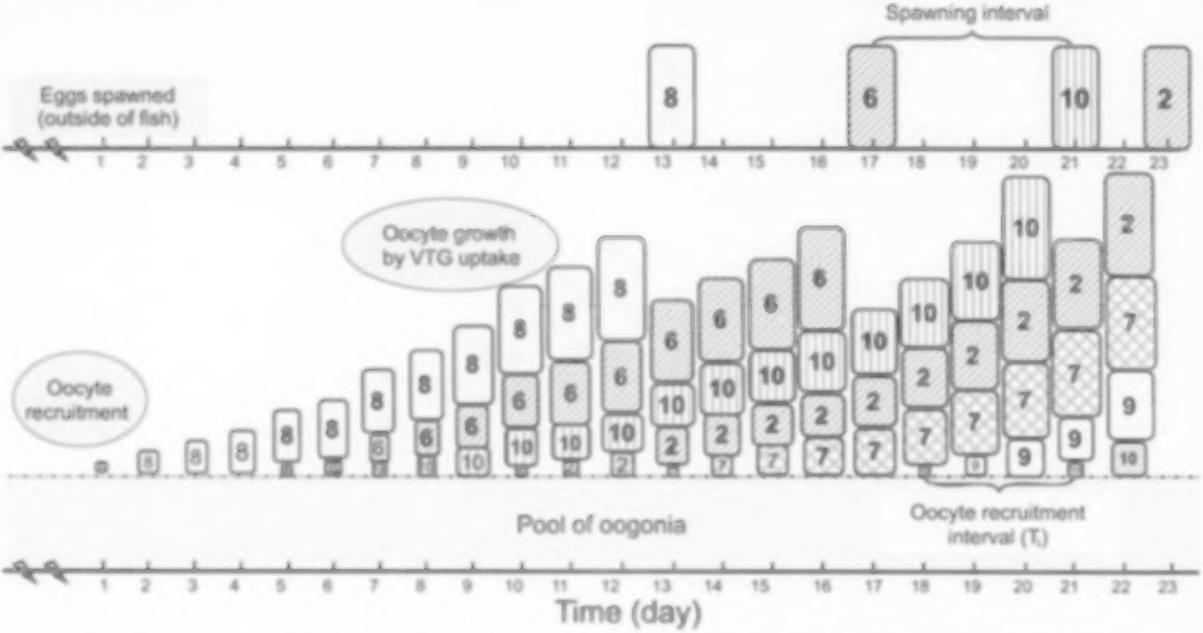

cytes in a batch reached the critical size, they were spawned, and the number of oocytes in the fish decreased.

Model evaluation

To evaluate the goodness of fit of the clutch size and spawning interval distributions, we simulated the number of eggs spawned as a function of time for unexposed FHMs with a PSD. To evaluate the predictive ability of our model, we simulated the number of eggs spawned as a function of time for unexposed FHMs with GSDs and for FHMs exposed to 17β-trenbolone for 21 days with a GSD. For simulation of the three data types above, measured FHM plasma VTG concentration was input as a model parameter. For each unexposed FHM from PSD or GSD studies, plasma VTG concentration was assumed to be a constant throughout the simulation, and its value was set to be the measured plasma VTG concentration recorded when the FHM was sacrificed. In unexposed, reproductively active FHMs, plasma VTG concentrations remain relatively constant over a spawning interval (Jensen et al. 2001), thus assuming that a constant plasma VTG concentration in unexposed FHMs is reasonable. For FHMs exposed to 17β-trenbolone, plasma VTG concentration before exposure was set to be the average plasma VTG concentration of the controls because we did not have preexposure plasma VTG data. At the start of a 17β-trenbolone exposure, plasma VTG concentration in the FHM was set to be the value measured at conclusion of the experiment.

To fully explore the distributions of oocyte recruitment size and spawning interval, 1000 simulations of each fish were performed in MCSim. That is, if an experiment measured data from 16 female FHMs, 16 000 simulation results were obtained (1000 simulations per fish). The MCSim output file was imported into MATLAB 7.1, and of 1000 results per fish, we randomly sampled one set of results. Based on the sampled results, we computed summary statistics for reproductive endpoints such as clutch size, spawning interval, and average fecundity. These statistics were then compared with the measured data.

In total, we had 50 unexposed FHMs from PSD studies with records of plasma VTG concentrations. Using the plasma VTG concentration as a model input, we predicted clutch sizes, spawning intervals, and average fecundities in each of the 50 fish, which were compared with experimental data visually. In addition, for each reproductive endpoint, we used a nonparametric two-sample Kolmogorov–Smirnov test in MATLAB 7.1 (The MathWorks Inc., Natick, Massachusetts) to test whether the distributions of model predictions and the measured data were different at a significance level of 0.01 ($\alpha = 0.01$). The null hypothesis was that the two samples were drawn from the same distribution; the alternative hypothesis was that they were drawn from different distributions.

The distributions used in our model (i.e., the distributions of oocyte recruitment size and recruitment interval) were derived from experimental data of FHMs from PSD studies, whereas the independent experimental data available to evaluate the model predictions were from FHMs in GSD studies. To evaluate whether there are statistically significant differences in average fecundity from a GSD (number of fish = 77, number of groups = 20, number of average fecundity data points = 20) versus a PSD, we performed a nonparametric two-sample Kolmogorov–Smirnov test ($\alpha = 0.01$). We could not reject the hypothesis that the two average fecundity data

Fig. 3. A timeline for model simulations. FHM, fathead minnows; TB, 17β-trenbolone.

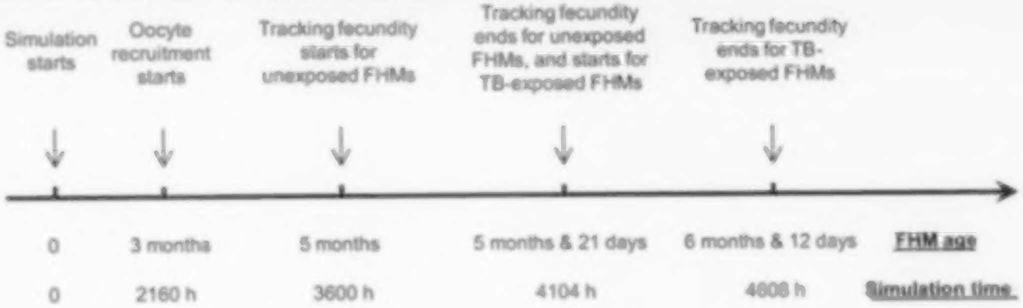
Simulation starts
Oocyte recruitment starts
Tracking fecundity starts for unexposed FHMs
Tracking fecundity ends for unexposed FHMs, and starts for TB-exposed FHMs
Tracking fecundity ends for TB-exposed FHMs
0
3 months
5 months
5 months & 21 days
6 months & 12 days
FHM age
0
2160 h
3600 h
4104 h
4608 h
Simulation time

sets were from the same distribution, i.e., the two data sets were not significantly different.

To determine whether our model could predict average fecundity in FHMs with a GSD, we simulated spawning in 77 unexposed FHMs from GSD studies. Model predictions for the 77 FHMs were divided into 20 groups consistent with the experimental design. The average fecundity of each group was calculated and compared visually and statistically with experimental data.

To evaluate whether our model could predict the average fecundity in FHMs exposed to 17β-trenbolone, we simulated spawning in the 71 FHMs exposed to 17β-trenbolone for 21 days. Model predictions for the 71 FHMs were divided into 18 groups consistent with the experimental design. The average fecundity of each group was calculated, grouped based on the different 17β-trenbolone concentrations, and compared with experimental data visually.

We created a timeline for our model simulations (Fig. 3). For all simulations, we set three months (2160 h after hatch) as the time that female FHMs start to recruit oocytes. For unexposed FHMs, we started tracking fecundity at five months (3600 h) and continued tracking it for 21 days (3600 to 4104 h). This was intended to simulate the actual age of reproductive maturity, as well as the actual age of FHMs used in the studies providing experimental data. For the 17β-trenbolone exposure study, we started tracking FHM fecundity at five months and continued for 21 days before the exposure. Then, we simulated the 17β-trenbolone exposure starting at five months and 22 days and tracked fecundity from 4104 to 4608 h (21 days totally).

Results

Distribution fitting

For the 60 unexposed FHMs from the PSD studies, clutch sizes fit a lognormal distribution, with mean and standard deviation (SD) in log space equal to 4.11 and 0.96, respectively (Table 2). The spawning intervals fit a lognormal distribution, with mean and SD in log space equal to 1.21 and 0.57, respectively (Table 2).

Model calibration results for unexposed FHMs with a PSD

We compared model predictions with the experimental data for the 50 unexposed female FHMs from PSD studies (Fig. 4). The mean and median model predictions were within 0.5- to 2.0-fold, respectively, of the mean and median measurements for clutch size (Fig. 4*a*), spawning interval (Fig. 4*b*), and average fecundity (Fig. 4*c*). The 95% confidence intervals (CIs) of model predictions encompassed the mean and median measurements, and the mean and median model predictions were within the 95% CIs of experimental data for each endpoint. Using nonparametric two-sample Kolmogorov–Smirnov tests ($\alpha = 0.01$), we concluded that there was no significant difference between the model predictions and experimental data for the three reproductive endpoints.

Model predictions for unexposed FHMs with a GSD

We compared model predictions with experimental data for the 77 unexposed female FHMs (20 groups) from GSD studies (Fig. 5), which were not used in the model calibration. Although the model predictions had a variance (4.0) slightly smaller than that of the experimental data variance (7.1), the two data sets were generally comparable. The 95% CIs of model predictions (11.7, 24.7) encompassed the mean (16.7) and median (16.3) measurements, and the mean (18.3) and median (17.9) model predictions were within the 95% CIs (5.1, 28.0) of the experimental data. Using a nonparametric two-sample Kolmogorov–Smirnov test ($\alpha = 0.01$), we concluded that there were no significant differences between the model predictions and experimental data.

Model predictions for 17β-trenbolone-exposed FHMs with a GSD

We compared model-predicted average fecundity with experimental data for 71 female FHMs (18 groups) exposed to 0, 0.005, 0.05, 0.5, 5, and 50 $\mu g \cdot L^{-1}$ 17β-trenbolone for 21 days (Fig. 6). Predicted average fecundity followed the same trend as the experimental data, i.e., with increasing 17β-trenbolone concentrations, the average fecundity of FHMs decreased, and the model predictions overlapped the experimental data. For each concentration of 17β-trenbolone, the predicted medians were 20.5, 13.8, 9.6, 0, 0, and 1.5 $eggs \cdot female^{-1} \cdot day^{-1}$, respectively, and the medians of measured data were 11.5, 11.6, 6.8, 0.4, 0, and 0 $eggs \cdot female^{-1} \cdot day^{-1}$, respectively. The model predicted an increase in average fecundity for the highest 17β-trenbolone exposure concentration (50 $\mu g \cdot L^{-1}$) that was not observed experimentally. At exposure concentrations of 0.5 $\mu g \cdot L^{-1}$ and 5 $\mu g \cdot L^{-1}$, all three predicted average fecundity values were zero, whereas at an exposure concentration of 50 $\mu g \cdot L^{-1}$, two of the three predicted average fecundity values were greater than zero.

Fig. 4. Model-predicted reproductive endpoints compared with experimental data from 50 unexposed (control) female fathead minnows (FHMs) with a paired-spawning experimental design: (*a*) clutch size, (*b*) spawning interval, and (*c*) average fecundity. Open boxes represent model predictions; shaded boxes represent measured data. The solid line within the box marks the median; the broken line within the box marks the mean; the boundary of the box farthest from zero indicates the 75th percentile; the boundary of the box closest to zero indicates the 25th percentile; the whisker (error bar) farthest from zero marks the 90th percentile; the whisker (error bar) closest to zero marks the 10th percentile; the circle farthest from zero marks the 95th percentile; and the circle closest to zero marks the 5th percentile.

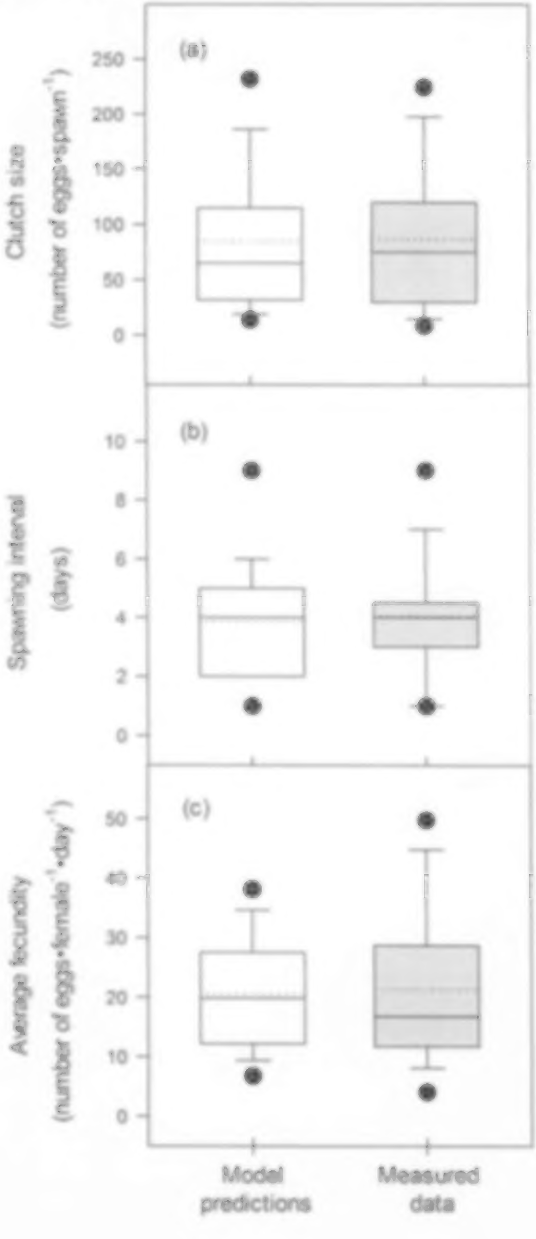

Fig. 5. Model-predicted average fecundity compared with experimental data from 77 unexposed female fathead minnows (FHMs) with a group-spawning experimental design. Open boxes represent model predictions; shaded boxes represent measured data. The solid line within the box marks the median; the broken line within the box marks the mean; the boundary of the box farthest from zero indicates the 75th percentile; the boundary of the box closest to zero indicates the 25th percentile; the whisker (error bar) farthest from zero marks the 90th percentile; the whisker (error bar) closest to zero marks the 10th percentile; the circle farthest from zero marks the 95th percentile; and the circle closest to zero marks the 5th percentile.

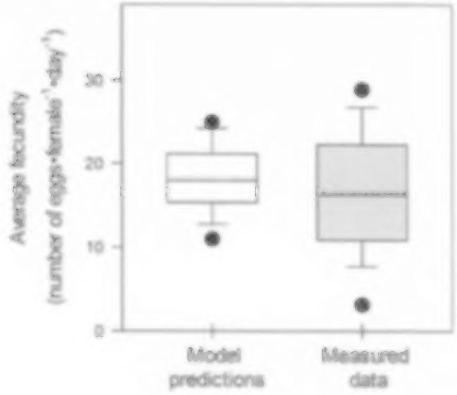

Discussion

In this study, we used data from studies with two different experimental designs, paired and group spawning. In a PSD experiment, it is clear that all eggs collected within a tank are spawned from a single female. Thus, these data were used to develop our computational model. In a GSD experiment, the eggs collected in one tank may be from one of four females or even from more than one female in the tank because multiple females might spawn on the same day. As a result, only average fecundity is determined for GSD experiments, which masks the variability in individual FHM fecundity. Moreover, it is possible that clutch sizes and spawning intervals are different in PSD and GSD studies. Despite its limitations, average fecundity data from GSD experiments were the only independent data available for model evaluation.

In our model evaluation, the distributions of oocyte recruitment size and oocyte recruitment interval were those derived from FHMs with a PSD. With these distributions, our model successfully predicted the average fecundity of FHMs from studies with a GSD. The simulated GSD experiments produced predictions for individual FHM fecundity, which were then used to compute averages for the group. Thus, if individual fecundity data from GSD experiments become available, we could compare model predictions with those data as well. Results from this study show that clutch sizes and spawning intervals from individual FHMs in PSD studies are able to explain the average fecundity observed in GSD studies. Further, these results suggest that the clutch sizes and spawning intervals for individual fish are not affected by the experimental design.

Model-predicted average fecundity in 17β-trenbolone-

Fig. 6. Model-predicted average fecundity compared with experimental data from 71 female fathead minnows (FHMs) exposed to 17β-trenbolone for 21 days with a group-spawning experimental design. Open circles correspond to model predictions; shaded circles correspond to measured data. Group numbers are shown next to each marker: underlined for model predictions, and regular for experimental data. Broken lines separate the comparisons based on different 17β-trenbolone concentrations.

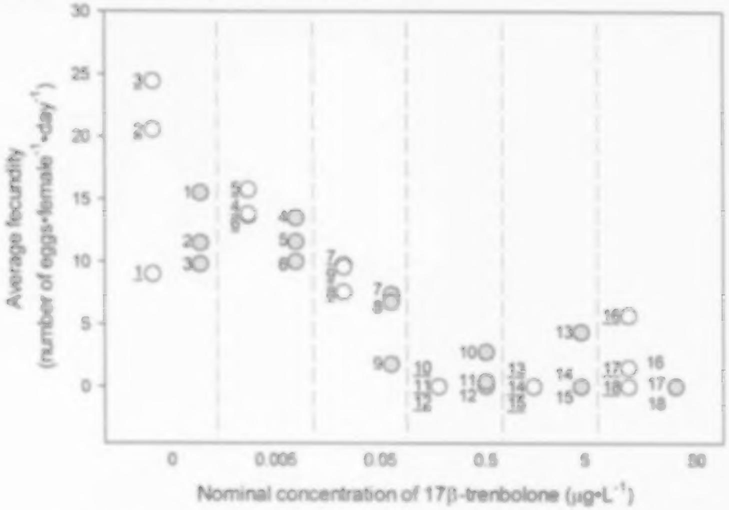

exposed FHMs followed the trend of the experimental data, which suggests that our model captured the relationship between VTG concentrations and oocyte growth dynamics. That is, the U-shaped curve in our model-predicted average fecundity was influenced by the U-shaped curve in the plasma VTG measurements (Ankley et al. 2003). For the 50 μg·L⁻¹ 17β-trenbolone exposure, the dependence of fecundity on plasma VTG concentrations resulted in a predicted average fecundity that was greater than the experimentally measured values. One possible explanation for the overpredictions is atresia, the process of oocyte reabsorption, which occurs in many vertebrates and plays an important role in regulating the number of oocytes that are eventually spawned (Tyler and Sumpter 1996). Although atresia occurs under ideal environmental conditions, it is not a common event in healthy females (Wallace and Selman 1981). In our model, we did not include the process of atresia because of the absence of quantitative information. However, exposure to environmental stressors may increase the rate of atresia, and in the 17β-trenbolone-exposed FHMs, atresia was indeed one of the major histological lesions (Ankley et al. 2003). As a result, without simulating atresia, our model tends to predict higher fecundity in the exposed FHMs, especially for the FHMs exposed to high levels of 17β-trenbolone.

An alternative explanation for the fecundity overprediction in the exposed FHMs is that the plasma VTG concentrations used in the simulations were not a continuous function of time. In the model, we input the plasma VTG concentration prior to exposure as the average plasma VTG concentration of the control FHMs; the VTG concentration after the start of exposure was input as the value measured at the end of the 21-day test. However, this simulation setting may lead to an overprediction of fecundity. In reality, prior to exposure, different FHMs have different VTG concentrations (e.g., plasma VTG concentrations in the control FHMs ranged from 0.12 to 0.24 nmol·μL⁻¹). After the start of the exposure, VTG concentrations probably changed as a function of time. For example, as shown by Seki et al. (2006), plasma VTG concentrations in spawning fish exposed to 17β-trenbolone were lower on day 14 than on day 21. Similarly, time-course studies by Villeneuve et al. (2009) and Ankley et al. (2009*b*) showed gradual declines, rather than an abrupt decrease, in average plasma VTG concentrations occurring over the first 4–8 days of exposure to EDCs that inhibit aromatase activity. Hence, the fixed VTG concentration for each exposed FHM in our simulations may overestimate or underestimate the plasma concentration of VTG available for oocyte growth. Thus, having a time course of plasma VTG concentrations would likely improve the model predictions. Measured plasma VTG concentrations would be optimal, but connecting the oocyte growth dynamics model to other computational models predicting plasma VTG concentrations as a function a time would also work (Murphy et al. 2009; Li et al. 2011).

A study by Murphy et al. (2009) linked a physiologically based model predicting plasma VTG concentrations in Atlantic croaker to the linear statistical model by Miller et al. (2007). That study represents a very good example of connecting two computational models. However, as stated by Murphy et al. (2009, p. 1300), "VTG concentration is in a state of flux", so assuming a simple direct relationship between fecundity and VTG concentration measured or predicted at a certain time point might introduce extra errors into model predictions. Furthermore, we speculate that there might be a delay in the effects of changes in VTG on fecundity because both VTG uptake and oocyte spawning are dynamic processes, i.e., the present plasma VTG concentration may not affect a clutch of oocytes currently being spawned. If our oocyte growth dynamics model was linked to the model for Atlantic croaker, plasma VTG concentrations as a function of time predicted by the croaker physiological model would be used as input for the oocyte growth dynamic model, and the effect of continuously changing VTG concentrations on fecundity could be predicted.

Linking the oocyte growth dynamics model to physiologically based computational models, or incorporating physiological processes directly, would extend the model's ability to simulate hormonal regulation of oocyte growth and maturation. In vertebrates such as fish, oocyte development is under the regulation of multiple hormones (e.g., follicle-stimulating hormone, luteinizing hormone, 17β-estradiol, and $17\alpha,20\beta$-dihydroxy-4-pregnen-3-one), and oocytes at different developmental stages provide different feedback signals to the regulatory system (Kim et al. 2006; Schulz et al. 2001). Presently, the oocyte growth dynamics model simplifies the mechanisms controlling oocyte development in FHMs leaving hormonal regulation to future work. For example, we do not know the mechanism controlling oocyte recruitment in FHMs, thus, we assumed that oocyte recruitment size and interval followed the distributions of clutch size and spawning interval, respectively. Similarly, we did not include atresia because of a shortage of quantitative information. In the future, as quantitative information on these processes becomes available, it will be possible to extend the model.

Although the best application of this model is for modeling egg production in unexposed laboratory FHMs, it can be adapted for other applications. For unexposed FHMs, model predictions matched the experimental data accurately. This is not surprising as the data used to calibrate the model were from unexposed FHMs. As an extension, the model predicted well the average fecundity in 17β-trenbolone-exposed FHMs. A possible future application is to simulate wild FHMs, though certain challenges exist in simulating a mixed-age group of FHMs. If plasma vitellogenin concentrations and empirical distributions for spawning intervals and clutch sizes are known in wild FHMs, the model algorithm could be evaluated with the new data. Without empirical distributions for wild FHMs, the model would need to be modified to account for environmental factors (e.g., water temperature, photoperiod, and nutrition) and the effect of age upon fecundity.

Another application of our model is to adapt it to other batch- and total-spawning fishes. For batch-spawning fishes (e.g., Japanese medaka), the fish-specific parameters (e.g., oocyte recruitment size, oocyte recruitment interval, and critical size for spawning) would need to be modified for the fish species of interest. For total-spawning fishes, after assigning fish-specific values to oocyte recruitment size and critical size for oocytes to spawn, the model algorithm can be used to simulate one batch of oocytes.

In summary, our oocyte growth dynamics model links plasma VTG concentration to fecundity in FHMs, which connects a molecular biomarker of EDC exposure with reproductive effects in individuals and populations. This is important, because a greater number of toxicological studies are evaluating changes in molecular-level endpoints, whereas ecological risk assessments focus on endpoints (e.g., fecundity) that affect a population (Forbes et al. 2006). In addition, our oocyte growth dynamics model presents a novel algorithm for oocyte growth and spawning that can be adapted and applied to other fish species, including both batch and total spawners. Linking the model to a physiologically based model of the HPG axis would enable research on hormone regulation of oocyte development and provide additional connections between EDC effects at a molecular level and effects at the individual level to contribute to ecological risk assessment.

Acknowledgments

This research was supported, in part, by grants from the U.S. Environmental Protection Agency (USEPA) Science to Achieve Results program (Cooperative Agreement RD-83184801–0) and by resources from the National Center for Computational Toxicology of the USEPA Office of Research and Development awarded to the Ecological Exposure Research and Ecosystem Research Divisions (National Exposure Research Laboratory) in Cincinnati, Ohio, and Athens, Georgia, respectively, and the Mid-Continent Ecology Division (National Health and Environmental Effects Research Laboratory) in Duluth, Minnesota. Although the research described in this article has been funded in part by the USEPA, it has not been subjected to any formal USEPA review and does not necessarily reflect the views of the Agency. No official endorsement should be inferred. The authors greatly appreciate input and insight from members of the Small Fish Computational Toxicology Team at the USEPA and from academe, Nancy D. Denslow (University of Florida) and María S. Sepúlveda (Purdue University). The authors also thank two CJFAS reviewers, who helped to improve the quality of this manuscript, and the Division of Environmental and Biomolecular Systems at Oregon Health & Science University for their support.

References

Ankley, G.T., and Villeneuve, D.L. 2006. The fathead minnow in aquatic toxicology: past, present and future. Aquat. Toxicol. **78**(1): 91–102. doi:10.1016/j.aquatox.2006.01.018. PMID:16494955.

Ankley, G.T., Jensen, K.M., Kahl, M.D., Korte, J.J., and Makynen, E.A. 2001. Description and evaluation of a short-term reproduction test with the fathead minnow (*Pimephales promelas*). Environ. Toxicol. Chem. **20**(6): 1276–1290. PMID:11392137.

Ankley, G.T., Kahl, M.D., Jensen, K.M., Hornung, M.W., Korte, J.J., Makynen, E.A., and Leino, R.L. 2002. Evaluation of the aromatase inhibitor fadrozole in a short-term reproduction assay with the fathead minnow (*Pimephales promelas*). Toxicol. Sci. **67**(1): 121–130. doi:10.1093/toxsci/67.1.121. PMID:11961225.

Ankley, G.T., Jensen, K.M., Makynen, E.A., Kahl, M.D., Korte, J.J., Hornung, M.W., Henry, T.R., Denny, J.S., Leino, R.L., Wilson, V. S., Cardon, M.C., Hartig, P.C., and Gray, L.E. 2003. Effects of the androgenic growth promoter 17-beta-trenbolone on fecundity and reproductive endocrinology of the fathead minnow. Environ. Toxicol. Chem. **22**(6): 1350–1360. doi:10.1002/etc.5620220623. PMID:12785594.

Ankley, G.T., Jensen, K.M., Durhan, E.J., Makynen, E.A., Butterworth, B.C., Kahl, M.D., Villeneuve, D.L., Linnum, A., Gray, L.E., Cardon, M., and Wilson, V.S. 2005*a*. Effects of two fungicides with multiple modes of action on reproductive endocrine function in the fathead minnow (*Pimephales promelas*). Toxicol. Sci. **86**(2): 300–308. doi:10.1093/toxsci/kfi202. PMID:15901916.

Ankley, G.T., Kuehl, D.W., Kahl, M.D., Jensen, K.M., Linnum, A., Leino, R.L., and Villeneuve, D.A. 2005*b*. Reproductive and developmental toxicity and bioconcentration of perfluorooctanesulfonate in a partial life-cycle test with the fathead minnow (*Pimephales promelas*). Environ. Toxicol. Chem. **24**(9): 2316–2324. doi:10.1897/04-634R.1. PMID:16193761.

Ankley, G.T., Jensen, K.M., Kahl, M.D., Makynen, E.A., Blake, L.S., Greene, K.J., Johnson, R.D., and Villeneuve, D.L. 2007. Ketoconazole in the fathead minnow (*Pimephales promelas*): reproductive toxicity and biological compensation. Environ. Toxicol. Chem. **26**(6): 1214–1223. doi:10.1897/06-428R.1. PMID:17571688.

Ankley, G.T., Bencic, D.C., Breen, M.S., Collette, T.W., Conolly, R.B., Denslow, N.D., Edwards, S.W., Ekman, D.R., Garcia-Reyero, N., Jensen, K.M., Lazorchak, J.M., Martinovic, D., Miller, D.H., Perkins, E.J., Orlando, E.F., Villeneuve, D.L., Wang, R.-L., and Watanabe, K.H. 2009*a*. Endocrine disrupting chemicals in fish: developing exposure indicators and predictive models of effects based on mechanism of action. Aquat. Toxicol. **92**(3): 168–178. doi:10.1016/j.aquatox.2009.01.013. PMID:19261338.

Ankley, G.T., Bencic, D.C., Cavallin, J.E., Jensen, K.M., Kahl, M.D., Makynen, E.A., Martinovic, D., Mueller, N.D., Wehmas, L.C., and Villeneuve, D.L. 2009*b*. Dynamic nature of alterations in the endocrine system of fathead minnows exposed to the fungicide prochloraz. Toxicol. Sci. **112**(2): 344–353. doi:10.1093/toxsci/kfp227. PMID:19767443.

Bois, F.Y., and Maszle, D.R. 1997. MCSim: a Monte Carlo simulation program. J. Stat. Softw. **2**(9): 1–56.

Coward, K., and Bromage, N.R. 1998. Histological classification of oocyte growth and the dynamics of ovarian recrudescence in *Tilapia zillii*. J. Fish Biol. **53**(2): 285–302. doi:10.1111/j.1095-8649.1998.tb00981.x.

Durhan, E.J., Lambright, C.S., Makynen, E.A., Lazorchak, J., Hartig, P.C., Wilson, V.S., Gray, L.E., and Ankley, G.T. 2006. Identification of metabolites of trenbolone acetate in androgenic runoff from a beef feedlot. Environ. Health Perspect. **114**(S-1): 65–68. doi:10.1289/ehp.8055. PMID:16818248.

Forbes, V.E., Palmqvist, A., and Bach, L. 2006. The use and misuse of biomarkers in ecotoxicology. Environ. Toxicol. Chem. **25**(1): 272–280. doi:10.1897/05-257R.1. PMID:16494252.

Gilbert, S.F. 2000. Developmental biology. Sinauer Associates, Sunderland, Massachusetts.

Hirao, Y., and Miyano, T. 2008. In vitro growth of mouse oocytes: oocyte size at the beginning of culture influences the appropriate length of culture period. J. Mammal. Ova Res. **25**(1): 56–62. doi:10.1274/jmor.25.56.

Jensen, K.M., Korte, J.J., Kahl, M.D., Pasha, M.S., and Ankley, G.T. 2001. Aspects of basic reproductive biology and endocrinology in the fathead minnow (*Pimephales promelas*). Comp. Biochem. Physiol. C Toxicol. Pharmacol. **128**(1): 127–141. doi:10.1016/S1532-0456(00)00185-X. PMID:11166681.

Jensen, K.M., Kahl, M.D., Makynen, E.A., Korte, J.J., Leino, R.L., Butterworth, B.C., and Ankley, G.T. 2004. Characterization of responses to the antiandrogen flutamide in a short-term reproduction assay with the fathead minnow. Aquat. Toxicol. **70**(2): 99–110. doi:10.1016/j.aquatox.2004.06.012. PMID:15522428.

Jensen, K.M., Makynen, E.A., Kahl, M.D., and Ankley, G.T. 2006. Effects of the feedlot contaminant 17alpha-trenbolone on reproductive endocrinology of the fathead minnow. Environ. Sci. Technol. **40**(9): 3112–3117. doi:10.1021/es052174s. PMID:16719119.

Kim, J., Hayton, W.L., and Schultz, I.R. 2006. Modeling the brain–pituitary–gonad axis in salmon. Mar. Environ. Res. **62**(Suppl. 1): S426–S432. doi:10.1016/j.marenvres.2006.04.022. PMID:16716390.

Leino, R.L., Jensen, K.M., and Ankley, G.T. 2005. Gonadal histology and characteristic histopathology associated with endocrine disruption in the adult fathead minnow (*Pimephales promelas*). Environ. Toxicol. Pharmacol. **19**(1): 85–98. doi:10.1016/j.etap.2004.05.010.

Li, Z., Kroll, K., Jensen, K.M., Villeneuve, D.L., Ankley, G.T., Brian, J.V., Sepulveda, M.S., Orlando, E.F., Lazorchak, J.M., Kostich, M., Armstrong, B., Denslow, N.D., and Watanabe, K.H. 2011. A computational model of the hypothalamic–pituitary–gonadal axis in female fathead minnows (*Pimephales promelas*) exposed to 17alpha-ethynylestradiol and 17beta-trenbolone. BMC Syst. Biol. **5**(1): 63. doi:10.1186/1752-0509-5-63. PMID:21545743.

Milla, S., Jalabert, B., Rime, H., Prunet, P., and Bobe, J. 2006. Hydration of rainbow trout oocyte during meiotic maturation and in vitro regulation by 17,20β-dihydroxy-4-pregnen-3-one and cortisol. J. Exp. Biol. **209**(6): 1147–1156. doi:10.1242/jeb.02094. PMID:16513941.

Miller, D.H., Jensen, K.M., Villeneuve, D.L., Kahl, M.D., Makynen, E.A., Durhan, E.J., and Ankley, G.T. 2007. Linkage of biochemical responses to population-level effects: a case study with vitellogenin in the fathead minnow (*Pimephales promelas*). Environ. Toxicol. Chem. **26**(3): 521–527. doi:10.1897/06-318R.1. PMID:17373517.

Murphy, C.A., Rose, K.A., Rahman, M.S., and Thomas, P. 2009. Testing and applying a fish vitellogenesis model to evaluate laboratory and field biomarkers of endocrine disruption in Atlantic croaker (*Micropogonias undulatus*) exposed to hypoxia. Environ. Toxicol. Chem. **28**(6): 1288–1303. doi:10.1897/08-304.1. PMID:19642826.

Nagahama, Y., Yoshikuni, M., Yamashita, M., Tokumoto, T., and Katsu, Y. 1995. Regulation of oocyte growth and maturation in fish. Curr. Top. Dev. Biol. **30**: 103–145. doi:10.1016/S0070-2153(08)60565-7. PMID:7555044.

Perazzolo, L.M., Coward, K., Davail, B., Normand, E., Tyler, C.R., Pakdel, F., Schneider, W.J., and Le Menn, F. 1999. Expression and localization of messenger ribonucleic acid for the vitellogenin receptor in ovarian follicles throughout oogenesis in the rainbow trout, *Oncorhynchus mykiss*. Biol. Reprod. **60**(5): 1057–1068. doi:10.1095/biolreprod60.5.1057. PMID:10208965.

Schulz, R.W., Vischer, H.F., Cavaco, J.E., Santos, E.M., Tyler, C.R., Goos, H.J., and Bogerd, J. 2001. Gonadotropins, their receptors, and the regulation of testicular functions in fish. Comp. Biochem. Physiol. B Biochem. Mol. Biol. **129**(2–3): 407–417. doi:10.1016/S1096-4959(01)00339-6. PMID:11399475.

Seki, M., Fujishima, S., Nozaka, T., Maeda, M., and Kobayashi, K. 2006. Comparison of response to 17β-estradiol and 17β-trenbolone among three small fish species. Environ. Toxicol. Chem. **25**(10): 2742–2752. doi:10.1897/05-647R.1. PMID:17022416.

Specker, J.L., and Sullivan, C.V. 1994. Vitellogenesis in fishes: status and perspectives. *In* Perspectives in comparative endocrinology. *Edited by* K.G. Davey, R.E. Peter, and S.S. Tobe. National Research Council of Canada, Ottawa, Canada. pp. 304–315.

Tyler, C.R., and Sumpter, J.P. 1996. Oocyte growth and development in teleosts. Rev. Fish Biol. Fish. **6**(3): 287–318. doi:10.1007/BF00122584.

Tyler, C.R., Sumpter, J.P., and Bromage, N.R. 1988. In vivo ovarian uptake and processing of vitellogenin in the rainbow trout, *Salmo gairdneri*. J. Exp. Zool. **246**(2): 171–179. doi:10.1002/jez.1402460209.

Tyler, C.R., Sumpter, J.P., and Witthames, P.R. 1990. The dynamics of oocyte growth during vitellogenesis in the rainbow trout (*Oncorhynchus mykiss*). Biol. Reprod. **43**(2): 202–209. doi:10.1095/biolreprod43.2.202. PMID:2378932.

Tyler, C.R., Pottinger, T.G., Santos, E., Sumpter, J.P., Price, S.A., Brooks, S., and Nagler, J.J. 1996. Mechanisms controlling egg size and number in the rainbow trout, *Oncorhynchus mykiss*. Biol. Reprod. **54**(1): 8–15. doi:10.1095/biolreprod54.1.8. PMID:8837994.

Villeneuve, D.L., Murphy, M.B., Kahl, M.D., Jensen, K.M., Butterworth, B.C., Makynen, E.A., Durhan, E.J., Linnum, A., Leino, R.L., Curtis, L.R., Giesy, J.P., and Ankley, G.T. 2006. Evaluation of the methoxytriazine herbicide prometon using a short-term fathead minnow reproduction test and a suite of in vitro bioassays. Environ. Toxicol. Chem. **25**(8): 2143–2153. doi:10.1897/05-604R.1. PMID:16916034.

Villeneuve, D.L., Miracle, A.L., Jensen, K.M., Degitz, S.J., Kahl, M.D., Korte, J.J., Greene, K.J., Blake, L.S., Linnum, A.L., and Ankley, G.T. 2007. Development of quantitative real-time PCR assays for fathead minnow (*Pimephales promelas*) gonadotropin β subunit mRNAs to support endocrine disruptor research. Comp. Biochem. Physiol. C Toxicol. Pharmacol. **145**(2): 171–183. doi:10.1016/j.cbpc.2006.11.003. PMID:17236816.

Villeneuve, D.L., Mueller, N.D., Martinovic, D., Makynen, E.A., Kahl, M.D., Jensen, K.M., Durhan, E.J., Cavallin, J.E., Bencic, D., and Ankley, G.T. 2009. Direct effects, compensation, and recovery in female fathead minnows exposed to a model aromatase inhibitor. Environ. Health Perspect. **117**(4): 624–631. PMID: 19440503.

Villeneuve, D.L., Garcia-Reyero, N., Martinovic, D., Mueller, N.D., Cavallin, J.E., Durhan, E.J., Makynen, E.A., Jensen, K.M., Kahl, M.D., Blake, L.S., Perkins, E.J., and Ankley, G.T. 2010. I. Effects of a dopamine receptor antagonist on fathead minnow, *Pimephales promelas*, reproduction. Ecotoxicol. Environ. Saf. **73**(4): 472–477. doi:10.1016/j.ecoenv.2009.09.007. PMID:19783049.

Wallace, R.A., and Selman, K. 1981. Cellular and dynamic aspects of oocyte growth in teleosts. Am. Zool. **21**(2): 325–343. doi:10.1093/icb/21.2.325.

Watanabe, K.H., Jensen, K.M., Orlando, E.F., and Ankley, G.T. 2007. What is normal? A characterization of the values and variability in reproductive endpoints of the fathead minnow, *Pimephales promelas*. Comp. Biochem. Physiol. C Toxicol. Pharmacol. **146**: 348–356. doi:10.1016/j.cbpc.2007.04.015. PMID:17600770.

Wolf, J.C., Dietrich, D.R., Friederich, U., Caunter, J., and Brown, A.R. 2004. Qualitative and quantitative histomorphologic assessment of fathead minnow *Pimephales promelas* gonads as an endpoint for evaluating endocrine-active compounds: a pilot methodology study. Toxicol. Pathol. **32**(5): 600–612. doi:10.1080/01926230490515201. PMID:15603544.

Yaron, Z., Gur, G., Melamed, P., Rosenfeld, H., Elizur, A., and Levavi-Sivan, B. 2003. Regulation of fish gonadotropins. Int. Rev. Cytol. **225**: 131–185. doi:10.1016/S0074-7696(05)25004-0. PMID:12696592.

Do exotic salmonids feed on native fauna after escaping from aquaculture cages in Tasmania, Australia?

Kátya Gisela Abrantes, Jeremy Martin Lyle, Peter D. Nichols, and Jayson Mark Semmens

Abstract: Atlantic salmon, *Salmo salar*, and rainbow trout, *Oncorhynchus mykiss*, are farmed in Tasmania, Australia, where fish sometimes escape into the natural environment. If escapees are able to survive and feed on native fauna, it is likely that they will have ecosystem impacts. Stomach content, body condition (muscle lipid content and Fulton' *K*), stable isotope, and fatty acid analysis were used to determine if escaped salmonids feed on native fauna. Results indicate that, in general, escaped salmonids do not feed on native fauna. Salmonids loose condition after escaping, and escapee stomachs were mostly empty or contained non-nutritious material or feed pellets. Nevertheless, almost a quarter of rainbow trout stomachs contained native fauna. The majority of escapees had biochemical composition similar to caged animals, indicating that these fish had not switched to feed on local food sources. However, a small fraction of escapees conclusively showed changes in biochemical parameters indicative of a shift to feeding on native fauna. Given the numbers and frequency of escapes, this can have an important impact on native species and on the ecology of Macquarie Harbour.

Résumé : On fait l'élevage du saumon atlantique, *Salmo salar*, et de la truite arc-en-ciel, *Oncorhynchus mykiss*, en Tasmanie, Australie, où les poissons s'échappent parfois vers le milieu naturel. Si les poissons qui s'échappent réussissent à survivre et se nourrir de la faune indigène, il est vraisemblable qu'ils aient un impact sur l'écosystème. Nous avons déterminé les contenus stomacaux et la condition corporelle (contenu lipidique des muscles et *K* de Fulton) et analysé les isotopes stables et les acides gras afin de vérifier si les salmonidés échappés se nourrissaient de la faune indigène. Après leur évasion, les poissons perdent de leur condition et les estomacs des poissons échappés sont en majorité vides ou alors contiennent du matériel non nutritif ou des granulés alimentaires. Néanmoins, presque un quart des estomacs de truites arc-en-ciel contenait de la faune indigène. Les poissons échappés ont pour la plupart une composition biochimique semblable à celle des animaux encagés, indiquant que ces poissons n'ont pas fait la transition vers les sources alimentaires locales. Cependant, une petite fraction des poissons échappés montre clairement des changements de variables biochimiques qui indiquent une transition vers l'alimentation à partir de la faune indigène. Étant donné le nombre et la fréquence des fuites, cela peut avoir un impact important sur les espèces indigènes et sur l'écologie de Macquarie Harbour.

[Traduit par la Rédaction]

Introduction

Atlantic salmon, *Salmo salar*, and rainbow trout, *Oncorhynchus mykiss*, are native to the North Atlantic and North Pacific, respectively, and were introduced to Australia in the late 1800s as sportfish for recreational anglers. Commercial farming of salmonids commenced in Australia in the mid-1980s and today Tasmania produces ~30 000 t of salmonids per annum. Salmonids are grown in sea cages, but fish occasionally escape into the natural environment as a consequence of human error, net breakages, or natural causes such as predator (seals and sharks) or storm damage to cages (Gausen and Moen 1991; McKinnell et al. 1997). Although exact numbers and frequency of escapes are not known, it is estimated that 2%–3% of stocked fish are lost owing to low-level leakage in Tasmania (DPIPWE 2006), along with occasional large-scale (>1000 individuals) losses. In other parts of the world, the numbers of escaped individuals (from here

Received 28 May 2010. Accepted 26 March 2011. Published at www.nrcresearchpress.com/cjfas on 2 September 2011.
J21840

Paper handled by Associate Editor Marc Trudel.

K.G. Abrantes,* J.M. Lyle, and J.M. Semmens. Tasmanian Aquaculture and Fisheries Institute, University of Tasmania, Private Bag 49, Hobart, Tasmania 7001, Australia.
P.D. Nichols. CSIRO Marine and Atmospheric Research, Wealth from Oceans Flagship, GPO Box 1538, Hobart, Tasmania 7001, Australia; CSIRO Wealth from Oceans Flagship, Division of Marine and Atmospheric Research, GPO Box 1538, Hobart, Tasmania 7000, Australia.

Corresponding author: Kátya Gisela Abrantes (e-mail: Katya.Abrantes@gmail.com).

*Present address: Department of Earth and Environmental Sciences, Katholieke Universiteit Leuven, 20 Kasteelpark Arenberg, 3001-Heverlee, Belgium.

Can. J. Fish. Aquat. Sci. **68**: 1539–1551 (2011)

doi:10.1139/F2011-057

on referred to as escapees) are sufficiently large as to contribute considerably to commercial and recreational fisheries (e.g., Lund et al. 1991; Youngson et al. 1997; Soto et al. 2001). In Tasmania, escaped Atlantic salmon and rainbow trout are targeted by anglers and recreational gillnetters in coastal marine waters.

There have been a number of studies examining the fate of escaped salmonids (Hansen et al. 1997; Jonsson et al. 2003; Hansen 2006), but relatively few have examined their feeding habits and potential impacts on native fauna (Hislop and Webb 1992; McKinnell et al. 1997; Jacobsen and Hansen 2001). Salmonids are opportunistic carnivores, feeding on crustaceans, mesopelagic fish, and squid (Jacobsen and Hansen 2001; Haugland et al. 2006). As predators, if escapees survive, feeding on native prey, this is likely to have a considerable impact on local ecosystems (Lodge 1993; Gross 1998). Although crossbreeding with wild salmonid populations is not a problem in Australia, impacts on native fauna and biodiversity can be important, either by direct predation or competition for food or habitat (Gross 1998; Soto et al. 2006; McDowall 2006).

Within their distributional range, escaped farmed Atlantic salmon appear to adapt well to feeding on natural prey (Hislop and Webb 1992; Jacobsen and Hansen 2001), although survival may be lower than for wild fish (Jonsson et al. 2003). Outside of their natural range, feeding success, as suggested by the high incidence of empty stomachs, tends to be poor (McKinnell et al. 1997; Morton and Volpe 2002). For rainbow trout, the ability to adapt to feeding on native fauna and subsequent survival appears dependent upon the size and age at escape, with younger fish being better able to adapt to the wild (Rikardsen and Sandring 2006).

Atlantic salmon is a poor colonizer and does not tend to form breeding populations after being introduced in foreign areas (McKinnell et al. 1997; Naylor et al. 2005). On the other hand, breeding populations of rainbow trout have been established in Australia (Ward et al. 2003), New Zealand (Crowl et al. 1992), Argentina (Soto et al. 2006), and Chile (Soto et al. 2006), as a result of escapes from aquaculture and stocking for recreational fisheries, but colonization success is generally low and highly variable with location (Fausch et al. 2001). Nevertheless, even if wild populations are not established, salmonids can still impact on the local ecosystems owing to the regular escapes from aquaculture facilities.

In the Southern Hemisphere, Chile and Australia (Tasmania) are the two main salmonid farming countries. In these areas, only one study on the fate of escapees based on stomach content and body condition analysis has been published (Chile; Soto et al. 2001). Results were inconclusive, as wild salmonids often have a high incidence of empty stomachs (Jacobsen and Hansen 2001) and their body condition is always lower than that of caged individuals (Thorstad et al. 1997; Johnston et al. 2006). Although stomach content analysis is an important method in the study of diets, it can lead to bias due to differences in detectability and digestibility among food sources, and it can confirm the diet in an animal only at a specific time. Consequently, a large number of stomachs would need to be analyzed to determine if salmonids survive by feeding on native fauna, and even then results may be inconclusive.

Biochemical techniques such as stable isotope and fatty acid analysis are more useful in determining if escaped salmonids feed on native fauna (Dempson and Power 2004; Martinez et al. 2009), and they have also been used to distinguish between fish of farmed or free-living origin, at least for as long as the isotopic signature is not affected by any shift in diet or other physiological processes (Schröder and Gacia de Leaniz 2010). These approaches provide information on the material that is assimilated and incorporated into an organisms' tissues and not just what is ingested, but reflects the diet over relatively long periods (weeks to months). This allows for the identification of food sources not easily detectable in stomach contents, and requires reduced sample sizes. For stable isotopes, δ^{13}C generally provides information on the base of the food web because different food sources can have distinct δ^{13}C, and especially because of the relatively small fractionation (~0.5‰–1.0‰; DeNiro and Epstein 1978) from food source to consumer. δ^{15}N is mostly used as an indicator of trophic position as it undergoes a much higher fractionation (2‰–5‰; DeNiro and Epstein 1981) between trophic levels. The fatty acid composition of a consumer is also a reflection of its food sources, as fatty acids with >14 carbons are deposited in consumer tissues in a relatively unmodified manner (Budge et al. 2006). Moreover, because animals cannot synthesize polyunsaturated fatty acids de novo, they can be used as biomarkers to trace the origin of nutrients to a specific source (Dalsgaard and John 2004).

In this study, stomach content analysis, body condition, stable isotope, and fatty acid analysis are used concurrently to determine if salmonids feed on native fauna after escaping from aquaculture cages in Tasmania, Australia.

Materials and methods

Study area

This study was conducted in Macquarie Harbour, western Tasmania, Australia (Fig. 1), one of the main salmonid marine farming areas in the Southern Hemisphere, producing ~6000 t of head-on, gutted salmonids per annum. Macquarie Harbour is a semi-enclosed ~32 km × 8 km estuarine system with an average depth of 20 m and area of ~276 km^2. The substrate is mostly sandy mud, with gravel, pebbles, and rocks along the margins. Macroalgae occur in very low abundance attached to pebbles and rocks. Small, sparse seagrass patches occur in shallow areas around the margins. The waters have a dark brown coloration due to a high concentration of tannins. Consequently, aquatic productivity is low (Edgar et al. 1999).

Animal collection

Macquarie Harbour was sampled for Atlantic salmon and rainbow trout escapees at two sites: Swan Basin and Table Head (Fig. 1). Swan Basin, ~10 km from the closest fish farms, is a shallow (max. 4 m) and relatively protected area in the northwest part of the system. Table Head is closer (~1 km) to farm leases. The two sites were selected for being at different distances from the farm leases. Sampling was conducted in November 2008 (Austral spring) and April 2009 (Austral autumn) to identify possible differences in feeding activity between the colder and warmer months. Each sampling trip consisted of 3 days and 2 nights of inten-

Fig. 1. Map showing Macquarie Harbour and the two sampling sites: Swan Basin and Table Head. Shaded square, approximate location of aquaculture leases; dotted line, approximate area netted in 2003–2004.

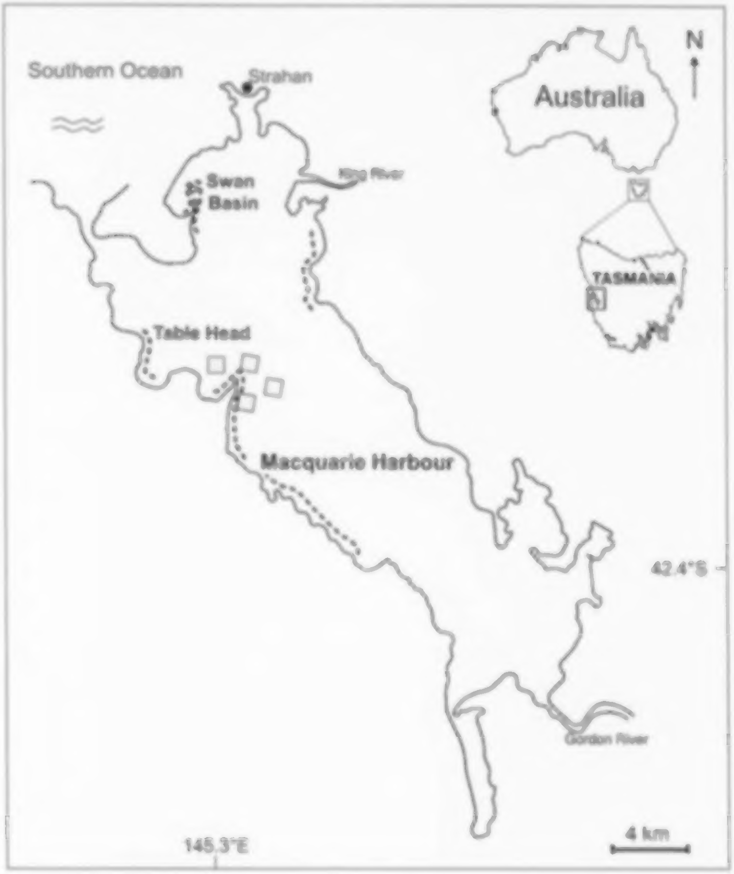

sive fishing using six monofilament gillnets, each comprised of three 30–50 m long nets of different mesh sizes (75, 105, and 140 mm stretched mesh). Nets were set perpendicular to the shoreline, and soak times varied between 6 and 12 h. Although no mass escapes of salmonids had been reported for at least 12 months prior to sampling, unreported small leakages did occur with some regularity.

All salmonids collected were retained, including wild brown trout, *Salmo trutta*, a species introduced to Tasmania in the mid-1800s for the recreational fishery. Upon capture, fish were stunned with a blow to the head and their brains spiked. Animals were then measured to the nearest 0.5 cm (FL, fork length), the viscera were removed, and the carcasses were weighed to the nearest 0.1 g. A ~3 g piece of muscle tissue was then excised from just below the dorsal fin. Four caged Atlantic salmon (555–640 mm FL), five rainbow trout (510–565 mm FL), and artificial feed pellets were also sampled in November 2008 to provide information on the stable isotope and fatty acid composition of caged animals and their feed.

In addition to salmonids, native fish and invertebrates were sampled to give an indication of what the stable isotope and fatty acid composition of salmonids would be in case of a diet switch to native fauna. Carnivorous fish, considered as potential competitors, were caught in the same gillnets as salmonids, and included red cod (*Pseudophycis bachus*), juvenile blue grenadier (*Macruronus novaezelandiae*), and Australian salmon (*Arripis trutta*). Potential prey were collected with seine nets and fish traps, and included crustaceans such as grapsid crabs (*Paragrapsus gaimardii*) and caridean shrimps (*Macrobrachium* sp. and an unidentified species); small fish (<100 mm FL) such as jollytails (*Galaxias* sp.), silverfish (*Leptatherina presbyteroides*), pilchards (*Sardinops sagax*), and short-headed hardyheads (*Kestratherina brevirostris*); two unidentified Gobiidae species; and small juveniles (<100 mm FL) of greenback flounder (*Rhombosolea tapirina*), yellow-eye mullet (*Aldrichetta forsteri*), and Australian salmon. Isopods and blue mussels (*Mytilus edulis*) were picked from between rocks and pebbles along the shore. Gammarid amphipods were collected from the substrate by sieving surface sediment through a 500 µm sieve and picking animals with tweezers. Potential fish competitors and the grapsid crab were collected in both sampling periods, while other invertebrates and small fish were only collected in April 2009. Large fish were killed as for the salmonids; whereas, small animals were killed by immersion in an ice-seawater slurry. All tissue samples were kept in liquid nitrogen until transported to the laboratory, where they were stored at –20 °C until analysis.

Primary producers were also collected at each site to obtain the baseline $\delta^{15}N$ for the food web at Macquarie Harbour and used as a point of comparison with the $\delta^{15}N$ of feed pellets. At each site, green leaves of the seagrass *Zostera muelleri* were collected from three to five individual plants and pooled for analysis. Phytoplankton was collected at each site with a 125 µm plankton net. Epilithic microalgae, mainly filamentous green algae, diatoms, and cyanobacteria, were collected by scraping 5–10 well-separated (>5 m) greenish pebbles with a scalpel. The scraped material was then passed through a 125 µm sieve, washed, and collected on a 5 µm Nuclepore membrane filter. Brown and red epiliths were collected from rocks with a pair of tweezers. In the laboratory, these algae were washed with distilled water and all possible debris were removed under a dissecting microscope. For each algae group, material collected at each site was pooled for analysis.

Stomach content analysis

Stomachs of salmonids were dissected and contents were sorted and identified. Food items were placed into the following categories: artificial feed pellets that were readily recognized, fish, crustaceans (caridean shrimps and grapsid crabs), bivalves (blue mussel), algae/seagrass, leaves/twigs, sand/pebbles, and “other”. Stomach content analysis was based on frequency of occurrence, i.e., as percentage of individuals that contained a particular food type (Hyslop 1980).

Stomach content data were supplemented with samples collected between July 2003 and May 2004, following two large escapes in March and April 2003 (J. Lyle, unpublished data). These fish were collected using the same sampling methodology but were sampled over a greater area within Macquarie Harbour (Fig. 1).

Body condition

Body condition was compared between caged and escaped salmonids using Fulton's *K*, an index based on the length–mass relationship and total lipid content in white muscle (% wet mass). Fulton's *K* was calculated as $K = (100 \times GW) \times FL^{-3}$, where GW is gutted mass (g) and FL is fork length (cm). For Atlantic salmon and rainbow trout, Fulton's *K* were compared between caged and escaped living conditions with a one-way analyses of variance (ANOVA), after the assumptions of normality and homogeneity of variances were met.

For the analyses of muscle lipid content, as for stable isotope and fatty acid analyses, only 39 out of the 47 rainbow trout were considered owing to cost constraints. The eight excluded individuals were captured in November 2008 from Table Head. Lipid samples were extracted overnight by a modification of the Bligh and Dyer (1959) method, using a chloroform–methanol–water solvent solution (1:2:0.8 by volume). Chloroform – saline water (10:10 *v/v*) was added to break phase for 2 h, after which the lower chloroform layer, containing lipids, was collected, concentrated, and weighed to obtain total lipid content (% wet mass). For each species, muscle lipid content was compared between caged and escaped animals with a one-way ANOVA. For rainbow trout, data were first inverse-transformed to meet the assumption of homogeneity of variances. The relationship between muscle lipid content and Fulton's *K* was also analyzed with regression analysis.

Stable isotope analysis

Sample processing and analysis

Muscle tissue was excised from the trunk behind the pectoral fin in small fish, from claws and legs in crabs, from abdominal muscles in shrimp, and from adductor muscles in bivalves. Because of their small size, peracarid crustaceans were processed whole. For salmonids and large fish, each individual was analysed separately. To reduce intraspecific variability in isotopic values, material from three to five individuals were pooled per sample for small fish prey and decapod crustaceans, and 10–30 for small invertebrates (bivalves and peracarid crustaceans).

Because tissue lipid content affects its $\delta^{13}C$ (DeNiro and Epstein 1977) and since salmonids are typically rich in lipids, lipids were removed from samples before $\delta^{13}C$ analysis with a chloroform–methanol–water solvent solution (1:2:0.8 by volume) for 12 h. Lipids were also removed from the artificial feed pellets before $\delta^{13}C$ analysis; because, owing to isotopic routing (Schwarcz 1991), the isotopic composition of a tissue is a reflection of the particular nutrients from which it is formed (Gannes et al. 1997; Bearhop et al. 2002), and not of the overall diet. $\delta^{15}N$ analysis was conducted on untreated samples because lipid extraction can cause fractionation in $\delta^{15}N$ (Sotiropoulos et al. 2004). Separate analyses were not conducted for other species; instead, $\delta^{13}C$ was mathematically normalized based on the C/N ratios using the equation: $\delta^{13}C_{\mathrm{normalized}} = \delta^{13}C_{\mathrm{untreated}} - 3.32 + 0.99 \times C/N$ (Post et al. 2007).

Samples were dried to constant mass at 60 °C and homogenized into a fine powder with a mortar and pestle. Then $\delta^{13}C$, $\delta^{15}N$, and carbon and nitrogen concentrations were measured with an Isoprime mass spectrometer coupled with an element analyser. Results are expressed as per mil (‰) deviations from the standards, PeeDee Belemnite (PDB) for carbon and atmospheric air for nitrogen, as defined by the equation: $\delta^{13}C, \delta^{15}N = [(R_{\mathrm{sample}}/R_{\mathrm{reference}}) - 1] \times 10^3$, where $R = {}^{13}C/{}^{12}C$ for carbon and ${}^{15}N/{}^{14}N$ for nitrogen. Secondary standards were Australian National University (ANU) sucrose for $\delta^{13}C$ and ammonium sulfate for $\delta^{15}N$. Duplicates were run every 12 samples and two standards were also run after every 12 samples. Results had a precision of ±0.1‰ (1 SD) for both $\delta^{13}C$ and $\delta^{15}N$.

Data analysis

$\delta^{13}C$ and $\delta^{15}N$ were compared between caged and escaped animals with a one-way ANOVA to identify differences in isotopic profiles likely due to changes in diet after escapement. This was done for Atlantic salmon and rainbow trout separately. Here, data from escapees captured at both sites and in both sampling trips were pooled, as there were no statistically significant differences in mean stable isotope composition between sites or time of collection.

$\delta^{13}C$ and $\delta^{15}N$ of primary producers, native species, artificial pellets, and salmonids was graphed to give an indication of the stable isotopic composition escaped salmonids would

Table 1. Diet (% occurrence) of escaped rainbow trout, Atlantic salmon, and of wild brown trout collected in Macquarie Harbour in 2003–2004 and in 2008–2009.

Species	*n*	Empty	Pellets	Fish	Crustaceans	Bivalves	Algae/ seagrass	Leaves/ twigs	Pebbles/ sand	Other
2008–2009										
Rainbow trout	47	38.1	21.4	2.4	14.3	9.5	21.4	31.0	19.0	7.1
Atlantic salmon	13	78.6	0.0	0.0	0.0	0.0	0.0	21.4	0.0	7.1
Brown trout	12	16.7	8.3	58.3	16.7	0.0	0.0	0.0	0.0	0.0
2003–2004										
Rainbow trout	312	38.0	17.6	0.0	4.8	4.5	1.3	26.5	16.6	3.2*
Atlantic salmon	553	77.4	6.1	1.2	0.2	0.5	0.2	13.0	0.7	1.8
Brown trout	10	40.0	0.0	50.0	10.0	0.0	0.0	0.0	0.0	0.0

*Terrestrial insects.

have if they successfully fed on native fauna. For animals, stable isotope results of individuals collected at both sites and on both sampling occasions were combined. This was only done after verifying, with a two-way ANOVA, that there were no spatial or temporal differences in δ^{13}C or δ^{15}N for the two species (grapsid crab and red cod) that were collected at both sites and both sampling occasions (Abrantes and Sheaves 2008).

Since δ^{15}N can increase with starvation (Hobson et al. 1993; Adams and Sterner 2000), lipid content of escapees was also correlated with δ^{15}N. A negative relationship would mean that any changes in δ^{15}N could be a result of starvation and not of a change in diet.

Fatty acid analysis

Sample processing and analysis

Fatty acid composition of artificial feed pellets, caged and escaped salmonids, and native species was analysed by gas chromatography (GC). Lipids were extracted as described above, and analyses were conducted on aliquots of the total lipid extracts, which were treated with a solution of methanol – hydrochloric acid – chloroform (10:1:1 by volume) at 100 °C for 2 h to produce fatty acid methyl esters (FAME). FAME were separated by an addition of 1 mL water and extracted with a 1.8 mL of 4:1 *v/v* hexane–chloroform solution. FAME were analyzed using a Agilent Technologies 7890A GC Palo Alto, Calif., USA) equipped with a Supelco Equity-1 fused silica capillary column (15 m × 0.1 mm i.d., 0.1 μm film thickness), a flame ionization detector, a split–splitless injector, and an Agilent Technologies 7683B Series auto sampler and injector. Helium was the carrier gas and inlet pressure was maintained at 425 kPa. Samples were injected in splitless mode with an oven temperature of 120 °C, and temperature was increased to 250 °C at 10 °C·min^{-1} and then to 270 °C at 3 °C·min^{-1}. Peaks were quantified with Agilent Technologies ChemStation software. Individual fatty acids were identified by mass spectral data and comparing retention times with those of authentic and laboratory standards. Results are expressed as percentage of the total fatty acids.

Data analysis

The fatty acid profiles of feed pellets, caged and escaped salmonids, and native fish and crustaceans were compared using principal component analysis (PCA) in PRIMER v.6 (Primer-E Ltd., Ivybridge, UK). Only fatty acids that contributed at >1% for any of the species were included. The proportion of saturated fatty acids (SFA), monounsaturated fatty acids (MUFA), and polyunsaturated fatty acids (PUFA) was considered in this analysis. Data were first arcsine transformed. Fatty acids responsible for separation of organisms were identified, and the diet of escapees were inferred by comparing the principal component scores with those from caged salmonids and native fish.

For escaped Atlantic salmon and rainbow trout, changes in fatty acid composition with lipid content (a proxy for time in the wild) were explored by regression analysis. Each fatty acid was considered individually in the regression. Since there were differences in MUFA and PUFA contents as well as the ω6:ω3 and eicosapentaenoic acid / docosahexaenoic acid (EPA/DHA) ratios between caged salmonids and native species, the relationships between lipid content and these sums and ratios were analysed. Since marine fish are typically rich in DHA and EPA, and feed based on non-marine oils is richer in oleic and linoleic acids, the relationship between the proportions of fatty acids of these different origins (DHA + EPA vs. 18:1ω9c+18:2ω6) was also analysed for each species with regression analysis. Since a total of 59 regression analyses were conducted for each species, the significance level was reduced using the Bonferroni correction for multiple comparisons. This is done by dividing the standard significance level of $\alpha = 0.05$ by the total number of individual comparisons (118), which leads to a Bonferroni-corrected significance level of $\alpha = 0.0004$.

Results

Stomach content analysis

Stomach contents of 47 escaped rainbow trout, 13 escaped Atlantic salmon, and 12 wild brown trout were collected in October 2008 and April 2009 (Table 1). For each species, results were combined between sampling periods. For rainbow trout, 63.2% of the stomachs was empty or contained non-nutritious material. The remaining 36.8% contained nutritious material such as artificial feed pellets (21%) or native animals (23.7%). From individuals that fed on artificial feed pellets, half was collected from Swan Basin. No nutritious material was identified in Atlantic salmon stomachs. The majority of the stomachs (79%) were empty, and three stomachs contained large quantities of leaves of the terrestrial plant myrtle, *Nothofagus cunninghamii* (Table 1). The proportion of brown trout containing fish in their diet was 58%,

Table 2. Size range, mass range, muscle lipid content (% wet mass; mean ± SD) and Fulton's *K* (mean ± SE) of caged and escaped Atlantic salmon and rainbow trout, and of wild brown trout.

	n	Fork length (mm)	Gutted mass (g)	Lipid content (%)	Fulton's *K*
Caged Atlantic salmon	4	555–640	2130–2720	15.4±2.3	1.1±0.1
Caged rainbow trout	5	510–565	2310–3510	21.2±2.9	1.6±0.1
Escaped Atlantic salmon	13	510–690	905–3000	5.0±4.4	0.9±0.1
Escaped rainbow trout	47	335–570	580–2725	12.0±7.3*	1.4±0.0
Brown trout	12	350–560	470–1880	2.8±1.6	1.1±0.0

*n = 39.

whereas 17% contained crabs, and one stomach contained high quantities of feed pellets.

Stomach content data from fish collected in 2003–2004 showed similar results (Table 1). For both farmed species, the majority of stomachs were empty or contained non-nutritious material such as twigs and pebbles (Table 1). A lower proportion (13.3% vs. 21.4%) of rainbow trout stomachs contained feed pellets than in 2008–2009, and only 6% had consumed crabs and (or) bivalves, while none had consumed fish. Interestingly, 2.4% of rainbow trout stomachs contained remains of terrestrial insects such as crickets, beetles, bees, wasps, and flies. For Atlantic salmon, unlike in 2008–2009, 6.1% of animals had consumed feed pellets and 1.6% of stomachs contained native fauna, including seven stomachs that contained teleost remains.

Body condition

For both caged and escaped individuals, Fulton's *K* was higher for rainbow trout than for Atlantic salmon (Table 2). For rainbow trout, escapees had significantly lower *K* values than caged individuals ($F_{[1,50]} = 4.70$, $p = 0.035$), but for Atlantic salmon *K* values were only slightly lower for escaped than caged individuals, and the difference was not significant ($F_{[1,15]} = 1.86$, $p = 0.192$) (Table 2). Fulton's *K* of wild brown trout was lower than that of both caged and escaped rainbow trout, and similar to that of caged and escaped Atlantic salmon (Table 2).

Atlantic salmon (0.6%–15.6%; SD = 4.4) and rainbow trout (2.1%–27.3%; SD = 7.3) escapees had highly variable muscle lipid content, and for both species, caged individuals had much higher mean lipid content than escapees and wild brown trout (Table 2). The difference between caged and escaped individuals was significant for Atlantic salmon ($F_{[1,16]} = 10.89$, $p = 0.005$). For rainbow trout, the variability in lipid content was much higher in escapees (Table 2) and included very high values, close to caged individuals, and very low values, close to wild brown trout. Given this high variability, no significant differences were detected for this species ($F_{[1,41]} = 2.99$, $p = 0.091$).

There was a weak significant relationship between Fulton's *K* and muscle lipid content for rainbow trout (Fulton's $K = 0.016 \times \%\text{lipid} + 1.258$; $R^2 = 0.23$, $p = 0.007$), but not for Atlantic salmon ($p = 0.047$; Bonferroni-adjusted $\alpha = 0.025$).

Stable isotope analysis

Stable isotope composition of native and introduced organisms

Primary producers varied in $\delta^{13}C$ from –27.0‰ for epilithic green microalgae to –12.5‰ for the seagrass *Zostera muelleri* (Fig. 2). Regarding $\delta^{15}N$, primary producers had similar values, averaging 4.1 ± 0.5‰ (±SE) (Fig. 2). There was no effect of site or time of collection on $\delta^{13}C$ or $\delta^{15}N$ for the grapsid crab or red cod ($p > 0.1$ in all cases), and therefore samples collected from both sites and field seasons were combined for each species in the following statistical analyses. Invertebrates and fish ranged in $\delta^{13}C$ from –23.7‰ to –20.1‰ and –23.3‰ to –19.2‰, respectively (Fig. 2*a*). Carnivorous fish had very close $\delta^{13}C$ and $\delta^{15}N$ (ranges: $\delta^{13}C$ = 1.5‰; $\delta^{15}N$ = 0.7‰) (Fig. 2*a*). The phytodetritivore yellow-eye mullet was similar to caged Atlantic salmon and rainbow trout (Fig. 2*a*).

Atlantic salmon and rainbow trout feed pellets had similar $\delta^{13}C$ and $\delta^{15}N$ (Fig. 2*a*). Caged Atlantic salmon were 1.0‰ more enriched in $\delta^{13}C$ and 4.0‰ more enriched in $\delta^{15}N$ than its feed, and for caged rainbow trout the difference was 1.2‰ and 3.0‰ for $\delta^{13}C$ and $\delta^{15}N$, respectively. There were no significant differences in $\delta^{13}C$ or $\delta^{15}N$ between caged and escaped animals for either species (Atlantic salmon: $F_{[1,15]}$ = 1.10, $p = 0.311$ for $\delta^{13}C$, and $F_{[1,15]} = 0.57$, $p = 0.463$ for $\delta^{15}N$; rainbow trout: $F_{[1,42]} = 0.30$, $p = 0.590$ for $\delta^{13}C$, and $F_{[1,42]} = 1.74$, $p = 0.194$ for $\delta^{15}N$).

While $\delta^{13}C$ of escaped Atlantic salmon ranged between –23.0‰ and –18.2‰, only one of the tested individuals had $\delta^{13}C$ lower than –20.0‰ (Fig. 2*b*). Escaped rainbow trout had lower variability in $\delta^{13}C$, ranging from –19.8‰ to –17.9‰ (Fig. 2*b*). $\delta^{15}N$ ranged from 10.5‰ to 13.2‰ and 9.8‰ to 12.7‰ for escaped Atlantic salmon and rainbow trout, respectively. There was no relationship between muscle lipid content (a proxy for time since escapement) and $\delta^{15}N$ of Atlantic salmon or rainbow trout ($p > 0.05$).

Fatty acid profiles

Fifty-seven individual fatty acids were identified. Feed pellets were rich in 18:1ω9*c* (oleic acid; 26%–31%) and 16:0 (palmitic acid; 20%–21%) (Appendix A). Caged and escaped Atlantic salmon and rainbow trout were also rich in 18:1ω9*c* (up to 35%), a fatty acid that occurred in much higher proportions than in native species, and contained more 16:1ω7*c* (palmitoleic acid) and 18:2ω6 (linoleic acid) than native species (Appendix A). In contrast, native fish were much richer in 22:6ω3 (DHA) and were slightly more enriched in 20:4ω6 (arachidonic acid, AA) and 20:5ω3 (EPA) (Appendix A). Native species had much lower ω6/ω3 and EPA/DHA ratios, and were richer in PUFA and poorer in MUFA than artificial pellets and caged and escaped salmonids (Appendix A).

The different animal groups were well separated in the PCA (Fig. 3). The first PCA component, explaining 73.2% of variability, was positively correlated with oleic acid and the sum of MUFA, and negatively correlated with DHA and

Fig. 2. Carbon and nitrogen stable isotope composition of organisms collected in Macquarie Harbour. Data for November 2008 and April 2009, and for Swan Basin and Table Head is pooled. (A) $\delta^{13}C$ and $\delta^{15}N$ (mean ± SE) of all native organisms analysed including primary producers, artificial feed pellets, caged and escaped Atlantic salmon (AS) and rainbow trout (RT), native invertebrates (white symbols), and fish (grey symbols). Producers: Epiliths, epilithic microalgae; Fil algae, red and brown filamentous algae; Phytopl; phytoplankton; seagrass, *Zostera muelleri*. (B) Isotopic results of each individual escaped Atlantic salmon, rainbow trout, and wild brown trout in relation to artificial feed pellets, caged individuals, and the three native carnivores: juvenile blue grenadier (BG), Australian salmon (AustS), and red cod (RC). YEM, yellow-eye mullet. Note the differences in scale in the *x* and *y* axes.

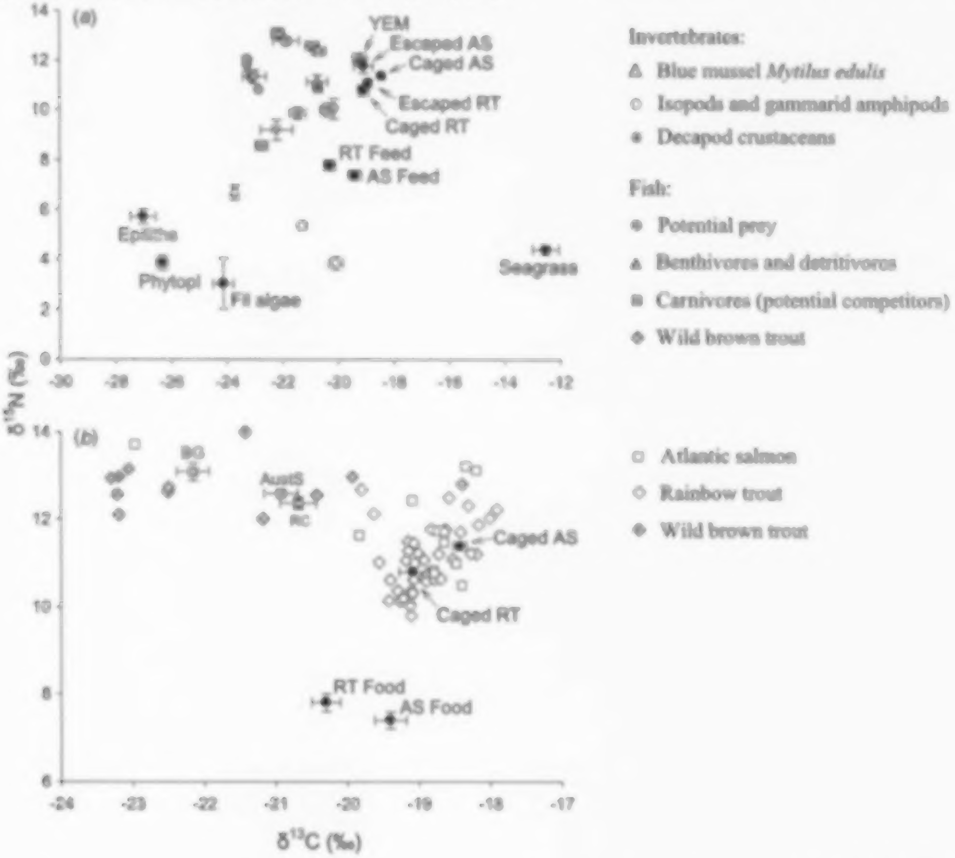

the sum of PUFA (Fig. 3). The second component was positively correlated with EPA and negatively correlated with DHA. Artificial feed pellets, caged salmonids and the majority of escaped Atlantic salmon, and rainbow trout formed a very tight group in the PCA, and were well separated from native species (Fig. 3). This separation was explained by the higher level of oleic acid and MUFA, and lower percentages of PUFA, DHA, EPA, and AA in relation to native species. Among native species, EPA, DHA, and AA separated carnivorous fish and small fish prey from the benthic species (Fig. 3). The first group had lower on the principal component (PC) 2 scores, indicating higher levels of DHA, whereas benthic species were richer in EPA and AA (Fig. 3).

As for stable isotopes, the fatty acid composition of brown trout was variable between individual fish. Consequently, brown trout individuals were scattered along the principal component 1, with one individual falling close to farmed salmonids, others falling close to carnivorous species, and the majority in between (Fig. 3).

Benthic fish species were well separated in the principal component 1 (Fig. 3). Apart from three benthic individuals collected from Table Head that had similar fatty acid composition to farmed salmonids, there was no pattern in the variation of fatty acid composition to indicate that animals collected closer to fish farms were more similar to caged fish than those collected further away from farms.

Two escaped Atlantic salmon (*a* and *b* in Fig. 3) and one escaped rainbow trout (*c* in Fig. 3) were separated from the salmonid group. The two Atlantic salmon were those with the lowest fat content (3.2% for individual *a*; 0.8% for individual *b*). Individual *a* was richer in 16:0, and slightly richer in DHA and EPA (Fig. 3). This individual also had the lowest $\delta^{13}C$ of all farmed salmonids (Fig. 2*b*). Individual *b* was in poorer condition and was separated from other farmed salmonids owing to the higher percentage of DHA and EPA. However, it was similar in both $\delta^{13}C$ (−18.4‰) and $\delta^{15}N$ (10.5‰) to caged and the majority of escaped salmonids.

In contrast, the separated rainbow trout (*c* in Fig. 3) was in

Fig. 3. Scores and factor loadings of principal component analysis (PCA) showing the first two components based on fatty acid data of feed pellets and animals from Macquarie Harbour. *a*, *b*, two Atlantic salmon that were separated from the Atlantic salmon group (3.2% and 0.8% lipid content, respectively); *c*, rainbow trout separated from the rainbow trout group (17.1% lipid content).

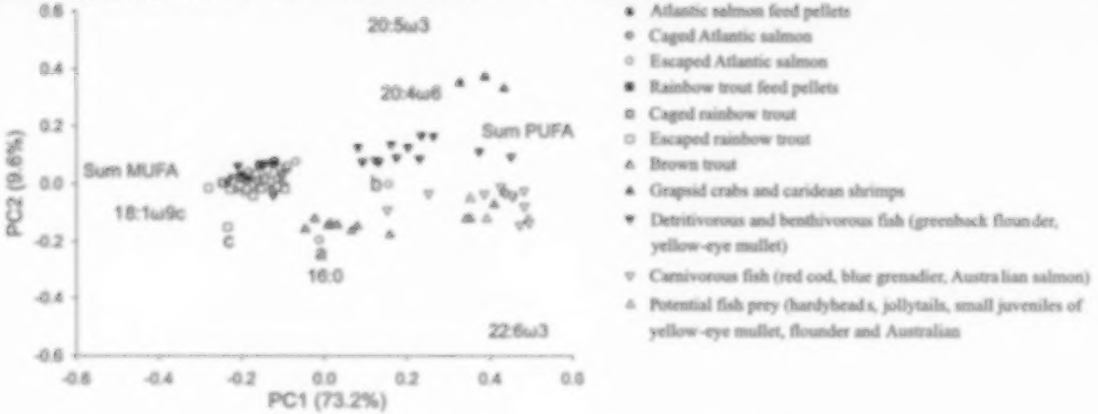

very good condition, with a lipid content of 17.1%. Although this individual had slightly different fatty acid composition, it was still much closer to farmed salmonids than to native fish (Fig. 3), and its stable isotope composition was also similar to caged fish ($\delta^{13}C = -19.1‰$; $\delta^{15}N = 10.3‰$).

For Atlantic salmon, there was a significant positive relationship between lipid content and the fatty acid 14:0 (Table 3), indicating that the proportion of these fatty acids decreased with loss of condition (lipid content). For rainbow trout, relationships were significant for three fatty acids: 16:1ω7 (positive relationship), AA and DHA (negative relationships), and a positive relationship between lipid content and EPA/DHA ratio was observed (Table 3). There were no significant relationships between lipid content and any other fatty acids, or among lipid content and sum of SFA, sum of MUFA, or ω6 and ω3 PUFA. For Atlantic salmon, there was also a significant negative relationship among the sum of oleic acid and linoleic acid ($(18{:}1 + 18{:}2) = -0.76 \times (\mathrm{EPA} + \mathrm{DHA}) + 44.43$; $R^2 = 0.782$, $p < 0.0001$), the fatty acids present at high relative levels in feed including non-marine oils (and (or) animals feeding on feeds incorporating non-marine oils), and EPA and DHA, fatty acids characteristic of marine organisms. This was not observed for rainbow trout.

Discussion

This study demonstrates that the contribution of native fauna on the diet of escaped salmonids can be determined using stable isotope and fatty acid analyses, especially when used in conjunction with traditional methods of diet analysis (stomach content analysis) and body condition. The majority of farmed salmonids did not feed on native fauna after escaping from aquaculture cages in Tasmania. Overall, these fish lost condition after escaping, as they either starve or take time to learn to feed on much less nutritious, live prey (Soto et al. 2001).

Body condition of the majority of escapees was higher (possibly indicating a more recent escape) or within the range of wild brown trout from Macquarie Harbour and of wild salmonids in their native ranges (Thorstad et al. 1997; Jacobsen and Hansen 2001). Only one of the Atlantic salmon examined had very low lipid content (0.8%) and exhibited obvious external signs of starvation. This could mean that the majority of the salmonids had been at liberty for relatively short periods or had been feeding in the wild, and illustrates that the analysis of body condition alone is not useful to determine if an exotic species is surviving in the wild by feeding on native sources. Although there is no information on the time required for differences in body condition to be noticeable under the temperature conditions of Tasmanian waters, at ~2–6 °C, 2 months are enough to detect differences in lipid content due to starvation in Atlantic salmon muscle (Einen et al. 1998). In Tasmania, salmonids are farmed in waters that can reach up to 19 °C. Since metabolic, growth, and fat deposition rates increase with water temperature (Cho and Bureau 1995; Ruyter et al. 2000), it is likely that differences in body condition would be noticeable in less than 2 months.

For escaped Atlantic salmon, in addition to lower body condition, the majority had empty stomachs or stomachs containing non-nutritious food like twigs or myrtle leaves, and only a very small number contained native fauna. The proportion of empty stomachs alone is not sufficient to determine if these fish feed, as carnivorous fish generally have high proportions of empty stomachs (Arrington et al. 2002), a phenomenon that has also been reported for salmonids even in areas where they are known to survive (e.g., Hislop and Webb 1992; Jacobsen and Hansen 2001). Nevertheless, both stable isotope and fatty acid results confirmed that the majority of Atlantic salmon escapees did not feed on native fauna.

For escaped rainbow trout, a relatively large proportion of stomachs contained readily recognizable feed pellets. From these fish, about half were collected in Swan Basin, ~10 km away from the closest fish farms, indicating that rainbow trout move throughout the system, but return to the farms to feed on the highly nutritious pellets. The dispersal of rainbow trout escapees and their return to farms to feed on pellets has been previously reported for a Canadian lake (Blanchfield et al. 2009), where animals dispersed ~1 km. The present study provides evidence of a much larger dispersal area, ~10 km, before returning to the proximity of the farms to feed. Salmonids, like most fish species, need a certain period of time to adjust to differences in taste, smell, texture, and behavior of

Table 3. Linear regression equations and diagnostic statistics for the relationships between lipid content (% wet mass) and relative levels of individual fatty acids (FA).

	Regression equation	Significance level (p values)	Variance explained (R^2)
Atlantic salmon (1%–19% lipid content, n = 17)			
14:0	%FA = 0.08 × % lipid + 1.09	<0.001	0.575
Rainbow trout (2%–27% lipid content; n = 44)			
16:1ω7*c*	%FA = 0.069 × % lipid + 7.090	<0.001	0.351
20:4ω6 (AA)	%FA = –0.010 × % lipid + 0.868	<0.001	0.383
22:6ω3 (DHA)	%FA = –0.11 × % lipid + 8.87	<0.001	0.353
EPA/DHA ratio	EPA/DHA = 0.01 × % lipid + 0.21	<0.001	0.283

Note: Only significant relationships (at Bonferroni-corrected α = 0.0004) are presented.

new food sources. This may explain the return of some rainbow trout individuals to the proximity of cages to feed on pellets. In contrast to rainbow trout, Atlantic salmon escapees do not return to the fish farms to feed, and animals rapidly disperse away from the cages (Whoriskey et al. 2006), explaining the lower incidence of stomachs containing feed pellets.

In southern Chile, ~15% of Atlantic salmon stomachs contained pellets (Soto et al. 2001). Native fish and crustaceans occurred in much higher proportions in both Atlantic salmon (over 10% for each group) and rainbow trout (~15% for fish and 30% for crustaceans) stomachs in that Chilean study. This difference between locations could be a result of higher prey availability in the coastal systems of Chile in comparison to Tasmanian estuaries, where the invertebrate and fish species diversity (Edgar et al. 1999, 2000), biomass, and abundance (Edgar et al. 1999) are very low. On the other hand, salmonids are visual predators with reduced prey detection and predation capabilities in low light conditions (Mazur and Beauchamp 2003). Hence, it is possible that a combination of factors, including the low light levels in Macquarie Harbour due to the tannin-stained waters, relatively low prey availability, and the availability of abundant, easy to obtain, nutrient rich, and highly palatable feed pellets in the area are contributing factors to the lower incidence of successful feeding on native fauna by escapees, compared with the situation in Chile. Nevertheless, the majority of wild brown trout stomachs analysed contained fish or crustaceans, indicating that potential prey items were available, and thus the differences observed cannot be attributed solely to low prey availability.

Regarding the biochemical analyses, the majority of native fish and invertebrate prey were collected in April 2009 whereas the majority of salmonid escapees were captured in November 2008, and this difference could influence results and limit the ability to detect consumption of native fauna. However, red cod and grapsid crabs were collected at both sites and on both sampling occasions yet exhibited no spatial or temporal variability in stable isotope and fatty acid composition. For stable isotopes, if there was a variation in primary producer baseline $\delta^{13}C$ or $\delta^{15}N$, this would have been detected as a shift in consumer isotopic composition, at least for low trophic level species such as grapsid crabs, which are small in size and have a fast muscle turnover, rapidly tracking any changes in source $\delta^{13}C$ and $\delta^{15}N$ (K. Abrantes, unpublished data). The major fatty acids responsible for the separation of native fish and salmonids were those characteristic of producers from marine environments (DHA + EPA) and those that occur in fish food based on non-marine oils (oleic and linoleic acids). Given the large differences in the proportion of these fatty acids between native fauna and artificial feed, no natural temporal or spatial differences in the levels of these fatty acids in the marine fish – invertebrate prey would ever be large enough to affect the results of this study.

A single Atlantic salmon had both stable isotope and fatty acid composition that indicated feeding on native fauna. Two other individuals also had relatively high $\delta^{15}N$, with values that could result from feeding on native species such as caridean shrimps and galaxiids. Given the small difference between $\delta^{15}N$ of feed pellets and local sources, and because of the natural variability in $\delta^{15}N$ trophic fractionation (McCutchan et al. 2003) and the increase in $\delta^{15}N$ with starvation (Hobson et al. 1993; Doucett et al. 1999), it is not possible to confirm that these latter individuals had been feeding on native fauna. Nevertheless, $\delta^{15}N$ was not correlated to lipid content, meaning that the high $\delta^{15}N$ values were not a result of starvation. It is possible that different individuals had different feeding success, making any relationship difficult to detect.

An additional Atlantic salmon and one rainbow trout also differed in fatty acid composition from the rest of the salmonid group. This could mean that these escapees had switched to feed on native fauna, or alternatively that the changes in fatty acid composition were a result of differential mobilization of the different fatty acids as a consequence of starvation (Kiessling and Kiessling 1993; Einen et al. 1998). In salmonid muscle, MUFA are preferentially mobilized during starvation (Jezierska et al. 1982; Kiessling and Kiessling 1993; Einen et al. 1998), whereas essential PUFA are preferentially retained or spared (Kiessling and Kiessling 1993; Kiessling et al. 2001). Hence, the higher PUFA levels found in the escaped Atlantic salmon could be a result of starvation, and not due to a diet switch to marine fauna. In contrast, the separated rainbow trout had relatively high MUFA content, suggesting that it was not starving, confirmed by condition indices, and that the difference in fatty acid composition was a result of consuming native fauna.

For both stable isotope (Hesslein et al. 1993) and fatty acid (Robin et al. 2003) composition, a certain time period under different food conditions is necessary for animal tissues to reflect the isotopic composition of a new food source. After a change in diet, differences in biochemical profiles can be detectable within 2–6 weeks for large fish (Hesslein et al. 1993; Jobling et al. 2002; Robin et al. 2003), but it is not known how long it takes for the isotopic and fatty acid composition to fully equilibrate and reflect the new food sources. The extent of these changes and of the amount of time to reach equilibrium will depend on differences between the old and new diets, differences in food nutrient composition and quality, feeding rates, and whether there is a total or only a partial change in diet. Hence, there is a need to determine the rate and nature of change in biochemical composition with starvation and with diet changes for fish under different temperature conditions. This information is crucial to better interpret variations in biochemical composition with time after escapement, and to aid interpretation in future studies.

As isotopic turnover rates in muscle are primarily dependent on growth and only a small proportion to metabolism, changes in stable isotope composition are relatively slow for large fish such as salmonids, and it can take over a year of feeding on a different diet before reaching equilibrium (Hesslein et al. 1993). Moreover, stable isotopes mainly reflect the composition of protein, which has a lower turnover rate compared with lipid, especially in large fish with slow growth (note that lipids were removed from δ^{13}C samples). Owing to isotopic routing (Schwarcz 1991), different nutrients in food are directed to similar compartments in the consumer (Podlesak and McWilliams 2006); i.e., lipids in food are mostly incorporated as lipid in a consumer, while amino acids are used to synthesize protein. This can explain the lack of relationship found between δ^{15}N and lipid content. Since protein and lipids have different turnover rates, stable isotope and fatty acid analysis can provide complementary information on diet. For example, the large (4.6‰) difference in δ^{13}C between the most ^{13}C-depleted Atlantic salmon escapee and caged individuals indicates that this animal had been feeding in the wild for a relatively long period, although its fatty acid composition indicated that the majority of the lipid was derived from artificial pellets, which are very rich in lipid.

In conclusion, stomach content analysis shows that about a quarter of rainbow trout escapees consumed native fauna. Given the numbers and frequency of escapes, this can have an important impact on the local ecology. For example, it is estimated that 2%–3% of stocked fish is lost owing to low-level leakage in Tasmania (DPIPWE 2006), which added to the large-scale (>1000 individuals) losses and adds up to many thousands of exotic predators introduced into Tasmanian waters each year. However, given that salmonids are targeted by anglers and recreational gillnetters in Tasmania, it is unlikely that these fish will survive long enough, even if they are consuming native prey, to have a significant impact on these ecosystems. Nevertheless, biochemical analyses indicate that 2.6% of rainbow trout and 15% Atlantic salmon had survived on a diet based on native fauna for a long period of time, as their tissues already reflected the biochemical composition of their new food sources.

Acknowledgements

The authors thank Graeme Ewing, Adam Barnett, and Michael Steer for help in the field. Zack Wingfield from Tassal Pty Ltd. provided farmed Atlantic salmon and Barry McClure from Petuna Seafarms farmed rainbow trout. Justin Clarke, Matt Gaby, Andrew Blenkhorn, and Doug Keep, recreational fishers, willingly provided muscle and stomach samples from their catch. Research was conducted under the General Fisheries Permit No. 7068 (DPIPWE, Tasmania, Australia). Research procedures received approval from the Animal Ethics Committee, University of Tasmania (Ethics Approval A0010272). The project was supported by Cradle Coast Natural Resource Management through funding from the Australian Government's Natural Heritage Trust. We are also very grateful to the helpful comments of the editor and two anonymous referees that greatly improved the quality of the manuscript.

References

Abrantes, K., and Sheaves, M. 2008. Incorporation of terrestrial wetland material into aquatic food webs in a tropical estuarine wetland. Estuar. Coast. Shelf Sci. **80**(3): 401–412. doi:10.1016/j.ecss.2008.09.009.

Adams, T.S., and Sterner, R.W. 2000. The effect of dietary nitrogen content on trophic level ^{15}N enrichment. Limnol. Oceanogr. **45**(3): 601–607. doi:10.4319/lo.2000.45.3.0601.

Arrington, D.A., Winemiller, K.O., Loftus, W.F., and Akin, S. 2002. How often do fishes "run empty"? Ecology, **83**: 2145–2151.

Bearhop, S., Waldron, S., Votier, S.C., and Furness, R.W. 2002. Factors that influence assimilation rates and fractionation of nitrogen and carbon stable isotopes in avian blood and feathers. Physiol. Biochem. Zool. **75**(5): 451–458. doi:10.1086/342800. PMID:12529846.

Blanchfield, P.J., Tate, L.S., and Podemski, C.L. 2009. Survival and behaviour of rainbow trout (*Oncorhynchus mykiss*) released from an experimental aquaculture operation. Can. J. Fish. Aquat. Sci. **66**(11): 1976–1988. doi:10.1139/F09-127.

Bligh, E.G., and Dyer, W.J. 1959. A rapid method for total lipid extraction and purification. Can. J. Biochem. Physiol. **37**(8): 911–917. PMID:13671378.

Budge, S.M., Iverson, S.J., and Koopman, H.N. 2006. Studying trophic ecology in marine ecosystems using fatty acids: a primer on analysis and interpretation. Mar. Mamm. Sci. **22**(4): 759–801. doi:10.1111/j.1748-7692.2006.00079.x.

Cho, Y., and Bureau, D.P. 1995. Determination of the energy requirements of fish with particular reference to salmonids. J. Appl. Ichthyology, **11**(3–4): 141–163. doi:10.1111/j.1439-0426.1995.tb00015.x.

Crowl, T.A., Townsend, C.R., and McIntosh, A.R. 1992. The impact of introduced brown and rainbow trout on native fish: the case of Australasia. Rev. Fish Biol. Fish. **2**(3): 217–241. doi:10.1007/BF00045038.

Dalsgaard, J., and John, M.S. 2004. Fatty acid biomarkers: validation of food web and trophic markers using ^{13}C-labelled fatty acids in juvenile sandeel (*Ammodytes tobianus*). Can. J. Fish. Aquat. Sci. **61**(9): 1671–1680. doi:10.1139/f04-095.

Dempson, J.B., and Power, M. 2004. Use of stable isotopes to distinguish farmed from wild Atlantic salmon, *Salmo salar*. Ecol. Freshwat. Fish, **13**(3): 176–184. doi:10.1111/j.1600-0633.2004.00057.x.

DeNiro, M.J., and Epstein, S. 1977. A mechanism of carbon isotope fractionation associated with lipid synthesis. Science, **197**(4300): 261–263. doi:10.1126/science.327543. PMID:327543.

DeNiro, M.J., and Epstein, S. 1978. Influence of diet in the distribution of carbon isotopes in animals. Geochim. Cosmochim. Acta, **42**(5): 495–506. doi:10.1016/0016-7037(78)90199-0.

DeNiro, M.J., and Epstein, S. 1981. Influence of diet on the distribution of nitrogen isotopes in animals. Geochim. Cosmochim. Acta, **45**(3): 341–351. doi:10.1016/0016-7037(81)90244-1.

Doucett, R.R., Booth, R.K., Power, G., and McKinley, R.S. 1999.

Effects of the spawning migration on the nutritional status of anadromous Atlantic salmon (*Salmo salar*): insights from stable-isotope analysis. Can. J. Fish. Aquat. Sci. **56**(11): 2172–2180. doi:10.1139/cjfas-56-11-2172.

Department of Primary Industries, Parks, Water and Environment (DPIPWE). 2006. An overview of escaped salmonids and their potential impacts in Tasmania. Tasmanian Department of Primary Industries, Parks, Water and Environment, Hobart, Tasmania, Australia.

Edgar, G.J., Barrett, N.S., and Last, P.R. 1999. The distribution of macroinvertebrates and fishes in Tasmanian estuaries. J. Biogeogr. **26**(6): 1169–1189. doi:10.1046/j.1365-2699.1999.00365.x.

Edgar, G.J., Barrett, N.S., Graddon, D.J., and Last, P.R. 2000. The conservation significance of estuaries: a classification of Tasmanian estuaries using ecological, physical and demographic attributes as a case study. Biol. Conserv. **92**(3): 383–397. doi:10.1016/S0006-3207(99)00111-1.

Einen, O., Waagan, B., and Thomassen, M.S. 1998. Starvation prior to slaughter in Atlantic salmon (*Salmo salar*) I. Effects on weight loss, body shape, slaughter- and fillet-yield, proximate and fatty acid composition. Aquaculture, **166**(1–2): 85–104. doi:10.1016/S0044-8486(98)00279-8.

Fausch, K.D., Taniguchi, Y., Nakano, S., Grossman, G.D., and Townsend, C.R. 2001. Flood disturbance regimes influence rainbow trout invasion success among five holarctic regions. Ecol. Appl. **11**(5): 1438–1455. doi:10.1890/1051-0761(2001)011[1438:FDRIRT]2.0.CO;2.

Gannes, L.Z., O'Brien, D.M., and del Rio, C.M. 1997. Stable isotopes in animal ecology: assumptions, caveats and a call for more laboratory experiments. Ecology, **78**(4): 1271–1276. doi:10.1890/0012-9658(1997)078[1271:SIIAEA]2.0.CO;2.

Gausen, D., and Moen, V. 1991. Large-scale escapes of farmed Atlantic salmon (*Salmo salar*) into Norwegian rivers threaten natural populations. Can. J. Fish. Aquat. Sci. **48**(3): 426–428. doi:10.1139/f91-055.

Gross, M.R. 1998. One species with two biologies: Atlantic salmon (*Salmo salar*) in the wild and in aquaculture. Can. J. Fish. Aquat. Sci. **55**(S1): 131–144. doi:10.1139/cjfas-55-S1-131.

Hansen, L.P. 2006. Migration and survival of farmed Atlantic salmon (*Salmo salar* L.) released from two Norwegian fish farms. ICES J. Mar. Sci. **63**(7): 1211–1217. doi:10.1016/j.icesjms.2006.04.022.

Hansen, L.P., Reddin, D.G., and Lund, R.A. 1997. The incidence of reared Atlantic salmon (Salmo salar L) of fish farm origin at West Greenland. ICES J. Mar. Sci. **54**(1): 152–155. doi:10.1006/jmsc.1996.0178.

Haugland, M., Holst, J.C., Holm, M., and Hansen, L.P. 2006. Feeding of Atlantic salmon (*Salmo salar* L.) post-smolts in the Northeast Atlantic. ICES J. Mar. Sci. **63**(8): 1488–1500. doi:10.1016/j.icesjms.2006.06.004.

Hesslein, R.H., Haland, K.A., and Ramlal, P. 1993. Replacement of sulfur, carbon and nitrogen in tissue of growing broad whitefish (*Coregonus nasus*) in response to a change in diet traced by δ^{34}S, δ^{13}C, and δ^{15}N. Can. J. Fish. Aquat. Sci. **50**: 2071–2076. doi:10.1139/f93-230.

Hislop, J.R.G., and Webb, J.H. 1992. Escaped farmed Atlantic salmon (*Salmo salar* L.) feeding in Scottish coastal waters. Aquacult. Fish. Manage. **23**: 721–723.

Hobson, K.A., Alisauskas, R.T., and Clark, R.G. 1993. Stable-nitrogen isotope enrichment in avian tissues due to fasting and nutritional stress: implications for isotopic analyses of diet. Condor, **95**(2): 388–394. doi:10.2307/1369361.

Hyslop, E.J. 1980. Stomach contents analysis: a review of methods and their application. J. Fish Biol. **17**(4): 411–429. doi:10.1111/j.1095-8649.1980.tb02775.x.

Jacobsen, J.A., and Hansen, L.P. 2001. Feeding habits of wild and escaped farmed Atlantic salmon, *Salmo salar* L., in the Northeast Atlantic. ICES J. Mar. Sci. **58**(4): 916–933. doi:10.1006/jmsc.2001.1084.

Jezierska, B., Hazel, J.R., and Gerking, S.D. 1982. Lipid mobilization during starvation in the rainbow trout, *Salmo gairdneri* Richardson, with attention to fatty acids. J. Fish Biol. **21**(6): 681–692. doi:10.1111/j.1095-8649.1982.tb02872.x.

Jobling, M., Larsen, A.V., Andreassen, B., Sigholt T., Olsen, R.L., and 2002. Influence of a dietary shift on temporal changes in fat deposition and fatty acid composition of Atlantic salmon post-smolt during the early phase of seawater rearing. Aquacult. Res. **33**(11): 875–889. doi:10.1046/j.1365-2109.2002.00727.x.

Johnston, I.A., Li, X., Vieira, V.L.A., Nickell, D., Dingwall, A., Alderson, R., Campbell, P., and Bickerdike, R. 2006. Muscle and flesh quality traits in wild and farmed Atlantic salmon. Aquaculture, **256**(1–4): 323–336. doi:10.1016/j.aquaculture.2006.02.048.

Jonsson, N., Jonsson, B., and Hansen, L.P. 2003. The marine survival and growth of wild and hatchery-reared Atlantic salmon. J. Appl. Ecol. **40**(5): 900–911. doi:10.1046/j.1365-2664.2003.00851.x.

Kiessling, A., and Kiessling, K.-H. 1993. Selective utilization of fatty acids in rainbow trout (*Oncorhynchus mykiss* Walbaum) red muscle mitochondria. Can. J. Zool. **71**(2): 248–251. doi:10.1139/z93-035.

Kiessling, A., Pickov, J., Johansson, L., Åsgård, T., Storebakken, T., and Kiessling, K.-H. 2001. Changes in fatty acid composition in muscle and adipose tissue of farmed rainbow trout (*Oncorhynchus mykiss*) in relation to ration and age. Food Chem. **73**(3): 271–284. doi:10.1016/S0308-8146(00)00297-1.

Lodge, D.M. 1993. Biological invasions: lessons for ecology. Trends Ecol. Evol. **8**(4): 133–137. doi:10.1016/0169-5347(93)90025-K. PMID:21236129.

Lund, R.A., Okland, F., and Hansen, L.P. 1991. 1991. Farmed Atlantic salmon (*Salmo salar*) in fisheries and rivers in Norway. Aquaculture, **98**(1–3): 143–150. doi:10.1016/0044-8486(91)90379-L.

Martinez, I., Standal, I.B., Axelson, D.E., Finstad, B., and Aursand, M. 2009. Identification of the farm origin of salmon by fatty acid and HR 13C NMR profiling. Food Chem. **116**(3): 766–773. doi:10.1016/j.foodchem.2009.03.026.

Mazur, M.M., and Beauchamp, D.A. 2003. A comparison of visual prey detection among species of piscivorous salmonids: effects of light and low turbidities. Environ. Biol. Fishes, **67**(4): 397–405. doi:10.1023/A:1025807711512.

McCutchan, J.H., Lewis, W.M., Jr, Kendall, C., and McGrath, C.C. 2003. Variation in trophic shift for stable isotope ratios of carbon, nitrogen and sulfur. Oikos, **102**(2): 378–390. doi:10.1034/j.1600-0706.2003.12098.x.

McDowall, R.M. 2006. Crying wolf, crying foul, or crying shame: alien salmonids and a biodiversity crisis in southern cool-temperate galaxoid fishes? Rev. Fish Biol. Fish. **16**(3–4): 233–422. doi:10.1007/s11160-006-9017-7.

McKinnell, S., Thomson, A.J., Black, E.A., Wing, B.L., Guthrie, C.M., Koerner, J.F., and Helle, J.H. 1997. Atlantic salmon in the North Pacific. Aquacult. Res. **28**(2): d145–d157. doi:10.1111/j.1365-2109.1997.tb01027.x.

Morton, A., and Volpe, J. 2002. A description of escaped farmed Atlantic salmon *Salmo salar* captures and their characteristics in one Pacific salmon fishery area in British Columbia, Canada, in 2000. Alaska Fish. Res. Bull. **9**: 102–110.

Naylor, R., Hindar, K., Fleming, I., Goldburg, R., Williams, S., Volpe, J., Whoriskey, F., Eagle, J., Kelso, D., and Mangel, M. 2005. Fugitive salmon: assessing the risks of escaped fish from net-pen aquaculture. Bioscience, **55**(5): 427–437. doi:10.1641/0006-3568(2005)055[0427:FSATRO]2.0.CO;2.

Podlesak, D.W., and McWilliams, S.R. 2006. Metabolic routing of dietary nutrients in birds: effects of diet quality and macronutrient composition revealed using stable isotopes. Physiol. Biochem. Zool. **79**(3): 534–549. doi:10.1086/502813. PMID:16691519.

Post, D.M., Layman, C.A., Arrington, D.A., Takimoto, G., Quattrochi, J., and Montaña, C.G. 2007. Getting to the fat of the matter: models, methods and assumptions for dealing with lipids in stable isotope analyses. Oecologia (Berl.), **152**(1): 179–189. doi:10.1007/s00442-006-0630-x. PMID:17225157.

Rikardsen, A.H., and Sandring, S. 2006. Diet and size-selective feeding by escaped hatchery rainbow trout *Oncorhynchus mykiss* (Walbaum). ICES J. Mar. Sci. **63**(3): 460–465. doi:10.1016/j.icesjms.2005.07.014.

Robin, J.H., Regost, C., Arzel, J., and Kaushik, S.J. 2003. Fatty acid profile of fish following a change in dietary fatty acid source: model of fatty acid composition with a dilution hypothesis. Aquaculture, **225**(1–4): 283–293. doi:10.1016/S0044-8486(03)00296-5.

Ruyter, B., Røsjø, C., Einen, O., and Thomassen, M.S. 2000. Essential fatty acids in Atlantic salmon: time course of changes in fatty acid composition of liver, blood and carcass induced by a diet deficient in n-3 and n-6 fatty acids. Aquacult. Nutr. **6**(2): 109–117. doi:10.1046/j.1365-2095.2000.00136.x.

Schröder, V., and Garcia de Leaniz, C. 2010. Discrimination between farmed and free-living invasive salmonids in Chilean Patagonia using stable isotope analysis. Biol. Invasions, **13**: 203–213.

Schwarcz, H.P. 1991. Some theoretical aspects of isotope paleodiet studies. J. Archaeol. Sci. **18**(3): 261–275. doi:10.1016/0305-4403(91)90065-W.

Sotiropoulos, M.A., Tonn, W.M., and Wassenaar, L.I. 2004. Effects of lipid extraction on stable carbon and nitrogen isotope analyses of fish tissues: potential consequences for food web studies. Ecol. Freshwat. Fish, **13**(3): 155–160. doi:10.1111/j.1600-0633.2004.00056.x.

Soto, D., Jara, F., and Moreno, C. 2001. Escaped salmon in the inner seas, southern Chile: facing ecological and social conflicts. Ecol. Appl. **11**(6): 1750–1762. doi:10.1890/1051-0761(2001)011[1750:ESITIS]2.0.CO;2.

Soto, D., Arismendi, I., González, J., Sanzana, J., Jara, F., Jara, C., Guzman, E., and Lara, A. 2006. Southern Chile, trout and salmon country: invasion patterns and threats for native species. Rev. Chil. Hist. Nat. **79**(1): 97–117. doi:10.4067/S0716-078X2006000100009.

Thorstad, E.B., Finstad, A.G., Økland, F., McKinley, R.S., and Booth, R.K. 1997. Endurance of farmed and sea-ranched Atlantic salmon *Salmo salar* L. at spawning. Aquacult. Res. **28**(8): 635–640. doi:10.1111/j.1365-2109.1997.tb01084.x.

Ward, R.D., Jorstad, K.E., and Maguire, G.B. 2003. Microsatellite diversity in rainbow trout (*Oncorhynchus mykiss*) introduced to Western Australia. Aquaculture, **219**(1–4): 169–179. doi:10.1016/S0044-8486(02)00569-0.

Whoriskey, F.G., Brooking, P., Doucette, G., Tinker, S., and Carr, J.W. 2006. Movements and survival of sonically tagged farmed Atlantic salmon released in Cobscook Bay, Maine, USA. ICES J. Mar. Sci. **63**(7): 1218–1223. doi:10.1016/j.icesjms.2006.04.002.

Youngson, A.F., Webb, J.B., MacLean, J.C., and Whyte, B.M. 1997. Frequency of occurrence of reared Atlantic salmon in Scottish salmon fisheries. ICES J. Mar. Sci. **54**(6): 1216–1220. doi:10.1016/S1054-3139(97)80028-8.

Appendix A

Table A1 follows on the next page.

Table A1. Percent fatty acid composition (mean ± SE) and lipid content of feed pellets, caged and escaped Atlantic salmon and rainbow trout, wild brown trout, native fish, and crustaceans collected in Macquarie Harbour.

Fatty acid	Atlantic salmon feed (n = 3)	Rainbow trout feed (n = 3)	Caged Atlantic salmon (n = 4)	Caged rainbow trout (n = 5)	Escaped Atlantic salmon (n = 13)	Escaped rainbow trout (n = 39)	Brown trout (n = 12)	Red cod (n = 7)	Blue grenadier (n = 1)	Australian salmon (n = 3)	Yellow-eyed mullet (n = 7)	Greenback flounder (n = 4)	Fish prey (n = 7)	Crustacean prey (n = 3)
14:0	2.0±0.5	2.0±0.2	2.3±0.2	1.6±0.1	1.7±0.2	1.6±0.1	1.5±0.2	0.0±0.0	0.0	0.3±0.2	1.0±0.2	0.9±0.5	0.2±0.1	0.0±0.0
15:0	0.3±0.0	0.3±0.0	0.1±0.1	0.2±0.0	0.2±0.0	0.2±0.0	0.4±0.0	0.1±0.1	0.0	0.2±0.1	0.2±0.1	0.2±0.1	0.1±0.0	0.0±0.0
16:0	21.4±0.1	19.7±0.1	17.7±0.4	16.4±0.6	17.9±0.8	18.4±0.4	21.8±0.7	20.2±0.7	18.6	20.8±0.5	21.1±0.5	16.4±0.8	17.3±0.8	11.0±3.7
18:0	5.6±0.2	5.4±0.2	4.9±0.2	4.5±0.1	5.8±0.4	5.3±0.1	5.3±0.3	7.6±0.4	7.3	8.5±0.4	6.5±0.7	8.1±1.4	6.7±0.5	8.2±0.2
22:0	0.1±0.0	0.2±0.0	0.0±0.0	0.1±0.0	0.1±0.0	0.0±0.0	0.1±0.0	0.0±0.0	3.3	0.0±0.0	0.0±0.0	0.0±0.0	0.1±0.1	0.6±0.3
Σ SFA	29.8±0.5	28.1±0.1	25.9±0.3	23.3±0.1	26.1±0.9	26.1±0.4	29.7±0.8	28.6±0.7	30.0	31.4±0.8	27.0±0.4	26.4±0.5	25.8±1.0	21.5±2.5
16:1ω7c	7.1±0.1	7.5±0.2	7.5±0.3	8.3±0.3	6.5±0.5	8.0±0.2	4.6±0.4	2.1±0.2	1.8	2.5±0.7	6.7±1.0	5.3±0.9	2.9±0.9	2.2±0.6
17:1ω8c+a17:0	0.3±0.0	0.3±0.0	0.2±0.1	0.3±0.0	0.3±0.1	0.3±0.0	0.4±0.1	0.2±0.1	0.0	0.3±0.2	0.5±0.1	0.6±0.3	0.3±0.2	1.0±0.5
18:1ω9c	30.1±0.4	27.1±0.6	26.0±0.6	33.6±0.8	27.1±0.9	30.9±0.5	20.8±1.8	11.7±0.6	9.0	15.9±3.3	13.3±0.5	21.5±3.5	11.0±0.4	12.2±1.8
18:1ω7c	3.3±0.0	3.3±0.0	4.0±0.0	3.7±0.1	3.6±0.3	3.9±0.1	2.9±1.2	3.1±0.2	3.1	3.2±0.4	4.6±0.3	6.3±0.2	3.4±0.4	4.9±0.1
20:1ω9+11c	1.5±0.1	0.9±0.1	1.5±0.1	1.7±0.1	1.8±0.1	1.6±0.02	1.1±0.2	0.2±0.1	0.0	0.5±0.3	0.6±0.2	1.2±0.4	1.1±0.3	0.0±0.0
20:1ω7c	0.2±0.0	0.2±0.0	0.3±0.1	0.2±0.0	0.3±0.0	0.2±0.0	0.2±0.1	0.0±0.0	0.0	0.0±0.0	0.9±0.2	0.3±0.2	0.5±0.2	0.3±0.2
24:1ω9c	0.3±0.0	0.2±0.0	0.3±0.1	0.1±0.0	0.5±0.1	0.2±0.0	1.1±0.0	1.2±0.2	1.8	1.5±0.3	0.6±0.1	0.4±0.2	1.3±0.2	0.0±0.0
Σ MUFA	42.8±0.4	39.6±0.6	41.0±1.0	49.1±0.5	40.1±1.4	45.8±0.5	31.1±2.1	19.2±0.5	17.4	25.0±3.8	28.7±4.5	36.6±4.5	21.5±1.2	21.0±2.1
18:4ω3	0.8±0.0	1.2±0.1	1.3±0.1	0.9±0.0	1.0±0.1	0.9±0.0	0.8±0.1	0.1±0.1	1.1	0.1±0.1	1.1±0.2	3.9±0.4	0.9±0.3	0.2±0.1
18:2ω6	9.0±0.1	9.2±0.0	7.6±0.0	8.7±0.6	7.2±0.5	7.9±0.1	2.5±0.4	2.2±0.4	1.5	3.2±1.1	1.9±0.3	3.2±0.5	2.4±0.6	3.2±0.5
18:3ω3	0.8±0.0	1.0±0.0	0.7±0.0	0.7±0.1	0.7±0.1	0.6±0.0	1.1±0.2	0.2±0.1	0.9	0.1±0.1	0.9±0.3	0.6±0.4	0.5±0.2	0.4±0.4
20:4ω6 (ARA)	0.6±0.0	0.8±0.0	0.8±0.0	0.6±0.0	1.2±0.3	0.7±0.0	1.4±0.3	5.7±0.4	2.2	2.6±0.5	4.4±0.5	5.8±1.1	3.1±0.8	6.5±0.1
20:5ω3 (EPA)	6.4±0.3	9.1±0.3	7.6±0.3	4.3±0.1	6.8±0.5	5.1±0.1	5.2±0.4	9.6±0.6	6.1	7.7±0.8	12.8±0.8	9.5±1.3	11.8±1.9	27.8±1.2
20:3ω6	0.2±0.0	0.2±0.0	0.4±0.1	0.4±0.1	0.3±0.1	0.3±0.0	0.1±0.0	0.0±0.0	0.0	0.0±0.0	0.2±0.1	0.0±0.0	0.0±0.0	0.1±0.1
20:4ω3	0.1±0.0	0.3±0.1	0.2±0.0	0.4±0.1	0.4±0.1	0.4±0.0	1.0±0.2	0.1±0.1	0.0	0.3±0.1	0.4±0.1	0.4±0.2	0.8±0.3	0.2±0.1
20:2ω6	0.1±0.0	0.2±0.0	0.3±0.1	0.4±0.1	0.5±0.1	0.4±0.0	0.3±0.0	0.1±0.1	0.0	0.2±0.1	0.2±0.1	0.1±0.1	0.3±0.1	0.5±0.5
21:5ω3	0.2±0.0	0.4±0.0	0.6±0.1	0.3±0.0	0.3±0.0	0.3±0.0	0.2±0.0	0.0±0.0	0.0	0.1±0.1	0.2±0.1	0.0±0.0	0.2±0.1	0.0±0.0
22:5ω6	0.1±0.0	0.2±0.0	0.1±0.0	0.2±0.0	0.2±0.0	0.1±0.0	0.3±0.0	0.2±0.1	0.8	0.7±0.1	0.3±0.1	0.4±0.2	0.5±0.1	0.6±0.4
22:6ω3 (DHA)	3.7±0.2	3.9±0.1	7.7±0.8	6.8±0.1	8.8±1.2	7.6±0.2	21.7±2.4	30.5±1.1	36.0	26.0±5.5	13.3±0.8	9.9±1.9	28.3±3.6	14.5±0.7
22:4ω6	0.0±0.0	0.0±0.0	0.1±0.0	0.1±0.0	0.1±0.0	0.1±0.0	0.3±0.1	0.6±0.2	0.0	0.3±0.2	0.3±0.1	0.7±0.3	0.2±0.1	0.0±0.0
22:5ω3	1.0±0.1	1.1±0.0	3.2±0.0	2.0±0.1	2.9±0.2	1.8±0.1	2.4±0.2	2.9±0.3	1.1	3.0±0.8	4.1±0.3	4.8±0.9	3.4±0.9	2.1±1.2
Σ PUFA	23.1±0.7	27.6±0.6	32.4±0.9	32.4±0.9	30.5±0.3	27.2±0.4	37.3±2.5	52.2±0.9	51.1	44.1±4.5	41.0±1.4	36.6±4.7	52.3±1.6	55.5±1.5
Others	11.4±0.2	12.0±0.1	11.2±0.6	11.2±0.6	10.5±0.6	10.6±0.3	7.5±0.6	4.1±0.3	4.3	4.7±0.7	10.4±1.2	7.2±1.5	5.8±1.1	4.2±0.5
ω6/ω3	0.8±0.2	0.6±0.0	0.4±0.0	0.4±0.2	0.5±0.0	0.6±0.0	0.2±0.0	0.2±0.0	0.1	0.2±0.0	0.2±0.0	0.4±0.1	0.2±0.0	0.2±0.0
EPA/DHA	1.7±0.0	2.3±0.0	0.9±0.1	1.0±0.0	0.9±0.1	0.7±0.0	0.3±0.0	0.3±0.0	0.2	0.3±0.1	1.0±0.1	1.0±0.1	0.5±0.1	1.9±0.1
Lipid content (% wet mass)	27.9±0.4	25.4±0.5	15.4±1.3	21.2±1.3	5.0±1.1	12.0±1.2	3.3±0.8	0.5±0.0	0.7	1.0±0.1	1.1±0.1	1.3±0.2	1.3±0.2	0.7±0.1

Note: Crustacean prey includes grapsid crabs (n = 2, each composed by 10 individuals) and caridean shrimps (n = 1, composed by 10 individuals). Fish prey includes galaxids (n = 1), hardyheads (n = 1), and juveniles of greenback flounder (n = 2), yellow-eyed mullet (n = 1), and Australian salmon (n = 1), with each sample composed by 5 individuals.

What drives dynamics in the Gulf of Alaska? Integrating hypotheses of species, fishing, and climate relationships using ecosystem modeling

Sarah K. Gaichas, Kerim Y. Aydin, and Robert C. Francis

Abstract: We use a dynamic ecosystem model to evaluate the relative effects of fishing history, climate change, and predator–prey interactions in determining biomass trajectories for 12 species groups ranging from marine mammals through commercially exploited fish and invertebrates in the Gulf of Alaska (GOA). Ecosystem model fits under six alternative hypotheses relating fishing, climate, and predation were evaluated. Fishing alone explained few GOA biomass trajectories; it was necessary to both estimate specific predator–prey relationships and provide some mechanism for increased production. No single control hypothesis explained all species dynamics simultaneously, suggesting that in the GOA, there is no single main driver of the ecosystem. Furthermore, the alternative control hypotheses implied contrasting sets of predator–prey relationships (estimated functional response parameters). Therefore, a single set of "best fit" parameters for a given control hypothesis is unlikely to be useful in forecasting. Future modeling efforts supporting ecosystem-based fishery management could retain multiple working models to accommodate complex forcing (fishing, keystone species production, and environmental) differentially affecting components of the ecosystem.

Résumé : Un modèle écosystémique dynamique nous a servi à évaluer les effets relatifs de l'histoire de la pêche, du changement climatique et des interactions prédateurs–proies sur la trajectoire des biomasses chez 12 groupes d'espèces, allant de mammifères marins jusqu'à des poissons et des invertébrés exploités commercialement, dans le golfe de l'Alaska (GOA). Nous avons évalué l'ajustement du modèle écosystémique en fonction de six hypothèses de rechange qui relient la pêche, le climat et la prédation. La pêche seule explique peu des trajectoires de biomasses du GOA; il est nécessaire d'estimer des relations spécifiques prédateurs–proies et aussi de fournir un mécanisme quelconque pour l'accroissement de la production. Aucun mécanisme unique de contrôle n'explique simultanément toutes les dynamiques des espèces, ce qui laisse croire que dans le GOA il n'existe pas un facteur explicatif unique de l'écosystème. De plus, les hypothèses de contrôle de rechange présupposent des séries contradictoires de relations prédateurs–proies (paramètres estimés des réponses fonctionnelles). C'est pourquoi, il est peu vraisemblable qu'une seule série de paramètres « d'ajustement optimal » pour une hypothèse de contrôle donnée puisse être utile pour faire des prédictions. Les efforts futurs de modélisation pour appuyer la gestion des pêches basée sur l'écosystème pourraient retenir plusieurs modèles de travail afin d'accommoder le forçage complexe (pêche, production des espèces phares et environnement) qui affecte de manière différente les divers compartiments de l'écosystème.

[Traduit par la Rédaction]

Introduction

In addition to the dynamics of fished populations, the dynamics of ecosystems are increasingly of interest to fisheries management (Pikitch et al. 2004). Changes in the Gulf of Alaska (GOA) continental shelf assemblage of invertebrates and fish, including groundfish (Anderson and Piatt 1999; Hare and Mantua 2000), crabs (Orensanz et al. 1998), zooplankton (Brodeur et al. 1996), and salmon (Mantua et al. 1997; Francis et al. 1998), have been well documented separately, but have yet to be analyzed quantitatively in an integrated framework. There is a long history of indigenous and industrial fishing and whaling in this ecosystem (Browning 1980; Antonson and Hanable 1984; Mizroch and Rice 2006), and current fishery management enforces catch limits for exploited species (DiCosimo et al. 2010). The trajectories for GOA commercial species vary widely over time (Fig. 1*a*). The fish biomass has been dominated by groundfish (demersal offshore roundfish and flatfish) species from 1960 to 2005, in particular by walleye pollock (*Theragra chalcogramma*) between 1970 and 1990, and in the most recent decade by arrowtooth flounder (*Atheresthes stomias*). However, at the beginning of the 1960s the configuration was completely different; groundfish biomass was dominated by Pacific ocean perch (POP, *Sebastes alutus*), with much lower biomass of other groundfish than at any other time in the

Received 13 October 2010. Accepted 27 April 2011. Published at www.nrcresearchpress.com/cjfas on 31 August 2011.
J2011-0135

Paper handled by Associate Editor John Post.

S.K. Gaichas and K.Y. Aydin. Resource Ecology and Fisheries Management Division, NOAA NMFS Alaska Fisheries Science Center, 7600 Sand Point Way NE, Building 4, Seattle, WA 98115, USA.
R.C. Francis. University of Washington, School of Fisheries and Aquatic Sciences, 1122 NE Boat Street, Seattle, WA 98105, USA.

Corresponding author: Sarah K. Gaichas (e-mail: Sarah.Gaichas@noaa.gov).

Can. J. Fish. Aquat. Sci. **68**: 1553–1578 (2011) doi:10.1139/F2011-080 Published by NRC Research Press

Fig. 1. (*a*) Biomass trajectories estimated from single-species stock assessments for Gulf of Alaska (GOA) fish stocks, 1935–2005. (*b*) Annual exploitation rates for GOA groundfish species, calculated as catch in metric tonnes (t) divided by stock assessment estimated biomass (t) (see Table 2 for all time series references).

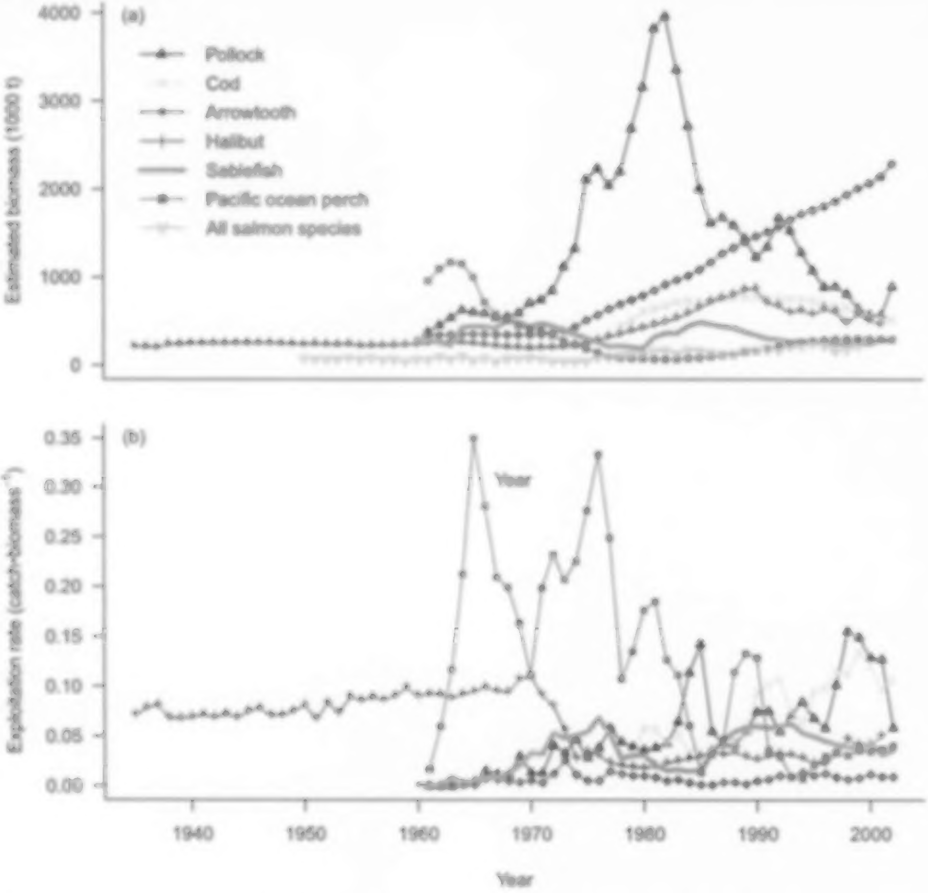

modeled period. The remaining groundfish (sablefish (*Anoplopoma fimbria*) and Pacific cod (*Gadus macrocephalus*)) have increased and declined between the late 1970s and the 1990s, with sablefish showing another increase and decline earlier in the period from 1960 to the mid-1970s. Pacific herring (*Clupea pallasii*) maintained relatively low biomass throughout the time period, whereas Pacific salmon (*Oncorhynchus* spp.) and Pacific halibut (*Hippoglossus stenolepis*) biomass has increased from the mid-1970s through the 1990s.

Control of ecosystem dynamics has been described as top-down (predator or fishery mediated; Baum and Worm 2009; Essington 2010), bottom-up (physically mediated), and as more complex combinations (e.g., the "wasp waist" of Cury et al. 2000). While some GOA population trajectories show top-down effects related to the exploitation history of each species — POP (Fig. 1*b*) and red king (*Paralithodes camtschaticus*, hereafter called king crab) and Tanner (*Chionoecetes bairdi*) crab declines (Orensanz et al. 1998) follow periods of extremely high catch and exploitation rates — not all of the trajectories show clear top-down effects. The increases in Pacific salmon and Pacific halibut followed periods of high exploitation and were concurrent with increased catches (but lower exploitation rates, Fig. 1*b*). Conversely, the Steller sea lion (*Eumetopias jubatus*) decline cannot be fully explained by fishing-related mortality (Atkinson et al. 2008). However, their decline was concurrent with an increase in groundfish exploitation, suggesting possible top-down effects of fisheries on Steller sea lion prey, a hypothesis subject to ongoing debate and investigation (e.g., National Research Council 2003; Atkinson et al. 2008; Berman 2008).

Many authors suggest that ecosystem changes are driven from the bottom up by climate regime shifts. In the GOA, the clearly defined 1977 shift in the Pacific Decadal Oscillation (PDO; Francis and Hare 1994; Mantua et al. 1997) has been implicated most often. The open ocean mechanism for the change in productivity at higher trophic levels is a change in phytoplankton and zooplankton production in response to changed physical condition such as mixed layer depth and temperature (Polovina et al. 1995; Francis et al.1998; Haigh et al. 2001). However, mechanisms on the GOA continental shelf are unclear, as even physical indicators lack a clear PDO signal there (Stabeno et al. 2004).

Despite uncertainty in how the PDO operates on the GOA continental shelf, several biological time series correlate with it, directly (Hare and Mantua 2000) and indirectly. Nearshore shrimp (Pandalidae) declined after large catches had been taken during the late 1960s and early 1970s, but this change has been attributed to the climate regime shift (Anderson and Piatt 1999). The trajectories of exploited flatfish such as arrowtooth flounder and Pacific halibut show a steady increase from the late 1970s through the present, suggesting a connection, though not a mechanism, for climate regime control (Clark et al. 1999). Through correlation analysis, Williams and Quinn (2000*a*, 2000*b*) suggest that GOA Pacific herring recruitment is best estimated with the aid of environmental time series. More complex mechanisms combining climate and predation-mediated control of GOA walleye pollock population dynamics have been suggested by Bailey (2000). Some have hypothesized that high historical fishing rates for the previously biomass-dominant POP altered population productivity and therefore altered pelagic predator–prey interactions that were formerly dominated by this pelagic zooplankton feeder (Outer Continental Shelf Environmental Assessment Program 1986).

Our objective is to apply ecosystem modeling to evaluate multiple hypotheses of ecosystem control in the GOA, a system that has both a long history of fishing and clear environmental signals. We compare hypotheses ranging from relatively simple top-down or bottom-up controls (e.g., either fishing or environment drive dynamics directly) through more complex control involving relationships among fishing, predator–prey interactions, competition for prey, and climate-induced productivity changes at various trophic levels. If fishing is the main ecosystem driver, we might expect most biomass trajectories to decline with increased directed or incidental fishing mortality and recover when fishing mortality decreases. If environmental drivers dominate, we would expect most trajectories to increase and decline with primary production changes or other physical changes. Indirect and combined effects of fishing and environment may also explain dynamics; for example, fishing might suppress species recovery because of prey fisheries or habitat impacts, or a climate-mediated change in single-species production combined with fishing mortality might drive trajectories. Finally, a single important species (or a set of similar species) may have connections to many other species throughout the ecosystem so that top-down or bottom-up forcing of these "keystone" species may disproportionately affect the ecosystem dynamics (e.g., Paine 1995; Cury et al. 2000).

Materials and methods

Dynamic ecosystem modeling framework

We use a modeling framework equivalent to Ecopath with Ecosim (EwE), originally based on the work of Polovina (1984) and extended by Walters et al. (1997). Aydin et al. (2007) implemented an independent version of EwE to allow more flexible parameter estimation and evaluation of fits to data as described in Burnham and Anderson (2002). We focus on the specifics of the implementation for the GOA here, as the basic EwE algorithms are described in detail elsewhere (e.g., Christensen and Walters 2004).

The modeling framework uses a static mass balance model (detailed in Gaichas et al. 2010) to initialize the dynamic model. The basin-wide spatial scale of our model, representing 291 840 km^2 of continental shelf (Fig. 2), was selected for compatibility with the single-species stock assessments currently applied in North Pacific fishery management. The model characterizes the state of the system in the early 1990s, with 122 living groups (4 producer and 118 consumer), 5 detritus groups, and 14 fishing fleets (Aydin et al. 2007). Twelve species including fur seals, sea lions, and all major commercial groundfish are modeled with age-structured dynamics in two stages: juvenile and adult (Aydin et al. 2007).

The translation of the static mass balance to the dynamic system of differential equations is described in Walters et al. (1997). Biomass dynamics equations are linked by functional relationships predicting how predator consumption of prey is altered by changing biomass in both groups. The change in biomass for a particular consumer group i is modeled as

$$(1)\qquad \frac{\mathrm{d}B_i}{\mathrm{d}t} = \mathrm{GE}_i \sum_{\text{prey}} Q(B_i, B_{\text{prey}}) - F_i B_i - M0_i B_i - \sum_{\text{pred}} Q(B_{\text{pred}}, B_i)$$

(See Table 1 for parameter descriptions.) To specify the changing consumption represented by the functional response, $Q(B_i, B_j)$, we use the EwE "Arena Foraging Model" (Walters et al. 1997). This functional response modifies the traditional Lotka–Volterra (mass action) predator–prey model using the hypothesis that only a subset of prey biomass is "vulnerable" to predation at any given time. It can be parameterized with low or high vulnerabilities to span a range of behaviors from pure donor-controlled "bottom-up" dynamics to pure Lotka–Volterra "top-down" predator–prey interactions, respectively. The consumption equation for a predator with a given predator–prey interaction at time t can be expressed as (Aydin 2004)

$$(2)\qquad \left(\frac{Q}{B_{\text{pred}}}\right)_{\text{pred, prey},t} = \frac{\left[\left(\frac{Q}{B_{\text{pred}}}\right)^{*} \cdot X^{*}_{\text{predprey}}\right] \cdot \mathrm{DC}^{*}_{\text{predprey}} \cdot \frac{(B_{\text{prey}})_t}{B^{*}_{\text{prey}}}}{(X^{*}_{\text{predprey}} - 1) + \frac{(B_{\text{pred}})_t}{B^{*}_{\text{pred}}}}$$

Here, we estimate the key functional response parameter X^{*}_{predprey} ("vulnerability" in EwE) for each predator–prey interaction by fitting the full dynamic ecosystem model to the available time series under each control hypothesis. All other functional response parameters available in EwE, including foraging time adjustment, handling time, mediation of predator–prey interactions by a third species, and seasonal forcing (described in Walters et al. 1997; Christensen and Walters 2004; and Walters and Martell 2004), are held at default multiplicative values of 1.

GOA time series

Twelve time series of biomass and 19 time series of catch were used as observational "data" for comparing hypotheses (detailed sources for all time series are listed in Table 2). Biomass time series for adult and juvenile Steller sea lions

Fig. 2. Spatial extent of the Gulf of Alaska (GOA) static mass balance and dynamic ecosystem model. 100 m depth contours are indicated with lines.

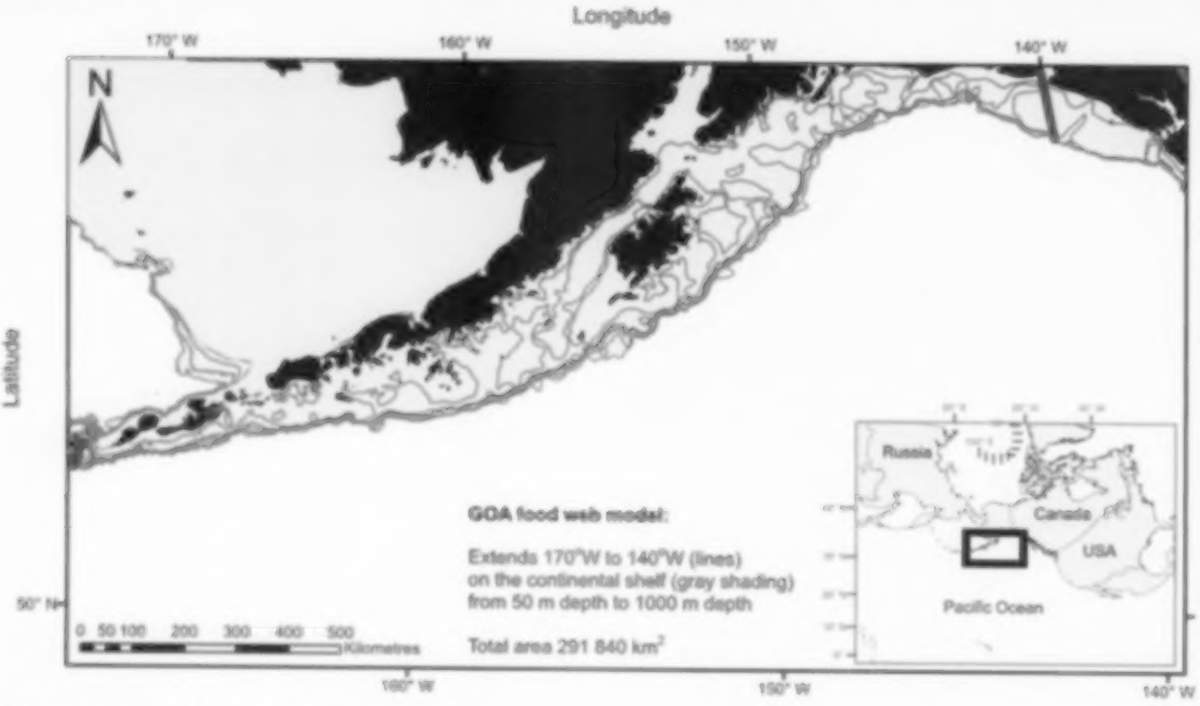

Table 1. Parameters of the dynamic ecosystem model.

Parameter	Abbreviation (units)	Parameter source
Biomass	*B* (t·km^{-2})	Estimated each time step for subscript group, where subscripts prey or pred represent all prey or all predators, respectively, of group *i*
Growth efficiency	GE (dimensionless)	Derived from mass balance; production rate divided by consumption rate (or other estimate)
Consumption	*Q* (t·km^{-2}·year^{-1})	Estimated each time step by eq. 2
Fishing mortality	*F* (year^{-1})	Estimated each time step from fishing effort forcing as catch/biomass at time *t*
Unexplained mortality	M0 (year^{-1})	Mass balance model estimate: derived as M0 = [production rate·(1 – energy used in the ecosystem)]
Biomass start	*B** (t·km^{-2}, used to estimate relative biomass at each time step)	Input to mass balance model, derived from survey estimates, sampling programs, stock assessments, or other methods
Consumption/biomass	*Q*/*B* (year^{-1})	Estimated each time step
Consumption/biomass start	*Q*/*B** (year^{-1})	Input to mass balance model, derived from bioenergetics models, gut content analysis
Vulnerability	*X** (dimensionless parameter determining the strength of the predator–prey interaction)	Estimated from fit to time series data
Diet composition	DC* (proportion of the prey in the diet (by mass) of consumer *j*; dimensionless)	Input to mass balance model, derived from gut content analysis

were derived from surveys and a simple population model. Biomass time series for walleye pollock, Pacific cod, Pacific herring, arrowtooth flounder, Pacific halibut, sablefish, POP, and shortspine thornyhead (*Sebastolobus alascanus*) were derived from age-structured stock assessment models, and the biomass time series for returning spawning Pacific salmon was derived from Rogers (1987). While stock assessment-derived time series assume constant natural mortality and our model estimates varying predation mortality, these assessments are currently used as the best representation of stock dynamics for fishery management. We use them in that spirit here, recognizing the potential conflicts between model assumptions and resulting nonindependent error patterns. The biomass time series for pandalid shrimp was derived by scaling up Anderson and Piatt's (1999) small mesh survey results to the full GOA to reflect the hypothesis that the shrimp de-

Table 2. Sources of biomass and catch time series.

Species	Sources	Comments
Biomass		
Juvenile steller sea lion	Fay 2004; Winship et al. 2001; York 1994	See Aydin et al. 2007 for complete methods
Adult steller sea lion	Fay 2004; Winship et al. 2001; York 1994	See Aydin et al. 2007 for complete methods
Walleye pollock	Dorn et al. 2003	
Pacific cod	Thompson et al. 2003	
Pacific herring	M. Foster[a], R. Merizon[b], and T. Otis[c], personal communication, 2004	Assembled from regional ADFG data
Arrowtooth flounder	Turnock et al. 2003	
Pacific halibut	S. Hare[d], personal communication, 2002	Combination of historical and recent stock assessments
Sablefish	Sigler et al. 2004	
Pacific ocean perch (POP)	Hanselman et al. 2003	
Shortspine thornyhead	Gaichas and Ianelli 2003	
Pacific salmon	Rogers 1987	
Pandalid shrimp	Anderson and Piatt 1999	Scaled up to full GOA
Catch		
Sea otter	Kenyon 1969; Lensink 1960	
Northern fur seal	Anonymous 1906 and 1910	
Right whale	Scarff 1991 and 2001; D. Rice[e], personal communication, 2005; Mizroch and Rice 2006	All 20th century shore-based whaling catch from D. Rice, personal communication, 2005; offshore whaling from Mizroch and Rice 2006
Fin whale	D. Rice, personal communication, 2005; Mizroch and Rice 2006	
Humpback whale	D. Rice, personal communication, 2005; Mizroch and Rice 2006	
Sei whale	D. Rice, personal communication, 2005; Mizroch and Rice 2006	
Sperm whale	D. Rice, personal communication, 2005; Mizroch and Rice 2006	
Walleye pollock	Dorn et al. 2003	
Pacific cod	W. Palsson[f], personal communication, 2006; Thompson et al. 2003	Pre-1977 catch from W. Palsson, personal communication, 2006
Pacific herring	M. Plotnick[g], personal communication, 2004	
Arrowtooth flounder	Turnock et al. 2003	
Pacific halibut	Bell 1981; International Pacific Halibut Commission 2005	International Pacific Halibut Commission "legacy" plus current catch data
Sablefish	Sigler et al. 2004	
Pacific ocean perch (POP)	Ito 1982; Hanselman et al. 2003	
Shortspine thornyhead	Gaichas and Ianelli 2003	
Pacific salmon	M. Plotnick, personal communication, 2005	
Tanner crab (*C. bairdi*)	M. Ruccio[h] and C. Trowbridge[i], personal communication, 2004	Assembled from regional ADFG data
King crab	M. Ruccio and C. Trowbridge, personal communication, 2004	Assembled from regional ADFG data
Pandalid shrimp	M. Ruccio and C. Trowbridge, personal communication, 2004	Assembled from regional ADFG data
Recruitment		
POP	Hanselman et al. 2003	Pre-1960s recruitment hypothesized (see text)
Pacific herring	Williams and Quinn 2000*a*	
Walleye pollock	Dorn et al. 2003	
Climate index		
PDO	Mantua 2005	

Note: ADFG, Alaska Department of Fish and Game; GOA, Gulf of Alaska.

[a] Alaska Department of Fish and Game, 211 Mission Road, Kodiak, AK 99615, USA.

[b] Alaska Department of Fish and Game, 1800 Glenn Hwy #4, Palmer, AK 99645, USA.

[c] Alaska Department of Fish and Game, 3298 Douglas Place, Homer, AK 99603, USA.

[d] International Halibut Commission, 2320 W. Commodore Way, Suite 300, Seattle, WA 98199, USA.

[e] Alaska Fisheries Science Center, 7600 Sand Point Way NE, Seattle, WA 98115, USA.

[f] Washington Department of Fish and Wildlife, 16018 Mill Creek Boulevard, Mill Creek, WA 98012, USA.

[g] Alaska Department of Fish and Game, P.O. Box 25526, Juneau, AK 99802, USA.

[h] Alaska Department of Fish and Game, 211 Mission Road, Kodiak, AK 99615, USA.

[i] Alaska Department of Fish and Game, 3298 Douglas Place, Homer, AK 99603, USA.

cline was GOA-wide. Catches recorded from 1802 through the 1975 Marine Mammal Protection Act were included for sea otters (*Enhydra lutris*), adult northern fur seals (*Callorhinus ursinus*), northern right whales (*Eubalaena glacialis*), fin whales (*Balaenoptera physalus*), humpback whales (*Megaptera novaeangliae*), sei whales (*Balaenoptera borealis*), and sperm whales (*Physeter macrocephalus*) to account for historical GOA marine mammal exploitation. Total catch time series for walleye pollock, Pacific cod, Pacific herring, arrowtooth flounder, Pacific halibut, sablefish, POP, shortspine thornyhead, and Pacific salmon represent the exploited fish species, beginning as early as the late 1880s (Pacific salmon) and early 1900s (Pacific herring) and spanning the more recent groundfish fisheries through 2001. Catch time series for Tanner crabs, king crabs, and pandalid shrimp from 1960 through the late 1980s round out the exploitation history.

The model was forced with identical fishing effort for all runs (see Appendix A for details) and was "spun up" from 1802 with no fishing to allow sufficient time for biomass to build up to historical unexploited levels from the 1990s baseline for currently exploited species. We exclude results from the spin up (1802–1902) and focus on results for the 1950s onwards.

Top-down, bottom-up, and mixed control hypotheses

While fishing effort time series can be viewed as top-down effects in an ecosystem, production time series were used to explore alternative hypotheses about bottom-up and more complex effects acting on specific groups within the ecosystem. We explored six working hypotheses, represented by alternative forcing functions, in this study: (1) "Fishing", where fishing explains ecosystem dynamics. This base model is forced top-down only with fishing time series while predator prey vulnerabilities remain at the default EwE value for all species. (2) "Fishing, PredPrey", where fishing and particular predator–prey interactions explain system dynamics. This is implemented as Model 1 with added estimation of predator and prey vulnerabilities for all species. (3) "Fishing, PredPrey, Historical Recruitment", where fishing and particular predator–prey interactions combined with high historical POP and Pacific herring production explain system dynamics. This is implemented as Model 2 with added Pacific herring and POP production forced by recruitment time series (see below and Appendix A). (4) "Fishing, PredPrey, All Recruitment", where fishing and particular predator–prey combined with high historical POP and Pacific herring production and recent walleye pollock production explain system dynamics. This is implemented as Model 3 with added walleye pollock production forced by recruitment time series. (5) "Fishing, Climate", where fishing and physically mediated changes in primary production at decadal time scales explain system dynamics. This is implemented as Model 1 with added primary production time series forced by the PDO (see below and Appendix A). (6) "Fishing, PredPrey, Climate", where fishing and physically mediated changes in primary production at decadal time scales combined with particular predator–prey interactions explain system dynamics. This is implemented as Model 5 with added estimation of predator and prey vulnerabilities.

We implemented climate-mediated production hypotheses (5 and 6) separately from the species-specific production hypotheses (3 and 4) to provide maximal contrast (detailed methods for recruitment and climate forcing are presented in Appendix A). Pacific herring and walleye pollock recruitment time series were estimated by Williams and Quinn (2000*a*) and Dorn et al. (2003), respectively. POP recruitment for 1960 to the present was estimated by Hanselman et al. (2003). We simulated increased historical POP production using a prefishery recruitment time series for 1939–1959, where recruitment varied between those estimated by the single-species stock assessment for the initial 5 years of the fishery (1960–1965) and double the highest observed from the stock assessment estimated time series. The PDO time series for 1901–2001 (Mantua 2005) was assumed to drive production for large and small phytoplankton.

Parameter estimation and model selection

For each of Models 2, 3, 4, and 6, we estimated a set of vulnerability parameters minimizing the negative log likelihood of the data using a Microsoft Visual Basic implementation of the Davidson–Fletcher–Powell algorithm (Press et al. 1992). (For Models 1 and 5, the negative log likelihood was calculated without parameter estimation.) A lognormal likelihood was assumed for fitting to both biomass and catch time series. While each predator–prey link in the ecosystem is potentially governed by an independent vulnerability parameter, we rewrite each predator–prey link X_{predprey} as a function of prey-specific (χ_{prey}) and predator-specific (χ_{pred}) vulnerabilities for each species such that

$$X_{\text{predprey}} = 1 + \exp\left(\chi_{\text{prey}} + \chi_{\text{pred}}\right) \tag{3}$$

where the range of χ is $(-\infty,+\infty)$ and X_{predprey} is the X from Walters et al. (1997; range $(1,+\infty)$). Note that if $\chi_{\text{pred}} = 0$ and $\chi_{\text{prey}} = 0$, then $X_{\text{predprey}} = 2$, the default value used in the EwE software. A χ range of ± 4 gives the full range of values for X_{predprey} used in EwE from donor control ($X_{\text{predprey}} \sim 1.0003$) to Lotka–Volterra ($X_{\text{predprey}} \sim 2982$). To reduce the number of simultaneously estimated parameters, models were fit iteratively by estimating all χ_{pred} while holding all χ_{prey} constant at 0. When that model converged, fitting was restarted by estimating all χ_{prey} while holding all χ_{pred} constant at previously estimated values. This process continued, alternating fitting by predator and then by prey vulnerabilities, until no further improvement in overall negative log likelihood was possible, at which point the model was considered fully converged. The Akaike information criterion (AIC; Burnham and Anderson 2002) was used as an index of model fit corrected for the number of parameters estimated.

Results

Overall, fits were poorest for models corresponding to hypotheses 1 (Fishing) and 5 (Fishing, Climate), suggesting that at a minimum, specific sets of predator–prey relationships are required to explain GOA ecosystem dynamics (Table 3; Figs. 3–8). Of the models with estimated vulnerability parameters (corresponding to hypotheses 2, 3, 4, and 6), none was clearly supported by all data time series, although each hypothesis received some support from different species' biomass data sets. Model 2 (Fishing, PredPrey) had the best fit for Pacific halibut, but poor fits for most other species. Models 3 and 4 (Fishing, PredPrey, Historical Recruitment; and

Table 3. Negative log likelihoods estimated for each modeled alternative forcing hypothesis for biomass and catch time series.

	Hypothesis					
Group	1: Fishing	2: Fishing, PredPrey	3: Fishing, PredPrey, Historical Recruitment	4: Fishing, PredPrey, All Recruitment	5: Fishing, Climate	6: Fishing, PredPrey, Climate
Fit to biomass						
Juvenile steller sea lion	44.33	53.26	51.74	36.32	162.96	56.08
Adult steller sea lion	62.60	67.78	61.33	66.12	194.51	119.22
Walleye pollock	230.65	313.02	295.19	130.55	233.78	179.52
Pacific cod	66.23	8.42	16.45	–12.40	283.14	8.66
Pacific herring	20 061.59	188.14	53.68	43.61	19 432.91	27.95
Arrowtooth flounder	335.39	780.98	691.69	642.27	460.54	11.43
Pacific halibut	20 387.76	–1.23	99.53	67.03	37 547.54	451.63
Sablefish	1 495.09	118.63	103.56	110.00	1 627.72	17.81
Pacific ocean perch (POP)	119 821.10	981.78	861.15	806.68	150 761.90	575.78
Shortspine thornyhead	41 443.02	13.98	–8.50	–17.70	47 856.55	508.36
Pacific salmon	65.66	57.47	56.13	57.10	5 885.64	5 892.15
Pandalid shrimp	441.97	401.30	434.63	326.52	720.83	494.99
Fit to catch						
Sea otter	101.06	101.06	101.06	101.06	101.06	101.06
Northern fur seal	157.38	157.38	157.38	157.38	157.38	157.38
Right whale	33.80	33.80	33.80	33.80	33.80	33.80
Fin whale	1 029.36	1 029.36	1 029.36	1 029.36	1 029.36	1 029.36
Humpback whale	40.47	40.47	40.47	40.47	40.47	40.47
Sei whale	60.32	60.32	60.32	60.32	60.32	60.32
Sperm whale	36.46	36.46	36.46	36.46	36.46	36.46
Walleye pollock	28.26	28.12	28.13	28.13	28.19	28.12
Pacific cod	79.43	78.42	78.42	78.42	79.22	78.41
Pacific herring	109.16	108.40	105.86	106.00	108.21	109.07
Arrowtooth flounder	32.40	30.22	30.22	30.21	30.32	30.20
Pacific halibut	0.42	–1.71	–1.71	–1.71	0.43	–1.72
Sablefish	29.87	29.64	29.64	29.64	31.95	29.65
POP	52.21	52.04	52.03	52.03	54.98	52.03
Shortspine thornyhead	16.64	16.64	16.64	16.64	15.31	16.64
Pacific salmon	83.67	83.67	83.67	83.67	93.80	94.16
Tanner crab	26.34	26.34	26.37	26.34	26.38	26.34
King crab	529.08	529.08	529.08	529.08	529.03	529.08
Pandalid shrimp	47.51	47.51	47.51	47.51	47.51	47.51
Sum biomass negative log likelihood	204 455.39	2 983.53	2 716.58	2 256.10	265 168.02	8 343.58
Sum catch negative log likelihood	2 493.84	2 487.22	2 484.71	2 484.81	2 504.18	2 498.34
Total negative log likelihood	206 949.23	5 470.75	5 201.29	4 740.91	267 672.20	10 841.92
Predator–prey vulnerabilities	0	250	250	250	0	250
Production forcing parameters	0	0	2	3	2	2
Total parameters	0	250	252	253	2	252
AIC	413 898	11 442	10 907	9 988	535 348	22 188

Note: Lower values indicate better fits. See text for model descriptions.

Fishing, PredPrey, All Recruitment, respectively) had improved fits for several species, with Model 4 having the best overall AIC and the best fits for walleye pollock, Pacific cod, shortspine thornyhead, and juvenile Steller sea lions. Model 6 (Fishing, PredPrey, Climate) had the best fits to 4 of the 12 time series (arrowtooth flounder, sablefish, POP, and Pacific herring), but the worst AIC for the models estimating vulnerability. Across all hypotheses, fits were poor for pandalid shrimp, adult Steller sea lion, and Pacific salmon biomass. We present detailed results for each modeled hypothesis individually (Appendix B). Below, we briefly present results specific to total catch time series, then compare results across models for estimated vulnerability parameters and for selected individual species.

Catch time series fits were remarkably similar between alternative models, with fin whale and king crab showing consistently poor fits (Table 3). In both cases, these catch time series could never be fit in any model because the unrealisti-

Fig. 3. Model 1: Fishing. Comparison of biomass ($t\cdot km^{-2}$) time series (points) with model-estimated biomass trajectories (lines) forced with fishing, but with no fitting of vulnerability parameters.

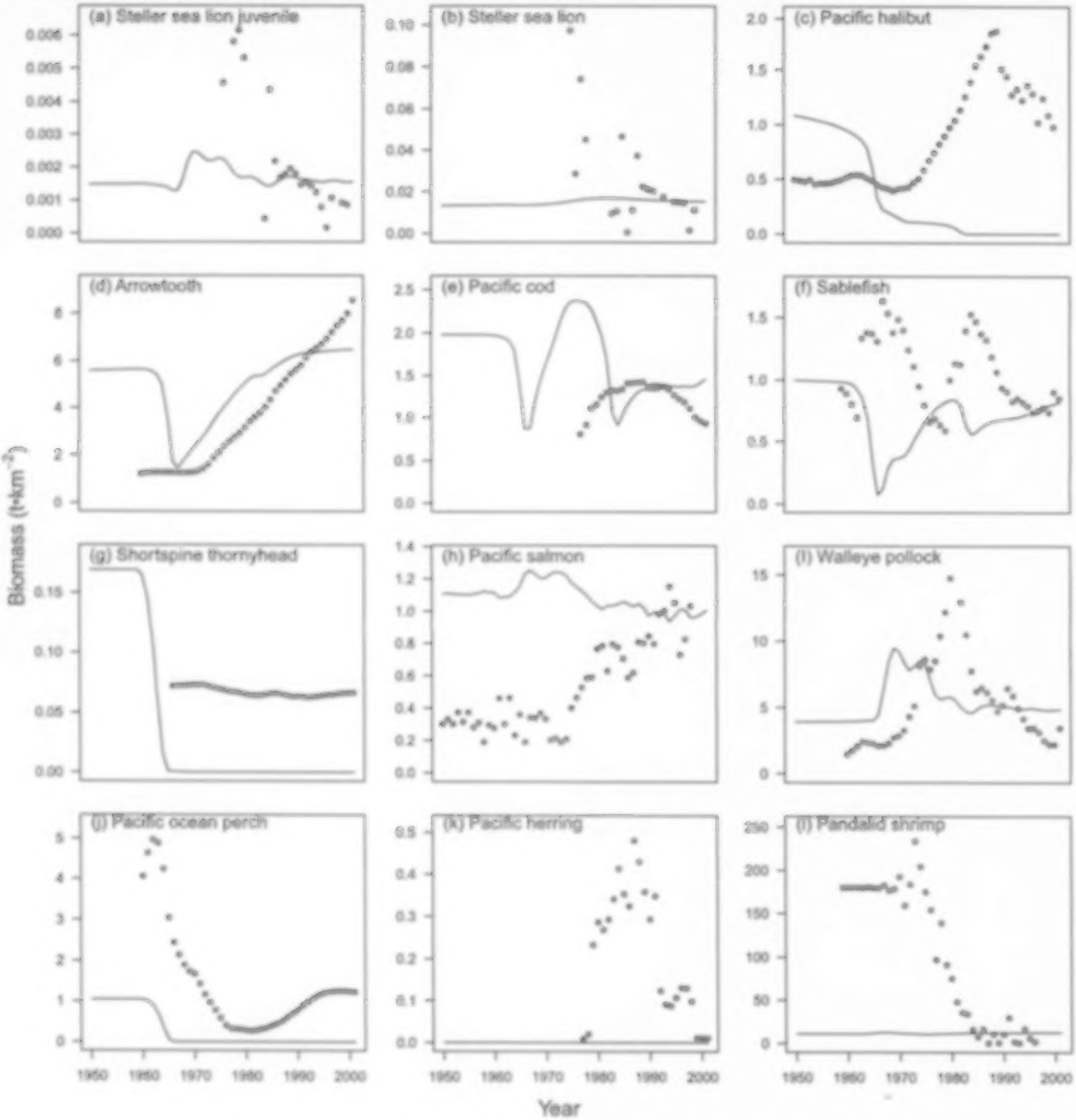

cally high effort estimated to take the first observed catch for each group was sufficient to drive the population permanently extinct, indicating that model-estimated biomass or production for each group was far too low to support observed catches, even after over 100 years of model spin up without exploitation. Similarly, the fit to Pacific salmon catch was poorest in Model 6, where the population is driven extinct under that hypothesis. Aside from these results penalizing extinction, fits to catch series seemed relatively uninformative about the alternative hypotheses or general model behavior. Removing the fin whale and king crab likelihood components from the model left other results unaffected.

Estimated parameter comparisons

Vulnerability parameters were estimated for all species in the GOA ecosystem model (rather than the limited set with time series data) to improve fits to biomass time series. However, the extent to which all species' vulnerability parameters

Fig. 4. Model 2: Fishing, PredPrey. Best model fits (lines) to biomass (t·km^{-2}) time series (points) for the GOA ecosystem model forced with fishing.

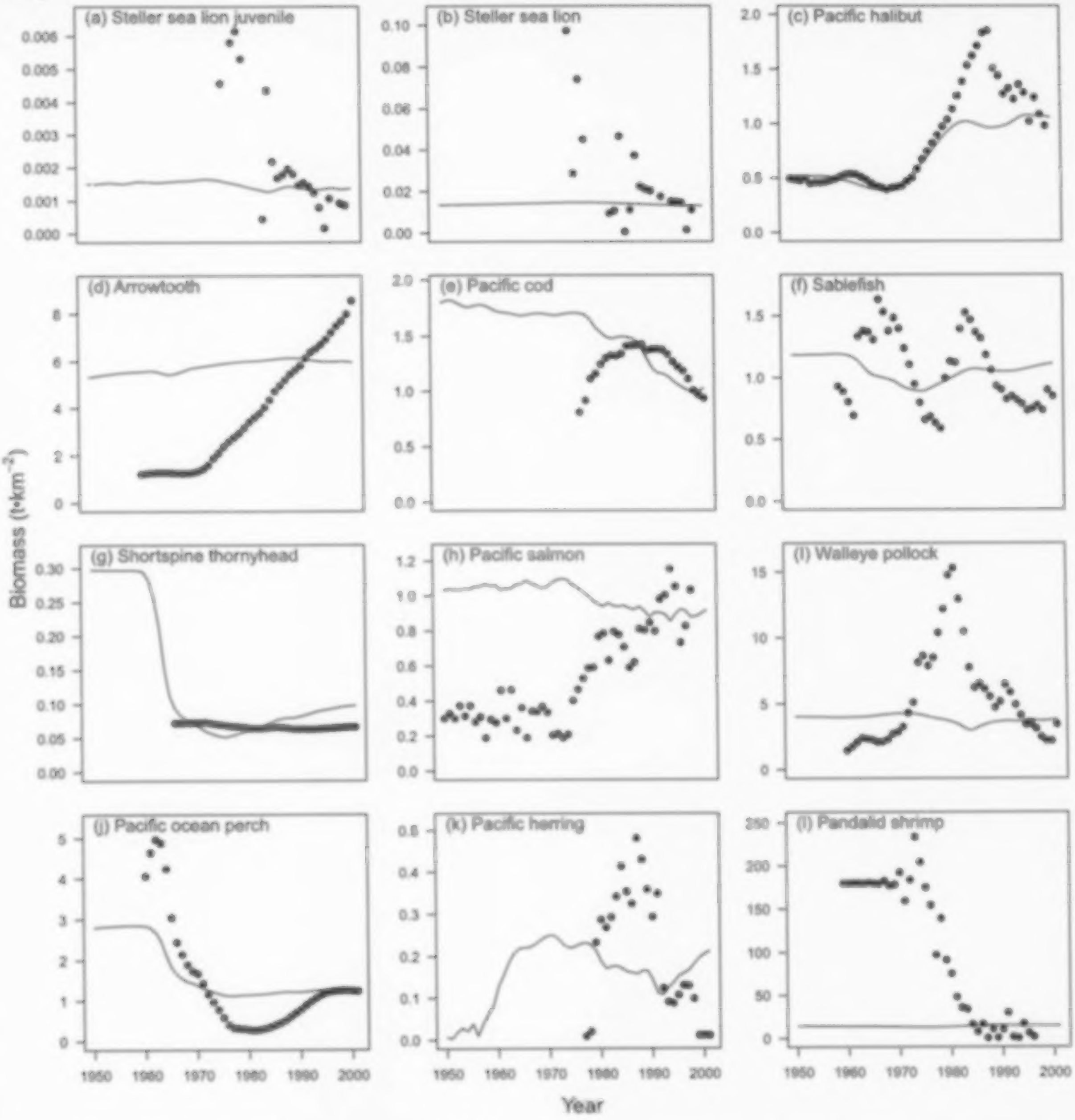

changed from default values differed between modeled hypotheses (Fig. 9). To facilitate comparison, we show the prey-specific (χ_{prey}) and predator-specific (χ_{pred}) vulnerability components estimated for each species with 0 as the default value and a range of ±4. Model 2 (Fishing, PredPrey), with top-down forcing only, had small changes from default vulnerabilities for many marine mammals and seabirds, as well as lower trophic-level benthic species groups (Fig. 9*a*). A minority (18) of predator vulnerabilities and even fewer (6) prey vulnerabilities are pushed past ±2 towards the extremes of functional response behavior. Model 6 (Fishing, PredPrey, Climate), with bottom-up and top-down forcing, had more extreme values of predator (38) and prey (10) vulnerability exceeding ±2, and several of these were fit for very low and high trophic-level groups, including some whales, seals, seabirds, all sharks, and most pelagic zooplankton (Fig. 9*b*).

Vulnerabilities estimated in the recruitment-forced models (3 and 4) also had more extreme values relative to the top-

Fig. 5. Model 3: Fishing, PredPrey, Historical Recruitment. Best model fits (lines) to biomass (t·km^{-2}) time series (points) for the GOA ecosystem model forced with fishing and hypothesized historical recruitment time series for Pacific herring and Pacific ocean perch.

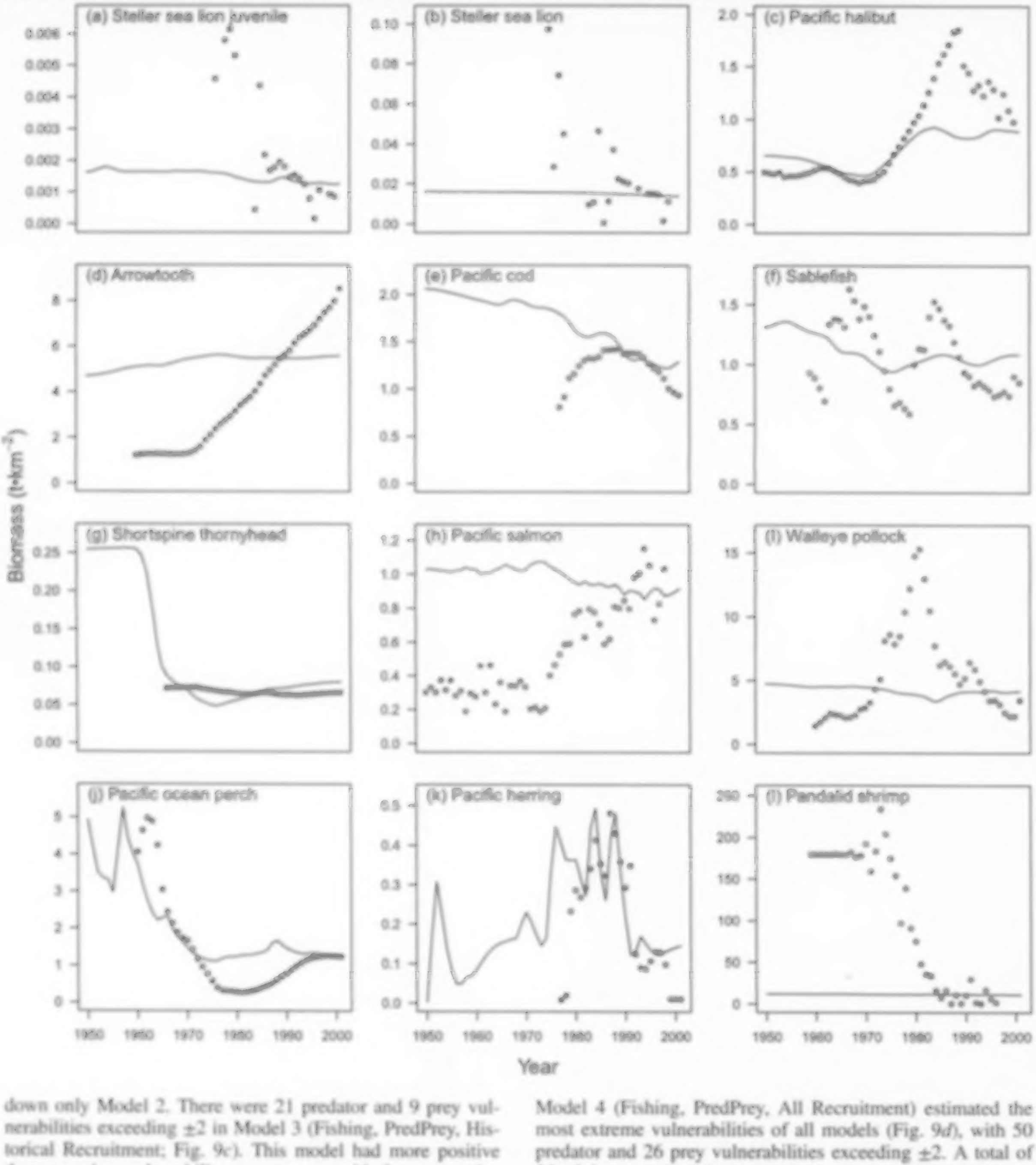

down only Model 2. There were 21 predator and 9 prey vulnerabilities exceeding ±2 in Model 3 (Fishing, PredPrey, Historical Recruitment; Fig. 9*c*). This model had more positive than negative vulnerability parameters, with large negative vulnerabilities estimated only for Pacific herring and POP (whose recruitment series forced the model) and a handful of other species including sablefish, grenadiers, skates, and rex sole (*Glyptocephalus zachirus*). This suggests a model-wide tendency towards Lotka–Volterra functional responses. Model 4 (Fishing, PredPrey, All Recruitment) estimated the most extreme vulnerabilities of all models (Fig. 9*d*), with 50 predator and 26 prey vulnerabilities exceeding ±2. A total of 25 of these reached the constrained parameter bounds of ±4. These extreme values appeared throughout all trophic levels, as was the case with Model 6 (Fishing, PredPrey, Climate). However, some signs were reversed between the two models; for example, pelagic zooplankton had extreme predator vulnerabilities in both models, but in the climate-driven Model 6

Fig. 6. Model 4: Fishing, PredPrey, All Recruitment. Best model fits (lines) to biomass (t·km^{-2}) time series (points) for the GOA ecosystem model forced with fishing, hypothesized historical recruitment time series for Pacific herring and Pacific ocean perch, and stock assessment estimated time series of walleye pollock recruitment.

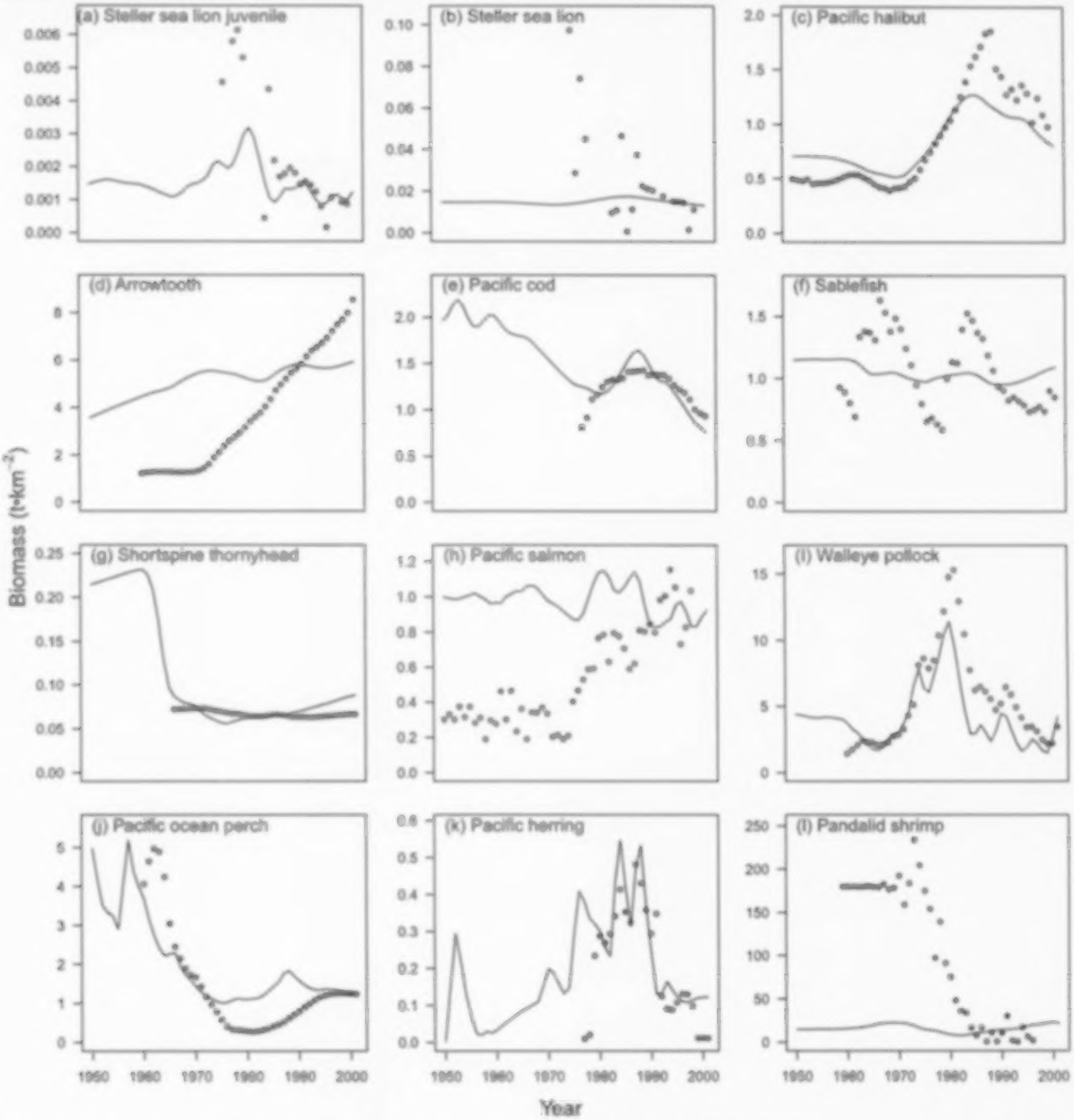

these were highly negative, indicating a tendency towards donor-controlled functional responses, and in the recruitment-driven Model 5 the pelagic zooplankton predator vulnerabilities were highly positive, indicating a tendency towards top-down functional responses (Fig. 9*b* vs. 9*d*).

Key species comparisons

We compare results across modeled hypotheses for two species directly forced by recruitment time series in at least one model, POP and walleye pollock (Fig. 10), and two that were never recruitment-forced, Pacific halibut and arrowtooth flounder (Fig. 11) to provide insight into the interactions of forcing parameters and estimated vulnerability parameters. The assessment time series for POP was fit fairly well using the hypothesized historical recruitment time series, although the model forced with fishing and PDO-driven primary pro-

Fig. 7. Model 5: Fishing, Climate. Comparison of biomass ($t \cdot km^{-2}$) time series (points) and model-estimated biomass trajectories (lines) forced with fishing and primary production following the PDO index (see text), but with no fitting of vulnerability parameters.

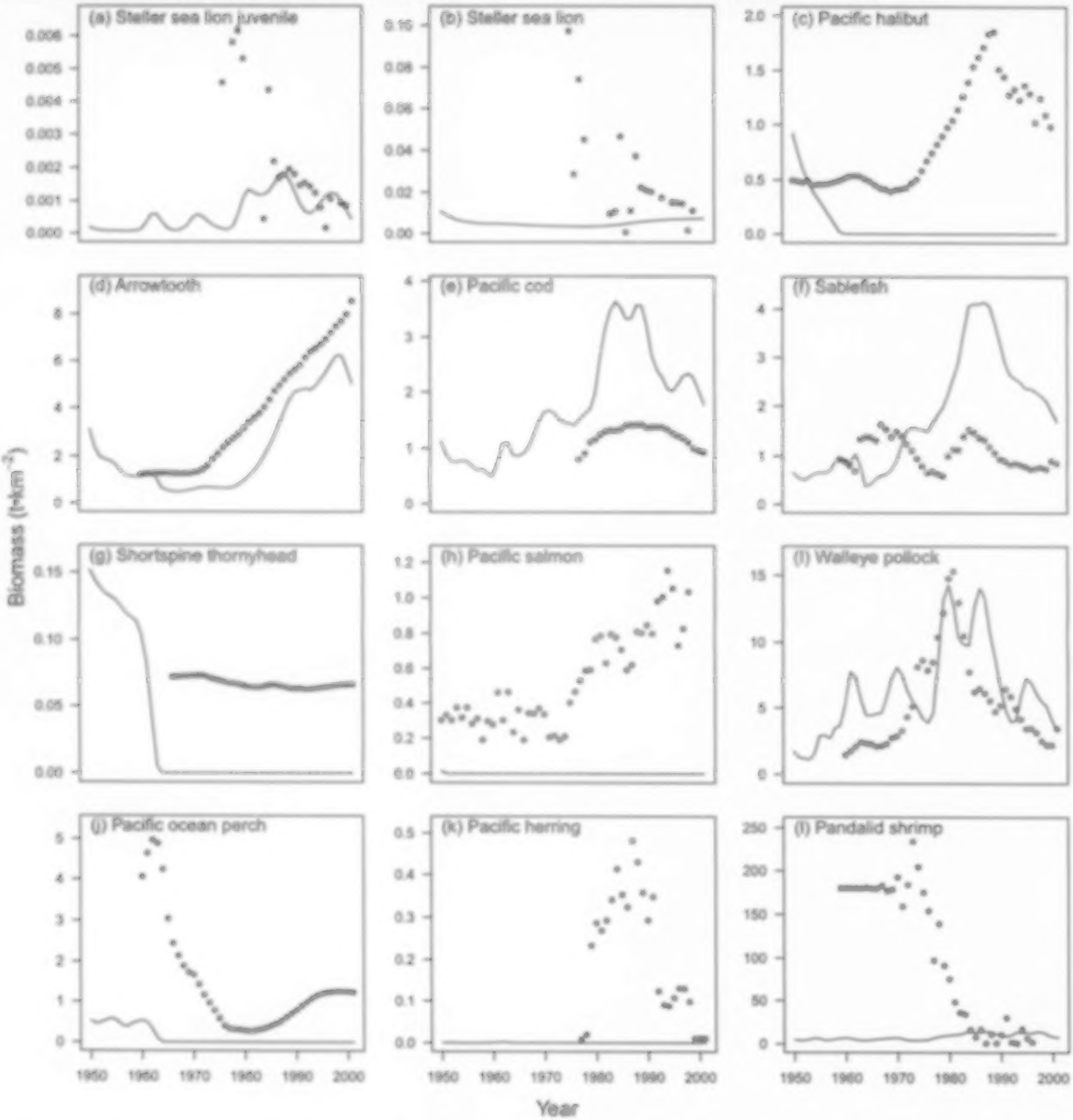

duction resulted in the best fit (Fig. 10*a*). Similarly, walleye pollock were best fit with their own recruitment time series and secondarily by the PDO (Fig. 10*b*). However, divergent vulnerability parameters were estimated to achieve similar fits. For POP, vulnerabilities estimated in the worst (Model 2, Fishing, PredPrey) and best (Model 6, Fishing, PredPrey, Climate) fits are similar; POP predator vulnerability is extremely high and prey vulnerability is extremely low in both cases (Figs. 9*a* and 9*b*). Conversely, the second-best fit in Model 4 (Fishing, PredPrey, All Recruitment) has extremely low values of both predator and prey vulnerability for POP (Fig. 9*d*). Similarly, walleye pollock predator and prey vulnerabilities estimated in the best-fitting Model 4 both approached the +4 parameter boundary (Fig. 9*d*), but those estimated in the second-best fit for walleye pollock (Model 6) were both about –2 (Fig. 9*b*).

The pattern changes for Pacific halibut and arrowtooth flounder, which had fairly divergent fits to their assessment

Fig. 8. Model 6: Fishing, PredPrey, Climate. Best model fits (lines) to biomass (t·km^{-2}) time series (points) for the GOA ecosystem model forced with fishing and the hypothesized PDO forcing of primary producer groups from 1901 to 2002.

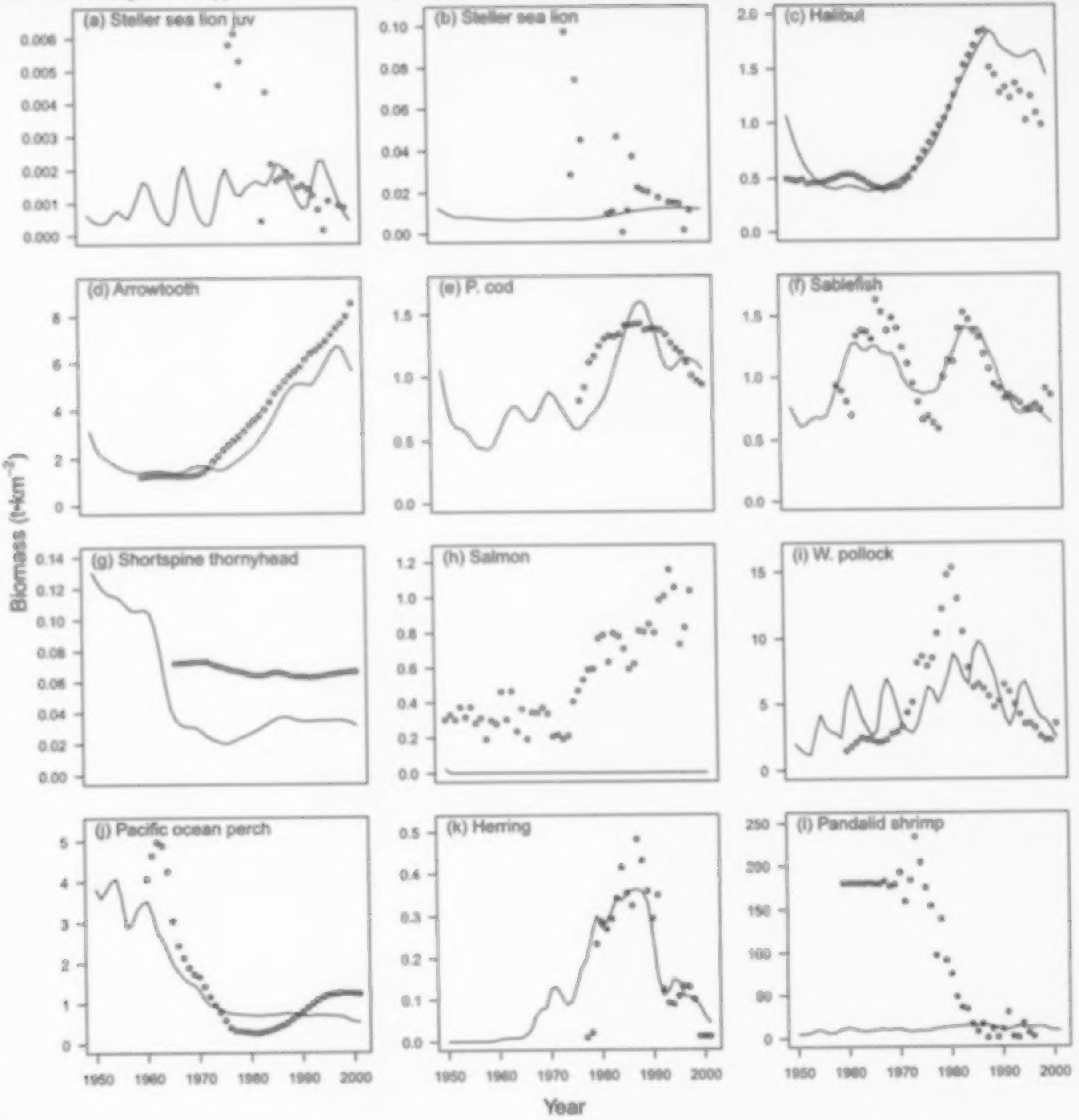

Fig. 9. Comparison of fitted predator vulnerabilities (vulnerability of all of that groups' prey to that group; light bars) and prey vulnerabilities (vulnerability of that group to all its predators; dark bars) for each species in the GOA ecosystem model under each modeled alternative forcing hypothesis. Species are ordered from highest to lowest trophic level from the top to the bottom of each plot. A vulnerability of 0 represents the default assumption, and fitted vulnerabilities were permitted to range from −4 to +4 on a unitless scale. Panel *a* shows vulnerabilities from Model 2 (Fishing, PredPrey), panel *b* shows Model 6 (Fishing, PredPrey, Climate), panel *c* shows Model 3 (Fishing, PredPrey, Historical Recruitment), and panel *d* shows Model 4 (Fishing, PredPrey, All Recruitment).

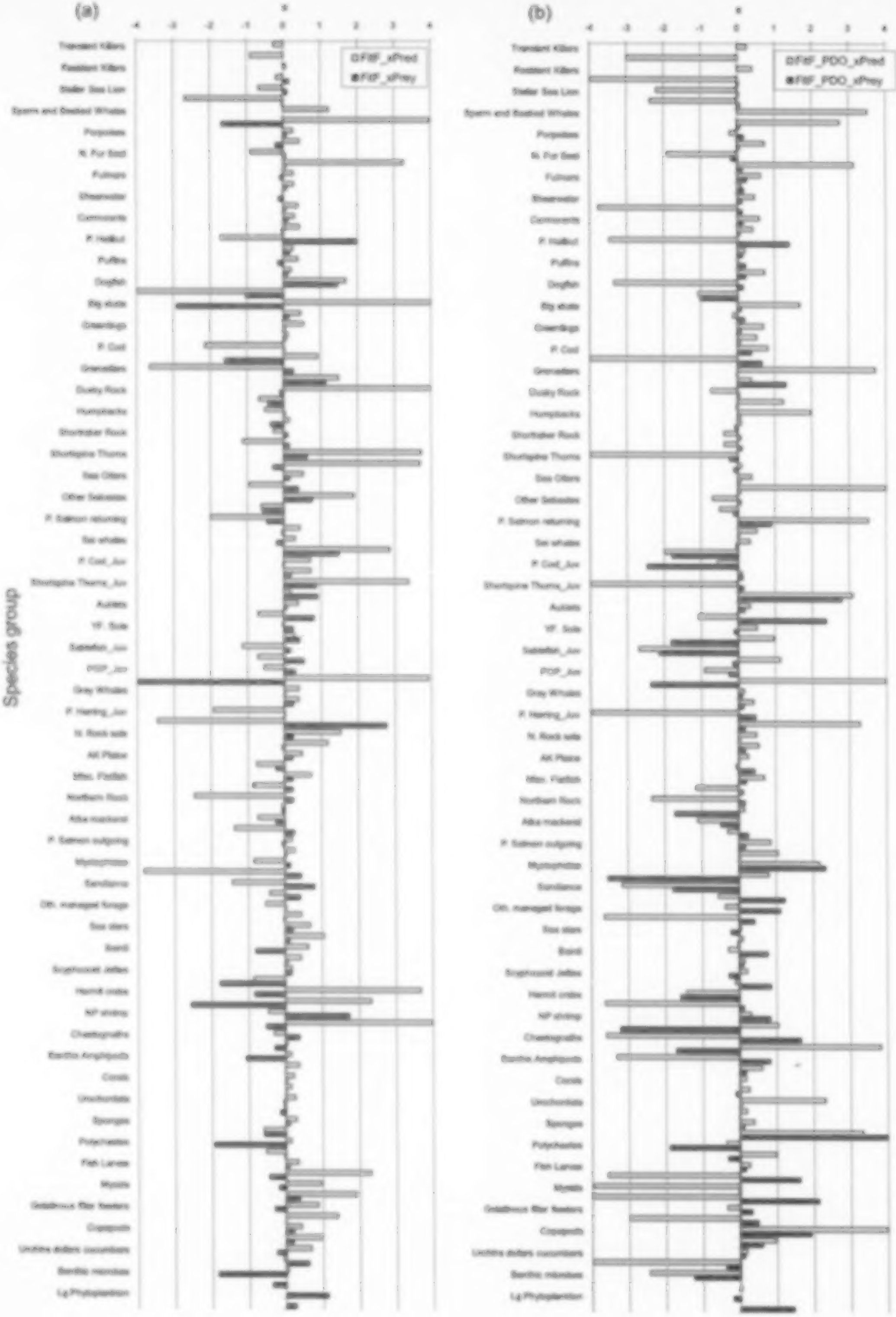
(a)
(b)
-4
-3
-2
-1
0
1
2
3
4
FitF_xPred
FitF_xPrey
FitF_PDO_xPred
FitF_PDO_xPrey
Species group
Transient Killers
Resident Killers
Steller Sea Lion
Sperm and Beaked Whales
Porpoises
N. Fur Seal
Fulmars
Shearwater
Cormorants
P. Halibut
Puffins
Dogfish
Big skate
Greenlings
P. Cod
Grenadiers
Dusky Rock
Humpbacks
Shortraker Rock
Shortspine Thorns
Sea Otters
Other Sebastes
P. Salmon returning
Sei whales
P. Cod_Juv
Shortspine Thorns_Juv
Auklets
YF. Sole
Sablefish_Juv
POP_Juv
Gray Whales
P. Herring_Juv
N. Rock sole
AK Plaice
Misc. Flatfish
Northern Rock
Atka mackerel
P. Salmon outgoing
Myctophidae
Sandlance
Oth. managed forage
Sea stars
Squid
Scyphozoid Jellies
Hermit crabs
NP shrimp
Chaetognaths
Benthic Amphipods
Corals
Urochordata
Sponges
Polychaetes
Fish Larvae
Mysids
Gelatinous filter feeders
Copepods
Urchins dollars cucumbers
Benthic microbes
Lg Phytoplankton

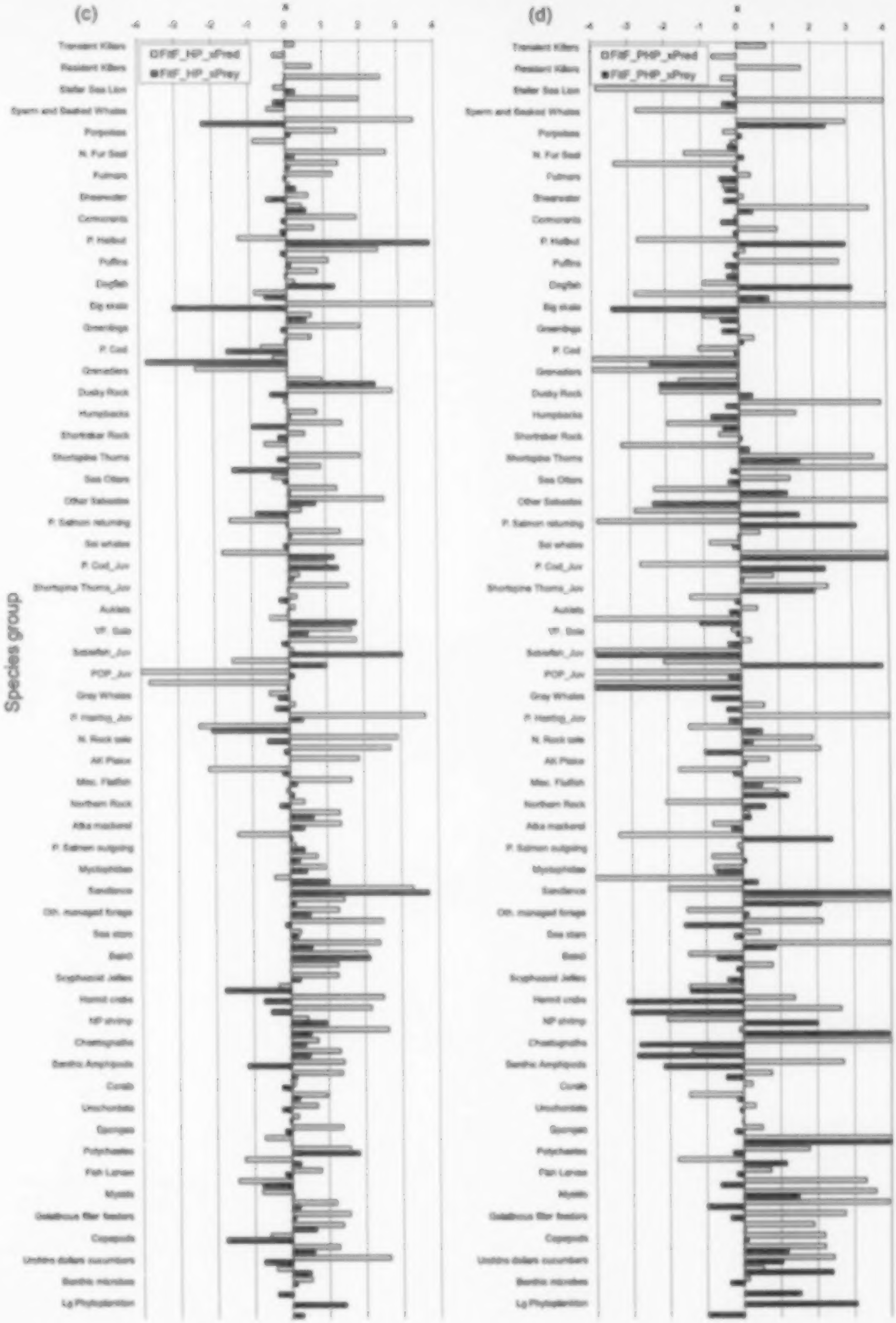
(c)
-4
-3
-2
-1
0
1
2
3
4
FIF_HP_xPred
FIF_HP_xPrey
Species group
Transient Killers
Resident Killers
Steller Sea Lion
Sperm and Beaked Whales
Porpoises
N. Fur Seal
Fulmars
Shearwater
Cormorants
P. Halibut
Puffins
Dogfish
Big skate
Greenlings
P. Cod
Grenadiers
Dusky Rock
Humpbacks
Shortraker Rock
Shortspine Thorns
Sea Otters
Other Sebastes
P. Salmon returning
Sei whales
P. Cod_Juv
Shortspine Thorns_Juv
Auklets
YF. Sole
Sablefish_Juv
POP_Juv
Gray Whales
P. Herring_Juv
N. Rock sole
AK Plaice
Misc. Flatfish
Northern Rock
Atka mackerel
P. Salmon outgoing
Myctophidae
Sandlance
Oth. managed forage
Sea stars
Bairdi
Scyphozoid Jellies
Hermit crabs
NP shrimp
Chaetognaths
Benthic Amphipods
Corals
Urochordata
Sponges
Polychaetes
Fish Larvae
Mysids
Gelatinous filter feeders
Copepods
Urchins dollars cucumbers
Benthic microbes
Lg Phytoplankton
(d)
-4
-3
-2
-1
0
1
2
3
4
FIF_PHP_xPred
FIF_PHP_xPrey
Transient Killers
Resident Killers
Steller Sea Lion
Sperm and Beaked Whales
Porpoises
N. Fur Seal
Fulmars
Shearwater
Cormorants
P. Halibut
Puffins
Dogfish
Big skate
Greenlings
P. Cod
Grenadiers
Dusky Rock
Humpbacks
Shortraker Rock
Shortspine Thorns
Sea Otters
Other Sebastes
P. Salmon returning
Sei whales
P. Cod_Juv
Shortspine Thorns_Juv
Auklets
YF. Sole
Sablefish_Juv
POP_Juv
Gray Whales
P. Herring_Juv
N. Rock sole
AK Plaice
Misc. Flatfish
Northern Rock
Atka mackerel
P. Salmon outgoing
Myctophidae
Sandlance
Oth. managed forage
Sea stars
Bairdi
Scyphozoid Jellies
Hermit crabs
NP shrimp
Chaetognaths
Benthic Amphipods
Corals
Urochordata
Sponges
Polychaetes
Fish Larvae
Mysids
Gelatinous filter feeders
Copepods
Urchins dollars cucumbers
Benthic microbes
Lg Phytoplankton

Fig. 10. Comparison of model fits for individual species: (*a*) Pacific ocean perch (POP) and (*b*) walleye pollock. Lines represent alternative modeled forcing hypotheses (solid: Model 2 (Fishing, PredPrey); dashed: Model 3 (Fishing, PredPrey, Historical Recruitment; dotted: Model 4 (Fishing, PredPrey, All Recruitment); dot-dash-dot: Model 6 (Fishing, PredPrey, Climate)); the heavy line indicates which hypothesis best fit the biomass time series (points) for each species.

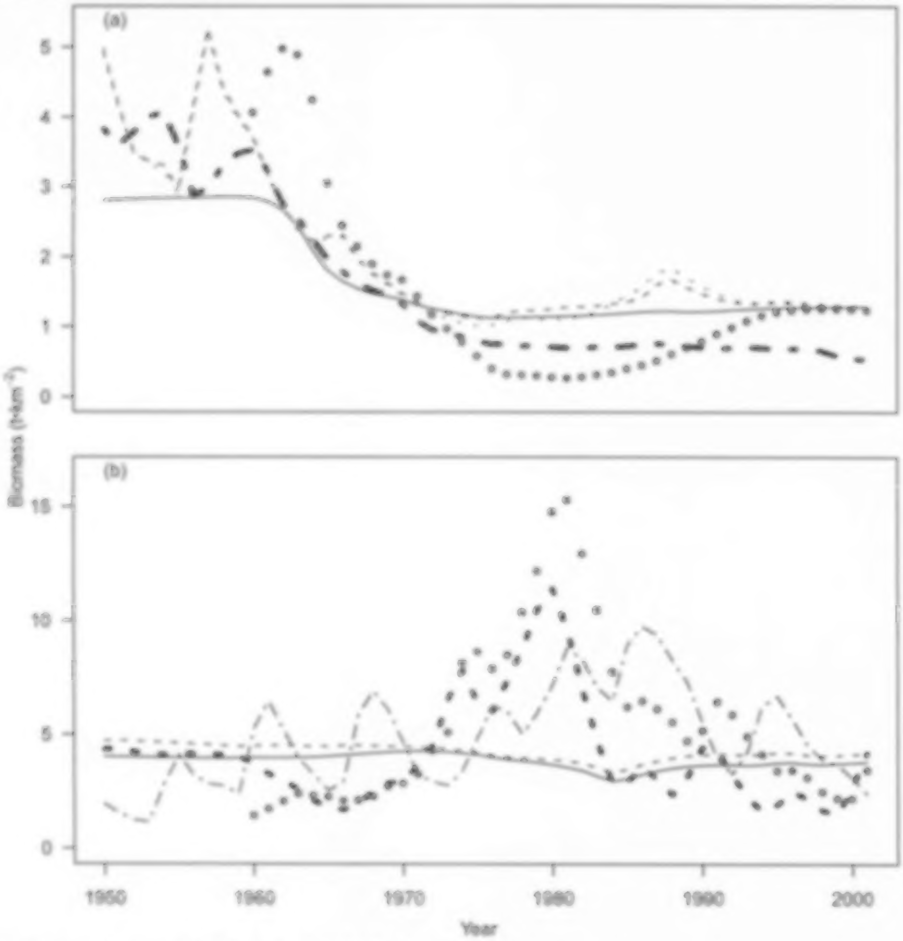

time series depending on the model (Fig. 11), but had relatively consistent estimated vulnerability parameters between models. Pacific halibut always had positive prey vulnerabilities and negative predator vulnerabilities estimated; the only difference between models was the magnitude of change. Pacific halibut vulnerabilities were closest to defaults in the Model 2 (Fishing, PredPrey), were extreme in Model 4 (Fishing, PredPrey, All Recruitment), the predator vulnerability was extremely negative in Model 6 (Fishing, PredPrey, Climate), and the prey vulnerability was extremely positive in Model 3 (Fishing, PredPrey, Historical Recruitment; Fig. 9). The biggest differences in vulnerability estimates for Pacific halibut are accompanied by the two best fits to the data in Models 2 and 4 (Fig. 11*a*). Arrowtooth flounder were consistently estimated to have negative predator vulnerabilities across all models and negative prey vulnerabilities in all models except for Model 4 (Fig. 9). The most extreme negative vulnerability estimates for arrowtooth flounder were in Models 2 and 4, which resulted in different fits to the biomass time series (Fig. 11*b*).

Discussion

Our dynamic ecosystem modeling framework showed considerable contrast among competing hypotheses of GOA ecosystem drivers. A few species were never explained well by any hypothesis, and some species could be explained well by very different hypotheses, but no dominant driver of the ecosystem was apparent. Further, the alternative control hypotheses implied very different sets of predator–prey relationships (estimated functional response parameters) within the ecosystem. Finally, fishing alone did not explain most biomass trajectories in the GOA; it was necessary to both estimate specific predator–prey relationships and provide some mechanism for increased production. We discuss each of these results in detail below, providing suggestions for future modeling efforts to support ecosystem-based fishery management.

First, we note that some important hypotheses are not directly testable within our modeling framework. These include climate-driven habitat changes (Agostini 2005), climate-

Fig. 11. Comparison of fits for individual species: (*a*) Pacific halibut and (*b*) arrowtooth flounder. Lines represent alternative modeled forcing hypotheses (solid: Model 2 (Fishing, PredPrey); dashed: Model 3 (Fishing, PredPrey, Historical Recruitment); dotted: Model 4 (Fishing, PredPrey, All Recruitment); dot-dash-dot: Model 6 (Fishing, PredPrey, Climate)); the heavy line indicates which hypothesis best fit the biomass time series (points) for each species.

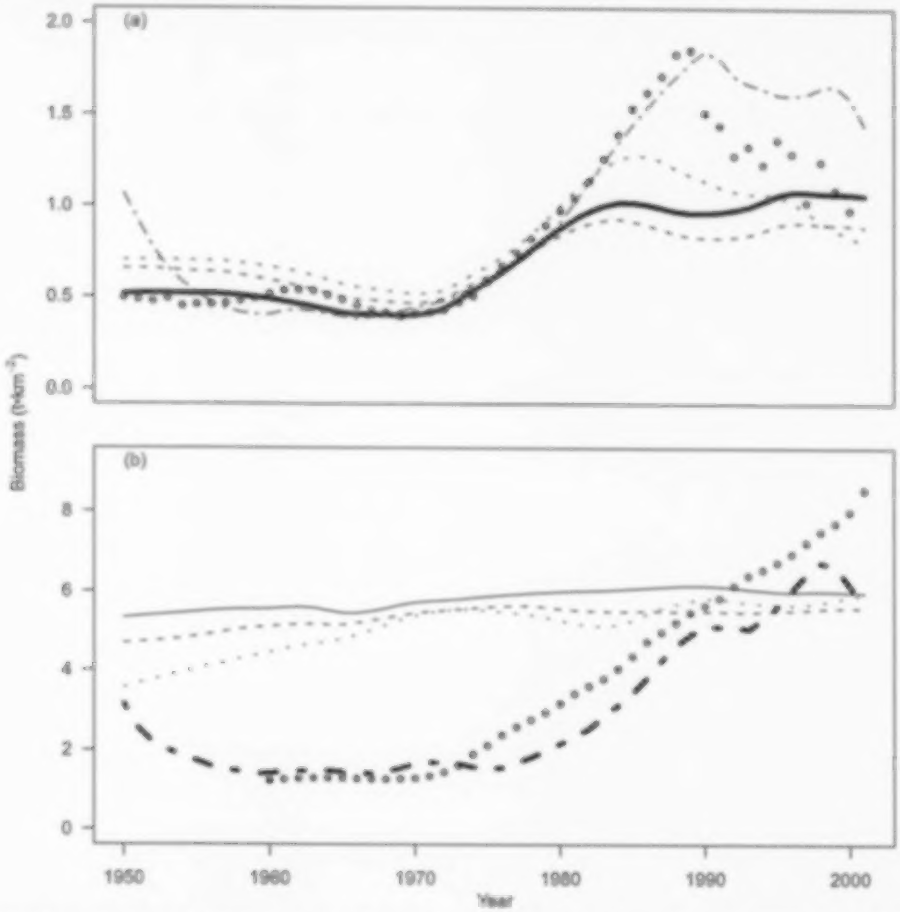

driven changes in the transport of larvae to optimal areas (Wilderbuer et al. 2002), fishery-driven habitat changes from fishing gear altering sediments or physical structure (Hermsen et al. 2003), and fishery-driven serial depletion of spatially discrete populations (Orensanz et al. 1998), all of which affect population trajectories. While spatial modeling is possible in the EwE extension Ecospace (Pauly et al. 2000) or in Atlantis (Fulton et al. 2004), we limited our study to similar spatial scales as stock assessments currently used in GOA fishery management. Some spatial and habitat effects on populations, whether climate- or fishery-driven, were likely incorporated within the spatially averaged time series and forcing functions used in this analysis (e.g., increased fishing effort may drive both increased fishing mortality and increased habitat alteration; a fitted climate forcing signal may suggest altered production when in fact altered transport was the mechanism for population change). Our analysis was unable to resolve these mechanisms, but it may lend support to general hypotheses regarding the relative dominance of climate versus fishing signals in ecosystem trends.

Consistency of poor fits: information for future efforts

Walters (1986) suggested that dynamic ecosystem modeling acts as a first-pass consistency check on the assumptions behind the time series. Similar to the findings of Gaichas et al. (2010) for the static mass balance model, this consistency check indicates which single-species hypotheses (reconstructed biomass time series) remain compatible when feeding relationships between species, detailed system-wide exploitation history, and alternative production hypotheses are taken into account. The clearest example of this comes from the biomass and catch time series that were never fit under any modeled scenario: pandalid shrimp and king crabs at low trophic levels and fin whales and Steller sea lions at high trophic levels.

Our pandalid shrimp time series was derived from the suggestion in Anderson and Piatt (1999) and Anderson (2000) that benthic communities in the GOA had been dominated by shrimp in the 1960s prior to the physical regime shift of the PDO in 1977 and that shrimp had declined precipitously after that shift to be replaced by high populations of groundfish. This suggestion was based on observations from a coastal GOA small mesh trawl survey and was supported by observed declines in shrimp fishery catches with concurrent increases in groundfish biomass. However, none of our modeled hypotheses fit the scaled-up shrimp biomass. In additional fitting experiments not reported here, the pandalid shrimp biomass time series was used to force the ecosystem model to test the hypothesis that shrimp biomass really was that high historically, which resulted in extremely high biomass estimates for groundfish predators of shrimp, such as Pacific cod, Pacific halibut, and shortspine thornyhead. These high, shrimp-forced, groundfish biomass estimates were inconsistent with all other available time series data for the GOA. Taken together, these results indicate that the coastal small mesh trawl survey results are unlikely to apply to the entire GOA continental shelf ecosystem. Eliminating this simple shrimp biomass hypothesis allows exploration of more realistic hypotheses involving more extensive spatial sampling of shrimp for Gulf-wide ecosystem investigations. Alternatively, future work could model only nearshore, spatially explicit ecosystem dynamics in areas well-sampled by the small mesh trawl survey.

The consistent ecosystem model failures to fit the recorded catch histories for both king crabs and fin whales suggest potential alternative parameters to estimate in future studies. Both groups died out of the model as soon as historical exploitation began for each, suggesting the biomass or the productivity (or both) specified for fin whales and king crabs in the base mass balance model was insufficient to support the historical catch. This situation is very similar to that observed for POP in the Model 1 (Fishing) with no fitting of vulnerability parameters; however, no models were able to estimate vulnerabilities capable of increasing fin whale or king crab biomass sufficiently before exploitation began. Fin whales have substantial biomass in the GOA at present (Zerbini et al. 2006), but still apparently much less than unexploited biomass, while king crab biomass remains low even in areas of high historical abundance (Stichert 2010). It is also possible that like POP, a difference in productivity between pre-exploited and exploited populations of fin whales and king crabs would improve fits to historical catches and allow fin whales and king crabs to escape extinction. This hypothesis could be explored in future modeling by estimating initial production, biomass, or unexplained mortality parameters conditional on the other input data.

Explaining Steller sea lion dynamics has been problematic (National Research Council 2003; Atkinson et al. 2008), and our study is no exception. The 1950s high biomass of juvenile and adult Steller sea lions is not explained by any of our ecosystem-wide hypotheses. This is consistent with the findings of one modeling study specifically designed to address the Steller sea lion decline (National Research Council 2003), but inconsistent with another (Guénette et al. 2006). In the study by National Research Council (2003), the decline of Steller sea lions in Alaska could only be explained by including increased adult mortality, which the authors attributed to undocumented culling of these predators, increased mortality of small pelagic fish due to disease outbreaks, or decreased vulnerability of Steller sea lion prey by an unidentified mechanism resulting from 1977 regime shift (National Research Council 2003). In the study by Guénette et al. (2006), increased predation mortality on sea lions by killer whales (*Orcinus orca*) was included in a model of the Aleutian Islands ecosystem, adjacent to the GOA. Models attempting to implement specific sea lion mortality hypotheses relied on many assumptions, as time series data are not available for undocumented culling, small pelagic fish dynamics, killer whale population trajectories, or even killer whale diet (National Research Council 2003; Guénette et al. 2006). In our study, we limited ourselves to control hypotheses that could be based on documented time series and therefore did not implement those listed above. Although our objective was not to address Steller sea lion declines specifically, our results still reveal a potential linkage between walleye pollock recruitment and juvenile sea lions. Our best fit to juvenile Steller sea lion biomass was forced by GOA walleye pollock recruitment (Model 4, Fishing, PredPrey, All Recruitment), in contrast with the National Research Council (2003) study, which found no such relationship using data for Bering Sea walleye pollock (see Ianelli et al. 2005). The strength of this linkage may be important for fishery and protected species management in the GOA and could be investigated with further refinement of ecosystem-specific modeling and research.

Best fits from multiple hypotheses: dealing with multiple ecosystem drivers

While fitting failures provide important insights for using dynamic ecosystem models in fishery management, successful fits provide equally important, if more complex, insights into ecosystem relationships. Fitting the model to data by estimating vulnerability parameters implies that a certain set of predator–prey interactions described by those parameters "best" explains the dynamics observed in the ecosystem. However, forcing with different production time series resulted in very different sets of estimated vulnerability parameters. Fitting to the fishing only forcing hypothesis (Model 2) resulted in a system where many groups had vulnerabilities implying balanced bottom-up and top-down forcing and a handful of groups with extreme top-down or bottom-up influence. Conversely, fitting while forcing with three individual species production time series (Model 4) resulted in a system where many species groups had extreme top-down or bottom-up influence. The other models had intermediate vulnerability characteristics as described above. One important management implication of this result is that projecting any of these models forward with these divergent parameterizations would result in different predictions of system dynamics. In particular, low vulnerability values imply productivity and stock compensation dynamics that are the multispecies equivalent of steep single-species recruitment curves: stocks with high productivity at low stock sizes (Aydin 2004). Conversely, high vulnerabilities imply weaker compensatory dynamics at low stock size. Therefore, the divergent parameterizations imply great differences in stocks' ability to recover from declines.

Future modeling could address this difficulty by narrowing the range of possible predator and prey vulnerabilities by fitting to or forcing with additional data types. For example, food habits collections for major predators in the GOA show trends in diet over time (Dorn et al. 2005; Gaichas et al. 2010), which could be fit within the dynamic ecosystem model along with biomass and catch time series. Another approach is to force with a low trophic-level time series. Field et al. (2006) fit Northern California Current ecosystem time series by forcing with an index of juvenile coho salmon (*Oncorhychus kisutch*) survival representing general low trophic-level productivity (Logerwell et al. 2003), which accounted for Pacific hake (*Merluccius productus*) dynamics as well. There is no equivalent time series for the GOA continental shelf. An approach suggested by Christensen et al. (2005) is to use a parameterized dynamic ecosystem model along with time series data to generate a single primary production "anomaly" that explains all time series not explained by fishing and vulnerability (e.g., Heymans et al. 2005). This was attempted using an early version of our GOA model implemented in EwE, but failed. Alternatively, model-generated time series of primary and secondary production derived from physical models of the GOA (e.g., Hermann et al. 2002) could be useful for further hypothesis testing in the GOA. Ultimately, a monitoring program to index broad-scale primary and secondary productivity in the GOA would be most useful to address fisheries management questions within an ecosystem modeling context.

Another approach to provide strategic management advice would be to retain a full range of feasible hypotheses in models used by implementing multimodel inference (MMI) methods (Burnham and Anderson 2002). Because no single forcing function explains all observed dynamics in the GOA, it seems appropriate to introduce modeling approaches that incorporate a realistic range of uncertainty as well as all feasible hypotheses rather than attempting to choose between them. Uncertainty in model parameters could be incorporated using a probabilistic approach that evaluates the prior probability of both the base food web parameters and the dynamic parameters in a Bayesian framework (Gelman et al. 1995). Givens et al. (1993) outlined a procedure using prior probability distributions for model inputs, parts of which have already been implemented for the GOA, Eastern Bering Sea (EBS), and Aleutian Islands ecosystem models (Aydin et al. 2007). The MMI framework is particularly appealing when several alternative models are best supported for different but equally commercially important species in an ecosystem, as was the case with the Models 4 (Fishing, PredPrey, All Recruitment) and 6 (Fishing, PredPrey, Climate) here. Rather than abandoning the good explanatory power for arrowtooth flounder, sablefish, POP, and Pacific herring in Model 6, this information would be included in system-wide predictions, although at a low weight relative to the best-fitting Model 4. Our work could form the basis for such inference, although a larger set of models should be tested, and the weighting procedure would require careful attention to prevent a large AIC contrast from selecting a single modeled hypothesis.

Relative complexity of the GOA

This study allows us to classify the GOA within a range of ecosystems with fairly simple to more complex control mechanisms. The forcing-without-fitting models 1 and 5 (Fishing; and Fishing, Climate, respectively) demonstrate that biomass trajectories cannot be explained without including predator–prey interactions considerably different from default EwE assumptions. Further, comparing results from fishing-only models with fishing-plus-production models suggests that the historical biomass of the ecosystem cannot be recovered from the current biomass simply by eliminating fishing. Some change in productivity, either at the population level or at the ecosystem level, must be included to force populations initialized from early 1990s data to "recover" to prefishing biomass levels over the course of a century or more. This contrasts with modeling exercises conducted in other systems where forcing with fishing alone or with fishing and secondary production time series achieved reasonably good agreement between model-estimated biomass trajectories and biomass time series data from each system. In the Central North Pacific (CNP; Cox et al. 2002*a*, 2002*b*), Eastern Tropical Pacific (ETP; Olson and Watters 2003), and Northern California Current (NCC; Field 2004 and Field et al. 2006), fishing mortality on major species was sufficient to produce EwE biomass trends strikingly similar to single-species assessments for most species. In the CNP, no formal nonlinear estimation of vulnerabilities was attempted, but a sensitivity analysis demonstrated that most fits were not affected by changing vulnerability parameters (Cox et al. 2002*b*). In the ETP and NCC, the addition of climate forcing functions known to affect lower trophic-level production improved agreement between model estimates and time series data to the few exploited species not fully explained by fishing mortality alone, while changing system-wide vulnerability parameters did not affect fits (Olson and Watters 2003; Field et al. 2006). In ecosystems outside the Pacific such as the Gulf of Mexico (GOM; Walters et al. 2008) and the Ionian Sea (IS; Piroddi et al. 2010), similarly dominant fishing signals have been found through ecosystem modeling, even though estimation of primary production and vulnerability parameters were employed in those studies.

In contrast, in the EBS (Aydin et al. 2002) and GOA (Aydin et al. 2007 and this study), fishing mortality alone generally did not reproduce the dynamics estimated from single-species assessments, and the understanding of specific climate forcing mechanisms is less advanced than in the ETP and NCC. In these Alaskan systems, stock assessment results were most closely reproduced only when production time series were included as forcing functions along with fishing mortality and when vulnerabilities were estimated. In single-species assessments, recruitment estimates absorb climate signals and other interactions that are not well explained by the models, and these functions currently serve the same purpose in the Alaskan dynamic ecosystem models. This places the Alaskan ecosystems in a similar category with the Strait of Georgia (SOG; Martell et al. 2001), the Northern Humboldt Current (NHC; Taylor et al. 2008), the South Catalan Sea (SCS; Coll et al. 2008), and the Northern Benguela Current (NBC; Heymans et al. 2009), where fishing, climate, and estimated predator–prey vulnerabilities were all required to explain observed ecosystem dynamics.

Our results also demonstrate that within each system there are species showing greater and lesser degrees of fishing effects and climate effects, as evidenced by the degree of agreement between single-species assessment models and ecosystem model results. In particular, the Pacific models give similarly good fits for species such as marlins (CNP) and rockfishes (NCC) where fishing mortality has clearly driven a strong decline. For other species, such as yellowfin tuna (*Thunnus albacares*) (CNP) and arrowtooth flounder

(GOA), fishing mortality rates have been low to virtually nonexistent, resulting in substantial divergence between the ecosystem models forced with fishing and single-species models. The pattern becomes more complex for species such as Pacific halibut and Pacific salmon (GOA), which have been heavily exploited for over a century, but which also display clear climate signals even in single-species analyses (Francis et al. 1998; Clark et al. 1999) and can be fit using multiple forcing hypotheses.

The relative importance of including feeding interactions, fishing, and production forcing may be used to place modeled marine ecosystems along a continuum from those that are more fishing-dominated (e.g., the CNP, ETP, NCC, GOM, and IS) to those where fishing mortality must be viewed within the more uncertain context of strong predator–prey interactions and climate forcing (the EBS, GOA, SOG, NHC, SCS, and NBC). Considering this complexity, in turn, changes our view of optimal fishing policies, as demonstrated in a recent analysis for the North Sea (Mackinson et al. 2009). The results of our model-based hypothesis testing suggest that in the GOA, there is no single main driver of the system; climate, fishing, and food web dynamics interact here in ways that are not yet fully captured in the dynamic ecosystem model or in the single-species assessments. But even this has important management implications. While fishing clearly has effects in the GOA, fishing effects do not damp out all other ecosystem processes. Might we consider the systems without clear fishing dominance to be ecologically healthier relative to those with a single dominant fishing driver? Fishery management is still necessary in a system with multiple drivers — in fact it is crucial to preventing fishing from becoming the dominant driver.

Acknowledgements

This work was initiated during NCEAS (National Center for Ecological Analysis and Synthesis) project 4160, "Models of Alternative Management Policies for Marine Ecosystems," led by Robert Francis and James Kitchell. Our approach was inspired by the "adaptive environmental assessment" described in Walters (1986). Sally Mizroch provided historical catch data for whales. Steven Hare provided the extended the historical time series of Pacific halibut biomass. Todd TenBrink assembled time series of catch for GOA crabs and Pacific herring. Jim Ianelli, Buck Stockhausen, Carl Walters, and three anonymous reviewers provided helpful comments on eariler drafts of this manuscript. Reference to trade names does not imply endorsement by the National Marine Fisheries Service, NOAA. The findings and conclusions in the paper are those of the authors and do not necessarily represent the views of the National Marine Fisheries Service, NOAA.

References

Agostini, V. 2005. Climate, ecology and productivity of Pacific sardine and hake in the California Current ecosystem. Ph.D. dissertation, School of Aquatic and Fishery Sciences, University of Washington, Seattle, Wash.

Anderson, P.J., and Piatt, J.F. 1999. Community reorganization in the Gulf of Alaska following ocean climate regime shift. Mar. Ecol. Prog. Ser. **189**: 117–123. doi:10.3354/meps189117.

Anderson, P.J. 2000. Pandalid shrimp as indicators of ecological regime shift. J. Northw. Atl. Fish. Sci. **27**: 1–10.

Anonymous. 1906. Alaskan seal fisheries. Vol. I. Compilation of documents and other printed matter relating thereto. Government Printing Office, Washington, D.C.

Anonymous. 1910. Alaskan seal fisheries. Vol. XVI. Compilation of documents and other printed matter relating thereto. Assembled by the Bureau of Fisheries. Government Printing Office, Washington, D.C.

Antonson, J.M., and Hanable, W.S. 1984. Alaska's heritage. Alaska Historical Commission Studies in History No. 133. The Alaska Historical Society for the Alaska Historical Commission, Department of Education, State of Alaska, Anchorage, Alaska.

Atkinson, S., DeMaster, D.P., and Calkins, D.G. 2008. Anthropogenic causes of the western Steller sea lion *Eumetopias jubatus* population decline and their threat to recovery. Mammal Rev. **38**(1): 1–18. doi:10.1111/j.1365-2907.2008.00128.x.

Aydin, K.Y. 2004. Age structure or functional response? Reconciling the energetic of surplus production between single species models and ECOSIM. Afr. J. Mar. Sci. **26**: 289–301. doi:10.2989/18142320409504062.

Aydin, K., Gaichas, S., Ortiz, I., Kinzey, D., and Friday, N. 2007. A comparison of the Bering Sea, Gulf of Alaska, and Aleutian Islands large marine ecosystems through food web modeling. US Department of Commerce, Washington, D.C. NOAA Tech. Memo. NMFS-AFSC-178.

Aydin, K.Y., Lapko, V.V., Radchenko, V.I., and Livingston, P.A. 2002. A comparison of the eastern Bering and western Bering Sea shelf and slope ecosystems through the use of mass-balance food web models. US Department of Commerce, Washington, D.C. NOAA Tech. Memo. NMFS-AFSC-130.

Bailey, K.M. 2000. Shifting control of recruitment of walleye pollock *Theragra chalcogramma* after a major climatic and ecosystem change. Mar. Ecol. Prog. Ser. **198**: 215–224. doi:10.3354/meps198215.

Baum, J.K., and Worm, B.W. 2009. Cascading top-down effects of changing oceanic predator abundances. J. Anim. Ecol. **78**(4): 699–714. doi:10.1111/j.1365-2656.2009.01531.x. PMID:19298616.

Bell, F.H. 1981. The Pacific halibut: the resource and its fishery. Alaska Northwest Publishing Company, Anchorage, Alaska.

Berman, M.D. 2008. Endangered species, threatened fisheries: science to the rescue! Evaluating the Congressionally designated Steller sea lion research program. Mar. Policy, **32**(4): 580–591. doi:10.1016/j.marpol.2007.10.007.

Brodeur, R.D., Frost, B.W., Hare, S.R., Francis, R.C., and Ingraham, W.J. 1996. Interannual variations in zooplankton biomass in the Gulf of Alaska, and covariation with California current zooplankton biomass. CalCOFI Rep. **37**: 80–99.

Browning, R. 1980. Fisheries of the North Pacific: history, species, gear and processes. Alaska Northwest Publishing Company, Anchorage, Alaska.

Burnham, K.P., and Anderson, D.R. 2002. Model selection and multimodel inference: a practical information-theoretic approach. 2nd ed. Springer, New York.

Christensen, V., and Walters, C. 2004. Ecopath with Ecosim: methods, capabilities, and limitations. Ecol. Model. **172**(2–4): 109–139. doi:10.1016/j.ecolmodel.2003.09.003.

Christensen, V., Walters, C.J., and Pauly, D. 2005. Ecopath with Ecosim: a user's guide. Fisheries Centre, The University of British Columbia, Vancouver. November 2005 ed. Available from http://www.ecopath.org/.

Clark, W.G., Hare, S.R., Parma, A.M., Sullivan, P.J., and Trumble, R.J. 1999. Decadal changes in growth and recruitment of Pacific halibut (*Hippoglossus stenolepis*). Can. J. Fish. Aquat. Sci. **56**(2): 242–252. doi:10.1139/f98-163.

Coll, M., Palomera, I., Tudela, S., and Dowd, M. 2008. Food-web dynamics in the South Catalan Sea ecosystem (NW Mediterranean) for 1978–2003. Ecol. Model. **217**(1–2): 95–116. doi:10.1016/j.ecolmodel.2008.06.013.

Cox, S.P., Martell, S.J.D., Walters, C.J., Essington, T.E., Kitchell, J.F., Boggs, C., and Kaplan, I. 2002*a*. Reconstructing ecosystem dynamics in the central Pacific Ocean, 1952–1998. I. Estimating population biomass and recruitment of tunas and billfishes. Can. J. Fish. Aquat. Sci. **59**(11): 1724–1735. doi:10.1139/f02-137.

Cox, S.P., Essington, T.E., Kitchell, J.F., Martell, S.J.D., Walters, C.J., Boggs, C., and Kaplan, I. 2002*b*. Reconstructing ecosystem dynamics in the central Pacific Ocean, 1952–1998. II. A preliminary assessment of the trophic impacts of fishing and effects on tuna dynamics. Can. J. Fish. Aquat. Sci. **59**(11): 1736–1747. doi:10.1139/f02-138.

Cury, P., Bakun, A., Crawford, R.J.M., Jarre, A., Quiñones, R.A., Shannon, L.J., and Verheye, H.M. 2000. Small pelagics in upwelling systems: patterns of interaction and structural changes in "wasp-waist" ecosystems. ICES J. Mar. Sci. **57**(3): 603–618. doi:10.1006/jmsc.2000.0712.

DiCosimo, J., Methot, R.D., and Ormseth, O.A. 2010. Use of annual catch limits to avoid stock depletion in the Bering Sea and Aleutian Islands management area (Northeast Pacific). ICES J. Mar. Sci. **67**(9): 1861–1865. doi:10.1093/icesjms/fsq060.

Dorn, M., Barbeaux, S., Guttormsen, M., Megrey, B., Hollowed, A., Wilkins, M., and Spalinger, K. 2003. Assessment of walleye pollock in the Gulf of Alaska. Section 1 in Stock Assessment and Fishery Evaluation Report for the Groundfish Resources of the Gulf of Alaska, November 2003. North Pacific Fishery Management Council, Anchorage, Alaska, USA. pp. 33–148. Available from http://www.afsc.noaa.gov/refm/docs/2003/GOApollock.pdf.

Dorn, M., Aydin, K., Barbeaux, S., Guttormsen, M., Megrey, B., Spalinger, K., and Wilkins, M. 2005. Assessment of walleye pollock in the Gulf of Alaska. Section 1 in Stock Assessment and Fishery Evaluation Report for the Groundfish Resources of the Gulf of Alaska, November 2005. North Pacific Fishery Management Council, Anchorage, Alaska, USA. Available from http://www.afsc.noaa.gov/refm/docs/2005/GOApollock.pdf.

Essington, T. 2010. Trophic cascades in open ocean ecosystems. Chapter 6. *In* Trophic cascades: predators, prey and the changing dynamics of nature. *Edited by* J. Terborgh and J.A. Estes. Island Press, Washington, D.C.

Fay, G. 2004. A Bayesian stochastic metapopulation model for Steller sea lions in Alaska. M.Sc. thesis, School of Aquatic and Fishery Sciences, University of Washington, Seattle, Wash.

Field, J.C. 2004. Application of ecosystem-based fishery management approaches in the northern California Current. Ph.D. dissertation, School of Aquatic and Fishery Sciences, University of Washington, Seattle, Wash.

Field, J.C., Francis, R.C., and Aydin, K.Y. 2006. Top-down modeling and bottom-up dynamics: linking a fisheries-based ecosystem model with climate hypotheses in the Northern California Current. Prog. Oceanogr. **68**: 238–270.

Francis, R.C., and Hare, S.R. 1994. Decadal-scale regime shifts in the large marine ecosystems of the north-east Pacific: a case for historical science. Fish. Oceanogr. **3**(4): 279–291. doi:10.1111/j.1365-2419.1994.tb00105.x.

Francis, R.C., Hare, S.R., Hollowed, A.B., and Wooster, W.S. 1998. Effects of interdecadal climate variability on the oceanic ecosystems of the NE Pacific. Fish. Oceanogr. **7**(1): 1–21. doi:10.1046/j.1365-2419.1998.00052.x.

Fulton, E.A., Smith, A.D.M., and Punt, A.E. 2004. Ecological indicators of the ecosystem effects of fishing: final report. Report No. R99/1546, Australian Fisheries Management Authority, Canberra, Australia.

Gaichas, S.K., Aydin, K.Y., and Francis, R.C. 2010. Using food web model results to inform stock assessment estimates of mortality and production for ecosystem-based fisheries management. Can. J. Fish. Aquat. Sci. **67**(9): 1490–1506. doi:10.1139/F10-071.

Gaichas, S., and Ianelli, J. 2003. Assessment of thornyheads (*Sebastolobus* spp.) in the Gulf of Alaska. *In* Stock assessment and fishery evaluation report for the groundfish resources of the Gulf of Alaska, November 2003, Section 12. North Pacific Fishery Management Council, Anchorage, Alaska, USA. pp. 659–698. Available from http://www.afsc.noaa.gov/refm/docs/2003/GOAthornyheads.pdf.

Gelman, A., Carlin, J.B., Stern, H.S., and Rubin, D.B. 1995. Bayesian data analysis. Chapman & Hall, London, UK.

Givens, G.H., Raftery, A.E., and Zeh, J.E. 1993. Benefits of a Bayesian approach for synthesizing multiple sources of evidence and uncertainty linked by a deterministic model. Rep. Int. Whaling Comm. **43**: 495–500.

Guénette, S., Heymans, S.J.J., Christensen, V., and Trites, A.W. 2006. Ecosystem models show combined effects of fishing, predation, competition, and ocean productivity on Steller sea lions (*Eumetopias jubatus*) in Alaska. Can. J. Fish. Aquat. Sci. **63**(11): 2495–2517. doi:10.1139/f06-136.

Haigh, S.P., Denman, K.L., and Hsieh, W.W. 2001. Simulation of the planktonic ecosystem response to pre- and post-1976 forcing in an isopycnic model of the North Pacific. Can. J. Fish. Aquat. Sci. **58**(4): 703–722. doi:10.1139/f01-010.

Hanselman, D., Heifetz, J., Fujioka, J.T., and Ianelli, J.N. 2003. Gulf of Alaska Pacific ocean perch. *In* Stock assessment and fishery evaluation report for the groundfish resources of the Gulf of Alaska, November 2003, Section 7. North Pacific Fishery Management Council, Anchorage, Alaska, USA. pp. 429–480. Available at http://www.afsc.noaa.gov/refm/docs/2003/GOAPOP.pdf.

Hare, S.R., and Mantua, N.J. 2000. Empirical evidence for North Pacific regime shifts in 1977 and 1989. Prog. Oceanogr. **47**(2–4): 103–145. doi:10.1016/S0079-6611(00)00033-1.

Hermann, A.J., Haidvogel, D.B., Dobbins, E.L., and Stabeno, P.J. 2002. Coupling global and regional circulation models in the coastal Gulf of Alaska. Prog. Oceanogr. **53**(2–4): 335–367. doi:10.1016/S0079-6611(02)00036-8.

Hermsen, J.M., Collie, J.S., and Valentine, P.C. 2003. Mobile fishing gear reduces benthic megafaunal production on Georges Bank. Mar. Ecol. Prog. Ser. **260**: 97–108. doi:10.3354/meps260097.

Heymans, J.J., Guénette, S., Christensen, V., and Trites, A. 2005. Changes in the Gulf of Alaska ecosystems due to ocean climate change and fishing. ICES CM, **2005**: 1–31.

Heymans, J.J., Sumaila, U.R., and Christensen, V. 2009. Policy options for the northern Benguela ecosystem using a multispecies, multifleet ecosystem model. Prog. Oceanogr. **83**(1–4): 417–425. doi:10.1016/j.pocean.2009.07.013.

Ianelli, J., Barbeaux, S., Honkalehto, T., Lauth, B., and Williamson, N. 2005. Assessment of Alaska pollock stock in the Eastern Bering Sea. Section 1. *In* Stock assessment and fishery evaluation report for the groundfish resources of the Bering Sea and Aleutian Islands, November 2005. North Pacific Fishery Management Council, Anchorage, Alaska, USA. Available from http://www.afsc.noaa.gov/refm/docs/2005/EBSPollock.pdf.

International Pacific Halibut Commission. 2005. Commercial landings of Pacific halibut, 1929–1990 [available from http://www.iphc.washington.edu/component/content/article/12-stock-assessment/122-his-comm-landings.html] and 1974–2002 catch data [available from http://www.iphc.washington.edu/halcom/research/sa/sa.data/rem.y.txt].

Ito, D.H. 1982. A cohort analysis of Pacific Ocean perch stocks from the Gulf of Alaska and Bering Sea regions. M.Sc. thesis, University of Washington, Seattle, Wash.

Kenyon, K.W. 1969. The sea otter in the eastern Pacific Ocean. N. Am. Fauna, **68**: 1–352. doi:10.3996/nafa.68.0001.

Lensink, C.J. 1960. Status and distribution of sea otters in Alaska. J. Mammal. **41**(2): 172–182. doi:10.2307/1376352.

Logerwell, E.A., Mantua, N., Lawson, P.W., Francis, R.C., and Agostini, V.N. 2003. Tracking environmental processes in the coastal zone for understanding and predicting Oregon coho (*Oncorhynchus kisutch*) marine survival. Fish. Oceanogr. **12**(6): 554–568. doi:10.1046/j.1365-2419.2003.00238.x.

Mackinson, S., Deas, B., Beveridge, D., and Casey, J. 2009. Mixed-fishery or ecosystem conundrum? Multispecies considerations inform thinking on long-term management of North Sea demersal stocks. Can. J. Fish. Aquat. Sci. **66**(7): 1107–1129. doi:10.1139/F09-057.

Mantua, N. 2005. PDO Index for 1900–2001. Available from http://jisao.washington.edu/pdo/PDO.latest.

Mantua, N.J., Hare, S.R., Zhang, Y., Wallace, J.M., and Francis, R.C. 1997. A Pacific interdecadal climate oscillation with impacts on salmon production. Bull. Am. Meteorol. Soc. **78**(6): 1069–1079. doi:10.1175/1520-0477(1997)078<1069:APICOW>2.0.CO;2.

Martell, S.D., Walters, C.J., Beattie, A., Nayar, T., and Briese, R. 2001. Simulating historical changes in the Strait of Georgia ecosystem using Ecopath with Ecosim. *In* Report of the 2000 BASS Workshop on the development of a conceptual model of the Subarctic. Pacific basin ecosystems, PICES-GLOBEC International Program On Climate Change And Carrying. Capacity Report of the 2000 BASS, MODEL, MONITOR and REX workshops, and the 2001 BASS/MODEL workshop. PICES Scientific Report, Sidney, B.C., Canada. pp. 9–16.

Mizroch, S.A., and Rice, D.W. 2006. Have North Pacific killer whales switched prey species in response to the depletion of the great whale populations? Mar. Ecol. Prog. Ser. **310**: 235–246. doi:10.3354/meps310235.

National Research Council. 2003. Decline of the Steller sea lion in Alaskan waters: untangling food webs and fishing nets. National Research Council of the National Academies of Science, National Academies Press, Washington, D.C.

Olson, R.J., and Watters, G.M. 2003. A model of the pelagic ecosystem in the eastern tropical Pacific Ocean. Inter-Am. Trop. Tuna Comm. Bull. **22**(3): 133–218.

Orensanz, L.M., Armstrong, J., Armstrong, D., and Hilborn, R. 1998. Crustacean resources are vulnerable to serial depletion — the multifaceted decline of crab and shrimp fisheries in the greater Gulf of Alaska. Rev. Fish Biol. Fish. **8**(2): 117–176. doi:10.1023/A:1008891412756.

Outer Continental Shelf Environmental Assessment Program. 1986. Marine fisheries: resources and environments. Chapter 14. *In* The Gulf of Alaska, physical environment and biological resources. *Edited by* D.W. Hood and S.T. Zimmerman. US Department of Commerce, NOAA, Office of Marine Pollution Assessment, University of Washington Press, Seattle, Wash. pp. 417–458.

Paine, R.T. 1995. A conversation on refining the concept of keystone species. Conserv. Biol. **9**(4): 962–964. doi:10.1046/j.1523-1739.1995.09040962.x.

Pauly, D., Christiensen, V., and Walters, C. 2000. Ecopath, Ecosim and Ecospace as tools for evaluating ecosystem impact of fisheries. ICES J. Mar. Sci. **57**(3): 697–706. doi:10.1006/jmsc.2000.0726.

Pikitch, E.K., Santora, C., Babcock, E.A., Bakun, A., Bonfil, R., Conover, D.O., Dayton, P., Doukakis, P., Fluharty, D., Heneman, B., Houde, E.D., Link, J., Livingston, P.A., Mangel, M., McAllister, M.K., Pope, J., and Sainsbury, K.J. 2004. Ecosystem-based fishery management. Science, **305**(5682): 346–347. doi:10.1126/science.1098222. PMID:15256658.

Piroddi, C., Bearzi, G., and Villy, C. 2010. Effects of local fisheries and ocean productivity on the northeastern Ionian Sea ecosystem. Ecol. Model. **221**(11): 1526–1544. doi:10.1016/j.ecolmodel.2010.03.002.

Polovina, J.J. 1984. Model of a coral reef ecosystem I. The ECOPATH model and its application to French Frigate Shoals. Coral Reefs, **3**(1): 1–11. doi:10.1007/BF00306135.

Polovina, J.J., Mitchum, G.T., and Evans, G.T. 1995. Decadal and basin-scale variation in mixed layer depth and the impact on biological production in the Central and North Pacific, 1960–1988. Deep-Sea Res. **42**(10): 1701–1716. doi:10.1016/0967-0637(95)00075-H.

Press, W.H., Teukolsky, S.A., Vetterling, W.T., and Flannery, B.P. 1992. Numerical recipes in C: the art of scientific computing. 2nd ed. Cambridge University Press, Cambridge, UK.

Rogers, D.E. 1987. Pacific salmon. Chapter 15. *In* The Gulf of Alaska, physical environment and biological resources. *Edited by* D.W. Hood and S.T. Zimmerman. US Department of Commerce, NOAA, Office of Marine Pollution Assessment, University of Washington Press, Seattle, Wash. pp. 461–476.

Scarff, J.E. 1991. Historic distribution and abundance of right whale (*Eubalaena glacialis*) in the North Pacific, Bering Sea, Sea of Okhotsk and Sea of Japan from the Maury whale charts. Rep. Int. Whaling Comm. **41**: 467–489.

Scarff, J.E. 2001. Preliminary estimates of whaling induced mortality in the 19th century North Pacific right whale (*Eubalaena japonicus*) fishery, adjusting for struck-but-lost whales and non-American whaling. J. Cetacean Res. Manag. **2**(Special issue): 261–268.

Sigler, M.F., Lunsford, C.R., Fujioka, J.T., and Lowe, S.A. 2004. Alaska Sablefish Assessment for 2005. *In* Stock assessment and evaluation report for the groundfish resources of the Bering Sea, Aleutian Islands, and Gulf of Alaska, November 2004, Section 3. North Pacific Fishery Management Council, Anchorage, Alaska, USA. pp. 303–368. Available from http://www.afsc.noaa.gov/refm/docs/2004/BSAIsablefish.pdf.

Stabeno, P.J., Bond, N.A., Hermann, A.J., Kachel, N.B., Mordy, C.W., and Overland, J.E. 2004. Meteorology and oceanography of the northern Gulf of Alaska. Cont. Shelf Res. **24**(7–8): 859–897. doi:10.1016/j.csr.2004.02.007.

Stichert, M.A. 2010. Annual management report for shellfish fisheries in the Kodiak, Chignik, and Alaska Peninsula Areas, 2009. Alaska Department of Fish and Game, Anchorage, Alaska. Fish. Manage. Rep. 10-32. Available from http://www.sf.adfg.state.ak.us/FedAidpdfs/FMR10-32.pdf.

Taylor, M.H., Tam, J., Blaskovic, V., Espinoza, P., Ballon, R.M., Wosnitza-Mendo, C., Arguelles, J., Diaz, E., Purca, S., Ochoa, N., Ayon, P., Goya, E., Gutierrez, D., Quipuzcoa, L., and Wolff, M. 2008. Trophic modeling of the Northern Humboldt Current Ecosystem, Part II: Elucidating ecosystem dynamics from 1995 to 2004 with a focus on the impact of ENSO. Prog. Oceanogr. **79**(2–4): 366–378. doi:10.1016/j.pocean.2008.10.008.

Thompson, G.G., Zenger, H.H., and Dorn, M.W. 2003. Chapter 2: Assessment of the Pacific cod stock in the Gulf of Alaska. *In* Stock assessment and fishery evaluation report for the groundfish resources of the Gulf of Alaska, November 2003, Section 2. North Pacific Fishery Management Council, Anchorage, Alaska, USA. pp. 149–242. Available from http://www.afsc.noaa.gov/refm/docs/2003/GOApcod.pdf.

Turnock, B.J., Wilderbuer, T.K., and Brown, E.S. 2003. Arrowtooth flounder. *In* Stock Assessment and fishery evaluation report for the groundfish resources of the Gulf of Alaska, November 2003, Section 5. North Pacific Fishery Management Council, Anchorage, Alaska, USA. pp. 369–406. Available from http://www.afsc.noaa.gov/refm/docs/2003/GOAatf.pdf.

Walters, C.J. 1986. Adaptive management of renewable resources. [Reprint of first edition in 2001.] The Blackburn Press, Caldwell, N.J.

Walters, C., Christensen, V., and Pauly, D. 1997. Structuring dynamic models of exploited ecosystems from trophic mass-balance assessments. Rev. Fish Biol. Fish. **7**(2): 139–172. doi:10.1023/A:1018479526149.

Walters, C.J., and Martell, S.J.D. 2004. Fisheries ecology and management. Princeton University Press, Princeton, N.J.

Walters, C., Martell, S.J.D., Christensen, V., and Mahmoudi, B. 2008. An ecosim model for exploring Gulf of Mexico ecosystem management options: Implications of including multistanza life-history models for policy predictions. Bull. Mar. Sci. **83**(1): 251–271.

Wilderbuer, T.K., Hollowed, A.B., Ingraham, W.J., Jr, Spencer, P.D., Conners, M.E., Bond, N.A., and Walters, G.E. 2002. Flatfish recruitment response to decadal climatic variability and ocean conditions in the eastern Bering Sea. Prog. Oceanogr. **55**(1–2): 235–247. doi:10.1016/S0079-6611(02)00081-2.

Williams, E.H., and Quinn, T.J., II. 2000*a*. Pacific herring, *Clupea pallasi*, recruitment in the Bering Sea and north-east Pacific Ocean, II: relationships to environmental variables and implications for forecasting. Fish. Oceanogr. **9**(4): 300–315. doi:10.1046/j.1365-2419.2000.00146.x.

Williams, E.H., and Quinn, T.J., II. 2000*b*. Pacific herring, *Clupea pallasi*, recruitment in the Bering Sea and north-east Pacific Ocean, I: relationships among different populations. Fish. Oceanogr. **9**(4): 285–299. doi:10.1046/j.1365-2419.2000.00145.x.

Winship, A.J., Trites, A.W., and Calkins, D.G. 2001. Growth in body size of the Steller sea lion (*Eumetopias jubatus*). J. Mammal. **82**(2): 500–519. doi:10.1644/1545-1542(2001)082<0500:GIBSOT>2.0.CO;2.

York, A. 1994. The population dynamics of northern sea lions, 1975–1985. Mar. Mamm. Sci. **10**(1): 38–51. doi:10.1111/j.1748-7692.1994.tb00388.x.

Zerbini, A.N., Waite, J.M., Laake, J.L., and Wade, P.R. 2006. Abundance, trends and distribution of baleen whales off western Alaska and the central Aleutian Islands. Deep Sea Res. Part I Oceanogr. Res. Pap. **53**(11): 1772–1790. doi:10.1016/j.dsr.2006.08.009.

Appendix A. Detailed methods

Modeling the top-down driver: fishing

The GOA ecosystem model is parameterized with 14 fishing fleets that are described in terms of their target species and gear (e.g., walleye pollock trawl, Pacific halibut longline, etc.; Aydin et al. 2007). Target species are defined as the predominant commercially important species in the catch for a particular fleet. Bycatch species in a particular fleet are defined as all species other than the target species, regardless of commercial value or retention (and many are retained). For example, walleye pollock are the target species in the walleye pollock trawl fleet, but they are still caught and retained in the Pacific cod trawl and flatfish trawl fleets, where we would define them as a bycatch species. To initialize the static model, the average annual catch of all target and bycatch species in each modeled fishing fleet was estimated using detailed at-sea observations in groundfish fisheries or using survey information to estimate fishery bycatch for Pacific halibut and other fisheries (see Aydin et al. 2007). The catch data available in Alaska is of very high quality because of the extensive groundfish monitoring and management program (Cahalan et al. 2010; DiCosimo et al. 2010), so for dynamic modeling we condition our model on this catch (i.e., we assume catch indices to be absolute, not relative).

The dynamic model was forced from the top-down with fishing effort in each of the 14 fleets and fit to the sum of catch across these fleets for each commercial species. While there is good catch data in Alaska, effort data is inconsistent, so we used the following method to estimate effort consistently from catch. For each fleet, we first obtained a time series of annual fleet-specific catch for the target species from the National Marine Fisheries Service (NMFS) Alaska Region catch accounting system (for example, catch of walleye pollock in the walleye pollock trawl fleet, a subset of total walleye pollock catch; see http://www.fakr.noaa.gov/sustainablefisheries/inseason/catchaccounting.htm and Cahalan et al. 2010). For each of the 14 fleets, the model then estimates the effort (E_{fleet}) required to remove the fleet-specific catch of the target species ($C_{\text{fleet, target}}$, divided into equal monthly increments summing to the annual total) from the estimated biomass of the target species (B_{target}) in each monthly time step and applies that estimated effort to estimate each bycatch species catch (C_{bycatch}) in that fleet:

$$q_{\text{fleet}} = \frac{C^*_{\text{fleet, target}}}{B^*_{\text{target}}} \tag{A.1}$$

$$E_{\text{fleet}} = \frac{C_{\text{fleet, target}}}{q_{\text{fleet}} \cdot B_{\text{target}}} \tag{A.2}$$

$$C_{\text{bycatch}} = E_{\text{fleet}} \cdot q_{\text{fleet}} \cdot B_{\text{bycatch}} \tag{A.3}$$

where q_{fleet} is the fleet-specific catchability, derived from the 1990s static food web model fleet-specific catch of the target species ($C^*_{\text{fleet, target}}$) and the static food web model biomass of the target species (B^*_{target}; Aydin et al. 2007). If catch calculated in this manner was greater than $0.99B$, catch was set to $0.99B$. Using this approach, under modeled scenarios with insufficient biomass to satisfy the catch, the stock would collapse and tended to remain at low levels. However, a fit criterion was added, fitting the total catch for each species to its observed total; so situations in which the stock was insufficiently productive or at insufficiently high biomass to satisfy catches were penalized heavily in the fitting procedure.

This method allows both direct fishing effects on target species and indirect effects on incidentally caught species to be captured by the model. For example, Pacific cod are caught as target species by three distinct fleets in the GOA model: cod longline, cod trawl, and cod pot. Pacific cod are also caught by several other fleets where they are bycatch species, including Pacific halibut longline, walleye pollock trawl, and flatfish trawl. Therefore, the catches of Pacific cod in the three cod-targeted fleets are used to estimate effort drivers for those fleets, but we fit to the times series of total catch of Pacific cod with the sum of all catches estimated from the effort in all 14 fleets in the GOA model.

This fishing effort calculation assumes that the bycatch observed per unit target species in each modeled fleet is similar to that observed in the early 1990s, which may be inaccurate for earlier time periods because of changes in gear efficiency, availability, etc. However, we lack information on these changes, and representing possibly inaccurate bycatch was thought to be better than assuming no bycatch in groundfish fisheries. Historical fisheries for whales, seals, Pacific salmon, Pacific herring, crab, and shrimp have no information on the bycatch of nontarget species, so they were assumed to have no bycatch. While this is reasonable for the highly selective exploitation of whales, seals, and sea otters, and also perhaps for Pacific salmon and Pacific herring fisheries that target dense spawning aggregations at fixed locations along the shore, this assumption may be poor for the trawl fisheries targeting invertebrates. Illegal, unregulated, or unreported (IUU) fishing was included when published reconstructed time series were available, such as for Soviet whaling in the 1960s and 1970s (Mizroch and Rice 2006). We were unable to find similar time series for IUU fishing on finfish or invertebrates and therefore included no potential impacts of IUU fishing on them here.

Modeling the bottom-up drivers: recruitment and climate

We represent bottom-up effects using two types of information: species-specific recruitment and system-wide primary production. From an ecosystem standpoint, species-specific recruitment integrates mixed effects such as top-down, density-dependent mortality on prerecruits and bottom-up ecosystem productivity for a particular species. However, in a single-species stock assessment sense, recruitment reflects the production (or bottom-up effect) for the fishable adult stock of that species. Recruitment forcing in our study asks what effect changes in the forced species have on the rest of the ecosystem, but cannot distinguish the sources of change for the forced species. Therefore, the recruitment-forced hypotheses are a mix of bottom-up and top-down forcing from an ecosystem point of view, but we use them to evaluate the influence of key species production on ecosystem dynamics.

Recruitment forcing was only attempted for age-structured commercial fish. We implemented delay-difference age structure accounting in this model, which accounts for juvenile population dynamics in monthly time steps and "graduates" juveniles into the adult biomass pool at the defined recruitment age (Walters and Martell 2004). To force the juvenile groups with recruitment time series, we assumed that the stock assessment model-derived recruitment estimates for each year class represented the relative abundance of newly hatched juveniles in that year. Recruitment time series were scaled relative to the numbers of juveniles estimated to comprise the biomass in the 1990s mass balance (Aydin et al. 2007). These relative recruitment time series were then used to force the numbers (and hence the biomass using the equations in Walters and Martell 2004, their box 10.2) of juvenile groundfish under hypotheses 3 (Fishing, PredPrey, Historical Recruitment) and 4 (Fishing, PredPrey, All Recruitment).

There were seven time series of recruitment available for commercial fish species, including walleye pollock, Pacific cod, Pacific herring, arrowtooth flounder, Pacific halibut, Pacific ocean perch (POP), and sablefish (Table 2). The rationale for including only POP, Pacific herring, and walleye pollock are as follows. Some have hypothesized that high historical fishing rates for the previously biomass-dominant POP altered population productivity from that specified using current population parameters from the 1990s and therefore altered system dynamics that were formerly dominated by this pelagic zooplankton feeder (Outer Continental Shelf Environmental Assessment Program 1986). POP had very high historical fishing rates relative to present exploitation rates, and they are long-lived and slow-growing, so they represent a generalized "fishing altered production" hypothesis. A hypothesis applicable to both Pacific herring and walleye pollock suggests that variability in the production of key commercially exploited forage species that is largely independent of fishing explains long-term and recent system dynamics (Bailey 2000; Williams and Quinn 2000). To examine this "keystone environmentally driven forage species" hypothesis, recruitment time series were used to force the system for one commercial forage fish that was heavily exploited historically (Pacific herring) and one commercial forage fish that has only recently been exploited (walleye pollock). Initial fitting experiments led us to combine POP and Pacific herring into one historical recruitment hypothesis and add walleye pollock in a nested all recruitment hypothesis to streamline presentation.

Changing production in the entire ecosystem can be represented by changes in primary productivity, which propagates throughout the food web via predator–prey interactions. The PDO time series was assumed to directly drive changes in production of the large and small phytoplankton groups in the GOA model, reflecting physically forced production hypotheses first raised in Francis and Hare (1994) and indirectly by Bailey (2000). The PDO time series for 1901–2001 (Mantua 2005) was rescaled to have an average value of 1 for the period 1990–1993 so that all previous and subsequent forcing years were relative to the primary production estimated in the base mass balance model (Aydin et al. 2007). The production (*P*/*B*) of the two phytoplankton groups was assumed to be directly proportional to this rescaled PDO time series.

References

Aydin, K., Gaichas, S., Ortiz, I., Kinzey, D., and Friday, N. 2007. A comparison of the Bering Sea, Gulf of Alaska, and Aleutian Islands large marine ecosystems through food web modeling. US Department of Commerce, Washington, D.C. NOAA Tech. Memo. NMFS-AFSC-178.

Bailey, K.M. 2000. Shifting control of recruitment of walleye pollock *Theragra chalcogramma* after a major climatic and ecosystem change. Mar. Ecol. Prog. Ser. **198**: 215–224. doi:10.3354/meps198215.

Cahalan, J., Mondragon, J., and Gasper, J. 2010. Catch sampling and estimation in the Federal groundfish fisheries off Alaska. US Department of Commerce, NOAA Tech. Memo. NMFS-AFSC-205.

DiCosimo, J., Methot, R.D., and Ormseth, O.A. 2010. Use of annual catch limits to avoid stock depletion in the Bering Sea and Aleutian Islands management area (Northeast Pacific). ICES J. Mar. Sci. **67**(9): 1861–1865. doi:10.1093/icesjms/fsq060.

Francis, R.C., and Hare, S.R. 1994. Decadal-scale regime shifts in the large marine ecosystems of the north-east Pacific: a case for historical science. Fish. Oceanogr. **3**(4): 279–291. doi:10.1111/j.1365-2419.1994.tb00105.x.

Mantua, N. 2005. PDO Index for 1900–2001. Available from http://jisao.washington.edu/pdo/PDO.latest.

Mizroch, S.A., and Rice, D.W. 2006. Have North Pacific killer whales switched prey species in response to the depletion of the great whale populations? Mar. Ecol. Prog. Ser. **310**: 235–246. doi:10.3354/meps310235.

Outer Continental Shelf Eenvironmental Assessment Program. 1986. Marine fisheries: resources and environments. Chapter 14. *In* The Gulf of Alaska, physical environment and biological resources. *Edited by* D.W. Hood and S.T. Zimmerman. US Department of Commerce, NOAA, Office of Marine Pollution Assessment, University of Washington Press, Seattle, Wash. pp. 417–458.

Walters, C.J., and Martell, S.J.D. 2004. Fisheries ecology and management. Princeton University Press, Princeton, N.J.

Williams, E.H., and Quinn, T.J., II. 2000. Pacific herring, *Clupea pallasi*, recruitment in the Bering Sea and north-east Pacific Ocean, II: relationships to environmental variables and implications for forecasting. Fish. Oceanogr. **9**(4): 300–315. doi:10.1046/j.1365-2419.2000.00146.x.

Appendix B. Detailed results for each hypothesis

1. Fishing: fishing explains system dynamics

This base model configuration fit the biomass time series poorly overall (Fig. 3) and resulted in extinctions for one third of the modeled species, including Pacific halibut, shortspine thornyhead, POP, and Pacific herring (Fig. 3). However, arrowtooth flounder and walleye pollock show some dynamics similar to their assessed time series, with arrowtooth flounder increasing to current levels after a sharp decline, which is not reflected in the assessment (Fig. 3*d*), and with walleye pollock rapidly increasing over this same period and then declining to previous levels (Fig. 3*i*). Precipitous declines were predicted over the same period for Pacific cod (Fig. 3*e*) and sablefish (Fig. 3*f*). These declines (and the extinctions for POP and shortspine thornyhead in the same years; Figs. 3*j* and 3*g*) coincided because of the high observed catch of POP for those years (over 1 million metric tonnes total; Ito 1982; Hanselman et al. 2003). Model 1 estimated a POP biomass five times smaller than that estimated by the POP stock assessment, so a very high fishing effort was applied to this low biomass to achieve the POP catch, resulting in high bycatch of arrowtooth flounder, sablefish, Pacific cod, and shortspine thornyhead in the rockfish trawl fishery. The model-estimated fishing removal of half the biomass of arrowtooth flounder and Pacific cod in those years (as well as the extinction of Pacific halibut), in turn, appears to release walleye pollock from predation pressure temporarily, as these three fish account for over 70% of walleye pollock mortality in the base food web model (Gaichas et al. 2010). Juvenile Steller sea lion model-estimated biomass mirrors this increase in walleye pollock (Fig. 3*a*). When POP are driven extinct in this base model, the rockfish trawl fishery bycatch of arrowtooth flounderand Pacific cod stops, the populations recover, and walleye pollock populations decline.

2. Fishing, PredPrey: fishing and particular predator–prey interactions explain system dynamics

Estimating vulnerability parameters in Model 2 eliminated the extinctions for Pacific halibut, shortspine thornyhead, and POP observed in Model 1. However, Pacific herring still experienced virtual extinction (and therefore no catches) between 1919 and 1951 (Fig. 4*k*) when large Pacific herring catches were taken in the GOA (Macy et al. 1978). The best fit under this hypothesis was for the Pacific halibut biomass time series (Fig. 4*c*), which was also the best fit to the Pacific halibut time series under any modeled hypothesis (Table 3). Fits to Pacific cod and shortspine thornyhead biomass time series were also reasonable, contributing a small proportion of total negative log likelihood (Table 3). This model fit poorly for arrowtooth flounder, sablefish, Pacific salmon, walleye pollock, Steller sea lions, and pandalids. While the Model 2 POP biomass does not reach the level in the POP stock assessment biomass time series, estimated biomass is sufficient to support the catches removed from the population during the 1960s, so the estimated fishing effort is no longer so intense as to drive other populations extinct or remove sufficient arrowtooth flounder, Pacific cod, and Pacific halibut from the system to release the walleye pollock population (as it was in Model 1 above).

3. Fishing, PredPrey, Historical Recruitment: fishing, particular predator–prey interactions, and POP and Pacific herring production explain system dynamics

This model had improved fits to the POP and Pacific herring biomass time series (as expected), as well as for shortspine thornyhead to a lesser extent (Fig. 5). The hypothesized recruitment for POP prior to the beginning of the 1960s fishery resulted in a good match to the POP stock assessment biomass time series and thus allowed high catches without invoking unreasonably high levels of effort. This resulted in less bycatch of arrowtooth flounder, sablefish, Pacific cod, and shortspine thornyhead. This model failed to match the extent of the decline observed in the POP data (Fig. 5*j*). Similarly, adding a historical recruitment time series for Pacific herring resulted in better agreement with the Pacific herring stock assessment biomass time series (Fig. 5*k*). However, the short overlap between the low or missing points in the hypothesized Pacific herring recruitment time series and the heavy Pacific herring fishing of the early 1920s still contributed to a near-extinction event for Pacific herring in the ecosystem model biomass trajectory, from which observed catches could not have been taken. This model estimated high Pacific halibut biomass relative to the stock assessment between 1930s and the early 1970s (Fig. 5*c*), likely because Pacific halibut eat Pacific herring (at a rate three to four times higher than they eat POP; Aydin et al. 2007). The arrowtooth flounder model fit is also moderately improved under this hypothesis (Table 3), although it is still far from matching the biomass time series. Fits to walleye pollock and sablefish are marginally improved, and the Pacific cod fit is marginally degraded (Figs. 5*i*, 5*f*, 5*e*, and Table 3).

4. Fishing, PredPrey, All Recruitment: fishing, particular predator–prey interactions, and POP, Pacific herring, and walleye pollock production explain system dynamics

As expected, this model resulted in the best fit to walleye pollock in any model (Fig. 6*i*). The fit for juvenile Steller sea lions was best in this model (Fig. 6*a*), mirroring the juvenile walleye pollock trajectory similarly to the Model 1 (Fishing) result. Fits to Pacific cod (Fig. 6*e*) and shortspine thornyhead (Fig. 6*g*) were also the best among all modeled hypotheses.

The fit to arrowtooth flounder also improved when walleye pollock, Pacific herring, and POP recruitment were used as forcing; the ecosystem model biomass trajectory takes a shape similar to the biomass time series, although the rise of arrowtooth flounder is approximately 30 years too early in the ecosystem model. Fits to Pacific halibut, Pacific herring, POP, and pandalid shrimp were slightly improved using this model relative to the Model 3 (Table 3), although the overall and visual fit to the shrimp time series remains poor (Fig. 6*l*). Pacific salmon and sablefish fits were slightly degraded under this hypothesis relative to Model 3, but remained comparably poor across these two models and the first fit only to fishing.

5. Fishing, Climate: fishing and physically mediated changes in primary production at decadal time scales explain system dynamics

Results for this model were similar to those from Model 1 (Fishing). Both result in extinction for Pacific halibut, shortspine thornyhead, POP, and Pacific herring, but in the PDO-forced model Pacific salmon also go extinct in 1951 (Fig. 7). The regime shift of 1946–1947 would translate into lower primary production after that time, but Pacific salmon catches increased from 1942 to 1947 (M. Plotnick, Alaska Department of Fish and Game, personal communication, 2005), so the modeled Pacific salmon population is apparently sensitive to these changes in system productivity. Another similarity between this default vulnerability model and the first forced only with fishing is the inverse relationship between the arrowtooth flounder trajectory (Fig. 7*d*) and the walleye pollock trajectory (Fig. 7*i*). In addition, the juvenile Steller sea lion biomass trajectory (Fig. 7*a*) mirrors that of walleye pollock, as in Model 1. PDO forcing of primary production results in the highest historical biomass of Steller sea lions of any hypothesis examined, although the fit was still poor (Table 3).

6. Fishing, PredPrey, Climate: fishing, physically mediated changes in primary production at decadal time scales, and particular predator–prey interactions explain system dynamics

Estimating vulnerabilities in this model substantially improved fits for Pacific halibut, shortspine thornyhead, POP, and Pacific herring (Fig. 8) relative to Model 5. However, Pacific herring experienced virtual extinction for a slightly longer period than in Model 2 (Fishing, PredPrey), extending from 1921 to 1958. Despite this, the negative log likelihood for the fit to the Pacific herring biomass time series is best for this model (Table 3), as is the fit for POP; both are better fit by the PDO-driven primary production time series than by their own hypothesized recruitment time series. Fits to arrowtooth flounder and sablefish biomass time series are also best in this model (Table 3; Figs. 8*d*, 8*f*). Fitted biomass trajectories for Pacific halibut, Pacific cod, and walleye pollock appear qualitatively similar to each groups' biomass time series (Figs. 8*c*, 8*e*, 8*i*), but the fits are worse than the best fits from Model 2 for Pacific halibut and Model 4 (Fishing, PredPrey, All Recruitment) for Pacific cod and walleye pollock (Table 3). This model's overall fit is greatly degraded by the extinction of Pacific salmon in 1951 (Fig. 8*h*). Over half of the total negative log likelihood for the model comes from the poor fit to the Pacific salmon biomass time series (Table 3).

References

Aydin, K., Gaichas, S., Ortiz, I., Kinzey, D., and Friday, N. 2007. A comparison of the Bering Sea, Gulf of Alaska, and Aleutian Islands large marine ecosystems through food web modeling. US Department of Commerce, Washington, D.C. NOAA Tech. Memo. NMFS-AFSC-178.

Gaichas, S.K., Aydin, K.Y., and Francis, R.C. 2010. Using food web model results to inform stock assessment estimates of mortality and production for ecosystem-based fisheries management. Can. J. Fish. Aquat. Sci. **67**(9): 1490–1506. doi:10.1139/F10-071.

Hanselman, D., Heifetz, J., Fujioka, J.T., and Ianelli, J.N. 2003. Gulf of Alaska Pacific ocean perch. *In* Stock assessment and fishery evaluation report for the groundfish resources of the Gulf of Alaska, November 2003, Section 7. North Pacific Fishery Management Council, Anchorage, Alaska, USA. pp. 429–480. Available from http://www.afsc.noaa.gov/refm/docs/2003/GOAPOP.pdf.

Ito, D.H. 1982. A cohort analysis of Pacific Ocean perch stocks from the Gulf of Alaska and Bering Sea regions. M.Sc. thesis, University of Washington, Seattle, Wash.

Macy, P.T., Wall, J.M., Lampsakis, N.D., and Mason, J.E. 1978. Resources of non-salmonid pelagic fishes of the Gulf of Alaska and eastern Bering Sea. Part 1: Introduction, General fish resources and fisheries, Review of literature on non-salmonid pelagic fish resources. US Department of Commerce, submitted as part of the Outer Continental Shelf Environmental Assessment Program. Northwest and Alaska Fisheries Science Center, National Marine Fisheries Service, NOAA, Seattle, Wash.

Weakened portfolio effect in a collapsed salmon population complex

Stephanie Marie Carlson and William Hallowell Satterthwaite

Abstract: Recent research has highlighted the importance of interpopulation diversity in fostering the stability of population complexes. Here we focus on California's recently collapsed fall-run Chinook salmon (*Oncorhynchus tshawytscha*) and ask whether portfolio effect induced buffering is observed across the complexity hierarchy from individual populations to populations within a river basin (Sacramento, San Joaquin) to the entire Central Valley. Some buffering was observed when comparing the coefficient of variation in adult returns to a given river basin with its constituent populations but not when comparing returns to the entire Central Valley with its constituent basins because of disproportionately many fish returning to the Sacramento Basin. Moreover, we report that positive correlations in population dynamics between rivers were stronger in the last 25 years of the study compared with the first 25 years. Together, these results suggest evidence of only a weak portfolio effect that has deteriorated in recent years. Nonetheless, we also report that correlations between rivers decreased significantly with distance, suggesting that some biocomplexity remains. Our results suggest that the greatest potential for strengthening the portfolio effect would come through restoration of San Joaquin Basin populations, which at low abundance currently contribute little to the overall buffering capacity despite low cross-basin correlations.

Résumé : Des travaux récents ont souligné l'importance de la diversité entre les populations pour favoriser la stabilité des complexes de populations. Nous nous intéressons ici à la montaison d'automne de saumons chinook (*Oncorhynchus tshawytscha*) qui s'est récemment effondrée en Californie et nous cherchons à savoir s'il se produit un phénomène tampon causé par un effet portefeuille dans la hiérarchie de la complexité à partir des populations individuelles, aux populations d'un bassin versant (Sacramento, San Joaquin) et à l'ensemble de la Vallée centrale. On observe un certain effet tampon lorsqu'on compare le coefficient de variation des retours d'adultes dans un bassin versant donné à ses populations constituantes, mais non lorsqu'on compare les retours de l'ensemble de la Vallée centrale à ses bassins constituants, parce qu'un nombre disproportionnellement élevé de poissons retournent au bassin de Sacramento. De plus, nous signalons que les corrélations positives dans la dynamique des populations entre les rivières sont plus fortes durant les 25 dernières années de l'étude que durant les 25 premières. Dans leur ensemble, ces résultats fournissent des indications de l'existence de seulement un faible effet portefeuille qui s'est atténué ces dernières années. Néanmoins, nous signalons aussi que les corrélations entre les rivières décroissent significativement en fonction de la distance, ce qui laisse croire qu'il demeure de la biocomplexité. Nos résultats indiquent que la façon la plus prometteuse de renforcer l'effet portefeuille serait de restaurer les populations du bassin de San Joaquin qui, à faible abondance, contribuent actuellement peu à la capacité tampon globale, malgré les faibles corrélations entre les bassins versants.

[Traduit par la Rédaction]

Introduction

The potential importance of species diversity in fostering stability has been long appreciated in community ecology (MacArthur 1955; Elton 1958; Tilman and Downing 1994). Recently, there has been a growing appreciation for the importance of interpopulation diversity to the stability of population complexes. Much of this latter work has focused on fish stocks, which often display considerable phenotypic diversity and, consequently, decoupled population dynamics, resulting in greater stability in annual returns (e.g., Hilborn et al. 2003; Hutchinson 2008; Schindler et al. 2010) or reduced recruitment variability (e.g., Rogers and Schindler 2008; Greene et al. 2010; Moore et al. 2010). Such biocomplexity (sensu Hilborn et al. 2003) has been shown to be important for long-term sustainability of the larger stock complex and the fisheries that exploit these stocks (Hilborn et al. 2003; Anderson et al. 2008) because of a stabilizing portfolio effect (PE), wherein the variability of the aggregate of stocks is considerably less than the variability of the constituent stocks (Greene et al. 2010; Schindler et al. 2010).

Perhaps the best example of this stabilizing PE comes

Received 10 May 2011. Accepted 31 May 2011. Published at www.nrcresearchpress.com/cjfas on 30 August 2011.
J2011-0003

Paper handled by Associate Editor Ian A. Fleming.

S.M. Carlson. University of California, Department of Environmental Science, Policy, and Management, 130 Mulford Hall #3114, Berkeley, CA 94720, USA.
W.H. Satterthwaite. University of California, Center for Stock Assessment Research, Department of Applied Mathematics and Statistics, Santa Cruz, CA 95064, USA; MRAG Americas, P.O. Box 1490, Capitola, CA 95010, USA.

Corresponding author: Stephanie M. Carlson (e-mail: smcarlson@berkeley.edu).

Can. J. Fish. Aquat. Sci. **68**: 1579–1589 (2011) doi:10.1139/F2011-084 Published by NRC Research Press

from research on the Bristol Bay sockeye salmon (*Oncorhynchus nerka*) complex (e.g., Hilborn et al. 2003; Greene et al. 2010; Schindler et al. 2010). This research has revealed that spatially aggregated returns to Bristol Bay were 41%–77% more stable (as measured by reduction in coefficient of variation (CV) in production) than individual stocks (Schindler et al. 2010), because of the diverse life histories within this complex (Greene et al. 2010). This work highlights the importance of population diversity for stabilizing resource flows to industries and ecosystems and contributes to a growing body of research emphasizing the importance of biocomplexity among fish stocks in promoting stability (e.g., Hutchinson 2008; Olsen et al. 2008). Aggregated stocks are buffered to changing conditions by a diversity of responses made possible by behavioral (Kerr et al. 2010) and life history diversity (Greene et al. 2010), which reflects both genetic diversity and phenotypic plasticity in the constituent stocks, as well as habitat heterogeneity (Oliver et al. 2010). However, it is also important to realize that some degree of stabilization should be expected in any aggregate measure made by summing variable components unless those components are perfectly correlated. In fact, this is a statistical inevitability (Doak et al. 1998).

Here we ask, what happens when biocomplexity is lost? We address this question by focusing on California's recently collapsed Central Valley fall-run Chinook salmon (*Oncorhynchus tshawytscha*), which support the California and southern Oregon Chinook salmon fishery. In spring 2008, state and federal fishery managers imposed an emergency closure of this fishery because of anticipated poor returns (Lindley et al. 2009). The fishery closure represented the first in the fishery's 157 year history. California's Central Valley Chinook salmon have been impacted by various anthropogenic activities (e.g., dams, habitat loss, hatcheries), all of which have likely contributed to a loss of biocomplexity.

We use long-term time series data for multiple populations of fall-run Chinook salmon breeding in California's Central Valley to test for evidence of a weak PE in this collapsed stock complex. We expect much biocomplexity has been lost because of degradation of the system, but the potential for a PE remains because the Central Valley contains multiple rivers with remaining stocks. Here we quantify variation in returns across the complexity hierarchy from individual rivers to the aggregated stocks and quantify the degree of independence in dynamics between the different rivers. We hypothesize that there should be some buffering even in a degraded system because the component stocks will not be perfectly correlated. We thus predict that there will be a measurable PE in the Central Valley despite its degraded state and that the degree of buffering will increase with an increasing number of component stocks making up a stock complex. In addition, we hypothesize that degraded basins will contain populations exhibiting little biocomplexity, resulting in higher mean correlations between their constituent rivers and less buffering.

Materials and methods

The system

Pacific salmon are structured into discrete breeding populations because of their natal homing behavior (e.g., Dittman and Quinn 1996). These reproductively isolated populations are then subject to local selection pressures, including a suite of local biotic and abiotic factors. Many fitness-related traits are heritable (Carlson and Seamons 2008), thus allowing for natural selection to drive adaptation to local conditions. The combination of natal homing and their use of a diversity of breeding and rearing habitats results in considerable intraspecific variation in phenotypic traits and population productivity. Historically, Chinook salmon breeding in the Central Valley rivers displayed extraordinary life history diversity (e.g., Fisher 1994; Yoshiyama et al. 2000; Williams 2006). Indeed, this is the only system across the entire range of the species known to contain four distinct breeding migrations or "runs" (fall, late fall, winter, and spring). Moreover, each of the four major Central Valley runs was historically composed of several distinct stocks, each breeding in distinct sites and, thus, encountering distinct local conditions and exhibiting distinct life histories (Lindley et al. 2007).

Construction of dams on nearly all of the major rivers in the Central Valley resulted in a selective loss of habitats, which disproportionately affected certain life history components (e.g., Lindley et al. 2007; McClure et al. 2008). Dam construction resulted in a rapid loss of Central Valley winter-run and spring-run Chinook (now federally endangered and threatened, respectively), because of a lack of access to historic breeding sites and modified flow and temperature regimes. To mitigate for lost breeding habitat, five hatcheries were established to propagate fall-run Chinook salmon, which naturally breed in low-elevation reaches of large rivers (Moyle 2002). Recent work suggests that the fall-run populations breeding in the different river systems are now genetically indistinguishable (e.g., Williamson and May 2005), presumably because of a long history of movement of individuals (gametes) among hatcheries as well as considerable and ongoing straying of hatchery-produced fish as adults (CDFG/NOAA 2001). Even more alarming is the recent finding that over 90% of the fish captured in the ocean fishery are of hatchery origin (Barnett-Johnson et al. 2007), suggesting that the fall-run stock is composed largely of hatchery-produced fish. An overall goal of ours is to understand the extent of buffering achieved in this system given the current state of the habitat and management activities, and consequently we focus our analyses on total adult returns, which includes both natural and hatchery production.

Adult production data

All of the analyses described herein are based on estimates of total (natural and hatchery production combined) adult returns for fall-run Chinook salmon to rivers in the Central Valley of California, USA (Fig. 1). These numbers were obtained from the CHINOOKPROD data set, maintained by the US Fish and Wildlife Service's Anadromous Fish Restoration Program (http://www.fws.gov/stockton/afrp). This data set is an attempt to estimate both natural production ("wild" fish) and total production (natural production + hatchery production), and we focused on the latter. These totals reflect escapement as well as ocean and in-river harvest. These data have been collected over a period of over five decades by multiple researchers using multiple methods. There are many caveats (e.g., different sampling methods in different time periods and sites) and many sim-

Fig. 1. Map of the Central Valley in California, USA, with our study rivers indicated. The five populations supported by hatchery production are denoted with an asterisk.

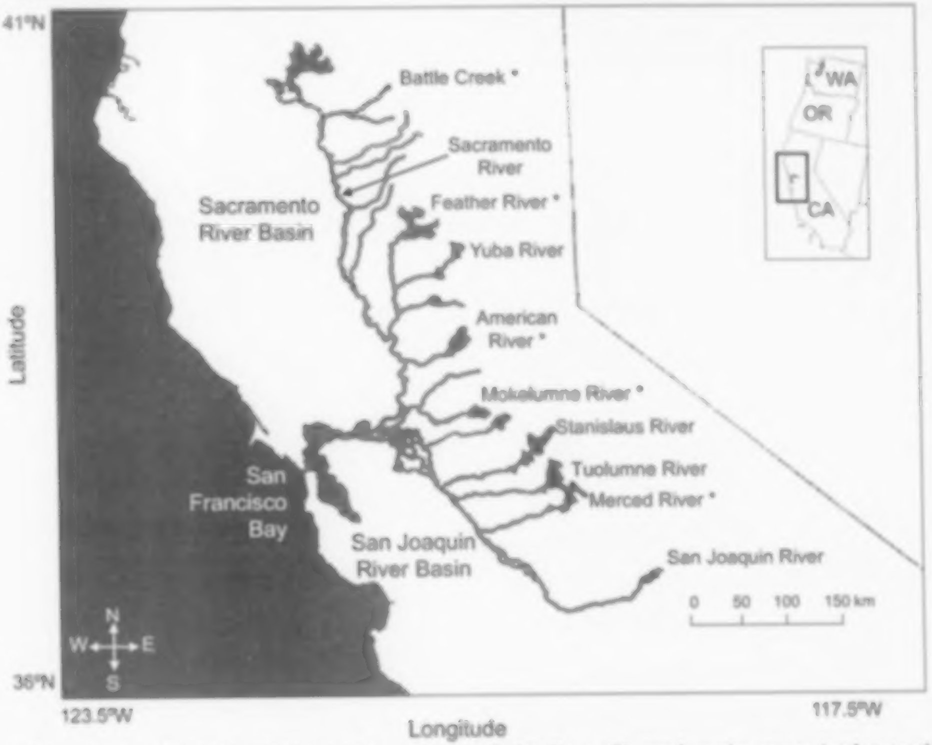

plifying assumptions (e.g., all stocks subject to the same ocean harvest rates) that clearly have the potential to influence the final estimates of adult returns to different sites. We relied on expert opinion to guide our choice of which data to use for analyses, for example, the underlying escapement data (i.e., GRANDTAB data, also available from http://www.fws.gov/stockton/afrp) are those used by management agencies, such as NOAA Fisheries (e.g., Lindley et al. 2007; Williams et al. 2007; NMFS 2010). Additionally, we performed simulations to explore the possible impacts of observation error on our analyses, which we found to be minimal (Appendix A).

We restricted our analysis to nine rivers, representing both river basins, for which data were available for at least 51 of the 52 years from 1957 to 2008. From the Sacramento River Basin (hereafter SAC Basin), we included the mainstem Sacramento River (Princeton Ferry to Keswick Dam), Battle Creek, the Feather River, the Yuba River, and the American River. From the San Joaquin River Basin (hereafter SJ Basin), we included the Mokelumne River, the Stanislaus River (missing data for 1982), the Tuolumne River, and the Merced River (Fig. 1). Five of these populations are supported by hatchery production: American, Battle, Feather, Merced, and Mokelumne.

We were thus able to assess buffering across the full complexity hierarchy from individual rivers to the two river basins to the entire Central Valley. We note two special cases: the Mokelumne River (SJ Basin) and Battle Creek (SAC Basin). The Mokelumne River is a special case because although it naturally flows into the San Joaquin River, the Delta Cross Channel carries water (and potentially fish) from the Sacramento River into it as well. Battle Creek also represents a special case because counts on this river show an obvious upward trend since the 1980s that may inflate our estimate of variation in that system. Thus, we repeated all analyses of the SJ Basin with and without the Mokelumne River and all analyses of the SAC Basin with and without Battle Creek.

Quantifying buffering induced by the PE

Pooling all years together, we calculated the CVs in adult returns for each river separately. We quantified potential buffering induced by the PE by comparing the mean CV for individual rivers with the CV calculated at larger scales, first pooling together all production within each basin and finally pooling together all rivers in our data set (see also Schindler et al. 2010). We used total adult returns rather than an index of productivity (e.g., recruits per spawner) because our data did not allow distinguishing among returning adults from different birth-year cohorts. Because we are missing data from the Stanislaus River in 1982, we excluded 1982 from all calculations of CV. We excluded 1982 regardless of whether the Stanislaus River was included in a calculation to avoid confounding effects of using different data sets for the other rivers for calculations including and excluding the Stanislaus.

To assess the importance of the number of substocks in buffering the total stock complex, within each basin we also compared the CV calculated for each river independently with that calculated for each possible grouping of two, three, four, and five rivers. We did not attempt to assess this rela-

Fig. 2. The absolute contributions of fall-run Chinook salmon from the two major river basins (black area: San Joaquin; grey area: Sacramento) within California's Central Valley to the total adult production (catch plus escapement). Note that this is a stacked plot so that the sum of the black plus grey areas represents the total returns to the Central Valley.

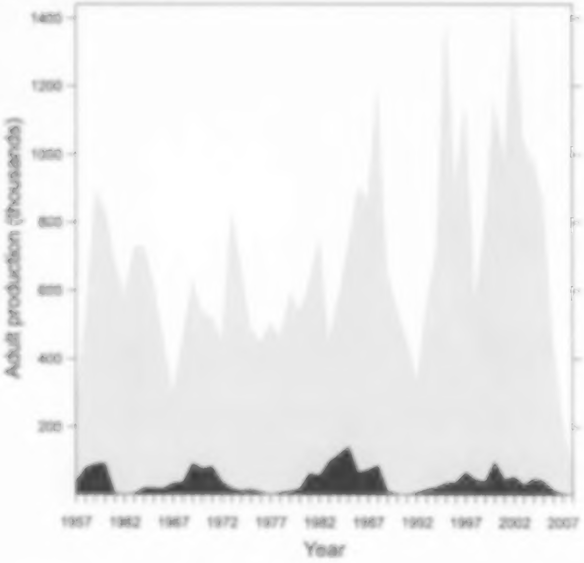

tionship statistically because the data violated several assumptions of regression and other common model-fitting tools: the variance is nonhomogeneous, the number of replicates varied across values of the independent variable, and there was non-independence among data points since the populations in each river contribute to multiple data points.

Quantifying degree of independence in dynamics between different rivers

To assess the degree of independence between dynamics in the different rivers, we calculated Pearson's correlation coefficients between all pairs of rivers. When testing the statistical significance of each correlation coefficient, we used one-tailed tests because we were specifically interested in positive correlations between rivers that would indicate synchronous dynamics. In testing for the significance of correlations, we adjusted the degrees of freedom to account for temporal autocorrelation in return numbers using the methods of Pyper and Peterman (1998).

We compared the mean level of correlation between basins and across basins using Wilcoxon rank sum tests because correlations were typically not normally distributed. We used one-tailed tests on the hypotheses that mean correlation would be higher within basins than across basins, and that mean correlation would be higher in the more degraded SJ Basin. We examined the relationship between the distance between rivers and correlations in their dynamics using Mantel tests (Legendre and Legendre 1998) on the entire Central Valley and within each basin separately. The distance between each river was calculated based on the river distances between the confluences of each river with the mainstem Sacramento or San Joaquin rivers, with three exceptions. First, we defined the "confluence" for the mainstem Sacramento to be Princeton Ferry, the location above which censuses were taken for the mainstem Sacramento return numbers. Second, as Battle Creek flows into the mainstem Sacramento above this point, we considered Battle Creek and the mainstem Sacramento to be coincident in space. Finally, we considered the Feather and Yuba rivers coincident because the Feather flows into the Yuba upstream of its confluence with the mainstem Sacramento. We obtained these distances from the NHDPlus data set (http://www.horizon-systems.com/nhdplus/).

Fig. 3. Estimated number of fall-run Chinook adults produced each year on the focal rivers in the Sacramento River (*a*) or San Joaquin River (*b*) basins.

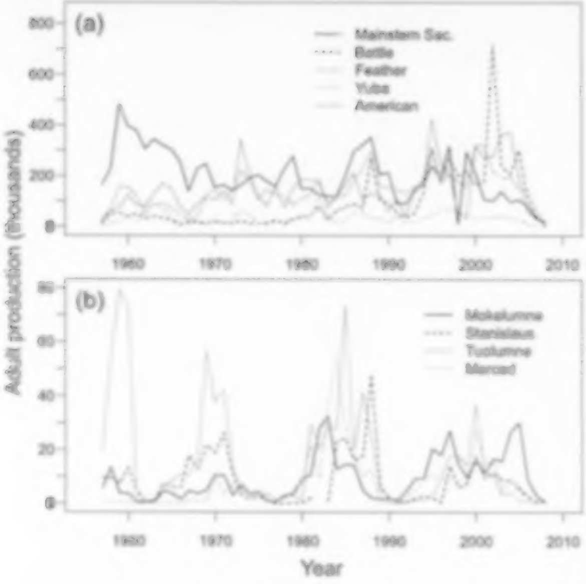

We performed an additional comparison between the first 25 years and last 25 years of our data set to explore whether there was evidence for a weakened PE over time. We calculated correlations among river returns and reductions in CV at various levels of aggregation as before. In addition, we checked for a temporal change in the evenness of the system by computing the Shannon diversity index (Shannon 1948; Krebs 1989) for mean returns to rivers in the various basins in both time periods.

All statistical analyses used R (R Development Core Team 2010). For Mantel tests, we used the "mantel" function in package "vegan" (Oksanen et al. 2011). Tests of the significance of correlation coefficients used R code modified from Rogers and Schindler 2008, available upon request.

Results

Buffering induced by the PE

The total return to the SAC Basin was typically an order of magnitude larger than that to the SJ Basin (Fig. 2). Estimated production for each river varied somewhat asynchronously through time (Fig. 3), with a range of means and variability (Table 1).

Table 1. Mean, standard deviation (SD), and coefficient of variation (CV) in the estimated number of fall-run Chinook adults produced each year on the focal streams in the Sacramento River (*i*) or San Joaquin River (*ii*) basins.

	Sacramento River Basin					San Joaquin River Basin			
	Mainstem	Battle	Feather	Yuba	American	Mokelumne	Stanislaus	Tuolumne	Merced
Mean	200 270	95 818	137 791	33 156	149 707	8 791	8 417	16 493	7 551
SD	100 309	123 449	75 013	20 201	93 604	8 060	9 223	20 868	10 369
CV	0.501	1.288	0.544	0.609	0.625	0.917	1.096	1.265	1.373

The mean CV for returning adult numbers for individual SAC Basin rivers was 0.714 ± 0.325 (mean ± standard deviation, SD) or 0.570 ± 0.058 when excluding Battle Creek. Pooling all rivers within the SAC Basin together reduced the CV to 0.440 (Fig. 4*a*), a 38% reduction compared with the individual river mean (or to 0.375 for a 34% reduction when excluding Battle Creek). The mean CV for returning adult numbers for individual SJ Basin rivers was 1.163 ± 0.200 (or 1.245 ± 0.140 when excluding the Mokelumne River). Pooling all rivers within the SJ Basin together reduced the CV to 0.850 (Fig. 4*a*), a 27% reduction compared with the individual mean (or to 0.987 for a 21% reduction when excluding the Mokelumne River). By this measure, buffering is more effective in the SAC Basin, although some of this increased buffering may be attributable to the larger number of rivers pooled in our data set for the SAC Basin. (Similarly, this may explain why we observed less CV reduction when excluding Battle Creek or the Mokelumne River.) We can remove this sample size effect by considering how much reduction in CV we would expect after pooling together different numbers of rivers in an ideal system, with zero correlation between rivers and equal average abundances. According to eq. 1 of Doak et al. (1998), we would expect a 55.3% reduction in CV when pooling together five ideal rivers and 50.0% reduction in CV when pooling together four ideal rivers; thus we would expect a 10.6% larger reduction in the CV for the SAC Basin before accounting for the effects of evenness and correlation structure. Instead, we observed a 40.7% larger reduction in CV for the SAC Basin, suggesting stronger buffering effects in the SAC Basin even after accounting for the number of rivers in each system. Pooling all rivers together yielded a CV of 0.430 (Fig. 4*a*), a 2% reduction compared with pooling just the SAC Basin rivers, which numerically dominated total production (Fig. 2), and a 49% reduction compared with pooling just the SJ Basin rivers.

In general, the buffering effect, as measured by percent decrease in CV, increased with the number of stocks making up a stock complex (Fig. 4*b*). While we were unable to rigorously compare the fit of alternate model formulations, it would appear that there are diminishing returns in the amount of additional buffering achieved as additional rivers are added (a result expected from theory, see Doak et al. 1998). Note that for both basins, the minimum possible CV is achieved by pooling only a subset of the available rivers (Fig. 4*b*).

Degree of independence in dynamics between different rivers

Taking data from all years together, the mean pairwise correlation between rivers within the SAC Basin was 0.268 ± 0.260 (mean ± SD) compared with 0.313 ± 0.190 for the SJ Basin, 0.285 ± 0.230 for all within-basin pairings, and 0.135 ± 0.258 for rivers from different basins (Table 2). The difference in mean correlations for within-basin versus across-basin pairings was significant (Wilcoxon $W = 216$, $p = 0.039$ one-tailed), while the difference in mean correlations within each basin was not. Excluding Battle Creek and the Mokelumne River from this analysis reduced the mean pairwise correlation among SAC Basin rivers to 0.257 ± 0.258 and increased the mean for SJ Basin rivers to 0.390 ± 0.142, a statistically significant difference ($W = 126$, $p = 0.047$ one-tailed).

Taking all rivers together, there was a statistically significant decrease in pairwise correlation with increasing distance between rivers, but this effect was slight and only explained a small amount of total variation (Fig. 5; Mantel test $r = 0.3432$, $p = 0.0409$). Within basins, there was no significant effect of distance between rivers on their pairwise correlations ($r < 0.128$ for both basins). With Battle Creek and the Mokelumne River excluded, the relationships between geographical distance and correlation remained statistically insignificant ($p = 0.255$ for SAC Basin, $p = 0.331$ for SJ Basin).

Testing for evidence of a weakened PE

To test for changes in the strength of the PE through time, we compared the strength of the PE in the first and last 25 years of our data set. This does not represent a comparison with pristine conditions, but could detect evidence for ongoing deterioration of the PE. We found that for the SAC Basin, pooling rivers together reduced CV by 46% in the first 25 years but only 28% in the last 25 years, suggesting ongoing deterioration of the PE. By contrast, reduction in CV was similarly small in both halves of our data set for the SJ Basin (19% in first half, 23% in second half). The weakening PE in the SAC Basin seems to have been driven largely by increasing correlation among rivers (from 0.23 to 0.39), since evenness increased only slightly during this period (Shannon diversity index increased from 1.34 to 1.51). Correlations also increased somewhat for the San Joaquin system (from a mean of 0.31 to 0.37), but this was offset by increasing evenness (Shannon diversity index increased from 1.15 to 1.37).

Discussion

Our analysis of California's recently collapsed Central Valley fall-run Chinook salmon yielded several salient results. First, despite the genetically homogeneous (Williamson and May 2005) and collapsed (Lindley et al. 2009) state of this stock complex, some variance buffering in adult returns was achieved. For example, adult returns to the Central Valley were 2%–53% more stable (as measured by reduction in the CV of returns at various scales of aggregation) than the variability in component stocks. This reduction suggests that

Fig. 4. Coefficient of variation (CV) in production as a function of the number of rivers pooled together to represent stock complex dynamics. In panel (*a*), we show the CV for individual rivers as well as the mean CV for individual rivers within each basin (error bars are ±1 standard error, SE), for each basin with all rivers pooled, and for the entire Central Valley with all rivers from both basins pooled together. In panel (*b*), we show the CV of each possible grouping of one, two, three, four, or five rivers from within each basin. Circles are from the SAC Basin; squares are from the SJ Basin.

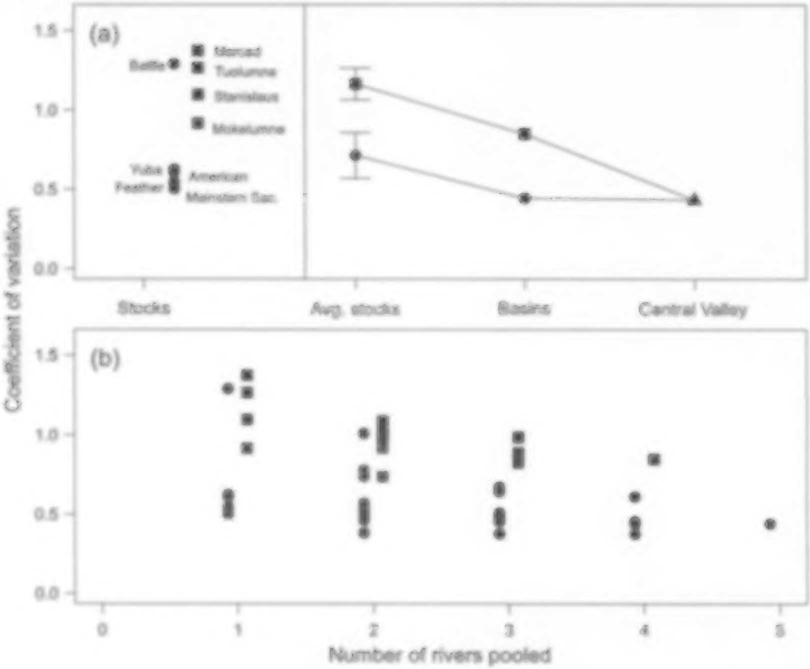

Table 2. Pairwise correlations between each pair of rivers, for all years combined.

	Main.	Battle	Feather	Yuba	American	Stanislaus	Tuolumne	Merced
Mainstem	—	–0.110	0.085	0.188	–0.063			
Battle		—	0.487*	0.213	0.552*			
Feather			—	0.242	0.668*			
Yuba				—	0.422*			
Mokelumne					—	0.084	0.122	0.498*
Stanislaus	0.225	0.177	0.273	–0.062	0.02	—	0.551*	0.339
Tuolumne	0.374*	–0.098	0.062	–0.131	–0.105		—	0.281
Merced	–0.185	0.21	0.275	0.037	0.252			—

Note: An asterisk (*) indicates significant correlation at $p < 0.05$ in a one-tailed test after accounting for temporal autocorrelation. Within-basin correlations are shown above the diagonal (highlighted with dashes), across-basin correlations are shown below the diagonal. Note that the Mokelumne does not appear as a column and the American does not appear as a row, as this allows the most compact table.

some buffering exists against reaching dangerously low abundances and effective economic extinction of the fishery. The weak PE that we observed was due largely to the nonperfect correlations in returns among rivers even in the face of reduced genetic diversity (Williamson and May 2005). Moreover, we observed a weak but statistically significant decrease in pairwise correlations with increasing distance between the focal rivers and lower correlations across basins than within. It is possible that observation error may inflate our estimate of PE strength, but as noted earlier, some degree of buffering is a statistical inevitability — even in degraded systems. Moreover, observation error would only weaken our ability to find significant geographic patterns in correlations (see Appendix A). Together, these results underscore the importance of maintaining multiple stocks even within degraded systems and highlight the possibility of improving buffering in degraded systems by fostering biocomplexity.

Second, despite the fact that some buffering was achieved in this degraded system, several lines of evidence suggest that the Central Valley fall-run Chinook stock complex represents a weak portfolio of stocks. For example, adult returns to the Central Valley as a whole were only 2% more stable (as measured by reduction in CV) than returns to the SAC Basin. This result reflects the considerable difference in adult returns to the two river basins. In particular, the SJ Basin contributes only a small amount to total adult returns to the Central Valley, and consequently, the variability in Central Valley production is driven largely by the variability in pro-

Fig. 5. Pairwise correlations between rivers within basins and across basins. The horizontal line at $y = 0$ indicates a correlation of zero and divides the plot into those correlations that are positive (above) versus negative (below). Circles are from the SAC Basin, squares are from the SJ Basin, and triangles represent cross-basin pairings.

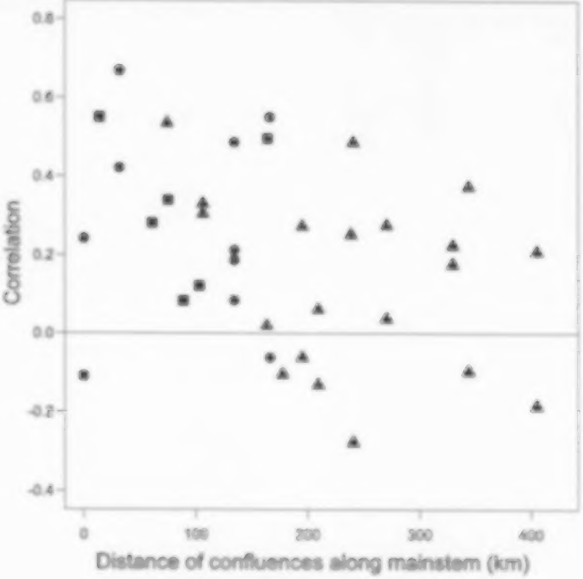

duction from the SAC Basin, and the small San Joaquin stocks contribute little buffering to the system. Moreover, production of rivers within the SJ Basin were more correlated (all pairwise correlations were positive, and 3/6 were significant) compared with production of rivers within the SAC Basin (all pairwise correlations were positive, and 4/10 were significant). One explanation for the apparently linked demography of the San Joaquin stocks is a shared environmental stressor that disproportionately impacts SJ Basin salmon. In general, salmon migrating downstream through the SAC Basin have a relatively direct downstream migration path to San Francisco Bay. In contrast, salmon migrating from the SJ Basin have to outmigrate through the south–middle delta to reach San Francisco Bay. This seemingly more difficult migration pathway (e.g., Brandes and McLain 2001) is a shared obstacle that the San Joaquin stocks must overcome and likely contributes to the higher observed correlations among the San Joaquin stocks.

Additional support for our conclusion of a weak PE in the Central Valley system derives from a comparison of the observed degree of reduction in CV to what would be achievable in an ideal system (even abundances with zero correlation). We found that pooling together the five rivers of the SAC Basin reduced CV by 38%, pooling together the four rivers of the SJ Basin reduced CV by 27%, and pooling together all nine rivers of the Central Valley reduced CV by 40%. In an ideal case, Doak et al. (1998, their eq. 1) show that the achievable reduction in CV would be 55%, 50%, and 67% for pooling together five, four, and nine populations, respectively. Thus, considerably less reduction in variance is achieved than in the ideal case, especially when pooling together the SAC and SJ basins. This is despite the possibility that measurement error inflated our estimate of CV reduction.

Of course, even in a pristine system, we would not necessarily expect exactly equal abundances or lack of correlation among streams, since returns would be strongly affected by shared ocean conditions. Unfortunately, there are no data available to quantify how much buffering this system was capable of in the past or even how well correlated and how even in abundance the component rivers were. However, our comparison of the estimated strength of the PE in the first and last 25 years of our data set suggests a weakened PE in this stock complex in more recent years. This result seems to have been driven largely by increasing correlation among rivers within the SAC Basin — a pattern that was also observed among rivers of the SJ Basin although to a lesser degree. This does not represent a comparison with pristine conditions but nevertheless suggests evidence of recent deterioration of the PE in this stock complex.

Third, we observed “diminishing returns” in terms of how much buffering was achieved through the addition of more stocks, as measured by the CV, although of course adding rivers has the added benefit of increasing the total stock complex size. Additionally, we found that a careful choice of a few uncorrelated stocks actually produced better buffering, as measured by the CV, than all stocks combined. This latter result was unexpected and leads us to suggest that caution is warranted when interpreting buffering results using the CV approach.

Coefficient of variation as a metric of stability

Earlier work quantifying the PE in Bristol Bay sockeye salmon focused on a system with few anthropogenic impacts beyond harvest (e.g., Hilborn et al. 2003; Greene et al. 2010; Schindler et al. 2010). In stark contrast, Central Valley Chinook salmon are subject to multiple anthropogenic impacts that interact in complex ways, including loss of breeding and rearing habitat due to an extensive network of dams, extensive flow alterations both in rivers and through the Sacramento–San Joaquin Delta, substantial influence of hatchery-reared salmon, and the presence of mixed-stock fisheries that do not discriminate between relatively strong (hatchery-produced) and weak (naturally produced) stocks (for another example from a system experiencing multiple anthropogenic impacts, see Moore et al. 2010). Our expectation was that there would be little evidence of portfolio-induced buffering across the complexity hierarchy for the degraded Central Valley stocks, but this was not always the case — a result that led us to consider some of the weaknesses of the CV as a metric of stability.

Somewhat unexpectedly, for example, we observed a high degree of variance buffering in the severely degraded SJ Basin stocks, as measured by reduction in CV. Returns to the SJ Basin are typically an order of magnitude less than returns to the SAC Basin, and yet pooled returns to the SJ Basin were reduced by nearly as much as pooled returns to the SAC Basin (38% vs. 27% reduction in CV compared with the mean CV for individual rivers within a basin for the SAC and SJ basins, respectively). Because the CV is calculated as the standard deviation divided by the mean, variation in the CV among stocks can reflect differences in standard deviation about the mean or differences in the means themselves. In the case of the SJ Basin stocks, the high CVs observed for these stocks appear to be the consequence of the low mean returns.

Moreover, the buffering observed in the SJ Basin extended across the full complexity hierarchy from individual rivers to the basin (described above) and from the basin to the Central Valley. In contrast, efficient buffering within the SAC Basin was observed only when comparing individual rivers with the basin but not when comparing CVs for the SAC Basin with the Central Valley. This result highlights an important point, which is that effective buffering requires both low correlation among constituent stocks and comparable means. In other words, fluctuations in a large stock complex, like the Sacramento, will not be buffered through the addition of a small stock complex, like the San Joaquin, even if the two are negatively correlated (see also Doak et al. 1998, their eq. 6). Shared ocean conditions may limit the extent to which river dynamics can be decoupled, even if their environments and hatchery production practices are quite different. To that end, it is interesting to note that reduced correlations across basin boundaries may reflect differential use of the ocean by different stocks. Within the Central Valley, Myers et al. (1998) noted a tendency toward maturation at younger ages along with spawning later in the year for San Joaquin salmon, suggesting some difference in their ocean ecology. In other systems, Koseki and Fleming (2006) suggested that ocean dynamics operating at different spatial scales may be important in determining the dynamics of jack versus hooknose coho (*Oncorhynchus kisutch*). In a follow-up paper, Koseki and Fleming (2007) suggest differential importance of freshwater versus ocean conditions in synchronizing naturally produced versus hatchery fish. A better understanding of the spatial distribution of different components of population complexes would greatly improve our ability to understand the factors driving variation in their dynamics.

For all of these reasons, we suggest some caution in using CV as a metric of stability. Other important metrics that could be monitored include those with mechanistic links to reduced variability, such as (*i*) correlations among components of a stock complex (e.g., Rogers and Schindler 2008), (*ii*) life history diversity including age composition (e.g., Greene et al. 2010) or the timing of migrations, and (*iii*) evenness among components of a stock complex (e.g., this study) — all of which could be monitored through time. Of course, evenness that results from a uniform decrease in mean abundance is not an effective buffer against risk, and negative trends in overall abundance are an obvious sign of trouble regardless of CV.

Management implications

Our results suggest that for the most effective buffering in this system, restoring the SJ Basin populations should be prioritized. If even a single population within this basin could be increased to a size comparable to one of the SAC Basin populations, this would contribute substantial buffering to the system because of the generally low correlations across basins. One major question then becomes whether it is better to improve production in the SJ Basin by improving the environment, which may take a long time, or through hatchery production, which may foster homogeneity among rivers. Here we argue that restoring environmental heterogeneity, which is the template that gives rise to local adaptations and diverse life history portfolios, will pay larger dividends in the long run. Projects designed to improve access to rivers in the southern part of the SJ Basin, for example, could restore populations with different life histories than those in the northern SJ Basin rivers, thereby improving the buffering capacity of the system. It is believed that the San Joaquin once supported a very large (but since extirpated) spring run (Yoshiyama et al. 1998). Both spring- and fall-run fish were found on multiple rivers in the SJ Basin, with "very large" populations on the Merced, Tuolumne, and upper San Joaquin rivers (Yoshiyama et al. 1998). A late fall run may have occurred on some rivers as well. Even partially restoring these numbers and this life history diversity would considerably aid buffering in the Central Valley Chinook salmon complex.

Moreover, ameliorating passage through the Sacramento–San Joaquin Delta holds substantial promise for improving the buffering capacity of the larger stock complex. If indeed difficult passage is why the San Joaquin run sizes are currently low, improving passage has the potential to increase run sizes on several San Joaquin rivers simultaneously, assuming they have adequate habitat to support larger populations. In addition, removing this shared bottleneck may lead to different limiting factors on the different rivers, thereby reducing correlations between them. Having multiple rivers with larger, less correlated runs will greatly increase buffering induced by the PE within this salmon stock complex. In general, managers of other systems need to consider how restoring a particular part of a system will contribute to the evenness and correlation structure of the complex and target restoration accordingly.

Finally, because one of our goals was to understand the buffering capacity in this collapsed stock complex given the current state of habitat and management activities in the Central Valley, we did not treat differently rivers with (n = 5) and without (n = 4) hatcheries. In the future, we plan to explicitly test how hatchery management activities influence evenness and correlation structure among these populations to illuminate the impact of management on the buffering capacity and stability of this stock complex.

Acknowledgements

We thank Eric Huber for assistance with data organization, Ethan Mora for calculating distances between rivers, Rachel Barnett-Johnson for providing the map, Lauren Rogers for sharing R code, and Rick Burmester with US Fisheries and Wildlife Service for answering questions about the available data sets. The manuscript was improved greatly through comments by Josh Israel, Steve Lindley, John Williams, and Ron Yoshiyama. S.M. Carlson was supported by National Science Foundation (DEB-0915173).

References

Anderson, C.N.K., Hsieh, C.H., Sandin, S.A., Hewitt, R., Hollowed, A., Beddington, J., May, R.M., and Sugihara, G. 2008. Why fishing magnifies fluctuations in fish abundance. Nature, **452**(7189): 835–839. doi:10.1038/nature06851. PMID:18421346.

Barnett-Johnson, R., Grimes, C.B., Royer, C.F., and Donohoe, C.J. 2007. Identifying the contribution of wild and hatchery Chinook salmon (*Oncorhynchus tshawytscha*) to the ocean fishery using otolith microstructure as natural tags. Can. J. Fish. Aquat. Sci. **64**(12): 1683–1692. doi:10.1139/f07-129.

Brandes, P.L., and McLain, J.S. 2001. Juvenile Chinook salmon abundance, distribution, and survival in the Sacramento–San Joaquin estuary. Calif. Dep. Fish Game Fish Bull. **179**(2): 39–138.

Carlson, S.M., and Seamons, T.R. 2008. A review of quantitative genetic components of fitness in salmonids: implications for adaptation to future change. Evol. Appl. **1**(2): 222–238. doi:10.1111/j.1752-4571.2008.00025.x.

CDFG/NOAA. 2001. Final report on anadromous salmonid fish hatcheries in California [online]. Available from https://nrmsecure.dfg.ca.gov/FileHandler.ashx?DocumentID=3346.

Dittman, A.H., and Quinn, T.P. 1996. Homing in Pacific salmon: mechanisms and ecological basis. J. Exp. Biol. **199**(1): 83–91. PMID:9317381.

Doak, D.F., Bigger, D., Harding, E.K., Marvier, M.A., O'Malley, R.E., and Thomson, D. 1998. The statistical inevitability of stability–diversity relationships in community ecology. Am. Nat. **151**(3): 264–276. doi:10.1086/286117. PMID:18811357.

Elton, C.S. 1958. The ecology of invasions by plants and animals. Chapman and Hall, London, UK.

Fisher, F.W. 1994. Past and present status of Central Valley Chinook salmon. Conserv. Biol. **8**(3): 870–873. doi:10.1046/j.1523-1739.1994.08030863-5.x.

Greene, C.M., Hall, J.E., Guilbault, K.R., and Quinn, T.P. 2010. improved viability of populations with diverse life-history portfolios. Biol. Lett. **6**(3): 382–386. doi:10.1098/rsbl.2009.0780. PMID:20007162.

Hilborn, R., Quinn, T.P., Schindler, D.E., and Rogers, D.E. 2003. Biocomplexity and fisheries sustainability. Proc. Natl. Acad. Sci. U.S.A. **100**(11): 6564–6568. doi:10.1073/pnas.1037274100. PMID:12743372.

Hutchinson, W.F. 2008. The dangers of ignoring stock complexity in fishery management: the case of the North Sea cod. Biol. Lett. **4**(6): 693–695. doi:10.1098/rsbl.2008.0443. PMID:18782730.

Kerr, L.A., Cadrin, S.X., and Secor, D.H. 2010. The role of spatial dynamics in the stability, resilience, and productivity of an estuarine fish population. Ecol. Appl. **20**(2): 497–507. doi:10.1890/08-1382.1. PMID:20405802.

Koseki, Y., and Fleming, I.A. 2006. Spatio-temporal dynamics of alternative male phenotypes in coho salmon populations in response to ocean environment. J. Anim. Ecol. **75**(2): 445–455. doi:10.1111/j.1365-2656.2006.01065.x. PMID:16637997.

Koseki, Y., and Fleming, I.A. 2007. Large-scale frequency dynamics of alternative male phenotypes in natural populations of coho salmon (*Oncorhynchus kisutch*): patterns, processes, and implications. Can. J. Fish. Aquat. Sci. **64**(4): 743–753. doi:10.1139/f07-046.

Krebs, C. 1989. Ecological methodology. Harper Collins, New York.

Legendre, P., and Legendre, L. 1998. Numerical ecology. Elselvier, Amsterdam.

Lindley, S.T., Grimes, C.B., Mohr, M.S., Peterson, W., Stein, J., Anderson, J.T., Botsford, L.W., Bottom, D.L., Busack, C.A., Collier, T.K., Ferguson, J., Garza, J.C., Grover, A.M., Hankin, D.G., Kope, R.G., Lawson, P.W., Low, A., MacFarlane, R.B., Moore, K., Palmer-Zwahlen, M., Schwing, F.B., Smith, J., Tracy, C., Webb, R., Wells, B.K., and Williams, T.H. 2009. What caused the Sacramento River fall Chinook stock collapse? NOAA Tech. Memo. NOAA-TM-NMFS-SWFSC-447.

Lindley, S.T., Schick, R.S., Mora, E., Adams, P.B., Anderson, J.J., Greene, S., Hanson, C., May, B.P., McEwan, D.R., MacFarlane, R.B., Swanson, C., and Williams, J.G. 2007. Framework for assessing viability of threatened and endangered Chinook salmon and steelhead in the Sacramento–San Joaquin Basin. San Francisco Estuary & Watershed Science, **5**(1): Article 4.

MacArthur, R. 1955. Fluctuations of animal populations and a measure of community stability. Ecology, **36**(3): 533–536. doi:10.2307/1929601.

McClure, M.M., Carlson, S.M., Beechie, T.J., Pess, G.R., Jorgensen, J.C., Sogard, S.M., Sultan, S.E., Holzer, D.M., Travis, J., Sanderson, B.L., Power, M.E., and Carmichael, R.W. 2008. Evolutionary consequences of habitat loss for Pacific anadromous salmonids. Evol. Appl. **1**(2): 300–318. doi:10.1111/j.1752-4571.2008.00030.x.

Moore, J.W., McClure, M., Rogers, L.A., and Schindler, D.E. 2010. Synchronization and portfolio performance of threatened salmon. Conserv. Lett. **3**(5): 340–348. doi:10.1111/j.1755-263X.2010.00119.x.

Moyle, P.B. 2002. Inland fishes of California — revised and expanded. University of California Press, Berkeley and Los Angeles, Calif.

Myers, J.M., Kope, R.G., Bryant, G.J., Teel, D., Lierheimer, L.J., Wainwright, T.C., Grant, W.S., Waknitz, F.W., Neely, K., Lindley, S.T., and Waples, R.S. 1998. Status review of Chinook salmon from Washington, Idaho, Oregon, and California [online]. US Dept. Comm. NOAA Tech. Memo. NMFS-NWFSC-35. Available from http://www.nwfsc.noaa.gov/publications/techmemos/tm35/index.htm.

NMFS. 2010. Endangered Species Act Section 7 Consultation Biological Opinion: Authorization of ocean salmon fisheries pursuant to the Pacific coast salmon fishery management plan and additional protective measures as it affects Sacramento River winter Chinook salmon [online]. Protect Resources Division, Southwest Region, National Marine Fisheries Service. Available from http://www.cio.noaa.gov/Policy_Programs/prplans/ID144_Final_Harvest_BiOp.pdf.

Oksanen, J., Blanchet, F.G., Kindt, R., Legendre, P., O'Hara, R.B., Simpson, G.L., Solymos, P., Stevens, H.H., and Wagner, H. 2011. vegan: community ecology package. R package version 1.17-10.

Oliver, T., Roy, D.B., Hill, J.K., Brereton, T., and Thomas, C.D. 2010. Heterogeneous landscapes promote population stability. Ecol. Lett. **13**(4): 473–484. doi:10.1111/j.1461-0248.2010.01441.x. PMID:20148927.

Olsen, E.M., Knutsen, H., Gjøsæter, J., Jorde, P.E., Knutsen, J.A., and Stenseth, N.C. 2008. Small-scale biocomplexity in coastal Atlantic cod supporting a Darwinian perspective on fisheries management. Evol. Appl. **1**(3): 524–533. doi:10.1111/j.1752-4571.2008.00024.x.

Pyper, B.J., and Peterman, R.M. 1998. Comparison of methods to account for autocorrelation in correlation analyses of fish data. Can. J. Fish. Aquat. Sci. **55**(9): 2127–2140. doi:10.1139/f98-104.

R Development Core Team. 2010. R: a language and environment for statistical computing. R Foundation for Statistical Computing, Vienna, Austria.

Rogers, L.A., and Schindler, D.E. 2008. Asynchrony in population dynamics of sockeye salmon in southwest Alaska. Oikos, **117**(10): 1578–1586. doi:10.1111/j.0030-1299.2008.16758.x.

Schindler, D.E., Hilborn, R., Chasco, B., Boatright, C.P., Quinn, T.P., Rogers, L.A., and Webster, M.S. 2010. Population diversity and the portfolio effect in an exploited species. Nature, **465**(7298): 609–612. doi:10.1038/nature09060. PMID:20520713.

Shannon, C.E. 1948. A mathematical theory of communication. Bell Syst. Tech. J. **27**: 379–423, 623–656. [July and October.]

Tilman, D., and Downing, J.A. 1994. Biodiversity and stability in grasslands. Nature, **367**(6461): 363–365. doi:10.1038/367363a0.

Williams, J.G. 2006. Central Valley salmon: a perspective on Chinook and steelhead in the Central Valley of California. San Francisco Estuary & Watershed Science, **4**(3): Article 2.

Williams, J.G., Anderson, J.J., Greene, S., Hanson, C., Lindley, S.T., Low, A., May, B.P., McEwan, D., Mohr, M.S., MacFarlane, R.B., and Swanson, C. 2007. Monitoring and research needed to manage the recovery of threatened and endangered Chinook and steelhead in the Sacramento–San Joaquin Basin. NOAA Tech. Memo. NOAA-TM-NMFS-SWFSC-399. pp. 1–11.

Williamson, K.C., and May, B. 2005. Homogenization of fall-run Chinook salmon gene pools in the Central Valley of California, USA. N. Am. J. Fish. Manage. **25**(3): 993–1009. doi:10.1577/M04-136.1.

Yoshiyama, R.M., Fisher, F.W., and Moyle, P.B. 1998. Historical abundance and decline of Chinook salmon in the Central Valley region of California. N. Am. J. Fish. Manage. **18**(3): 487–521. doi:10.1577/1548-8675(1998)018<0487:HAADOC>2.0.CO;2.

Yoshiyama, R.M., Gerstung, E.R., Fisher, F.W., and Moyle, P.B. 2000. Chinook salmon in the California Central Valley: an assessment. Fisheries, **25**(2): 6–20.

Appendix A

Simulations exploring the impact of observation error on estimated portfolio effect (PE) strength and power to detect geographic patterns in correlations among rivers

Because of varying degrees of documentation of the individual estimates making up the GRANDTAB data set, we cannot directly model observation error in our production estimates. However, we can attempt to remove some of the effect of observation error by smoothing our production estimates via a moving average. This builds upon part of the method described by Holmes (2001) for population viability analysis of noisy data. Although our analysis does not require every step of a method originally focused on estimates of mean and variance in growth rate, we do take the first step of estimating total population size (including both returning spawners and fish in the ocean) as a weighted sum of sequential counts, with the side benefit of reducing observation error. An equivalent approach (through scaling outputs back down to the magnitude of annual returns rather than total population size) using a moving average rather than a moving sum has previously been used to smooth salmon counts for comparisons across watersheds (e.g., Fujiwara 2008). We chose to use the running average approach for easier comparison with the mean and SD in returns used in the body of the paper. Since we cannot estimate the temporally varying proportion of fall-run Central Valley Chinook, which return at different ages (primarily ages 2, 3, or 4), we took an unweighted moving average of estimated returns over 3 years to yield a smoothed trajectory. This averaging likely reduced the contributions of both observation error and real population changes to variation in estimated returns. The smoothing reduced the SD in returns for each river by 19%–26% (SAC Basin) or 10%–21% (SJ Basin).

As a conservative test of the influence of observation error on generating patterns documented in the main text, we repeated our analysis on this smoothed data, which likely had "true" variation removed as well. To examine the potential for observation error to create spurious results, we regard the smooth trajectories as "true" and compare the results of analyzing the smoothed trajectories with trajectories to which we have added normally distributed error with mean 0 and a SD equal to 5%–150% of the SD for each river in the original (presmoothing) data set. We chose normally distributed observation error since even though population sizes are often lognormally distributed (because of a multiplicative process and thus multiplicative process error), counts themselves are additive and thus likely have normally distributed errors. As a result, it is possible to generate a negative population size in our counts with large simulated error, which we convert to zero. For this reason, we excluded Battle Creek from our analysis, since (in addition to concerns raised in the main text) its large SD combined with low estimated returns prior to the 1980s meant that we would most often encounter negative population estimates when adding noise to Battle Creek.

Fig. A1. Estimated strength of portfolio effect (PE, as proportional reduction in coefficient of variation (CV), solid symbols and solid lines) and pairwise correlations (open symbols and dashed lines) among rivers for simulations based on smoothed trajectories as a function of the amount of simulated noise (as percentage of standard deviation (SD) in the raw data for each river) added back in. Circles are from the SAC Basin, squares are are from the SJ Basin, and triangles represent cross-basin pairings. Error bars are ±1 SD from 100 simulations at each level of added noise.

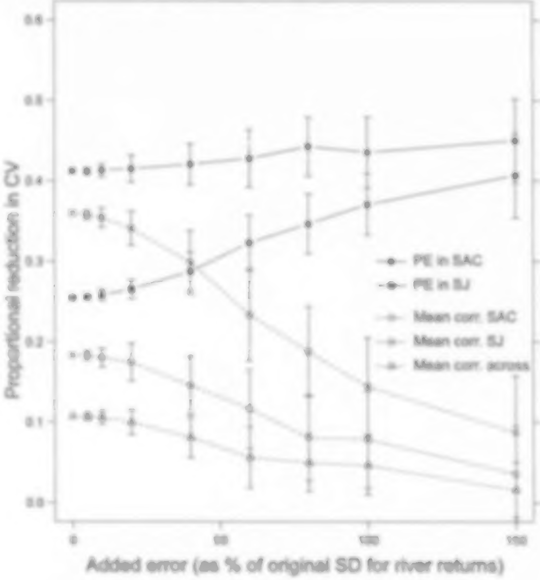

Our main results from the text are closely matched by an analysis of the smoothed data set (noting that numeric comparisons should be made with the analyses that exclude Battle Creek). We observed more reduction in the coefficient of variation in the SAC Basin (41%, was 34%) than in the SJ Basin (25%, was 21%), with mean correlations among rivers highest within the SJ Basin (0.36, was 0.31), lowest across basins (0.11, was 0.14), and intermediate within the SAC Basin (0.18, was 0.26).

As we increased the simulated observation error (Fig. A1), we tended to underestimate correlations among rivers and tended to overestimate the degree to which CV was reduced by the PE, although the effects were small for added error on the order of 20%–30% of the original SD. Both of these effects are to be expected — adding uncorrelated noise will reduce correlations between trajectories and as a result lead to more effective buffering when adding noisy trajectories together.

Thus it is possible that we overestimated the strength of the PE in the system — however we reiterate that some degree of PE is a statistical inevitability. Observation error would not lead us to find higher correlations or less buffering in the SJ Basin than in the SAC Basin, unless observation error made up a much larger proportion of variation in estimated SAC Basin returns. Likewise observation error might lead us to underestimate cross-basin correlations, but since it would similarly affect our estimates of within-basin correlations, it would not lead us to find lower correlations across basins than within either basin. It is possible that large observation error in the SAC Basin but not SJ Basin would lead us to underestimate within-SAC and across-basin correlations but not within-SJ correlations, with the result that when pooling together all within-basin correlations (half of which will be influenced by large observation error) they are higher than across-basin correlations (all of which will be influenced by large observation error). However, this seems unlikely since our main results are robust to an attempt to reduce the effects of observation error, and in fact we found a stronger PE (41% reduction in CV vs. 34%) and lower mean correlations (0.18 vs. 0.26) for the SAC Basin in the smoothed data set. Thus it appears that our smoothing removed more correlated signal (or bias) than uncorrelated noise. Also, despite whatever observation error was present, we still found statistically significant correlations for 4/10 (2/6 excluding Battle Creek) pairings in the SAC Basin.

References

Fujiwara, M. 2008. Identifying interactions among salmon populations from observed dynamics. Ecology, **89**(1): 4–11. doi:10.1890/07-1270.1. PMID:18376540.

Holmes, E.E. 2001. Estimating risks in declining populations with poor data. Proc. Natl. Acad. Sci. U.S.A. **98**(9): 5072–5077. doi:10.1073/pnas.081055898. PMID:11309483.

Sockeye salmon (*Oncorhynchus nerka*) return after an absence of nearly 90 years: a case of reversion to anadromy

L. Godbout, C.C. Wood, R.E. Withler, S. Latham, R.J. Nelson, L. Wetzel, R. Barnett-Johnson, M.J. Grove, A.K. Schmitt, and K.D. McKeegan

Abstract: We document the recent reappearance of anadromous sockeye salmon (*Oncorhynchus nerka*) that were thought to have been extirpated by the construction of hydroelectric dams on the Coquitlam and Alouette rivers in British Columbia, Canada, in 1914 and 1927, respectively. Unexpected downstream migrations of juveniles during experimental water releases into both rivers in 2005 and 2006 preceded upstream return migrations of adults in 2007 and 2008. Genetic (microsatellite and mitochondrial DNA) markers and stable isotope ($\delta^{34}S$ and $^{87}Sr/^{86}Sr$) patterns in otoliths confirm that both the juvenile downstream migrants and adult upstream migrants were progeny of nonanadromous sockeye salmon (kokanee) that inhabit Coquitlam and Alouette reservoirs. Low genetic diversity and evidence of genetic bottlenecks suggest that the kokanee populations in both reservoirs originated from relatively few anadromous individuals that residualized after downstream migration was largely prevented by the construction of dams. Once given an opportunity for upstream and downstream migration, both populations appear capable of reverting to a successful anadromous form, even after 25 generations.

Résumé : Nous apportons des informations sur la réapparition récente des saumons rouges (*Oncorhynchus nerka*) anadromes qu'on croyait extirpés par la construction de barrages sur les rivières Coquitlam et Alouette en Colombie-Britannique, Canada, respectivement en 1914 et en 1927. Des migrations inattendues vers l'aval de jeunes saumons durant des vidanges expérimentales d'eau dans les deux rivières en 2005 et 2006 ont précédé des migrations de retour vers l'amont en 2007 et 2008. Les marqueurs génétiques (microsatellites et ADN mitochondrial) et les patrons d'isotopes stables ($\delta^{34}S$ et $^{87}Sr/^{86}Sr$) dans les otolithes confirment que tant les jeunes migrateurs vers l'aval que les migrateurs adultes vers l'amont sont des rejetons de saumons rouges non anadromes (kokanis) qui habitent les réservoirs Coquitlam et Alouette. La faible diversité génétique et des indications de goulots d'étranglement génétiques laissent croire que les populations de kokanis des deux réservoirs sont issues d'un petit nombre d'individus anadromes qui sont demeurés sur place lorsque la migration vers l'aval a été en grande partie bloquée par la construction des barrages. Une fois la possibilité rétablie de migrations vers l'amont et l'aval, les deux populations semblent capables de revenir avec succès à une forme anadrome, même après 25 générations.

[Traduit par la Rédaction]

Introduction

Life history diversity contributes to population resilience in variable environments (e.g., Hilborn et al. 2003; Schindler et al. 2010), yet human actions and natural processes increasingly threaten migratory phenotypes in salmonids (Gustafson et al. 2007; Waples and Hendry 2008). The species sockeye salmon, *Oncorhynchus nerka*, is widely distributed throughout the North Pacific and occurs as three distinctive ecotypes: (*i*) anadromous lake-type sockeye salmon, which typically rear in lakes for 1 year before migrating to the ocean where they typically spend the next 2 years before returning to fresh water to spawn and die; (*ii*) anadromous sea- or river-type sockeye salmon, which usually rear in rivers for several weeks to months before migrating to the ocean where they spend 2 to 3 years and then return to fresh water; and (*iii*) nonanadromous kokanee, which spend their entire life in fresh water (Burgner 1991; Wood et al. 2008). Kokanee pop-

Received 31 August 2010. Accepted 12 May 2011. Published at www.nrcresearchpress.com/cjfas on 30 August 2011.
J2011-0061

Paper handled by Associate Editor Michael Bradford.

L. Godbout, C.C. Wood, and R.E. Withler. Fisheries and Oceans Canada, Pacific Biological Station, 3190 Hammond Bay Road, Nanaimo, BC V9T 6N7, Canada.
S. Latham. Pacific Salmon Commission, 600 - 1155 Robson Street, Vancouver, BC V6E 1B5, Canada.
R.J. Nelson. Fisheries and Oceans Canada, Institute of Oceans and Science, P.O. Box 6000, 9860 West Saanich Road, Sidney, BC V8L 4B2, Canada.
L. Wetzel. US Geological Survey, Western Fisheries Research Center, 6505 NE 65th Street, Seattle, WA 98115, USA.
R. Barnett-Johnson. US Department of Interior, 2800 Cottage Way, MP-151, Sacramento, CA 95825, USA.
M.J. Grove. Department of Geological and Environmental Sciences, Stanford University, Stanford, CA 94305, USA.
A.K. Schmitt and K.D. McKeegan. Department of Earth and Space Sciences, University of California, Los Angeles, CA 90095-1567, USA.

Corresponding author: Lyse Godbout (e-mail: lyse.godbout@dfo-mpo.gc.ca).

doi:10.1139/F2011-089

ulations are known to have evolved from anadromous lake-type sockeye salmon where barriers have impeded anadromous migration (Ricker 1938, 1959; Krogius 1981). Genetically distinct kokanee populations can also evolve and coexist in sympatry with the freshwater phase of lake-type sockeye salmon (Foote 1989; Wood and Foote 1996).

Because kokanee retain the ability to osmoregulate in seawater even after being land-locked for thousands of generations (Foote et al. 1994), it seems plausible that they could revert to an anadromous ecotype given the opportunity. Considerable evidence for such reversion exists, but well-documented examples of "sea-run kokanee" are rare. Foerster (1947) marked and released hatchery-reared age-1 kokanee from Kootenay Lake, B.C., into Sweltzer Creek (draining Cultus Lake, B.C.), forcing them to migrate downstream to the Fraser River. Of the 63 874 juveniles released, 0.12% survived to adulthood, with an estimated 74 caught in the fishery and 17 returning to the lake as 5-year-olds, 1 year older than the typical age of return for anadromous sockeye salmon (Foerster 1947). Hatchery-reared progeny of 1942 brood-year kokanee from Lake Chelan in Washington State were released as 18-month-old juveniles in the Entiat River, but only 0.004% survived to return as adults. The populations of kokanee in Kootenay and Chelan lakes must have been non-anadromous for about 10 000 years because high natural waterfalls block their return migration. In another experiment, hatchery-reared progeny of the 1944 brood-year kokanee from Wenatchee Lake, also in Washington State, were marked and planted back into Wenatchee Lake as 12-month-old juveniles and into Icicle Creek (a tributary of the Wenatchee River) as 18-month-old juveniles; 0.27% and 0.5% were later recovered as anadromous adults, respectively (Fulton and Pearson 1981). Ricker (1972) speculated that these kokanee had been recently derived from anadromous sockeye salmon in Wenatchee Lake and that Lake Wenatchee kokanee may have diverged from sockeye salmon only within the past 90 years. Up to 2.8% of hatchery-reared kokanee released in Lake Toro and forced to migrate to sea survived to return as anadromous adults (Urawa and Kaeriyama 1999). The parent kokanee had been transplanted from Lake Sikotshu, which in turn had originated from anadromous sockeye salmon that were transplanted from the Kuril Islands in the late 1800s and as recently as 1925–1940 (Urawa and Kaeriyama 1999). Although limited, these observations collectively suggest that adaptations to marine life are lost after a long period of isolation in fresh water.

Understanding the potential for kokanee to revert to anadromy could aid in the recovery of anadromous sockeye runs, many of which face imminent extirpation (Slaney et al. 1996; Gustafson et al. 2007; Waples and Hendry 2008). It is therefore important to document empirical evidence of the biotic and abiotic conditions under which one ecotype is favoured over another and to identify conditions under which kokanee can successfully revert to anadromy.

In this paper we investigate the extent to which kokanee in the Coquitlam and Alouette reservoirs may have reverted to anadromy under a modified regime of water outflow. Both rivers once drained natural lakes and supported sizeable runs of sockeye salmon that provided a major food supply to local aboriginal people in the area (Hirst 1991). The main runs in both rivers were early (April–May up to July), although later runs were also present (Bengeyfield et al. 2001; Koop 2001). Anadromous sockeye salmon used to spawn along the shores of the Alouette and Coquitlam lakes and adjoining tributaries (Hirst 1991; Koop 2001). Gold Creek, an inlet tributary of Alouette Lake, was one of the spawning grounds (Hirst 1991). By the 1930s, following construction of hydroelectric dams in the mid 1910s and late 1920s, native anadromous sockeye salmon had disappeared entirely from the Alouette and Coquitlam rivers, respectively.

In 2007 and 2008, for the first time in nearly 90 years, anadromous adults reappeared in both rivers migrating upstream as far as the dams. These adult upstream migrants (AUM) were presumed to be associated with unprecedented observations of *O. nerka* juvenile downstream migrants (JDM) in both rivers in 2005 and 2006, which apparently had been triggered by experimental manipulations of water releases past the dams (Baxter and Bocking 2006; Humble et al. 2006). Alternatively, the AUM might have been strays from nearby populations, or sea- or river-type sockeye salmon that evolved from lake-type Alouette sockeye salmon and persisted in the Alouette River after dam construction prevented access to the nursery lake.

Our first objective is to document these unusual events including relevant demographic information for AUM and JDM with respect to estimates of abundance, size, age, migration timing, and marine survival. We then compare these demographic characteristics with data available for other populations of sockeye salmon that emigrated from the Fraser River in the same year.

Our second objective is to assess, using genetic and isotopic markers, whether the JDM and the AUM were progeny of the kokanee known to inhabit each reservoir. We tested this hypothesis in two complementary ways. First, we compared the microsatellite DNA (μsatDNA) and mitochondrial DNA (mtDNA) of the unknown samples (i.e., JDM and AUM) with reference samples from kokanee in the reservoirs and from other populations of sockeye salmon and kokanee in nearby river systems. Second, we measured stable isotope ratios of sulfur ($^{34}S/^{32}S$, expressed as $\delta^{34}S$) and strontium ($^{87}Sr/^{86}Sr$) in otoliths to determine whether the isotopic signature was consistent with that expected in the anadromous progeny of kokanee (hereafter referred to as "sea-run kokanee"). The otolith core is formed from the yolk, which reflects the feeding environment of the maternal parent (Kalish 1990), so sea-run kokanee should not have a marine signature in the otolith core.

Our third objective is to elucidate the evolutionary history of sockeye salmon and kokanee in the Alouette and Coquitlam rivers by compiling historical accounts and examining genetic data. We searched the literature and government databases for stocking and catch records to assess whether Alouette and Coquitlam kokanee might have originated from a native or introduced kokanee population. Lastly, we compared indices of allelic richness and genetic diversity in Alouette and Coquitlam kokanee with indices for nearby sockeye salmon populations, looking for evidence of population bottlenecks or rapid genetic drift. Bottlenecks would be expected if the Alouette and Coquitlam kokanee populations had originated from "residual" sockeye salmon (the non-anadromous progeny of anadromous sockeye salmon), which were likely rare in the original population, but which could have survived to spawn after dams prevented spawning by anadromous fish.

Materials and methods

Study sites

Coquitlam and Alouette reservoirs are oligotrophic, relatively small (12 and 16 km^2) but deep (maximum depths of 187 and 140 m), located in the steep terrain of the Coast Mountains at 49.3°N latitude, at a distance to the ocean of 60 and 72 km, respectively (Fig. 1). Both are coastal reservoirs where the majority of the inflow results from seasonal storms and spring snow melt. The bulk of the outflow from both reservoirs is diverted to other water bodies via tunnels to produce hydroelectricity.

Alouette Reservoir is formed by a 21 m dam constructed at the south end of the original lake at the natural outlet into the Alouette River, which drains into the Pitt River before entering the Fraser River (Conlin et al. 2000*a*). The 17 km long reservoir comprises two basins separated by a narrow section corresponding to the former two lakes "Upper and Lower Lillooet Lake" (Conlin et al. 2000*a*). Most of the outflow is diverted through a 1 km tunnel at the north end of Alouette Lake into Stave Reservoir where power generation occurs. Outflow at the original outlet into the Alouette River is controlled by a low-level outlet (LLO, underwater release), a crest gate (surface water release), and a free crest weir (surface water release) (BC Hydro 2009). Water can spill over the free crest weir if the water level is greater than 125.5 m, but such spills are rare. Based on BC Hydro records from 1984, it occurred only in 1986 (3 days in November) and 1995 (5 days in November and December) (B. Wilson, BC Hydro Ruskin Dam & Generating Station, 10600 Wilson Street, Mission, BC V4S 1B4, unpublished data).

The 12 km long Coquitlam Reservoir is formed by a 30 m dam constructed across the original outlet into the Coquitlam River at the south end of the lake (Conlin et al. 2000*b*). In contrast with the Alouette Reservoir, there is no crest gate at the Coquitlam dam for releasing surface water into the river. Water spills to the Coquitlam River are solely controlled by the LLO and a free crest weir. Over the full length of the records, water spill over the free crest weir occurred only in 1990 (3 days in November), 1991 (3 days August–September), 1995 (15 days August–September), and 1996 (3 days in January). The Coquitlam River runs through the municipality of Port Coquitlam before entering the Fraser River and the Pacific Ocean. Most of the outflow is diverted for power generation into Buntzen Lake through a tunnel at the southwest side of the reservoir, 4 km from the dam. Public access to the Coquitlam watershed has been restricted since the 1880s because it supplies drinking water to the Greater Vancouver Metropolitan Area via a water intake 300 m from the dam on the east side of the lake (Conlin et al. 2000*b*; BC Hydro 2005).

Fish monitoring and collection and experimental water releases

As part of the Alouette and Coquitlam Water Use Plans, rotary screw traps (RSTs) have been used to monitor the downstream migrations of coho (*Oncorhynchus kisutch*), chum (*Oncorhynchus keta*), and Chinook salmon (*Oncorhynchus tshawytscha*) and steelhead trout (*Oncorhynchus mykiss*). In the Alouette River, RSTs were deployed 16 km downstream of the dam every year since 1998 (Cope 2010). In the Coquitlam River, RSTs were deployed at 1, 4, and 7 km downstream of the dam every year since 2000 (Derek et al. 2010). Returning adults were enumerated visually by stream walk in the Coquitlam River and by trapping in the Alouette River. After sockeye salmon were observed returning to the Alouette River trap in 2007, that trap was modified to better handle returns in 2008 (Backle 2008), and a new trap was installed in the Coquitlam River in 2008.

As part of a program to reintroduce coho salmon in 2005 and steelhead trout in 2006, the hydroelectric company of British Columbia (BC Hydro) in concert with the Alouette River Management Society experimentally manipulated water release from the Alouette Dam. In 2005, water was released via the crest gate over the spillway for 1 month (3 May – 3 June), and flow at the gate was maintained between 2.2 and 2.8 m^3·s^{-1} (Baxter and Bocking 2006). In 2006, the water was released over 2 weeks (11–31 May), with flow at the gate ranging from 2.2 to 3.5 m^3·s^{-1} (Humble et al. 2006). The water depth at the gate during surface water release averaged ~1 m (1 standard deviation (SD) = 0.26). The outflow through the LLO was gradually decreased when the experiment began and was maintained at zero flow for the majority of the experimental water releases. In both years, RSTs located approximately 1.5 km downstream of the Alouette Dam were used to obtain a sample of the salmonid migrants. Traps were checked daily in the morning, and all species of fish within the holding box were counted. Total numbers of JDM in 2005 and 2006 were based on estimates of trap efficiency obtained in mark and recapture experiments with coho (42%, 2005) and with JDM (35%, 2006). Experimental water releases in the Coquitlam Reservoir consisted of opening the LLO and fish valves. In 2005, water flow at the gate was maintained experimentally at ~6.5 m^3·s^{-1} for 10 days (21 April – 1 May). A second water release of 23 days (21 April – 14 May) occurred in 2006, when flow at the gate was ~6.1 m^3·s^{-1} (G. Lewis, 2755 Lougheed Highway, Port Coquitlam, BC V3B 5Y9, personal communication, 2010). The depth at which the LLO opened ranged from 5.0 to 6.7 m in 2005 and 3.0 to 3.7 m in 2006. In both years, RSTs were used to monitor all salmonid migrants, including the JDM.

In 2005 and 2006, tissue samples and fork length measurements were collected from a random sample of JDM in both the Alouette and Coquitlam rivers. Fish scales for ageing were collected from random samples of the Alouette JDM in 2005 and 2006. BC Hydro employees first noticed sockeye salmon-like spawners in the Alouette and Coquitlam rivers attempting to ascend past the dams in the late summer of 2007, and they collected tissues for DNA analysis, scales for ageing, otoliths, and postorbital fork lengths. In 2008, AUM from both rivers were sampled only for fork length, DNA, and scales for ageing before being transported and released upstream into their respective reservoirs (Table 1*a*). Corresponding samples were collected from kokanee in both reservoirs.

Genetic markers

Microsatellites (μsatDNA) and mitochondrial DNA (mtDNA) were analyzed to determine whether samples of JDM and AUM (Table 1*a*) were more closely related to kokanee in their respec-

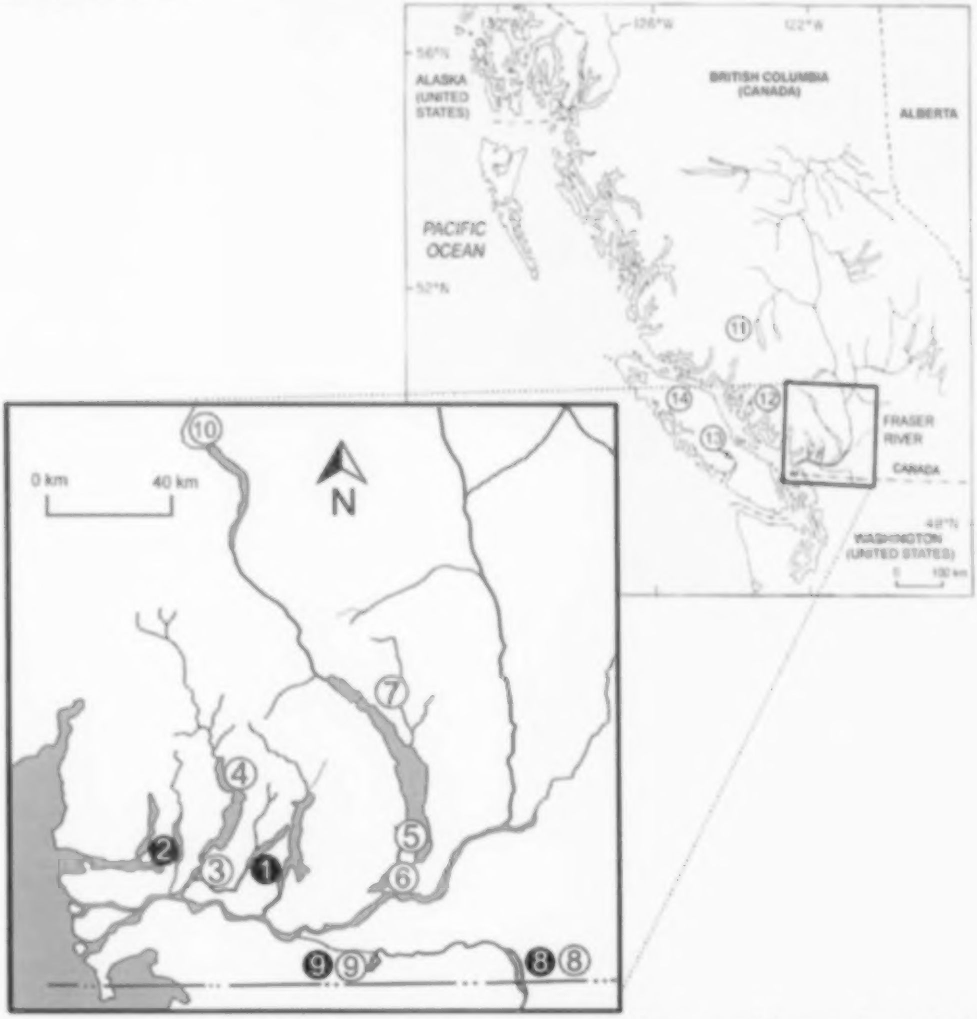

Fig. 1. Location of sockeye salmon (open circles) and kokanee (solid circles) populations sampled for the genetic and isotopic markers studies. Genetic study on the lower Fraser River and Chilko Lake sockeye salmon on the upper Fraser: Alouette Reservoir (1), Coquitlam Reservoir (2), Widgeon Slough (3), Pitt River (4), Weaver (5), Harrison Rapids (6), Big Silver Creek (7), Chilliwack Lake (8), Cultus Lake (9), Lillooet Lake – Birkenhead River (10), Chilko Lake (11). Isotopic markers study: Alouette Reservoir (1), Sakinaw Lake (12), Sproat Lake (13), and Nimpkish Lake (14).

tive river systems than to anadromous sockeye salmon spawning in neighbouring rivers (referred to as the reference populations; Table 1*b*). For each AUM sampled, we determined a multilocus genotype at 14 microsatellite loci (*Ots2*, *Ots3*, *Ots100*, *Ots103*, *Ots107*, *Ots108*, *Oki1a*, *Oki1b*, *Oki6*, *Oki10*, *Oki16*, *Oki29*, *One8*, and *Omy77*; Beacham et al. 2005) and a composite haplotype based on two genes (cytochrome *b* (*cytb*) and NADH dehydrogenase subunit 1(*ND1*)) in mitochondrial DNA (as described in Wood et al. 2008). Polymerase chain reaction (PCR) amplification of mitochondrial genes *ND1* and *cytb* was accomplished with primer pairs LGL 290 GGGCCTAAGCCCTTTTTCTCA, LGL 560 GGCRGCTTTTGGTTATTAG and LGL 287 GAGCTAGGGCAGGCTCA, LGL 765 GAAAAACCAYCGTTGTWATTCAACT, respectively. The *cytb* PCR product was approximately 1300 base pairs, whereas the amplified segment of the *ND1* gene was approximately 859 base pairs. Genetic data for the 10 reference populations are from published μsatDNA (Beacham et al. 2005) and mtDNA (Wood et al. 2008) databases and additional analyses conducted as part of this study.

The extent of genetic divergence between groups of fish was assessed by testing for differences in allelic and haplotypic frequencies based on pairwise F_{ST} values calculated for each sample over all loci or haplotypes combined. The pairwise F_{ST} value is the genetic variance attributable to differentiation between samples. F_{ST} values can range from 0 (no detectable divergence between samples) to 1 (complete divergence). Critical significance levels for simultaneous pairwise population differentiation one-tailed tests were evaluated using Bonferroni adjustment (0.05/240 × 2 = 0.000417) in FSTAT version 2.9.3.2 (Goudet 2001). An unrooted, consensus neighbor-joining tree based on 1000 replicate trees was generated with the CONSENSE program from PHYLIP (Fel-

Table 1. Sample collection data for (*a*) juvenile downstream migrants (JDM) and adult upstream migrants (AUM) caught in the Alouette and Coquitlam rivers; and (*b*) reference samples for genetic analysis from kokanee and anadromous sockeye salmon populations in the lower Fraser River.

(*a*) Samples of unknown origin (caught below reservoir).

	Year migration	µsatDNA (*n*)	mtDNA (*n*)	$\delta^{34}S$ (*n*)	$^{87}Sr/^{86}Sr$ (*n*)	Population estimate of the migrants (*N*)
JDM						
Alouette River	2005	190	25			7 900[a]
	2006	48	55			5 064[b]
	2007	44	0			62 923
	2008	10	0			8 257
Coquitlam River	2005	0	0			~1 500[c]
	2006	41	46			~800[c]
	2007	0	0			NA
	2008	3	0			NA
AUM						
Alouette River	2007	18	8	13	10	28[d]
	2008	53	27			54[d]
Coquitlam River	2007	2	1			NA
	2008	10	10			10[e]

(*b*) Samples of known origin.

	µsatDNA (*n*, years)	mtDNA (*n*, years)	$\delta^{34}S$ (*n*, years)	$^{87}Sr/^{86}Sr$ (*n*, years)
Kokanee				
Alouette Reservoir	86 (2000, 2002)	122 (2005, 2006)	3 (2007)	5 (2007)
Coquitlam Reservoir	59 (2004, 2005)	133 (2002, 2004, 2005, 2006)		
Cultus Lake	32 (2006, 2007)	21 (2007)		
Chilliwack Lake	100 (2004)	23 (2002, 2004)		
Sockeye				
Widgeon Slough	82 (2002)	45 (1997, 2003)		
Pitt River	68 (2005)	33 (2004)		
Weaver Creek	60 (1992)	48 (1992, 2000)		
Harrison Rapids	132 (1986)	25 (1997)		
Birkenhead River	100 (1998)	25 (1992)		
Big Silver Creek	95 (2002)	25 (2002)		
Chilliwack Lake	88 (2004)	25 (2001, 2004)		
Cultus Lake	161 (2005)	25 (1985)		
Chilko Lake (upper Fraser)	122 (1999)	23 (1992)		
Sproat Lake			5 (2006)	5 (2006)
Sakinaw Lake			2 (2005)	7 (2003, 2005)
Nimpkish Lake			1 (2006)	4 (2006)

Note: Sample size is represented by *n*; population estimates are represented by *N*. Data in part *b* include an outgroup (Chilko Lake sockeye salmon) from the upper Fraser River and reference otolith samples for isotope analysis from kokanee in the Alouette Reservoir and anadromous sockeye salmon in Sproat, Sakinaw, and Nimpkish lakes.

[a] Baxter and Bocking 2006.

[b] Humble et al. 2006.

[c] G. Lewis, 2755 Lougheed Highway, Port Coquitlam, BC V3B 5Y9, personal communication, January 2011.

[d] Backle 2008.

[e] M. Coulter-Boisvert, Fisheries and Oceans Canada, Delta, BC V3M 6A2, personal communication, January 2011.

senstein 1993). The Chilko River sockeye salmon population was included as an outgroup.

Genetic similarity among populations was also revealed by multidimensional scaling (MDS) with the monotonic Kruskal loss function in SYSTAT (2004). MDS allows genetic similarities among populations to be visualized in two dimensions without the added challenge of imposing a phylogenetic tree. Two similarity matrices were created, one for µsatDNA data and the other for mtDNA data, based on Cavalli-Sforza and Edwards (1967) chord distances between each pair of populations. This distance measure is appropriate when differences arise by genetic drift rather than by mutation (Felsenstein 2005). To facilitate comparison of grouping patterns in the µsatDNA and mtDNA data, MDS values from dimension 2 of the mtDNA analysis were plotted against MDS values from dimension 1 of the µsatDNA analysis. These particular dimensions were complementary (least redundant) in the sense that they provided the greatest separation of individual populations in a two-dimensional projection.

Assignment of individual genotypes for the unknown AUM samples was conducted using Bayesian methods from the program cBAYES (Neaves et al. 2005). The cBAYES program was run with eight chains through 20 000 iterations, and each fish was assigned to the baseline sample to which it had the highest probability of membership.

Standardized allelic richness (El Mousadik and Petit 1996) in the AUM samples was compared with that in the reference populations. The software program Bottleneck (Cornuet and Luikart 1996) was used to compare gene diversity (expected heterozygosity) at each locus in the AUM sample with that expected, given the same number of alleles assuming mutation–drift equilibrium. The calculation was performed using the infinite alleles model of locus evolution. For each sample, a one-tailed Wilcoxon test was performed to determine whether the observed number of loci showing excess heterozygosity was significantly higher than expected by chance, which would indicate a recent loss of alleles consistent with a bottleneck in population size. To correct for multiple tests, a P value less than 0.0042 was required to reject the null hypothesis with 95% confidence.

Isotopic markers

Otoliths from 13 AUM in the Alouette River in 2007 (Table 1*a*) were cleaned in de-ionized water, dried, embedded in resin (Buehler 20-8130 epoxide resin with Buehler 20-8132 hardener), cured overnight at 62 °C in a drying oven, and polished on both sides to expose growth bands and the core portion of the otolith accreted during juvenile growth. Distribution of sulfur isotopes in otoliths, from the core to the outer edge of the otoliths, was analyzed by secondary ion mass spectrometry (SIMS) at University of California – Los Angeles with methods similar to those reported by Godbout et al. (2010). Usually two spots were analyzed in each of three zones: the core (pre-exogenous), the first year of growth (exogenous feeding in fresh water), and the last 2 years of growth. Data were corrected for instrumental mass fractionation determined throughout each analytical session from replicate analysis of the outer edge of the sockeye salmon otolith assuming a marine $^{34}S/^{32}S$ of 0.04505, or $\delta^{34}S$ (V-CDT) = +20‰ relative to V-CDT $^{34}S/^{32}S$ = 0.044163 (Ding et al. 2001). All $^{34}S/^{32}S$ ratios were expressed as $\delta\,^{34}S$ values, the deviation in per mil (‰) relative to the Canyon Diablo Troilite (CDT) standard.

$$\delta^{34}S = \left[\frac{(^{34}S/^{32}S)_{\text{sample}}}{(^{34}S/^{32}S)_{\text{CDT}}} - 1\right] \times 1000$$

To supplement our comparison, we used $\delta^{34}S$ in otoliths from three kokanee caught in the Alouette Reservoir and eight wild adult sockeye salmon from Sakinaw, Sproat, and Nimpkish lakes (Godbout et al. 2010), hereafter referred to as kokanee and wild sockeye salmon of known maternal origin, respectively (Table 1*b*). We also measured the strontium isotope ratio ($^{87}Sr/^{86}Sr$) in otoliths of 10 AUM (Table 1*a*), 4 Alouette kokanee, and 16 wild sockeye salmon from Sakinaw, Sproat, Nimpkish lakes, respectively (Table 1*b*) by laser ablation multicollector inductively coupled plasma mass spectrometry (LA-MC-ICPMS; Agilent Technologies 7200A ICPMS, coupled with a Nd:YAG 213 nm laser, New Ware Research UP213 at University of California – Davis, Davis, California) with specific instrument, laser, and interference corrections as applied to otoliths (Barnett-Johnson et al. 2005). Two or three laser spots were analyzed in each of the three zones (core, first, and last 2 years of growth). Approximately 30 $^{87}Sr/^{86}Sr$ ratios were measured for each laser spot (60 μm). $^{87}Sr/^{86}Sr$ ratios were normalized to $^{88}Sr/^{86}Sr$ = 0.1194 to account for any natural or machine-induced fractionation. External precisions (reproducibility) were based on repeated measurements of an in-house gastropod shell standard. The daily mean value of $^{87}Sr/^{86}Sr$ measurements for the standard ranged from 0.70921 to 0.70924 (1 SD < 0.00006; daily n >5), which is close to the global marine $^{87}Sr/^{86}Sr$ value of 0.70918.

The life histories of the various groups (Alouette AUM, Alouette Lake kokanee, and wild sockeye salmon of known origin) were confirmed by testing for differences in $\delta^{34}S$ and $^{87}Sr/^{86}Sr$ in analyses of variance (ANOVAs in Proc GLM; SAS Institute Inc. 2008). Subsequently, multiple t tests with Tukey–Kramer adjustment (LSMEANS in Proc GLM; SAS Institute Inc. 2008) were used to test for differences in the mean values of $\delta^{34}S$ and $^{87}Sr/^{86}Sr$ in the core, in the last 2 years of growth, and in the mean differences between the core and last 2 years of growth (DIFF), among AUM, kokanee, and sockeye salmon.

Results

Evidence for anadromous migrations

Mark–recapture estimates of JDM abundance in the Alouette River were 7900 in 2005 and 5064 in 2006 (Table 1*a*) (Baxter and Bocking 2006; Humble et al. 2006). Mark–recapture estimation was not successful in the Coquitlam River, but tentative estimates of 1500 and 800 JDM have been suggested for 2005 and 2006, respectively (G. Lewis, 2755 Lougheed Highway, Port Coquitlam, BC V3B 5Y9, personal communication, 2010). In both 2005 and 2006, most JDM in the Alouette River were age 1 with a median fork length of 8.0 cm (Fig. 2). JDM in the Coquitlam River comprised three size groups with median fork lengths of 7.7, 16.1, and 19.9 cm. Although these fish have not been aged, the three size groups likely correspond to ages 1, 2, and 3 years of age, respectively. Sockeye salmon smolts from Chilko and Cultus lakes were primarily age 1 in both 2005 and 2006 (Fig. 2). In 2005, average size was similar in Alouette JDM and Chilko smolts (7 cm) and 3 cm longer in Cultus smolts (10 cm); in 2006, Alouette JDM averaged 1 cm less than Chilko smolts (8 cm), and again 3 cm less than Cultus smolts (10 cm) (Fig. 2).

Counts of AUM in the Alouette River were 28 in 2007 and 54 in 2008, but some might have been missed in 2007 as no monitoring program was in place (their return was unexpected). In 2007, all aged fishes were age 4 (or more specifically, 1.2, where the digits indicate the number of winters spent in fresh water and at sea, respectively, excluding the first winter, while the fish is an unhatched egg (Burgner 1991); in 2008, 32% were age 4 (both 1.2 and 2.1), 55% were age 5 (1.3 and 2.2), and 13% could not be aged (Table 2). The overall mean (±1 standard error, SE) length of

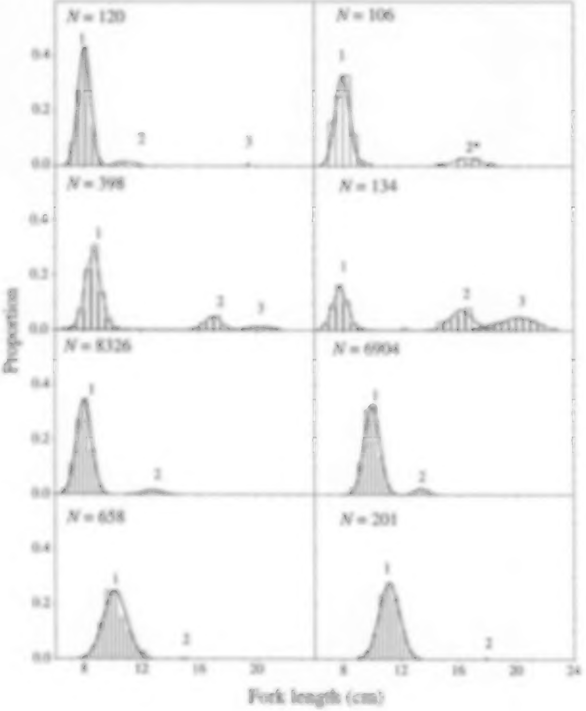

Fig. 2. Length distribution of juvenile downstream migrants (JDM) from the Alouette and Coquitlam rivers and anadromous sockeye smolts from Chilko and Cultus lakes in 2005 (left panels) and 2006 (right panels). Numbers beside each mode indicate estimated age. Note that the size distribution of the 2-year-old JDM from Alouette River in 2006 is based on fish selected to be larger than 14 cm (*).

the returning adults was 59.7 ± 0.66 cm. Regardless of freshwater age, returning adults that had spent 3 years at sea (age *x*.3) were on average 4 cm longer than those returning after only 2 years at sea (*x*.2) (Table 2).

No AUM were reported in the Coquitlam River in 2007, perhaps owing to a lack of monitoring as there was not yet any expectation of returns. In 2008, 10 AUM were observed (M. Coulter-Boisvert, Fisheries and Oceans Canada, Delta, British Columbia, personal communication, 2011), ranging in size from 56.0 to 69.5 cm; ages 4 and 5 adults were equally represented among the six fish that could be aged. Coquitlam and Alouette adults of the same sea age were similar in size (Table 2). In contrast, adult kokanee that remained within the Alouette reservoir their entire life were on average less than half the length of the AUM in Alouette River at the same total age (Fig. 3).

Evidence for sea-run kokanee

μsatDNA variation within samples

Allelic frequencies did not differ significantly among samples of kokanee, JDM, and AUM collected within the same drainage (Table 3). In contrast, allelic frequencies differed significantly in pairwise comparisons between all 12 reference populations of sockeye salmon and kokanee (Table 3; Fig. 4*a*). The mean F_{ST} value in pairwise comparisons between kokanee populations (0.13) was similar to that of sockeye salmon populations (0.11). Kokanee populations in the Alouette and Coquitlam reservoirs were more similar to one another than to other populations in the lower Fraser River (Table 3; Fig. 4*a*). Kokanee and sockeye salmon populations in the Chilliwack drainage were the most distinctive (although relatively similar to one another) because of their unusual allelic frequencies and low levels of diversity. The three populations within the Pitt River drainage (Alouette kokanee, Upper Pitt sockeye salmon, and Widgeon Slough sockeye salmon) were genetically diverse, with the Pitt sockeye salmon population being more similar to sockeye salmon populations of the Harrison River drainage than to the other Pitt River populations. This analysis confirms that genetic distinctions among populations are sufficient to permit accurate individual identifications of AUM and JDM fish.

mtDNA

F_{ST} values for pairwise comparisons based on mtDNA haplotype frequencies generally support inferences based on μsatDNA (Table 3). Plotting multidimensional scaling values for dimension 1 of μsatDNA against dimension 2 for mtDNA reveals nonoverlapping geographic clusters associated with seven distinct nursery lakes (Alouette, Coquitlam, Cultus, Chillliwack, Lillooet (the Birkenhead River sample), Harrison (the Big Silver and Weaver Creek samples), and Pitt lakes) and two sea-type populations (Widgeon Slough and Harrison Rapids) (Fig. 4*b*). This plot also shows that the Alouette group is more similar to the Coquitlam group than to any other group. JDM and AUM are more closely related to the kokanee within the same drainage. The greater variation along the *Y* axis within the Coquitlam samples is due to the small sample size (Table 1*a*); only 11 Coquitlam AUM were analyzed for mtDNA, which accounts for the apparent (but statistically insignificant) difference among Coquitlam kokanee, JDM, and AUM (Fig. 4).

Genetic assignment of AUM

cBAYES assigned all AUM specimens to the kokanee population within the same drainage after comparing their multilocus genotypes to genetic data for 12 reference populations. This result confirms that the AUM were not strays from other rivers.

Isotopic markers

Otoliths of AUM from the Alouette River typically had low values of $\delta^{34}S$ (~5‰) and $^{87}Sr/^{86}Sr$ (~0.7042) in the core and in the first year of growth, as in kokanee, but high values of $\delta^{34}S$ (20‰) and $^{87}Sr/^{86}Sr$ (~0.7093) in the last 2 years of growth, as in anadromous sockeye salmon (Figs. 5*a*, 5*b*). Plotting mean values of $\delta^{34}S$ and $^{87}Sr/^{86}Sr$ in the core against mean values in the last 2 years of growth reveals three distinct groups (Figs. 6*a*, 6*b*). Mean $\delta^{34}S$ and $^{87}Sr/^{86}Sr$ in the core of otoliths in AUM (~5.59‰, 0.7043) were not significantly different than that in kokanee (5.18‰, $P < 0.95$; and 0.7045, $P < 0.33$), but were lower than that in sockeye salmon (~19.2‰, $P < 0.0001$; and 0.7082, $P < 0.0001$), which confirms that the AUM were the progeny of nonanadromous females. It is therefore impossible for the AUM to have been the progeny of sea- or river-type sockeye salmon that might have persisted in the Alouette River after

Table 2. Age composition (x.x) and mean fork length (FL ± 1 standard error, SE) at age of the adult upstream migrants (AUM) in Alouette River and Coquitlam River in 2007 and 2008.

		Age proportion (FL±1 SE)				
Adults of unknown origin (AUM)	Migration year	1.2	2.1	1.3	2.2	Unknown
Alouette River	2007 (n = 28)	0.5 (58.5±0.53)	—	—	—	0.5
	2008 (n = 53)	0.30 (58.5±1.0)	0.02 (52.0)[a]	0.23 (62.6±0.8)	0.32 (58.4±1.0)	0.13 (61.4±1.9)
Coquitlam River	2007	NA	NA	NA	NA	NA
	2008 (n = 10)	0.10 (58.0)[a]	—	—	0.30 (57.8±1.6)	0.60 (60.8±1.9)

Note: Sample size is indicated by n.

[a] There was only one fish, so there is no SE.

Fig. 3. Box plot comparison of fork length (cm) of age 4 (1.2) adults returning to Chilko Lake, Cultus Lake, Coquitlam River, and Alouette River in 2007 (open diamonds) and 2008 (light grey diamonds) and Alouette kokanee collected from the lake in 2007 (open diamond, dotted line, lower right). Fork lengths (FL) for Chilko sockeye salmon were estimated from postorbital fork length (pof) based on a conversion equation specific to Chilko Lake: FL_{Chilko} (male) = 1.0054 × pof + 6.7876; FL_{Chilko} (female) = 1.0934 × pof + 0.39262 (S. Cox-Rogers, Fisheries and Oceans Canada, 417 – 2nd Avenue West, Prince Rupert, BC V8J 1G8, unpublished data). Fork lengths for anadromous adults returning to the Alouette River in 2007 and Cultus Lake in 2007 and 2008 were estimated using a general conversion equation: FL (male) = 1.0555 × pof + 4.6563; FL (female) = 1.0625 × pof +2.1976 (S. Cox-Rogers, unpublished data).

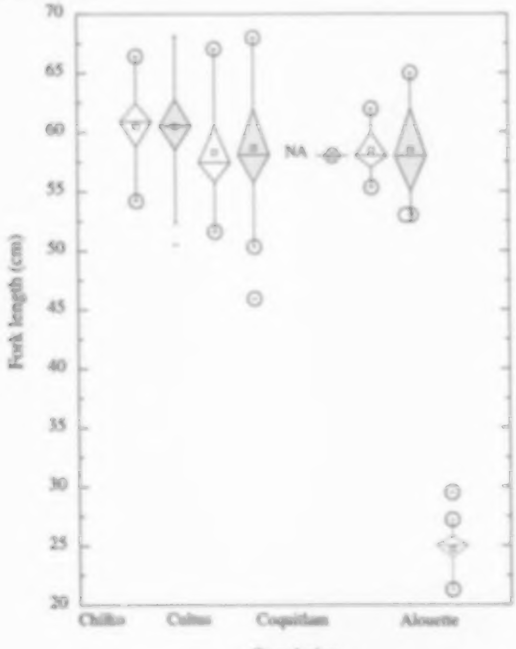

dam construction. The mean $\delta^{34}S$ and $^{87}Sr/^{86}Sr$ during the last 2 years of growth were also significantly higher in AUM (20.00‰ and 0.7091) than in kokanee (6.90‰, $P < 0.0001$; and 0.7048, $P < 0.0001$), but not significantly different than in anadromous sockeye salmon (21.15‰, $P = 0.76$; and 0.7092, $P = 0.92$). Finally, $\delta^{34}S$ DIFF of the AUM was significantly different from zero (DIFF = 14.41‰, $P < 0.0001$), which was not the case for kokanee (DIFF = –1.72‰, $P < 0.18$) or sockeye salmon (DIFF = –0.96‰, $P < 0.22$). The $^{87}Sr/^{86}Sr$ DIFF of both the AUM (0.0049, $P < 0.0001$) and sockeye salmon (0.00095, $P < 0.0001$) were significantly different than zero and significantly different from each other ($P < 0.0001$).

Evolutionary history of the Alouette and Coquitlam kokanee populations

Historical records

We attempted to assess whether kokanee existed sympatrically with sockeye salmon prior to dam construction or whether the existing kokanee population is recently derived from sockeye salmon since the construction of the dam. Historical records confirm that prior to the construction of the dams, natural lakes in both the Alouette and Coquitlam drainages supported sizeable populations of anadromous sockeye salmon (Wilson et al. 2003; Bengeyfield et al. 2001). After dam construction, sockeye salmon returning from the ocean in either system would have had no possibility to access the reservoirs (J. Bruce BC Hydro, 6911 Southpoint Drive (Floor E04), Burnaby, BC V3N 4X8, personal communication, 2010). We were unable to find any record of kokanee having existed in these natural lakes.

Kokanee were first documented in Alouette Lake in 1951. No sampling has been conducted in Coquitlam Reservoir (because of the restricted access), but kokanee were first documented in Buntzen Lake (immediately downstream via the tunnel) in 1955 (D. Jesson, BC Ministry of Environment, Surrey, British Columbia, unpublished data), which suggests that kokanee may have been in Coquitlam Reservoir by this time too. Our search of an electronic database (http://a100.gov.bc.ca/pub/fidq/stockedSpeciesSelect.do) and hardcopy files (D. Jesson, BC Ministry of Environment, Surrey, British Columbia, unpublished data) for either Coquitlam or Alouette produced no records that kokanee were stocked in either system from 1894 to present.

The fact that male kokanee in Alouette Reservoir resemble "residual sockeye salmon" (as described by Ricker 1938) in that they lack secondary sexual characteristics (Wilson et al. 2003) suggests a recent origin from anadromous sockeye salmon. Although we cannot rule out that kokanee existed sympatrically with sockeye salmon in the original natural lakes, as they do in some other lakes in the Lower Fraser (e.g., Chilliwack Lake), all the available evidence is consistent with a more recent origin.

Genetic data: genetic diversity and bottlenecks

Allelic richness was lower (<7) in all four kokanee popu-

Table 3. F_{ST} values for pairwise comparisons between juvenile downstream migrants (JDM), adult upstream migrants (AUM), and reference mitochondrial DNA (below diagonal).

	Alouette_K	Alouette_JDM	Alouette_AUM	Coquitlam_K	Coquitlam_JDM	Coquitlam_AUM
Alouette_K	—	0.002	0.004	**0.050**	**0.055**	**0.037**
Alouette_JDM	0.000	—	0.000	**0.045**	**0.051**	**0.036**
Alouette_AUM	0.000	0.000	—	**0.042**	**0.047**	**0.033**
Coquitlam_K	**0.143**	**0.120**	**0.088**	—	0.000	0.000
Coquitlam_JDM	**0.245**	**0.191**	**0.120**	–0.009	—	0.000
Coquitlam_AUM	**0.686**	**0.594**	**0.408**	0.045	0.021	—
Chilliwack_K	**0.986**	**0.981**	**0.966**	**0.651**	**0.697**	**0.735**
Cultus_K	**0.916**	**0.884**	**0.805**	**0.565**	**0.540**	**0.356**
Big Silver	**0.271**	**0.203**	0.110	0.020	0.014	0.076
Birkenhead	**0.955**	**0.938**	**0.894**	**0.598**	**0.607**	**0.533**
Chilliwack	**0.907**	**0.874**	**0.795**	**0.542**	**0.539**	**0.454**
Cultus	**0.820**	**0.764**	**0.643**	**0.411**	**0.369**	**0.155**
Harrison	**0.765**	**0.697**	**0.561**	**0.285**	**0.254**	0.102
Pitt	**0.474**	**0.393**	**0.269**	**0.043**	**0.047**	0.009
Weaver	**0.449**	**0.377**	**0.272**	**0.081**	**0.068**	–0.008
Widgeon	0.000	0.000	0.000	**0.096**	**0.138**	**0.463**

Note: Population is anadromous sockeye salmon unless denoted otherwise. Bold font indicates that the pairwise F_{ST} value is significantly greater than zero

Fig. 4. (*a*) Unrooted, consensus neighbour-joining dendrogram based on chord genetic distance showing phylogenetic relationships among reference samples of kokanee (solid circles) and anadromous sockeye salmon (open circles) from the lower Fraser River and juvenile downstream migrants (downward triangles) and adult upstream migrants (upward triangles) in the Alouette and Coquitlam rivers. The Chilko Lake sockeye salmon population is included as an outgroup. (*b*) Multidimensional scaling values (MDS) from matrix of chord distances among populations based on mitochondrial DNA (*Y* axis) plotted against corresponding MDS values based on microsatellite DNA (*X* axis). Location labels are as in Fig. 1. Dotted circles group populations rearing in the same nursery lake.

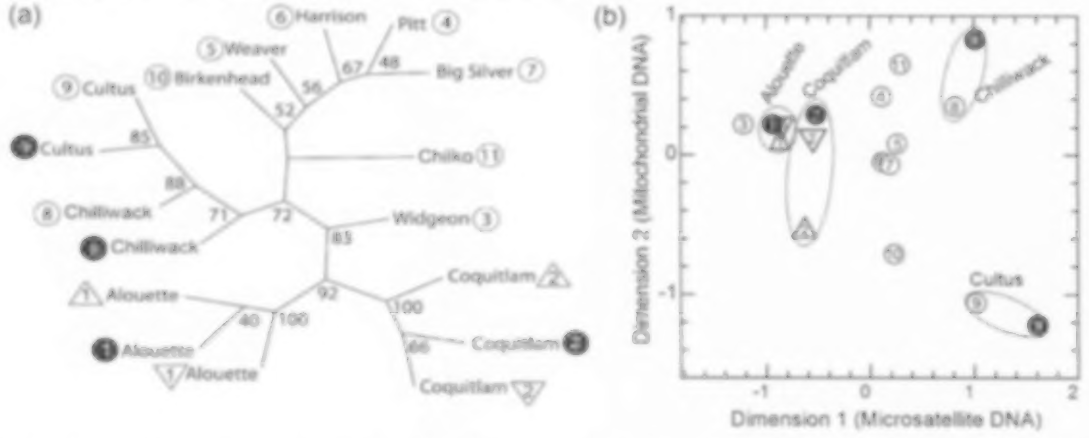

lations than in most sockeye salmon populations that we examined in the lower Fraser River (Table 4). Among sockeye salmon populations, Widgeon Slough in the Pitt River drainage and Cultus and Chilliwack lakes in the Chilliwack River drainage had unusually low levels of allelic richness and gene diversity. After accounting for multiple comparisons, four samples had significant levels of excess heterozygosity compared with expectations for populations in mutation–drift equilibrium (Table 4). These samples included kokanee in the Alouette and Coquitlam reservoirs, Cultus Lake kokanee, and Pitt River sockeye salmon.

The excess heterozygosity in the Alouette and Coquitlam kokanee samples suggests that abundance had been very low (i.e., bottlenecked) in the recent past, consistent with the hypothesis that they are recently derived from residual sockeye salmon that remained in the reservoir after dam construction. Low levels of diversity at microsatellite loci and fixation of a single mitochondrial haplotype in the Alouette kokanee population are also consistent with this scenario. The Coquitlam population has retained greater diversity at microsatellite loci and a greater diversity of mitochondrial haplotypes. These results suggest that the Alouette and Coquitlam kokanee populations were established independently, likely from distinct anadromous sockeye salmon populations that once inhabited the Alouette and Coquitlam rivers.

Discussion

Our results based on genetic and isotopic markers confirm that the anadromous AUM in the Alouette and Coquitlam populations of kokanee (K), and anadromous sockeye salmon in the lower Fraser River based on microsatellite DNA (above diagonal) and

Chilliwack_K	CultusK	Big Silver	Birkenhead	Chilliwack	Cultus	Harr	Pitt	Weaver	Widgeon
0.190	**0.148**	**0.092**	**0.113**	**0.134**	**0.184**	**0.096**	**0.096**	**0.112**	**0.186**
0.183	**0.141**	**0.089**	**0.105**	**0.129**	**0.172**	**0.091**	**0.091**	**0.105**	**0.187**
0.177	**0.138**	**0.085**	**0.102**	**0.127**	**0.169**	**0.085**	**0.087**	**0.105**	**0.203**
0.150	**0.108**	**0.068**	**0.070**	**0.095**	**0.147**	**0.073**	**0.071**	**0.084**	**0.196**
0.153	**0.104**	**0.071**	**0.072**	**0.089**	**0.139**	**0.072**	**0.073**	**0.085**	**0.206**
0.139	**0.099**	**0.053**	**0.057**	**0.085**	**0.136**	**0.058**	**0.054**	**0.072**	**0.200**
—	**0.145**	**0.123**	**0.115**	**0.164**	**0.166**	**0.126**	**0.116**	**0.162**	**0.257**
0.698	—	**0.089**	**0.081**	**0.098**	**0.091**	**0.090**	**0.069**	**0.099**	**0.265**
0.843	**0.638**	—	**0.036**	**0.102**	**0.129**	**0.023**	**0.023**	**0.040**	**0.180**
0.838	**0.532**	**0.721**	—	**0.090**	**0.119**	**0.034**	**0.038**	**0.045**	**0.180**
0.159	**0.453**	**0.640**	**0.538**	—	**0.099**	**0.110**	**0.103**	**0.090**	**0.224**
0.639	0.026	**0.455**	**0.476**	**0.423**	—	**0.126**	**0.124**	**0.106**	**0.278**
0.618	**0.360**	**0.311**	**0.184**	**0.335**	**0.250**	—	**0.026**	**0.044**	**0.186**
0.544	**0.426**	**0.097**	**0.479**	**0.346**	**0.276**	**0.118**	—	**0.050**	**0.174**
0.455	**0.309**	**0.132**	**0.397**	**0.283**	**0.172**	**0.094**	−0.004	—	**0.199**
0.971	**0.831**	**0.134**	**0.909**	**0.820**	**0.679**	**0.601**	**0.301**	**0.299**	—

($P < 0.05$ after Bonferroni correction).

Fig. 5. (*a*) Transmitted light micrograph of a polished otolith from an age-4 adult upstream migrant (AUM) to Alouette River in 2007. Ion probe pits (1–18, white circles) from sulfur isotope analysis and MC-ICPMS pits (1–8, white squares) from strontium isotope analysis. (*b*) Spatial distribution of the mean (±1 standard error, SE) ratio of strontium isotopes (open squares) and mean (±1 SE) ratio of sulfur isotopes (solid circles) in the (*i*) core–pre-exogenous, (*ii*) first year, and (*iii*) last 2 years of growth.

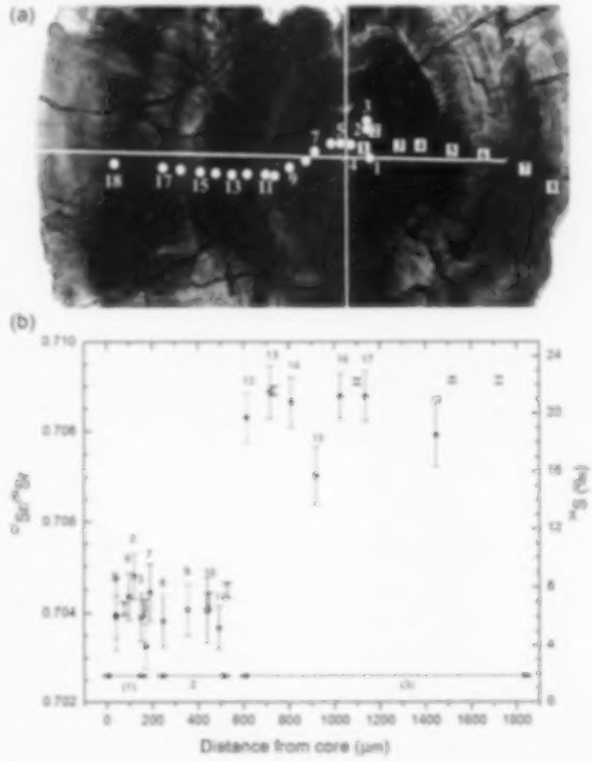

Fig. 6. Mean (±1 standard error, SE) ratio of stable isotopes of (*a*) $\delta^{34}S$ and (*b*) $^{87}Sr/^{86}Sr$ in the last 2 years of growth (*Y* axis) plotted against values in the core of the otolith (*X* axis) of Alouette adult upstream migrants (AUM), Alouette kokanee, and wild anadromous sockeye salmon from other populations in British Columbia. Ellipses illustrate groupings identified by analysis of variance (ANOVA).

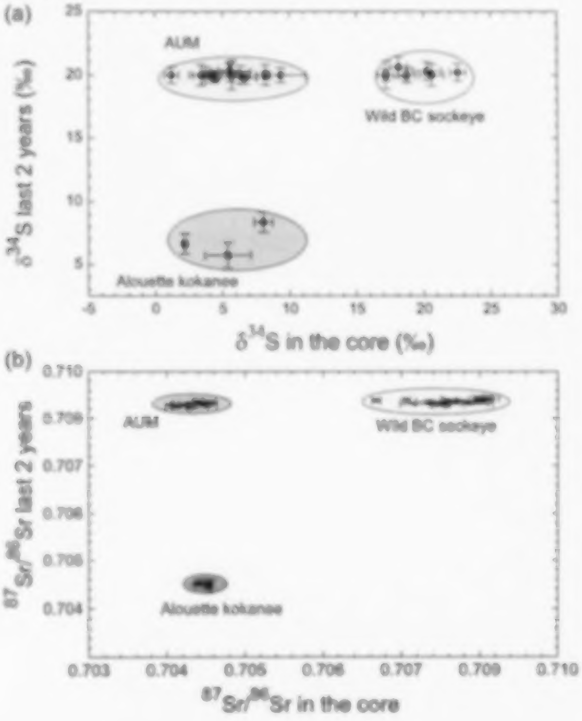

Table 4. Comparison of genetic diversity in reference populations of kokanee and sockeye salmon in the lower Fraser River.

Population	Mitochondrial DNA: No. of haplotypes	Mitochondrial DNA: Gene diversity	Microsatellite DNA: Allelic richness	Microsatellite DNA: Expected heterozygosity	Microsatellite DNA: Probability of bottleneck
Kokanee					
Alouette	1	0.00	5.8	0.64	**0.0004**
Coquitlam	5	0.40	6.9	0.67	**0.0006**
Chilliwack	2	0.09	6.2	0.63	0.0595
Cultus	3	0.50	6.8	0.69	**0.0017**
Sockeye					
Big Silver	2	0.22	8.1	0.71	0.0067
Birkenhead	2	0.22	8.7	0.72	0.0968
Chilliwack	3	0.48	6.0	0.62	0.0453
Cultus	3	0.61	6.7	0.59	0.1788
Harrison Rapids	3	0.59	8.8	0.71	0.1338
Pitt	4	0.58	9.4	0.73	**0.0021**
Weaver	5	0.69	8.3	0.66	0.0676
Widgeon	1	0.00	4.1	0.51	0.0290

Note: Sample sizes and descriptions are given in Table 1. Bold font indicates a statistically significant probability of a recent bottleneck (after correction for multiple comparisons).

rivers in 2007 and 2008 are sea-run kokanee originating from local nonanadromous (kokanee) populations. The possibility that these fish were strays is implausible because of the extent of genetic differentiation among populations in the lower Fraser River. In addition, the freshwater isotopic signature in otolith cores of the AUM ruled out the possibility of an Alouette sea- or river-type sockeye salmon. The genetic evidence for recent population bottlenecks in both the Alouette and Coquitlam kokanee populations, together with the lack of secondary sexual characteristics of Alouette male kokanee and the absence of historical records of kokanee in these reservoirs until mid-century, further suggests that these populations are recently derived from anadromous runs that were extirpated by the dams 20 to 25 generations ago.

The fact that JDM were ~5- to 10-fold more abundant in the Alouette River than in the Coquitlam River suggests that kokanee are more abundant in the Alouette Reservoir, perhaps as a result of lake fertilization that has occurred annually since 1999. Alternatively, given that sockeye salmon smolts migrate nocturnally and orient to the surface during downstream migration (Wood et al. 1993), the lower number of JDM in the Coquitlam River might be caused by the LLO being located 3 to 7 m below the water surface.

Whether nonanadromous ecotypes could be used to recreate anadromous populations that have become extinct depends in part on their survival and reproductive capacity. At this time, it is not known whether AUM transported in the Alouette Reservoir in 2008 reproduced successfully. Comparison of their body size, migration route, and marine survival to the corresponding data for other sea-run kokanee and anadromous sockeye salmon populations suggests that the AUM may contribute to the restoration of the anadromous ecotype of *O. nerka* in Alouette Reservoir.

Body size of adult sea-run kokanee from the Alouette Reservoir was similar to that of sockeye salmon returning to Chilko and Cultus lakes and to that of other North American sockeye salmon populations at the same latitude, and thus they could be expected to have similar fecundity (McGurk 2000). Migratory behaviour of sea-run kokanee juveniles seems to be similar to that of sockeye salmon. Acoustic tracking of 19 Alouette JDM showed that their migration rates to the lower Fraser River and into Juan de Fuca Strait were similar to that of juvenile salmon (Baxter and Bocking 2006). These results are consistent with the findings of Wood et al. (2011) that acoustically tagged sockeye salmon and kokanee dispersed from a marine release site near Sakinaw Lake, British Columbia, at the same rate and tended to follow the same migration route.

Smolt-to-adult survival of Alouette sea-run kokanee (corrected for harvest, including all age classes) was 0.57% in sea-entry year 2005 and 0.84% in 2006. These rates are lower than those observed in Chilko sockeye salmon (1.53% and 3.97%), but similar to those in Cultus sockeye salmon (0.68% and 1.35%) in the same years. Lower marine survival of sea-run kokanee may be related to the relatively late timing of the experimental water releases, as earlier downstream migration appeared to be associated with higher marine survival. Chilko smolts emigrated 10 days earlier in 2005 and 7 days earlier in 2006 than Cultus smolts (T. Cone, Fisheries and Oceans Canada, Annacis Island, British Columbia, unpublished data). Chilko smolts also migrated downstream at a faster pace, requiring only 7 days on average to reach the mouth of the Fraser River from Chilko Lake (Crittenden 1994; D. Welch, Kintama Research, Nanaimo, British Columbia, personal communication, 2011) compared with 4 to 5.6 days from Cultus Lake (Welch et al. 2009), despite the sevenfold greater travel distance from Chilko Lake. At this rate of travel, 50% and 60% of Chilko Lake smolts (compared with only 10% and 35% of Cultus Lake smolts) would have already reached the mouth of the Fraser River by the time water was first spilled from the Alouette Reservoir in 2005 and 2006, respectively.

Comparison of marine survival rates in different years is complicated by annual and decadal fluctuations in marine climate. We note that survival rates of Alouette sea-run kokanee that migrated volitionally in sea-entry years 2005 and 2006 were higher than those sea-run kokanee forced to migrate in experiments in the 1940s with kokanee populations that had been isolated for ~10 000 years (0.004% for Lake Chelan, 0.12% for Kootenay lake kokanee released from Cultus Lake; total sea-run kokanee in the fishery/number yearlings). However, within the same period (1933–1936; Foerster 1936), marine survival rate of the Kootenay Lake kokanee released from Cultus Lake was 15- to 24-fold lower than that of Cultus Lake sockeye salmon.

Our study confirms that kokanee isolated from anadromous sockeye salmon for at least 80 to 90 years can revert to anadromy. Additional work is needed to compare the marine survival, growth, migratory behaviour, and reproductive capacity of sea-run kokanee that have been isolated for various amounts of time.

Acknowledgements

This research benefited from substantial contributions by various individuals. We thank James Bruce, Dave Hunter, Brent Wilson, LGL Limited, Maurice Coulter-Boisvert, Matt Foy, the Alouette River Management Society, and Duane Jesson for providing data or information from lake surveys, and Jim Irvine for his support. Additionally, Tatiana Bruk helped with otolith imagery, Emma-Jane Johnson provided kokanee otoliths from Alouette Lake, Jim Cameron assisted in the field, and the staff of the Pacific Salmon Commission Scale Laboratory helped with age determination. Justin Glessner at University of California – Davis provided much appreciated help with the MC-ICPMS, and Frank Loge and the PBS Ageing Laboratory graciously loaned the use of microscopes and cameras. We also appreciate the helpful comments and suggestions by two anonymous reviewers. The UCLA ion microprobe laboratory is partially supported by a grant from the National Science Foundation Instrumentation and Facilities Program. Any use of trade names herein facilitates descriptive purposes only and does not imply endorsement by the Canadian or US governments.

References

Backle, A. 2008. Alouette River sockeye trap and truck, Maple Ridge, BC. 2008–2009 [online]. Prepared for BC Hydro Bridge Coastal Fish and Wildlife Restoration Program 08.ALU.04. Available from http://www.bchydro.com/bcrp/projects/docs/bridge_river/08.ALU.04.pdf [accessed January 2011].

Barnett-Johnson, R., Ramos, F.C., Grimes, C.B., and MacFarlane, R.B. 2005. Validation of Sr isotopes in otoliths by laser ablation multicollector inductively coupled plasma mass spectrometry (LA-MC-ICPMS): opening avenues in fisheries science applications. Can. J. Fish. Aquat. Sci. **62**(11): 2425–2430. doi:10.1139/f05-194.

Baxter, B.E., and Bocking, R.C. 2006. Field trials to assess coho smolt migration success through the Alouette Reservoir, 2005 [online]. Report prepared by LGL Limited for BC Hydro Bridge Coastal Fish and Wildlife Restoration Program. Available from http://www.bchydro.com/bcrp/projects/docs/bridge_river/05A102.pdf [accessed January 2011].

BC Hydro. 2005. Coquitlam–Buntzen Project water use plan [online]. Available from http://www.bchydro.com/etc/medialib/internet/documents/environment/pdf/wup_coquitlam_water_use_plan_pdf.Par.0001.File.wup_coquitlam_water_use_plan.pdf [accessed January 2011].

BC Hydro. 2009. Alouette Project water use plan (April 15, 2009) [online]. Available from http://www.bchydro.com/etc/medialib/internet/documents/environment/pdf/wup_-_alouette_wup.Par.0001.File.Alouette_WUP_Rev_for_Accept_15_Apr_2009.pdf [accessed January 2011].

Beacham, T.D., Candy, J.R., McIntosh, B., MacConnachie, C., Tabata, A., Kaukinen, K., Deng, L., Miller, K.M., Withler, R.E., and Varnavskaya, N.V. 2005. Estimation of stock composition and individual identification of sockeye salmon on a Pacific Rim basis using microsatellite and major histocompatibility complex variation. Trans. Am. Fish. Soc. **134**(5): 1124–1146. doi:10.1577/T05-005.1.

Bengeyfield, W., Hay, D., Joyce, S., and Greenbank, J. 2001. Evaluation of restoring historic fish passage for anadromous fish at BC Hydro facilities [online]. Report for Power Supply Environment, BC Hydro, Burnaby, B.C. Available from http://www.bchydro.com/bcrp/reports/docs/global_fish_passage.pdf [accessed January 2011].

Burgner, R.L. 1991. Life history of sockeye salmon (*Oncorhynchus nerka*). *In* Pacific salmon life histories. *Edited by* C. Groot and L. Margolis. University of British Columbia Press, Vancouver, B.C. pp. 3–117.

Cavalli-Sforza, L.L., and Edwards, A. 1967. Phylogenetic analysis: models and estimation procedures. Am. J. Hum. Genet. **19**(3 Part 1): 233–257. PMID:6026583.

Conlin, K., Lamont, C., and MacFarlane, S. 2000*a*. Chapter 6: Alouette River Watershed [online]. *In* Bridge-coastal fish and wildlife restoration program strategic plan. Vol. 2. Watershed plans. Available at http://www.bchydro.com/bcrp/about/docs/ch06_final.pdf [accessed February 2011].

Conlin, K., Lamont, C., and MacFarlane, S. 2000*b*. Chapter 8: Coquitlam River and Buntzen Lake watersheds [online]. *In* Bridge-coastal fish and wildlife restoration. Vol. 2. Watershed plans. Available at http://www.bchydro.com/bcrp/about/docs/ch08_final.pdf [accessed 15 February 2011].

Cope, S. 2010. Alouette River salmonid smolt migration enumeration: 2009 data report [online]. Prepared for Alouette Management Committee and BC Hydro Generation. Available from http://www.bchydro.com/etc/medialib/internet/documents/planning_regulatory/wup/lower_mainland/2010q2/alumon-1_yr2_jan_2010.Par.0001.File.ALUMON_1_Yr2_Jan_2010.pdf [accessed January 2011].

Cornuet, J.M., and Luikart, G. 1996. Description and power analysis of two tests for detecting recent population bottlenecks from allele frequency data. Genetics, **144**(4): 2001–2014. PMID:8978083.

Crittenden, R.M. 1994. A diffusion model for the downstream migration of sockeye salmon smolts. Ecol. Model. **71**(1–3): 69–84. doi:10.1016/0304-3800(94)90076-0.

Derek, S., Macnair, J., and Lewis, G. 2010. Coquitlam River fish monitoring program: 2000–2009 results. BC Hydro Lower Coquitlam Fish Productivity Index — Year 4 Reference: COQMON#7. BC Hydro, Burnaby, B.C.

Ding, T., Valkiers, S., Kipphardt, H., De Bièvre, P., Taylor, P.D.P., Gonfiantini, R., and Krouse, R. 2001. Calibrated sulfur isotope abundance ratios of three IAEA sulfur isotope reference materials and V-CDT with a reassessment of the atomic weight of sulfur. Geochim. Cosmochim. Acta, **65**(15): 2433–2437. doi:10.1016/S0016-7037(01)00611-1.

El Mousadik, A., and Petit, R.J. 1996. High level of genetic differentiation for allelic richness among populations of the argan tree (*Agrania spinosa* (L.) Skeels) endemic to Morocco. Theor. Appl. Genet. **92**(7): 832–839. doi:10.1007/BF00221895.

Felsenstein, J. 1993. PHYLIP (Phylogeny Inference Package) Version 3.5c [online]. Available from http://cmgm.stanford.edu/phylip/ [accessed September 2010].

Felsenstein, J. 2005. PHYLIP (Phylogeny Inference Package) Version 3.6. Department of Genome Sciences, University of Washington, Seattle, Wash.

Foerster, R.E. 1936. The return from the sea of sockeye salmon (*Oncorhynchus nerka*) with special reference to percentage survival, sex proportions and progress of migration. J. Fish. Res. Board Can. **3**: 26–42.

Foerster, R.E. 1947. Experiment to develop sea-run from land-locked sockeye salmon (*Oncorhynchus nerka kennerlyi*). J. Fish. Res. Board Can. **7**(2): 88–93. doi:10.1139/f47-010.

Foote, C.J. 1989. Female mate preference in Pacific salmon. Anim. Behav. **38**(4): 721–723. doi:10.1016/S0003-3472(89)80022-3.

Foote, C.J., Mayer, I., Wood, C.C., Clarke, W.C., and Blackburn, J. 1994. On the developmental pathway to nonanadromy in sockeye salmon, *Oncorhynchus nerka*. Can. J. Zool. **72**(3): 397–405. doi:10.1139/z94-056.

Fulton, L.A., and Pearson, R.E. 1981. Transplantation and homing experiments on salmon, *Oncorhynchus* spp., and steelhead trout, *Salmon airdneri*, in the Columbia River system: fish of the 1939–1944 broods. NOAA Tech. Memo. NMFS F/NWC 12.

Godbout, L., Trudel, M., Irvine, J., Wood, C.C., Grove, M.J., Schmitt, A.K., and McKeegan, K.D. 2010. Sulfur isotopes in otoliths allow discrimination of anadromous and non-anadronous ecotypes of sockeye salmon, *Oncorhynchus nerka*. Environ. Biol. Fishes, **89**(3–4): 521–532. doi:10.1007/s10641-010-9689-7.

Goudet, J. 2001. FSTAT, a program to estimate and test gene diversities and fixation indices (version 2.9.3) [online]. Available from http://www2.unil.ch/popgen/softwares/fstat.htm [accessed January 2011].

Gustafson, R.G., Waples, R.S., Myers, J.M., Weitkamp, L.A., Bryant, G.J., Johnson, O.W., and Hard, J.J. 2007. Pacific salmon extinctions: quantifying lost and remaining diversity. Conserv. Biol. **21**(4): 1009–1020. doi:10.1111/j.1523-1739.2007.00693.x. PMID:17650251.

Hilborn, R., Quinn, T.P., Schindler, D.E., and Rogers, D.E. 2003. Biocomplexity and fisheries sustainability. Proc. Natl. Acad. Sci. U.S.A. **100**(11): 6564–6568. doi:10.1073/pnas.1037274100. PMID:12743372.

Hirst, S.M. 1991. Impacts of the operation of existing hydroelectric developments on fishery resources in British Columbia. Inland fisheries news. Volume 1. Can. Manuscr. Rep. Fish. Aquat. Sci. **2093**.

Humble, S.R., Blakley, A.C., and Bocking, R.C. 2006. Field trials to assess steelhead smolt migration success through the Alouette Reservoir, 2006 [online]. LGL Limited Prepared for BC Hydro Bridge Coastal Fish and Wildlife Restoration Program. Available from http://www.bchydro.com/bcrp/projects/docs/bridge_river/06.ALU.02.pdf [accessed January 2011].

Kalish, J.M. 1990. Use of otolith microchemistry to distinguish progeny of sympatric anadromous and non-anadromous salmonids. Fish. Bull. **88**(4): 657–666.

Koop, W. 2001. Red fish up the river. A report on the former Coquitlam salmon migrations and the hydro-electric developments at Coquitlam Lake, British Columbia, pre-1914 [online]. Presented by the Kwikwetlem Nation through BCRP and Coquitlam/Buntzen Water Use Plan. Available from http://www.bchydro.com/bcrp/reports/docs/RedFishUpTheRiver.pdf [accessed January 2011].

Krogius, F.V. 1981. The role of resident fish in the reproduction of anadromous sockeye salmon, *Oncorhynchus nerka*. J. Ichthyol. **21**: 14–21.

McGurk, M.D. 2000. Comparison of fecundity–length–latitude relationships between nonanadromous (kokanee) and anadromous sockeye salmon (*Oncorhynchus nerka*). Can. J. Zool. **78**(10): 1791–1805.

Neaves, P.I., Wallace, C.G., Candy, J.R., and Beacham, T.D. 2005. CBayes: computer program for mixed stock analysis of allelic data. Version v4.02 [online]. Available from http://www.pac.dfo-mpo.gc.ca/science/facilities-installations/pbs-sbp/mgl-lgm/apps/index-eng.htm [accessed September 2010; updated 26 March 2010].

Ricker, W.E. 1938. "Residual" and kokanee salmon in Cultus lake. J. Fish. Res. Board Can. **4**(3): 192–218. doi:10.1139/f38-018.

Ricker, W.E. 1959. Additional observations concerning residual sockeye and kokanee (*Oncorhynchus nerka*). J. Fish. Res. Board Can. **16**(6): 897–902. doi:10.1139/f59-063.

Ricker, W.E. 1972. Hereditary and environmental factors affecting certain salmonid populations. *In* The stock concept in Pacific salmon. *Edited by* R.C. Simon and P.A. Larkin. MacMillan Lectures in Fisheries, The University of British Columbia, Vancouver, B.C. pp. 19–160.

SAS Institute Inc. 2008. SAS/STAT 9.2 user's guide: the GLM procedure. SAS Publishing, Cary, N.C.

Schindler, D.E., Hilborn, R., Chasco, B., Boatright, C.P., Quinn, T.P., Rogers, L.A., and Webster, M.S. 2010. Population diversity and the portfolio effect in an exploited species. Nature, **465**(7298): 609–612. doi:10.1038/nature09060. PMID:20520713.

Slaney, T.L., Hyatt, K.D., Northcote, T.G., and Fielden, R.J. 1996. Status of anadromous salmon and trout in British Columbia and Yukon. Fisheries, **21**(10): 20–35.

SYSTAT. 2004. SYSTAT 11 [online]. SYSTAT Software, Inc. Richmond, Calif. Available from http://www.systat.com [accessed November 2007].

Urawa, S., and Kaeriyama, M. 1999. Temporary residence of precocious sockeye salmon (*Oncorhynchus nerka*) in the ocean. Bull. Natl. Salmon Resour. Cent. No. 2. pp. 9–13.

Waples, R.S., and Hendry, A.P. 2008. Evolutionary perspectives on salmonid conservation and management. Evol. Appl. **1**(2): 183–188. doi:10.1111/j.1752-4571.2008.00035.x.

Welch, D.W., Melnychuk, M.C., Rechisky, E.R., Porter, A.D., Jacobs, M.C., Ladouceur, A., McKinley, R.S., and Jackson, G.D. 2009. Freshwater and marine migration and survival of endangered Cultus Lake sockeye salmon (*Oncorhynchus nerka*) smolts using POST, a large-scale acoustic telemetry array. Can. J. Fish. Aquat. Sci. **66**(5): 736–750. doi:10.1139/F09-032.

Wilson, G., Ashley, K., McCusker, M., Land, R., Stockner, J., Scholten, G., Dolecki, D., and Sebastian, D. 2003. The Alouette fertilization experiment: Year 1998–2002, Final Report. Fisheries Science Section. RD99. Ministry of Water, Land, and Air Protection Aquatic Ecosystem Section. Surrey, B.C.

Wood, C.C., and Foote, C.J. 1996. Evidence for sympatric genetic divergence of anadromous and nonanadromous morphs of sockeye salmon (*Oncorhynchus nerka*). Evolution, **50**(3): 1265–1279. doi:10.2307/2410667.

Wood, C.C., Hargreaves, N.B., Rutherford, D.T., and Emmett, B.T. 1993. Downstream and early marine migratory behaviour of sockeye salmon (*Oncorhynchus nerka*) smolts entering Barkley Sound, Vancouver Island. Can. J. Fish. Aquat. Sci. **50**(6): 1329–1337. doi:10.1139/f93-151.

Wood, C.C., Bickham, J.W., Nelson, R.J., Foote, C.J., and Patton, J.C. 2008. Recurrent evolution of life history ecotypes in sockeye salmon: implications for conservation and future evolution. Evol. Appl. **1**(2): 207–221. doi:10.1111/j.1752-4571.2008.00028.x.

Wood, C.C., Welch, D.W., Godbout, L., and Cameron, J. 2011. Marine migratory behavior of hatchery-reared anadromous and wild non-anadromous sockeye salmon revealed by acoustic tags. *In* Advances in fish tagging and marking technology. *Edited by* J. McKenzie, Q. Phelps, R. Kopf, M. Mesa, B. Parsons, and A. Seitz. American Fisheries Society, Symposium 76, Bethesda, Md.

Bayesian fishable biomass dynamics models incorporating fished area and relative fish density

Shijie Zhou, Andre E. Punt, Roy Deng, Marco Kienzle, and Wayne Rochester

Abstract: Fisheries typically experience large changes over time in fishing effort. The size of the area fished may also change substantially over time, mimicking the trend in fishing effort, and may have major effects on the population dynamics and fishing process. We extend a biomass dynamics model to incorporate fished area and relative fish density in fished and unfished areas. The fishable population is defined as those individuals in the fished area and those that are sufficiently close to the fished area that they could potentially move into fished area during the fishing season. We estimate fishable biomass using three models assuming different level of population mixing between fished and unfished areas (i.e., partial mixing, full mixing, and no mixing). The models are implemented within a hierarchical Bayesian framework. Model performance is explored using simulations, and the approach is illustrated using logbook data for two tiger prawn species in Australia's Northern Prawn Fishery. The partial mixing model that involves estimating a mixing parameter performs better than the models that assume no or full mixing. The methods could be applied to other fisheries where the area fished has changed substantially over the history of the fishery.

Résumé : Les pêches commerciales connaissent typiquement de grands changements temporels de leur effort de pêche. La surface de la zone de pêche peut aussi changer de manière substantielle dans le temps, mimant la tendance de l'effort de pêche, et peut avoir un effet majeur sur la dynamique de la population et sur le processus de pêche. Nous faisons l'extension d'un modèle de la dynamique de la biomasse afin d'inclure la surface pêchée et la densité relative des poissons dans les zones pêchées et non pêchées. Nous définissons la population capturable comme contenant les individus dans la zone pêchée et ceux qui sont suffisamment proches de la zone de pêche qu'ils pourraient pénétrer dans la zone de pêche durant la saison de capture. Nous estimons la biomasse capturable à l'aide de trois modèles qui présupposent des niveaux différents de mélange entre les zones pêchées et non pêchées (c.-à-d. mélange partiel, mélange total et mélange nul). Les modèles sont utilisés dans un cadre hiérarchique bayésien. Nous explorons la performance des modèles à l'aide de simulations et illustrons la méthode à partir de données tirées des journaux de pêche sur deux espèces de crevettes tigrées de la pêche commerciale de crevettes du nord de l'Australie. Le modèle de mélange partiel qui estime un paramètre de mélange fonctionne mieux que les modèles qui présupposent un mélange complet ou nul. Ces méthodes peuvent s'appliquer à d'autres pêcheries commerciales dans lesquelles la zone de pêche a considérablement changé durant l'histoire de cette pêche.

[Traduit par la Rédaction]

Introduction

Industrial fisheries typically experience substantial changes in fishing effort and catch over their history. This has been conceptualized as the "fisheries cycle" (Food and Agriculture Organization of the United Nations 1984). A typical fisheries cycle may include a pre-industrial phase, an expansion phase, a mature phase, and a senescent phase. Fishing effort grows to a peak and then reduces to a more or less sustainable level during this cycle. An expansion and later contraction of the area fished may be associated with changes in fishing effort. Fish stock assessments often attempt to use all of the available data that have been collected during the history of a fishery, which would include changes over time in fishing effort and the area fished. Standardization of catch rate (i.e., catch per unit effort, CPUE) data (Maunder and Punt 2004; Bishop et al. 2008) is one common way to attempt to ensure that data from different sources or time periods are comparable. However, area fished is seldom included as a factor when standardizing catch and effort data, in particular because it is usually difficult to adjust for changes over time in area fished (Campbell 2004). CPUE standardization considers only the data from the area fished and hence relates only to the component of the stock within the area fished and not to components of the stock that are outside this area. The size of the area fished will affect both the population dynamics and the impact of fishing on the stock. Further, organisms are typically not randomly distributed in space over their suit-

Received 17 November 2010. Accepted 4 June 2011. Published at www.nrcresearchpress.com/cjfas on 6 September 2011.
J2011-0150

Paper handled by Associate Editor Kenneth Rose.

S. Zhou, R. Deng, M. Kienzle, and W. Rochester. CSIRO Wealth from Oceans Flagship, Division of Marine and Atmospheric Research, GPO Box 2583, Brisbane, QLD 4001, Australia.
A.E. Punt. CSIRO Wealth from Oceans Flagship, Division of Marine and Atmospheric Research, GPO Box 1538, Hobart TAS 7001, Australia; School of Aquatic and Fishery Sciences, Box 355020, University of Washington, Seattle, WA 98195-5020, USA.

Corresponding author: S. Zhou (e-mail: Shijie.zhou@csiro.au).

Can. J. Fish. Aquat. Sci. **68**: 1603–1614 (2011) doi:10.1139/F2011-083 Published by NRC Research Press

Fig. 1. The number of grids where grooved and brown tiger prawns were caught (1970–2007). Solid line, grooved tiger prawns; dotted line, brown tiger prawns.

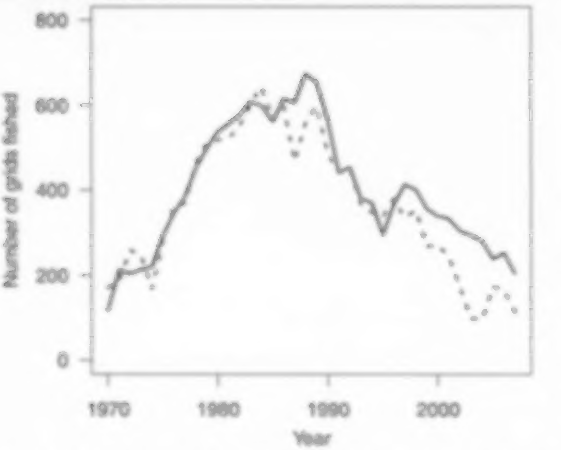

able habitat. Variation in density across the area occupied by a stock further complicates assessing the impact of area fished on population dynamics and hence the impact of fishing. Few studies have quantitatively explored these potential issues within the context of a stock assessment (but see Die et al. 1990).

In this paper we extend a biomass dynamics model to explore the effect of changes in area fished and relative fish density on the performance of a stock assessment method. We base the analysis on a non-equilibrium biomass dynamics model implemented within a multistock, multifleet, hierarchical Bayesian estimation framework because this method is particularly pertinent to species that move slowly and the fishing season is relatively short so that individuals in fished and unfished areas may not have time to fully mix. The population being assessed can be considered to be a single biological unit. However, some components of the population may be more susceptible to fishing than others. For example, components within the area fished will be directly affected by fishing, those close to the area fished could interact (exchange) with those in the area fished, and there may be some components that are too far away from the area fished to be affected by fishing. The model, referred to as the "fishable biomass dynamics model", distinguishes between "fishable" and "total" biomass to enable the impacts of fishing to be captured in a fairly simple way.

Simulation is first used to evaluate the performance of the fishable biomass dynamics model as well as the consequences of not accounting for the impact of changes over time in the area fished on the key outputs from a stock assessment. Time series of catch and effort are generated from a fishable biomass dynamics model with known parameters. The fishable biomass dynamics model is then fitted to these data in a manner similar to its application to actual fishery data, and the estimates of key model outputs are compared with the known values for these outputs (Punt 2003). The method is then demonstrated by applying it to data for two prawn species (grooved tiger prawn, *Penaeus semisulcatus*; and brown tiger prawn, *Penaeus esculentus*) in Australia's Northern Prawn Fishery (NPF).

Materials and methods

Tiger prawns and the NPF

The tiger prawn fishery off northern Australia targets two species of tiger prawns, *P. semisulcatus* and *P. esculentus*. This fishery has generally been open between April and November with midseason closures during the last two decades. The area fished, expressed in 6 × 6 nautical mile grids (1 n.mi = 1.852 km; the finest resolution at which historical catch and effort data have been reported), has changed substantially over the history of the fishery, from less than 300 grids at the start of the fishery to more than 1100 grids during the early 1980s, after which the number of grids fished dropped to fewer than 300 in recent years (Fig. 1). The logbook data show a clear linear relationship between catch and area fished (Fig. 2).

Assessments of the two tiger prawn species are based primarily on catch and effort data from commercial logbooks. The two species of tiger prawns in the NPF have each been divided into seven putative "stocks" based on geographic and biological information (Dichmont et al. 2005). However, these seven stocks have been combined into four stocks for assessment purposes primarily because the abundance in some of these putative stocks is so low that the data are uninformative, precluding the application of assessment models (Dichmont et al. 2005). For simplicity, we follow Zhou et al. (2009*a*) and refer to these four stocks as follows: Outside Gulf of Carpentaria — Stock 1; Groote — Stock 2; Vanderlins — Stock 3; and Weipa — Stock 4.

The reported catch and effort data are aggregated across tiger prawn species. A statistical model has been developed that is able to allocate the catches to species and identify "fleets" that target each tiger prawn species (Venables and Dichmont 2004). The four fleets considered in this study are a grooved tiger fleet targeting *P. semisulcatus*, a brown tiger fleet targeting *P. esculentus*, a red legged banana fleet targeting *Penaeus indicus*, and a common banana fleet targeting *Penaeus merguiensis*. These four fleets all catch some tiger prawns, so their catch is included in the analyses. However, the catch rate indices for the two banana prawn fleets are not used for parameter estimation because their catches of tiger prawns are very small.

Biomass dynamics models incorporating fished area and relative fish density

Prawns in each of the four stock regions (hereafter denoted "stocks") are assumed to be biologically independent (i.e., there is no spawner or larval migration among the four stocks; Dichmont et al. 2005). For stock *s*, the stochastic version of the standard biomass dynamics model can be written as

$$(1) \qquad B_{s,y} = \left[B_{s,y-1} + r_s B_{s,y-1}\left(1 - \frac{B_{s,y-1}}{K_s}\right) - \sum_f C_{s,f,y-1}\right] e^{\varepsilon^B_{s,y}}$$

where $B_{s,y}$ is the biomass of stock *s* during year *y* (in metric tonnes), r_s is the intrinsic rate of growth for stock *s*, K_s is the carrying capacity for stock *s*, and $C_{s,f,y}$ is the observed catch of prawns of stock *s* by fleet *f* during year *y*. $\varepsilon^B_{s,y}$ is the process error for stock *s* during year *y*, and we assume $\varepsilon^B_{s,y} \sim N\left(0;\sigma^2_{B,s}\right)$, where the variance $\sigma^2_{B,s}$ determines the extent of process error in the dynamics.

Fig. 2. Annual catch of grooved (*a*) and brown (*b*) tiger prawns versus the number of grids fished (1970–2007).

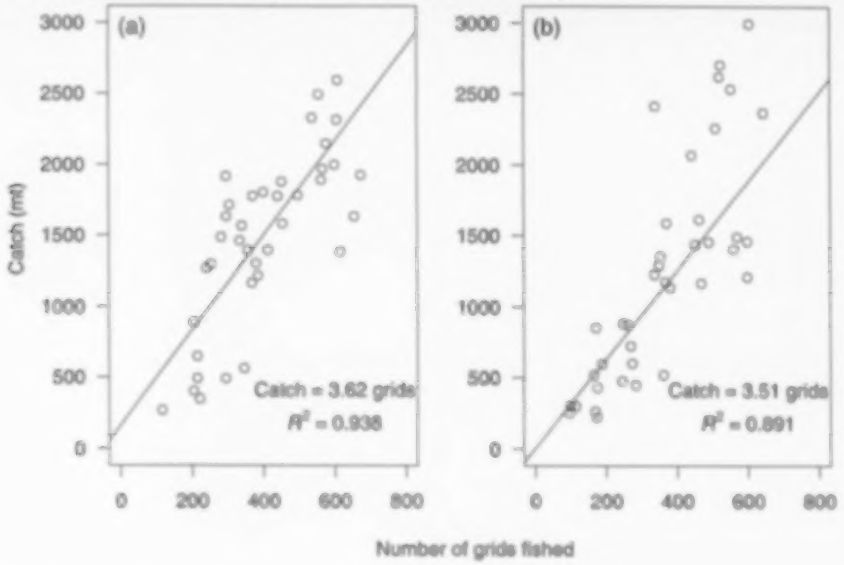

Fig. 3. Illustration of population components mixing between fished and unfished areas. Individuals in the outer white area belong to the component that is not affected by fishing during the fishing season; *d* is the maximum distance that individuals could move during the fishing season.

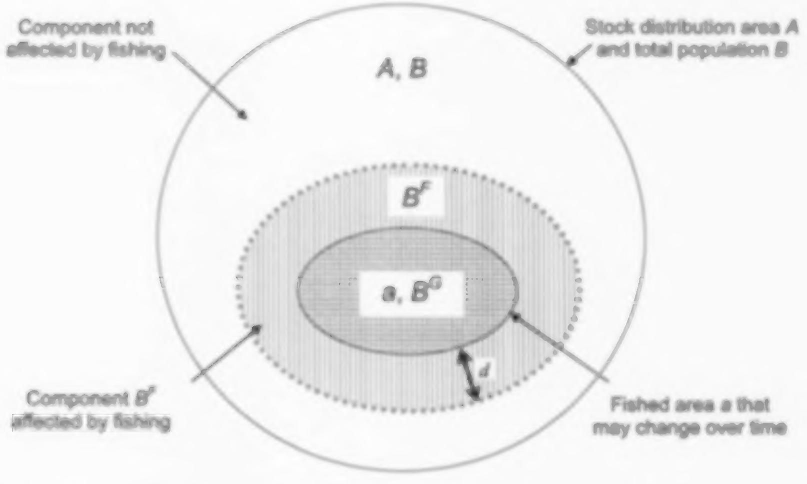
Component not affected by fishing
Stock distribution area *A* and total population *B*
A, *B*
B^F
a, B^G
d
Component B^F affected by fishing
Fished area *a* that may change over time

A fishery may not be able to access the entire population when fishing occurs on a subset of the total stock distribution area and the fishing season is relatively short. Only the fraction of population that is affected by fishing can be captured by the fishery. The fishable biomass consists of the mass of individuals within the area fished and that of individuals that are sufficiently close to the area fished that they can move into the area fished during the fishing season (Fig. 3). This terminology is similar to the concept of "available biomass" (Marr 1951). There are three possible assumptions regarding how prawns in the fished and unfished areas mix during the fishing season: no mixing, full mixing, and partial mixing. The fishable biomass may be calculated as follows if prawn density is the same in the fished and unfished areas:

$$(2) \qquad B^F_{s,f,y} = \left(\frac{a_{s,f,y}}{A_s}\right)^{\phi_s} B_{s,y}$$

where $B^F_{s,f,y}$ is the fishable biomass for stock *s* fished by fleet *f* during year *y*, A_s is the total area where stock *s* has been caught during the history of the fishery, and $a_{s,f,y}/A_s$ is the fraction of A_s that was fished by fleet *f* during year *y*. The parameter ϕ determines the mixing process: no mixing when $\phi = 1$, full mixing when $\phi = 0$, and partial mixing when $0 < \phi < 1$. Note this equation assumes there are two population components: one fishable and another unfishable. However, these two population components are assumed to belong to the same biological stock in terms of reproduction, growth, and natural mortality. This is a reasonable assumption for ti-

Table 1. Parameters, priors, and hyperpriors.

Parameter	Treatment
Estimated	
Growth rate r_s	$r_s \sim \text{lognormal}(\mu_r, \sigma_r^2)$
Carrying capacity K_s	$K_s \sim \text{lognormal}(\mu_K, \sigma_K^2)$
Catchability $q_{s,f}$	$q_{s,f} \sim \text{lognormal}(\mu_{q,f}, \sigma_{q,f}^2)$
Mixing parameter ϕ	$\phi_s \sim N(\mu_\phi, \sigma_\phi^2)$
Process error	$\varepsilon_{s,y}^B \sim N(0, \sigma_{B,s}^2)$
Observation error	$\varepsilon_{s,f,y}^U \sim N(0, \sigma_{U,s,f}^2)$
Hyperparameters	
r_s prior mean μ_r	$\mu_r \sim \text{normal}(M_r, \Sigma_r)$
K_s prior mean μ_K	$\mu_K \sim \text{normal}(M_K, \Sigma_K)$
ϕ_s prior mean μ_ϕ	$\mu_\phi \sim \text{normal}(M_\phi, \Sigma_\phi)$
$q_{s,f}$ prior mean $\mu_{q,f}$	$\mu_{q,f} \sim \text{normal}(M_{q,f}, \Sigma_{q,f})$
Variance Σ_θ (for r, K, and q)	$\Sigma_\theta^2 \sim \text{half-Couchy}, \dfrac{\lvert\vartheta_\theta\rvert}{\sqrt{v_\theta}}$
Parameters of the half-Cauchy	$\vartheta_\theta \sim N(0, 5)$; $v_\theta \sim \text{inverse gamma}(0.5, 0.5)$
Variance in growth rate	$\sigma_r^2 \sim \text{inverse gamma}(0.001, 0.001)$
Variance in carrying capacity	$\sigma_K^2 \sim \text{inverse gamma}(0.001, 0.001)$
Variance in catchability	$\sigma_{q,f}^2 \sim \text{inverse gamma}(0.001, 0.001)$
Variance in mixing parameter	$\sigma_\phi^2 \sim \text{inverse gamma}(0.001, 0.001)$
Variance in process error	$\sigma_{B,s}^2 \sim \text{inverse gamma}(0.001, 0.001)$
Variance in observation error	$\sigma_{U,s,f}^2 \sim \text{inverse gamma}(0.001, 0.001)$

ger prawns because eq. 1 has an annual time step, the fishery only occurs over a relatively short period during the year, and particularly because natural mortality is very high for tiger prawns (~0.05 week^{-1}).

The catch rate (catch per unit effort U) relates to the fishable biomass:

$$U_{s,f,y} = \frac{C_{s,f,y}}{E_{s,f,y}} = B_{s,f,y}^F q_{s,f} P_y e^{\varepsilon_{s,f,y}^U} \tag{3}$$

where $E_{s,f,y}$ is the fishing effort targeted by fleet f at prawns in stock s during year y, $q_{s,f}$ is catchability coefficient for fleet f for prawns in stock s, and P_y is efficiency of 1 day of fishing in year y relative to that in 1993, set for this paper to the "base case high" series of Bishop et al. (2008). The observation error is assumed to be stock- and fleet-specific, and we assume $\varepsilon_{s,f,y}^U \sim N(0, \sigma_{U,s,f}^2)$.

Fish (including prawns) are typically not randomly or evenly distributed within their distribution area, so it is reasonable to assume that average fish density differs across the distribution area. The biomass within the area fished of stock s during year y is given by

$$B_{s,f,y}^G = \sum_{g \in G} \varsigma D_{s,y,g} = a_{s,f,y} \overline{D}_{s,y}^G \tag{4}$$

where ς is the area of one grid cell, $D_{s,y,g}$ is density (biomass per unit area) in grid cell g fished in stock s during year y, $a_{s,f,y}$ is the area in which stock s with mean density $\overline{D}_{s,y}^G$ is fished by fleet f during year y, and $G = a_{s,f,y}$. The biomass in the fished area ($B_{s,f,y}^G$) may differ from fishable biomass ($B_{s,f,y}^F$), depending on the mixing parameter ϕ.

Equation 4 can be expressed in terms of CPUE according to eq. 5 if there was a year y' when the whole distribution area of stock s was fished (using the historically largest area fished may underestimate the true whole distribution area), the exchange rate (i.e., the proportion of individuals moving among grids within the area fished) was constant, and catchability was the same for each fleet in all grids during that year (these two assumptions are reasonable for prawns):

$$B_{s,f,y'}^G = \sum_{g \in G} \varsigma D_{s,y',g} = \frac{1}{q_{s,f,y'}} \sum_{g \in G} U_{s,f,y',g} \tag{5}$$

The summed CPUE, $\sum_{g \in G} U_{s,f,y',g}$, can therefore be considered as a biomass index for the component of stock s within the area fished. Similarly, the total biomass of stock s during year y is given by

$$B_{s,y} = \sum_{g \in A_s} \varsigma D_{s,y,g} = A_s \overline{D}_{s,y} \tag{6}$$

The total biomass and the biomass in the area fished can be obtained using the following formulae if the distribution pattern in y' remains same in other years:

$$\begin{aligned} B_{s,f,y}^F &= \left(\frac{\sum_{g \in G,y'} \varsigma D_{s,y',g}}{\sum_{g \in A,y'} \varsigma D_{s,y',g}} \right)^{\phi_s} B_{s,y} \\ &= \left(\frac{\sum_{g \in G,y} \overline{U}_{s,f,y',g}}{\sum_{g \in A,y'} \overline{U}_{s,f,y',g}} \right)^{\phi_s} B_{s,y} \end{aligned} \tag{7}$$

Fig. 4. Relative error distributions for the posterior means for key model parameters and outputs for three models. B_{cur} is the biomass in 2007. (*a*) Model 1, ϕ estimated; (*b*) Model 2, $\phi = 0$; (*c*) Model 3, $\phi = 1$.

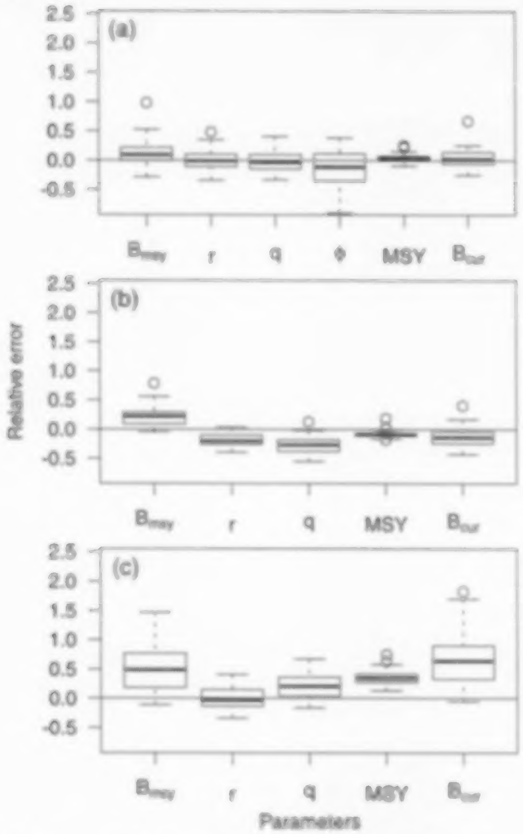

Fig. 5. Relative error distributions for the posterior medians for the time series of B_t/B_{msy} values for three models. (*a*) Model 1, ϕ estimated; (*b*) Model 2, $\phi = 0$; (*c*) Model 3, $\phi = 1$.

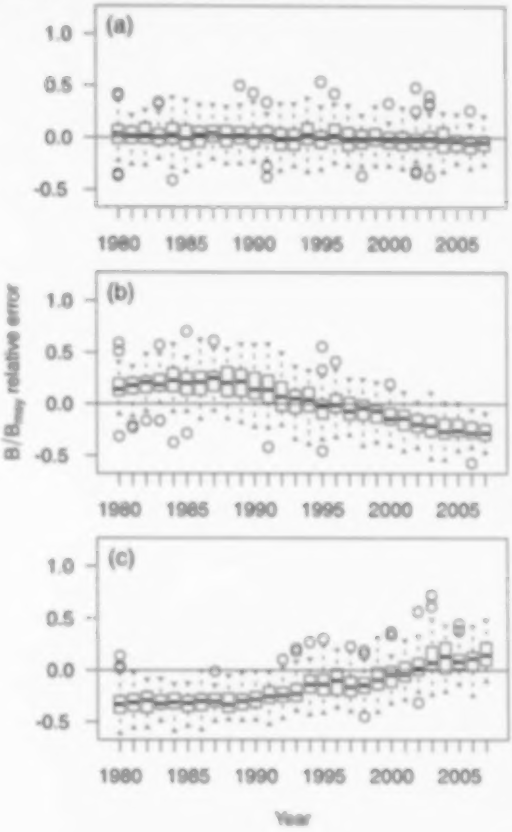

where $\overline{U}_{s,f,y',g}$ is the CPUE for grid g averaged over the period y' (if y' is longer than a single year). Equation 7 is based on the observed mean CPUE ratio between the fished and total areas, where errors measuring CPUE should cancel out to some extent. Because the density and CPUE between the fished area and the total area are relative each other, their corresponding biomass can be referred to as relative biomass. Equation 7 is the same as eq. 2 if the catch rates in the fished and unfished areas are the same, that is, $\overline{U}^{G}_{s,f,y',\bullet} = \overline{U}^{A}_{s,f,y',\bullet}$, where • means "across all grids in the area fished or in both the fished and unfished areas". An equation for the catch rate for fleet f, stocks s, and year y can be obtained by substituting eq. 7 into eq. 3:

$$(8)\qquad U_{s,f,y} = q_{s,f}P_y\left(\frac{\sum\limits_{g\in G,y}\overline{U}_{s,f,y',g}}{\sum\limits_{g\in A,y'}\overline{U}_{s,f,y',g}}\right)^{\phi_s} B_{s,y}\mathrm{e}^{\varepsilon^{U}_{s,f,y}}$$

The total number of grids fished in the NPF was highest between 1982 and 1989, so these years are used to define y'. The area fished in eq. 2 and the relative density in eq. 7 exhibit a similar trend over time, but the fishery tends to concentrate effort in areas with higher prawn density.

Bayesian model implementation

The models are implemented using a hierarchical Bayesian framework similar to the procedure outlined in Zhou et al. (2009*a*). The parameters are r, K, B_1, q, ϕ, and their associated variances, $\sigma^2_{B,s}$ and $\sigma^2_{U,s,f}$ (see Table 1 for the assumed priors). Parameters r, K, q, and ϕ are assumed to be distributed about common means μ_θ (θ can be r, K, q, or ϕ). These means are known as hyperparameters, which have their own distributions, $\mu_\theta \sim N(M_\theta, \Sigma_\theta)$, for μ_θ. We specify values for the means of these hyperpriors, M_θ, by considering the results of other studies (Die et al. 1990; Wang 1999; Zhou et al. 2009*a*) and assume a half-Cauchy distribution for the hypervariance parameter Σ_θ. Other variances, including those of key parameters, as well as the priors for the observation and process errors, are set to proper, but reasonably noninformative, inverse gamma distributions with mean 1 and variance 1000. The parameters are sampled from the joint posterior distribution using a Markov chain Monte Carlo algorithm, as implemented in WinBUGS (Spiegelhalter et al. 2003) similar to Zhou et al. (2009*a*).

The Bayesian analyses for each model were based on three chains of 60 000 cycles. The first 10 000 cycles for each chain were discarded, with the samples used for inference

Fig. 6. Observed catch rates (dots) and posterior median predicted catch rates for grooved tiger prawns from three models. The dotted lines denote 95% credibility intervals for Model 1. (*a*) Target (grooved) fleet; (*b*) bycatch (brown) fleet.

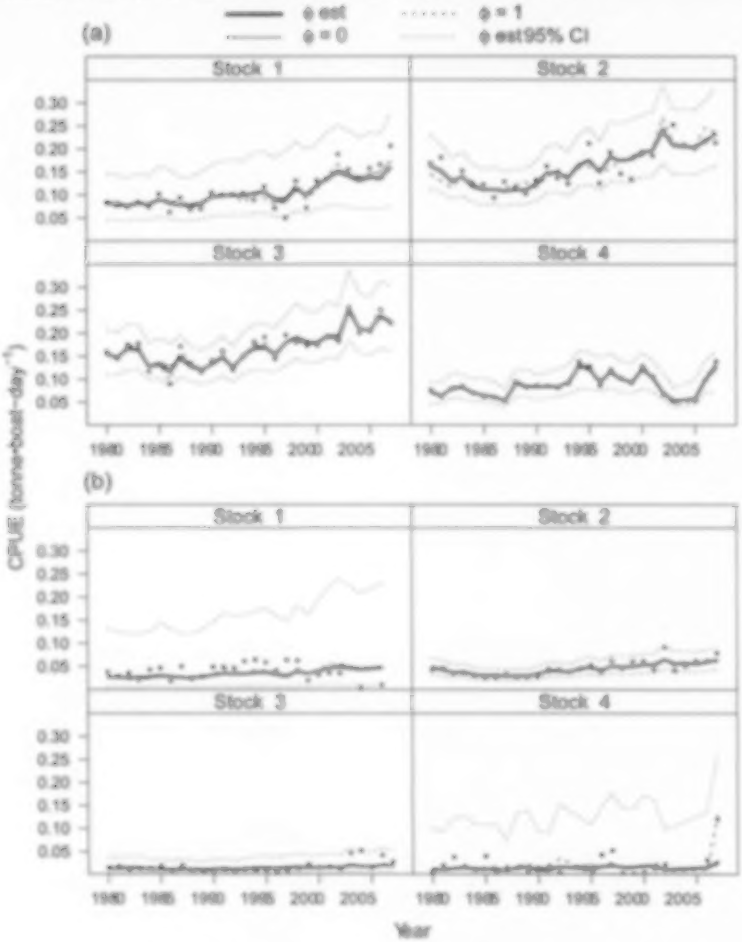

Table 2. Mean square predictive error for the three models and the two species.

Species	Model	2.5%	Median	97.5%
Grooved tiger	1: ϕ estimated	0.325	0.461	0.681
	2: $\phi = 0$	0.327	0.464	0.683
	3: $\phi = 1$	0.418	0.609	0.940
Brown tiger	1: ϕ estimated	0.227	0.297	0.399
	2: $\phi = 0$	0.229	0.304	0.416
	3: $\phi = 1$	0.277	0.357	0.470

based on every 10th cycle of the remaining chains. Trace plots were evaluated as an initial way to determine whether convergence had taken place.

Three alternative models based on assumptions of how fishable biomass is related to total biomass were explored: Model 1: partial mixing, ϕ estimated; Model 2: fully mixing, $\phi = 0$; and Model 3: no mixing, $\phi = 1$. Model 2 is the standard approach in traditional stock assessment, where the biomass of the entire stock is assumed to be accessible when modelling CPUE.

Model diagnostics and comparison

The fits of the three models to the data were evaluated using a graphical assessment of the 95% prediction credibility intervals (95% CIs). These statistics were calculated from posterior predictive distributions for the stock- and fleet-specific catch rates. The posterior predictive distribution for each CPUE data point was obtained by sampling parameters from the joint posterior distribution, which summarizes all of the information about a "new" CPUE point, $U_{s,f,y}^{\text{pred}}$, given the observed data, priors, and likelihood:

$$(9)\qquad P\left(U_{s,f,y}^{\text{pred}}\right) = \int P\left(U_{s,f,y}^{\text{pred}}, \underline{\theta}\right) P(\underline{\theta}|\mathbf{U})\, d\underline{\theta}$$

where $\underline{\theta}$ denotes all parameters, including model parameters and hyperparameters. The 2.5th, 50th, and 97.5th percentiles from the posterior predictive distribution were plotted together with the observed CPUE, $U_{s,f,y}$.

The mean square predictive error loss function (MSPE) on the log-scale (Ghosh and Norris 2005; Webster et al. 2008) was also used to compare among the three models:

Fig. 7. Posterior distributions for the mixing parameter ϕ for grooved tiger (*a*) and brown tiger (*b*) prawns in four stock areas. Thin solid line, Stock 1; thin dashed line, Stock 2; thick solid line, Stock 3; thick dashed line, Stock 4.

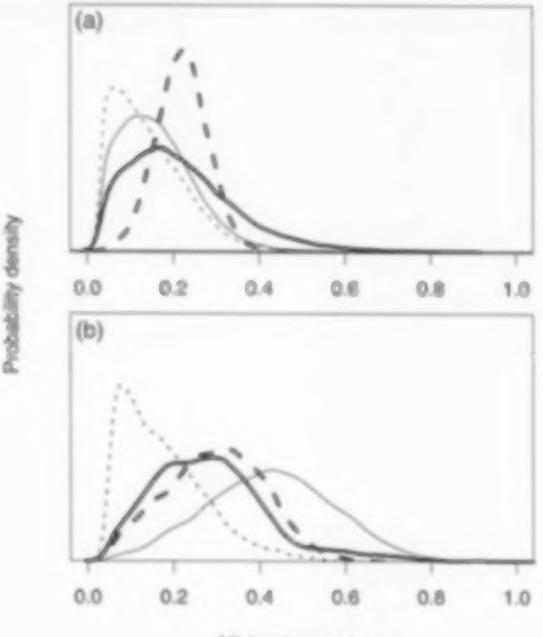

$$\text{MSPE} = \frac{1}{n}\sum_{s}\sum_{f}\sum_{y}\left[\ln(U_{s,f,y}^{\text{pred}}) - \ln(U_{s,f,y})\right]^2 \tag{10}$$

where n is the total number of data points, and $U_{s,f,y}^{\text{pred}}$ is sampled from eq. 9. The best model is the one that has the smallest values for MSPE.

Simulations

Monte Carlo simulations were conducted to evaluate the performance of the Bayesian fishable biomass dynamics method. These simulations involved three steps: data generation, parameter estimation, and evaluation of estimation performance. Data generation involved applying eqs. 1 and 2 in which there was a single stock and one fleet. The results of the simulation exercise likely underestimate the potential performance of the method because the actual application involves multiple stocks and fleets and hence more data.

The values for K, r, and σ_B were set to 5000, 0.5, and 0.1, respectively (values that are similar to the posterior means for these parameters for the actual tiger prawn species). The proportion of the area fished (a_y/A) and the annual effort were set to the actual values for two tiger prawns in the NPF (1980–2007; Fig. 1). Five scenarios ($\phi = 0.2$, 0.4, 0.5, 0.6, and 0.8) were used to examine the impact of the true value of the mixing parameter on model performance. The two extreme scenarios of full and no mixing ($\phi = 0$ and 1.0) are deemed unrealistic, but were considered to examine model behaviour across the full set of possibilities. Catchability (q) was set to 8.8×10^{-5} (Wang 1999), and the extent of observations error (σ_U) was set to 0.15. One hundred data sets, each with a 28-year time series of data, were generated. The Bayesian fishable biomass dynamics method was applied assuming (*i*) ϕ estimated; (*ii*) $\phi = 0$; and (*iii*) $\phi = 1$. The priors were set to those in Table 1, and the process for running WinBUGS was similar to that outlined above.

The performance of the method was evaluated by the mean and distribution for the relative error of the posterior means for K, r, q, ϕ, maximum sustainable yield (MSY), B_{cur} (biomass in year 2007), and B_y/B_{msy}, that is, for some quantity θ:

$$\text{RE}_i^{\theta} = \frac{\theta_i|\text{data}_i - \theta_{\text{true},i}}{\theta_{\text{true},i}} \times 100, \quad i = 1 \ldots 100 \tag{11}$$

$$\text{MRE}^{\theta} = \frac{1}{100}\sum_{i=1}^{100}\text{RE}_i^{\theta} \tag{12}$$

Results

Simulations

Examinations of model convergence, posterior distributions for estimated parameters, and the Gelman–Rubin statistic indicate no undesirable estimation behaviour for any of the models. There was also no evidence for high correlations among the parameters.

Model 2 (full mixing) leads to smaller mean relative errors than Model 3 (no mixing) when the value of ϕ used to generate the data is small (e.g., 0.2). The opposite is true when ϕ is set to a large value (e.g., 0.8). This is expected because Model 2 assumes $\phi = 0$ while Model 3 assumes $\phi = 1$. Also, as expected, when the data are generated with $\phi = 1$ (no mixing), Model 3 performs well while Model 2 performs poorly. In these two extreme cases, Model 1 results in a posterior mean for ϕ of 0.07 when the true value of ϕ is 0 and 0.88 when the true value of ϕ is 1.0.

However, Model 1, which treats ϕ as a random variable, outperforms Models 2 and 3 in all scenarios with ϕ ranging from 0.2 to 0.8. Detailed results are shown for the case in which $\phi = 0.5$ (Figs. 4 and 5; these results are representative of those for all five values for ϕ). Model 1 performs well for most key parameters (Fig. 4*a*), but it tends to underestimates the mixing parameter ϕ. The underestimation of ϕ by about 9% leads to overestimation of fishable biomass. This makes the results for Model 1 appear more similar to those for Model 2 than to those for Model 3 (see below). Model 1 provides accurate estimates of MSY, but tends to slightly overestimate B_y/B_{msy} during the earlier years while slightly underestimating B_y/B_{msy} for the final several years (Fig. 5*a*).

In contrast, the two other models, assuming full mixing or no mixing, perform poorly (Figs. 4*b*, 4*c* and Figs. 5*b*, 5*c*). Model 2 underestimates MSY by an average of 10%, while Model 3 overestimates it by 34%. The estimated time series of B_y/B_{msy} values either starts positively biased and becomes negatively biased or vice versa (Figs. 5*b*, 5*c*). These trends in bias are due mainly to the trend in a_y/A (Fig. 1); the proportion of the area fished increased from 1980 to a peak in the mid-1980s and gradually declined. This pattern led Model 2, which assumes full mixing between the fished and unfished areas, to overestimate biomass during early years and underestimate biomass during recent years.

Fig. 8. Fraction of the species distribution area and biomass fished for grooved (*a*) and brown (*b*) tiger prawns.

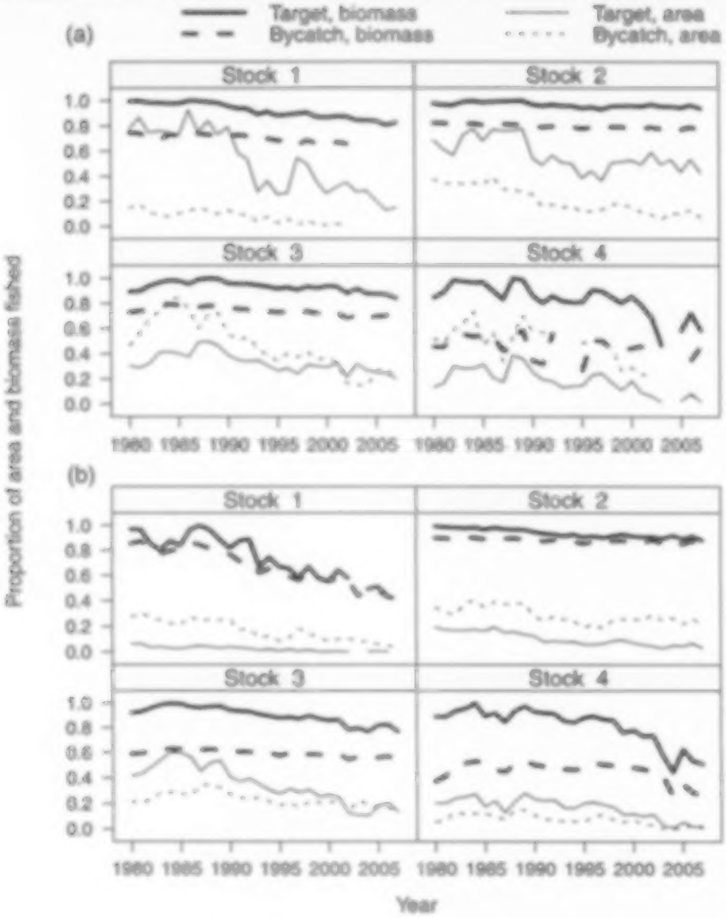

Fig. 9. Posterior medians and 95% credibility intervals for MSY for grooved and brown tiger prawns from the three models (mixing parameter ϕ estimated, 0, and 1).

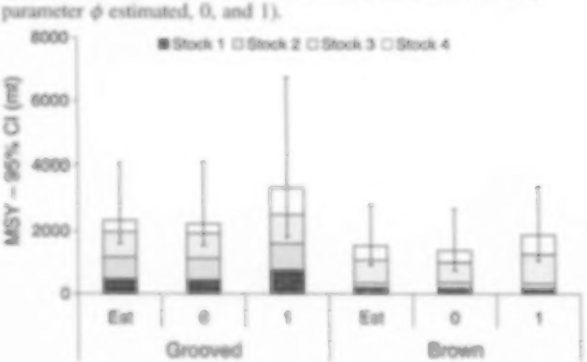

Application to grooved tiger prawns

Model diagnosis and comparison

The posterior predictive distributions show that the three models assuming different mixing rates mimic the observed catch rate data very well (Fig. 6), although (and as expected) the posterior predictive distributions for the bycatch fleet are poorer than those for the target fleet. It was difficult to visually distinguish the posterior median time trajectories of CPUE among the three models, especially between Model 1 (ϕ estimated) and Model 2 ($\phi = 0$) (Fig. 6). However, the MSPE (Table 2) suggests that Models 1 and 2 are superior to Model 3.

Fishable biomass

The posterior distributions for ϕ from Model 1 are similar among stocks (Fig. 7). They have most of their mass between 0 and 0.4, which suggests a high rate of mixing between the fished and unfished areas. This mixing, and a higher density of grooved tiger prawns in the fished area, results in a higher proportion of the total biomass that is fishable than the proportion of grids fished would suggest (Fig. 8). Also shown is that the fishable biomass is always higher for the target fleet than for the bycatch fleet, which coincides with inferences from CPUE data (Fig. 8; Zhou et al. 2011). This is because the target fleet fishes in the grids with a higher density of grooved prawns than those fished by the bycatch fleet, and the target fleet also fishes a higher proportion of the grids in which grooved tiger prawns are found.

Fig. 10. Time trajectories for the posterior distributions for B_t/B_{msy} from three models for grooved (*a*) and brown (*b*) tiger prawns.

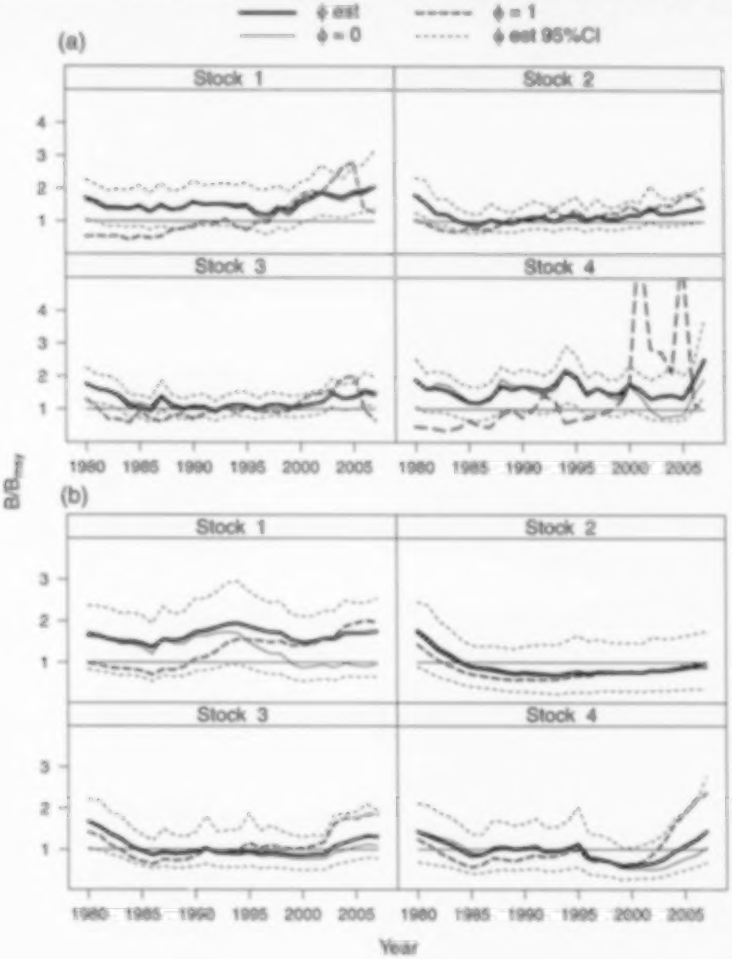

Key parameters

The posterior distributions for r and K are more similar between Models 1 and 2, while Model 3 results in a smaller r and a larger K than Models 1 and 2 (results not shown). The MSY, which is a function of r and K, is similar between Models 1 and 2 (Fig. 9). The time trajectories for the posterior distribution of B_t/B_{msy} are also more similar between Models 1 and 2 (Fig. 10). One interesting difference between the results for Models 1 and 2 is that the latter, which assumes that all prawns are available to the fishery, results in a more optimistic appraisal of stock status in the early years, but a more pessimistic appraisal in recent years than the former. Model 3 leads to the opposite pattern. This phenomenon is clearer when the four stocks are combined (Fig. 11). Models 1 and 2 indicate that the total biomass (across all stocks) has been above B_{msy} since 1980 with high probability.

Application to brown tiger prawns

Model diagnosis and comparison

The posterior predictive distributions show that the three models fit observed catch rate data for brown tiger prawns reasonably well (Fig. 12), although the posterior predictive distributions for brown tiger prawns are less precise than those for grooved tiger prawns (higher observation error). This is not unexpected because biological information (e.g., reproduction cycle, natural mortality, migration pattern) and fishery knowledge (i.e., catchability) is more sparse for brown tiger prawns than for grooved tiger prawns. Stock assessments for brown tiger prawns often need to "borrow" information from those for grooved tiger prawns (Dichmont et al. 2005). Again, Models 1 and 2 are more similar than Model 3. The MSPE (Table 2) again provides strong evidence against Model 3, but in contrast with grooved tiger prawns, the MSPE provides more support for Model 1.

Fishable biomass

The posterior distributions for ϕ are wider for brown than for grooved tiger prawns (Fig. 7, lower panel). The results again suggest that a higher proportion of the total biomass is in the area fished than the proportion of grids fished would suggest (Fig. 8). The target fleet again has higher fishable bi-

Fig. 11. Time trajectories of the posterior medians for B_t/B_{msy} from three models in which the results are aggregated across stocks. The horizontal line is $B = B_{msy}$. (*a*) Grooved tiger prawn; (*b*) brown tiger prawn.

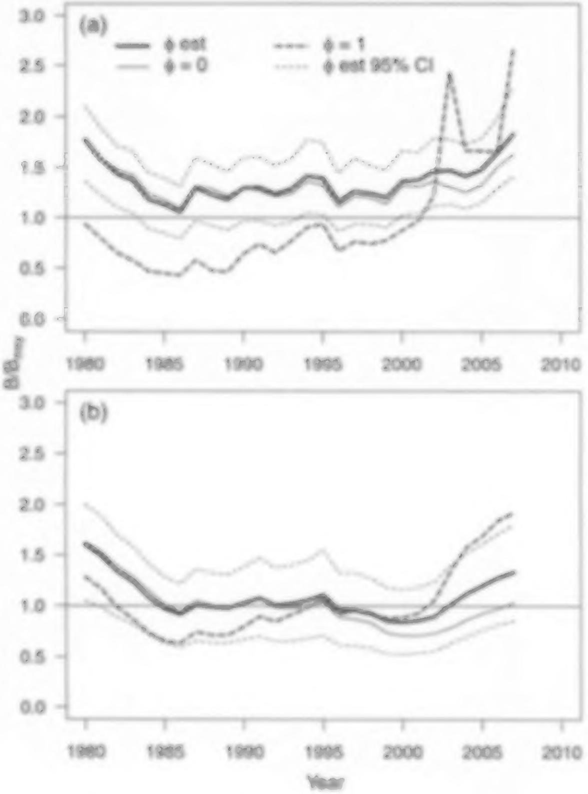

omass than the bycatch fleet, and the fraction of biomass available to the fishery could be very high even when the amount of area fished is relatively small (Fig. 8).

Key parameters

The posterior distributions for *r* and *K* are similar among the three models (results not shown). Model 1 leads to a higher posterior median for MSY than Model 2, but this median is less than that for Model 3 (Fig. 9). The posterior distributions for the time series of B_t/B_{msy} values from Models 1 and 2 are again more similar than that from Model 3 (Fig. 10). Model 2 again produces a more optimistic appraisal of stock status in the early years and a more pessimistic appraisal in recent years than Model 1, while Model 3 results in lower biomass during the early years, but higher biomass in recent years than Model 1. Based on Model 1, there were 11 years when the probability that the biomass was less than B_{msy} exceeded 0.5 for the whole brown tiger prawn stock in the NPF (Fig. 11). The lowest median B_t/B_{msy} ratio was about 0.85 in 3 years from 1999 to 2001.

Discussion

Fishing can affect the population outside of the area actually fished, but the impacts will not be uniform throughout the population. Such a partial impact on individuals in the unfishable area is obvious and is the underlying basis of extensive debates on marine reserves (Gerber et al. 2002). The size of a protected area is the key to determine whether it would achieve the objective of protecting species affected by fishing. Increasing fishing intensity outside a reserve can be a major concern because of mixing between populations inside and outside of the protected area. Interaction between fish inside and outside reserves affects population dynamics and should be considered for stock assessment (Law and Polunin 1995). In the NPF, fishers have indicated that they try to repeatedly trawl a track until the catch rate drops to a certain level, and this practice has been confirmed by analysing vessel monitoring system data (Deng et al. 2005). Although the trawl will pass over only a small area, prawns near the trawl track could move into the trawled area and feed on the disturbed seabed. This behaviour has been observed in the field for other species. For example, Kaiser and Spencer (1994) observed a greater concentration of fish marks (acoustic signals from side-scan sonar) around new trawl tracks than in adjacent unfished areas. Their study indicated that fish rapidly migrate into beam-trawled areas to feed on benthic animals that have been either damaged or disturbed by fishing. They also found some mobile invertebrate scavengers, such as *Pandalus* spp., only occurred in fish diets after the area had been fished, suggesting that these animals were also scavenging over the trawl tracks.

A linear relationship is often assumed between catch rate and fishable biomass when conducting stock assessments. By incorporating fished area and relative density, eqs. 7 and 8 are equivalent to assuming a nonlinear relationship between catch rate and the area fished. These equations are similar to a general relationship among CPUE, effort, and abundance (Shardlow and Hilborn 1985; Quinn and Deriso 1999). However, the general nonlinear relationship between catch rate and abundance (or effort) relates to density-dependent catchability. Weak evidence for density-dependent catchability within a fishing season has been found for the aggregated banana prawn *P. merguiensis* (Zhou et al. 2007). Our results show that models with and without area fished lead to different outcomes. We assume that there are no major changes to the spatial distribution of the stock over time, primarily because we lack annual species distribution data outside the fished area, although such changes would lead to biased outcomes irrespective of the choice of model. Such changes may be due to a range contraction of the fished stock or changes in environmental–oceanographic conditions from year to year. Nevertheless, information on species distribution, if available, can be incorporated into the model so that the assumption of constant distribution range is not needed. For example, fishery-independent surveys outside the fished area or bycatch from other fisheries may provide auxiliary information for species distribution in some fisheries. In NPF, tiger prawns are not restricted to the fished area (Ye et al. 2007).

Many factors may affect the mixing process between fished and unfished areas, including the size of the area fished, the duration of the fishing season, the relative density in the fished and unfished areas, and the mobility of the species. The rate of mixing (represented in the biomass dynamics model by the parameter ϕ) should be a function of these quantities. The maximum distance an animal can move de-

Fig. 12. Observed catch rates and posterior median predicted catch rates from three models for brown tiger prawns. The dotted lines denote 95% credibility intervals for Model 1. (*a*) Target (brown) fleet; (*b*) bycatch (grooved) fleet.

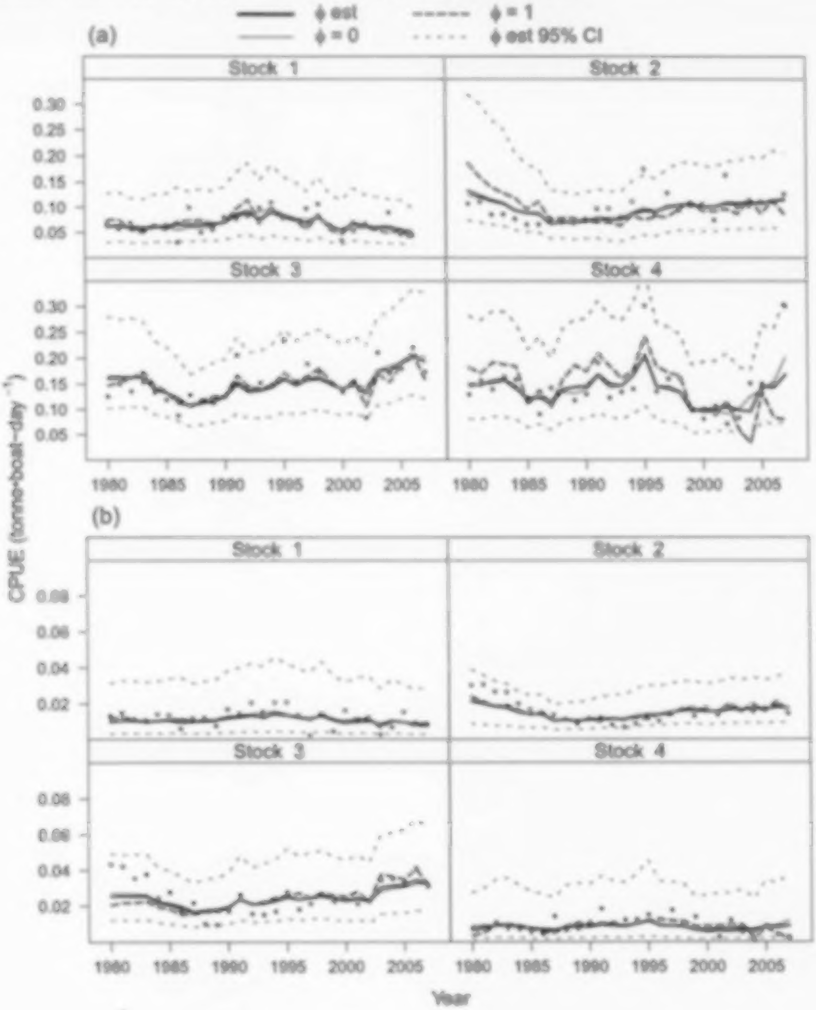

pends on swimming speed and the length of the fishing season. This parameter is difficult to estimate owing to confounding with other parameters, particularly the catchability coefficient. The simulations of this paper indicate that the mixing rate is overestimated (resulting a smaller estimate of ϕ), while catchability q is underestimated. Two consequences of this are that fishable biomass is overestimated, and the difference between models that estimate mixing and that assume full mixing appear to be less than is actually the case.

Despite these concerns, the model that estimates the relationship between area fished and the fraction of the total population available to the fishery leads to better estimates of management-related quantities when the area fished changes appreciably over time, the fishing season is relatively short, and the species of interest does not swim fast. Interaction between populations in fished and unfished area is a concern even for fast swimming species such as tuna (Die et al. 1990). It is not uncommon that the area fished changes substantially over time (Larcombe et al. 2001; Ragnarsson and Steingri 2003; Zhou et al. 2009*b*), but it is common that this factor is not taken into consideration in stock assessments. Our study suggests that ignoring the effect of area fished on the biomass available to the fishery may result in serious biases, and the simple approach described in this paper could be used for stock assessment in such cases.

Acknowledgements

This research is supported by CSIRO Wealth from Ocean Flagship. We thank Chris Legault and two anonymous reviewers for their comments on an earlier version of the paper.

References

Bishop, J., Venables, W.N., Dichmont, C.M., and Sterling, D.J. 2008. Standardizing catch rates: is logbook information by itself enough? ICES J. Mar. Sci. **65**(2): 255–266. doi:10.1093/icesjms/fsm179.

Campbell, R.A. 2004. CPUE standardisation and the construction of indices of stock abundance in a spatially varying fishery using general linear models. Fish. Res. **70**(2–3): 209–227. doi:10.1016/j.fishres.2004.08.026.

Deng, R., Dichmont, C., Milton, D., Haywood, M., Vance, D., Hall, N., and Die, D. 2005. Can vessel monitoring system data also be used to study trawling intensity and population depletion? The example of Australia's northern prawn fishery. Can. J. Fish. Aquat. Sci. **62**(3): 611–622. doi:10.1139/f04-219.

Dichmont, C.M., Deng, A.R., Venables, W.N., Punt, A.E., Haddon, M., and Tattersall, K. 2005. A new approach to assessment in the NPF: spatial models in a management strategy environment that includes uncertainty. Fisheries Research and Development Corporation Report 2001/002.

Die, D.J., Restrepo, V.R., and Fox, W.W., Jr. 1990. Equilibrium production models that incorporate fished area. Trans. Am. Fish. Soc. **119**(3): 445–454. doi:10.1577/1548-8659(1990)119<0445:EPMTIF>2.3.CO;2.

Food and Agriculture Organization of the United Nations. 1984. Papers presented at the Expert Consultation on the regulation of fishing effort (fishing mortality), Rome, 17–26 January 1983. A preparatory meeting for the FAO World Conference on fisheries management and development. FAO Fish. Rep. 289 Suppl. 2.

Gerber, L.R., Kareiva, P.M., and Bascompte, J. 2002. The influence of life history attributes and fishing pressure on the efficacy of marine reserves. Biol. Conserv. **106**(1): 11–18. doi:10.1016/S0006-3207(01)00224-5.

Ghosh, S.K., and Norris, J.L. 2005. Bayesian capture–recapture analysis and model selection allowing for heterogeneity and behavioural effects. J. Agric. Biol. Environ. Stat. **10**(1): 35–49. doi:10.1198/108571105X28651.

Kaiser, M.J., and Spencer, B.E. 1994. Fish scavenging behaviour in recently trawled areas. Mar. Ecol. Prog. Ser. **112**: 41–49. doi:10.3354/meps112041.

Larcombe, J.W.P., McLoughlin, K.J., and Tilzey, R.D.J. 2001. Trawl operations in the South East Fishery, Australia: spatial distribution and intensity. Mar. Freshw. Res. **52**(4): 419–430. doi:10.1071/MF99169.

Man, A., Law, R., and Polunin, N.V.C. 1995. Role of marine reserves in recruitment to reef fisheries: a metapopulation model. Biol. Conserv. **71**(2): 197–204. doi:10.1016/0006-3207(94)00047-T.

Marr, J.C. 1951. On the use of the terms, abundance, availability and apparent abundance in fishery biology. Copeia, **1951**(2): 163–169. doi:10.2307/1437549.

Maunder, M.N., and Punt, A.E. 2004. Standardizating catch and effort data: a review of recent approaches. Fish. Res. **70**(2–3): 141–159. doi:10.1016/j.fishres.2004.08.002.

Punt, A.E. 2003. Extending production models to include process error in the population dynamics. Can. J. Fish. Aquat. Sci. **60**(10): 1217–1228. doi:10.1139/f03-105.

Quinn, T.J., and Deriso, R.B. 1999. Quantitative fish dynamics. Oxford University Press, New York.

Ragnarsson, S.A., and Steingri, S.A. 2003. Spatial distribution of otter trawl effort in Icelandic waters: comparison of measures of effort and implications for benthic community effects of trawling activities. ICES J. Mar. Sci. **60**(6): 1200–1215. doi:10.1016/S1054-3139(03)00143-7.

Shardlow, T., Hilborn, R., Peterman, R.M., Steer, G.J., and Bradford, M.J. 1985. Density-dependent catchability coefficients. Trans. Am. Fish. Soc. **114**(3): 436–440.

Spiegelhalter, D., Thomas, A., Best, N., and Lunn, D. 2003. WinBUGS user manual, Version 1.4. MRC Biostatistics Unit, Cambridge, UK.

Venables, W., and Dichmont, C.M. 2004. A generalized linear model for catch allocation: an example from Australia's Northern Prawn Fishery. Fish. Res. **70**(2–3): 409–426. doi:10.1016/j.fishres.2004.08.017.

Wang, Y.G. 1999. A maximum-likelihood method for estimating natural mortality and catchability coefficient from catch-and-effort data. Mar. Freshw. Res. **50**(4): 307–311. doi:10.1071/MF97140.

Webster, R.A., Pollock, K.H., Ghosh, S.K., and Hankin, D.G. 2008. Bayesian spatial modelling of data from unit-count surveys of fish in streams. Trans. Am. Fish. Soc. **137**(2): 438–453. doi:10.1577/T06-138.1.

Ye, Y., Kenyon, R.A., Burridge, C., Dichmont, C.M., Pendrey, R., van der Velde, T., Vance, D., Bishop, J., Donovan, A., and Zhou, S. 2007. An integrated monitoring program for the Northern Prawn Fishery 2005/06. Project AFMA R05/0599.

Zhou, S., Dichmont, C., Burridge, C.Y., Venables, W.N., Toscas, P.J., and Vance, D. 2007. Is catchability density-dependent for schooling prawns? Fish. Res. **85**(1–2): 23–36. doi:10.1016/j.fishres.2006.11.034.

Zhou, S., Punt, A.E., Deng, R., Dichmont, C.M., Ye, Y., and Bishop, J. 2009*a*. Modified hierarchical Bayesian biomass dynamics model for assessment of short-lived invertebrates: a comparison for tropical tiger prawns. Mar. Freshw. Res. **60**(12): 1298–1308. doi:10.1071/MF09022.

Zhou, S., Fuller, M., and Smith, A.D.M. 2009*b*. Rapid quantitative risk assessment for seven Commonwealth fisheries. Final Report on AFMA project. CSIRO Cleveland, Australia. Available from http://www.environment.gov.au/coasts/fisheries/commonwealth/southern-bluefin-tuna/pubs/sbt-attachmentd-safe.pdf.

Zhou, S., Punt, A.E., Deng, R., and Bishop, J. 2011. Estimating multifleet catchability coefficients and natural mortality from fishery catch and effort data: comparison of Bayesian state–space and observation error models. Can. J. Fish. Aquat. Sci. **68**(7): 1171–1181.

Influence of pinniped-caused injuries on the survival of adult Chinook salmon (*Oncorhynchus tshawytscha*) and steelhead trout (*Oncorhynchus mykiss*) in the Columbia River basin

George P. Naughton, Matthew L. Keefer, Tami S. Clabough, Michael A. Jepson, Steven R. Lee, Christopher A. Peery, and Christopher C. Caudill

Abstract: Increasing pinniped abundance in the Pacific Northwest has coincided with population declines of Pacific salmon (*Oncorhynchus* spp.) and steelhead trout (*Oncorhynchus mykiss*), and concentrated predation may affect the recovery of some threatened and endangered salmonid stocks. We used radiotelemetry to evaluate pinniped-caused injury effects on migration survival of 17 007 adult Columbia River Chinook salmon (*Oncorhynchus tshawytscha*) and steelhead trout. Injuries from pinnipeds were common (mean injury rate across 29 run-years = 36.5%) and were most common for spring Chinook salmon and steelhead trout. Injury was not consistently associated with adult survival to spawning tributaries, but some negative survival effects were detected. Pinniped-caused injury rates decreased as annual run sizes increased, indicating density-dependent or saturation effects. Within a run, large fish generally had a higher injury incidence than small fish, suggesting pinnipeds targeted large fish or more efficiently captured small fish. Seasonal, size-dependent, and density-dependent results imply that pinniped effects likely differ widely among salmonid populations within the Columbia River basin. A better understanding of these effects is needed to guide management and conservation strategies.

Résumé : L'augmentation d'abondance des pinnipèdes dans le Nord-Ouest Pacifique coïncide avec les déclins démographiques des saumons du Pacifique (*Oncorhynchus* spp.) et de la truite arc-en-ciel anadrome (*Oncorhynchus mykiss*) et la concentration de la prédation peut affecter le rétablissement de quelques stocks de salmonidés menacés et en péril. La radiotélémétrie nous a servi à évaluer les effets des blessures causées par les pinnipèdes sur la survie durant la migration de 17 007 saumons chinook (*Oncorhynchus tshawytscha*) et truites arc-en-ciel anadromes adultes dans le fleuve Columbia. Les blessures dues aux pinnipèdes sont communes (taux moyen de blessures dans 29 montaisons-années = 36,5 %) et sont plus abondantes chez les saumons chinook et truites arc-en-ciel anadromes de printemps. Il n'y a pas d'association constante entre les blessures et la survie des adultes jusqu'aux tributaires de fraie, mais on peut déceler des effets négatifs sur la survie. Les taux de blessures dues aux pinnipèdes diminuent à mesure que la taille des montaisons annuelles augmente, ce qui indique des effets de densité dépendance ou de saturation. Dans une montaison, les poissons plus grands ont généralement une incidence plus élevée de blessures que les poissons plus petits, ce qui laisse croire que les pinnipèdes ciblent les poissons plus grands ou alors capturent plus efficacement les plus petits. Ces résultats saisonniers et dépendants de la taille et de la densité amènent à croire que les effets des pinnipèdes diffèrent vraisemblablement beaucoup d'une population de salmonidés à une autre au sein du bassin versant du Columbia. Une meilleure compréhension de ces effets est requise pour orienter les stratégies de gestion et de conservation.

[Traduit par la Rédaction]

Introduction

Members of the Order Pinnipedia evolved >20 million years ago, and their distributions have likely overlapped those of Pacific anadromous salmonids (*Oncorhynchus* spp.) for much of their existence. Many pinnipeds (seals and sea lions) were hunted until only small fractions of their former populations remained in the late 19th and early 20th centuries for both the fur trade and to reduce fishery interactions (Beddington et al. 1985). However, since passage of the Marine Mammal Protection Act in 1972, many pinniped populations in the Pacific Northwest (e.g., California sea lion (*Zalophus californicus*), Steller sea lion (*Eumetopias jubatus*), and Pacific harbor seal (*Phoca vitulina*)) have steadily increased (e.g., Barlow et al. 1995; Baraff and Loughlin 2000) and may be reaching historically high levels (Jeffries et al. 2003;

Received 1 June 2010. Accepted 11 April 2011. Published at www.nrcresearchpress.com/cjfas on 30 August 2011.
J21849

Paper handled by Associate Editor Michael Bradford.

G.P. Naughton, M.L. Keefer, T.S. Clabough, M.A. Jepson, S.R. Lee, C.A. Peery,* and C.C. Caudill. Department of Fish and Wildlife Resources, University of Idaho, Moscow, ID 83844-3141, USA.

Corresponding author: G.P. Naughton (e-mail: naughton@uidaho.edu).

*Present address: USFWS, Idaho Fishery Resource Office, 4147 Ahsahka Road, Ahsahka, ID 82520, USA.

doi:10.1139/F2011-064

Fig. 1. Columbia and Snake rivers showing dams monitored with radiotelemetry (inset map shows the location of the study region in the northwestern United States). For this study, the hydrosystem was bounded by Bonneville, Lower Granite, and Priest Rapids dams. Other monitored dams include The Dalles (TD), John Day (JD), McNary (MN), Ice Harbor (IH), Lower Monumental (LM), and Little Goose (GO). Major Columbia River tributaries within the studied hydrosystem that were monitored with radio antennas are indicated: 1, Wind; 2, Little White Salmon; 3, White Salmon; 4, Hood; 5, Klickitat; 6, Deschutes; 7, John Day; 8, Umatilla; 9, Walla Walla; 10, Snake; 11, Yakima. Fish were released 9.5 km downstream from Bonneville Dam.

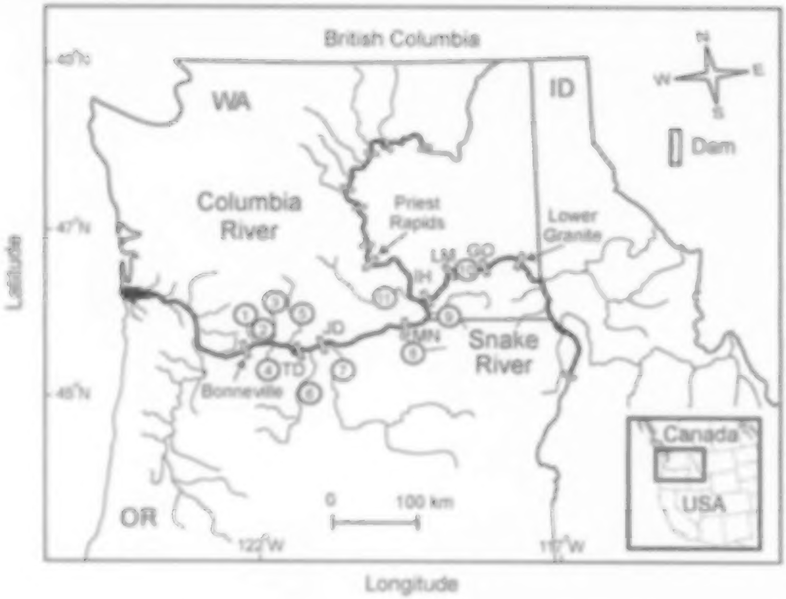

Carretta et al. 2005). Pinnipeds are effective and conspicuous marine predators, and coincident with recent increases in pinniped abundance, many salmon and steelhead trout (*Oncorhynchus mykiss*, hereafter called steelhead) populations have declined dramatically in the Pacific Northwest (Nehlsen et al. 1991; McClure et al. 2003; Wright et al. 2007). It is unlikely that pinniped predation has been a major cause of Columbia River salmonid declines, but predation by locally abundant pinnipeds has the potential to affect the recovery of many threatened and endangered stocks (National Marine Fisheries Service 1999) through both direct mortality and sublethal effects such as injury-related delayed mortality.

Adult salmonids are vulnerable to pinniped predation during their spawning migrations through estuaries and river mouths and especially where salmonids concentrate or where passage is constricted (National Marine Fisheries Service 1997). The risk of predation depends on a number of factors, including predator and prey density (Ricker 1952; Holling 1965; Abrams and Ginzburg 2000), predator attack or satiation rates, and physical habitat characteristics (i.e., water clarity, availability of escape routes, etc.). For example, predation on steelhead by California sea lions at the Ballard Locks, a man-made constriction in Seattle, Washington, was estimated to be as high as 65% of the annual returning adult population (Scordino and Pfeifer 1993). California sea lions have also been observed preying on adult salmonids near Willamette Falls in the Willamette River, Oregon (National Marine Fisheries Service 1998). In the Columbia River, recent increases in pinniped abundance have been associated with increases in injury rate and estimates of direct mortality. Fryer (1998) demonstrated an increase in pinniped abrasions from 2.8% in 1991 to 25.9% in 1996 for sockeye salmon (*Oncorhynchus nerka*) and 10.5% in 1991 to 31.8% in 1994 for spring–summer Chinook salmon (*Oncorhynchus tshawytscha*) sampled at Bonneville Dam, although only 3% of the injuries were considered severe enough to affect survival. More recently, Columbia River surveys conducted from 2002 through 2008 in the tailrace of Bonneville Dam (river kilometre 235) suggest that the percentage of the spring Chinook salmon run consumed by pinnipeds has increased from <1% to >4% at this single site (Stansell 2004; Tackley et al. 2008).

Pinniped predation in the lower Columbia River illustrates the challenges of multispecies management because both salmonids and pinnipeds are species of conservation concern. Fisheries managers, tribal and commercial fishers, and sport anglers have expressed concern about the effects of increasing pinniped populations on Columbia River salmonids, including evolutionary significant units listed under the Endangered Species Act (ESA). The National Marine Fisheries Service (NMFS) is responsible for recovery of ESA-listed salmonids. Simultaneously, the NMFS Office of Protected Species is responsible for protecting marine mammals under the Marine Mammal Protection Act. These joint responsibilities create a management conflict because marine mammals are seen as direct competitors to commercial and other human fisheries and as a potential hindrance to salmonid recovery. In 2000, the Federal Columbia River Power System Biological Opinion (National Marine Fisheries Service 2000) called for an evaluation of pinniped predation in the tailrace of Bonneville Dam. These studies resulted in pin-

Table 1. Estimated percentages of Chinook salmon (*Oncorhynchus tshawytscha*) and steelhead trout (*Oncorhynchus mykiss*) with and without pinniped-caused injuries that successfully reached spawning tributaries in 1996–2004.

		Marine mammal injury type					
		No injury		Any injury		Major new injury	
Run	Year	Survival (%)	*n*	Survival (%)	*n*	Survival (%)	*n*
Chinook							
Spring	1996	69	167	75	309	74	59
	1997	84	132	75*	335	83	66
	1998	82	208	79	291	78	65
	2000	86	363	86	282	86	53
	2001	91	442	92	213	90	28
	2002	90	442	91	266	88	59
	2003	81	316	77	264	79	81
	2004	82	202	75	61	66*	19
Summer	1996	97	35	88	98	87	26
	1997	74	150	82	100	79	19
	1998	82	104	82	112	82	23
	2000	85	144	86	130	77	13
	2001	90	218	85	39	90	1
	2002	88	225	90	37	88	7
	2003	92	262	89	54	92	12
	2004	77	120	93	14	100	5
Fall	1998	76	396	78	274	78	31
	2000	74	424	75	187	71	34
	2001	77	545	76	58	73	11
	2002	76	568	76	55	72	18
	2003	68	329	78	55	82	18
	2004	63	315	65	15	100	2
Steelhead	1996	70	57	63	380	69	120
	1997	66	150	69	373	69	111
	2000	78	316	72*	370	66*	57
	2001	82	629	81	200	80	61
	2002	81	693	79	203	76	69
	2003	75	310	69	93	74	39
	2004	81	162	85	35	100	2

Note: Fish harvested in lower Columbia River fisheries were excluded from the analyses.

*Indicates significant differences in percent survival between fish with and without injuries (Pearson χ^2 tests, $P < 0.05$).

niped deterrents such as fishway exclusion devices, acoustic deterrents, hazing (M.A. Jepson, unpublished data), and use of lethal population control (National Oceanic and Atmospheric Administration 2008). Ongoing visual surveys estimate minimum pinniped predation rates at Bonneville Dam each year. Some attacked fish escape with injuries, and there is concern that these fish may die before reaching spawning areas (National Marine Fisheries Service 2000).

In this paper, we describe associations between pinniped-caused injuries and the upstream survival of radio-tagged Chinook salmon and steelhead in the Columbia River system. The injury, radiotelemetry, and fish fate data were collected for more than 17 000 fish over 8 years (1996–1998, 2000–2004) as part of a large-scale, multi-objective adult migration evaluation (e.g., Keefer et al. 2005; Goniea et al. 2006; Caudill et al. 2007). The specific objectives of this retrospective analysis were to evaluate (*i*) the seasonal abundance, age, and severity of pinniped-caused injuries on Chinook salmon and steelhead, (*ii*) the relationships among pinniped injuries, fish traits, and fish run size, and (*iii*) the effects of pinniped injuries on salmonid survival to spawning tributaries. We hypothesized that injury rates would differ seasonally and among runs in response to pinniped abundance downstream from Bonneville Dam, that injury rates would decrease with increasing run size (i.e., density-dependent effects), and that injured fish would have lower survival than uninjured fish.

Materials and methods

Fish trapping, tagging, and monitoring

Adult steelhead and spring, summer, and fall Chinook salmon were trapped at Bonneville Dam in the adult fish facility adjacent to the Washington shore fish ladder as they migrated upstream in the Columbia River (Fig. 1). Run dates for Chi-

Fig. 2. Differences in survival to tributaries between Chinook salmon (*Oncorhynchus tshawytscha*) and steelhead trout (*Oncorhynchus mykiss*) with and without pinniped-caused injuries, 1996–2004, stratified by week of collection, tagging, and release. Fish were grouped by release week, where week 1 started 1 March. Points above the horizontal line indicate fish without pinniped-caused injuries had higher survival percentages than fish with injuries. Solid circles indicate spring Chinook salmon, open circles are summer Chinook salmon, solid triangles show fall Chinook salmon, and open triangles are steelhead.

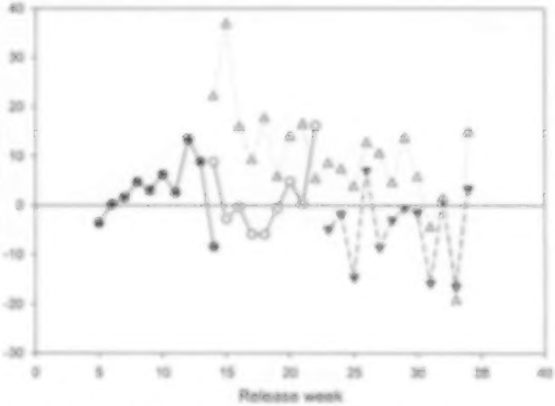

nook salmon followed those established by US Army Corps of Engineers (2005).

Each day that fish were tagged, a weir was lowered into the ladder to divert fish into the adult fish facility via a short secondary ladder. Once inside the facility, fish were either diverted into anesthetic tanks for tagging or returned to the main ladder without handling. The methods used for trapping, intragastric tagging, and radiotelemetry monitoring have been described in detail by Reischel and Bjornn (2003); Keefer et al. (2004*b*), and Naughton et al. (2005).

Overall 17 007 fish were used in this analysis: 5193 spring Chinook salmon (April–May, 8 years), 2163 summer Chinook salmon (June–July, 8 years), 4369 fall Chinook salmon (August–November, 6 years), and 5282 summer steelhead (June–October, 7 years). After tagging, fish were released at locations ~9.5 km downstream from Bonneville Dam (n = 14 581) on both sides of the river or in the Bonneville Dam forebay or Washington shore fish ladder (n = 2426).

Inferences about radio-tagged Chinook salmon and steelhead survival were made primarily using data from fixed-site radiotelemetry antennas and receivers. We used SRX receivers (Lotek Wireless, Inc., Newmarket, Ontario) with aerial Yagi antennas to monitor tailrace areas at dams and tributary mouths and also used digital spectrum processors added to SRX receivers with underwater antennas made of coaxial cable to monitor fishways and ladder tops at dams. We also monitored main stem and tributary sites with mobile radio-tracking units, and additional data were collected from hatcheries, fisheries returns, and spawning ground surveys (see Keefer et al. 2005).

Pinniped-caused injuries and survival

During tagging, we examined fish for head and body injuries attributable to pinnipeds. Head injuries included cuts and scrapes and torn opercula or maxillaries. We recorded bite and scrape wounds as described by Fryer (1998). We also differentiated between major and minor injuries and whether the injuries were old or new. We did not attempt to differentiate between seal and sea lion marks. Light skin scrapes that did not penetrate the skin were considered minor injuries, whereas cuts and bites that penetrated the skin were considered major injuries. Injuries where healing appeared to have occurred were considered old, while injuries with raw surfaces and (or) bleeding were considered new. We used five different injury categories: (*i*) no injury; (*ii*) minor, old injuries; (*iii*) minor, new injuries; (*iv*) major, old injuries; and (*v*) major, new injuries. Fish with severe injuries (e.g., gashes penetrating to the coelomic cavity) accounted for <1% of all fish trapped, and these were not tagged. The exclusion of these fish may have led to a slight (<1%) overestimation of survival. In 1996 if a fish had both a new and an old injury, only the new injury was recorded but both injury categories were recorded in subsequent years.

We used a combination of radiotelemetry records, spawning ground surveys, and radio tag returns from fisheries to classify fish as successful migrants or as prespawn migration mortalities. Successful migrants included fish that entered spawning tributaries, those found as carcasses in spawning ground surveys, those that returned to hatcheries or traps, and those that passed the upstream extent of the study area (Lower Granite Dam or Priest Rapids Dam). We also considered interbasin strays to be successful migrants regardless of their ultimate destination. Permanent strays were those last detected inside non-natal tributaries downstream from Lower Granite Dam either at fixed-site aerial radiotelemetry antennas or while mobile tracking (see Keefer et al. 2008). Mortalities included salmon and steelhead whose final radiotelemetry records were in reservoirs or at dams. We excluded 2825 fish (579 spring Chinook salmon, 113 summer Chinook salmon, 1115 fall Chinook salmon, and 1018 steelhead) that were captured in tribal and sport fisheries, because it was unknown whether these fish would have survived to spawning grounds had they not been harvested. Mortalities may have included unreported main stem harvest, though this potential bias would be unlikely to substantially affect the analyses unless injured fish were more (or less) likely to be harvested.

Statistical analysis

We used logistic regression (Hosmer and Lemeshow 2000) to test whether salmon and steelhead survival to a spawning ground was related to the following: pinniped injuries, year, fork length (FL), sex, whether the fish had fin clips, and (or) the tagging day of year at Bonneville Dam. We first fit a model that included all the variables except injury that might explain variation in survival to a tributary:

$$\text{Survival (yes/no)} = \text{year} + \text{FL} + \text{sex} + \text{date} + \text{clip}$$

We then added the injury indicator variable and an injury × year interaction variable (because the percentage of injured fish among all runs tended to decline over the study period) to determine its effect on the model:

$$\text{Survival (yes/no)} = \text{year} + \text{FL} + \text{sex} + \text{date} + \text{clip} + \text{injury} + (\text{injury} \times \text{year})$$

Table 2. Annual and total run-specific estimates of the percentages of radio-tagged Chinook salmon (*O. tshawytscha*) and steelhead trout (*O. mykiss*) with pinniped-caused injuries, with injury age and severity.

				Pinniped injury type (%)				
				Minor		Major		
Run	Year	Run size	*n*	Old	New	Old	New	Total
Chinook								
Spring	1996	51 635	651	0.0	51.0	0.0	12.3	63.3
	1997	114 235	607	0.0	60.8	0.0	13.2	74.0
	1998	38 359	623	0.0	45.7	0.0	13.3	59.1
	2000	178 336	751	0.0	34.9	0.9	8.3	44.1
	2001	391 818	717	0.1	23.3	4.6	4.3	32.4
	2002	269 428	784	0.0	28.8	0.0	8.5	37.4
	2003	195 671	731	2.1	26.3	4.5	14.1	46.9
	2004	170 291	329	0.6	14.3	0.9	8.8	24.6
	Total	1 409 773	5193	0.3	36.2	1.5	10.3	48.3
Summer	1996	16 034	148	0.0	55.4	0.0	20.3	75.7
	1997	27 936	324	0.0	30.2	0.0	7.4	37.7
	1998	21 433	263	0.0	41.1	0.0	10.6	51.7
	2000	30 616	321	0.6	40.5	0.6	5.3	47.0
	2001	76 156	283	1.8	6.7	5.3	0.4	14.1
	2002	127 436	298	0.0	11.1	0.0	2.7	13.8
	2003	114 808	355	2.0	4.8	6.2	3.7	16.6
	2004	92 143	171	0.6	4.7	0.6	2.9	8.8
	Total	506 562	2163	0.7	22.9	1.8	5.8	31.3
Fall	1998	189 108	872	0.0	35.6	0.0	4.6	40.1
	2000	193 006	820	0.0	24.0	0.6	5.9	30.5
	2001	400 423	784	0.1	6.8	0.9	1.9	9.7
	2002	474 666	818	0.0	5.7	0.0	3.1	8.8
	2003	640 464	554	1.8	4.5	2.5	4.0	12.8
	2004	583 617	521	0.0	4.0	0.0	0.4	4.4
	Total	2 481 284	4369	0.3	14.9	0.6	3.5	19.3
Steelhead	1996	203 583	686	0.0	62.8	0.0	25.2	88.0
	1997	258 509	767	0.0	49.3	0.0	21.0	70.3
	2000	275 806	919	0.0	45.7	1.0	9.5	56.1
	2001	636 006	1009	0.6	15.1	1.2	7.5	24.4
	2002	482 071	1112	0.1	14.9	0.0	8.2	23.2
	2003	363 369	547	2.0	8.8	4.2	9.7	24.7
	2004	312 523	242	0.4	15.7	0.0	0.8	16.9
	Total	2 531 867	5282	0.4	30.9	0.8	12.2	44.3

Note: Scrapes and abrasions were considered minor injuries, and cuts and bites were considered major injuries. All harvested fish were excluded.

We used a likelihood ratio test to determine if the addition of the two injury variables significantly improved the model fit (Ramsey and Schafer 2002; SAS Institute Inc. 2008).

We also used Pearson χ^2 tests to examine whether survival to tributaries was associated with injuries. Separate tests were conducted for (*i*) any pinniped-caused injury, (*ii*) minor injuries, (*iii*) major injuries, (*iv*) years separately for each run, and (*v*) years combined for each run.

To evaluate seasonal survival patterns, we calculated differences in percent survival by weekly release cohort between fish with and without pinniped-caused injuries. The weekly survival difference was calculated by subtracting the percent survival of fish without injuries from the percent survival of fish with injuries for each Chinook salmon and steelhead run. We tested whether the incidence of pinniped-caused abrasions was related to run size using linear regression and used Kolmgorov–Smirnov two-sample tests to compare length–frequency distributions of fish with and without pinniped-caused injuries.

Results

Pinniped injuries and survival

There was little overall difference in survival to tributaries between fish with and without pinniped-caused injuries (Table 1). Results of the χ^2 tests indicated that there were no differences other than those expected by chance alone. (Among the 32 run-years, the relationship was statistically significant ($P < 0.05$) only for spring Chinook salmon with any injury in 1997 and major new injuries in 2004 and steelhead with

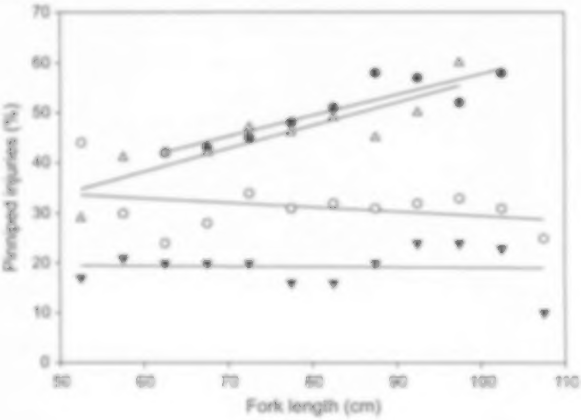

Fig. 3. Linear relationships between adult Chinook salmon (*O. tshawytscha*) and steelhead trout (*O. mykiss*) fork length and the percentages of each run with pinniped-caused injuries. Fork length was binned in 5 cm increments, and all years were combined within each run. Bins with $n < 10$ are not shown. Solid circles indicate spring Chinook salmon, open circles are summer Chinook salmon, solid triangles show fall Chinook salmon, and open triangles are steelhead.

any injury and major new injuries in 2000.) With all years combined, steelhead and spring Chinook salmon showed more negative survival effects from injuries than summer or fall Chinook salmon (Fig. 2). Fish without injuries survived at higher rates in 8 of 10 (80%) bi-weeks for spring Chinook salmon and 19 of 21 (90.4%) bi-weeks for steelhead. In contrast, survival differences were positive in 4 of 9 (44%) bi-weeks for summer Chinook salmon and 3 of 12 (25%) bi-weeks for fall Chinook salmon.

Logistic regression models and maximum likelihood tests for each run also indicated that pinniped-caused injuries were not strongly associated with survival to a spawning tributary. The addition of the injury terms to the model (survival = year + FL + sex + date + clip + injury + (injury × year) resulted in statistically significant improvement for spring Chinook salmon (Wald's $\chi^2 = 8.2$; $P = 0.0412$) but not for summer Chinook salmon (Wald's $\chi^2 = 4.9$; $P = 0.1771$), fall Chinook salmon (Wald's $\chi^2 = 2.1$; $P = 0.5585$), or steelhead (Wald's $\chi^2 = 3.3$; $P = 0.3451$). Year was a significant predictor of survival to a tributary for all runs ($10.1 \leq \chi^2 \leq 121.5$; $P < 0.05$). Day of year was significant for summer Chinook salmon ($\chi^2 = 21.9$; $P = 0.0015$), while day of year ($\chi^2 = 46.7$; $P < 0.0001$), FL ($\chi^2 = 16.2$; $P < 0.0001$), and clip ($\chi^2 = 16.3$; $P = 0.0001$) were also significant for fall Chinook salmon. The injury and injury × year terms were not significant predictors of survival to a tributary for any run.

Pinniped injury incidence among runs

Overall, injuries from pinnipeds were common (mean percent injured across 29 run-years = 36.5%; range = 4.4%–88.0%), and the percent injured varied among runs and years. With all years combined, the percentage of fish with pinniped-caused injuries ranged from 19.3% for fall Chinook salmon to 48.3% for spring Chinook salmon (Table 2). The 1996 steelhead run had the highest percentage of major new injuries (25.2%) followed by 1997 steelhead (21.0%) and 1996 summer Chinook salmon (20.3%; Table 2). With all years combined, 10.3% of spring Chinook salmon had major new injuries compared with 3.5% of fall Chinook salmon. For all years, old injuries comprised relatively small percentages (≤6%) of both minor and major injury categories. The percentage of old injuries recorded in 1996 are minimum estimates because if a fish had both a new and an old injury, only the new injury was recorded. New minor injuries ranged from 14.9% for fall Chinook salmon to 36.2% for spring Chinook salmon (all years combined). In general, the percentage of injured fish was highest early in the study period for all runs but declined substantially over the study period.

Pinniped injuries and fish length

Injured fish were larger than uninjured fish in most years. The difference was significant in 31% of the run-years, including spring Chinook salmon (2002, 2003), summer Chinook salmon (1996), and steelhead (all years except 2004) (Kolmgorov–Smirnov two-sample tests, $P < 0.05$). There were no significant differences for fall Chinook salmon. When fish within a run were combined across years and binned using 5 cm increments, FL was significantly ($P < 0.05$) positively associated with injury percentage for spring Chinook salmon (weighted linear regression, $F = 27.1$, $r^2 = 0.73$, P, 0.001) and steelhead ($F = 15.5$, $r^2 = 0.87$, $P = 0.003$), but not for summer or fall Chinook salmon ($P > 0.30$) (Fig. 3).

Pinniped injuries, run size, and migration timing

Within each run, the percentage of fish with pinniped injuries decreased as run size increased (Fig. 4). Linear regressions were significant for summer Chinook salmon ($n = 8$, $P = 0.006$, $r^2 = 0.70$) and fall Chinook salmon ($n = 6$, $P = 0.022$, $r^2 = 0.71$), but not for spring Chinook salmon ($n = 8$, $P = 0.060$, $r^2 = 0.47$) or steelhead ($n = 7$, $P = 0.086$, $r^2 = 0.48$). Migration timing effects were also evident in the percentage of salmon and steelhead with pinniped injuries. Larger, late-migrating steelhead similarly had a higher percentage of pinniped-caused injuries compared with either smaller or early timed steelhead (Fig. 5*a*). Early-migrating spring Chinook salmon had substantially higher injury rates than later-timed summer- and fall-run fish (Fig. 5*b*).

Discussion

The primary conclusions from this study are (*i*) injuries from pinnipeds occurred on a high proportion of Columbia River anadromous migrants but did not consistently influence migration survival of Chinook salmon or steelhead to spawning areas; (*ii*) steelhead and spring Chinook salmon showed more negative survival effects from injuries than summer and fall Chinook salmon, at least partially reflecting relatively high springtime abundance of pinnipeds in the lower Columbia River; (*iii*) pinniped-caused injury incidence tended to decrease with increasing run size, indicating density-dependent predation effects; and (*iv*) injury was less common in smaller adults in many run years, providing indirect evidence of size-selective predation by pinnipeds.

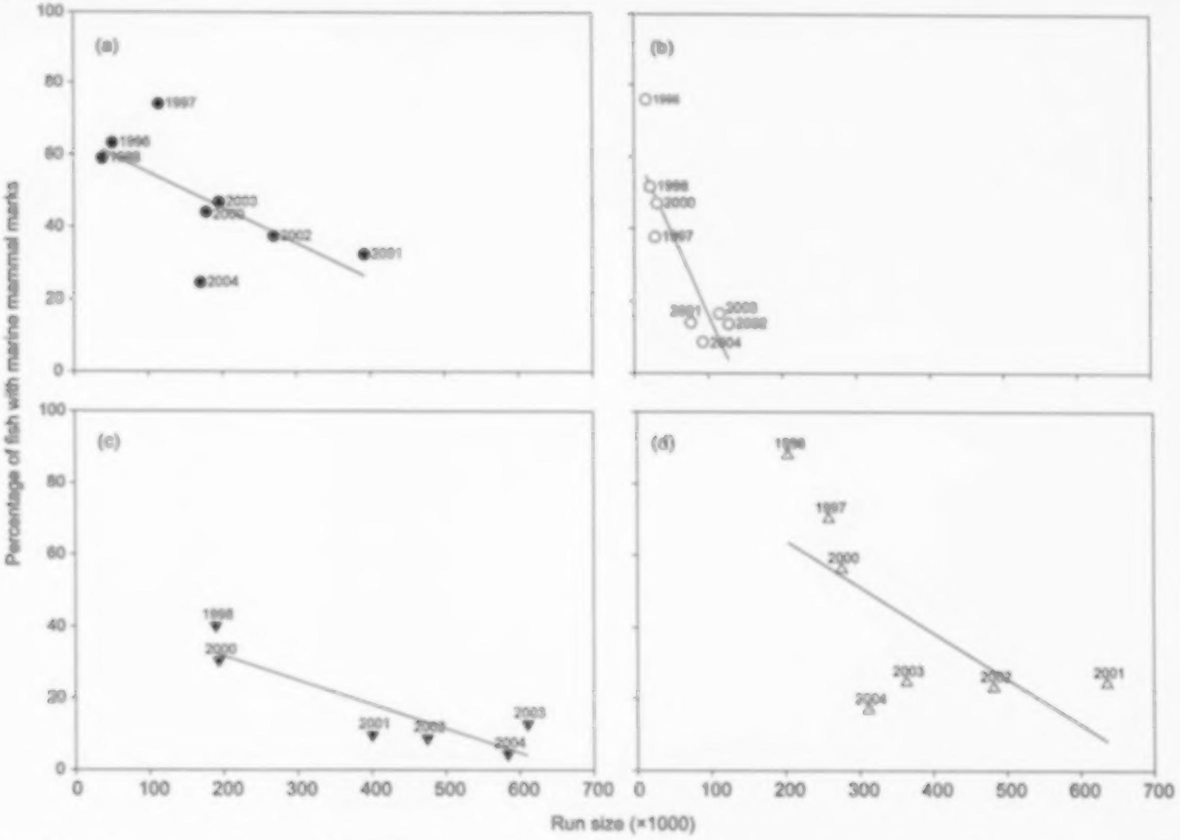

Fig. 4. Linear regression relationships between annual (1996–2004) run size and the percentages of pinniped-caused injuries on Chinook salmon (*O. tshwaytscha*) and steelhead trout (*O. mykiss*): (*a*) spring Chinook salmon, (*b*) summer Chinook salmon, (*c*) fall Chinook salmon, (*d*) steelhead.

Relationship between injury and survival

Contrary to our survival hypothesis, pinniped-caused injuries were not or were only weakly associated with survival of adult salmon and steelhead to spawning tributaries, once accounting for multiple comparisons. Among the four runs, the addition of injury variables to the logistic regression models resulted in a statistically significant improvement in the model only for spring Chinook salmon (uncorrected P value = 0.0412). Although the overall model fit improved, neither the injury nor injury × year interaction variable were significant. Thus we conclude that while there was some statistical evidence for an association between injury and fate, the overall magnitude of the injury effect was small in the run years with evidence of statistical differences when considering uncorrected χ^2 results, and there were many run years where survival rates were similar or higher for both categories of injured fish compared with uninjured adults. This result was in contrast with previously reported survival relationships described for other injury types. For example, there is evidence that injuries from gill nets and angling can cause significant delayed mortality in salmonids (e.g., Chopin and Arimoto 1995; Lindsay et al. 2004). The sample sizes of our study suggest that the observed lack of relationship was not the result of a lack of statistical power or else that the effect size was very small.

Importantly, the radiotelemetry studies were not designed to confirm spawning success, and as such we may not have captured all of the delayed effects from injuries on fitness. Injured adults last detected in tributaries or at the top of Lower Granite or Priest Rapids dams may not have reached spawning sites or may have died prior to spawning. For example, Keefer et al. (2010) found that prespawn mortality of spring Chinook salmon in the Willamette River was strongly dependent on salmon condition before they entered spawning areas. It was also possible that pinniped-caused injuries contributed to, or were partially masked by, losses attributed to other sources (i.e., disease, illegal or unreported harvest, lost transmitters, or undetected main stem exit), though we have no reason to believe injured fish would be lost at higher rates than uninjured fish. Assuming the lack of a difference in survival during migration was not an artifact, the equivalent survival of injured adults implies that adults are robust to attack because predator attacks have long been a selective pressure, and salmon have developed the ability to maintain their upstream migration even after sustaining injuries.

Injury incidence

The pinniped-caused injury incidence rates reported here are higher than those reported in other regional studies. The

Fig. 5. Bubble plots showing the relationships among tagging date, fork length, and the percentage of pinniped-caused injuries among (*a*) steelhead trout (*O. mykiss*) and (*b*) Chinook salmon (*O. tshawytscha*), all years combined. Data were binned by increments of 5 cm for fork length and 10 days for tagging date. Bins with $n < 10$ are not shown. Larger bubbles indicate a higher proportion with injuries and are scaled the same for both species (minimum = 0%, maximum = 74%).

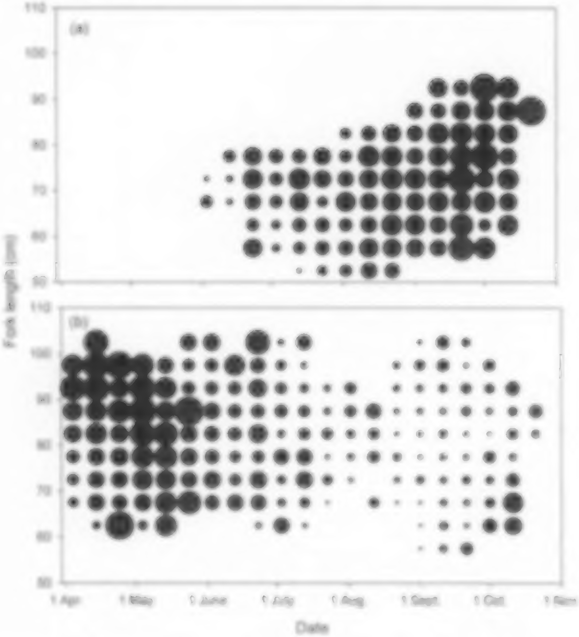

increased incidence rates are consistent with the hypothesis that recent increases in pinniped abundance in the lower Columbia River have resulted in increased attack and predation rates on adult salmonids. Across all years, about 42%–45% of spring Chinook salmon and steelhead had pinniped-caused injuries, considerably higher than the 10%–32% rates reported for spring–summer Chinook salmon sampled at Bonneville Dam from 1991 to 1994 (Fryer 1998). The current results were also higher than pinniped injury rates reported by Harmon et al. (1994) on the Snake River about 450 km upstream from Bonneville Dam (14%–18% of spring–summer Chinook salmon and 5%–14% of steelhead). Both Fryer (1998) and Harmon et al. (1994) suggested that marine mammals were targeting the earlier migrating spring–summer Chinook salmon. Although our study was not directly comparable to those of Fryer and Harmon et al., we did record the highest incidence of pinniped-caused injuries in spring Chinook salmon. The spring Chinook run coincides with the highest abundance of observed pinnipeds at Bonneville Dam, supporting our migration timing hypothesis. Pinniped sightings in the Bonneville Dam tailrace were highest from 15 March through 31 May 2005–2007, and few sightings occurred outside this time frame (Tackley et al. 2008). While spring Chinook salmon had the highest percentage of injuries in our study, the later migrating steelhead and summer and fall Chinook salmon also had relatively high incidences of pinniped-caused injuries. The springtime increase in sea lion presence at Bonneville Dam probably cannot explain the injury incidence in these runs. Instead, most of the injuries in the later runs presumably were incurred further downstream in the estuary or nearshore ocean.

Although the incidence of injuries was higher than in previous studies, the percentage of injuries for all four runs declined substantially over the study period. This is likely due to higher per capita risk of injury during years with relatively small run sizes. For example, the percentage of spring Chinook salmon with injuries was approximately 60% or higher between 1996 and 1998 when salmon run sizes were low. Paradoxically, the high injury incidence in the late 1990s was prior to the large influx of sea lions that occurred in the 2000s. While this is confounded by changes in run size, it suggests the marks may mostly be due to harbor seals, which are year-round residents near the Columbia River mouth.

Relationship between injury and fork length

Across years and runs, larger fish tended to have a higher incidence of injuries than smaller fish. There were few statistically significant results for Chinook salmon, but steelhead with injuries were significantly larger than fish without injuries in 6 of 7 study years. This suggests size-related predation effects that may be related to predator selection, escape rates, or other factors. Fryer (1998) also found that large-bodied spring–summer Chinook salmon had significantly more abrasions than smaller sockeye salmon and suggested that larger fish may be more visible to pinnipeds and thus more likely to be attacked. Alternatively, because smaller fish are generally slower swimmers and are weaker than larger fish (e.g., Brett 1965; Weihs 1973), they may be more easily captured and killed. Body size is important in mediating predator–prey interactions (Werner and Gilliam 1984), and capture success has been shown to decline with increasing prey size in a variety of species (e.g., Christensen 1996; Lundvall et al. 1999).

Relationship between injury and run size

Evidence for our density-dependence hypothesis was found for all four study runs, with lower pinniped-caused injury rates in years with larger run sizes. This relationship was significant for both spring and summer Chinook salmon. In contrast, Fryer (1998) did not find any significant relationships between the incidence of pinniped-caused abrasions and run size. Fryer (1998) suggested that the increase in injuries was related to an increase in pinniped population size. It is likely that both effects occur below Bonneville Dam, with some countervailing impacts. For example, seasonally increasing numbers of pinnipeds in the Bonneville Dam tailrace (Stansell 2004; Tackley et al. 2008) and increasing presence in the Columbia River estuary (e.g., Wright et al. 2010) likely explain the overall higher injury rates in this study compared with earlier studies.

Relationships between pinniped and salmonid abundance have been found in other riverine and estuarine study areas in the USA and UK (e.g., Brown and Mate 1983; Roffe and Mate 1984; Greenstreet et al. 1993). In some cases, pinniped abundance has been directly related to the abundance of returning salmon (e.g., Middlemas et al. 2006). Nevertheless, our results are more consistent with Quinn et al. (2003), who found the number of sockeye salmon killed by Alaska brown bears increased with salmon abundance, but the proportion killed generally decreased with salmon abundance. Describing predator–prey dynamics was beyond the scope of our study, but the results suggest that Columbia River salmonid injury and direct mortality rates vary as a function of both pinniped density and run size. Importantly, these effects likely differ seasonally, and some early-run populations are probably the most vulnerable to predation, especially in years with low salmon returns.

Management implications

Because both salmonids and pinnipeds are federally protected, finding management solutions in the Columbia River basin will be challenging. The frequencies of new injuries and scarred fish suggest that attack rates on adult salmonids are high, and the increases in both injury rates and observed predation rates (e.g., Tackley et al. 2008) prompted lethal pinniped management in 2008–2010. However, considerable uncertainty remains regarding the direct and delayed effects of pinniped predation, particularly with regard to impacts on ESA-listed salmon and steelhead populations. Moreover, because we did not attempt to differentiate seal from sea lion bites, we may have missed spatio-temporal differences in foraging behavior of the three pinniped species in the Columbia River. The seasonal difference in pinniped species composition and relative abundance (e.g., Beach et al. 1985; Laake et al. 2002; Wright et al. 2010) almost certainly has differential impacts on the spring, summer, and fall runs. The challenges and conflicts between salmonids and pinniped management will likely increase should adult run sizes of salmonids decline to the levels that led to listing under the US ESA.

More information is needed on the relationships among injury rates, attack rates, and predation rates. In addition, better quantification of the fitness effects on individual salmon and steelhead populations is needed through the spawning period, as impacts likely vary widely among populations, seasons, and years. Estimating stock-specific impacts, particularly for early-run threatened populations (e.g., Keefer et al. 2004*a*; Anderson and Beer 2009), should be a high management priority.

Acknowledgements

Many people provided time and assistance during the course of this study. We are especially indebted to T. Bjornn, R. Ringe, and K. Tolotti. C. Boggs, B. Daigle, M. Feeley, E. Johnson, D. Joosten, M. Heinrich, P. Keniry, M. Morasch, C. Morat, C. Naumann, and C. Williams helped with field operations and collection and processing of telemetry data at the University of Idaho. B. Burke, K. Frick, A. Matter, and M. Moser (National Marine Fisheries Service) helped with data processing and project management. Funding for this project was provided by the US Army Corps of Engineers under the administration of D. Clugston, M. Langeslay, M. Shutters, R. Kalamacz, and R. Dach. Two anonymous reviewers provided valuable and constructive comments.

References

Abrams, P.A., and Ginzburg, L.R. 2000. The nature of predation: prey dependent, ratio dependent, or neither? Trends Ecol. Evol. **15**(8): 337–341. doi:10.1016/S0169-5347(00)01908-X. PMID:10884706.

Anderson, J.J., and Beer, W.N. 2009. Oceanic, riverine, and genetic influences on spring Chinook salmon migration timing. Ecol. Appl. **19**(8): 1989–2003. doi:10.1890/08-0477.1. PMID:20014573.

Baraff, L.S., and Loughlin, T.R. 2000. Trends and potential interactions between pinnipeds and fisheries of New England and the U.S. west coast. Mar. Fish. Rev. **62**: 1–40.

Barlow, J., Brownell Jr., R.L., DeMaster, D.P., Forney, K.A., Lowry, M.S., Osmek, S., Ragen, T.J., Reeves, R.R., and Small, R.J. 1995. U.S. Pacific marine mammal stock assessments. NOAA Tech. Memo. NMFS-SWFSC-219.

Beach, R.J., Geiger, A.C., Jeffries, S.J., Treacy, S.D., and Troutman, B.L. 1985. Marine mammals and their interactions with fisheries of the Columbia River and adjacent waters, 1980–1982. Alaska Fisheries Science Center, National Marine Fisheries Service – NOAA, Seattle, Wash., USA. Processed Rep. 85-04.

Beddington, J.R., Beverton, R.J.H., and Lavigne, D.M. 1985. Marine mammals and fisheries. George Allen and Unwin, London, UK.

Brett, J.R. 1965. The relation of size to the rate of oxygen consumption and sustained swimming speed of sockeye salmon (*Oncorhynchus nerka*). J. Fish. Res. Board Can. **22**(6): 1491–1501. doi:10.1139/f65-128.

Brown, R.F., and Mate, B.R. 1983. Abundance, movements, and feeding-habits of harbor seals, *Phoca vitulina*, at Netarts and Tillamook Bays, Oregon. Fish Bull. **81**: 291–301.

Carretta, J.V., Forney, K.A., Muto, M.M., Barlow, J., Baker, J., Hanson, B., and Lowry, M.S. 2005. U.S. Pacific marine mammal stock assessments: 2005. US Dept. Comm. Tech. Memo. NOAA-TM-NMFS-SWFSC-375.

Caudill, C.C., Daigle, W.R., Keefer, M.L., Boggs, C.T., Jepson, M. A., Burke, B.J., Zabel, R.W., Bjornn, T.C., and Peery, C.A. 2007. Slow dam passage in adult Columbia River salmonids associated with unsuccessful migration: delayed negative effects of passage obstacles or condition-dependent mortality? Can. J. Fish. Aquat. Sci. **64**(7): 979–995. doi:10.1139/f07-065.

Chopin, F.S., and Arimoto, T. 1995. The condition of fish escaping from fishing gears-a review. Fish. Res. **21**(3–4): 315–327. doi:10.1016/0165-7836(94)00301-C.

Christensen, B. 1996. Predator foraging capabilities and prey antipredator behaviours: pre- versus postcapture constrains on sizedependent predator–prey interactions. Oikos, **76**(2): 368–380. doi:10.2307/3546209.

Fryer, J.K. 1998. Frequency of pinniped-caused scars and wounds on adult spring–summer chinook and sockeye salmon returning to the Columbia River. N. Am. J. Fish. Manage. **18**(1): 46–51. doi:10.1577/1548-8675(1998)018<0046:FOPCSA>2.0.CO;2.

Gonica, T.M., Keefer, M.L., Bjornn, T.C., Peery, C.A., Bennett, D. H., and Stuehrenberg, L.C. 2006. Behavioral thermoregulation and slowed migration by adult fall Chinook salmon in response to high Columbia River water temperatures. Trans. Am. Fish. Soc. **135**(2): 408–419. doi:10.1577/T04-113.1.

Greenstreet, S.P.R., Morgan, R.I.G., Barnett, S., and Redhead, P. 1993. Variation in the numbers of shags *Phalacrocorax aristotelis* and common seals *Phoca vitulina* near the mouth of an Atlantic salmon *Salmo salar* river at the time of the smolt run. J. Anim. Ecol. **62**(3): 565–576. doi:10.2307/5205.

Harmon, J.R., Thomas, K.L., McIntyre, K.W., and Paasch, N.N. 1994. Prevalence of marine-mammal tooth and claw abrasions on adult anadromous salmonids returning to the Snake River. N. Am. J. Fish. Manage. **14**(3): 661–663. doi:10.1577/1548-8675(1994)014<0661:POMMTA>2.3.CO;2.

Holling, C.S. 1965. The functional response of predators to prey density and its role in mimicry and population regulation. Mem. Entomol. Soc. Can. **97**(45): 1–60. doi:10.4039/entm9745fv.

Hosmer, D.W., and Lemeshow, S. 2000. Applied logistic regression. 2nd ed. Wiley-InterScience, Hoboken, N.J.

Jeffries, S., Huber, H., Calambokidis, J., and Laake, J. 2003. Trends and status of harbor seals in Washington state: 1978–1999. J. Wildl. Manage. **67**(1): 207–218. doi:10.2307/3803076.

Keefer, M.L., Peery, C.A., Jepson, M.A., Tolotti, K.R., Bjornn, T.C., and Stuehrenberg, L.C. 2004*a*. Stock-specific migration timing of adult spring–summer Chinook salmon in the Columbia River basin. N. Am. J. Fish. Manage. **24**(4): 1145–1162. doi:10.1577/M03-170.1.

Keefer, M.L., Peery, C.A., Ringe, R.R., and Bjornn, T.C. 2004*b*. Regurgitation rates of intragastric radio transmitters by adult Chinook salmon and steelhead during upstream migration in the Columbia and Snake rivers. N. Am. J. Fish. Manage. **24**(1): 47–54. doi:10.1577/M02-128.

Keefer, M.L., Peery, C.A., Daigle, W.R., Jepson, M.A., Lee, S.R., Boggs, C.T., Tolotti, K.R., and Burke, B.J. 2005. Escapement, harvest, and unknown loss of radio-tagged adult salmonids in the Columbia River – Snake River hydrosystem. Can. J. Fish. Aquat. Sci. **62**(4): 930–949. doi:10.1139/f04-246.

Keefer, M.L., Caudill, C.C., Peery, C.A., and Lee, S.R. 2008. Transporting juvenile salmonids around dams impairs adult migration. Ecol. Appl. **18**(8): 1888–1900. doi:10.1890/07-0710.1. PMID:19263886.

Keefer, M.L., Taylor, G.A., Garletts, D.F., Gauthier, G.A., Pierce, T. M., and Caudill, C.C. 2010. Prespawn mortality in adult spring Chinook salmon outplanted above barrier dams. Ecol. Freshw. Fish, **19**(3): 361–372. doi:10.1111/j.1600-0633.2010.00418.x.

Laake, J.L., Browne, P., DeLong, R.L., and Huber, H.R. 2002. Pinniped diet composition: a comparison of estimation models. Fish Bull. **100**: 434–447.

Lindsay, R.B., Schroeder, R.K., Kenaston, K.R., Toman, R.N., and Buckman, M.A. 2004. Hooking mortality by anatomical location and its use is estimating mortality of spring Chinook salmon caught and released in a river sport fishery. N. Am. J. Fish. Manage. **24**(2): 367–378. doi:10.1577/M02-101.1.

Lundvall, D., Svanbck, R., Persson, L., and Byström, P. 1999. Size-dependent predation in piscivores: interactions between predator foraging and prey avoidance abilities. Can. J. Fish. Aquat. Sci. **56**(7): 1285–1292. doi:10.1139/cjfas-56-7-1285.

McClure, M.M., Holmes, E.E., Sanderson, B.L., and Jordan, C.E. 2003. A large-scale, multispecies status, assessment: anadromous salmonids in the Columbia River Basin. Ecol. Appl. **13**(4): 964–989. doi:10.1890/1051-0761(2003)13[964:ALMSAA]2.0.CO;2.

Middlemas, S.J., Barton, T.R., Armstrong, J.D., and Thompson, P. 2006. Functional and aggregative responses of harbour seals to changes in salmonid abundance. Proc. Biol. Sci. **273**(1583): 193–198. doi:10.1098/rspb.2005.3215. PMID:16555787.

National Marine Fisheries Service. 1997. Investigation of scientific information on the impacts of California sea lions and Pacific harbor seals on salmonids and on the coastal ecosystems of Washington, Oregon, and California. US Dept. Comm. NOAA Tech. Memo. NMFS-NWFSC-28.

National Marine Fisheries Service. 1998. Marine mammals; environmental assessment on preventing California sea lion foraging and predation on salmonids at Willamette Falls, Oregon. Fed. Regist. **63**: 56–60.

National Marine Fisheries Service. 1999. Report to Congress: impacts of California sea lion and Pacific harbor seals on salmonids and West Coast ecosystems. US Department of Commerce, National Marine Fisheries Service, Silver Spring, Md., USA.

National Marine Fisheries Service. 2000. Federal Columbia River Power System Biological Opinion (section 9.6.1.5.3, action Item 106). Seattle, Wash.

National Oceanic and Atmospheric Administration. 2008. Authority for states to remove sea lions under Marine Mammal Protection Act Section 120. Available from http://www.nwr.noaa.gov/Publications/FR-Notices/2008/upload/73FR15483.pdf.

Naughton, G.P., Caudill, C.C., Keefer, M.L., Bjornn, T.C., Stuehrenberg, L., and Peery, C.A. 2005. Late-season mortality during migration of radio-tagged adult sockeye salmon (*Oncorhynchus nerka*) in the Columbia River. Can. J. Fish. Aquat. Sci. **62**(1): 30–47. doi:10.1139/f04-147.

Nehlsen, W., Williams, J.E., and Lichatowich, J.A. 1991. Pacific salmon at the crossroads: stocks at risk from California, Oregon, Idaho, and Washington. Fisheries, **16**: 4–21.

Quinn, T.P., Gende, S.M., Ruggerone, G.T., and Rogers, D.E. 2003. Density-dependent predation by brown bears (*Ursus arctos*) on sockeye salmon (*Oncorhynchus nerka*). Can. J. Fish. Aquat. Sci. **60**(5): 553–562. doi:10.1139/f03-045.

Ramsey, F.L., and Schafer, D.W. 2002. The statistical sleuth. 2nd ed. Duxbury, Pacific Grove, Calif., USA.

Reischel, T.S., and Bjornn, T.C. 2003. Influence of fishway placement on fallback of adult salmon at the Bonneville Dam on the Columbia River. N. Am. J. Fish. Manage. **23**(4): 1215–1224. doi:10.1577/M02-113.

Ricker, W.E. 1952. Numerical relations between abundance of predators and survival of prey. Can. Fish. Cult. **13**: 5–9.

Roffe, T.J., and Mate, B.R. 1984. Abundances and feeding habits of pinnipeds in the Rogue River, Oregon. J. Wildl. Manage. **48**(4): 1262–1274. doi:10.2307/3801787.

SAS Institute Inc. 2008. SAS/STAT user's guide version 9.2. SAS Institute Inc., Cary, N.C., USA.

Scordino, J., and Pfeifer, B. 1993. Sea lion/steelhead conflict at the Ballard Locks. A history of control efforts to date and a bibliography of technical reports. Washington Department of Fish and Wildlife Report. [Available from Northwest Regional Office, National Marine Fisheries Service – NOAA, 7600 Sand Point Way NE, Seattle, WA 98115, USA.]

Stansell, R. 2004. Evaluation of pinniped predation on adult salmonids and other fish in the Bonneville Dam tailrace, 2002–2004. US Army Corps of Engineers. Bonneville Lock and Dam, Cascade Locks, Ore.

Tackley, S., Stansell, R., and Gibbons, K. 2008. Pinniped predation on adult salmonids and other fish in the Bonneville Dam tailrace, 2005–2007. US Army Corps of Engineers, CENWP-OP-SRF, Bonneville Lock and Dam, Cascade Locks, Ore.

US Army Corps of Engineers. 2005. Annual fish passage report. USACE, Portland, Ore.

Weihs, D. 1973. Optimal fish cruising speed. Nature, **245**(5419): 48–50. doi:10.1038/245048a0.

Werner, E.E., and Gilliam, J.F. 1984. The ontogenetic niche and species interactions in size-structured populations. Annu. Rev. Ecol. Syst. **15**(1): 393–425. doi:10.1146/annurev.es.15.110184.002141.

Wright, B.E., Riemer, S.D., Brown, R.F., Ougzin, A.M., and Bucklin, K.A. 2007. Assessment of harbor seal predation on adult salmonids in a Pacific Northwest estuary. Ecol. Appl. **17**(2): 338–351. doi:10.1890/05-1941. PMID:17489243.

Wright, B.E., Tennis, M.J., and Brown, R.F. 2010. Movements of California sea lions captured in the Columbia River. Northwest Sci. **84**(1): 60–72. doi:10.3955/046.084.0107.

Including mark–recapture data into a spatial age-structured model: walleye pollock (*Theragra chalcogramma*) in the eastern Bering Sea

Peter-John F. Hulson, Sara E. Miller, James N. Ianelli, and Terrance J. Quinn II

Abstract: Integrated assessment models used to evaluate fish stocks are becoming increasingly complex, with some capable of incorporating spatial considerations. Such a model has been developed to estimate movement of walleye pollock (*Theragra chalcogramma*) between the northwestern and southeastern eastern Bering Sea. In this study, we investigate the feasibility of estimating movement using spatially disaggregated data supplemented by tagging data. Monte Carlo simulation was used to test accuracy and variability of parameter estimation in model scenarios with and without tagging information. Total biomass estimates for models with and without tagging data were unbiased, but uncertainty was smaller when tagging data were available. Uncertainty was also reduced in regional biomass and movement parameters when including tagging data. Our findings indicate that tagging information would be important to provide reliable spatially explicit fisheries management advice for eastern Bering Sea pollock.

Résumé : Les modèles intégrés d'estimation utilisés pour évaluer les stocks de poissons deviennent de plus en plus complexes, certains étant capables d'incorporer des considérations spatiales. Un tel modèle a été mis au point pour estimer les déplacements de la goberge d'Alaska (*Theragra chalcogramma*) entre le nord-ouest et le sud-est de la mer de Béring orientale. Dans notre étude, nous examinons la faisabilité d'estimer les déplacements en utilisant des données spatialement désagrégées, additionnées de données de marquage. Une simulation de Monte Carlo sert à tester l'exactitude et la variabilité de l'estimation des paramètres dans les scénarios du modèle avec et sans données de marquage. Les estimations de la biomasse totale dans les modèles avec et sans marquage sont non biaisées, mais l'incertitude est plus petite quand des données de marquage sont disponibles. L'incertitude est aussi réduite dans les paramètres de biomasse régionale et de déplacement lorsqu'on inclut les données de marquage. Nos résultats indiquent que les données de marquage pourraient être importantes lorsqu'on veut fournir des avis de gestion fiables et spatialement explicites sur la goberge de la mer de Béring.

[Traduit par la Rédaction]

Introduction

Because the true mechanisms and processes underlying the natural world are unknown, researchers describe the system using models based on available observations. These data sets typically lack the contrast needed to estimate more complex parameterizations because parameters can become confounded due to the statistical models employed. For example, natural mortality parameters are often confounded with movement parameters in spatial models, in which case, tagging data have been proposed as a way to address parameter confounding (Anganuzzi 1996).

One of the most powerful tools available to test assessment models in fisheries science is simulation (Hilborn and Mangel 1997). Monte Carlo simulation has been used to determine model robustness from incorrectly specifying the error structure or parameter structure (e.g., Fu and Quinn 2000). By using simulated data, the researcher knows the true parameter values and can then evaluate model performance (Hilborn and Mangel 1997). Through realistic simulation that includes aspects of random variability in dynamics and observation, it is important to investigate the biases, effectiveness, and impacts on management procedures of new stock assessment methods (Hilborn and Walters 1992; Maunder 2001). This study presents an application of simulation-estimation tests for a relatively complex spatially explicit movement model.

Changes to a fish population structure over space or time can affect fish stock assessment estimates of potential fishery yields and mortality. Assuming that there is no movement in a fish population when movement actually occurs can lead to a loss in potential harvests (Tuck and Possingham 1994). Conversely, assuming movement when populations are relatively stationary over space or time can lead to depletion im-

Received 5 July 2010. Accepted 30 March 2011. Published at www.nrcresearchpress.com/cjfas on 6 September 2011.
J21907

Corresponding Editor: Josef Michael Jech.

P.-J.F. Hulson, S.E. Miller, and T.J. Quinn II. Juneau Center, School of Fisheries and Ocean Sciences, University of Alaska Fairbanks, 17101 Point Lena Loop Road, Juneau, AK 99801, USA.
J.N. Ianelli. Resource Ecology and Fisheries Management Division, Alaska Fisheries Science Center, NMFS 7600 Sand Point Way NE, Seattle, WA 98115, USA.

Corresponding author: Peter-John F. Hulson (e-mail: phulson@alaska.edu).

Can. J. Fish. Aquat. Sci. **68**: 1625–1634 (2011) doi:10.1139/F2011-060 **Published by NRC Research Press**

Table 1. Years of spatially disaggregated data sources available for the northwestern (NW) and southeastern (SE) regions of the eastern Bering Sea pollock. Total yield included all years (1977 to 2005).

Region	Season	Bottom-trawl survey abundance	Echo-integrated trawl survey abundance	Fishery (catch-at-age and yield)
NW	A	1982–2004	1994, 1996, 1997, 1999, 2000, 2002	1977–2005 (missing 1988–1990, 1997)
	B			1977–2005 (missing 1988–1990)
SE	A	1982–2004	1994, 1996, 1997, 1999, 2000, 2002	1977–2005 (missing 1988–1990)
	B			1977–2005 (missing 1988–1990)

Note: The "A" season fishery occurs subsequent to the start of the year from January to June with half-year natural mortality; the "B" season fishery is subsequent to the first regional movement and occurs from July to December with half-year natural mortality.

balances with fishing (Hilborn and Walters 1992). Incorporation of movement in fish stock assessment analysis is rare because of the lack of tagging information and added model complexity (Quinn and Deriso 1999). Consequently, spatial assessment models are uncommon in fishery management settings, but there have been some promising developments.

An age-structured movement model has been developed for eastern Bering Sea (EBS) walleye pollock (*Theragra chalcogramma*, hereafter referred to as pollock) that estimates movement based on spatially disaggregated survey and fishery data (Miller et al. 2008). A method for including tagging data into assessment models was provided by Maunder (2001). In this model, the tagged fish follow the same population dynamics of the entire population and are essentially modeled as a subset of the entire population within the assessment model. Other spatial models that include tagging data are those of Punt et al. (2000) and Hanselman et al. (2007). The first is a spatially explicit model for school shark (*Galeorhinus galeus*) off southern Australia that includes tagging data. The latter is a size-based migration model designed for the migratory Alaska sablefish (*Anaplopoma fimbria*) and uses mark–recapture data sets that began in 1979 (Heifetz and Fujioka 1991). Also, a size-structured model that includes mark–recapture information for South Australian rock lobster (*Jasus edwardsii*) has been developed (McGarvy et al. 2010) and is used for management advice.

The groundfish fishery for pollock in the EBS is one of the world's largest, and catch limits are managed by seasons. During spring and summer in the EBS, pollock are thought to migrate to feeding areas, and during the late fall and early winter, they migrate to spawning areas. Pollock distribution with respect to temperature obtained from EBS surveys shows that feeding migrations tend to follow a northward and shoreward movement, the extent of which increases with increasing size of pollock (Kotwicki et al. 2005). Currently, there is no movement information from a large-scale EBS pollock mark–recapture study, but feasibility studies for tagging of pollock have shown the potential for sufficient sample size and survival rates (Natural Resources Consultants, Inc., and Northwest Marine Technology, Inc. 1996; Miller 2007; Winter et al. 2007).

Using disaggregated survey and fishery catch data, age-specific pollock movement between the northwestern (NW) and southeastern (SE) EBS was estimated using an age-structured assessment movement model (ASM; Miller et al. 2008). This model differs from the present EBS pollock stock assessment that is based on a standard age-structured stock assessment model (Ianelli et al. 2009) and does not estimate movement. Under moderate assumptions for spatial structure (the number of regions in which movement was estimated), reasonable estimates of most population and movement parameters could be obtained. However, some parameter estimates were highly uncertain and correlated, and the analysis lacked a formal evaluation of accuracy and precision. In the current study, the utility of additional information from a hypothetical mark–recapture program is examined and compared with the ASM model constructed by Miller et al. (2008). We do not consider interpopulation movement, rather that the pollock "stock" exhibits intrapopulation movement between the two regions in the EBS. The ability to reliably estimate movement parameters was tested using Monte Carlo simulation (Hilborn and Mangel 1997). Given specified spatial and seasonal population characteristics, we investigated the bias and variability in parameters and population estimates across a variety of scenarios, including the addition of tagging data. The goals were to determine (*i*) the benefits of having tagging data sets for the ASM model, (*ii*) the sensitivity of results to tag-release protocols (e.g., season and area of releases), and (*iii*) the magnitude of bias and variability in population parameter estimates without tagging data.

Materials and methods

In this study the ASM model developed by Miller et al. (2008) was used as the operating model. Estimates based on the original data fit with the ASM model formed the "true" state of nature from which data were generated (with specified errors) for subsequent fitting by the estimation models (Table 1). The two regions considered for the EBS in Miller at al. (2008) were divided into NW and SE by the 170°W meridian (Fig. 1). The data sets used in the ASM model are described in Miller et al. (2008). The Aleutian Islands and the Gulf of Alaska were not included in the analysis.

As the primary focus of this study was to evaluate the effect of tagging data on ASM model estimates, tagging data by region and season were also generated and applied to an integrated tagging and catch-at-age analysis (ITCAAN) estimation model (Maunder 2001). Results from the simulation analyses were compared through bias and variability in the movement parameters and biomass estimates. The simulation procedure was executed with customized code in R language (R Development Core Team 2008) that integrated R with AD model builder (ADMB; Fournier 1996). The ASM and ITCAAN estimating models were written using ADMB, and the operating model and simulation–estimation loops were written using R. For each variance scenario, 1000 operating model simulations were evaluated; the number of simulations was selected to obtain robust estimates of variance (e.g., Efron and Tibshirani 1993). Further, the ASM and ITCAAN models in each simulation used the same generated data

Fig. 1. Map showing the northwestern (NW) and southeastern (SE) regions of the eastern Bering Sea considered in the spatial modeling of walleye pollock.

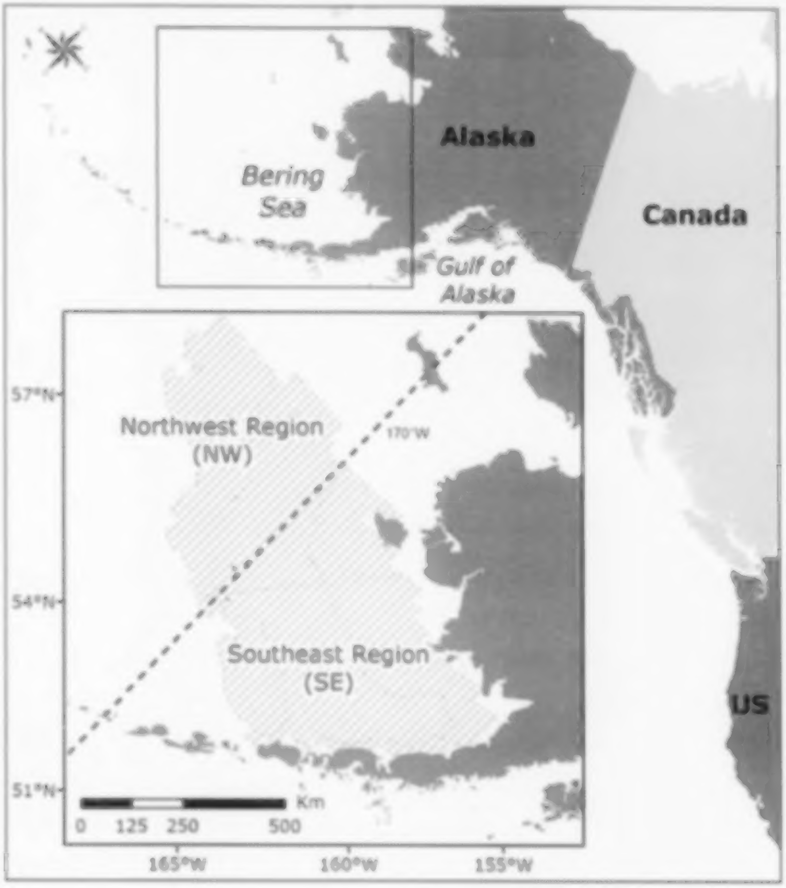

except the generated tag-recovery data because the ASM model does not fit tag-recovery data.

Operating model

In Miller et al. (2008), the population dynamics of EBS pollock was modeled with a discrete-time and region-specific ASM model (Quinn and Deriso 1999; Maunder 2001). The generalized dynamics of pollock in region r at age a in year y at the start of the year in the ASM model can be formulated as the sequence of spatial (regions NW, SE) and temporal (seasons A and B) events shown (Fig. 2). Pollock spawn in the winter, and this time period is used in the ASM model as the start of the modeling year (1 January). The A season fishery occurs subsequent to the start of the year from January to June. After the A season, the first regional movement between the NW and SE takes place to reflect movement of pollock from the spawning to summer feeding grounds. During this time, half of the year's natural mortality was applied to the population. The B season fishery is subsequent to the first regional movement and occurs from July to December. After the B season fishery, the second regional movement was modeled to reflect movement back to spawning grounds in the fall, and the second half of the year's natural mortality is applied. Note that when movement occurs, it is not the entire population moving from region to region, rather a proportion of the population that moves as determined by the probability of movement estimated by movement parameters. The population after the A fishing season at age a in year y was the first step (step 1) in the yearly population dynamics equation:

$$(1)\quad {}^{1}_{r}N_{a,y} = {}_{r}N_{a,y}e^{-{}_{r}F_{a,y,A}}$$

Movement from the winter spawning grounds to summer feeding grounds (step 2), with half-year natural mortality, was modeled as

$$(2)\quad {}^{2}_{r}N_{a,y} = ({}^{1}_{r}N_{a,y}\theta_{r\to r,A} + {}^{1}_{r'}N_{a,y}\theta_{r'\to r,A})e^{-M/2}$$

in which the abundance in region r is the sum of the numbers of fish that stay in region r ($r \to r$) and the numbers that leave region r' for region r ($r' \to r$). The B season fishing mortality was applied to the population in step 3:

$$(3)\quad {}^{3}_{r}N_{a,y} = {}^{2}_{r}N_{a,y}e^{-{}_{r}F_{a,y,B}}$$

Fig. 2. Depiction of the two-area, two-season model for pollock in the eastern Bering Sea showing the processes affecting the population. Figure modified from Miller et al. (2008).

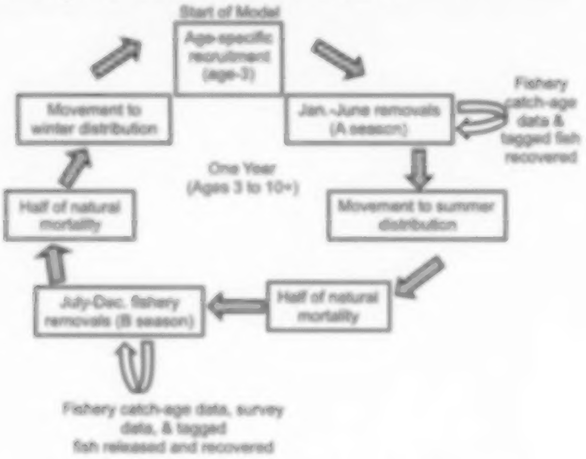
Start of Model
Age-specific recruitment (age-3)
Jan.-June removals (A season)
Fishery catch-age data & tagged fish recovered
One Year (Ages 3 to 10+)
Movement to summer distribution
Half of natural mortality
July-Dec. fishery removals (B season)
Fishery catch-age data, survey data, & tagged fish released and recovered
Half of natural mortality
Movement to winter distribution

After the B fishing season movement from the summer feeding grounds back to the spawning grounds, the final step in the yearly population dynamics (step 4) was estimated by

$$(4)\qquad {}^{4}_{r}N_{a,y} = \left({}^{3}_{r}N_{a,y}\theta_{r\to r,B} + {}^{3}_{r'}N_{a,y}\theta_{r'\to r,B}\right)e^{-M/2}$$

which becomes the population abundance at the beginning of the next year. The prime notation is used to describe the alternate region, that is, if r = NW then r' = SE. In these equations, F represents fishing mortalities for the A and B seasons, M is natural mortality, and θ is the probability of movement after fishing seasons A or B from region r to region r', which may also be a function of age.

Pollock are thought to move seasonally and with a general ontogenetic pattern that shifts southeastward with increasing age (Buckley et al. 2001). For the NW region, the operating model was conditioned such that the probability of movement from the NW to SE was an increasing linear function of age. For convenience, the modeling of movement was parameterized in terms of probability of staying in the same region (1 – probability of movement). Based on available knowledge, the probability that age 3 fish stayed in the NW after the A season was $\theta_{\mathrm{NW}\to\mathrm{NW,A}}$ = 99% and the probability after the B season was $\theta_{\mathrm{NW}\to\mathrm{NW,B}}$ = 75%. These amounts were multiplied by 80% for each successive age class for movement after the A fishing season and by 90% for the movement after the B fishing season (Miller et al. 2008). For the SE EBS, available knowledge suggests that the probability of staying in the SE region was constant for all ages, equal to $\theta_{\mathrm{SE}\to\mathrm{SE,A}}$ = 30% after the A season and $\theta_{\mathrm{SE}\to\mathrm{SE,B}}$ = 70% after the B season (Miller et al. 2008). These four parameters were estimated in the estimation model. The corresponding age-specific movement rates are shown (Fig. 3).

Data generation

Data were simulated by generating random variability about the expected values from the operating model and fitting the generated data with the estimation model structures. In the simulation analysis, a total of 13 data sets (Table 2) were generated and employed in the ASM model structure and 17 in the ITCAAN model structure. The four additional data sets in the ITCAAN model were tag-return data from the two regions and two fishery seasons (Table 3). Because the lognormal distribution was used in the ASM model fit by Miller et al. (2008), simulated data were structured to follow a lognormal distribution to provide a direct comparison with the prior study:

Fig. 3. Movement parameter estimates, by age, modified from Miller et al. (2008). $\theta_{\mathrm{NW}\to\mathrm{NW,A}}$ and $\theta_{\mathrm{NW}\to\mathrm{NW,B}}$, the probability that age 3 fish stayed in the NW after seasons A and B, respectively; $\theta_{\mathrm{SE}\to\mathrm{SE,A}}$ and $\theta_{\mathrm{SE}\to\mathrm{SE,B}}$, the probability that fish of all ages stayed in the SE after seasons A and B, respectively.

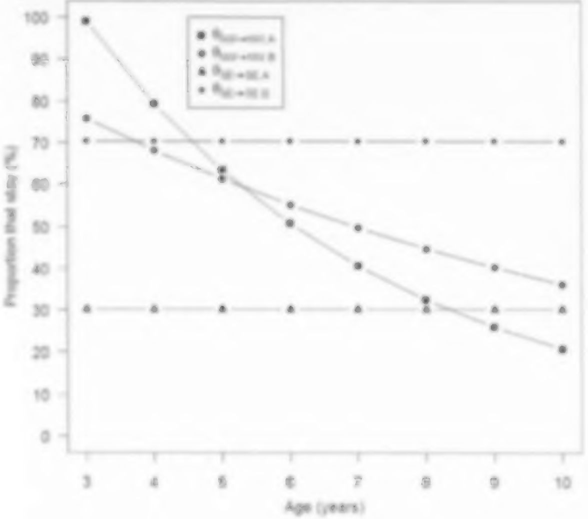

$$(5)\qquad x_i = \bar{x}e^{\left(\varepsilon_i - \frac{\sigma^2}{2}\right)},\quad \varepsilon_i \sim \mathrm{N}(0,\sigma)$$

in which $\bar{x}$ is the "true" value from an area and year, ε_i is the randomly generated normal deviation for simulation i, and σ is the prespecified standard deviation. The values for σ in the estimation model were set to a range of different values relative to the "true" operating model values (Tables 2 and 3).

Because tagging information was the key focus in this study, "observed" tag-recovery data were constructed in the operating model by a simulated tagging program. In this program, there were annual releases of tags into the marked population in both regions for all ages 3 to 10+ during the summer surveys. To evaluate the effect of the number of years that tag release and recovery were conducted, two cases were considered. In the first case (case I), tagged fish were released in each year from 2000 to 2002. In the second case (case II), tagged fish were released in each year from 1995 to 2002. Recoveries for both cases start in the first year of tagging and continue through 2004. We refer to a spatial model with both regular assessment data and mark–recapture data as an integrated tagging and catch-at-age analysis (ITCAAN) model after Maunder (2001).

In the ITCAAN model, the tagged and the total population (including both tagged and untagged fish) were modeled simultaneously with the same dynamics and parameter values

Table 2. Input values for σ (used in the lognormal distribution) relative to different spatially disaggregated data sources.

Data sources	Region	Season	σ
Fishery yield	NW	A	0.05
		B	0.05
	SE	A	0.05
		B	0.05
Total fishery yield	na	na	0.025
Fishery catch-at-age	NW	A	0.3
		B	0.2
	SE	A	0.2
		B	0.2
Bottom trawl survey	NW	na	0.2
	SE	na	0.2
Echo-integrated trawl survey	NW	na	0.2
	SE	na	0.2

Note: In the Region and Season columns, "na" means not applicable; NW and SE, northwestern and southeastern regions of the eastern Bering Sea, respectively. See Table 1 or text for explanation of seasons A and B.

Table 3. Standard deviations considered in the two uncertainty scenarios (*a* and *b*) for tag-recovery data.

		Scenario	
Region	Season	*a*	*b*
NW	A	0.05	0.7
	B	0.05	0.2
SE	A	0.05	0.1
	B	0.05	0.1

Note: NW and SE, northwestern and southeastern regions of the eastern Bering Sea, respectively. See Table 1 or text for explanation of seasons A and B.

(e.g., Maunder 2001), except that the initial tagged populations at the start of the mark–recapture program were the numbers of releases by regions and ages. It was assumed that the pollock would be implanted with magnetically detectable coded wire tags (CWT) by a research vessel in the summer during the bottom trawl survey (BTS) such that fish in different regions would receive different tags. In this study, we did not consider tag-induced mortality, as an actual tagging program has not been implemented for pollock and it would be difficult to presume what tag-induced mortality would be. It was further assumed that fish would be recovered by the commercial fishery in either fishery season A or B. There are three fishing sectors in the EBS: (1) fishing vessels with shoreside processors (50% of total acceptable catch (TAC)), (2) fishing vessels with offshore mothership processors (10% of TAC), and (3) vessels that both harvest and process their catch offshore (40% of TAC). Only the feasibility of installing electronic CWT detectors in shoreside processing plants has been determined (National Research Council 1996). Therefore, only the proportion of the catch typically caught by the fishing vessels with shoreside processors was considered in the tag-recovery process.

The number of recoveries (${}^rR_{a,y,s}$) at age a in year y from region r and season s was generated by

$$(6) \qquad {}^rR_{a,y,s} = {}^rp\,{}^rT_{a,y,s}\left(1 - e^{-{}^rF_{a,y,s}}\right)$$

in which ${}^rT_{a,y,s}$ is the number of marked individuals at age a in year y from region r and season s after one-half year of natural mortality, F is the fishing mortality, and ${}^rp$ is the proportion of the total catch delivered to shoreside processors from region r. For simplicity, this proportion was treated as constant over time, which is reasonable from examination of catch data. Recoveries are a function of the exploitation fraction of the fishery; incidental recoveries from survey effort were omitted as total catch during a survey is very low. The proportion of total catch from region r (${}^rp$) delivered to shoreside processors, derived from observed regional landings from 2003–2005, was set at 7% from the NW region and at 39% from the SE region (Miller 2007). As an actual tagging program has not been implemented for pollock, in this simulation study, it was assumed that there was no tag loss or tag-induced mortality for fish that were tagged with CWTs and that the total catch delivered to shoreside processors was examined for tags with a detection rate of 100%. Thus, to simplify, non-reporting rate, tag-induced mortality, and tag loss were considered negligible (e.g., Haist 1998).

Two methods of releasing tags during the survey were examined in the simulation analysis. In the first method, tags were released evenly across the NW and SE regions. In this case, 5000 tags were released in the NW and 5000 in the SE during the BTS survey. In the second method, tags were released proportionally to the BTS survey catch: 67% (6700) of the tags were released in the NW region and 33% (3300) were released in the SE during the survey. In both cases, it was assumed that the ages at the time of tagging were known, the tags were distributed uniformly across age classes, and the tagged fish mixed completely in the population with untagged fish. Fitting the ITCAAN model to even tagging is denoted by ITCAAN_E, and fitting to proportional tagging is denoted ITCAAN_P. The two cases for the number of years for which tags were released for each tagging method were denoted as (even tagging, for example) $\mathrm{ITCAAN}_{E,I}$ for case I and $\mathrm{ITCAAN}_{E,II}$ for case II.

Two uncertainty scenarios for the tag-recovery data were used in the simulation (Table 3). In the first scenario (*a*), the standard deviation for tag recoveries was set at 0.05 to represent a case in which the uncertainty in tag returns was low. The second scenario (*b*) used standard deviations that were proportional to the inverse of the number of tag recoveries. This scenario was selected to evaluate uncertainty that is related to the sample size of tag recoveries obtained.

Estimation models

In both the ASM and ITCAAN models, parameter estimates were obtained using an objective function that represented the negative log likelihood of normalized residuals. The objective function consisted of 13 data set sources for the ASM model (Table 2; Miller et al. 2008). For the ITCAAN model, there were the 13 data set sources fitted in the ASM, with an additional four data sets for tag recoveries by fishing season and region (Table 3). The weighting terms, or equivalently the data set standard deviations, were derived from either the 2009 stock assessment report (Ianelli et al. 2009) or were assigned a value consistent with available knowledge (Table 2).

In the ITCAAN estimation model, the tag-release data were directly input into the model, because this information would be known. The tag recovery data sets were fit in the

Fig. 4. Total, NW, and SE biomass in 2005 estimated by the ASM and ITCAAN models. Tag-recovery data uncertainty scenario *a* is shown in the left panel, and scenario *b* is shown in the right panel. The box represents the interquartile range from the estimation models, the whiskers (broken vertical lines) represent the 95% confidence interval, and values outside the 95% confidence intervals are shown with open circles. For the models, P and E refer to proportional and even tagging, respectively, and I and II refer to case I and case II release dates, respectively.

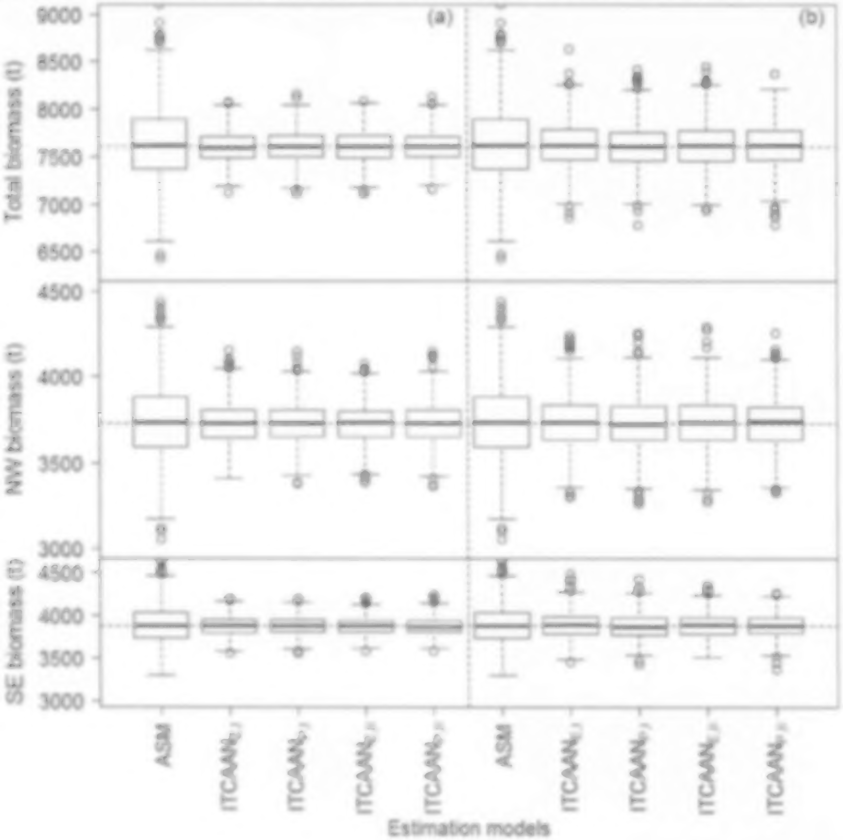

estimation model after being estimated following eq. 6 with a lognormal likelihood. We considered only region-specific tags rather than year- and region-specific tags; more sophisticated treatments of tagging data would potentially improve the ITCAAN model but are beyond the scope of this study. The lognormal distribution rather than discrete distributions (i.e., Poisson, multinomial) was used to provide more direct comparison with Miller et al. (2008), as the lognormal likelihood was used in that study. Further analysis is being conducted that uses discrete distributions to generate tagging data sets. In each tag-recovery data set uncertainty scenario, the standard deviations used in data simulation were subsequently used in the objective function as the likelihood variance to fit the generated data sets. We did not consider misspecification of variance in the estimation model.

For presentation, we focused on estimates of movement parameters and total and regional biomass in the results. For total and regional biomass, the results focus on the estimate in the last year of the model, as this is the crucial year from which forecasts and harvest recommendations are made to managers. Estimated asymptotic approximations to the standard deviations of the biomass and movement parameters were also provided. Box plots of these key parameters were used for presentation, the box represents the interquartile range from the estimation models and the whiskers (vertical broken lines) represent the 95% confidence interval. Bias was considered significant if the value from the operating model was outside the 95% confidence intervals.

Results

Overall, the variability in the estimates of total and regional biomass in the last year was reduced when tagging data sets were integrated into the stock assessment model (Fig. 4). Estimated total and regional biomass for both the ASM and ITCAAN models were not biased (Fig. 4). The estimated standard deviations in total and regional biomass from ADMB were smaller for the tag-recovery data set uncertainty scenario *a* as compared with scenario *b* for the ITCAAN models, but the estimated standard deviations from the ASM model were larger than either tag-recovery data set uncertainty scenario for the ITCAAN models (Fig. 5). Results were similar when tagging evenly between regions or proportionally to the BTS survey when considering the estimated standard deviations in total and regional biomass in the last year of the model (Fig. 5). Further, the estimated standard

Fig. 5. Standard deviations (SD) in total, NW, and SE biomass in 2005 estimated with ADMB for the ASM and ITCAAN models. Tag-recovery data uncertainty scenario *a* is shown in the left panel, and scenario *b* is shown in the right panel. The box represents the interquartile range from the estimation models, the whiskers (broken vertical lines) represent the 95% confidence interval, and values outside the 95% confidence intervals are shown with open circles. See Fig. 3 or text for movement parameter details and Fig. 4 or text for model details.

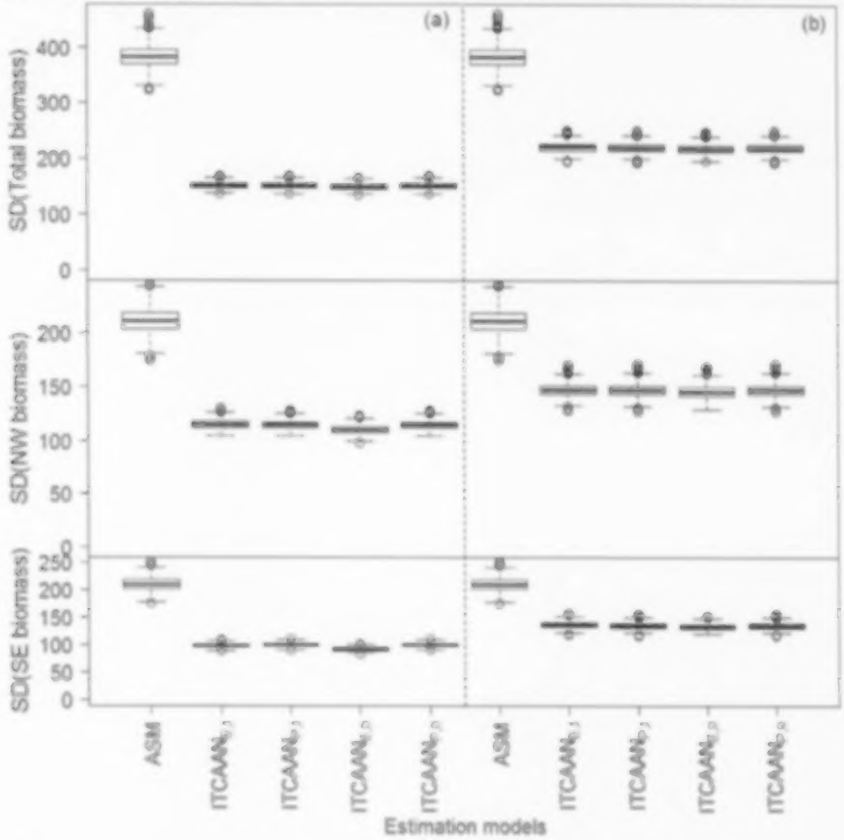

deviations in total and regional biomass were similar regardless of the length of the tag data set time series (Fig. 5).

Parameter estimates for regional and seasonal movement were unbiased for both the ASM and ITCAAN models (Fig. 6). The estimated standard deviations in the movement parameter estimate for the NW region after season A ($\theta_{NW\rightarrow NW,A}$) were similar for both the ASM and ITCAAN models (Fig. 7). Even though reduction in the estimated standard deviations was small, for all other movement parameters, the estimated standard deviations from ADMB were decreased in the ITCAAN models compared with the ASM model (Fig. 7). The largest differences in estimated standard deviations for movement parameters between the ASM and ITCAAN models occurred for tag-recovery data uncertainty scenario *a* compared with scenario *b*. In scenario *b*, the estimated standard deviations in movement parameters from the ITCAAN models were only slightly lower than from the ASM model, but the general patterns were similar to results from scenario *a* (Fig. 7). When uncertainty was low in the tag-return data in scenario *a* and tags were released evenly between regions, the estimated standard deviations of movement parameters were smaller when the time series of tag-recovery data were longer (case II compared with case I). When tagging proportionally to the BTS survey, the estimated standard deviations in movement parameters were similar regardless of the length of the tag-recovery data (Fig. 7). Comparing between tag-release methods, in tag-recovery data set uncertainty scenario *a*, the estimated standard deviations of movement parameters were smaller when tagging evenly across regions as compared with tagging proportionally to the BTS survey; the same resulted for tag-recovery data uncertainty scenario *b*, but the differences were not as notable (Fig. 7).

Discussion

The quality and quantity of data and the soundness of assumptions all directly affect the accuracy of models and their predictions (National Research Council 1998). Both the ASM and ITCAAN models resulted in significantly unbiased estimates of parameters and population biomass. This is a consequence of the operating and estimation models being the same, but it also shows that there was apparently no appreciable parameter confounding even in the absence of tagging data. Our simulation study showed that an advantage of including tagging data sets into a spatially

Fig. 6. Estimated movement parameters from the ASM and ITCAAN models. Tag-recovery data uncertainty scenario *a* is shown in the left panel, and scenario *b* is shown in the right panel. The box represents the interquartile range from the estimation models, the whiskers (broken vertical lines) represent the 95% confidence interval, and values outside the 95% confidence intervals are shown with open circles. See Fig. 3 or text for movement parameter details and Fig. 4 or text for model details.

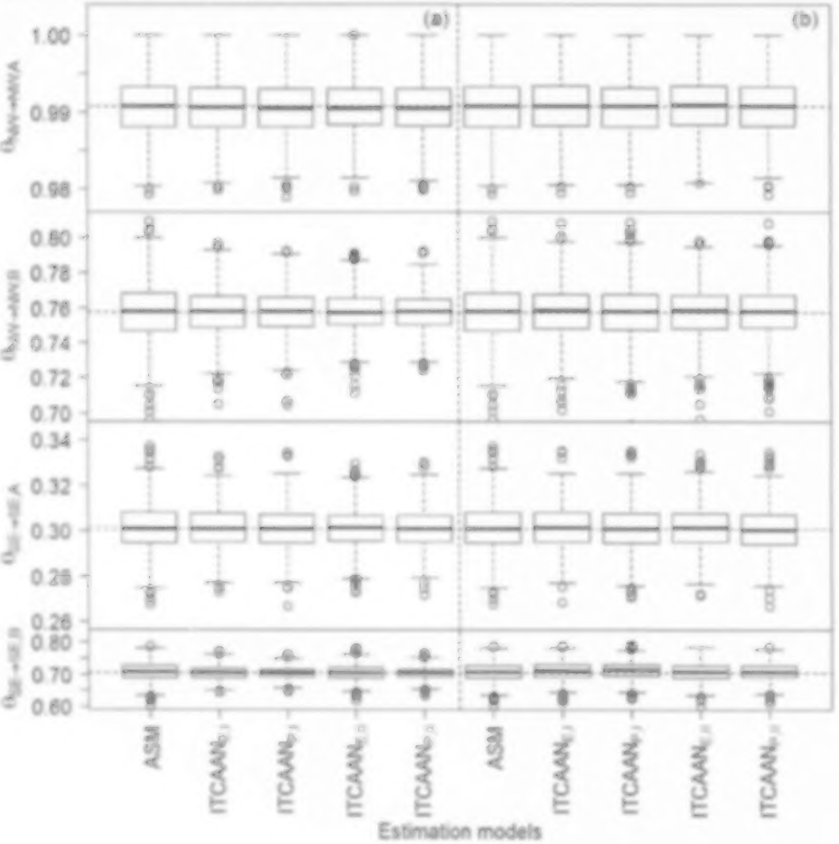

explicit age-structured stock assessment model is primarily reduced variability in population biomass estimates and movement parameters. Even with a small-scale tagging study, there was reduced variability in estimated total and regional biomass with the addition of tagging data. Thus, even if there is a large amount of uncertainty in observed data, the inclusion of tagging data will reduce the uncertainty in stock assessment estimates of biomass that are subsequently used for fishery management.

Variability was generally smaller in the movement parameter estimates when tagging data were included into the stock assessment model. When the movement parameter was near one (99%), however, variability was not affected, as shown with the movement parameter estimated after fishing season A in the NW region (which is actually the probability of staying in the NW region). For all other movement parameters, variability decreased when tagging data was used. We found that the number of years available for tag-return data also influenced variability in the movement parameters. The differences in movement parameter variability when considering the length of tag-return data were more evident when uncertainty was low in the tag-recovery data. When uncertainty in the tag-recovery data was larger, there was not a substantial improvement in movement parameter variability. Thus, the variability in the movement parameters decreased as the time series of tag data increased, but the magnitude of improvement in movement parameter variability depended on the uncertainty in the tag-recovery data and the tag-release protocol.

Releasing tags evenly between regions provided the largest reduction in movement parameter variability. When tagging proportionally to the BTS survey catch, we found that the variability in movement parameters was not largely affected by the number of years for which tag-recovery data were available. However, variability in movement parameters was reduced when tagging evenly between regions as the number of years for which tagging data sets were available increased. Thus, we found that it is better to release tags evenly among regions rather than proportionally to abundance in this example. However, in this study, we considered the simplified case in which complete mixing of tagged and nontagged fish occurs immediately after the tags were released. Perhaps, the spectrum of movement scenarios was too limited in this simulation; it may be that with alternative movement hypotheses such as random yearly movement, tagging proportionally may result in less uncertainty than tagging evenly. Also, the

Fig. 7. Standard deviations (SD) in movement parameters estimated by ADMB for the ASM and ITCAAN models. Tag-recovery data uncertainty scenario *a* is shown in the left panel, and scenario *b* is shown in the right panel. The box represents the interquartile range from the estimation models, the whiskers (broken vertical lines) represent the 95% confidence interval, and values outside the 95% confidence intervals are shown with open circles. See Fig. 3 or text for movement parameter details and Fig. 4 or text for model details.

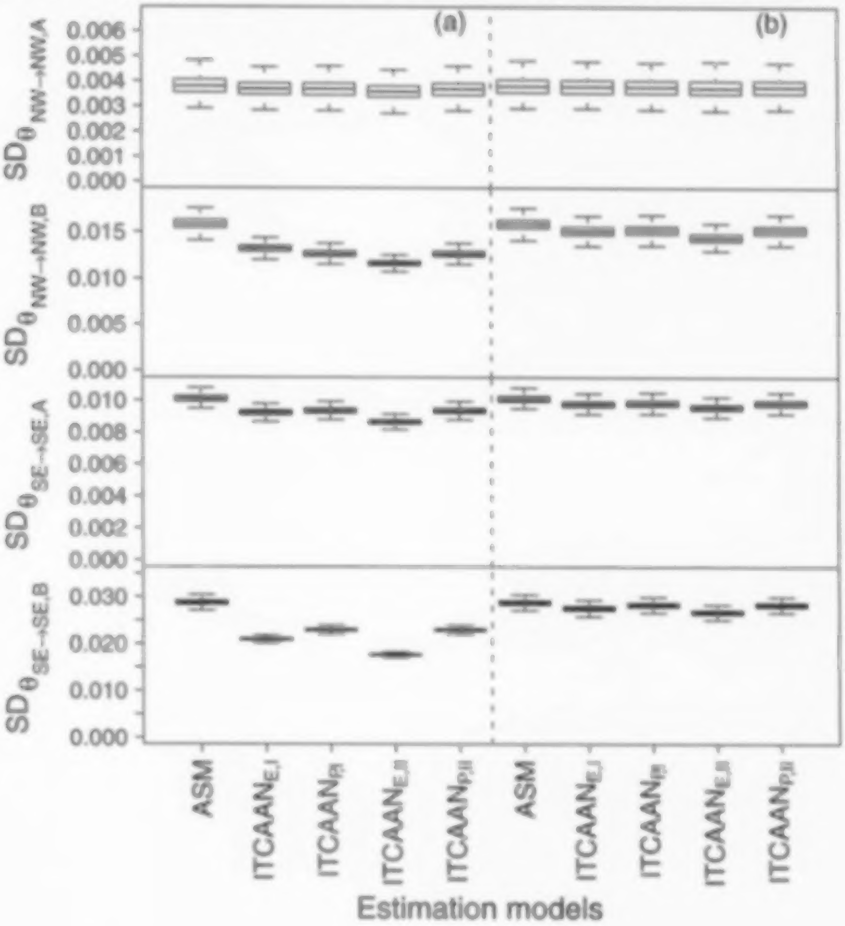

amount of mixing between tagged and untagged fish could identify differences between tag-release protocols, a topic that requires further study. Our model is ideally suited to evaluate alternative experimental designs and protocols.

Pollock migration patterns could vary in the future from historical patterns due to climate change forcing (e.g., Mueter and Litzow 2008). Temperature changes in the Bering Sea can affect pollock distribution between the US and Russian Exclusive Economic Zones and the availability of this species to each fishery. Temperature changes can also affect the timing of pollock migration and the proportion of the stock within the standard EBS survey area when the survey is conducted (Kotwicki et al. 2005). Because the EBS pollock stock migrates further north as Bering Sea temperatures rise, these pollock may be missed in the EBS survey estimates, caught by the Russian fishery, and create management complications when determining the EBS total acceptable biological catch (Ianelli et al. 2001). In this simulation, movement was assumed constant across years. However, because of reduced uncertainty in total and regional biomass estimates when comparing the ASM and ITCAAN models, we hypothesize that tagging data would provide more accurate and precise estimates from stock assessment models when movement is stochastic, a hypothesis that will be tested in future research. If this is the case with tagging data, management decisions would be made with less uncertainty, less likelihood of overharvesting, and potentially higher sustained yields.

Acknowledgements

This work was supported by funding from the Cooperative Institute For Alaska Research (CIFAR) / Alaska Fisheries Science Center (AFSC) and Alaska Sea Grant project R/31-16. We thank Kalei Shotwell for constructing the map shown in Fig. 1. We also thank referee André Punt and two anonymous referees for their helpful comments. The findings and conclusions in this paper are those of the authors and do not necessarily represent the views of the National Marine Fisheries Service, NOAA.

References

Anganuzzi, A. 1996. Some technical issues regarding the study of fisheries interactions. *In* Status of interactions of Pacific Tuna Fisheries in 1995. *Edited by* R. Shomura, J. Majkowski, and R. Harman. FAO Fish. Tech. Paper No. 365. pp. 21–37.

Buckley, T.W., Greig, A., Ianelli, J., Livingston, P., and Walters, G. 2001. Spatial distribution and ontogenetic movement of pollock in the eastern Bering Sea. Poster presented to North Pacific Marine Science Organization (PICES), Alaska Fisheries Science Center, Seattle, Washington.

Efron, B., and Tibshirani, R.J. 1993. An introduction to the Bootstrap. Chapman and Hall, New York.

Fournier, D. 1996. An introduction to AD Model Builder for use in nonlinear modeling and statistics. Otter Research Ltd., Nanaimo, British Columbia.

Fu, C., and Quinn, T.J., II. 2000. Estimability of natural mortality and other population parameters in a length-based model: *Pandalus borealis* in Kachemak Bay, Alaska. Can. J. Fish. Aquat. Sci. **57**(12): 2420–2432. doi:10.1139/cjfas-57-12-2420.

Haist, V. 1998. Integrated catch-age mark–recapture model: applications to B.C. sablefish stocks. *In* Fishery stock assessment models. *Edited by* F. Funk, T.J. Quinn II, J. Heifetz, J.N. Ianelli, J.E. Powers, J.F. Schweigert, P.J. Sullivan, and C.I. Zhang. Alaska Sea Grant Program Report No. AK-SG-98-01, University of Alaska Fairbanks, Fairbanks, Alaska. pp. 469–494.

Hanselman, D., Lunsford, C.R., Fujioka, J.T., and Rodgveller, C.J. 2007. Alaska Sablefish Assessment for 2008. *In* NPFMC Bering Sea, Aleutian Islands and Gulf of Alaska Stock Assessment and Fishery Evaluation Report for 2008. North Pacific Fishery Management Council, Anchorage, Alaska. pp. 195–312.

Heifetz, J., and Fujioka, J. 1991. Movement dynamics of tagged sablefish in the northeastern Pacific. Fish. Res. **11**(3–4): 355–374. doi:10.1016/0165-7836(91)90009-5.

Hilborn, R., and Mangel, M. 1997. The ecological detective: confronting models with data. Princeton University Press, Princeton, New Jersey.

Hilborn, R., and Walters, C. 1992. Quantitative fisheries stock assessment: choice, dynamics, and uncertainty. Chapman and Hall, New York.

Ianelli, J.N., Buckley, T., Honkalehto, T., Williamson, N., and Walters, G. 2001. Bering Sea – Aleutian Islands pollock assessment for 2002. *In* Stock Assessment and Fishery Evaluation Report for the Groundfish Resources of the Bering Sea/Aleutian Islands Regions. North Pacific Fishery Management Council, Anchorage, Alaska. pp. 1–105.

Ianelli, J.N., Barbeaux, S., Walters, G., Honkalehto, T., and Williamson, N. 2009. Eastern Bering Sea pollock stock assessment. *In* Stock assessment and fishery evaluation report for the groundfish resources of the Bering Sea/Aleutian Islands regions. North Pacific Fishery Management Council, Anchorage, Alaska. pp. 47–149.

Kotwicki, S., Buckley, T.W., Honkalehto, T., and Walters, G. 2005. Variation in the distribution of pollock (*Theragra chalcogramma*) with temperature and implications for seasonal migration. Fish. Bull. **103**: 574–587.

Maunder, M. 2001. Integrated Tagging and Catch-at-Age Analysis (ITCAAN): model development and simulation testing. *In* Spatial processes and management of marine populations. *Edited by* G. Kruse, N. Bez, A. Booth, M.W. Dorn, S. Hills, R.N. Lipcius, D. Pelletier, C. Roy, S.J. Smith, and D. Witherell. Alaska Sea Grant College Program No. AK-SG-01–02, University of Alaska, Fairbanks, Alaska. pp. 123–146.

McGarvey, R., Linnane, A.J., Feenstra, J.E., Punt, A.E., and Matthews, J.M. 2010. Integrating recapture-conditioned movement estimation into spatial stock assessment: a south Australian lobster fishery application. Fish. Res. **105**(2): 80–90. doi:10.1016/j.fishres.2010.03.006.

Miller, S. 2007. Estimating movement with a spatially explicit stock assessment model of eastern Bering Sea pollock (*Theragra chalcogramma*). M.S. thesis, School of Fisheries and Ocean Sciences, University of Alaska, Fairbanks, Alaska.

Miller, S., Ianelli, J., and Quinn, T.J., II. 2008. Estimation of age-specific migration in an age-structured model. *In* Resiliency of gadid stocks to fishing and climate change. *Edited by* G. Kruse, K. Drinkwater, J.N. Ianelli, J.S. Link, D.L. Stram, V. Wespestad, and D. Woodby. Alaska Sea Grant College Program Report AK-SG-08-01, University of Alaska, Fairbanks, Alaska. pp. 161–178.

Mueter, F.J., and Litzow, M.A. 2008. Sea ice retreat alters the biogeography of the Bering Sea continental shelf. Ecol. Appl. **18**(2): 309–320. doi:10.1890/07-0564.1. PMID:18488598.

National Research Council. 1998. Improving fish stock assessments. National Academy Press, Washington, D.C.

Natural Resources Consultants, Inc., and Northwest Marine Technology, Inc. 1996. Feasibility of tagging pollock, *Theragra chalcogramma*, with coded wire tags. NMFS Report prepared for Marine Resources Management Center and Resource Ecology and Fisheries Management Division, 7600 Sand Point Way N.E., Seattle, WA 98115, USA.

Punt, A., Pribac, F., Walker, T.I., Taylor, B.L., and Prince, J.D. 2000. Stock assessment of school shark, *Galeorhinus galeus*, based on a spatially explicit population dynamics model. Mar. Freshw. Res. **51**(3): 205–220. doi:10.1071/MF99124.

Quinn, T.J., II, and Deriso, R. 1999. Quantitative fish dynamics. Oxford University Press, Inc., New York.

R Development Core Team. 2008. R: a language and environment for statistical computing. R Foundation for Statistical Computing, Vienna, Austria.

Tuck, G., and Possingham, H. 1994. Optimal harvesting strategies for a metapopulation. Bull. Math. Biol. **56**(1): 107–127.

Winter, A., Foy, R.J., and Trussell, M. 2007. Factors influencing the mortality of tagged pollock captures using a trawl net. North Pacific Research Board Project 506 Final Report. Available at http://doc.nprb.org/web/05_prjs/506_final_report.pdf.

A model for estimating mortality of Atlantic salmon, *Salmo salar*, between spawning events

P. Bradford Hubley and A. Jamie F. Gibson

Abstract: We developed a Bayesian hierarchical model to estimate annual mortality of repeat-spawning Atlantic salmon, *Salmo salar*, that distinguishes between mortality rates and the confounding effects of consecutive-year and alternate-year repeat-spawning strategies. The model provides annual estimates of two mortality rates: mortality in the first year (Z1), a time period during which salmon are primarily in freshwater (staging, spawning, and overwintering) followed by a brief period at sea, and mortality in the second year (Z2) when salmon are predominantly at sea. When fit to data for the LaHave River (Nova Scotia, Canada) salmon population, Z1 showed an increasing trend throughout the time series, whereas Z2 also increased but in a single, stepwise manner. Once a time series of mortality rates was separated from the other life-history parameters, we were able to demonstrate how they could be used for examining the influence of environmental conditions by comparing the estimated mortality rate time series with the North Atlantic Oscillation Index (NAOI). This comparison uncovered a statistically significant correlation between the NAOI and the survival in the second year after spawning that would not have been evident had the mortality estimation model not been developed.

Résumé : Nous mettons au point un modèle hiérarchique bayésien afin d'estimer la mortalité annuelle chez le saumon atlantique, *Salmo salar*, itéropare qui distingue entre les taux de mortalité et les effets confondants des stratégies de fraie aux années consécutives ou aux deux ans. Le modèle fournit des estimations annuelles de deux taux de mortalité, la mortalité durant la première année (Z1), une période de temps pendant laquelle les saumons sont surtout en eau douce (halte migratoire, fraie et hivernage) suivie par une courte période en mer, et la mortalité durant la seconde année (Z2) pendant laquelle les saumons sont surtout en mer. Lorsque le modèle est ajusté à des données provenant de la population de saumons de la rivière LaHave (Nouvelle-Écosse, Canada), Z1 suit une tendance croissante dans la série chronologique, alors que Z2 augmente aussi, mais en un seul palier. Une fois qu'une série chronologique de taux de mortalité est séparée des autres variables du cycle biologique, nous avons pu démontrer comment ces taux de mortalité peuvent servir à examiner l'influence des conditions environnementales en comparant la série chronologique des taux de mortalité et l'indice de l'oscillation nord-atlantique (NAOI). Cette comparaison a révélé une corrélation statistiquement significative entre le NAOI et la survie dans la seconde année après la fraie qui n'aurait pas été évidente sans la mise au point du modèle d'estimation de la mortalité.

[Traduit par la Rédaction]

Introduction

Widespread declines in Atlantic salmon (*Salmo salar*) abundance in North America have not abated since the closure of the commercial fisheries (Friedland et al. 2003*a*; Gibson et al. 2006; International Council for the Exploration of the Sea (ICES) 2008). Identification and investigation of potential sources of mortality affecting various life stages are important steps in developing strategies to reverse the declines. Research into present-day population dynamics suggests that low at-sea survival is one of the main factors currently limiting recovery (Jonsson and Jonsson 2004*a*; Friedland et al. 2009; Gibson et al. 2009). Salmon survival at sea could be impacted by ecological conditions, e.g., a trophic cascade caused by the removal of top predators in the ecosystem (Frank et al. 2005), or environmental changes, e.g., decreasing primary production in northern latitudes associated with increasing sea-surface temperatures (Gregg et al. 2003). Adaptation may prove challenging for migrating Atlantic salmon during critical phases, especially if migration triggers are not synchronized with changing oceanographic conditions (Friedland et al. 2003*a*). Although mortality of Atlantic salmon in the marine phase has certainly increased since 1990, the specific mechanisms responsible for this have yet to be determined (Friedland et al. 2003*a*; Trzcinski et al. 2004; Todd et al. 2008).

To date, research on survival has fallen into two different categories: field programs and time series analysis. Field programs such as those that employ acoustic telemetry (e.g., Lacroix et al. 2005; Hubley et al. 2008; Welch et al. 2009) attempt to measure survival directly and relate it to local environmental conditions. These methods provide detailed in-

Received 10 September 2010. Accepted 28 April 2011. Published at www.nrcresearchpress.com/cjfas on 6 September 2011.
J22010

Paper handled by Associate Editor Bror Jonsson.

P.B. Hubley and A.J.F. Gibson. Department of Fisheries and Oceans, Science Branch, Population Ecology Division, Bedford Institute of Oceanography, P.O. Box 1006, Dartmouth, NS B2Y 4A2, Canada.

Corresponding author: Brad Hubley (e-mail: Brad.Hubley@dfo-mpo.gc.ca).

Can. J. Fish. Aquat. Sci. **68**: 1635–1650 (2011) doi:10.1139/F2011-074 Published by NRC Research Press

formation for specific times and places and are useful for identifying life stages when mortality is high and thus where mitigative measures might best be focused. The alternative method, comparison of historical abundance and growth time series with environmental indicators (e.g., Friedland et al. 2003*b*, 2005, 2009), provides information on how conditions have changed over time and are therefore useful for identifying the reasons for the decline in abundance. Unfortunately, time series analyses have been hampered by the lack of an index of mortality that is not confounded with other variables. Indices such as commercial landings and return rates are compromised by differing life-history strategies and mortality occurring in freshwater. It is therefore important to develop methods for producing direct estimates of age- or stage-specific annual mortality rates that can be compared with relevant environmental variables to best evaluate potential causes for the decline in survival.

Most research on at-sea survival of Atlantic salmon has been focused on survival between the time when smolts leave the river and when they first return to spawn as adults (Friedland et al. 1993, 2000; Jonsson et al. 2003). Although smolt abundance and adult return data series are available for many Atlantic salmon populations, the return rates (the proportion of smolt returning as adults) cannot directly be interpreted as mortality rates because salmon may mature after one, two, or three or more years at sea such that survival and the proportion maturing at age are confounded. One method for separating survival from the maturity probability is to use the ratio method, a variation of the Murphy method (Murphy 1952), in which the contrast in spawning strategies between males and females is used to estimate survival based on the assumption that the survival of males and females is the same (Ricker 1975). The ratio method has been used to estimate marine survival of farmed Atlantic salmon in Iceland (Jonasson et al. 1994) and of post-smolts in eastern Canada (Chaput et al. 2003). However, studies that use the contrast in age at maturity between the sexes to estimate survival from smolt to first spawning rely on having accurate estimates of smolt abundance, which can be difficult to obtain, as well as information on the sex ratios of smolts, which is not typically collected. The ratio method is very sensitive to bias in the sex ratio and is sensitive to random error in the data, especially when the sample size is small (Chaput et al. 2003), making it difficult to draw strong conclusions from these types of analyses when working with smolts. Previous analyses using this method have sometimes produced nonsensical results, i.e., survival fractions greater than one or less than zero (Ricker 1976; Jonasson et al. 1994). In these instances, the approach was generally to disregard nonsensical values and rely on large sample sizes or average results from a number of analyses (Ricker 1976; Jonasson et al. 1994).

Atlantic salmon are iteroparous, and survival of adult salmon between spawning events is another variable that could be informative about the causes of declines in abundance. However, repeat-spawning salmon can utilize either of two different life-history strategies: consecutive-year spawning (those that spawn each year after maturing) and alternate-year spawning (those that skip a year between spawning events). Here again, the proportion that return to spawn a second time cannot be directly interpreted as a survival rate because of the confounding effect of life-history strategy (whether to spawn in consecutive or alternate years).

In this study, our overall objective was to develop a model for estimating the mortality rate of adult salmon between spawning events that would remove the confounding effects of variable life-history strategies. As described below, we developed a Bayesian hierarchical model that allows for the incorporation of prior information and can be structured in such a way as to facilitate the integration of information across the data set. With the ratio method as a basis for our Bayesian analyses, we were able to address some problems identified when estimating mortality rates without accounting for variability in the process. Hierarchical structures have been found to be effective in improving inferences from models (Rivot and Prévost 2002). Particularly, Bayesian state–space models, structured around the stages of Atlantic salmon life history, have proven useful for evaluating different hypotheses regarding smolt-to-spawner return rates (Rivot et al. 2004). The Bayesian approach confines the estimates to the realm of plausibility by placing appropriate limits on the probability of consecutive spawning and on mortality parameters. Similarly, our approach incorporates realistic life-cycle transitions in a probabilistic framework. We developed and tested the model using Atlantic salmon data from the LaHave River, Nova Scotia, Canada. By utilizing a Bayesian hierarchical structure in a model in which the ratio method is implicit, we were able to produce a 29-year time series of mortality rate estimates for adult Atlantic salmon for both their first and second years after spawning. We then compared the time series of mortality rates with the North Atlantic Oscillation Index (NAOI) to examine the influence of environmental conditions on survival. The purpose of this comparison is to demonstrate how direct estimates of mortality are better for evaluating the impact of environmental factors on survival than measures of abundance, which are confounded with other variables.

Materials and methods

Study population

We used data from the Atlantic salmon population in the LaHave River, Nova Scotia, Canada (44°23′54″N, 64°32′34″W), from 1979 to 2008 to develop and test this model. Adult salmon are enumerated as they ascend a fish ladder bypassing Morgans Falls, a natural barrier on this river. After ascending the fishway, the fish enter a trap where they are sampled before being released above the falls. Sampling includes the collection of the weight, length, and sex of individual fish, as well as the collection of a scale sample from which the age of the fish is determined. Although fish may pass back down over the falls after passing through the fishway, they cannot get above the falls without being counted. To prevent fish from being double-counted, all sampled fish are marked to identify them in case they pass over the falls and re-ascend. Therefore, the count is considered to be a total census of the number of salmon returning to this location.

The status of Atlantic salmon in the LaHave River (above Morgans Falls) is one of the two main indicators of the status of Atlantic salmon populations along Nova Scotia's mainland Atlantic coast (Amiro et al. 2006). Abundance in this popula-

Fig. 1. Time series of the abundance of spawning Atlantic salmon (*Salmo salar*) as they passed through Morgan Falls fishway, LaHave River, Nova Scotia, Canada. Spawners are grouped by sex (male, △; female, ○) and those spawning after (*a*) one or (*b*) two winters at sea or (*c*) after an earlier spawning.

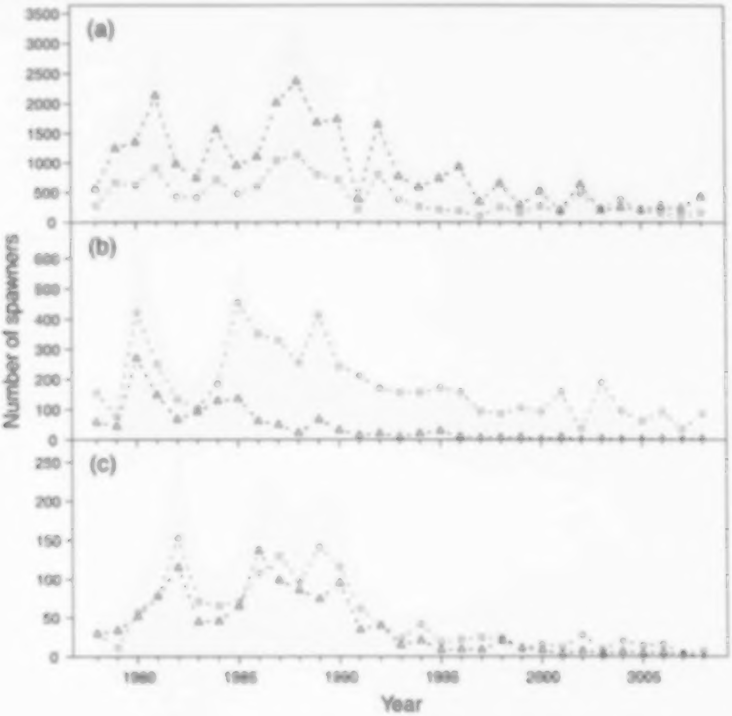

tion has declined from just under 4000 adult salmon in 1988 to 220 in 2009 (Fisheries and Oceans Canada 2010). The proportion of repeat spawners in the spawning run has fallen from 6.5% to 3% between the periods 1979–1992 and 1993–2008 (Fig. 1), potentially indicative of an increase in the mortality rate of adult salmon during this period. This change is of concern because, despite the fact that repeat spawners make up only a small proportion of the annual spawning run, their higher fecundity means that they contributed, on average, more than 15% of the total egg production prior to 1992 (determined from the fecundity equation in Amiro et al. 1996).

The age structure of the spawning Atlantic salmon population can be very complex, comprising different smolt ages, sea ages, and repeat spawners (Fig. 2). The presence of various age types in the spawning population, which is indicative of different life-history strategies, maximizes genetic diversity and enhances population stability (O'Connell et al. 2006). In the LaHave River, the spawning run consists primarily (81%) of salmon that mature after one winter at sea (1SW) and of salmon (13%) that spend two winters at sea (2SW) before spawning for the first time. Similar to many salmon populations, maturity schedules for LaHave River salmon differ between sexes: 2SW salmon are mostly female (80%) and 1SW salmon are mostly male (67%). The remainder of the spawning run consists of repeat spawners, for which there are also two different life-history strategies: consecutive-year and alternate-year spawning. After spawning in the fall, a large (but unknown) proportion of the population overwinters in freshwater and returns to the ocean in the spring. Consecutive spawners are characterized as having a short reconditioning period after returning to the ocean, typically 2 to 3 months in the marine environment. Alternate spawners have a longer reconditioning period, not returning to spawn until after approximately 14 months in the marine environment. In the LaHave River, the alternate-year spawning strategy is more common and provides a significant advantage over the consecutive-year spawning strategy in terms of growth because of the extended period spent in the marine environment. We used the numbers of 1SW and 2SW salmon spawning for the first and second times in these analyses; salmon spawning three or more times were not included in the analysis.

A proportion of the adult population in this study originated from hatchery-reared smolts. Progeny of adults captured at Morgans Falls were raised in a nearby hatchery facility for one and a half years and released as smolts in May. Although return rates of hatchery-origin smolts to spawning adults are much lower than for wild-origin smolts, hatchery-origin repeat spawners have successfully completed a previous marine–spawning migration and thus have been exposed to natural selection pressures. We found no significant differences in the return rates of hatchery-origin versus wild-origin repeat spawners from 1981 to 2000 in the LaHave River (Wilcoxon test, $p > 0.1$). We therefore included both hatchery- and wild-origin fish in our analysis, which substantially increased our sample size and statistical power.

Fig. 2. (*a*) Annual and (*b*) seasonal spawning schedules for the different age types of Atlantic salmon (*Salmo salar*) from the LaHave River, Nova Scotia, Canada. Labels indicate different spawning strategies (consecutive year (C) or alternate year (A)) and ages at maturity (1 sea winter (G) or 2 sea winters (S)). The colors of the lines in both panels represent various mortality parameters: immature mortality (purple), first-year mature mortality or Z1 (red), and second-year mature mortality or Z2 (green). The sizes of the fish in the upper panel are relative to the average size at a given age, and the arrowheads in the lower panel represent the median count date at the Morgans Falls fishway.

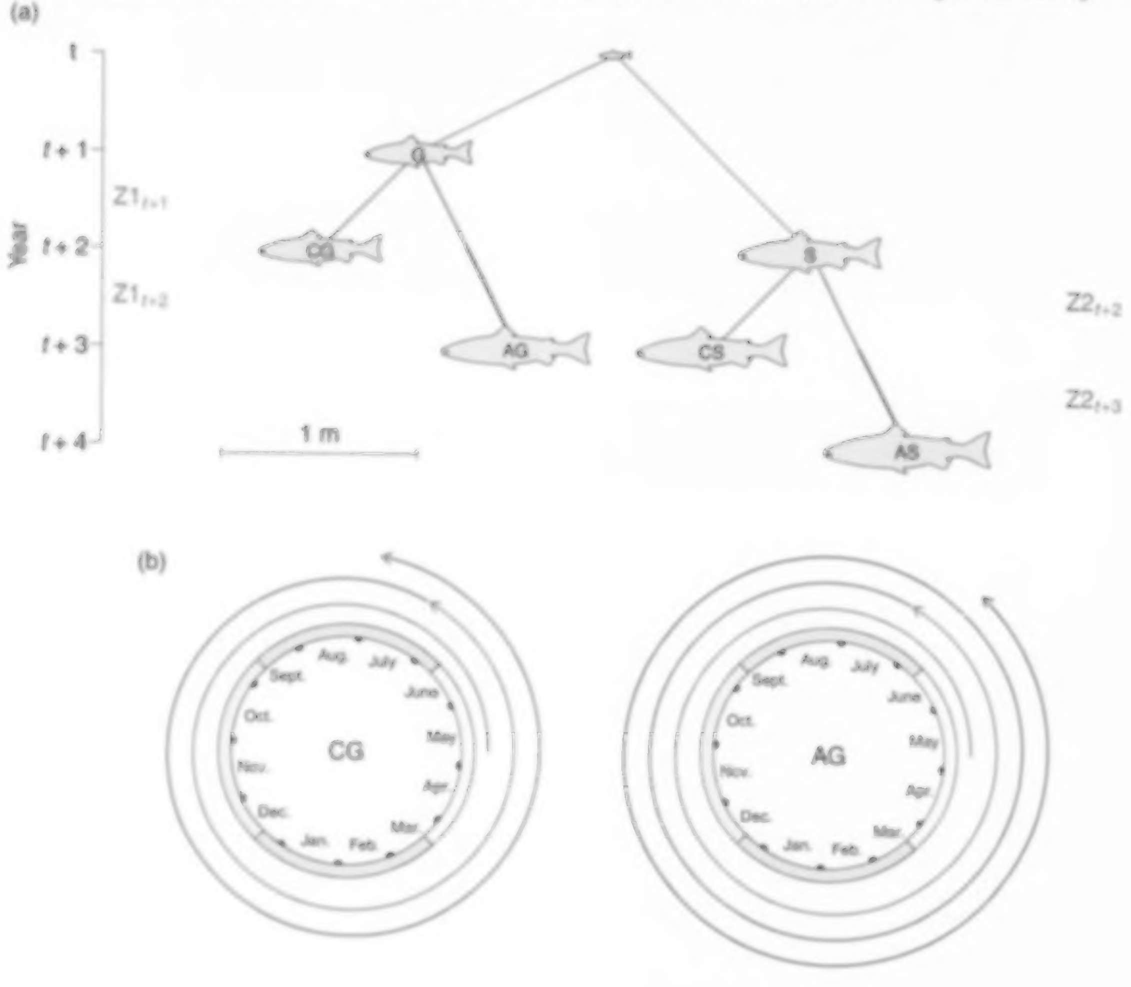

Interpretation of the mortality parameters

In the analyses that follow, the mortality rate of adult fish is divided into two parts: the first-year (Z1) and the second-year (Z2) instantaneous mortality rate. Because fish are enumerated as they ascend the fish ladder prior to spawning, Z1 occurs in the year following the summer spawning migration and includes mortality associated with staging prior to spawning, spawning during the fall, overwintering in freshwater, returning to sea after the spring melt, spending a couple of months in the marine environment, and, in the case of consecutive spawners, migrating upstream to spawn a second time (Fig. 2). The other parameter, Z2, applies only to alternate-year spawners and quantifies mortality associated with spending an extra year in the marine environment, as well as that during the short upstream migration in early summer prior to spawning the second time (Fig. 2).

Ratio method

We initially attempted to apply the ratio method to the adult count data from the LaHave River to estimate survival of previous spawners in the second year at sea. Underlying the ratio method are the mortality equations for the two different spawning strategies, i.e., the number (*N*) of consecutive (C) and alternate (A) repeat spawners in a given year (*t*) as a function of the number (*N*) of first-time spawners (V) in year *t* – 1, the probability of consecutive spawning (*p*), and the subsequent mortality rates (Z1 and Z2).

$$N_{\mathrm{C},t+1} = N_{\mathrm{V},t}p_t\mathrm{e}^{-Z1_t} \tag{1}$$

$$N_{\mathrm{A},t+2} = N_{\mathrm{V},t}(1 - p_t)\mathrm{e}^{-(Z1_t+Z2_{t+1})} \tag{2}$$

Fig. 3. Box plots showing the return rates of repeat-spawning Atlantic salmon (*Salmo salar*) from the LaHave River, Nova Scotia, Canada. The rates are given for every combination of spawning strategy (consecutive (C) or alternate (A)), sex (male (M) or female (F)), and age at maturity (one sea winter (G) or two sea winters (S)). Outliers (○) are those points that exceed the median by 1.5 times the interquartile range.

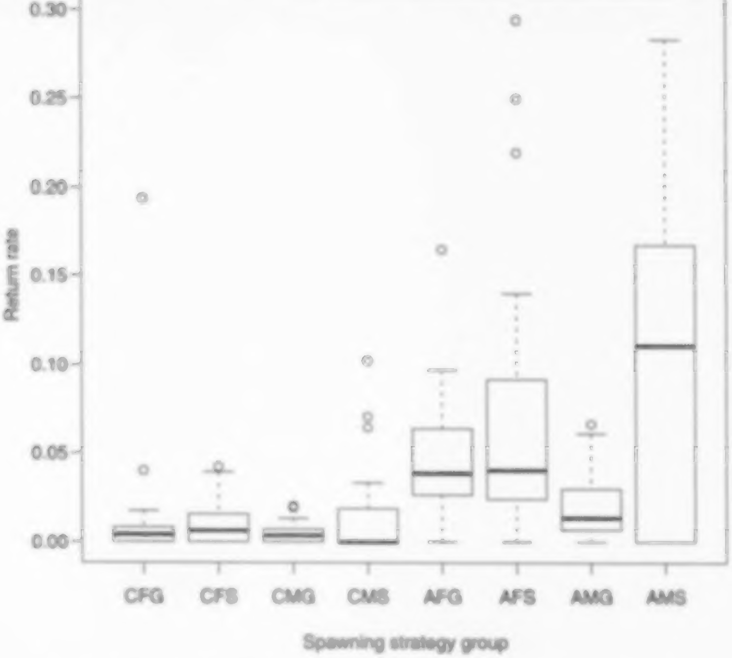

Assuming that mortality rates are the same for males (M) and females (F), an analytical solution for survival in the second year ($S2$) can be found by combining the mortality equations (eqs. 1 and 2) for both sexes (see Appendix A).

$$(3)\qquad S2 = \frac{N_{\mathrm{V,M}}N_{\mathrm{A,F}} - N_{\mathrm{V,F}}N_{\mathrm{A,M}}}{N_{\mathrm{V,F}}N_{\mathrm{C,M}} - N_{\mathrm{V,M}}N_{\mathrm{C,F}}}$$

The method requires that there are contrasting spawning schedules for the two groups in the ratio (i.e., the number of male 1SW > the number of female 1SW and the number of male 2SW < the number of female 2SW). A key assumption of the model is that mortality rates are the same for both sex groups and for both maturing and nonmaturing salmon during the first year at sea. However, some studies suggest that the assumptions of equal mortality between sex and age-at-maturity groups may not always hold (Jonsson et al. 1991*a*; Fleming 1998).

Our attempts to apply the ratio method (eq. 3) to LaHave River adult salmon produced nonsensical results. We tested different groups for calculating ratios such as sex (male to female) and smolt age (2 to 3). For previous spawners, there was little contrast in the repeat-spawning schedule of these groups and most survival estimates were impossible, with only 4% of values for $S2$ falling between 0 and 1. To avoid these problems, we estimated mortality within a Bayesian hierarchical structure using a variant of the ratio method as the predictive component of the model. This approach also allows for accounting for the uncertainties and process variability in the mortality equations

Mortality estimation model

The mortality equations (eqs. 1 and 2) that form the basis of the ratio method were fit to the data using a Bayesian approach with the appropriate limits placed on the parameters to eliminate the possibility of nonsense values and to incorporate an error structure in the process. By setting up equations with different groups and shared parameters, the ratio method becomes implicit within the model. For the purposes of grouping, the population was divided by sex (male (M) or female (F)) and age at maturity (1SW (G) or 2SW (S)).

An assumption of the ratio method is that the mortality rates are similar in the first year after spawning for both consecutive and alternate spawners and between groups. Hubley et al. (2008) demonstrated that these fish are found together at least until May (only two months prior to the spawning run), which supports the assumption for similar mortality rates among consecutive and alternate spawners up to this point. However, a two-month period remains during which, for at least some of this time, these fish are not found together and may experience differing mortality rates. This assumption is a necessary one in this case, so until future research can quantify the differences in mortality between consecutive and alternate spawners in the last two months of the first year, we must assume that these differences are negligible when compared with mortality of the previous 10 months of the first year and the following 12 months of the second year. Despite a G test (Sokal and Rohlf 2003) that did not reveal any significant differences ($p > 0.1$), an exploratory analysis of the return rates between sex and age-at-maturity groups suggests that mature 2SW males have

Table 1. Uniform priors and hyperpriors and the resulting posteriors of the parameters and hyperparameters.

	Prior		Posterior	
Parameter	Lower bound	Upper bound	Mean	SD
$Z1$	0	7	—	—
$Z2$	0	7	—	—
ξ_G	0	10	1.56	0.0932
ξ_S	0	10	0.532	0.0929
σ_τ	0	5	0.553	0.0441
$\mu_{p\text{MG}}$	0.001	0.5	0.0733	0.0225
$(\alpha + \beta)^{-1/2}{}_{p\text{MG}}$	0.001	$\sqrt{\mu_{p\text{MG}}}$	0.224	0.00294
$\mu_{p\text{MS}}$	0.001	0.5	0.0345	0.0129
$(\alpha + \beta)^{-1/2}{}_{p\text{MS}}$	0.001	$\sqrt{\mu_{p\text{MS}}}$	0.135	0.0486
$\mu_{p\text{FG}}$	0.001	0.5	0.0330	0.00915
$(\alpha + \beta)^{-1/2}{}_{p\text{FG}}$	0.001	$\sqrt{\mu_{p\text{FG}}}$	0.150	0.0331
$\mu_{p\text{FS}}$	0.001	0.5	0.0580	0.0170
$(\alpha + \beta)^{-1/2}{}_{p\text{FS}}$	0.001	$\sqrt{\mu_{p\text{FS}}}$	0.204	0.0451

Note: $Z1$ and $Z2$, first- and second-year instantaneous mortality rate, respectively; ξ, offset; σ, standard deviation; μ, mean; τ, error term; p, probability of consecutive spawning; M, male; F, female; G, one sea winter; S, two sea winters; α and β, hyperparameters.

lower mortality rates than mature 1SW males and that mature female mortality rates are somewhere in between (Fig. 3). The return rates are not considered synonymous with mortality, but they are an indication that the assumption in the ratio method that mortality rates are equal between groups does not hold. However, by assuming that the mortality rates between groups are at least proportional if not the same, offsets (ξ) can be used to relate mortality in the first year after spawning between groups. Offsets, as multipliers, were initially applied to all mortality parameters, but all except the offsets on $Z1$ for male 1SW (ξ_G) and 2SW (ξ_S) were estimated to be sufficiently close to one to be dropped from the final model. Finally, the ratio method calculations do not incorporate observation or process error. Because the counts are considered a complete census, we did not include observation error but did include an error term (τ) to allow for deviations in the processes described; τ was assumed to be a normally distributed random variable with a mean of zero and an estimated standard deviation (σ_τ) common to all groups (Table 1). Thus the equations for males become

$$N_{\text{M.C.G},t+1} = N_{\text{M.V.G},t}\,p_{\text{M.G},t}\,e^{-Z1_t\xi_G}e^{\tau_t} \tag{4}$$

$$N_{\text{M.A.G},t+2} = N_{\text{M.V.G},t}(1 - p_{\text{M.G},t})e^{-(Z1_t\xi_G + Z2_{t+1})}e^{\tau_t} \tag{5}$$

$$N_{\text{M.C.S},t+1} = N_{\text{M.V.S},t}\,p_{\text{M.S},t}\,e^{-Z1_t\xi_S}e^{\tau_t} \tag{6}$$

$$N_{\text{M.A.S},t+2} = N_{\text{M.V.S},t}(1 - p_{\text{M.S},t})e^{-(Z1_t\xi_S + Z2_{t+1})}e^{\tau_t} \tag{7}$$

and for females become

$$N_{\text{F.C.G},t+1} = N_{\text{F.V.G},t}\,p_{\text{F.G},t}\,e^{-Z1_t}e^{\tau_t} \tag{8}$$

$$N_{\text{F.A.G},t+2} = N_{\text{F.V.G},t}(1 - p_{\text{F.G},t})e^{-(Z1_t + Z2_{t+1})}e^{\tau_t} \tag{9}$$

$$N_{\text{F.C.S},t+1} = N_{\text{F.V.S},t}\,p_{\text{F.S},t}\,e^{-Z1_t}e^{\tau_t} \tag{10}$$

$$N_{\text{F.A.S},t+2} = N_{\text{F.V.S},t}(1 - p_{\text{F.S},t})e^{-(Z1_t + Z2_{t+1})}e^{\tau_t} \tag{11}$$

Bayesian analysis allows for existing information to be formally incorporated into an analysis through prior distributions of model parameters. The prior distributions are combined with information from the data to produce posterior distributions from which the parameter estimates are obtained. When information is lacking or there is uncertainty regarding a particular parameter, uninformative priors are typically used to get a baseline that can be used to evaluate the sensitivity of the model to a more informative prior. A Jeffrey's prior is often used as an uninformative prior because the probability density is conserved even when the parameter in question is transformed. Millar (2002) provides several default (Jeffrey's) priors for common fisheries models. One of these models, the Ricker stock–recruit curve with multiplicative lognormal errors is analogous to the above-mentioned mortality estimation model (eqs. 1, 2), and the derivation of the Jeffrey's prior is presented in detail by Millar (2002). For the Ricker model,

$$R_t = aS_te^{-bS_t}e^{\tau_t}$$

the parameter b is analogous to Z in eqs. 1, 2, 4–11, and a is analogous to p. Therefore, the Jeffery's priors for these parameters are as follows:

$$Z1 \sim \text{Uniform}[0, \infty)$$

$$Z2 \sim \text{Uniform}[0, \infty)$$

$$p \sim \text{Uniform}[0, 1]$$

The probability of consecutive spawning (p) was problematic to parameterize in the model because little is known of it and it is confounded with mortality. Given the lack of information and that other studies suggest that the timing of ma-

Fig. 4. Posteriors of the mean (μ) and standard deviation (σ) for the probability of consecutive spawning (p). There are separate parameters for each sex – age-at-maturity group: (*a*) male – one sea winter, (*b*) male – two sea winters, (*c*) female – one sea winter, and (*d*) female – two sea winters.

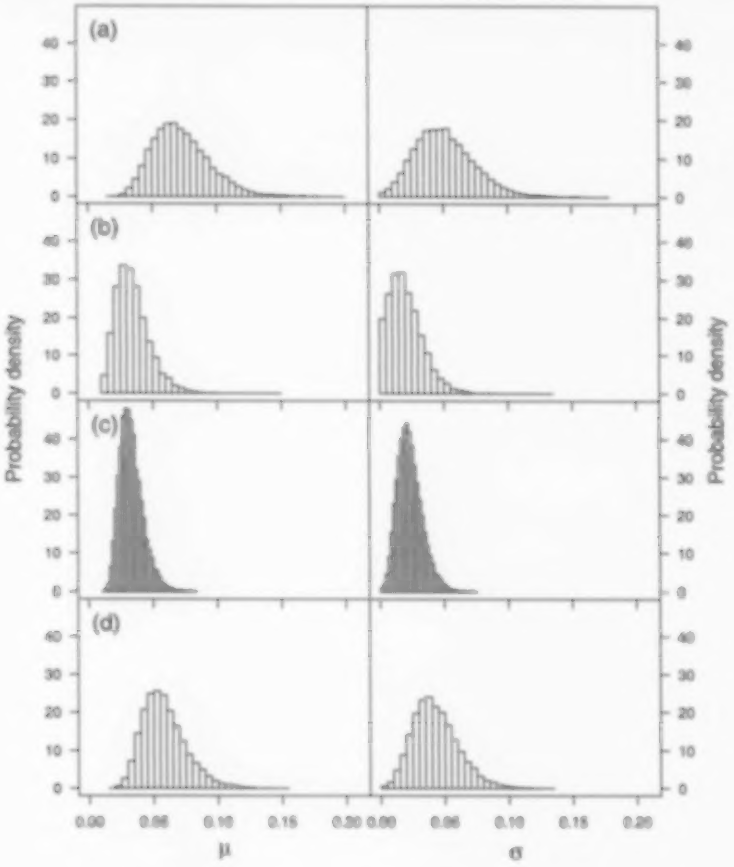

turity in immature salmon is linked to marine environmental variables (Reddin 2006), an annually varying p was desirable. However, a high degree of annual variation in p is unlikely as there are always more alternate spawners than consecutives throughout the time series, which also means that p must be less than 0.5.

When the uniform prior [0, 0.5] was used for p, the parameter estimates varied dramatically within these bounds and were not well estimated in years when sample size was small. As a consequence of this variation, most mortality was attributed to $Z1$, and the modes of the posterior distributions of $Z2$ were often zero. This mathematical solution did not make sense biologically; life-history parameters are unlikely to change dramatically from year to year. Furthermore, mortality in the marine environment is thought to be driving the declines currently being observed in many populations (Friedland et al. 2003*a*; Jonsson and Jonsson 2004*a*), making it highly unlikely that $Z2$ would be near zero. By placing a prior on the probability of consecutive spawning so that an annually varying estimate is drawn from a beta distribution, information from the whole time series can be used to estimate p while still allowing for slight changes from year to year. An uninformative hyperprior density that yields a proper posterior distribution dominated by the likelihood was used for the hyperpriors of the beta distribution (Gelman et al. 2004):

$$p(\alpha, \beta) \propto (\alpha + \beta)^{-5/2}$$

To avoid impropriety of the posterior, Gelman et al. (2004) suggests placing uniform priors on the mean, $\mu = \alpha(\alpha + \beta)^{-1}$ and $(\alpha + \beta)^{-1/2}$, where the upper bound for $(\alpha + \beta)^{-1/2}$ is the square root of the mean:

$$\alpha(\alpha + \beta)^{-1} \sim \mathrm{Uniform}[0.001, 0.5]$$

$$(\alpha + \beta)^{-1/2} \sim \mathrm{Uniform}[0.001, \sqrt{\mu}]$$

$$p_t \sim \mathrm{Beta}(\alpha, \beta)$$

These priors and the bounds selected were designed to restrict p to plausible values and constrain the hyperparameters (α, β) to be greater than 1, thus insuring a finite probability density of the beta prior. This approach yielded proper well-

Fig. 5. Posteriors of the hyperparameters (α, β) of the beta prior for the probability of consecutive spawning (p). Uniform hyperpriors placed on $\alpha(\alpha + \beta)^{-1}$, and $(\alpha + \beta)^{-1/2}$. There are separate hyperparameters for each sex – age-at-maturity group: (*a*) male – one sea winter, (*b*) male – two sea winters, (*c*) female – one sea winter, and (*d*) female – two sea winters.

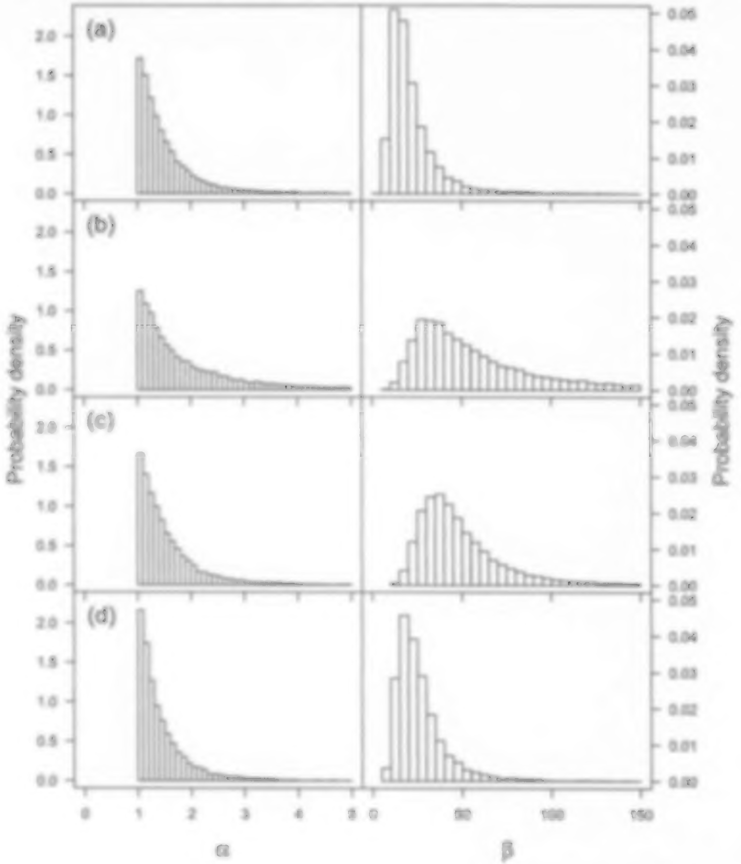

defined posteriors for the mean (μ) and standard deviation (σ) of each p (Fig. 4). Within the model, these estimates were then used to calculate α and β for the beta prior on an annually varying p. The posteriors of α and β show how the parameterization described above restricts α and β to values greater than 1 (Fig. 5).

The final mortality estimation model, with age at maturity and sex as grouping variables, used uninformative uniform priors for the mortality, offsets on the sex-specific mortality rates, and error parameters (Table 1). The hierarchical structure of the model involved beta priors for the annual p parameters derived from the posteriors of the beta hyperparameters α and β (Fig. 5), which had uninformative uniform priors placed on the mean (μ) and $(\alpha + \beta)^{-1/2}$ (Table 1). For the 29-year time series, the model estimated 185 parameters (six annual + 11 fixed) from 348 data points (12 per year). The output parameters of interest are the two vectors of annual estimates of mortality $Z1$ and $Z2$ (58 parameters), the mortality offset parameters that modify $Z1$ for male 1SW and 2SW (two parameters), and to a lesser extent the annual p parameters (116 parameters).

To evaluate how well the model estimates mortality rates, we tested the model on simulated data to see if it was able to recover known parameters. To generate realistic known parameters for our study population, we randomly selected five sets of mortality and p parameters from the posterior estimates of the model fit to the LaHave River data. Each of these sets was used to produce five time series of repeat spawners from a fixed number of virgin spawners (1000 1SW and 300 2SW). The model was then fit to the resulting 25 simulated data sets to evaluate how well the parameters were estimated. The median residuals for the mortality parameters were 0.15 for $Z1$ and 0.30 for $Z2$. In nearly all of the runs, the model estimated the known parameters within the expected margin of error (i.e., 23 of 29 known parameters fell within the 80% credible interval of their estimate, and 28 of 29 known parameters fell within the 95% credible interval of their estimate).

The model was fit with the WinBUGS software package (version 1.4; Lunn et al. 2000) using Markov chain Monte Carlo (MCMC) integration via Gibbs sampling. To be assured that convergence was reached in the model, two MCMC chains were initiated performing 150 000 iterations with only every 10th iteration sampled and the first 75 000 discarded. The potential scale reduction factor was monitored for each parameter and all were sufficiently close to one (Brooks and

Fig. 6. Fitted (–) versus observed (○) Atlantic salmon (*Salmo salar*) repeat-spawner abundance (*N*) from the LaHave River, Nova Scotia, Canada, presented on the log scale. The broken line is the 95% credible interval of the fitted abundance. Consecutive (C) and alternate (A) spawners are grouped by sex (male (M) or female (F)) and age at maturity (one sea winter (G) or two sea winters (S)).

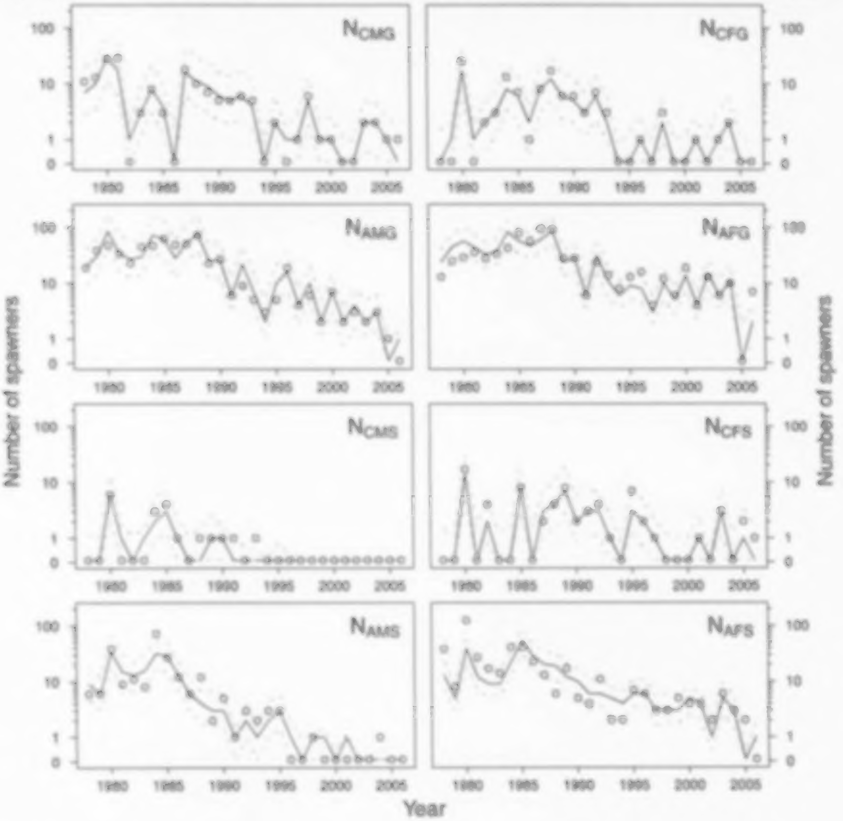

Gelman 1998). Autocorrelation of the MCMC samples for the first 40 lags was very small, ranging from –0.0311 to 0.0392 across all parameters.

We also compared the annual first- and second-year mortality estimates with the winter NAOI (Hurrell 1995), in part to provide evidence that the model does estimate mortality and in part as a preliminary look at the relationship between environmental conditions and mortality of salmon. The NAOI is a strong indicator of ocean climate in the North Atlantic (Dickson and Turrell 2000) that has been shown to correlate with growth and age at maturity in Atlantic salmon in Europe (Jonsson and Jonsson 2004*b*). In our correlation analysis using Pearson product-moment correlation, we accounted for autocorrelation by adjusting the effective degrees of freedom as suggested by Pyper and Peterman (1998). This approach has been used in similar analyses to correct for autocorrelation in comparisons of salmon abundance and environmental variables (Friedland et al. 2009).

Results

Overall, the predicted numbers of repeat spawners appear to be an appropriate fit to the observed data and capture the declining trend in abundance of each group (Fig. 6). The results indicate more clearly what was suspected from the return rates, different survival rates for each sex (Fig. 7). Based on the median of the posterior distributions for ξ_G and ξ_S (Fig. 7), the instantaneous mortality rate of male 1SW salmon ($Z1_{G,M}$) is 1.56 times that of female 1SW salmon ($Z1_{G,F}$), and the mortality rate of male 2SW salmon ($Z1_{S,M}$) is 0.525 times that of female 2SW salmon ($Z1_{S,F}$). For example, according to the parameter estimates from the model, if 20% of 1SW females survived the first year after the spawning migration, survival of male 1SW salmon would only be 8%; if 20% of 2SW females survived, survival of male 2SW salmon would be 43%. There is strong evidence from the model that the mortality offsets represent a real difference in mortality rates between the sexes at different ages. First, the resulting posterior distributions (Fig. 7) are well defined, indicating that the data are informative with respect to these parameters. Second, the ranges of the posteriors do not include 1 (which would indicate no difference in survival), even though the model used a uniform prior including a mortality offset of 1. As a consequence, the skewed sex ratios in first-time spawners, where more 1SW salmon are male and more 2SW salmon are female, are less pronounced in repeat spawners.

Although the hierarchical structure of the model allowed for annual variation in *p*, estimates were constantly low, and there did not appear to be any trend between the groups (Fig. 8). Median values of the annual estimates in all groups

Fig. 7. Posterior probability distributions of the mortality offset parameter (ξ) for (*a*) male one sea winter and (*b*) two sea winters Atlantic salmon (*Salmo salar*) relative to mortality of females from the LaHave River, Nova Scotia, Canada. The vertical dotted line shows an offset of 1, which would indicate no difference in survival.

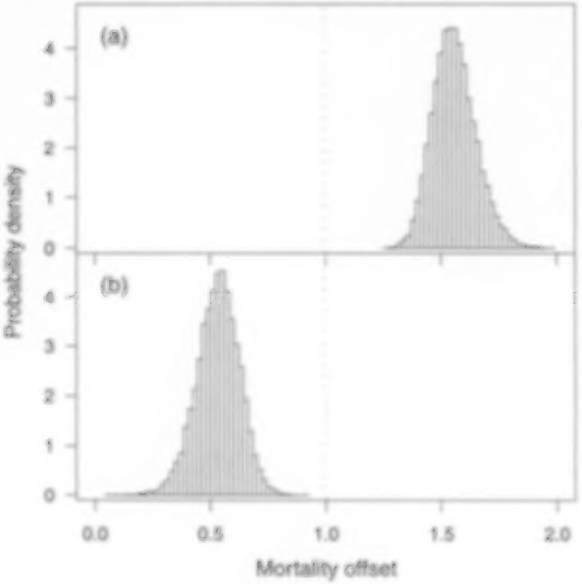

ranged from 0.00203 to 0.167, and there was little difference in the p when comparing the mean from three 10-year periods (Table 2). The probability distributions estimated in the model have a higher mean and variance for male 1SW salmon and female 2SW salmon than for female 1SW salmon and male 2SW salmon (Fig. 4). Estimates of p for male 2SW salmon after 1994 show little annual variation because no consecutive male 1SW salmon have been observed since 1994. When there is little information for p in a given year, the hierarchical structure of the model ensures that the annual p will reflect the prior for p, which is similar to an average for all years.

Estimates for both $Z1$ and $Z2$ have increased since the 1980s (Fig. 9). Although the magnitudes of $Z1$ are different among groups, note that an identical trend is a model assumption. The average annual mortality rate for all mature salmon groups is substantially higher in the last 10 years than in the first 10 years of the time series (Table 2). The trend in $Z1$ has been a consistent increase, with spikes of relatively high mortality rates occurring in 1995, 2003, and 2007 (Table 2; Fig. 9). The years that experienced the lowest mortality rates in each decade are 1981, 1992, and 2004 (Fig. 9). An increasing trend is also exhibited by $Z2$, but it appears to be more cyclical in nature, showing a decline in the 1980s, followed by a increase in the early 1990s, and remaining relatively high during the late 1990s until 2002 (Fig. 9). After 2001, $Z2$ was highly variable, and almost all salmon were estimated to have died in their second year in 2007. Overall, the annual mortality rate of mature salmon in their first year ($M1 = 1 - e^{-Z1}$) has increased gradually over the time series. In contrast, the average annual mortality rate in the second year at sea ($M2 = 1 - e^{-Z2}$) is much higher in the 1990s and 2000s than it was in the 1980s (with the exception of the year 2007) but does not appear to have increased during the 1990s and 2000s (Table 2).

The estimates of $M2$ from this model are correlated with the NAOI from the winter period (Fig. 10). A positive NAOI is associated with higher mortality rates, whereas lower mortality rates tend to occur when the NAOI is negative, a relationship that is statistically significant. The trends match quite closely until 2000, after which the highly variable mortality rates do not correspond well with the NAOI. However, the direction of change from the previous year remains the same in both $M2$ and NAOI since 2003. Based on the correlation with the NAOI until 2000 (Table 3), the annual mortality rate of salmon in the marine environment increases by 0.036 when the NAOI increases by one.

In contrast with the pattern observed for $M2$, the estimates of $M1$, which includes a significant period of freshwater residency, were not correlated with the NAOI (Fig. 10; Table 3). Additionally, no significant correlations were found between the NAOI and the return rates for 1SW or 2SW salmon of either sex (Table 3).

Discussion

In this paper, we presented a model for separating variability in repeat-spawning life-history strategies from the mortality rates of adult Atlantic salmon. Although the previously used ratio method is implicit within the model, the approach presented here is considerably more flexible than the direct calculation and allows for model assumptions to be explicitly evaluated. Our final model included a relaxation of the ratio model assumption of identical mortality rates for each life-history group to an assumption of a similar trend in mortality among groups. As a statistical model, it provides estimates of the uncertainty associated with the resulting parameter estimates in the form of posterior probability densities. As a Bayesian model, hierarchical structures can be used to share or borrow information among years. A hierarchical structure on the p_i parameters in the final model allowed for annual variation in each group's p and constrained its value in years when data were limited. When fit to data for LaHave River salmon, the resulting parameter estimates were all biologically plausible, which is often not the case when the mortality rates are calculated directly from smolt to adult data using the ratio method (Ricker 1976; Jonasson et al. 1994). The resulting mortality rate time series from the LaHave River indicate differing trends in the survival in the first and second years after spawning and show a relationship between mortality in the second year and a climate index that would not have been as evident without this model.

Separating spawners by both sex and age at maturity revealed some interesting biological aspects of salmon life history that might have been hidden had the groups been combined. The difference in survival of males in the first year revealed by the mortality offset parameters (ξ_G and ξ_S) could be related to breeding behaviour. With a biased sex ratio towards males common in many salmonids species, male competition for mates is intense (Fleming 1996, 1998) and fighting behaviour probably contributes to greater mortality in males than females during spawning (Jonsson and Jonsson 2003). This may be a contributing factor to male mortality

Fig. 8. Model estimates of the probability of consecutive spawning (p) for repeat-spawning Atlantic salmon (*Salmo salar*) from the LaHave River, Nova Scotia, Canada. The left column panels show the annual probabilities, with broken lines representing the 80% credible intervals. The right column panels show the priors for p resulting from an uninformative hyperprior on the hyperparamters of the beta distribution. There are different p parameters for each sex – age-at-maturity group: (*a*) male – one sea winter, (*b*) male – two sea winters, (*c*) female – one sea winter, and (*d*) female – two sea winters.

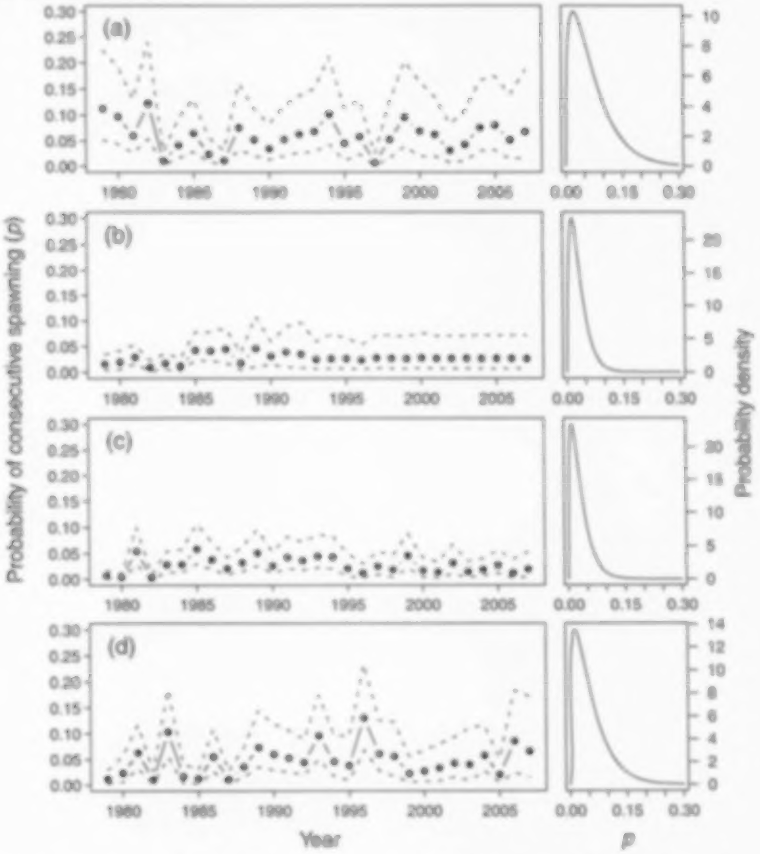

Table 2. Mean annual mortality rate in the first ($M1$) and second ($M2$) years following the first spawning migration and probability of consecutive spawning (p) of repeat-spawning Atlantic salmon (*Salmo salar*) from the LaHave River, Nova Scotia, Canada, during three time periods.

	Period		
Parameter	1979–1988	1989–1998	1999–2008
$M1_{\mathrm{MG}}$	0.88	0.92	0.95
$M1_{\mathrm{MS}}$	0.51	0.59	0.64
$M1_{\mathrm{F}}$	0.75	0.81	0.86
$M2$	0.60	0.73	0.74
p_{MG}	0.058	0.055	0.062
p_{MS}	0.022	0.026	0.022
p_{FG}	0.028	0.033	0.020
p_{FS}	0.033	0.071	0.043

Note: M, male; F, female; G, one sea winter; S, two sea winters.

during and immediately following spawning and could affect 1SW salmon disproportionately because of their smaller size. The lower mortality experienced by male 2SW salmon may reflect a lower cost of reproduction for large males, given that less energy is needed to produce gonads as compared with females and large males have an advantage over smaller males in mate competition.

Consecutive or alternate spawning is thought to reflect trade-offs in life-history strategy that could differ between the sexes. In other Atlantic salmon populations, there is a higher incidence of repeat spawning in females (Mills 1989; Niemel et al. 2000). This is also the case for the LaHave River because there are substantially more male 1SW salmon than 2SW salmon. Although the probability of consecutive spawning was estimated to be somewhat greater in the more common age-at-maturity strategy for each sex (1SW for males and 2SW for females), alternate spawning is really the dominant strategy for this population. It has been reported previously that 1SW salmon are more likely to be consecutive spawners, whereas 2SW salmon are more likely to be alternate spawners (Jonsson et al. 1991*b*). Our model did not produce sufficient evidence to support this for LaHave River salmon.

One of the main benefits of the model is that it provides annual estimates of mortality rates that are better for comparison with environmental variables than the proxies for survival

Fig. 9. Model estimates of the instantaneous mortality parameters and the resulting annual survival fraction for repeat-spawning Atlantic salmon (*Salmo salar*) from the LaHave River, Nova Scotia, Canada. Broken lines represent the 80% credible intervals. The different mortality parameters are as follows: (*a*) first-year mature mortality for male – one sea winter, (*b*) first-year mature mortality for male – two sea winters, (*c*) first-year mature mortality for female – one and two sea winters, (*d*) and second-year mature mortality for alternate spawners.

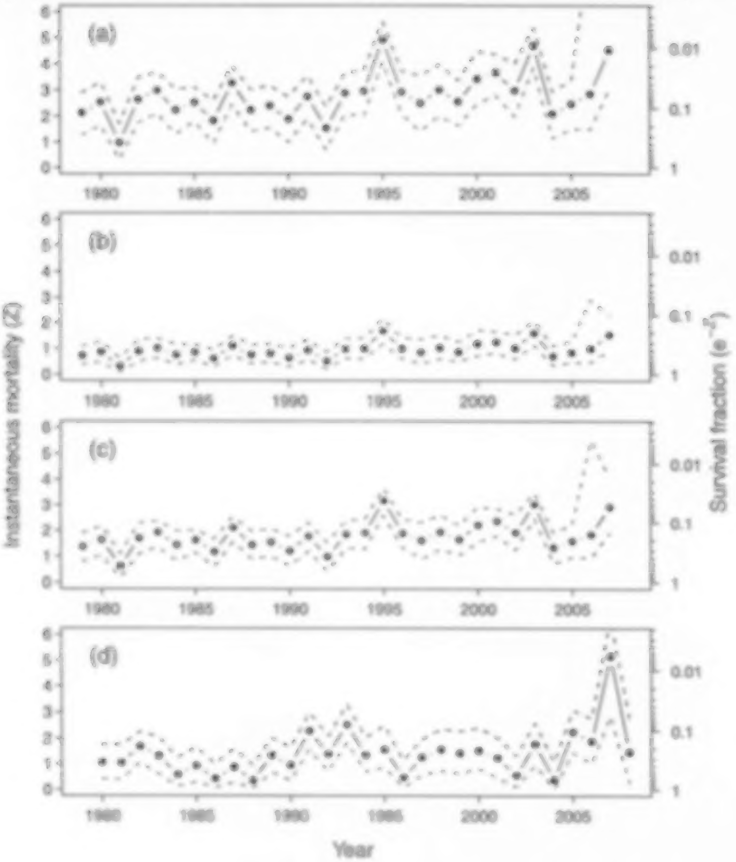

(either abundances or return rates) that are sometimes used (Friedland et al. 2003*a*, 2003*b*; Chaput 2008). Unlike these other indices, direct estimates of the second-year mortality rate are not confounded with the selection of life-history strategy or with mortality in the first year. This benefit is illustrated when we compared the correlations between NAOI and the return rates with the correlations between NAOI and the mortality estimates: correlations with the return rates were not significant at the 95% confidence level, whereas a significant correlation was found between *M*2 and the NAOI from 1979 to 2000. Had we not estimated mortality directly, no relationship with NAOI would have been observed. The reason that the relationship is less strong after 2000 may be related to a higher level of uncertainty in estimates of mortality caused by small sample size in recent years or other factors that affect survival when population sizes are small (Courchamp et al. 1999).

The similarity of the trends between NAOI and *M*2 suggest that variability in ocean climate plays a major role in natural mortality of Atlantic salmon in the marine environment. The NAO is a major driving force in the North Atlantic climate affecting current strength, direction, and many other factors (Hurrell 1995). The NAO has been shown to influence age at maturity in European stocks (Jonsson and Jonsson 2004*b*), but previous attempts to find correlations between the NAOI and abundance indices for North American populations of Atlantic salmon have been less successful (Friedland et al. 2003*a*; Reddin 2006). The mechanisms by which changes in ocean climate impact Atlantic salmon survival are not clear (Jonsson and Jonsson 2004*b*; Todd et al. 2008). Some studies have focused on the effects of sea-surface temperatures on recruitment and have found correlations that could indicate a direct physiological effect on survival (Martin and Mitchell 1985; Narayanan et al. 1995; Friedland et al. 2000). However, given certain conflicting correlations with temperature (Friedland et al. 2005), more indirect effects through ecosystem shifts may be more likely. Ecosystem shifts, reflected by changing species compositions that correspond with environmental variables, have been documented as beginning in the 1990s (Benoît and Swain 2008). An ecosystem shift could result from a cascade through the trophic web initially caused by climate change and eventually affecting species at higher trophic levels. For example, changes in zooplankton distribution as a result of climate forcing could result in a decline in sal-

Fig. 10. Annual mortality rate as the proportion of potential mature Atlantic salmon (*Salmo salar*) that die in a given first year plotted alongside the winter North Atlantic Oscillation Index (NAOI, squares), an environmental variable thought to influence the marine ecology of Atlantic salmon. The NAOI is compared with (*a*) mortality in the first year (triangles), which occurs mainly in freshwater, and (*b*) mortality in the second year (circles), which occurs mainly in the marine environment. A horizontal broken line is provided for reference and represents an NOAI of 0 or an annually mortality rate of 50%.

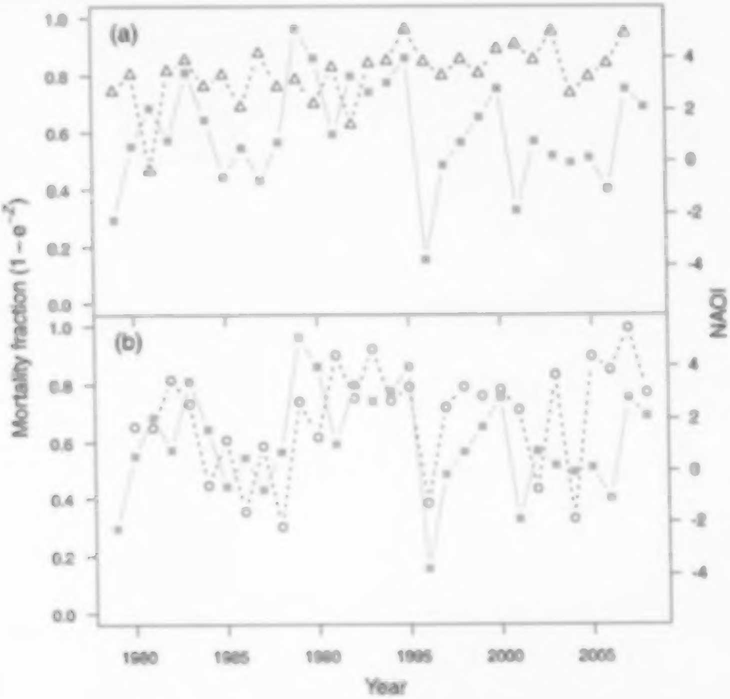

Table 3. Correlation between the North Atlantic Oscillation Index and the annual mortality rate in the first ($M1$) and second ($M2$) years following the first spawning migration estimated from the model, as well as the return rates of consecutive (C) and alternate (A) spawning one-sea-winter (G) and two-sea-winter (S) Atlantic salmon (*Salmo salar*).

Response variable	Correlation coefficient	p value
$M1$	−0.06	0.80
$M2$	0.44	0.04
CG return rate	−0.10	0.67
CS return rate	0.04	0.87
AG return rate	−0.34	0.13
AS return rate	−0.07	0.76

mon abundance (Beaugrand and Reid 2003). Alternatively, a shift could also result from changes in top-down control, potentially caused by the removal of a large biomass of predatory groundfish species in the commercial fisheries during the 1970s and 1980s associated with increased macroinvertebrates and changes in the zooplankton community (Frank et al. 2005).

The increase in overall adult salmon mortality is evident in the LaHave River but does not exist in all Atlantic salmon populations. Mature Atlantic salmon from the Miramichi River, in particular, appear to be experiencing increased survival in recent years (Chaput and Jones 2006; Chaput 2008). These differences most likely reflect mortality in the first year for two reasons. First, mortality in the second year is expected to be similar given that oceanic conditions act over a broad area and would likely impact both populations in the same manner. Second, the increase in repeat spawners seen in the Miramichi has been mostly consecutive spawners that have a brief marine reconditioning period (Chaput 2008). The reasons that the first-year mortality trends differ between the Gulf of St. Lawrence and Nova Scotia Atlantic coast populations is a key research area for understanding the plight of Atlantic salmon in Eastern Canada as a whole and is important in the context of recovery planning for populations in decline.

For adult salmon in the LaHave River, mortality rates have increased in both the marine and freshwater environment in recent years. The mortality rate of adult salmon in the first year varies for different populations and is likely related to local strategies and environmental conditions. In the LaHave River, it has been steadily increasing, and more research is needed in this and other troubled populations to find appropriate mitigating actions at the local level. The increase in mortality of adult salmon in their second year occurring around 1990 is consistent with a regime shift occurring in the ocean around that time (Choi et al. 2004; Benoît and Swain 2008). If broad-scale climate factors in the North Atlantic are influencing marine mortality, it would be expected to follow a similar trend in different populations and applying the model would be one way to independently test this. Additionally, although the comparison of *M*2 with the NAOI did provide evidence of climate influencing mortality at sea, comparison with other environmental and ecological data could lead to a better understanding of the mechanisms linking climate and survival of adult salmon. These linkages need to be established to understand how the recovery of salmon may be affected, the answer to which undoubtedly lies with continuing research into the threats that they face in the many ecosystems that they inhabit during the course of their lives.

Acknowledgements

We thank the efforts of our colleagues Heather Bowlby, Ian Jonsen, and Stephen Smith for their comments, suggestions, thoughts, and insights that improved this manuscript prior to submission. We also thank Nick Gayeski and another anonymous reviewer for their constructive comments. In particular, Nick Gayeski's thorough evaluation of the Bayesian methods led to an improvement in the construction of the hyperpriors for the beta distribution.

References

Amiro, P.G., Jefferson, E.M., and Harvie, C.J. 1996. Status of Atlantic salmon in Salmon Fishing Area 21, in 1995, with emphasis on the upper LaHave River, Lunenburg Co., Nova Scotia. DFO Atl. Fish. Res. Doc. 1996/126.

Amiro, P.G., Gibson, A.J.F., and Bowlby, H.D. 2006. Atlantic salmon (*Salmo salar*) overview for eastern Cape Breton, Eastern Shore, Southwest Nova Scotia and inner Bay of Fundy rivers (SFA 19 to 22) in 2005. Can. Sci. Advis. Sec. Res. Doc. 2006/024.

Beaugrand, G., and Reid, P.C. 2003. Long-term changes in phytoplankton, zooplankton and salmon related to climate. Glob. Change Biol. **9**(6): 801–817. doi:10.1046/j.1365-2486.2003.00632.x.

Benoît, H.P., and Swain, D.P. 2008. Impacts of environmental change and direct and indirect harvesting effects on the dynamics of a marine fish community. Can. J. Fish. Aquat. Sci. **65**(10): 2088–2104. doi:10.1139/F08-112.

Brooks, S.P., and Gelman, A. 1998. Alternative methods for monitoring convergence of iterative simulations. J. Comput. Graph. Statist. **7**(4): 434–455. doi:10.2307/1390675.

Chaput, G. 2008. Ecosystem driven variations in return rates to a second spawning for Atlantic salmon from the Miramichi River. *In* Report of the Working Group on North Atlantic Salmon (WGNAS), 1–10 April 2008, Galway, Ireland. ICES WGNAS Working Paper 2008/35.

Chaput, G., and Jones, R. 2006. Reproductive rates and rebuilding potential for two multi-sea-winter Atlantic salmon (*Salmo salar* L.) stocks of the Maritime Provinces. Can. Sci. Advis. Sec. Res. Doc. 2006/027.

Chaput, G., Caron, F., and Marshall, L. 2003. Estimates of survival of Atlantic salmon (*Salmo salar* L.) in the first and second years at sea. *In* Marine mortality of Atlantic salmon, *Salmo salar* L.: methods and measures. *Edited by* E.C.E. Potter, N.O. Maoileidigh, and G. Chaput. Can. Sci. Advis. Sec. Res. Doc. 2003/101. pp. 83–109.

Choi, J., Frank, K.T., Leggett, W.C., and Drinkwater, K. 2004. Transition to an alternate state in a continental shelf ecosystem. Can. J. Fish. Aquat. Sci. **61**(4): 505–510. doi:10.1139/f04-079.

Courchamp, F., Clutton-Brock, T., and Grenfell, B. 1999. Inverse density dependence and the Allee effect. Trends Ecol. Evol. **14**(10): 405–410. doi:10.1016/S0169-5347(99)01683-3. PMID:10481205.

Dickson, R.R., and Turrell, W.R. 2000. The NAO: the dominant atmospheric process affecting oceanic variability in home, middle, and distant waters of European Atlantic salmon. *In* The ocean life of Atlantic salmon. Environmental and biological factors influencing survival. *Edited by* D. Mills. Fishing News Books, Malden, Mass. pp. 92–115.

Fisheries and Oceans Canada. 2010. Status of Atlantic salmon in Salmon Fishing Areas (SFAs) 19–21 and 23. DFO Can. Sci. Advis. Sec. Sci. Rep. 2010/002.

Fleming, I.A. 1996. Reproductive strategies of Atlantic salmon: ecology and evolution. Rev. Fish Biol. Fish. **6**(4): 379–416. doi:10.1007/BF00164323.

Fleming, I.A. 1998. Pattern and variability in the breeding system of Atlantic salmon (*Salmo salar*), with comparisons to other salmonids. Can. J. Fish. Aquat. Sci. **55**(Suppl. 1): 59–76. doi:10.1139/d98-009.

Frank, K.T., Petrie, B., Choi, J.S., and Leggett, W.C. 2005. Trophic cascades in a formerly cod-dominated ecosystem. Science (Washington, D.C.), **308**(5728): 1621–1623. doi:10.1126/science.1113075. PMID:15947186.

Friedland, K.D., Reddin, D.G., and Kocik, J.F. 1993. Marine survival of North American and European Atlantic salmon: effects of growth and environment. ICES J. Mar. Sci. **50**(4): 481–492. doi:10.1006/jmsc.1993.1051.

Friedland, K.D., Hansen, L.P., Dunkley, D.A., and MacLean, J.C. 2000. Linkage between ocean climate, post-smolt growth, and survival of Atlantic salmon (*Salmo salar* L.) in the North Sea area. ICES J. Mar. Sci. **57**(2): 419–429. doi:10.1006/jmsc.1999.0639.

Friedland, K.D., Reddin, D.G., McMenemy, J.R., and Drinkwater, K.F. 2003*a*. Multidecadal trends in North American Atlantic salmon (*Salmo salar*) stocks and climate trends relevant to juvenile survival. Can. J. Fish. Aquat. Sci. **60**(5): 563–583. doi:10.1139/f03-047.

Friedland, K.D., Reddin, D.G., and Castonguay, M. 2003*b*. Ocean thermal conditions in the post-smolt nursery of North American Atlantic salmon. ICES J. Mar. Sci. **60**(2): 343–355. doi:10.1016/S1054-3139(03)00022-5.

Friedland, K.D., Chaput, G., and MacLean, J.C. 2005. The emerging role of climate in post-smolt growth of Atlantic salmon. ICES J. Mar. Sci. **62**(7): 1338–1349. doi:10.1016/j.icesjms.2005.04.013.

Friedland, K.D., MacLean, J.C., Hansen, L.P., Peyronnet, A.J., Karlsson, L., Reddin, D.G., Maoiléidigh, N.Ó., and McCarthy, J.L. 2009. The recruitment of Atlantic salmon in Europe. ICES J. Mar. Sci. **66**(2): 289–304. doi:10.1093/icesjms/fsn210.

Gelman, A., Carlin, J.B., Stern, H.S., and Rubin, D.B. 2004. Bayesian data analysis. 2nd ed. Chapman and Hall/CRC, New York.

Gibson, A.J.F., Hubley, P.B., Chaput, G.P., Dempson, J.B., Caron, F., and Amiro, P.G. 2006. Summary of status and abundance trends for eastern Canadian Atlantic salmon (*Salmo salar*) populations. Can. Sci. Advis. Sec. Res. Doc. 2006/026.

Gibson, A.J.F., Jones, R.A., and Bowlby, H.D. 2009. Equilibrium analysis of a population's response to recovery activities: a case study with Atlantic salmon. N. Am. J. Fish. Manage. **29**(4): 958–974. doi:10.1577/M08-006.1.

Gregg, W.W., Conkright, M.E., Ginoux, P., O'Reilly, J.E., and Casey, N.W. 2003. Ocean primary production and climate: global decadal changes. Geophys. Res. Lett. **30**(15): 1809. doi:10.1029/2003GL016889.

Hubley, P.B., Amiro, P.G., Gibson, A.J.F., Lacroix, G.L., and Redden, A.M. 2008. Survival and behaviour of migrating Atlantic salmon (*Salmo salar* L.) kelts in river, estuarine, and coastal habitat. ICES J. Mar. Sci. **65**(9): 1626–1634. doi:10.1093/icesjms/fsn129.

Hurrell, J.W. 1995. Decadal trends in the North Atlantic Oscillation: regional temperatures and precipitation. Science (Washington, D.C.), **269**(5224): 676–679. doi:10.1126/science.269.5224.676. PMID:17758812.

International Council for the Exploration of the Sea. 2008. Report of the Working Group on North Atlantic Salmon. ICES Document CM 2008/ACFM: 18.

Jonasson, J., Johannsson, V., and Oskarsson, S. 1994. Ocean mortality of ranched Atlantic salmon during the second year in the sea. Nord. J. Freshw. Res. **69**: 79–83.

Jonsson, N., and Jonsson, B. 2003. Energy allocation among developmental stages, age groups, and types of Atlantic salmon (*Salmo salar*) spawners. Can. J. Fish. Aquat. Sci. **60**: 506–516. doi:10.1139/f03-042.

Jonsson, B., and Jonsson, N. 2004*a*. Factors affecting marine production of Atlantic salmon (*Salmo salar*). Can. J. Fish. Aquat. Sci. **61**(12): 2369–2383. doi:10.1139/f04-215.

Jonsson, N., and Jonsson, B. 2004*b*. Size and age of maturity of Atlantic salmon correlate with the North Atlantic Oscillation Index (NAOI). J. Fish Biol. **64**(1): 241–247. doi:10.1111/j.1095-8649.2004.00269.x.

Jonsson, N., Jonsson, B., and Hansen, L.P. 1991*a*. Energetic cost of spawning in male and female Atlantic salmon (*Salmo salar* L.). J. Fish Biol. **39**(5): 739–744. doi:10.1111/j.1095-8649.1991.tb04403.x.

Jonsson, N., Hansen, L.P., and Jonsson, B. 1991*b*. Variation in age, size and repeat spawning of adult Atlantic salmon in relation to river discharge. J. Anim. Ecol. **60**(3): 937–947. doi:10.2307/5423.

Jonsson, B., Jonsson, N., and Hansen, L.P. 2003. The marine survival and growth of wild and hatchery-reared Atlantic salmon. J. Appl. Ecol. **40**(5): 900–911. doi:10.1046/j.1365-2664.2003.00851.x.

Lacroix, G.L., Knox, D., and Stokesbury, M.J.W. 2005. Survival and behaviour of post-smolt Atlantic salmon in coastal habitat with extreme tides. J. Fish Biol. **66**(2): 485–498. doi:10.1111/j.0022-1112.2005.00616.x.

Lunn, D.J., Thomas, A., Best, N., and Spiegelhalter, D. 2000. WinBUGS: a Bayesian modelling framework: concepts, structure, and extensibility. Stat. Comput. **10**(4): 325–337. doi:10.1023/A:1008929526011.

Martin, J.H.A., and Mitchell, K.A. 1985. Influence of sea temperature upon the numbers of grilse and multi-sea-winter Atlantic salmon (*Salmo salar*) caught in the vicinity of the River Dee (Aberdeenshire). Can. J. Fish. Aquat. Sci. **42**(9): 1513–1521. doi:10.1139/f85-189.

Millar, R.B. 2002. Reference priors for Bayesian fisheries models. Can. J. Fish. Aquat. Sci. **59**(9): 1492–1502. doi:10.1139/f02-108.

Mills, D.H. 1989. Ecology and management of Atlantic salmon. Chapman and Hall, London, UK.

Murphy, G.I. 1952. An analysis of silver salmon counts at Benbow Dam, South Fork of Eel River, California. Calif. Fish Game, **38**: 105–112.

Narayanan, S., Carscadden, J., Dempson, J.B., O'Connell, M.F., Prinsenberg, S., Reddin, D.G., and Shackell, N. 1995. Marine climate off Newfoundland and its influence on Atlantic salmon (*Salmo salar*) and capelin (*Mallotus villosus*). *In* Climate change and northern fish populations. *Edited by* R.J. Beamish. Can. Spec. Publ. Fish. Aquat. Sci. 121. pp. 461–474.

Niemel, J., Mkinen, T.S., Moen, K., Hassinen, E., Erkinaro, J., Lmman, M., and Julkunen, M. 2000. Age, sex ratio and timing of the catch of kelts and ascending Atlantic salmon in the subarctic River Teno. J. Fish Biol. **56**(4): 974–985. doi:10.1111/j.1095-8649.2000.tb00886.x.

O'Connell, M.F., Dempson, J.B., and Chaput, G. 2006. Aspects of the life history, biology, and population dynamics of Atlantic salmon (*Salmo salar* L.) in eastern Canada. Can. Sci. Advis. Sec. Res. Doc. 2006/014.

Pyper, B.J., and Peterman, R.M. 1998. Comparison of methods to account for autocorrelation in correlation analyses of fish data. Can. J. Fish. Aquat. Sci. **55**(9): 2127–2140. doi:10.1139/f98-104.

Reddin, D.G. 2006. Perspectives on the marine ecology of Atlantic salmon (*Salmo salar*) in the Northwest Atlantic. Can. Sci. Advis. Sec. Res. Doc. 2006/018.

Ricker, W.E. 1975. Computation and interpretation of biological statistics of fish populations. Bull. Fish. Res. Board Can. 191.

Ricker, W.E. 1976. Review of the rate of growth and mortality of Pacific salmon in salt water, and noncatch mortality caused by fishing. J. Fish. Res. Board Can. **33**(7): 1483–1524. doi:10.1139/f76-191.

Rivot, E., and Prévost, E. 2002. Hierarchical Bayesian analysis of capture–mark–recapture data. Can. J. Fish. Aquat. Sci. **59**(11): 1768–1784. doi:10.1139/f02-145.

Rivot, E., Prévost, E., Parent, E., and Baglinière, J.L. 2004. A Bayesian state–space modelling framework for fitting a salmon stage-structured population dynamic model to multiple time series of field data. Ecol. Model. **179**(4): 463–485. doi:10.1016/j.ecolmodel.2004.05.011.

Sokal, R.R., and Rohlf, F.J. 2003. Biometry. 3rd ed. W.H. Freeman and Co., New York.

Todd, C.D., Hughes, S.L., Marshall, S.T., MacLean, J.C., Lonergan, M.E., and Biuw, E.M. 2008. Detrimental effects of recent ocean surface warming on growth condition of Atlantic salmon. Glob. Change Biol. **14**(5): 958–970. doi:10.1111/j.1365-2486.2007.01522.x.

Trzcinski, M.K., Gibson, A.J.F., Amiro, P.G., and Randall, R.G. 2004. Inner Bay of Fundy Atlantic salmon (*Salmo salar*) critical habitat case study. Can. Sci. Advis. Sec. Res. Doc. 2004/114.

Welch, D.W., Melnychuk, M.C., Rechisky, E.R., Porter, A.D., Jacobs, M.P., Ladouceur, A., McKinley, R.S., and Jackson, G.D. 2009. Freshwater and marine migration and survival of endangered Cultus Lake sockeye salmon (*Oncorhynchus nerka*) smolts using POST, a large-scale acoustic telemetry array. Can. J. Fish. Aquat. Sci. **66**(5): 736–750. doi:10.1139/F09-032.

Appendix A. Ratio method derivation

The number of repeat spawners (consecutive or alternate) is equal to the number of initial spawners multiplied by the survival fraction (over one or two years) after the first spawning event:

$$N_{\mathrm{C}} = N_{\mathrm{V}} p e^{-Z1}; \quad N_{\mathrm{A}} = N_{\mathrm{V}}(1-p)e^{-(Z1+Z2)}$$

where N represents the number of fish; V, virgin spawners; C, consecutive spawners; A, alternate spawners; M, male; F, female; p, the probability of consecutive spawning; $Z1$, instantaneous mortality rate during first year; and $Z2$, instantaneous mortality rate during second year. Then,

$$N_{\mathrm{C}} e^{Z1} = N_{\mathrm{V}} p; \quad N_{\mathrm{A}} e^{Z1+Z2} = N_{\mathrm{V}}(1-p)$$

$$N_{\mathrm{V}} p + N_{\mathrm{V}}(1-p) = N_{\mathrm{C}} e^{Z1} + N_{\mathrm{A}} e^{Z1+Z2}$$

$$N_{\mathrm{V}} = N_{\mathrm{C}} e^{Z1} + N_{\mathrm{A}} e^{Z1+Z2}$$

This equation can then be specified for two groups within the population. Here we show the derivation of the solution for mortality using the male to female ratio.

$$N_{\mathrm{V,M}} = N_{\mathrm{C,M}}e^{Z1} + N_{\mathrm{A,M}}e^{Z1+Z2}$$

$$N_{\mathrm{V,F}} = N_{\mathrm{C,F}}e^{Z1} + N_{\mathrm{A,F}}e^{Z1+Z2}$$

$$\frac{N_{\mathrm{V,M}}}{N_{\mathrm{V,F}}} = \frac{N_{\mathrm{C,M}}e^{Z1} + N_{\mathrm{A,M}}e^{Z2+Z1}}{N_{\mathrm{C,F}}e^{Z1} + N_{\mathrm{A,F}}e^{Z2+Z1}}$$

$$\frac{N_{\mathrm{V,M}}}{N_{\mathrm{V,F}}} = \frac{N_{\mathrm{C,M}} + N_{\mathrm{A,M}}e^{Z2}}{N_{\mathrm{C,F}} + N_{\mathrm{A,F}}e^{Z2}} \times \frac{e^{Z1}}{e^{Z1}}$$

$$\frac{N_{\mathrm{V,M}}}{N_{\mathrm{V,F}}} = \frac{N_{\mathrm{C,M}} + N_{\mathrm{A,M}}e^{Z2}}{N_{\mathrm{C,F}} + N_{\mathrm{A,F}}e^{Z2}}$$

$$N_{\mathrm{V,M}}(N_{\mathrm{C,F}} + N_{\mathrm{A,F}}e^{Z2}) = N_{\mathrm{V,F}}(N_{\mathrm{C,M}} + N_{\mathrm{A,M}}e^{Z2})$$

$$N_{\mathrm{V,M}}N_{\mathrm{C,F}} + N_{\mathrm{V,M}}N_{\mathrm{A,F}}e^{Z2} = N_{\mathrm{V,F}}N_{\mathrm{C,M}} + N_{\mathrm{V,F}}N_{\mathrm{A,M}}e^{Z2}$$

$$N_{\mathrm{V,M}}N_{\mathrm{A,F}}e^{Z2} - N_{\mathrm{V,F}}N_{\mathrm{A,M}}e^{Z2} = N_{\mathrm{V,F}}N_{\mathrm{C,M}} - N_{\mathrm{V,M}}N_{\mathrm{C,F}}$$

$$e^{Z2}(N_{\mathrm{V,M}}N_{\mathrm{A,F}} - N_{\mathrm{V,F}}N_{\mathrm{A,M}}) = N_{\mathrm{V,F}}N_{\mathrm{C,M}} - N_{\mathrm{V,M}}N_{\mathrm{C,F}}$$

$$S2 = e^{-Z2} = \frac{N_{\mathrm{V,M}}N_{\mathrm{A,F}} - N_{\mathrm{V,F}}N_{\mathrm{A,M}}}{N_{\mathrm{V,F}}N_{\mathrm{C,M}} - N_{\mathrm{V,M}}N_{\mathrm{C,F}}}$$

$$S1_{\mathrm{M}} = e^{-Z1} = \frac{N_{\mathrm{C,M}} + N_{\mathrm{A,M}}e^{Z2}}{N_{\mathrm{V,M}}}$$

$$S1_{\mathrm{F}} = e^{-Z1} = \frac{N_{\mathrm{C,F}} + N_{\mathrm{A,F}}e^{Z2}}{N_{\mathrm{V,F}}}$$

Does size matter? A bioeconomic perspective on optimal harvesting when price is size-dependent

Fabian Zimmermann, Mikko Heino, and Stein Ivar Steinshamn

Abstract: Body size is a key parameter influencing demographic characteristics of fish populations as well as market value of landed catch. Yet in bioeconomic modelling, body size is often an overlooked biological and economic parameter. Here we evaluate how size-dependent pricing influences optimal harvest strategies in a model parameterized for two pelagic fisheries, those targeting Atlantic herring (*Clupea harengus*) and Atlantic mackerel (*Scomber scombrus*), in Norway. In our model, positively size-dependent pricing clearly shifts optimal harvest strategies towards lower harvest rates and higher mean body size of caught fish. The results are relatively insensitive to biological (e.g., natural mortality) and economic details of the model (e.g., discount rate or demand function). These findings show that size-dependent pricing influences optimal harvest strategies aiming at maximum economic yield and, hence, requires more attention in resource economics and in fisheries management.

Résumé : La taille corporelle est une variable clé qui influence certaines caractéristiques démographiques des populations de poissons ainsi que la valeur marchande des débarquements. Néanmoins, la taille corporelle est souvent une variable biologique et économique négligée dans les modèles bioéconomiques. Nous évaluons ici comment la fixation des prix en fonction de la taille influence les stratégies de récolte optimale dans un modèle paramétrisé pour deux pêches pélagiques, celles qui ciblent le hareng atlantique (*Clupea harengus*) et le maquereau bleu (*Scomber scombrus*) en Norvège. Dans notre modèle, une fixation positive des prix en fonction de la taille fait déplacer les stratégies de récolte optimale vers des taux de récolte plus faibles et vers une taille moyenne plus grande des poissons récoltés. Les résultats sont relativement insensibles aux détails biologiques (par ex., la mortalité naturelle) et économiques (par ex., le taux d'escompte ou la fonction de demande). Ces résultats montrent que la fixation des prix en fonction de la taille influence les stratégies de capture optimale qui recherchent un rendement économique maximal et qu'ainsi elle mérite plus d'attention dans l'étude économique des ressources et la gestion des pêches.

[Traduit par la Rédaction]

Introduction

It is common that price of fish depends on their size; typically, large individuals fetch a higher price per kilogram than small individuals of the same species. When present, such size dependence should be considered when evaluating harvest strategies (Hilborn and Walters 1992). While size-dependent pricing is occasionally included in bioeconomic models, it is very rare that the consequences of size-dependent pricing per se have been studied in any detail. We are aware of only few studies where this question has been touched; Gallagher et al. (2004) and Holland et al. (2005) showed that for Oregon ocean shrimp (*Pandalus jordani*) and rock lobster (*Jasus edwardsii*), respectively, size-related pricing indeed influences management strategies. Similarly, Tahvonen (2009) demonstrated in a generic age-structured model how equilibrium revenue and stock size are affected by size-dependent pricing. More typically, size-dependent pricing has been either overlooked, acknowledged but not analyzed (Anderson 1989), or taken as an extrinsically determined model component that is kept fixed in the analysis (e.g., Thunberg et al. 1998; De Leo and Gatto 2001; Katsukawa 2005). Some studies also acknowledge other biological factors influencing price (e.g., seasonal changes in fish quality; Larkin and Sylvia 1999). Size-dependent pricing is also important in aquaculture (Bjørndal 1988; Asche and Guttormsen 2001). Thus, we have all reasons to expect that the size dependency of the price is widespread and highly relevant for optimal utilization of fish stocks.

Here our aim is to quantify how size-dependent pricing influences optimal harvest strategies. We use Atlantic herring (*Clupea harengus*) and Atlantic mackerel (*Scomber scombrus*) as case studies. Specifically, we focus on the Norwegian

Received 9 November 2010. Accepted 4 June 2011. Published at www.nrcresearchpress.com/cjfas on 9 September 2011.
J2011-0219

Paper handled by Associate Editor Ray Hilborn.

F. Zimmermann. University of Bergen, Department of Biology, P.O. Box 7803, N-5020 Bergen, Norway.
M. Heino. University of Bergen, Department of Biology, P.O. Box 7803, N-5020 Bergen, Norway; Institute of Marine Research, P.O. Box 1870 Nordnes, N-5817 Bergen, Norway; International Institute for Applied Systems Analysis, A-2361, Laxenburg, Austria.
S.I. Steinshamn. Samfunns- og næringslivsforskning AS (SNF; Norwegian School of Economics), Breiviksveien 40, N-5045 Bergen, Norway.

Corresponding author: Fabian Zimmermann (e-mail: fabian.zimmermann@bio.uib.no).

Can. J. Fish. Aquat. Sci. **68**: 1651–1659 (2011) doi:10.1139/F2011-093 Published by NRC Research Press

spring spawning herring stock and the northeast Atlantic mackerel stock, following the stock definitions used in the management (ICES 2010). Herring and mackerel are of major importance for the fisheries of several European countries, with a total catch of about 1.7 and 0.7 million tonnes, respectively, in 2009 (ICES 2010). Moreover, herring and mackerel are key species in the northeast Atlantic pelagic ecosystem (Skjoldal et al. 2004), making their sustainable management even more important.

We utilize an age-structured, discrete-time population model with size-dependent harvesting. Price data are based on Norwegian market data for herring and mackerel. For simplicity we assume that the relationship between size and price is linear; this allows us to smoothly vary the strength of size dependency, in contrast with earlier studies that only considered a limited set of fixed pricing scenarios (Gallagher et al. 2004; Holland et al. 2005) The cost of harvesting is output-regulated and depends on yield. In the optimization, the main target is to maximize the net present value over a long time scale with discount rates on an efficient market level, while high discount factors are used to emulate an open-access situation. We show how optimal fishing mortality and resulting mean individual mass in the catch depends on the size dependency of pricing. We also estimate the shadow cost (i.e., the opportunity costs for applying a suboptimal harvest regime and the lost margin of benefit due to ignoring the size dependency of pricing).

Materials and methods

Biological model

The biological model is based on an age-structured population dynamics model with annual time steps. Sexes are combined because male and female life histories are similar in herring and mackerel (the parameters and their values are listed in Appendix Table A1).

There are n discrete age classes, denoted by N_a with $a = 1, 2, \ldots, n$, and there is no senescence. The last age class is a so-called plus-group representing all fish n years of age or older. Population dynamics is then described by

$$N_a(t+1) = \begin{cases} r[\mathrm{SSB}(t)] \\ s_a N_{a-1}(t) \\ s_n[N_{n-1}(t) + N_n(t)] \end{cases} \quad \text{if} \quad \begin{cases} a = 1 \\ 1 < a < n \\ a = n \end{cases}$$

where SSB is the spawning stock biomass, $r(\mathrm{SSB})$ is the stock–recruitment function, and s_a is age-specific survival probability defined below.

The connection between age and size is defined through the von Bertalanffy growth model $l(a) = L_\infty(1 - \mathrm{e}^{-ka})$, where L_∞ is the asymptotic length and k is the growth coefficient. Furthermore, we assume an allometric mass–length relationship $w(l) = vl^u$, where v is the length–mass coefficient and u is the allometric exponent.

Reaching maturity is based on the age of the individual and defined by the age-maturity ogive $o(a) = \left[1 + \mathrm{e}^{-(a - a_{50})/a_\mathrm{width}}\right]^{-1}$, where a_{50} is the age where 50% of the individuals have reached maturity and a_width is the coefficient describing width of the maturity envelope. Mature individuals constitute the spawning stock, and SSB is defined as $\mathrm{SSB} = \sum_a w_a o_a N_a(t)$. For herring, recruitment follows the Beverton–Holt stock–recruitment model as defined by (Fiksen and Slotte 2002), $r(\mathrm{SSB}) = \frac{b_1\,\mathrm{SSB}}{b_2 + \mathrm{SSB}}$, where b_1 is asymptotic maximum recruitment and b_2 determines how fast the asymptote is approached. For mackerel, we use the hockey-stick recruitment model estimated by ICES (2010), implying that below a threshold $\mathrm{SSB}_\mathrm{max}$ recruitment is a linear, increasing function of SSB, $r(\mathrm{SSB}) = b_3\mathrm{SSB}$, whereas above the threshold recruitment is assumed to be constant, $r(\mathrm{SSB}) = r_\mathrm{max}$.

The fishing mortality is assumed to be length-dependent. Catchability usually increases with size until levelling off at some intermediate size, a relationship usually described by a sigmoid curve. However, in our study stocks, no such levelling off can be detected between fishing mortality (mean fishing mortality at age from 1984–2009; ICES 2010) and length-at-age (from the growth model described above); for mackerel, the three-parameter sigmoid model fails to converge, whereas for herring the inflection point in the resulting fit is far outside the range of observed lengths. Within the range of observed lengths, a two-parameter power function and the sigmoid function predict similar fishing mortalities for mackerel, but the power function gives a lower Akaike information criterion (AIC) (difference = 2.0) than the sigmoid function. The relationship between fishing mortality and length is therefore most parsimoniously described as a power function for both stocks. Here we normalize length relative to mean catch length $\bar{l}$, such that

$$(1) \qquad F_a = F[l(a)] = F_0(l/\bar{l})^\eta$$

where F_0 is fishing mortality at mean catch length and η is a selectivity parameter that determines the strength of length dependency; the function is convex for $\eta > 1$. The equation was fitted to fishing mortality at age data from (ICES 2010), transforming age into length using the von Bertalanffy model described above. Mean catch length $\bar{l}$ used in the normalization was estimated through back calculation of mean catch mass based on mass at age in the International Council for the Exploration of the Sea (ICES) catch from 2009 (ICES 2010).

The natural mortality M is based on the values used in the stock assessment (ICES 2010). The survival probability s is determined by the total mortality Z, which is the sum of fishing mortality F and natural mortality M: $s_a = \mathrm{e}^{-Z_a} = \mathrm{e}^{-(F_a + M_a)}$

The link between the biological and economic part of the model is the catch equation $H_a = N_a(1 - \mathrm{e}^{-Z_a})F_a/Z_a$, where H_a is catch numbers at age. Total catch in terms of biomass, or yield, is catch numbers times the mean age-specific individual mass, $Y = \sum_a H_a w_a$.

Economics

We assume that the relationship between size and price can be expressed as a simple linear function of mass, such that we can easily change the strength of size dependence. To make the parameters easily interpretable, we standardize mass relative to the mean observed individual catch mass over all age classes, $\bar{w}$. Furthermore, we standardize the price–mass coefficient relative to the observed coefficient,

Fig. 1. Linear mass–price functions (solid lines) estimated from real price data (dots) and step functions based on price per mass categories for herring (*a*, *c*) and mackerel (*b*, *d*). The actual price slopes β_0 are 2.43 (herring) and 8.97 Norwegian krones (NOK)·kg^{-1} (mackerel). For reference, the case with constant price ($\beta = 0$; grey line) is also shown. The pivot point of these lines corresponds to the observed mean individual catch mass, $\overline{w}$ (dotted line) and price per kilogram for this mass, $p_{\overline{w}}$. The price data are annual mean prices per mass class from Norwegian spring spawning herring and northeast Atlantic mackerel in 2000–2010 provided by the Norwegian Fisheries Directorate (Per Sandberg, Fiskeridirektoratet, Postboks 185 Sentrum, 5804 Bergen, Norway, personal communication, 2011). We use annual catch mass distributions (ICES 2010) to transform mass classes into mean mass of each mass class (*a*, *b*). Step functions (*c*, *d*) represent prices per mass class in 2009 (dashed line) and 2010 (solid line).

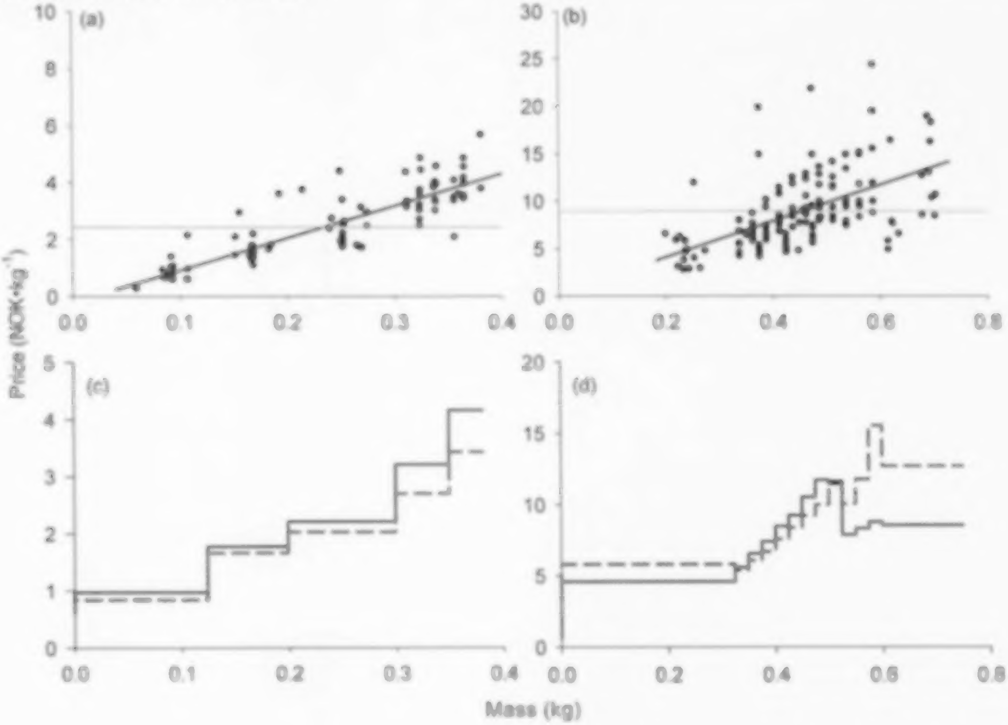

β_0. The price function is then $p(w) = p_{\overline{w}} + \beta\beta_0\left(\frac{w-\overline{w}}{\overline{w}}\right)$, where the intercept $p_{\overline{w}}$ is the price per unit biomass for $\overline{w}$, the observed slope β_0 gives the price increase when individual mass is increased by $\overline{w}$, and β is the relative deviation from the observed slope. $\overline{w}$ thus acts as the pivot point in this function. The parameters $p_{\overline{w}}$ and β_0 of the price function (Fig. 1) were estimated with linear regression using data provided by the Norwegian Fisheries Directorate (Per Sandberg, Fiskeridirektoratet, Postboks 185 Sentrum, 5804 Bergen, Norway, personal communication, 2011). The data comprise total annual yield and value per mass class in 2000–2010 as registered by the sales organizations. Average prices per mass class are derived from these data. To obtain mean mass for each mass class, we assumed that mass at age in the catch is normally distributed, with mean taken from ICES (2010) and a coefficient of variation of 30%. We then multiplied the age-specific mass distributions with catch numbers at age (ICES 2010) to obtain total mass distribution in a given year, which allows estimating the mean mass for a certain mass class as well as the overall mean mass $\overline{w}$. Mean price $p_{\overline{w}}$ was derived from the data from the Norwegian Fisheries Directorate.

We also considered constraining the influence of size on price. As the minimum price, we used the minimum price set by the Norwegian pelagic fish sales organization, which was 0.60 Norwegian krones (NOK)·kg^{-1} for both herring and mackerel in 2010 (Norges Sildesalgslaget 2011). As the maximum, we used the highest mean price in 2010, which was 4.16 NOK·kg^{-1} for herring and 11.7 NOK·kg^{-1} for mackerel.

The total revenue is the sum of the annual yield times the mass-dependent price for each age class, $R_t = \sum_a p(w_a)Y_a$. The cost function is derived from the model of Touzeau et al. (2000). To avoid potential complications due to the nonlinearity of this cost curve, a simplified cost function with a linear relationship between yield and cost based on a linear regression of the cost function of Touzeau et al. (2000), $C_t = C_0 + \upsilon Y_t$, has been used. Here the intercept C_0 represents fixed costs, and the term υY_t represents variable costs. The net revenue is then $\Pi_t = R_t - C_t$. With d denoting discount rate, the net present value (NPV) is the sum of annual discounted net revenues:

$$\text{(2)} \qquad \text{NPV} = \sum_{0}^{t} \frac{\Pi_t}{(1+d)^t}$$

We tested a demand function estimated from Norwegian yield and price data in 2000–2009. However, the resulting fit

Fig. 2. Net present value (NPV) for herring (*a*) and mackerel (*b*) fisheries as a function of harvest proportion under the current pricing regime (solid line), no size-dependent pricing ($\beta = 0$; long dashed line) and a twofold price slope ($\beta = 2$; short dashed line). The distance between vertical grey lines illustrates the difference in the NPV-maximizing harvest strategies in the presence and absence of size-dependent pricing. Discount rate (d) is equal to 0.05. Harvest proportion is calculated from the mean fishing mortality over reference ages as defined by ICES (ages 5–14 years for herring, 4–8 years for mackerel; ICES 2010).

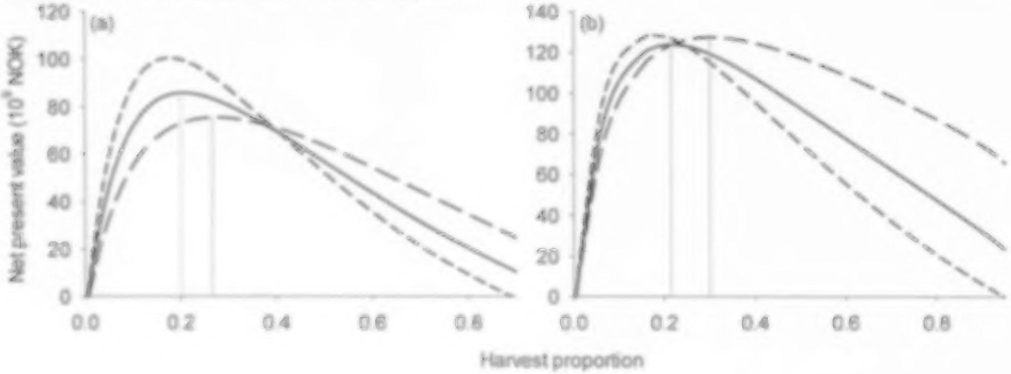

was poor because of the lack of information about willingness to pay outside the narrow range of actual production volumes and because of other factors influencing the price. Sensitivity analysis showed no significant influence on the results, and therefore demand effects were not considered further in this study. However, because of this and the simple cost function used, we emphasize that we do not expect the model to give precise quantitative predictions, even though the results shown are qualitatively robust.

Simulations

The model was run over 1000 years, an essentially infinite time horizon unless discount rate is very low ($d < 0.01$). The first 200 years were used to establish prefishing equilibrium. Fishing started from the virgin stock at year 200, causing the stock to decline towards a new equilibrium. It is assumed that size selectivity of the fisheries is fixed, but that the managers can adjust the overall level of fishing mortality such that NPV of the stock is maximized. Harvest strategies in our model are therefore defined through the parameter F_0, fishing mortality at mean catch length. The optimal F_0 was identified using the function "optimize" in R (R Development Core Team 2010).

Results

The effect of size-dependent pricing is to shift harvest rate that maximizes NPV towards lower values (Fig. 2). Comparing the harvest strategy optimized for size dependency of the current pricing regime and one without any size dependency, the shadow cost of omitting the size dependency in the current pricing regime is found to be about 3.3% for herring and 3.8% for mackerel relative to the optimal NPV (discount rate $d = 0.05$). Shadow costs define here the difference in NPV between the optimal harvest strategy with the current, size-dependent price regime and the one that would be optimal when we assume no size-dependent pricing (i.e., the opportunity cost of ignoring size dependency in price).

With increasing effect of size on price (increasing β), the mean fishing mortality that maximizes NPV decreases and the corresponding mean individual size increases (Fig. 3); for herring the effect is almost linear within the considered range, whereas for mackerel the effect is levelling off for strong size dependence. Mean fishing mortalities (age groups 4–8 for mackerel and 5–14 weighted by stock numbers for herring) yielding maximum NPV (with discount rate $d = 0.05$) are 0.146 year^{-1} in the current pricing regime ($\beta = 1$) compared with 0.189 year^{-1} without size-dependent pricing for herring and 0.242 year^{-1} compared with 0.357 year^{-1} for mackerel. For reference, the latest stock assessments estimated fishing mortalities at 0.154 year^{-1} for herring and 0.233 year^{-1} for mackerel (ICES 2010). In our model, the decrease in mean fishing mortality between no size dependency and a realistic size-dependent pricing is about 23% for herring and 32% for mackerel, and the mean catch mass increases by about 6% and 8%, respectively. The patterns remain similar if the initial stock states are changed from the pristine levels to lower population abundances estimated in the latest stock assessments (ICES 2010).

The discount rate has no influence on the qualitative effect that size-dependent pricing has on optimal fishing mortality and the corresponding mean size (Fig. 3), even when very high discount rates emulating an open-access situation are considered (Fig. 4). Nevertheless, the discount rate has a considerable quantitative effect on the optimal fishing mortality; the optimal value increases almost threefold between the extreme cases of no discounting and a very high discount rate of one, mimicking an open-access situation. As theory suggests, the biggest effect on optimal fishing mortality is found on low to intermediate discounting levels.

Because natural mortality is an important parameter in age-structured models, we investigate its influence further. For both species, changing natural mortality results in changes in optimal fishing mortality and, to a somewhat lesser extent, in the resulting mean catch mass (Fig. 5). These changes are opposite for the two species; higher natural mortality leads to higher optimal fishing mortality for mackerel but lower optimal fishing mortality for herring. These effects are slightly more pronounced for low β; an increasing β

Fig. 3. The influence of relative price slope β on optimal fishing mortality (black) and the resulting mean individual mass (grey) in the catch of herring (*a*) and mackerel (*b*) with respect to different discount rates *d*. Discount rate takes values $d = 0.05 \pm 0.05$ ($d = 0$ long dashed line; $d = 0.1$ short dashed line; $d = 0.05$ solid line). Optimal strategy is the one maximizing the net present value of a pristine stock. Strength of size dependence of price is expressed as the relative price slope β, with $\beta = 1$ corresponding to the current price dependence shown in Fig. 1, and $\beta = 0$ corresponding to no price dependence. Fishing mortality is the mean fishing mortality over reference ages as defined by ICES (ages 5–14 years weighted by stock numbers for herring, 4–8 years for mackerel; ICES 2010).

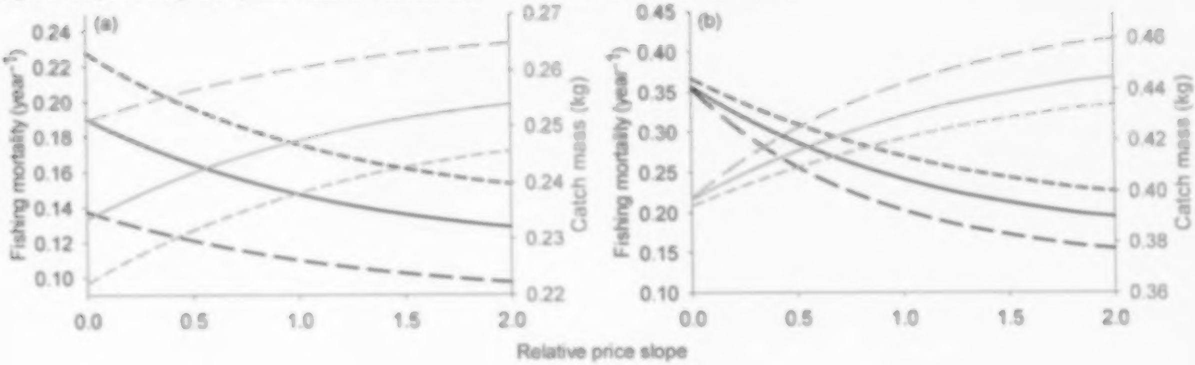

Fig. 4. Mean fishing mortality optimized for net present value in herring (*a*) and mackerel (*b*) fisheries under the assumptions of discount rates between 0 and 1. The solid line shows results for the real size dependence of pricing. The envelope with dashed lines shows the case of no size dependency (long dashed) and doubled slope (short dashed). Optimal strategy is the one maximizing the net present value of a pristine stock. Fishing mortality is the mean fishing mortality over reference ages as defined by ICES (ages 5–14 years weighted by stock numbers for herring, 4–8 years for mackerel; ICES 2010).

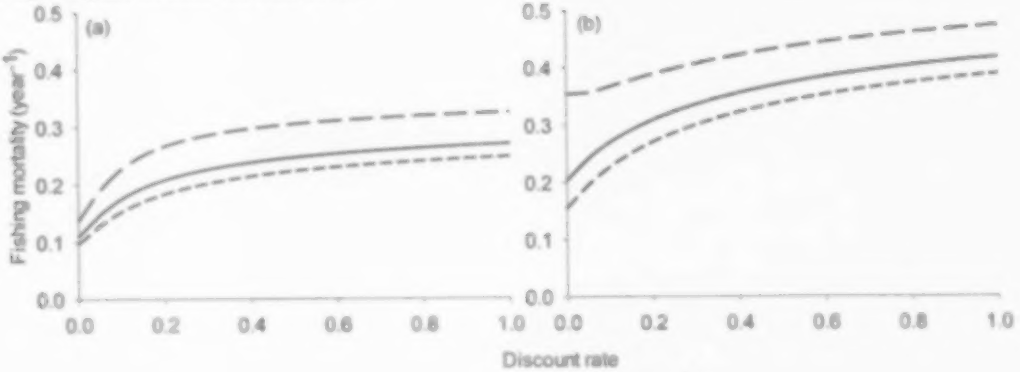

tends to dampen the influence of changing natural mortality. The qualitative difference between the species is caused by the age-dependent natural mortality in herring; assuming a constant natural mortality for herring leads to mackerel-like results. For catch masses, the influence of changing natural mortality is qualitatively the same for both species; mean catch mass is increased (decreased) by higher (lower) natural mortality.

Comparing the continuous price function with the empirical step functions either in 2009 or 2010 given in Fig. 1 shows that the differences are negligible; optimization with discrete price classes displays the same shift between constant price and size dependency and similar quantitative results. The same applies when applying minimum and (or) maximum price caps. Additionally, optimal fishing mortality depends on the selectivity parameter η, but the effect is minor and does not influence the qualitative pattern (Fig. 6).

Discussion

The size of fish is a key parameter from biological as well as technical and economic perspectives. In terms of biology, size is closely linked with growth, maturation, reproductive output, and survival. Avoidance of growth overfishing — catching fish too small, before a cohort has realized its growth potential — has been a crucial part of fisheries management since Beverton and Holt (1957). Using minimum size restrictions and mesh size regulations as management tools to protect the productivity of a fish stock reflects this idea. Likewise, the fishing industry has a strong interest in fish size both to optimize the industrial utilization and to serve consumer preferences. Ultimately, these market incentives are a key driver for size-dependent pricing. Yet the connection between price and body size is an understudied issue in fisheries economics. This is surprising given that size-

Fig. 5. Mean fishing mortality (black) that maximizes net present value (NPV) in herring (*a*) and mackerel (*b*) fisheries and the corresponding mean catch mass (grey) as functions of the relative price slope. The lines represent the default natural mortality M_a (solid) and M_a decreased (long dashed) or increased (short dashed) by 20%. The discount rate is $d = 0.05$. Optimal strategy is the one maximizing the NPV of a pristine stock. Strength of size dependence of price is expressed as the relative price slope β, with $\beta = 1$ corresponding to the current price dependence shown in Fig. 1 and $\beta = 0$ corresponding to no price dependence. Fishing mortality is the mean fishing mortality over reference ages as defined by ICES (ages 5–14 years weighted by stock numbers for herring, 4–8 years for mackerel; ICES 2010).

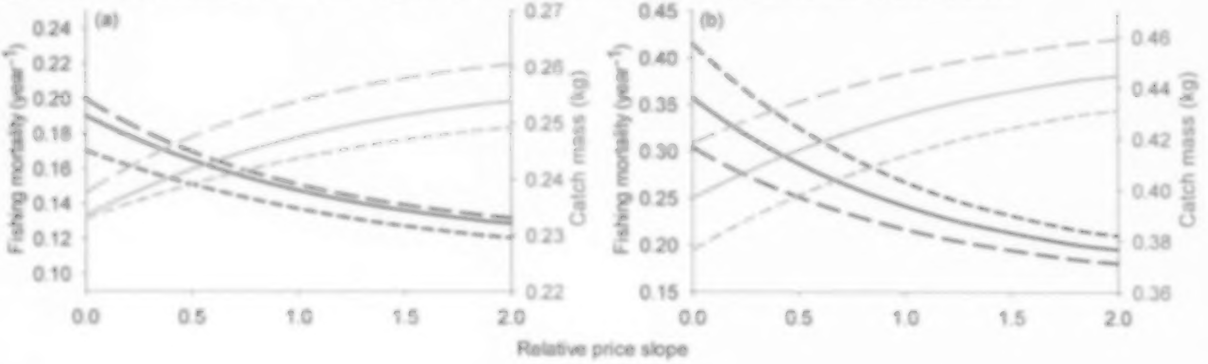

Fig. 6. Mean fishing mortality (black) optimized for net present value (NPV) in herring (*a*) and mackerel (*b*) fisheries and the corresponding mean catch mass (grey) as functions of the relative price slope. The lines represent the default selectivity parameter η (solid line) and η decreased (long dashed line) or increased (short dashed line) by 20%. The discount rate is $d = 0.05$. Optimal strategy is the one maximizing the NPV of a pristine stock. Strength of size dependence of price is expressed as the relative price slope β, with $\beta = 1$ corresponding to the current price dependence shown in Fig. 1 and $\beta = 0$ corresponding to no price dependence. Fishing mortality is the mean fishing mortality over reference ages as defined by ICES (ages 5–14 years weighted by stock numbers for herring, 4–8 years for mackerel; ICES 2010).

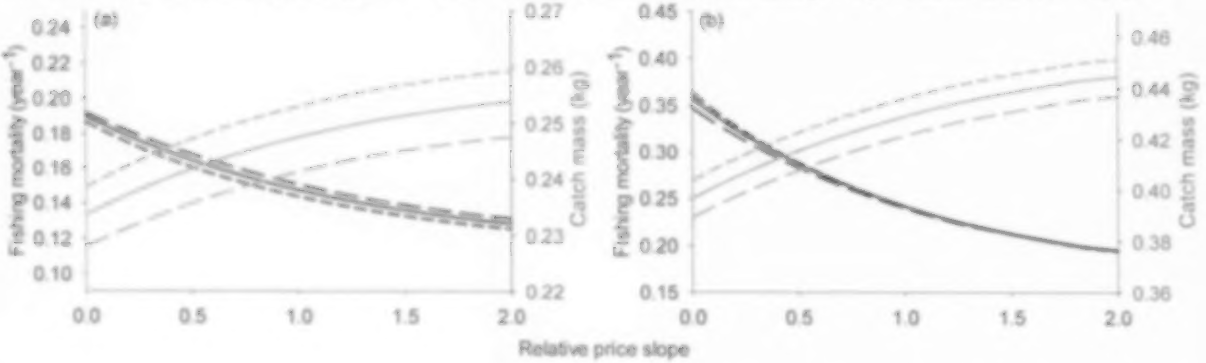

dependent pricing is ubiquitous and that its role in rational harvest management has in theory been acknowledged for a long time (Hilborn and Walters 1992). While a number of studies on capture fisheries have included size-dependent pricing, the majority of these have only considered a single scenario, without studying the effects of size-dependent pricing per se (e.g., Helser et al. 1996; Thunberg et al. 1998; Katsukawa 2005). A few studies have included a small number of alternative size-dependent pricing scenarios when analysing specific fisheries (Gallagher et al. 2004; Holland et al. 2005). There are also a few generic models that have included size-dependent pricing (Anderson 1989; Tahvonen 2009). While Anderson (1989) did not elaborate on the importance of size-dependent pricing, Tahvonen (2009) showed with a concrete example how positively (or negatively) size-dependent pricing leads to equilibrium revenues to be maximized at a higher (or respectively lower) stock biomass level. The topic has also been discussed outside fisheries economics. For example, price of fish produced in aquaculture is size-dependent, and this has consequences for optimizing the production cycle (Bjørndal 1988; Asche and Guttormsen 2001).

Our goal here was to demonstrate the importance of size-dependent pricing for economically optimal harvest strategies using simple age-structured models parameterized for two important pelagic fish stocks. The results confirm our expectations; fishing pressure maximizing economic yield in terms of revenue and NPV depends on the applied size-based pricing regime, with implications for mean size of fish in the catches and equilibrium stock abundance. The results reveal potential for overestimation of future profits and rent dissipation due to the application of suboptimal harvest strategies when ignoring size-dependent pricing; the effect in the examples studied here is nevertheless quantitatively modest. However, the effect on the resultant harvest strategy is appreciable. Considering that in most commercially important fish stocks the price is size-dependent, the insights presented here call for broader utilization of size-dependent pricing in economic modelling.

When the size–price relationship is monotonic and positive, maximum economic yields are obtained through higher stock sizes and smaller catches than when such size dependence is absent. In other words, positive size–price relationships imply that lower fishing mortalities optimize the NPV. It is acknowledged that catches below maximum sustainable yield typically maximize the resource rent (Clark 2006; Grafton et al. 2007; Tietenberg and Lewis 2008). Our results suggest that this effect might even be stronger than maximum economic yield estimates ignoring size-dependent pricing would suggest. Therefore, taking positively size-dependent pricing into account would result in lower harvest rates, which would not only ultimately increase society's direct economic benefits from fisheries, but also reduce the negative effects fisheries might have on the ecosystems. This is in accord with the precautionary approach to fisheries management, calling for more conservative harvest policies that lead to an increased overall stock abundance. This would enhance population resilience, harvest productivity, and efficiency.

Our results resonate with calls to save the big fish for the sake of improved biological sustainability (Birkeland and Dayton 2005; Francis et al. 2007; Diekert et al. 2010). This statement may seem counterintuitive, since we emphasize the high market value of large-sized fish. However, we have focused on a single-owner fishery where the manager adopts a long time perspective, avoiding the short-sighted temptation of targeting the large fish. In our model, the opportunity cost of choosing a suboptimal harvest strategy can only be mitigated by reducing the overall fishing mortality, therefore allowing more fish to reach large sizes and, ultimately, leaving more big fish in the sea.

We emphasize that in general, mesh size regulations and other means of modifying size-dependent catchability can be important levers of optimizing the harvest, even though we did not consider them here. Our model applies to pelagic fisheries where effective regulation of size-dependent catchability is difficult; gears like purse seines are weakly size-selective, and pelagic fish have low survival after slipping through meshes or being strangled in a net. However, demersal fish are often more robust and have better chances of surviving if slipping through meshes or sorting grids or if discarded after the capture. Mesh size regulations can therefore be a means to ensure that enough fish have chance to grow to the most valuable size classes. In such cases, economic implications of considering size-dependent pricing are likely larger than what we have found for herring and mackerel here.

We have used the simplest possible price function, a linear relationship between price and mass, as the default price function. While this is a good approximation for herring and mackerel, more complex relationships occur in some fisheries (Thunberg et al. 1998). There is also some evidence that the price premium for larger size disappears for very large mackerel, a situation that may not be uncommon if very large fish have lower flesh quality, higher concentrations of contaminants, or are less suited for industrial processing. Similarly, if small-sized fish are destined to fish meal production instead of human consumption, their precise size may become unimportant. We therefore also tried constraining the price between certain minimum and (or) maximum levels, but this did not change the results in any essential way (the bulk of the harvest comes from medium-sized fish). Additionally, our price function implies continuously increasing effect of size on price, whereas real markets commonly operate with discrete mass classes. While using the real mass classes should give more precise results, our simulations suggest that a linear function is a good approximation. Moreover, market mass classes often vary over time and space. For these reasons we consider a linear approximation justified here.

Our study has several general limitations. We rely on a single-species approach and focus in the steady state scenario without environmental oscillations. Size structure in the model is determined by the age structure using a static age–length relationship. In reality, size structure of the harvestable stock is determined by intra- and inter-specific interactions (availability of resources and presence of predators). In particular, density-dependent body growth (e.g., Lorenzen and Enberg 2002) might counter the increase in average size that is expected to occur when fishing is reduced and therefore influence management strategies (Helser and Brodziak 1998). A major source of uncertainty is natural mortality. This is modelled as constant (mackerel) or age-dependent (herring); both assumptions are crude approximations of reality, but unfortunately data for more realistic choices are not available. Also, our economic model is rather simplistic, apart from inclusion of size-dependent price. We assume a simple yield-determined cost function and absence of market feedbacks on price. Our initial explorations suggested that considering effort-dependent costs or demand curves is not important for the questions addressed here. Moreover, developing a more detailed bioeconomic model for mackerel would have been a major task on its own, whereas for herring, more detailed information exists (e.g., Touzeau et al. 2000; Sandberg 2006). Finally, the model does not account for practical challenges in balancing stakeholder interests nor policy implementation and enforcement; in reality, suboptimal management due to political and social pressures and illegal fishing are more a rule than an exception (Beddington et al. 2007; Agnew et al. 2009; Mora et al. 2009).

Another angle worth discussing is that of fisheries-induced adaptive changes. Statistical, experimental, and modelling approaches are giving increasing support to the hypothesis that fishing causes evolutionary shifts in life-history traits (Jørgensen et al. 2007; Dunlop et al. 2009; Sharpe and Hendry 2009). Because these changes typically involve reduced adult body size (Heino 1998; Enberg et al. 2011), size-dependent pricing is relevant also when trying to estimate the possible economic impacts of fisheries-induced evolution.

To conclude, this study has highlighted that size-dependent pricing has important implications for fisheries management. Because markets usually value large fish more than small fish, harvest strategies should consider how the harvest influences size structure of the catch: the higher the harvest pressure, the lower the mean size of fish. Therefore, harvest policies that aim at maintaining harvest of large-sized fish lead to lower harvest levels than those that ignore the quality of the catch; ultimately, this might lead to more sustainable harvest and increased economic benefits from the fisheries.

We encourage further explorations into consequences of size-dependent pricing on fisheries management, both in the direction of further generalizations and towards more detailed studies on specific fish stocks and fisheries.

Acknowledgements

We thank C. Jørgensen and Ø. Fiksen for discussions, two reviewers for helpful comments, P. Sandberg at the Norwegian Directorate of Fisheries for providing the price data, and the Norwegian Research Council for funding (184951/S40). MH and FZ also acknowledge funding from the Bergen Research Foundation.

References

Agnew, D.J., Pearce, J., Pramod, G., Peatman, T., Watson, R., Beddington, J.R., and Pitcher, T.J. 2009. Estimating the worldwide extent of illegal fishing. PLoS ONE, **4**(2): e4570. doi:10.1371/journal.pone.0004570. PMID:19240812.

Anderson, L.G. 1989. Optimal intra- and interseasonal harvesting strategies when price varies with individual size. Mar. Resour. Econ. **6**(2): 145–162.

Asche, F., and Guttormsen, A.G. 2001. Patterns in the relative price for different sizes of farmed fish. Mar. Resour. Econ. **16**(3): 235–248.

Beddington, J.R., Agnew, D.J., and Clark, C.W. 2007. Current problems in the management of marine fisheries. Science, **316**(5832): 1713–1716. doi:10.1126/science.1137362. PMID:17588923.

Beverton, R., and Holt, S. 1957. On the dynamics of exploited fish populations. Fish. Invest. London Ser. 2. Ministry of Agriculture, Fisheries and Food, London.

Birkeland, C., and Dayton, P. 2005. The importance in fishery management of leaving the big ones. Trends Ecol. Evol. **20**(7): 356–358. doi:10.1016/j.tree.2005.03.015. PMID:16701393.

Bjørndal, T. 1988. Optimal harvesting of farmed fish. Mar. Resour. Econ. **5**: 139–159.

Clark, C. 2006. The worldwide crisis in fisheries: economic models and human behavior. Cambridge University Press, Cambridge, UK.

De Leo, G.A., and Gatto, M. 2001. A stochastic bioeconomic analysis of silver eel fisheries. Ecol. Appl. **11**(1): 281–294. doi:10.1890/1051-0761(2001)011[0281:ASBAOS]2.0.CO;2.

Diekert, F.K., Hjermann, D., Nævdal, E., and Stenseth, N.C. 2010. Spare the young fish: optimal harvesting policies for north-east Arctic cod. Environ. Resour. Econ. **47**(4): 455–475. doi:10.1007/s10640-010-9388-z.

Dunlop, E.S., Enberg, K., Jørgensen, C., and Heino, M. 2009. Toward Darwinian fisheries management. Evol. Appl. **2**(3): 245–259. doi:10.1111/j.1752-4571.2009.00087.x.

Enberg, K., Jørgensen, C., Dunlop, E.S., Varpe, Ø., Boukal, D.S., Baulier, L., Eliassen, S., and Heino, M. 2011. Fishing-induced evolution of growth: concepts, mechanisms, and the empirical evidence. Mar. Ecol. [In press.] doi: 10.1111/j.1439-0485.2011.00460.x.

Fiksen, Ø., and Slotte, A. 2002. Stock–environment recruitment models for Norwegian spring spawning herring (*Clupea harengus*). Can. J. Fish. Aquat. Sci. **59**(2): 211–217. doi:10.1139/f02-002.

Francis, R., Hixon, M., Clarke, M., Murawski, S., and Ralston, S. 2007. Ten commandments for ecosystem-based fisheries scientists. Fisheries, **32**(5): 217–233.

Gallagher, C., Hannah, R., and Sylvia, G. 2004. A comparison of yield per recruit and revenue per recruit models for the Oregon ocean shrimp, *Pandalus jordani*, fishery. Fish. Res. **66**(1): 71–84. doi:10.1016/S0165-7836(03)00147-4.

Grafton, R.Q., Kompas, T., and Hilborn, R.W. 2007. Economics of overexploitation revisited. Science, **318**(5856): 1601. doi:10.1126/science.1146017. PMID:18063793.

Heino, M. 1998. Management of evolving fish stocks. Can. J. Fish. Aquat. Sci. **55**(8): 1971–1982. doi:10.1139/f98-089.

Helser, T.E., and Brodziak, J.K.T. 1998. Impacts of density-dependent growth and maturation on assessment advice to rebuild depleted U.S. silver hake (*Merluccius bilinearis*) stocks. Can. J. Fish. Aquat. Sci. **55**(4): 882–892. doi:10.1139/f97-290.

Helser, T.E., Thunberg, E.M., and Mayo, R.K. 1996. An age-structured bioeconomic simulation of U.S. silver hake fisheries. N. Am. J. Fish. Manage. **16**(4): 783–794. doi:10.1577/1548-8675(1996)016<0783:AASBSO>2.3.CO;2.

Hilborn, R., and Walters, C. 1992. Quantitative fisheries stock assessment: choice, dynamics, and uncertainty. Chapman & Hall, New York.

Holland, D.S., Bentley, N., and Lallemand, P. 2005. A bioeconomic analysis of management strategies for rebuilding and maintenance of the NSS rock lobster (*Jasus edwardsii*) stock in southern New Zealand. Can. J. Fish. Aquat. Sci. **62**(7): 1553–1569. doi:10.1139/f05-059.

ICES. 2010. Report of the Working Group on Widely Distributed Stocks (WGWIDE). ICES CM 2010/ACOM:15. International Council for the Exploration of the Sea, Copenhagen, Denmark.

Jørgensen, C., Enberg, K., Dunlop, E.S., Arlinghaus, R., Boukal, D.S., Brander, K., Ernande, B., Gårdmark, A., Johnston, F., Matsumura, S., Pardoe, H., Raab, K., Silva, A., Vainikka, A., Dieckmann, U., Heino, M., and Rijnsdorp, A.D. 2007. Managing evolving fish stocks. Science, **318**(5854): 1247–1248. doi:10.1126/science.1148089. PMID:18033868.

Katsukawa, T. 2005. Evaluation of current and alternative fisheries management scenarios based on spawning-per-recruit (SPR), revenue-per-recruit (RPR), and yield-per-recruit (YPR) diagrams. ICES J. Mar. Sci. **62**(5): 841–846. doi:10.1016/j.icesjms.2005.04.002.

Larkin, S.L., and Sylvia, G. 1999. Intrinsic fish characteristics and intraseason production efficiency: a management-level bioeconomic analysis of a commercial fishery. Am. J. Agric. Econ. **81**(1): 29–43. doi:10.2307/1244448.

Lorenzen, K., and Enberg, K. 2002. Density-dependent growth as a key mechanism in the regulation of fish populations: evidence from among-population comparisons. Proc. Biol. Sci. **269**(1486): 49–54. doi:10.1098/rspb.2001.1853. PMID:11788036.

Mora, C., Myers, R.A., Coll, M., Libralato, S., Pitcher, T.J., Sumaila, R. U., Zeller, D., Watson, R., Gaston, K.J., and Worm, B. 2009. Management effectiveness of the world's marine fisheries. PLoS Biol. **7**(6): e1000131. doi:10.1371/journal.pbio.1000131. PMID:19547743.

Norges Sildesalgslaget. 2011. Norges Sildesalgslaget [online]. Available from http://www.sildelaget.no [accessed 10 April 2011].

R Development Core Team. 2010. R: a language and environment for statistical computing. R Foundation for Statistical Computing, Vienna, Austria.

Sandberg, P. 2006. Variable unit costs in an output-regulated industry: the fishery. Appl. Econ. **38**(9): 1007–1018. doi:10.1080/00036840500405912.

Sharpe, D.M.T., and Hendry, A.P. 2009. Life history change in commercially exploited fish stocks: an analysis of trends across studies. Evol. Appl. **2**(3): 260–275. doi:10.1111/j.1752-4571.2009.00080.x.

Skjoldal, H.R., Sætre, R., Fernø, A., Misund, O.A., and Røttingen, I. 2004. The Norwegian Sea ecosystem. Tapir Forlag, Trondheim, Norway.

Tahvonen, O. 2009. Optimal harvesting of age-structured fish populations. Mar. Resour. Econ. **24**(2): 281–299.

Thunberg, E., Helser, T., and Mayo, R. 1998. Bioeconomic analysis of alternative selection patterns in the United States Atlantic silver hake fishery. Mar. Resour. Econ. **13**: 51–74.

Tietenberg, T., and Lewis, L. 2008. Environmental and natural resource economics. Addison Wesley, Boston, Mass.

Touzeau, S., Lindroos, M., Kaitala, V., and Ylikarjula, J. 2000. Economic and biological risk analysis of the Norwegian spring-spawning herring fishery. Ann. Oper. Res. **94**(1–4): 197–217. doi:10.1023/A:1018973217951.

Appendix A

Table A1. List of parameters and their values.

			Value	
Parameter	Definition	Unit	Herring	Mackerel
n	Maximum age class[a]	year	15	12
M_a	Natural mortality[a]	year^{-1}	$\begin{cases} 0.9 \\ 0.15 \\ 0.5 \end{cases}$ for $a = \begin{cases} a \leq 2 \\ 2 < a < n \\ n \end{cases}$	0.15
b_1	Asymptotic recruitment[b]	—	1.9×10^{11}	—
b_2	Steepness of recruitment function[b]	kg	5.1×10^{9}	—
b_3	Initial slope of recruitment function[a]	kg^{-1}	—	1.811
$r_{\max}$	Maximum recruitment[a]	—	—	4.252×10^{9}
L_{∞}	Asymptotic length[c]	mm	370	418
k	von Bertalanffy growth parameter[c]	year^{-1}	0.26	0.43
v	Length–mass coefficient[c]	kg·mm^{-u}	2.32×10^{-5}	3.4×10^{-3}
u	Length–mass exponent	—	2.81	3.24
a_{50}	Age at 50% maturity[a]	year	4	3
a_{width}	Width of maturity envelope	year	0.3	0.2
η	Selectivity parameter[a]	—	4.3	3.3
β_0	Price function slope[d]	NOK·kg^{-1}	2.43	8.97
$\overline{w}$	Mean catch mass[a,d]	kg	0.235	0.454
C_0	Fixed costs[e]	NOK	3.4×10^{5}	3.4×10^{5}
υ	Cost function slope[f]	NOK·kg^{-1}	0.7	0.7

[a] ICES 2010.

[b] Fiksen and Slotte 2002.

[c] Jennings and Beverton 1991.

[d] Norwegian Directorate of Fisheries (P. Sandberg, Fiskeridirektoratet, Postboks 185 Sentrum, 5804 Bergen, Norway, personal communication, 2011).

[e] Touzeau et al. 2000.

[f] Froese and Pauly 2009.

References

Fiksen, O., and Slotte, A. 2002. Stock–environment recruitment models for Norwegian spring spawning herring (*Clupea harengus*). Can. J. Fish. Aquat. Sci. **59**(2): 211–217. doi:10.1139/f02-002.

Froese, R., and Pauly, D. 2009. FishBase. Available from www.fishbase.org [accessed 14 March 2009].

ICES. 2010. Report of the Working Group on Widely Distributed Stocks (WGWIDE). ICES CM 2010/ACOM:15. International Council for the Exploration of the Sea, Copenhagen, Denmark.

Jennings, S., and Beverton, R. 1991. Intraspecific variation in the life history tactics of Atlantic herring (*Clupea harengus* L.) stocks. ICES J. Mar. Sci. **48**(1): 117–125. doi:10.1093/icesjms/48.1.117.

Touzeau, S., Lindroos, M., Kaitala, V., and Ylikarjula, J. 2000. Economic and biological risk analysis of the Norwegian spring-spawning herring fishery. Ann. Oper. Res. **94**(1–4): 197–217. doi:10.1023/A:1018973217951.

Potential climate change impacts on thermal habitats of Pacific salmon (*Oncorhynchus* spp.) in the North Pacific Ocean and adjacent seas

Omar I. Abdul-Aziz, Nathan J. Mantua, and Katherine W. Myers

Abstract: We developed spatially explicit representations for seasonal high-seas (open ocean) thermal habitats for six species of Pacific salmon (*Oncorhynchus* spp.) and evaluated the effects of natural climate variability and projected changes under three Intergovernmental Panel on Climate Change scenarios of future greenhouse gas emissions. Changes in high-seas habitat due to natural climatic variation in 20th century were small relative to that under anthropogenic climate change scenarios for the middle to late 21st century. Under a multimodel ensemble average of global climate model outputs using A1B (medium) emissions scenario for the entire study area (North Pacific and part of Arctic Ocean), projected winter habitats of sockeye (*Oncorhynchus nerka*) decreased by 38%, and summer habitat decreased by 86% for Chinook (*Oncorhynchus tshawytscha*), 45% for sockeye, 36% for steelhead (*Oncorhynchus mykiss*), 30% for coho (*Oncorhynchus kisutch*), 30% for pink (*Oncorhynchus gorbuscha*), and 29% for chum (*Oncorhynchus keta*) salmon by 2100. Reductions were 25% lower for B1 (lower) emissions and 7% higher for A2 (higher) emissions scenarios. Projected habitat losses were largest in the Gulf of Alaska and western and central subarctic North Pacific. Nearly complete losses of Gulf of Alaska habitat for sockeye in both seasons and Chinook in summer raise important policy issues for North American fishery managers and governments.

Résumé : Nous mettons au point des représentations spatialement explicites des habitats thermiques saisonniers de haute-mer (au large) de six espèces de saumons du Pacifique (*Oncorhynchus* spp.) et évaluons les effets de la variabilité climatique naturelle et des changements prévus dans trois scénarios d'émissions futures de gaz à effets de serre produits par le Panel intergouvernemental sur le changement climatique. Les changements dans l'habitat de haute-mer dus à la variation climatique naturelle au 20^{ième} siècle sont faibles par comparaison aux scénarios de changements climatiques anthropiques prédits pour le milieu et la fin du 21^{e} siècle. Dans la moyenne d'un ensemble multi-modèles de projections faites par des modèles de climat global, utilisant le scénario A1B (moyen) pour les émissions dans l'ensemble de la région (Pacifique Nord et partie de l'Océan Arctique), les habitats d'hiver prédits pour le saumon rouge (*Oncorhynchus nerka*) diminuent de 38 % et les habitats d'été sont réduits de 86 % pour le saumon chinook (*Oncorhynchus tshawytscha*), 45 % pour le saumon rouge, 36 % pour la truite arc-en-ciel anadrome (*Oncorhynchus mykiss*), 30 % pour le saumon coho (*Oncorhynchus kisutch*), 30 % pour le saumon rose (*Oncorhynchus gorbuscha*) et 29 % pour le saumon kéta (*Oncorhynchus keta*) vers l'année 2100. Les réductions sont 25 % plus basses avec le scénario B1 (plus faible) d'émissions et 7 % plus fortes pour le scénario (plus élevé) A2. Les pertes prédites d'habitat sont les plus importantes dans le golfe de l'Alaska et les portions ouest et centrales du Pacifique Nord arctique. Les pertes presque complètes de l'habitat pour le saumon rouge dans le golfe de l'Alaska pendant les deux saisons et pour le saumon chinook en été représentent des problèmes importants de politique pour les gouvernements et les gestionnaires des pêches en Amérique du Nord.

[Traduit par la Rédaction]

Introduction

Scenarios for potential changes in ocean distributions of economically important species of fish such as Pacific salmon (*Oncorhynchus* spp.) can contribute valuable information to natural resource policy design and management (Schindler et al. 2008). The high-seas (open ocean) waters of the North Pacific Ocean and its adjacent seas provide vast summer foraging and overwintering habitats for most major species and stocks of Pacific salmon. As visual foragers, salmon in the open

Received 19 April 2010. Accepted 9 May 2011. Published at www.nrcresearchpress.com/cjfas on 6 September 2011.
J2011-0141

Paper handled by Associate Editor Michael Bradford.

O.I. Abdul-Aziz* and N.J. Mantua. School of Aquatic and Fishery Sciences, University of Washington, 1122 Boat Street, Box 355020, Seattle, WA 98195-5020, USA; Climate Impacts Group, Joint Institute for the Study of the Atmosphere and Ocean (JISAO), University of Washington, 3737 Brooklyn Avenue NE, Box 355672, Seattle, WA 98105-5672, USA.
K.W. Myers. School of Aquatic and Fishery Sciences, University of Washington, 1122 Boat Street, Box 355020, Seattle, WA 98195-5020, USA.

Corresponding author: Omar I. Abdul-Aziz (e-mail: oabdulaz@fiu.edu).

*Present address: Department of Civil and Environmental Engineering, Florida International University, 10555 W Flagler Street, Miami, FL 33174, USA.

Can. J. Fish. Aquat. Sci. **68**: 1660–1680 (2011) doi:10.1139/F2011-079 Published by NRC Research Press

ocean exhibit diurnal patterns of vertical migration, largely within the surface layer (0–60 m depth) during daylight hours, while they remain at or near the ocean surface at night (Sakai et al. 1997; Walker et al. 2007). Because anthropogenic climate change is predicted to substantially increase upper ocean temperatures globally in the 21st century (Intergovernmental Panel on Climate Change 2007), a reasonable assumption is that future increases in sea surface temperatures (SSTs) will affect open ocean distributions of salmon.

In pioneering research on the potential effects of anthropogenic climate warming on the high-seas distributions of Pacific salmon, Welch et al. (1995, 1998*a*, 1998*b*) argued for sharp upper thermal limits in the distribution of high-seas research vessel catches of salmon and speculated that thermal limits resulted from behavioral avoidance of salmon to bioenergetically unfavorable temperatures. Upper ocean temperatures are known to impact the metabolic rates and aerobic scope for salmon (Pörtner and Farrell 2008). Welch et al.'s (1998*a*, 1998*b*) analyses identified a substantial northward shift of the warmest (i.e., southern) thermal boundary and a potential exclusion of sockeye salmon (*Oncorhynchus nerka*) from the entire North Pacific Ocean in summer, as well as a substantial reduction in thermal habitat of steelhead trout (*Oncorhynchus mykiss*), by the middle of the 21st century under an equilibrium climate change scenario with doubled atmospheric CO_2 concentrations. Azumaya et al. (2007) also used research vessel catch data to identify upper and lower thermal limits for five species of Pacific salmon. Under a scenario with a spatially uniform 1.5 °C warming of SST and 0.2 psu reduction in upper ocean salinity, they reported a northward shift in preferred high-seas salmon habitat in the North Pacific Ocean. Using the Intergovernmental Panel on Climate Change (IPCC) A1B (medium) greenhouse gas emissions scenario (Nakicenovic et al. 2000), Kaeriyama (2008) predicted a large reduction of chum salmon (*Oncorhynchus keta*) distributional area, resulting in a northward displacement towards the Arctic Ocean, as well as loss of migration routes in the Okhotsk Sea by the end of the 21st century.

Our objectives in this paper are to extend previous studies by developing spatially explicit representations of seasonal (summer and winter) thermal habitats for six species of Pacific salmon and to use the framework for evaluating and comparing the effects of natural interdecadal climate variability on these thermal habitats with that of anthropogenic climate warming through 2100.

Materials and methods

Study area and stratification of data

The study area included the North Pacific Ocean, Bering Sea, and part of the Arctic Ocean (Fig. 1*a*). The entire domain was divided into the five subdomains of Arctic Ocean, Bering Sea, Gulf of Alaska, Subarctic, and Okhotsk Sea (Fig. 1*b*). The Eastern Subarctic, as represented by the Gulf of Alaska, was separated from the rest of the Subarctic North Pacific because of the importance of the Gulf of Alaska region for North American salmon. The term "Subarctic", therefore, refers to the combined regions of Central and Western Subarctic. Our historical SST reference period was the 30-year average centered on the 1980s (1970–1999). Three 30-year average periods centered on the 2020s (2010–2039), 2040s (2030–2059), and 2080s (2070–2099) were used to evaluate the projected changes in temperatures and reference thermal habitats. The Pacific Decadal Oscillation (PDO) (Mantua et al. 1997) warm and cool phase eras of 1925–1946 (termed here as 1925s; warm), 1946–1976 (1947s; cool), and 1977–1997 (1977s; warm) were also considered to assess the impacts of natural, interdecadal climate variability on the historical, thermally defined high-seas habitat areas for Pacific salmon in the 20th century.

Observations and global climate models (GCMs)

Observed historical mean monthly SSTs were obtained from the National Oceanic and Atmospheric Administration's (NOAA) extended reconstructed SST (ersst version 3b) data (Smith et al. 2008). Simulated SSTs (mean monthly skin temperature data) for the "climate of the 20th century experiment (20c3m)", as well as for three warming scenarios of lower (SRES B1), medium (SRES A1B), and higher (SRES A2) greenhouse gas emissions, were obtained from the world wide web site of the Program for Climate Model Diagnosis and Intercomparison (PCMDI) (http://www-pcmdi.llnl.gov/). Further details on the greenhouse gas emissions scenarios can be found in Nakicenovic et al. (2000). The names, sources, climate sensitivities, and approximate spatial data resolutions of the 18 GCMs used in this study are presented (Table 1). As indicated, four GCMs did not provide SSTs for the A2 emissions scenario; therefore, only 14 models contributed to the A2 scenario multimodel average.

The observed, historical reference SST climatology of the 1980s was calculated by averaging SST time series at each grid cell for each calendar month within the 1970–1999 period. Likewise, historical mean monthly SSTs were calculated for the 1925s, 1947s, and 1977s. Multimodel average monthly SST projections for the 2020s, 2040s, and 2080s were calculated for each of the three emission scenarios (B1, A1B, and A2) after regridding and correcting projected SSTs for model biases.

Regridding and bias correction

Skin temperature is defined as the SST for "open ocean" in PCMDI's "IPCC standard output from coupled ocean-atmosphere GCMs" (table A1a; available at http://www-pcmdi.llnl.gov/ipcc/standard_output.html). Spatial resolution of the global, historical SST field was 2° × 2°, while model resolutions for the "surface skin temperature" simulations varied approximately from 1.4° × 1.4° to 4° × 5° (latitude by longitude). Processing of the SST projections of finer spatial resolutions from more detailed oceanographic model components of the GCMs is computationally more expensive and not rewarding here given the coarse resolution of the historical SST field and the open ocean focus of the paper. Defining the historical data resolution as the reference resolution, the time-averaged mean monthly SSTs of 2020s, 2040s, and 2080s were regridded to the 2° × 2° reference grids for consistency with the historical 1980s period (refer to Appendix A for details on the regridding algorithm used).

The regridded model SSTs were corrected for biases (the differences between model simulations and historical observations for the 30 year average centered on the 1980s) of all individual GCMs. Because each GCM has unique biases in simulated SST fields, we use a simple delta method to com-

Fig. 1. Study area representing (*a*) the North Pacific and Arctic oceans and (*b*) a coarse delineation of five subdomains within the whole domain using a historical 2° × 2° grid.

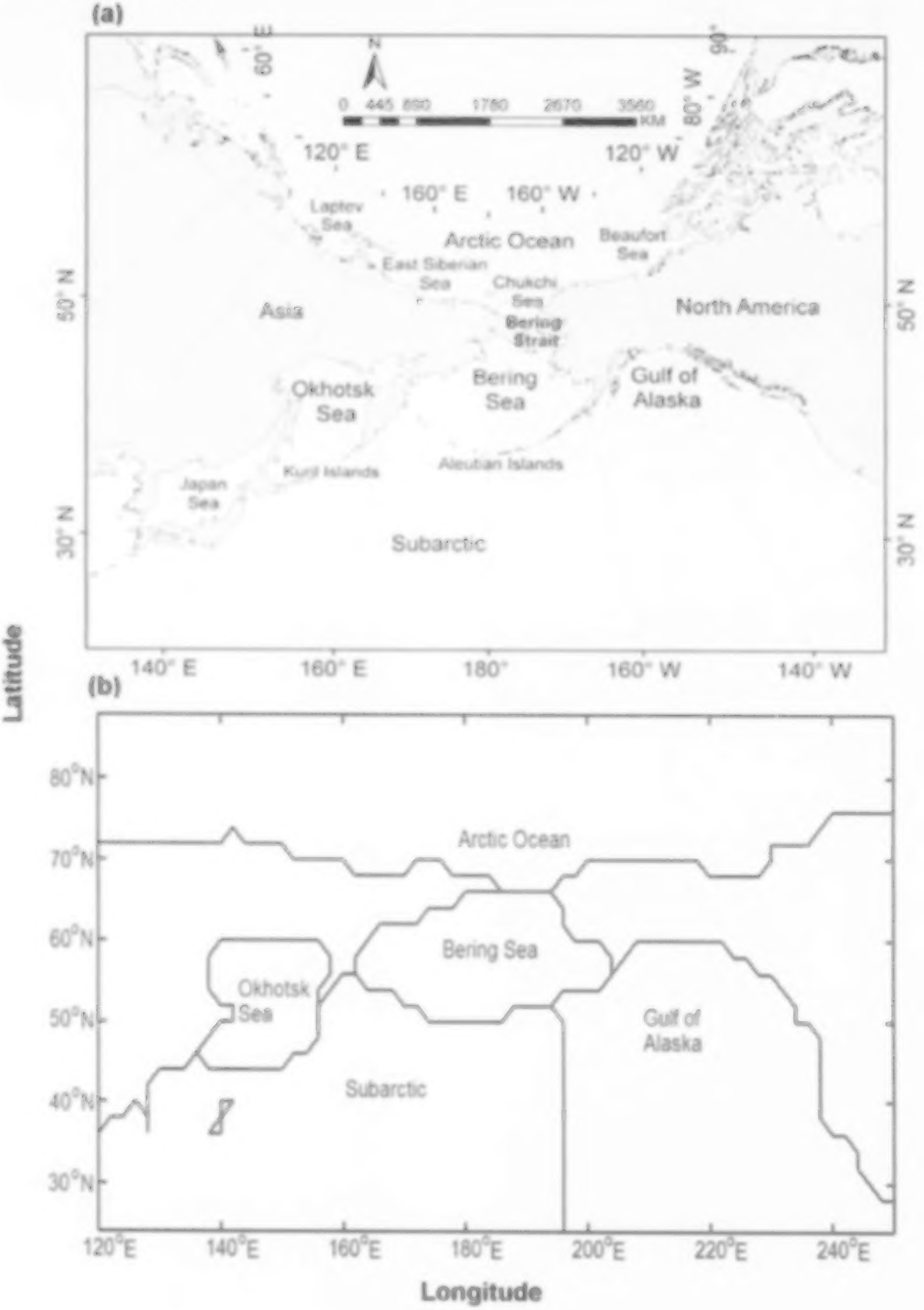
(a)
N
0 445 890 1780 2670 3560 KM
60° E
90° W
80° W
120° E
120° W
160° E
160° W
Laptev Sea
Arctic Ocean
Beaufort Sea
East Siberian Sea
Chukchi Sea
Bering Strait
Asia
North America
Okhotsk Sea
Bering Sea
Gulf of Alaska
Kuril Islands
Aleutian Islands
Japan Sea
Subarctic
50° N
30° N
140° E
160° E
180°
160° W
140° W
Latitude
(b)
80°N
70°N
60°N
50°N
40°N
30°N
Arctic Ocean
Bering Sea
Okhotsk Sea
Gulf of Alaska
Subarctic
120°E
140°E
160°E
180°E
200°E
220°E
240°E
Longitude

Table 1. List of global climate models (GCMs) for sea surface temperature simulation outputs used in the study.

Model	Source	TCR (°C)*	Resolution (Lat. × Long.)[†]
BCCR-BCM2.0	University of Bergen, Norway	NA	2.8° × 2.8°
CCSM3[‡]	University Corporation for Atmospheric Research, USA	1.5	1.4° × 1.4°
CGCM (T47)	Centre for Climate Modelling and Analysis, Canada	1.9	3.75° × 3.75°
CGCM (T63)[‡]	Centre for Climate Modelling and Analysis, Canada	NA	2.8° × 2.8°
CNRM (CM3)	Centre National de Recherches Météorologiques, France	1.6	2.8° × 2.8°
CSIRO (Mk3.5d)	Commonwealth Scientific and Industrial Research Organisation, Australia	1.4	1.9° × 1.9°
ECHAM5	Max Planck Institute for Meteorology, Germany	2.2	1.9° × 1.9°
ECHO-G	University of Bonn, Germany	1.7	3.75° × 3.75°
FGOALS[‡]	Institute of Atmospheric Physics, China	1.2	3.0° × 2.8°
GFDL-CM2.0	Geophysical Fluid Dynamics Laboratory, USA	1.6	2.0° × 2.5°
GFDL-CM2.1	Geophysical Fluid Dynamics Laboratory, USA	1.5	2.0° × 2.5°
GISS-AOM (c4×3)[‡]	Goddard Institute for Space Studies, USA	NA	3.0° × 4.0°
GISS-ER	Goddard Institute for Space Studies, USA	1.5	3.9° × 5.0°
HADCM3	Met Office, Exeter, UK	2.0	2.5° × 3.75°
INMCM3.0	Institute for Numerical Mathematics, Russia	1.6	4.0° × 5.0°
IPSL	Institut Pierre Simon Laplace, France	2.1	2.5° × 3.75°
MIROC-medres	Center for Climate System Research – National Institute for Environmental Studies – Frontier Research Center for Global Change, Japan	2.1	2.8° × 2.8°
PCM	National Center for Atmospheric Research (NCAR), USA	1.3	2.8° × 2.8°

*Transient climate response (TCR) is a measure of modeled climate sensitivity. It is defined as the global mean temperature change at the time of CO_2 doubling when CO_2 is increased at a rate of 1% per year in a simulation (Randall et al. 2007).

[†] GCMs' atmospheric model component resolutions are approximate and given in order of latitude (Lat.) × longitude (Long.). Resolutions vary from approximately 1.4° × 1.4° to 4° × 5°.

[‡] CCSM3, CGCM (T63), FGOALS, and GISS-AOM did not provide SST projections for A2 scenario.

Table 2. Thermal limits for Pacific salmon based on high-seas data from the North Pacific Ocean and adjacent seas.

		Frequently observed range (°C)	
Major salmon species	Absolute range (°C; all seasons)	Spring–Summer–Fall (April–October)	Winter (November–March)
Sockeye (*O. nerka*)	1.0–17.3*, 3.3–13.3^{a}, 4.0–17.3^{c}, >1–17.3^{f}	**1–12**, 1–10^{f}, 2–7^{m}, –12^{h}, 3–9^{j}	**1.5–7**, 1.5–6^{e}, 2–6^{a}, –7^{b}
Chum (*O. keta*)	0–15.6*, 2.7–15.6^{e}, 0–15^{c}	**1–13**^{m}, 3–11^{f,n}, 8–12^{d}	**1.5–10**^{r}
Pink (*O. gorbuscha*)	2.8–17*, 2.8–16.6^{e}, 3–17^{f,a}	**3–13**^{m}, 4–11^{l}, 3–11^{f}	**3.5–8.5**^{r}
Coho (*O. kisutch*)	3–16.9^{*,a,h}, 3.7–15.7^{a}	**6–13**^{f}, 8–12^{h}, 7–12^{f}, 7–11^{m}	**5.5–9**^{r}
Chinook (*O. tshawytscha*)	1–18.5^{*,h,i}, –13.4^{a}	**1–10**, 7–10^{f}, 6–8^{i}, 4–10^{j}, 1–9^{m}	**1.5–12**, 1.5^{r}, –12^{s}
Steelhead (*O. mykiss*)	2.8–15.8^{*,j,k}	**6–12.5**, 8–11.4^{e}, 6–10^{f}, 7–11^{l}, 6–11.9^{k}, 7–12.5^{r}	**5–11**^{r}

Note: Lower and upper limits, respectively, refer to the coldest and warmest thermal limits. A single temperature with a dash in front indicates the upper limit of a range. All ranges mainly represent high-seas data. The reference ranges for mapping and analyses in this study were chosen from the most observed ranges and are highlighted in bold font. Superscript letters indicate the following sources of data: ^{a}Azumaya et al. (2007); ^{b}Welch et al. (1998*a*); ^{c}Welch et al. (1998*b*); ^{d}Kaeriyama (2008); ^{e}Walker et al. (2000*a*, 2000*b*); ^{f}Manzer et al. (1965); ^{g}Myers and Bernard (1993); ^{h}Godfrey et al. (1975); ^{i}Major et al. (1978); ^{j}Okazaki (1983); ^{k}Burgner et al. (1992); ^{l}Takagi (1983); ^{m}Ogura and Takagi (1987); ^{n}Neave et al. (1976); ^{o}Sutherland (1973); ^{p}Birman (1960); ^{q}French et al. (1976); ^{r}Katherine Myers (2009, unpublished data); ^{s}Hinke et al. (2005).

*Overall range.

pute model-specific changes in SSTs relative to each model's own reference climatology for the simulated 1980s (1970–1999) as obtained from their respective 20c3m experiments. Then, the multimodel average changes of monthly SSTs in different future periods relative to the 1980s were obtained by the ensemble averages of changes from 14 models for A2 scenario and 18 models for both B1 and A1B scenarios. The final bias-corrected mean monthly SST projections for each of the different periods and scenarios were constructed by adding the respective ensemble-average changes in mean monthly SSTs to the observed, historical mean monthly SSTs of 1980s.

Reference ocean thermal limits for Pacific salmon

High-seas salmon survey data collected over the last 50 years were used to identify reference thermal limits for different species of Pacific salmon. The sources and reported absolute (all seasons), as well as frequently observed, thermal ranges for spring through fall (April through October) and winter (November through March) seasons are presented (Table 2). Lower and upper limits, respectively, refer to the coldest (northern) and warmest (southern) thermal limits. To evaluate the historical changes and potential impacts of future anthropogenic warming on high-seas salmon habitat, we subjectively selected species-specific sets of "frequently observed" thermal ranges as reference ranges for mapping and analyses in this study. It is important to recognize that these thermal limits should not be taken as definitive boundaries for high-seas salmon habitat; instead, we choose these to in-

Table 3. Nondimensional sensitivity coefficients (percent changes in parentheses) in 1980s reference habitat areas for 1 °C increase in respective reference limits.

Limit	Sockeye	Chum	Pink	Coho	Chinook	Steelhead
July						
Coldest	–0.01 (–0.6%)	–0.01 (–0.6%)	–0.01 (–0.5%)	–0.12 (–2.1%)	–0.01 (–0.9%)	–0.13 (–2.2%)
Warmest	1.09 (9.1%)	1.24 (9.5%)	1.26 (9.7%)	1.28 (9.8%)	1.95 (19.5%)	0.90 (7.2%)
December						
Coldest	–0.18 (–11.8%)	–0.12 (–7.8%)	–0.58 (–16.7%)	–2.03 (–36.9%)	–0.10 (–6.6%)	–1.12 (–22.4%)
Warmest	1.30 (18.5%)	1.22 (12.2%)	1.57 (18.4%)	2.03 (22.6%)	1.05 (8.8%)	0.93 (8.4%)

vestigate the sensitivity of habitat areas for different species under historical climate variations and different future climate scenarios. The selected reference spring–summer–fall and winter ranges were, respectively, 1–12 and 1.5–7 °C for sockeye salmon, 1–13 and 1.5–10 °C for chum salmon, 3–13 and 3.5–8.5 °C for pink salmon (*Oncorhynchus gorbuscha*), 6–13 and 5.5–9 °C for coho salmon (*Oncorhynchus kisutch*), 1–10 and 1.5–12 °C for Chinook salmon (*Oncorhynchus tshawytscha*), and 6–12.5 and 5–11 °C for steelhead. Reference thermal habitats for different species in different seasons and periods were determined by applying these reference limits to the different SST fields (historical versus future scenarios).

The habitat ranges and areas for July and December are presented in this study as examples of those in summer and winter seasons, respectively. The computer codes for data analysis and area determination were written in a MATLAB platform (The MathWorks Inc., Natick, Massachusetts). SST contour (i.e., isotherms) and salmon range change maps were produced in an ArcGIS9.3 platform using Albers equal area conic projection. The reference habitat areas were obtained by summing the areas of the reference grids representing the respective reference temperature ranges.

Results

Sensitivity of reference limits

The reference July and December habitat areas of 1980s for different species were obtained from the total cell areas of the corresponding mean July and December SST fields (ersst averaged over 1970–1999) satisfying the respective reference thermal ranges (Table 2). For each species, the sensitivity of the habitat areas to the specified thermal boundaries was determined by the percent changes in the respective 1980s July and December habitat areas by separately increasing and decreasing one of the thermal limits at a time (i.e., either the warmest or coldest limit) by 1 °C while keeping the other limit unchanged. The ratios of the corresponding percent changes in the habitat areas and reference limits were defined as the sensitivity coefficients (Abdul-Aziz et al. 2010), which are nondimensional and show both the magnitude and direction of the sensitivity rates. Since both 1 °C increase and decrease resulted in similar estimates of sensitivity coefficients, we only reported sensitivity results obtained with the case of 1 °C increase in the thermal limits as examples (further details on sensitivity coefficients are given in Appendix A). Although these coefficients were calculated by increasing the thermal limits by 1 °C, they may be used to obtain the corresponding changes in habitat areas for any changes (both increases and decreases) in the thermal limits by applying appropriate multiplying factors.

For the change in the warmest thermal limits of July, Chinook salmon exhibited the highest sensitivity with a coefficient of 1.95, while the sensitivity of the other species ranged within 0.90 to 1.28 (Table 3). The 1980s July habitats of different species increased by around 7%–20% for a 1 °C increase in the warmest limits. However, they showed little sensitivity to a 1 °C increase in the coldest (northern) limits, leading to decreases of around 0.5%–2% in the respective 1980s habitat areas. This also indicated a limited region of habitat expansion to the north if the coldest thermal limits for July were decreased by 1 °C. The December 1980s habitat areas declined by 7%–37% for a 1 °C increase in the coldest (i.e., northern) reference temperatures, depending on the species. In this case, the sensitivity coefficient for coho salmon was –2.03, while that for the other species ranged from –0.10 to –1.12. An increase of 1 °C in the warmest limits for December showed sensitivity coefficients of 0.93 to 2.03 for all species, leading to increases of around 8%–23% in the 1980s December habitat areas.

Historical changes in reference ocean ranges and habitat areas of Pacific salmon

The ocean–atmosphere climate phenomenon of the PDO is expressed in part by basin-scale variations in North Pacific SSTs. The 20th century PDO variability has been shown to correspond with shifts in salmon production regimes in the North Pacific Ocean (Mantua et al. 1997; Hare et al. 1999). For evaluating the impacts of this natural interdecadal climate variability on high-seas habitat areas for Pacific salmon, historical July and December reference habitat ranges and areas of the six species were mapped and quantified for the warm (1925s: 1925–1946, and 1977s: 1977–1997) and cool (1947s: 1947–1976) PDO eras. The historical ranges of 1925s, 1947s, and 1977s are presented for July and December habitats (Figs. 2 and 3, respectively). The reference historical ranges of 1980s (i.e., 1970–1999) are not shown here, since they mostly coincided with those of 1977s. Both the July and December reference isotherms of different species generally showed very small displacements between the warm and cool PDO phases in the 20th century.

The reference historical July and December habitat areas of 1980s within the entire study area are presented (Table 4).

Fig. 2. Reference July thermal habitat ranges for six major species of Pacific salmon during the Pacific Decadal Oscillation (PDO) periods of 1925s, 1947s, and 1977s.

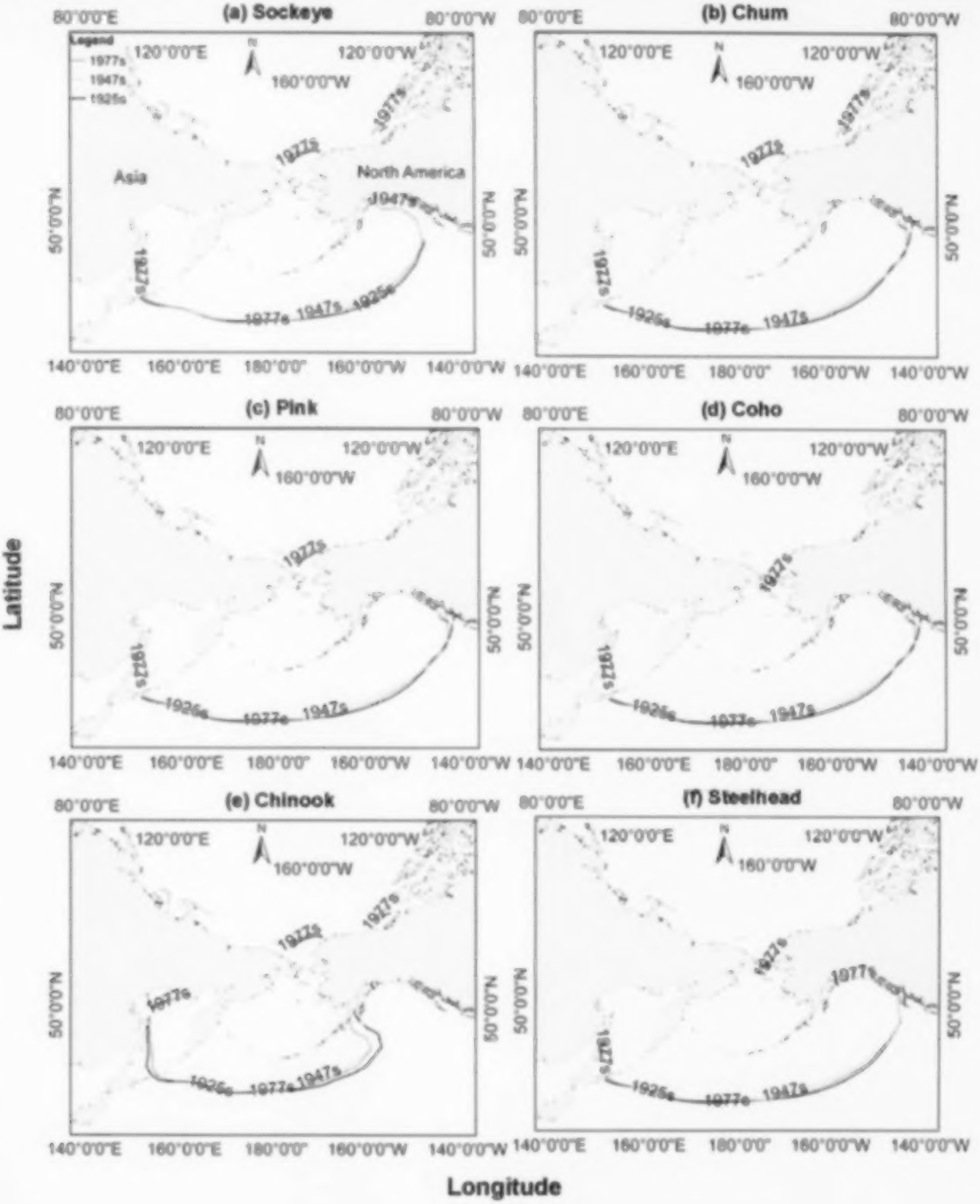
(a) Sockeye
(b) Chum
(c) Pink
(d) Coho
(e) Chinook
(f) Steelhead
Legend
1977s
1947s
1925s
Asia
North America
N
80°0'0"E
80°0'0"W
120°0'0"E
120°0'0"W
160°0'0"W
50°0'0"N
140°0'0"E
160°0'0"E
180°0'0"
160°0'0"W
140°0'0"W
1977s
1947s
1925s
Latitude
Longitude

Fig. 3. Reference December thermal habitat ranges for six major species of Pacific salmon during the Pacific Decadal Oscillation (PDO) periods of 1925s, 1947s, and 1977s.

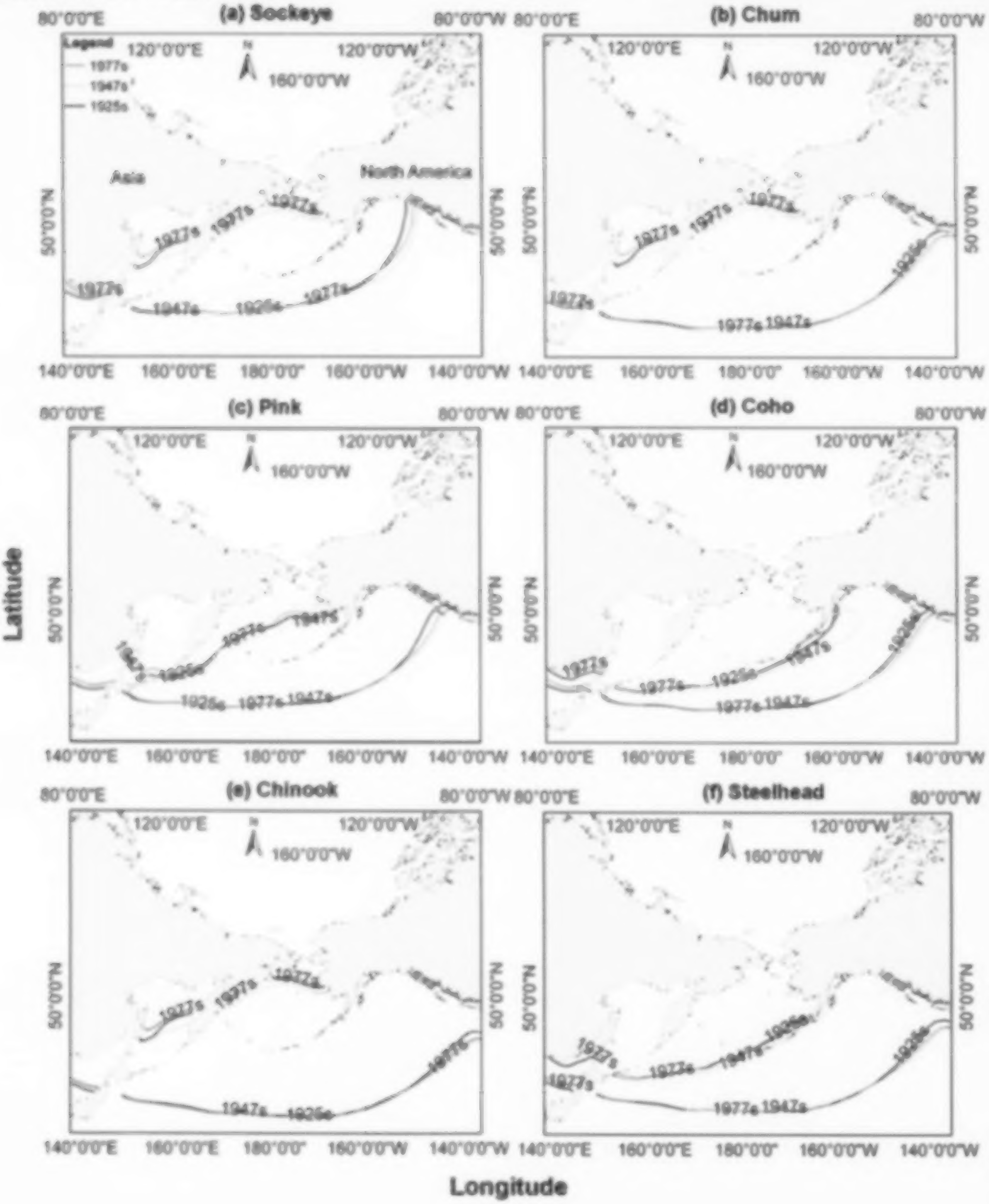
(a) Sockeye
(b) Chum
(c) Pink
(d) Coho
(e) Chinook
(f) Steelhead
Legend
1977s
1947s
1925s
Asia
North America
80°0'0"E
80°0'0"W
120°0'0"E
120°0'0"W
160°0'0"W
N
50°0'0"N
140°0'0"E
160°0'0"E
180°0'0"
160°0'0"W
140°0'0"W
1977s
1947s
1925s
Latitude
Longitude

Table 4. Changes in reference thermal habitat areas of Pacific salmon in the 20th century within the entire study area (North Pacific and Arctic oceans) during Pacific Decadal Oscillation (PDO) periods.

Time	Scenario	Sockeye	Chum	Pink	Coho	Chinook	Steelhead
July							
1980s	Hist. (million km^2)	10.06	10.98	10.80	10.63	6.98	10.23
	CV (%)	8	6	5	5	13	6
1925s	Hist. (%)	2	0	0	1	3	1
1947s	Hist. (%)	–3	–2	–2	–2	–3	–2
1977s	Hist. (%)	–3	–1	–1	–1	–1	–1
December							
1980s	Hist. (million km^2)	7.31	10.95	7.00	5.14	12.99	8.29
	CV (%)	5	4	6	11	4	7
1925s	Hist. (%)	–2	–1	–2	–1	–1	–4
1947s	Hist. (%)	–4	–5	–3	–9	–4	–7
1977s	Hist. (%)	1	1	2	1	0	1

Note: 1980s: 1970–1999; 1925s: 1925–1946; 1947s: 1947–1976; 1977s: 1977–1997. CV is the coefficient of variation defined as the standard deviation normalized by mean of the historical habitat areas. "Hist." refers to historical data.

Fig. 4. Potential increases in ensemble mean sea surface temperature (SST) of July and December in the North Pacific and Arctic oceans by 2040s and 2080s under IPCC A1B scenario relative to their observed counterparts in the 1980s historical period.

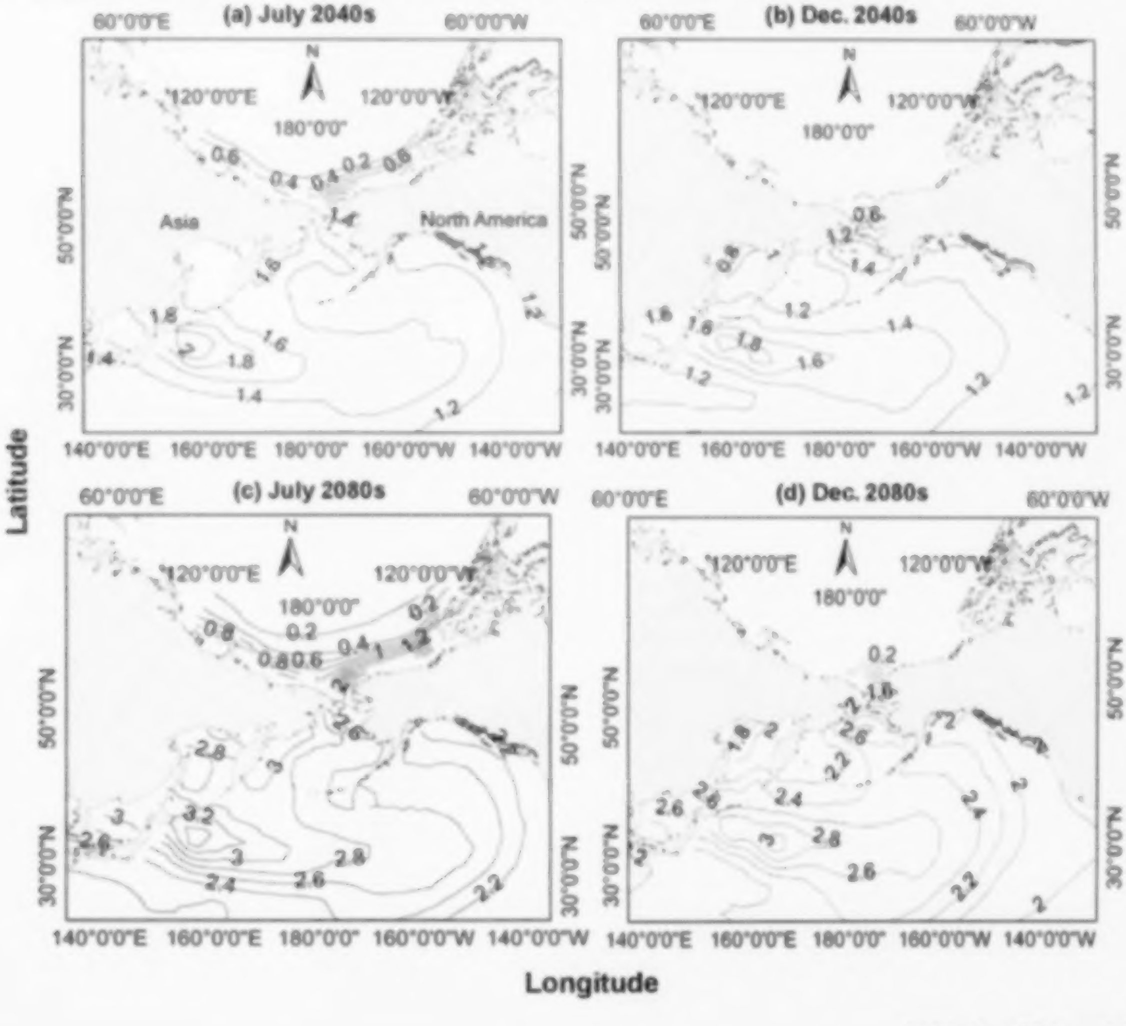
(a) July 2040s
(b) Dec. 2040s
(c) July 2080s
(d) Dec. 2080s
Asia
North America
N
60°0'0"E
60°0'0"W
120°0'0"E
120°0'0"W
180°0'0"
50°0'0"N
30°0'0"N
140°0'0"E
160°0'0"E
180°0'0"
160°0'0"W
140°0'0"W
Latitude
Longitude

Table 5. Projected changes (percent, based on multimodel averages) in reference thermal habitat areas of Pacific salmon in 21st century within the entire study area (North Pacific and Arctic oceans) under three IPCC climate change (i.e., greenhouse gas emissions) scenarios.

Time	Scenario	Sockeye	Chum	Pink	Coho	Chinook	Steelhead
July							
1980s	Hist. (million km^2)	10.06	10.98	10.80	10.63	6.98	10.23
	CV (%)	8	6	5	5	13	6
2020s	A2 (%)	–12	–5	–5	–5	–24	–8
	A1B (%)	–12	–5	–5	–5	–26	–8
	B1 (%)	–13	–7	–6	–7	–29	–10
2040s	A2 (%)	–18	–10	–10	–10	–41	–16
	A1B (%)	–20	–13	–13	–14	–48	–19
	B1 (%)	–18	–9	–9	–9	–40	–15
2080s	A2 (%)	–50	–31	–32	–33	–88	–43
	A1B (%)	–45	–29	–30	–30	–86	–36
	B1 (%)	–27	–20	–20	–21	–66	–24
December							
1980s	Hist. (million km^2)	7.31	10.95	7.00	5.14	12.99	8.29
	CV (%)	5	4	6	11	4	7
2020s	A2 (%)	–6	–2	3	2	0	–2
	A1B (%)	–7	–2	1	2	0	–1
	B1 (%)	–7	–2	1	2	0	–1
2040s	A2 (%)	–12	–7	–1	4	–4	–1
	A1B (%)	–16	–8	–2	3	–6	–1
	B1 (%)	–9	–4	0	5	–2	–2
2080s	A2 (%)	–41	–17	–10	4	–12	0
	A1B (%)	–38	–16	–10	–1	–10	–2
	B1 (%)	–24	–9	–6	0	–7	0

Note: 1980s: 1970–1999; 2020s: 2010–2039; 2040s: 2030–2059; 2080s: 2070–2099. CV is the coefficient of variation defined as the standard deviation normalized by mean of the historical habitat areas. "Hist." refers to historical data.

The species-specific coefficients of variation (CVs) of historical habitat areas during 1970–1999, as well as the percent differences of the respective habitat areas during the three PDO periods relative to the reference 1980s areas, are also shown. The habitat areas of each year during 1970–1999 for different species were calculated using the respective monthly SST fields and reference thermal ranges. A nonparametric, Lilliefors test (Conover 1980; Lilliefors 1967) for unknown population mean and variance showed that the null hypothesis of normal distribution of these species-specific historical areas (sample size = 30 for each season and species) could not be rejected at the 10% significance level. The CVs of the historical areas were obtained from the 30-year area time series as the standard deviations normalized by the respective means and are expressed in percent. The reference habitat areas during the PDO periods were calculated based on the mean (i.e., averaged over the respective periods) monthly SSTs from historical ersst fields and reference thermal ranges.

The magnitudes of changes in the PDO eras of the 20th century did not exceed the respective CVs for any species in July and for most species in December. Only the 1947s changes in December habitat relative to that of 1980s were either equal (for Chinook and steelhead) or marginally greater (for chum) than the respective CVs (Table 4). In general, the changes of habitat areas and ranges in the 20th century were within a few percent of the historical references of 1980s.

Projected changes in SST for the 2040s and 2080s

The GCM scenarios showed SST increases of up to ~3 °C by the 2080s, with the western North Pacific as well as the western and northern Bering Sea warming more than the other parts of the study domain (Fig. 4). Based on the median of SST increases over the entire study area, July and December temperatures were projected to increase by around 0.5 °C by 2020s and 1.0 °C by 2040s within the North Pacific and adjacent Arctic basins under all three emission scenarios. The A1B scenario showed median increases of around 2.0 °C both in July and December SSTs by 2080s. These projections were further corroborated by the plots of historical ersst and future SST changes at four North Pacific Ocean locations (Fig. 5). The 2080s increases in temperatures were around 12% higher for A2 and 31% lower for B1 scenarios, respectively, compared with those for A1B.

Potential changes in reference ocean ranges and habitat areas of Pacific salmon

Entire North Pacific and part of Arctic oceans

Potential changes in reference thermal habitat ranges and areas were quantified for all six salmon species under the lower (B1), medium (A1B), and higher (A2) greenhouse gas emission scenarios based on the reference thermal limits and the 30-year multimodel ensemble average SST fields for the future periods (Table 5). Range change maps for each species in July and December under the A1B emissions scenario are provided as examples (Figs. 6 and 7). These maps include isotherms that were developed based on the respective reference thermal limits for representing the reference historical

Fig. 5. Mean monthly sea surface temperatures (SSTs) in the 1980s (observed; solid line with boxes), 2040s (ensemble model; dotted line with circles), and 2080s (ensemble model; dotted line with squares) at North Pacific Ocean locations: (*a*) Bering Sea (54°N, 180°W), (*b*) Subarctic (44°N, 180°W), (*c*) Gulf of Alaska (54°N, 150°W), and (*d*) Okhotsk Sea (50°N, 150°E). Data for the future time frames represent the IPCC A1B (medium) emissions scenario. Boxes represent statistics of historical SSTs, with solid lines at the lower quartile, median, and upper quartile. Whiskers show the extent of SSTs within 1.5 times the interquartile ranges.

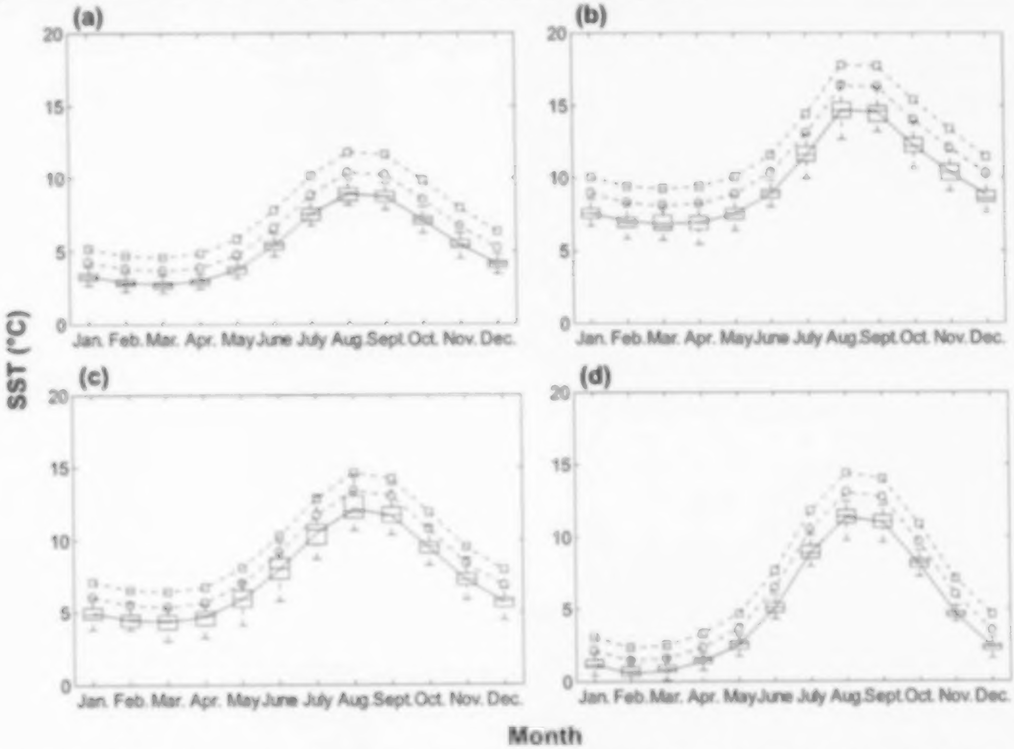

(1980s) ranges, as well as for identifying the projected future (2040s and 2080s) ranges. The future changes in thermal habitat ranges and areas of each species are described below. It should be noted that we treated the Gulf of Alaska separately from the rest of the Subarctic North Pacific (Central and Western Subarctic were together termed as "Subarctic") because of the importance of the Eastern Subarctic (represented by the Gulf of Alaska region) for North American salmon (Fig. 1*b*).

Sockeye salmon

The July 1980s habitat offered favorable thermal environment for sockeye salmon (Fig. 6*a*) from mid-latitudes of the Subarctic North Pacific in the south to the Beaufort, Chukchi, and Laptev seas in the Arctic Ocean in the north. The east–west expanse of this historical range extended from the Gulf of Alaska through the Okhotsk Sea. This range was projected to notably contract by the 2040s because of a northward movement of the warmest (southern) boundary, while the coldest (northern) boundary was little changed. By the 2080s, the warmest limit moved further northward towards the Bering Sea, essentially eliminating summertime favorable habitat from the Gulf of Alaska and substantially reducing the Subarctic and Okhotsk Sea habitats. A very small northern shift of the coldest boundary slightly increased reference habitat in the Arctic Ocean. The projected reductions in the overall July reference habitat for the 2080s were 50% under A2, 45% under A1B, and 27% under B1 scenarios (Table 5). Decreases were 12%–13% for the 2020s and 18%–20% for the 2040s under all three emission scenarios. Magnitudes of these reductions were much larger than the coefficient of variation (CV) of 8%, which refers to the standard deviation of potential habitat areas over the 1970–1999 period. Habitat reductions by the 2040s and 2080s were also higher than the equivalent percent changes of two standard deviations (i.e., 16%) and three standard deviations (i.e., 24%), respectively. The projected changes were, therefore, well beyond the range of historical experiences.

The December 1980s habitat for sockeye salmon (Fig. 7*a*) encompassed a relatively narrow east–west band that excluded the Arctic Ocean and included most of the Bering Sea and parts of the Gulf of Alaska, Subarctic North Pacific, and Okhotsk Sea. Both the warmest and coldest thermal boundaries showed large northward movements, leading to large habitat reductions by the 2040s and complete elimination by the 2080s in the Gulf of Alaska. Losses of available habitat areas in the Subarctic were large by the 2040s and substantial by the 2080s. However, large areas with favorable thermal regimes were developed in these future periods in the Okhotsk Sea through the northward shift of the coldest boundaries. The northward shift of the coldest boundary towards the Bering Strait opened up areas of new habitat in the Be-

Fig. 6. Reference July thermal habitat ranges in 1980s, 2040s, and 2080s for six major species of Pacific salmon under IPCC A1B (medium) emissions scenario.

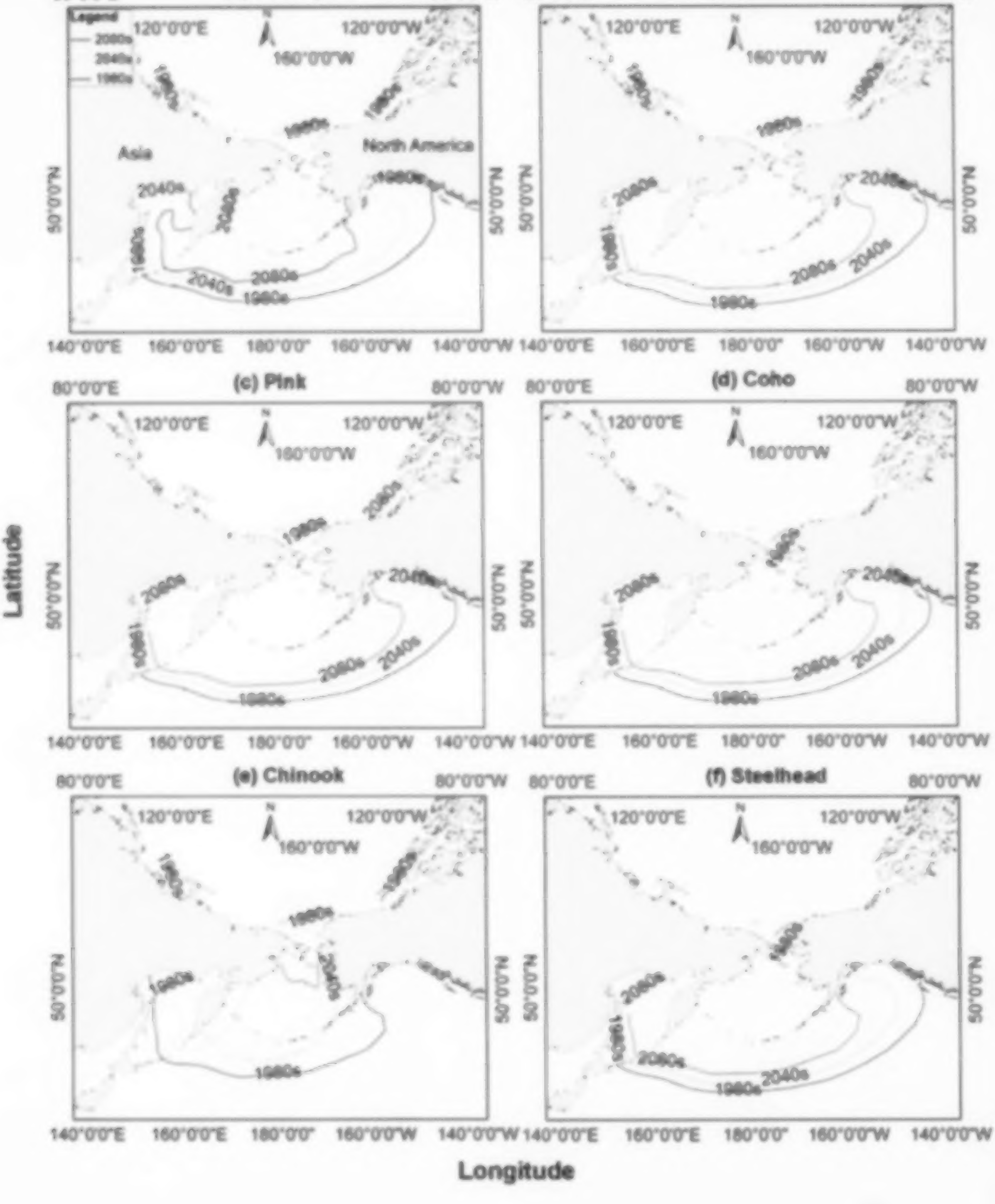
(a) Sockeye
(b) Chum
(c) Pink
(d) Coho
(e) Chinook
(f) Steelhead
Legend
2080s
2040s
1980s
Asia
North America
80°0'0"E
80°0'0"W
120°0'0"E
120°0'0"W
160°0'0"W
50°0'0"N
140°0'0"E
160°0'0"E
180°0'0"
160°0'0"W
140°0'0"W
Latitude
Longitude

Fig. 7. Reference December thermal habitat ranges in the 1980s, 2040s, and 2080s for six major species of Pacific salmon under the IPCC A1B (medium) emissions scenario.

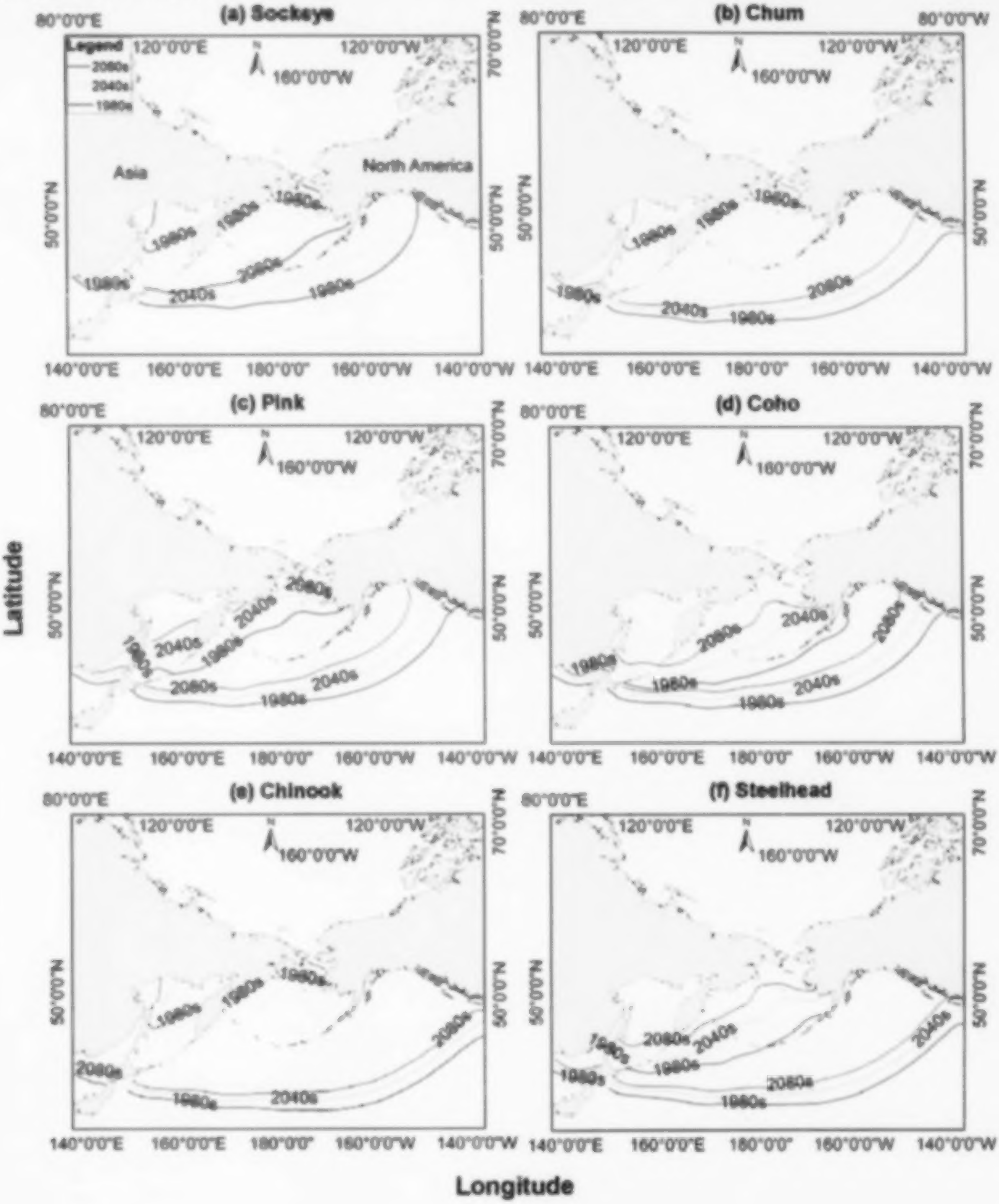
(a) Sockeye
(b) Chum
(c) Pink
(d) Coho
(e) Chinook
(f) Steelhead
Legend
2080s
2040s
1980s
Asia
North America
80°0'0"E
80°0'0"W
120°0'0"E
120°0'0"W
160°0'0"W
70°0'0"N
50°0'0"N
140°0'0"E
160°0'0"E
180°0'0"
160°0'0"W
140°0'0"W
Latitude
Longitude

ring Sea, while some southeastern Bering Sea habitats were lost because of a northward movement of the warmest boundary by the 2080s. Relative to the historical reference of 1980s, the overall December habitat losses were 41% (A2), 38% (A1B), and 24% (B1) for the 2080s. The losses were 6%–7% for the 2020s and 9%–16% for the 2040s. All of these reductions exceeded the habitat area CV of 5% from the 1970–1999 period, whereas losses by the 2080s also exceeded the equivalent three standard deviations (15%).

Chum salmon

The July 1980s habitat range for chum salmon (Fig. 6*b*) closely resembled that for sockeye except for a slightly more southern location of the warmest limit. This resulted in approximately 9% more reference habitat area for chum compared with sockeye salmon. Similar to the results for sockeye salmon, a very small northward movement of the coldest boundaries was apparent in the 21st century. In contrast, strong northward shifts in the warmest boundaries notably reduced the Gulf of Alaska, Subarctic, and Okhotsk Sea habitats by the 2040s. Reductions were substantial in the Gulf of Alaska, Subarctic, and the Okhotsk Sea by the 2080s. The reductions in the overall reference historical habitat for the 2040s under different emission scenarios were 9%–13%, all of which exceeded the CV (6%) of the 1970–1999 potential habitat areas. The 2080s habitat reductions were 20%–31%, which exceeded the equivalent three standard deviations (18%).

The December 1980s habitat range (Fig. 7*b*) represented a relatively wide east–west band, excluding the Arctic Ocean and including most of the Bering Sea, Gulf of Alaska, Subarctic, and Okhotsk Sea regions. A northward shift of the warmest boundary partially reduced the Gulf of Alaska and Subarctic habitats by the 2040s and 2080s, while large areas of new habitat opened up in the Bering and Okhotsk seas by a northward movement of the coldest boundary. The reductions in the total reference habitat area by the southern losses were substantially compensated by the northern gains. Relative to the 1980s habitat area, the reductions of 2% by the 2020s and 4%–8% by 2040s were smaller or only marginally larger than the CV of 4%. In contrast, the 2080s reductions were 17%, 16%, and 9% under A2, A1B, and B1 scenarios, respectively.

Pink salmon

The warmest boundary of pink salmon's (Fig. 6*c*) July 1980s habitat range was identical to that of chum salmon. The coldest boundary, however, excluded the Laptev and Beaufort seas, encompassing around 2% less in the reference habitat area of chum salmon. Northward movement, as well as east–west contraction, of the warmest boundary in the future periods resulted in reductions in habitat ranges, which were identical to those for chum salmon. Northward movement of the coldest boundary developed new habitat areas in the Arctic Ocean, including large areas in the Beaufort Sea for the 2040s and 2080s. The overall reference habitat area decreased by 5%–6% for the 2020s, 9%–13% for the 2040s, and 20%–32% for the 2080s. These habitat area reductions were all larger than the CV of 5% of the historical potential areas. The 2080s reductions also exceeded the equivalent three standard deviations (15%).

The 1980s December habitat range (Fig. 7*c*) encompassed a relatively narrow east–west band that included most of the Gulf of Alaska, much of Bering Sea and Subarctic, and part of Okhotsk Sea. The northward shift of the warmest boundary reduced much of the Gulf of Alaska and Subarctic habitats by the 2040s and 2080s. However, these northern losses were substantially compensated by habitat gains through the northward movement of the coldest boundary that developed new habitat areas in much of the Okhotsk Sea and most of the Bering Sea. The magnitudes of changes in the total habitat area by the 2020s and the 2040s under different emission scenarios were much less than the CV of 6% of the 1970–1999 potential habitat areas. The habitat reductions were 6%–10% by the 2080s. Only the 10% reductions from the A1B and A2 emissions scenarios exceeded the CV for the historical period.

Coho salmon

The warmest boundary of the July 1980s range for coho salmon (Fig. 6*d*) also resembled its chum salmon counterpart. The coldest boundary, however, was located near the Bering Strait and excluded thermal habitat from the Arctic Ocean. The reference coho habitat area was approximately 3.6% less than that for chum salmon. SST increases reduced the east–west extent and displaced the warmest boundary northward by the 2040s and 2080s, leading to habitat range reductions identical to those for chum salmon. Although the northward movement of the coldest boundary developed new habitats in the Chukchi Sea in the future periods, the overall reference habitat area decreased by 5%–7% for the 2020s, 9%–14% for the 2040s, and 21%–33% for the 2080s under different emission scenarios. The 2040s and 2080s habitat area reductions were greater than, respectively, the two standard deviations (10%; CV = 5%) and three standard deviations (15%) of the 1970–1999 potential habitat area variations.

Compared with other species, the reference 1980s December habitat range for coho (Fig. 7*d*) had a narrower east–west band, including only most of the Gulf of Alaska and parts of the Subarctic region. Northward movement of the coldest boundary opened new habitat areas in much of the Bering Sea and parts of the Okhotsk Sea by the 2040s and 2080s. These gains in total habitat area were, however, almost balanced by losses through the northward shift of the warmest boundary. The total habitat area showed mostly slight increases and occasionally very little decrease or no changes at all in the future periods. All of these changes were much less than the CV of 11% of the historical potential habitat areas.

Chinook salmon

The July 1980s habitat of Chinook salmon (Fig. 6*e*) encompassed a much smaller geographic range and area compared with that for other species. It included a small portion from the Gulf of Alaska in the east and extended through much of the Okhotsk Sea in the west. In the north–south dimension, it extended from the edge of Subarctic through the Beaufort, Chukchi, and Laptev seas in the Arctic Ocean. The drastic northward movement and east–west contraction of the warmest boundary caused a complete elimination of the Gulf of Alaska habitat, substantial reductions of the Okhotsk Sea and Subarctic habitats, and a large reduction of the Bering Sea habitat by the 2040s. The 2080s SST changes resulted in complete eliminations of the Okhotsk Sea and Subarctic habitats, as well as a substantial reduction of the Bering Sea habitat. The coldest boundary also moved slightly northward to contribute only a small increase in total habitat by opening new areas in the Arctic Ocean. The overall reductions in the total reference habitat area under different emission scenarios for the 2020s were 24%–29%, which were much larger than the CV of 13% of the historical areas. The 2040s habitat area reductions were 41%–48% and the 2080s reductions were 88% (A2), 86% (A1B), and 66% (B1), which by far exceeded the three standard deviations (39%) of the 1970–1999 potential habitat areas.

The December 1980s habitat range for Chinook salmon (Fig. 7*e*) exhibited a wider east–west band than that for other species. It excluded the Arctic Ocean while including the Gulf of Alaska, the Subarctic, most of the Bering Sea, and parts of the Okhotsk Sea. Climatic warming shifted both the warmest and coldest boundaries northward, which led to habitat losses in the Gulf of Alaska and Subarctic while opening new areas in the Bering and Okhotsk Seas. Although the total habitat area remained unchanged for the 2020s, it was reduced by 2%–6% by the 2040s. The reductions of 7%–12% by the 2080s were greater than the CV of 4%. However, only the reductions of 10%–12% under the medium (A1B) and higher (A2) emissions scenarios exceeded the equivalent two standard deviations (8%) of the potential historical areas.

Steelhead trout

The July 1980s range of steelhead (Fig. 6*f*) closely resembled that for coho salmon except for a slight northward extension of the warmest boundary, which resulted in approximately 3.7% less area in the reference habitat. A strong northward shift and east–west contraction in the warmest boundary caused notable reductions in the Subarctic, Okhotsk Sea, and Gulf of Alaska habitat areas for the 2040s. Habitat reductions for the 2080s were substantial in the Gulf of Alaska and high in the Subarctic and Okhotsk Sea, although small areas of new habitat opened up in the Chukchi Sea. Reductions in the overall habitat area were 8%–10% for the 2020s, 15%–19% for the 2040s, and 24%–43% for the 2080s, all of which exceeded the historical period CV of 6%. Further, the areal reductions by the 2040s exceeded two standard deviations (12%), while that for 2080s exceeded three standard deviations (18%).

The December 1980s habitat range (Fig. 7*f*) encompassed a relatively narrow east–west band, including most of the Gulf of Alaska and Subarctic, as well as a part of the Bering Sea. None of the Okhotsk Sea and Arctic Ocean habitats was included in this range. By the 2040s and 2080s, the northward shift of the coldest boundary opened up new habitat areas in much of the Bering and Okhotsk seas. These gains in the total habitat range and area were, however, nearly completely compensated by almost equal losses through the northward shift of the warmest boundary. Consequently, the total habitat area in future periods either remained unchanged or reduced slightly by 1%–2%, which was substantially smaller than the CV of 7% of the historical potential habitat areas.

Subdomains of North Pacific and Arctic oceans

The potential future changes in the reference thermal habitat areas of all six species were also quantified for the five subdomains of the entire study area: Arctic Ocean, Bering Sea, Gulf of Alaska, Subarctic, and Okhotsk Sea (Fig. 1*b*). Because the Gulf of Alaska is an important rearing area for North American salmon, we treated this region separately from the rest of the Subarctic North Pacific. The Central and Western Subarctic were evaluated together as the "Subarctic". The reference 1980s habitat areas (km^2) for the summer month of July and winter month of December and projected changes by the 2020s, 2040s, and 2080s under the three emission scenarios of B1, A1B, and A2 are presented (Tables 6–10). Unlike the previous section, the projected changes are presented here in units of million km^2, rather than in percentage (%) of the 1980s habitat to avoid any singularity arising from the absence of reference 1980s habitat for some species in some subdomains.

Arctic Ocean

This subdomain provided July 1980s thermal habitat areas of around 0.13–0.31 million km^2 for sockeye, chum, pink, and Chinook salmon (Table 6). The Arctic Ocean supported no July 1980s habitats for coho salmon and steelhead, as well as no December 1980s habitats for any species. Climatic warming developed new areas for the reference July habitat, leading to new habitat areas of 0.01–0.20 million km^2 for different species, including coho salmon and steelhead, for each of the future periods under all three emission scenarios. However, no reference December habitats appeared in the Arctic Ocean for any species under any emission scenarios for these periods.

Bering Sea

The reference July 1980s range provided suitable thermal habitat areas of around 2.49 million km^2 for each species throughout the entire Bering Sea area (Table 7). The reference habitat area for Chinook salmon was reduced by 0.13–2.22 million km^2 (5% to 89%) for the 2020s through 2080s. It remained unchanged for chum, pink, and coho salmon through the 2080s and for sockeye salmon and steelhead through the 2040s. By the 2080s, reference sockeye salmon habitat decreased by approximately 0.16 million km^2 (6%) under medium (A1B) and higher (A2) emission scenarios while remaining unchanged under the B1 emission scenario. There were no reductions by the 2080s for steelhead reference habitat under B1 and A1B scenarios, but a reduction of around 0.03 million km^2 (1%) occurred under the A2 scenario. The Bering Sea did not provide a favorable 1980s December habitat for coho salmon while offering substantial habitat areas for the other five species. Climatic warming developed new areas that increased the Bering Sea's reference December habitat areas by up to 1.49 million km^2 for the six species by the 2080s under different emissions scenarios.

Gulf of Alaska

The reference 1980s habitat areas of both July and December stayed within 0.41–4.57 million km^2 for different species in this region (Table 8). These reference areas decreased by around 0.26–2.09 million km^2 by the 2020s through 2080s under different emission scenarios. The most striking reductions were the complete (i.e., 100%) elimination of the July reference area for Chinook salmon under each of the three emission scenarios and the December reference area for sockeye salmon under A2 and A1B scenarios by the 2080s.

Table 6. Reference historical thermal habitat areas (million km^2) of Pacific salmon and projected changes (million km^2) in 21st century within the Arctic Ocean under three IPCC climate change scenarios.

Time	Scenario	Sockeye	Chum	Pink	Coho	Chinook	Steelhead
July							
1980s	Hist.	0.31	0.31	0.13	0.00	0.31	0.00
2020s	A2	0.03	0.03	0.08	0.04	0.03	0.04
	A1B	0.03	0.03	0.08	0.02	0.03	0.02
	B1	0.01	0.01	0.08	0.02	0.01	0.02
2040s	A2	0.05	0.05	0.08	0.04	0.05	0.04
	A1B	0.06	0.06	0.14	0.06	0.06	0.06
	B1	0.03	0.03	0.08	0.04	0.03	0.04
2080s	A2	0.20	0.20	0.15	0.07	0.20	0.07
	A1B	0.15	0.15	0.14	0.07	0.15	0.07
	B1	0.06	0.06	0.14	0.06	0.06	0.06
December							
1980s	Hist.	0.00	0.00	0.00	0.00	0.00	0.00
2020s	A2	0.00	0.00	0.00	0.00	0.00	0.00
	A1B	0.00	0.00	0.00	0.00	0.00	0.00
	B1	0.00	0.00	0.00	0.00	0.00	0.00
2040s	A2	0.00	0.00	0.00	0.00	0.00	0.00
	A1B	0.00	0.00	0.00	0.00	0.00	0.00
	B1	0.00	0.00	0.00	0.00	0.00	0.00
2080s	A2	0.00	0.00	0.00	0.00	0.00	0.00
	A1B	0.00	0.00	0.00	0.00	0.00	0.00
	B1	0.00	0.00	0.00	0.00	0.00	0.00

Note: 1980s: 1970–1999; 2020s: 2010–2039; 2040s: 2030–2059; 2080s: 2070–2099. "Hist." refers to historical data.

Table 7. Reference historical thermal habitat areas (million km^2) of Pacific salmon and projected changes (million km^2) in 21st century within the Bering Sea under three IPCC climate change scenarios.

Time	Scenario	Sockeye	Chum	Pink	Coho	Chinook	Steelhead
July							
1980s	Hist.	2.49	2.49	2.49	2.49	2.49	2.49
2020s	A2	0.00	0.00	0.00	0.00	–0.13	0.00
	A1B	0.00	0.00	0.00	0.00	–0.18	0.00
	B1	0.00	0.00	0.00	0.00	–0.13	0.00
2040s	A2	0.00	0.00	0.00	0.00	–0.32	0.00
	A1B	0.00	0.00	0.00	0.00	–0.50	0.00
	B1	0.00	0.00	0.00	0.00	–0.32	0.00
2080s	A2	–0.16	0.00	0.00	0.00	–2.22	–0.03
	A1B	–0.16	0.00	0.00	0.00	–2.10	0.00
	B1	0.00	0.00	0.00	0.00	–0.68	0.00
December							
1980s	Hist.	1.96	1.96	1.03	0.00	1.96	0.12
2020s	A2	0.24	0.24	0.35	0.18	0.24	0.46
	A1B	0.27	0.27	0.35	0.18	0.27	0.49
	B1	0.27	0.27	0.35	0.18	0.27	0.49
2040s	A2	0.29	0.29	0.58	0.52	0.29	0.66
	A1B	0.31	0.31	0.63	0.66	0.31	0.77
	B1	0.29	0.29	0.52	0.44	0.29	0.63
2080s	A2	0.04	0.47	1.20	1.45	0.47	1.49
	A1B	0.13	0.45	1.12	1.26	0.45	1.43
	B1	0.36	0.36	0.76	0.81	0.36	0.99

Note: 1980s: 1970–1999; 2020s: 2010–2039; 2040s: 2030–2059; 2080s: 2070–2099. "Hist." refers to historical data.

Subarctic

The Subarctic provided reference 1980s habitat areas of 1.77–4.43 million km^2 for different species during July and December (Table 9). The reference habitats decreased by around 0.04–1.77 million km^2 by the 2020s through the 2080s. The reference July habitat of Chinook salmon, in particular, was completely eliminated from this region by the 2080s under each of the three emission scenarios.

Okhotsk Sea

The reference July 1980s range for different species generally provided habitat areas of around 1.05–1.46 million km^2,

Table 8. Reference historical thermal habitat areas (million km^2) of Pacific salmon and projected changes (million km^2) in 21st century within the Gulf of Alaska under three IPCC climate change scenarios.

Time	Scenario	Sockeye	Chum	Pink	Coho	Chinook	Steelhead
July							
1980s	Hist.	2.16	2.83	2.83	2.83	0.41	2.50
2020s	A2	–0.66	–0.40	–0.40	–0.40	–0.32	–0.40
	A1B	–0.66	–0.43	–0.43	–0.43	–0.38	–0.49
	B1	–0.72	–0.53	–0.53	–0.53	–0.38	–0.64
2040s	A2	–0.97	–0.59	–0.59	–0.59	–0.41	–0.85
	A1B	–1.15	–0.86	–0.86	–0.86	–0.41	–1.06
	B1	–1.06	–0.74	–0.74	–0.74	–0.41	–0.97
2080s	A2	–1.97	–1.89	–1.89	–1.89	–0.41	–2.03
	A1B	–2.00	–1.97	–1.97	–1.97	–0.41	–2.09
	B1	–1.54	–1.34	–1.34	–1.34	–0.41	–1.43
December							
1980s	Hist.	1.41	3.39	2.45	2.68	4.57	4.03
2020s	A2	–0.40	–0.41	–0.43	–0.26	–0.40	–0.46
	A1B	–0.43	–0.41	–0.46	–0.30	–0.40	–0.46
	B1	–0.45	–0.45	–0.49	–0.30	–0.40	–0.46
2040s	A2	–0.72	–0.62	–0.70	–0.59	–0.62	–0.64
	A1B	–0.87	–0.75	–0.86	–0.75	–0.76	–0.74
	B1	–0.72	–0.62	–0.70	–0.55	–0.58	–0.64
2080s	A2	–1.41	–1.40	–1.50	–1.43	–1.39	–1.42
	A1B	–1.41	–1.43	–1.59	–1.46	–1.29	–1.42
	B1	–1.32	–0.91	–1.11	–0.97	–0.97	–1.01

Note: 1980s: 1970–1999; 2020s: 2010–2039; 2040s: 2030–2059; 2080s: 2070–2099. "Hist." refers to historical data.

Table 9. Reference historical thermal habitat areas (million km^2) of Pacific salmon and projected changes (million km^2) in 21st century within the Subarctic under three IPCC climate change scenarios.

Time	Scenario	Sockeye	Chum	Pink	Coho	Chinook	Steelhead
July							
1980s	Hist.	2.61	2.72	2.72	2.72	1.77	2.72
2020s	A2	–0.50	–0.04	–0.04	–0.04	–0.55	–0.36
	A1B	–0.50	–0.04	–0.04	–0.04	–0.57	–0.32
	B1	–0.50	–0.07	–0.07	–0.07	–0.64	–0.39
2040s	A2	–0.68	–0.36	–0.36	–0.36	–0.93	–0.64
	A1B	–0.68	–0.50	–0.50	–0.50	–1.19	–0.71
	B1	–0.64	–0.18	–0.18	–0.18	–0.93	–0.53
2080s	A2	–1.61	–1.02	–1.02	–1.02	–1.77	–1.40
	A1B	–1.49	–0.85	–0.85	–0.85	–1.77	–1.13
	B1	–0.81	–0.68	–0.68	–0.68	–1.77	–0.78
December							
1980s	Hist.	2.02	3.61	2.42	2.19	4.43	3.48
2020s	A2	–0.38	–0.33	–0.06	–0.30	–0.04	–0.36
	A1B	–0.45	–0.33	–0.10	–0.26	–0.11	–0.36
	B1	–0.45	–0.33	–0.06	–0.26	–0.15	–0.36
2040s	A2	–0.79	–0.88	–0.36	–0.32	–0.64	–0.56
	A1B	–0.92	–0.91	–0.37	–0.35	–0.78	–0.53
	B1	–0.55	–0.52	–0.18	–0.24	–0.38	–0.45
2080s	A2	–1.46	–1.55	–1.27	–0.81	–1.34	–1.07
	A1B	–1.36	–1.41	–0.95	–0.66	–1.12	–0.94
	B1	–1.09	–0.98	–0.58	–0.50	–0.89	–0.45

Note: 1980s: 1970–1999; 2020s: 2010–2039; 2040s: 2030–2059; 2080s: 2070–2099. The Central and Western Subarctic were lumped together and termed as "Subarctic". Eastern Subarctic was included in the Gulf of Alaska subdomain (Fig. 1*b*). "Hist." refers to historical data.

encompassing all or most of the Okhotsk Sea (Table 10). The reference areas decreased by 0.03–1.18 million km^2 in the 2020s through the 2080s under different emission scenarios for all species except steelhead. July reference habitat for steelhead remained unchanged through the 2020s while decreasing by 0.03–0.83 million km^2 (2% to 59%) in the 2040s and 2080s. By the 2080s, the reference July habitat of Chinook salmon was completely (i.e., 100%) eliminated from this region under the A1B and A2 scenarios. The December 1980s range provided habitat areas of approximately 0.17–

Table 10. Reference historical thermal habitat areas (million km^2) of Pacific salmon and projected changes (million km^2) in 21st century within the Okhotsk Sea under three IPCC climate change scenarios.

Time	Scenario	Sockeye	Chum	Pink	Coho	Chinook	Steelhead
July							
1980s	Hist.	1.39	1.46	1.46	1.46	1.05	1.39
2020s	A2	–0.03	–0.07	–0.07	–0.07	–0.53	0.00
	A1B	–0.03	–0.07	–0.07	–0.07	–0.53	0.00
	B1	–0.03	–0.07	–0.07	–0.07	–0.68	0.00
2040s	A2	–0.15	–0.07	–0.07	–0.07	–0.86	–0.03
	A1B	–0.15	–0.07	–0.07	–0.07	–0.92	–0.12
	B1	–0.12	–0.07	–0.07	–0.07	–0.83	–0.03
2080s	A2	–1.18	–0.54	–0.54	–0.54	–1.05	–0.83
	A1B	–0.82	–0.33	–0.33	–0.33	–1.05	–0.41
	B1	–0.32	–0.15	–0.15	–0.15	–0.99	–0.15
December							
1980s	Hist.	0.81	0.81	0.17	0.00	0.81	0.00
2020s	A2	0.23	0.23	0.23	0.00	0.23	0.07
	A1B	0.23	0.23	0.20	0.00	0.23	0.10
	B1	0.26	0.26	0.20	0.00	0.26	0.07
2040s	A2	0.51	0.51	0.30	0.07	0.51	0.17
	A1B	0.51	0.51	0.36	0.10	0.51	0.17
	B1	0.43	0.43	0.23	0.07	0.43	0.10
2080s	A2	0.62	0.72	0.88	0.41	0.72	0.57
	A1B	0.60	0.67	0.67	0.24	0.67	0.41
	B1	0.59	0.59	0.46	0.10	0.59	0.17

Note: 1980s: 1970–1999; 2020s: 2010–2039; 2040s: 2030–2059; 2080s: 2070–2099. "Hist." refers to historical data.

0.81 million km^2 for sockeye, chum, pink, and Chinook salmon. No December habitats for coho salmon and steelhead were present in this region. By the 2040s and 2080s, climatic warming developed new habitat areas of 0.07–0.57 million km^2 in the Okhotsk Sea for these two species. The reference winter habitat areas increased by 0.20–0.88 million km^2 for the other three species within the three future periods.

Discussion

This study raises some crucial concerns for managers of salmon fisheries and policy makers. For example, conservation and restoration efforts for Chinook salmon in the Columbia River Basin and sockeye salmon in British Columbia have largely been focused on freshwater habitats. Our results show that the high-seas ocean distributions of these two species are projected to be the most strongly impacted by anthropogenic climate change. Further, the high-seas Gulf of Alaska habitat for Chinook salmon (in summer) and sockeye salmon (in summer and winter) could be completely lost by the end of 21st century. This leads to extremely important public policy issues for North American governments because the Gulf of Alaska has historically been recognized as the primary foraging ground for many populations of North American sockeye salmon (e.g., stocks of British Columbia) and Chinook salmon (e.g., certain stocks from the Columbia River Basin, although their offshore distribution is not well known). High priority should, therefore, be given in the future to develop a better understanding of stock-specific distribution of salmon on the high seas.

Thermal limits were subjectively chosen from published data and defined as "reference", rather than "actual", thermal limits in this study. The choice of thermal limits is inherently subjective because there are no unique guidelines to define them. The habitat areas based on our choice of reference limits exhibited a range of sensitivities. For example, a 1 °C increase in the thermal limits resulted in approximately 0.5% to 37% changes in the 1980s reference habitat areas for different species. Although sensitivity coefficients were quantified based on the 1980s reference habitat areas, they are nondimensional and, therefore, can be applied for other time fames to approximately quantify any overestimations or underestimations caused by the choice of thermal limits. For example, our July reference upper thermal limit of 13 °C for chum, pink, and coho salmon would have overestimated their respective 2080s habitat areas by around 10% compared with the areas obtained by using 12 °C. Explicit tests of empirically derived thermal limits should be conducted in future research to assess the validity of these limits.

The projected declines in summer habitat area were least for chum, pink, and coho salmon. Because pink, chum, and sockeye salmon have substantial diet overlap on the high seas, differential impacts on total high-seas habitat areas may lead to an increased competitive dominance of pink and chum salmon over sockeye salmon (that has higher projected habitat decline), while greater density-dependent growth reductions from crowding should be expected for all species (e.g., Ruggerone et al. 2003; Ruggerone and Nielsen 2004, 2009).

Another interesting issue is the potential for the northward displacement of favorable thermal habitats at sea to influence the freshwater distribution and life history variants of Pacific salmon. Notably, ocean warming in the nearshore portions of the Bering, Chukchi, and Beaufort seas may enable more successful Pacific salmon colonizations of Arctic rivers or increases in the abundance for small populations that are currently spawning and rearing in Arctic watersheds

(Stephenson 2006; Irvine et al. 2009). The anadromous life history form of *O. mykiss* (steelhead trout) might also become more viable in southwestern Alaska streams (e.g., Bristol Bay) that currently are thought to host only resident rainbow trout (Burgner et al. 1992), but in the future will lie within the boundaries of steelhead thermal reference habitat in both summer and winter. In contrast, the west coast's North American salmon would have to travel longer through unfavorable thermal regimes to migrate back from the central North Pacific or Bering Sea to British Columbia watersheds or the Columbia River Basin. An assessment possibly through bioenergetics modeling would provide better insights into the energetic costs of this migration and subsequent successes under a warming climate.

The differences in the reference habitat ranges and areas among different salmon species were caused by the differences among their reference thermal limits. Projected reductions of the habitat ranges and areas in the 21st century were particularly influenced by the upper thermal limits. For example, the highest reductions in the reference July habitat of Chinook salmon, as well as that in the December habitat of sockeye salmon, corresponded to the lowest July and December upper thermal limits, respectively. These outcomes were expected, since the smaller upper thermal limits were located in regions of the North Pacific where the ocean basin narrows considerably to the north. Projected changes in the reference habitat areas of individual species were relatively insensitive to the choice of emissions scenario until the 2040s because the GCMs projected similar temperature increases under all three emission scenarios up to this time period.

The higher future habitat losses in the Gulf of Alaska and Subarctic for both seasons, as well as in the Bering and Okhotsk seas for summer, were caused by the relatively high historical SSTs and stronger SST increases in these regions. Additionally, some of the striking reductions in the Gulf of Alaska habitat areas in this study were related to our choice of upper thermal limits defined for the entire North Pacific and adjacent Arctic Ocean basins. For example, application of 15 °C as a regional upper limit for sockeye salmon in the Gulf of Alaska (as hinted at by Welch et al. 1998*a*) added around 2.28 million km^2 to the 1980s July habitat area obtained with the applied overall limit of 12 °C. This regional upper limit of 15 °C resulted in sockeye summer habitat area reductions of 31%–42% in the Gulf of Alaska for 2080s, rather than the 71%–93% area reduction based on the 12 °C upper thermal limit. Similar explanations may apply for the substantial reductions–eliminations of summer and winter habitats for other species from the Gulf of Alaska.

Our results largely agree with the results of the previous studies that used seasonally fixed thermal limits and SST projections from a limited number of future climate scenarios and GCM projections (e.g., Welch et al. 1998*a*; Azumaya et al. 2007; Kaeriyama 2008). These studies generally indicated large reductions of available summer habitats for Pacific salmon, particularly from the northeast Pacific Ocean – Gulf of Alaska regions. While Welch et al. (1998*a*, 1998*b*) anticipated a potential exclusion of sockeye summer habitat and substantial reductions of summer as well as winter habitats for steelhead in the North Pacific Ocean by the end of the 21st century, Azumaya et al. (2007) estimated average decreases of 13% in summer habitats and increases of 19% in winter habitats for five species (excluding steelhead). In contrast, our analysis showed substantial reductions of summer as well as winter habitats for sockeye salmon and only summer habitats for the other five species. These differences can be attributed to the application of different, season-specific thermal limits and multimodel average projected SST fields under different IPCC greenhouse gas emissions scenarios considered in this study. In particular, the year-round fixed upper thermal limits of Azumaya et al. (2007) were much higher than those used in this study, leading to smaller reductions in summer habitats and increases, rather than decreases, in winter habitats. Further, their study incorporated a climate scenario representing a spatially uniform 1.5 °C warming of SST and 0.2 psu reduction in upper ocean salinity, while our study used only SST projections from a large number of GCMs, leading to spatially nonuniform SST increases of up to 3 °C in both seasons.

Our results support the hypothesis that anthropogenic climate change in the 21st century may result in an increase in the Arctic habitat for salmon in the summer season. Although results of this analysis mainly apply to the high-seas thermal habitats, our analysis provides important insights into the potential changes in coastal habitats for Pacific salmon. For example, substantial reductions of summer habitats are indicated for all six species both from the eastern and western North Pacific nearshore ocean regions by 2040s and 2080s, while winter habitats appear to be predominantly lost from the eastern ocean basin and slightly gained in the western basin, particularly near the Okhotsk Sea region. This may indicate a possible redistribution of winter habitats for Pacific salmon between the eastern and western North Pacific coasts as a consequence of climatic warming.

This paper presents possible reference high-seas thermal habitats of Pacific salmon in the 20th and 21st centuries. This approach does not guarantee the presence or absence of salmon in any ocean domains because temperature is not likely the sole determinant of ocean distributions for Pacific salmon. Other factors such as salinity, acidity, ocean currents, predator–prey availability, prey quality, etc., are also important. The thermal habitat preferences identified in high-seas surveys are likely far from the species-specific lethal upper thermal limits. Salmon species might adapt to changing thermal conditions through acclimation, evolution, alternative migration timing or routes, and (or) other pathways to survive through the projected unfavorable temperature regimes. Some species might adapt behaviorally by reducing their surface orientation and finding refuge in the relatively cool deeper ocean if they can also satisfy requirements for feeding and predator avoidance. Reliable high-seas survey and monitoring data collected in the future with new and rapidly evolving technologies (e.g., archival and acoustic fish tags and tracking used in combination with autonomous underwater gliders that measure environmental conditions) can investigate these possibilities.

In conclusion, historical changes in the summer and winter thermal habitat areas of Pacific salmon species during the warm and cool PDO eras of the 20th century were within a few percent of their reference 1980s habitats. Interdecadal average habitat area changes were mostly much lower than the interannual CVs obtained from species-specific habitat area time series of the 30-year (1970–1999) historical reference period. Scenarios for climatic warming led to substantial northward displacements, as well as east–west contractions, of the warmest habitat boundaries of reference July habitats for all salmon species in the 21st century. The projected changes in July reference habitat ranges and areas for all species, as well as in December habitat for sockeye salmon, during the 21st century were much larger than those in the historical time frames. Chinook and sockeye salmon were projected to experience the greatest reductions relative to historical July and December habitat areas, respectively. According to the A1B scenario, the reference July thermal habitat was projected to decrease by around 86% for Chinook, 45% for sockeye, 36% for steelhead, 30% for coho, 30% for pink, and 29% for chum salmon by 2080s. The projected decrease in the reference winter habitat for sockeye salmon was around 38% by 2080s under the A1B scenario. The reductions were around 25% lower and 7% higher than those for B1 and A2 scenarios, respectively.

Research herein focused on the ensemble mean state of the habitat range and areas of Pacific salmon based on subjectively chosen reference thermal limits, historical SST fields, and multimodel (GCMs) ensemble SST projections. Although effects of uncertainties associated with the parameters of reference thermal limits were investigated with sensitivity analysis, a comprehensive analysis of all the uncertainties stemming from SST projections of individual, as well as ensemble, GCMs were beyond the scope of this paper. Additional study into the limiting factors on the high-seas behavior and distribution of salmon is necessary to better understand climate impacts on the high-seas ranges of Pacific salmon. These are important topics for future research.

Acknowledgements

The research described in this paper was funded by a grant from the Gordon and Betty Moore Foundation administered by the National Center for Ecological Analysis and Synthesis (NCEAS), University of California, Santa Barbara. Participation by Katherine Myers was funded by award No. NA04NMF4380162 from NOAA, administered by the Alaska Department of Fish and Game for the Arctic–Yukon–Kuskokwim Sustainable Salmon Initiative and a grant from the Washington Sea Grant Program, University of Washington, pursuant to National Oceanic and Atmospheric Administration Award No. NA07OAR4170007, Project No. R/F-160. This publication is partially funded by the Joint Institute for the Study of the Atmosphere and Ocean (JISAO) under NOAA Cooperative Agreement No. NA17RJ1232, Contribution No. 1835. The statements, findings, conclusions, and recommendations are those of the authors and do not necessarily reflect the views of NOAA or any of its subagencies. The SST projections for the GCMs were obtained from the PCMDI data portal (Table 1). Important suggestions from Robert V. Walker, Nancy D. Davis, Todd Mitchell, as well as GIS mapping tips from Robert Norheim and Yan Jiang, from the University of Washington are gratefully acknowledged. We thank David Welch and an anonymous reviewer for providing valuable critiques and insightful comments.

References

Abdul-Aziz, O.I., Wilson, B.N., and Gulliver, J.S. 2010. Two-zone model for stream and river ecosystems. Hydrobiologia, **638**(1): 85–107. doi:10.1007/s10750-009-0011-7.

Azumaya, T., Nagasawa, T., Temnykh, O.S., and Khen, G.V. 2007. Regional and seasonal differences in temperature and salinity limitations of Pacific salmon. N. Pac. Anadr. Fish Comm. Bull. 4. pp. 179–187. Available from http://www.npafc.org/new/pub_bulletin.html [accessed 28 October 2010].

Birman, I.B. 1960. New information on the marine period of life and the marine fishery of Pacific salmon. Tr. Soveshch. Ikhtiol. Kom. Akad. Nauk SSSR. **10**: 151–164. [Available on request from the Pacific Biological Station Library, Nanaimo, B.C.] [English translation, Fish. Res. Board Can. Transl. Ser. 357, 1962.]

Burgner, R.L., Light, J.T., Margolis, L., Okazaki, T., Tautz, A., and Ito, S. 1992. Distribution and origins of steelhead trout (*Oncorhynchus mykiss*) in offshore waters of the North Pacific Ocean. Int. N. Pac. Fish. Comm. Bull. 51.

Conover, W.J. 1980. Practical nonparametric statistics, John Wiley and Sons, Inc., New York.

French, R., Bilton, H., Osako, M., and Hartt, A. 1976. Distribution and origin of sockeye salmon (*Oncorhynchus nerka*) in offshore waters of the North Pacific Ocean. Int. N. Pac. Fish. Comm. Bull. 34.

Godfrey, H., Henry, K.A., and Machidori, S. 1975. Distribution and abundance of coho salmon in offshore waters of the North Pacific Ocean. Int. N. Pac. Fish. Comm. Bull. 31.

Hare, S.R., Mantua, N.J., and Francis, R.C. 1999. Inverse production regimes: Alaskan and west coast Pacific salmon. Fisheries, **21**(1): 6–14.

Hinke, J.T., Foley, D.G., Wilson, C., and Watters, G.M. 2005. Persistent habitat use by Chinook salmon *Oncorhynchus tshawytscha* in the coastal ocean. Mar. Ecol. Prog. Ser. **304**: 207–220. doi:10.3354/meps304207.

Intergovernmental Panel on Climate Change. 2007. Climate Change 2007: synthesis report. Contribution of Working Groups I, II and III to the Fourth Assessment Report of the Intergovernmental Panel on Climate Change. *Edited by* R.K. Pachauri and A. Reisinger. Core Writing Team, IPCC, Geneva, Switzerland.

Irvine, J.R., Macdonald, R.W., Brown, R.J., Godbout, L., Reist, J.D., and Carmack, E.C. 2009. Salmon in the Arctic and how they avoid lethal low temperatures. N. Pac. Anadr. Fish Comm. Bull. 5. pp. 39–50. Available from http://www.npafc.org/new/pub_bulletin.html [accessed 28 October 2010].

Kaeriyama, M. 2008. Ecosystem-based sustainable conservation and management of Pacific salmon. *In* Fisheries for global welfare and environment, memorial book of the 5th World Fisheries Congress 2008. *Edited by* K. Tsukamoto, T. Kawamura, T. Takeuchi, T.D. Bard, Jr., and M.J. Kaiser. TERRAPUB e-Library. ISBN No.: 978-4-88704-144-8. pp. 371–380. Available from http://www.terrapub.co.jp/onlineproceedings/fs/wfc2008/index.html [accessed 28 October 2010].

Lilliefors, H.W. 1967. On the Kolmogorov–Smirnov test for normality with mean and variance unknown. J. Am. Stat. Assoc. **62**(318): 399–402. doi:10.2307/2283970.

Major, R.L., Ito, J., Ito, S., and Godfrey, H. 1978. Distribution and origin of Chinook salmon (*Oncorhynchus tshawytscha*) in offshore waters of the North Pacific Ocean. Int. N. Pac. Fish. Comm. Bull. 38.

Mantua, N.J., Hare, S.R., Zhang, Y., Wallace, J.M., and Francis, F.C. 1997. A Pacific interdecadal climate oscillation with impacts on salmon production. Bull. Am. Meteorol. Soc. **78**(6): 1069–1079. doi:10.1175/1520-0477(1997)078<1069:APICOW>2.0.CO;2.

Manzer, J.I., Ishida, T., Peterson, A.E., and Hanavan, M.G. 1965. Salmon of the North Pacific Ocean. Part V. Offshore distribution of salmon. Int. North Pac. Fish. Comm. Bull. 15.

Myers, K.W., and Bernard, R.L. 1993. Biological information on Pacific salmon and steelhead trout in observer samples from the

Japanese squid driftnet fishery in 1990. Int. North Pac. Fish. Comm. Bull. 53 (II). pp. 217–238.

Nakicenovic, N., Alcamo, J., Davis, G., de Vries, B., Fenhann, J., Gaffin, S., Gregory, K., Grübler, A., Jung, T.-Y., Kram, T., Lebre La Rovere, E., Michaelis, L., Mori, S., Morita, T., Pepper, W., Pitcher, H., Price, L., Riahi, K., Roehrl, A., Rogner, H., Sankovski, A., Schlesinger, M., Shukla, P., Smith, S., Swart, R., van Rooijen, S., Victor, N., and Zhou, D. 2000. Special report on emissions scenarios: a special report of Working Group III of the Intergovernmental Panel on Climate Change. Cambridge University Press, Cambridge, UK.

Neave, F., Yonemori, T., and Bakkala, R.G. 1976. Distribution and origin of chum salmon in offshore waters of the North Pacific Ocean. Int. N. Pac. Fish. Comm. Bull. 35.

Ogura, M., and Takagi, K. 1987. Difference in area of distribution between salmon and flying squid based on data collected by Japanese salmon research vessels, 1983–1986. Document submitted to International North Pacific Fisheries Commission. Fisheries Agency of Japan, Tokyo, Japan. Available on request from the Secretariat, North Pacific Anadromous Fish Commission, Vancouver, B.C.

Okazaki, T. 1983. Distribution and seasonal abundance of *Salmo gairdneri* and *Salmo mykiss* in the North Pacific Ocean. Jpn. J. Ichthyol. **30**: 235–246.

Pörtner, H.O., and Farrell, A.P. 2008. Physiology and climate change. Science, **322**(5902): 690–692. doi:10.1126/science.1163156. PMID:18974339.

Randall, D.A., Wood, R.A., Bony, S., Colman, R., Fichefet, T., Fyfe, J., Kattsov, V., Pitman, A., Shukla, J., Srinivasan, J., Stouffer, R.J., Sumi, A., and Taylor, K.E. 2007. Climate models and their evaluation. *In* Climate Change 2007: the physical science basis. Contribution of Working Group I to the Fourth Assessment Report of the Intergovernmental Panel on Climate Change. Chapter 8. *Edited by* S. Solomon, D. Qin, M. Manning, Z. Chen, M. Marquis, K.B. Averyt, M. Tignor, and H.L. Miller. Cambridge University Press, Cambridge and New York. pp. 589–662.

Ruggerone, G.T., and Nielsen, J.L. 2004. Evidence for competitive dominance of pink salmon (*Oncorhynchus gorbuscha*) over other salmonids in the North Pacific Ocean. Rev. Fish Biol. Fish. **14**(3): 371–390. doi:10.1007/s11160-004-6927-0.

Ruggerone, G.T., and Nielsen, J.L. 2009. A review of growth and survival of salmon at sea in response to competition and climate change. Am. Fish. Soc. Symp. **70**: 241–265.

Ruggerone, G.T., Zimmermann, M., Myers, K.W., Nielsen, J.L., and Rogers, D.E. 2003. Competition between Asian pink salmon (*Oncorhynchus gorbuscha*) an Alaskan sockeye salmon (*O. nerka*) in the North Pacific Ocean. Fish. Oceanogr. **12**(3): 209–219. doi:10.1046/j.1365-2419.2003.00239.x.

Sakai, J., Ueno, Y., Ishida, Y., and Nakayama, K. 1997. Vertical distribution of salmon determined by an acoustic survey in the North Pacific Ocean in the winter of 1996. Salmon Rep. Ser. **42**: 72–76.

Schindler, D.E., Augerot, X., Fleishman, E., Mantua, N., Riddell, B., Ruckelshaus, M., Seeb, J., and Webster, M. 2008. Climate change, ecosystem impacts, and management for Pacific salmon. Fisheries, **33**(10): 502–506. doi:10.1577/1548-8446-33.10.502.

Smith, T.M., Reynolds, R.W., Peterson, T.C., and Lawrimore, J. 2008. Improvements to NOAA's historical merged land–ocean surface temperature analysis (1880–2006). J. Clim. **21**(10): 2283–2296. doi:10.1175/2007JCLI2100.1.

Stephenson, S.A. 2006. A review of the occurrence of Pacific salmon (*Oncorhynchus* spp.) in the Canadian Western Arctic. Arctic, **59**: 37–46.

Sutherland, D.F. 1973. Distribution, seasonal abundance, and some biological features of steelhead trout, *Salmo gairdneri*, in the North Pacific Ocean. Fish Bull. **71**: 787–826.

Takagi, K. 1983. Differences in areas of distribution between salmon and flying squid. Document submitted to International North Pacific Fisheries Commission. Fisheries Agency of Japan, Tokyo, Japan. Available on request from the Secretariat, North Pacific Anadromous Fish Commission, Vancouver, B.C.

Walker, R.V., Myers, K.W., Davis, N.D., Aydin, K.Y., Friedland, K.D., Carlson, H.R., Boehlert, G., Urawa, S., Ueno, Y., and Anma, G. 2000*a*. Diurnal variation in thermal environment experienced by salmonids in the North Pacific as indicated by data storage tags. Fish. Oceanogr. **9**(2): 171–186. doi:10.1046/j.1365-2419.2000.00131.x.

Walker, R.V., Myers, K.W., Davis, N.D., Aydin, K.Y., and Friedland, K.D. 2000*b*. Using temperature data from data storage tags to model potential salmon growth. N. Pac. Anadr. Fish. Comm. Bull. 2. pp. 301–308. Available from http://www.npafc.org/new/pub_bulletin.html [accessed 28 October 2010].

Walker, R.V., Sviridov, V.V., Urawa, S., and Azumaya, T. 2007. Spatio-temporal variation in vertical distributions of Pacific salmon in the ocean. N. Pac. Anadr. Fish Comm. Bull. 4. pp. 193–201. Available from http://www.npafc.org/new/pub_bulletin.html [accessed 28 October 2010].

Welch, D.W., Chigirinsky, A.I., and Ishida, Y. 1995. Upper thermal limits on the oceanic distribution of Pacific salmon (*Oncorhynchus* spp.) in the spring. Can. J. Fish. Aquat. Sci. **52**(3): 489–503. doi:10.1139/f95-050.

Welch, D.W., Ishida, Y., and Nagasawa, K. 1998a. Thermal limits and ocean migrations of sockeye salmon (*Oncorhynchus nerka*): long-term consequences of global warming. Can. J. Fish. Aquat. Sci. **55**(4): 937–948. doi:10.1139/f98-023.

Welch, D.W., Ishida, Y., Nagasawa, K., and Eveson, J.P. 1998b. Thermal limits on the ocean distribution of steelhead trout (*Oncorhynchus mykiss*). N. Pac. Anadr. Fish Comm. Bull. 1. pp. 396–404. Available from http://www.npafc.org/new/pub_bulletin.html [accessed 28 October 2010].

Appendix A

Regridding algorithm

The regridding was performed by developing and verifying a distance-weighted spatial interpolation formula, which can be stated in functional form as

$$\text{(A.1)} \qquad \mathrm{SST}_{\mathrm{ref},j} = \frac{\sum_{i=1}^{n} w_i \times \mathrm{SST}_{\mathrm{mod},i}}{\sum_{i=1}^{n} w_i}$$

where $\mathrm{SST}_{\mathrm{ref},j}$ is the temperature at reference grid point j, $\mathrm{SST}_{\mathrm{mod},i}$ is the temperature at model grid point i, $w_i = 1/d_{ij}$ is the weight assigned to the model grid i, d_{ij} is the great-circle distance between model grid i and reference grid j obtained by using Haversine formula (see below), and n is the total number of neighboring model grids (i) considered for each reference grid j. As apparent, the model grids closer to the reference grid get the higher weights. In general, $n = 4$ was used in this study. In the case of superposition between reference and model grid points (i.e., $d_{ij} = 0$), both n and w_i were assigned to 1.0 to avoid singularity. Contamination of coastal SSTs by land surface temperatures was minimized by excluding coastal grid points that contained 50% or more land surface compared with that of sea. These percent "land area fraction" data were available for all 18 GCMs except CGCM (T47) (Table 1). The land area fraction data from ECHO-G were used for CGCM (T47), as they had an identical spatial resolution.

Haversine formula for calculating distance on sphere

The great-circle distance *d* between any two points B and C with respective geographic coordinates of (λ_B, φ_B) and (λ_C, φ_C) on sphere can be determined as (Sinnott 1984)

$$d = 2 \times R \sin^{-1}\left[\sqrt{\sin^2\left(\frac{\varphi_B - \varphi_C}{2}\right) + \cos(\varphi_B) \times \cos(\varphi_C) \times \sin^2\left(\frac{\lambda_B - \lambda_C}{2}\right)}\right] \tag{A.2}$$

where λ and φ are, respectively, the longitudes and latitudes in radians, and *R* is the radius of the sphere. A mean radius of 6371 km was used for the Earth's sphere in this study.

Formula for calculating area of a grid on sphere

Assuming points B and C of the previous section form two opposite corners on a diagonal of a grid on the sphere, magnitude of the projected trapezoidal area of the grid (A_{grid}) can analytically be derived as

$$A_{grid} = R^2 \times \Delta\lambda \times \Delta\varphi \times \cos(\varphi) \times \cos(\Delta\varphi/2) \tag{A.3}$$

where $\Delta\lambda = \text{abs}(\lambda_B - \lambda_C)$, $\Delta\varphi = \text{abs}(\varphi_B - \varphi_C)$, $\varphi = (\varphi_B + \varphi_C)/2$, abs refers to the absolute value, and others are as previously defined.

Definition of sensitivity coefficients

Following Abdul-Aziz et al. (2010), the nondimensional sensitivity coefficient (S^*) can be defined as

$$S^* = \frac{\Delta A^*}{\Delta T^*} \tag{A.4}$$

where $\Delta A^* = \Delta A/A_{ref}$ and $\Delta T^* = \Delta T/T_{ref}$ are, respectively, the proportionate (i.e., nondimensional) changes in the reference habitat area (A_{ref}, km^2) and thermal limit (T_{ref}, °C); ΔA is the corresponding change (km^2) in the reference area for the change (°C) in the reference thermal limit, ΔT. Thus, ΔA (km^2) for any ΔT (°C) can be calculated by simply rearranging terms in eq. A.4 as

$$\Delta A = S^* \times \frac{\Delta T}{T_{ref}} \times A_{ref} \tag{A.5}$$

References

Abdul-Aziz, O.I., Wilson, B.N., and Gulliver, J.S. 2010. Two-zone model for stream and river ecosystems. Hydrobiologia, **638**(1): 85–107. doi:10.1007/s10750-009-0011-7.

Sinnott, R.W. 1984. Virtues of the Haversine. Sky Telescope, **68**(2): 159.

Accounting for fish shoals in single- and multispecies survey data using mixture distribution models

James T. Thorson, Ian J. Stewart, and André E. Punt

Abstract: A scientific bottom trawl survey targeting Pacific rockfishes (*Sebastes* spp.) occasionally yields extraordinary catch events (ECEs) in which catch-per-unit-area is much greater than usual. We hypothesize that ECEs result from trawl catches of fish shoals. We developed mixture distribution models for positive catch rates to identify spatial covariates associated with ECEs or normal trawl catches and used simulation modeling to contrast the performance of mixture distribution and conventional log-linear models for estimating an annual index of positive catch rates. Finally, mixed-effects modeling was applied to multispecies data to evaluate the hypothesis that ECEs are related to shoaling behaviors. Results show that mixture distribution models are often selected over conventional models for shoaling species and that untrawlable habitat has a positive effect on rockfish densities. Simulation shows that mixture distribution models can perform as well as or better than conventional models at predicting positive catch rates. Finally, model selection supports the hypothesis that shoaling behaviors contribute to the occurrence of ECEs. We propose that greater understanding of ECEs and shoaling habitat selection could be useful in future spatial management and survey design and that mixture distribution models could improve methods for estimating annual indices of abundance.

Résumé : Un inventaire scientifique au chalut de fond qui cible les sébastes du Pacifique (*Sebastes* spp.) produit à l'occasion un événement de capture exceptionnel (ECE) dans lequel les captures par unité d'effort sont beaucoup plus importantes que d'habitude. Nous émettons comme hypothèse que ces ECE résultent de la capture de bancs de poissons. Nous avons mis au point des modèles de mélanges de distributions pour les taux de captures positifs afin d'identifier les covariables spatiales associées aux ECE et aux captures normales au chalut; nous avons aussi utilisé des modèles de simulation pour comparer les performances des modèles de mélanges de distributions et les modèles log-linéaires conventionnels pour l'estimation d'un indice annuel de taux de captures positifs. Finalement, une modélisation d'effets mixtes avec les données multispécifiques a permis d'évaluer l'hypothèse selon laquelle les ECE sont reliés aux comportements de formation de bancs. Les résultats montrent que les modèles de mélanges de distributions sont souvent choisis de préférence aux modèles conventionnels pour les espèces qui forment des bancs et ils indiquent que l'habitat dans lequel on ne peut faire du chalutage a un effet positif sur les densités de sébastes. Les simulations montrent que les modèles de mélanges de distribution peuvent performer aussi bien ou mieux que les modèles conventionnels pour prédire les taux de captures positifs. Enfin, la sélection des modèles appuie l'hypothèse qui veut que les comportements de formation des bancs contribuent à l'avènement des ECE. Nous croyons qu'une meilleure compréhension des ECE et de la sélection des habitats pour la formation des bancs pourrait s'avérer utile dans le futur pour la gestion spatiale et la planification des inventaires; les modèles de mélanges de distributions pourraient améliorer les méthodes d'estimation des indices annuels d'abondance.

[Traduit par la Rédaction]

Introduction

Fishery-independent bottom trawl surveys conducted by the National Marine Fisheries Service Northwest Fisheries Science Center (NMFS-NWFSC) are an important data source for groundfishes off the US west coast. Data from this survey provide information regarding fish habitat selection and behavior, as well as for stock assessment and management of the seven stocks of Pacific rockfishes (*Sebastes* spp.) in this region that are currently designated by the NMFS as rebuilding from an overfished state. Bottom trawl survey data are collected during a randomized scientific survey of trawlable groundfish habitat using contracted fishing industry vessels (Keller et al. 2008). In some cases, however, the catch rates from individual hauls may be 50 times larger than average (Stewart 2008), termed extraordinary catch events (ECEs). ECEs represent extremely large groundfish aggregations that may be statistically anomalous, transient from nearby untrawlable refuges, or simply rare shoaling events.

Received 14 February 2011. Accepted 20 June 2011. Published at www.nrcresearchpress.com/cjfas on 8 September 2011.
J2011-0022

Paper handled by Associate Editor Josef Michael Jech.

J.T. Thorson and A.E. Punt. School of Aquatic & Fishery Sciences, Box 355020, University of Washington, Seattle, WA 98195-5020, USA.
I.J. Stewart. Northwest Fisheries Science Center, 2725 Montlake Boulevard East, Seattle, WA 98112, USA.

Corresponding author: James T. Thorson (e-mail: JimThor@uw.edu).

Can. J. Fish. Aquat. Sci. **68**: 1681–1693 (2011) doi:10.1139/F2011-086 Published by NRC Research Press

Data from this and other fishery-dependent and -independent surveys are often analyzed using statistical models to control for conflating spatial, environmental, or behavioral effects while estimating an annual index of abundance (Maunder and Punt 2004; Ye and Dennis 2009). NMFS-NWFSC trawl survey indices of abundance are currently computed using delta generalized linear models (delta-GLMs; Helser et al. 2004; Maunder and Punt 2004). Often called hurdle models (Rose et al. 2001; Zuur et al. 2009), these approaches combine two separate types of information to generate an index of abundance: the proportion of hauls containing some catch of the species of interest (modeled as a Bernoulli random variable and (or) using a logit link function for a linear model), and catch rates given that the catch is nonzero (modeled using a fixed- or mixed-effects GLM). The proportion of positive catches serves as a proxy for occupied habitat, while in certain cases, positive catch rates are an efficient estimator for stock density (Pennington 1983). Changes in either process may indicate abundance changes, which is why delta-GLM models are widely used for index standardization (Stefansson 1996).

The presence of aggregations for some rockfish species (e.g., canary rockfish (*Sebastes pinniger*); Stewart 2008) suggests that a third process (after range size and positive densities) also underlies observed catch rates: the probability of and density when encountering a large aggregation. Index standardization models can account for this third process using a mixture distribution for catch rates in positive hauls in which two separate models (one for collections of solitary individuals and one for shoals) are combined to create a potentially bimodal probability distribution for catch rates in each trawl haul. This mixture distribution model can incorporate explanatory variables for solitary (or potentially small aggregations) and ECE densities, as well as for the mixture component that determines the relative probability of finding aggregated or solitary individuals in a given trawl haul. It also allows a model-driven identification of ECEs instead of using an a priori (and possibly arbitrary) cutoff to distinguish between typical and extreme catches.

The development of a mixture distribution model for normal and ECE tows allows formal exploration of the hypothesis that ECEs are caused by shoaling behavior. Specifically, this hypothesis can be evaluated by identifying which species are shoaling a priori and using this information as a species-level explanatory variable within a mixed-effects model. Model selection methods can then be applied to assess the strength of evidence that shoaling behaviors are associated with differences in mixture distribution catch rates.

Similarly, mixture distribution models can be used to identify spatial variables that have an effect on shoaling behavior in multiple species. Specifically, model selection can be used to explore the hypothesis that ECEs are more likely near untrawlable habitat, as seems likely given that rockfish densities are known to be higher around rocky bottom habitats (Jagielo et al. 2003). Mixture distribution models could also be used to screen for other spatial covariates that might influence the relative probability of encountering an ECE.

Finally, ECEs violate the statistical assumptions of common modeling techniques for survey data and will cause several problems if used to develop abundance indices using conventional statistical estimators (Kappenman 1999) or, presumably, when using delta-GLMs. These problems include (*i*) imprecise or biased estimation of the coefficient of variation of the abundance index (Olsen and Schafer 2001), (*ii*) indices that vary substantially among years, and (*iii*) potentially subjective decision-making regarding the exclusion or inclusion of ECEs (which might appear to be statistical outliers) when computing abundance indices. In principle, ECEs can be handled by modifying analysis methods (Kyriazidou 1997; Kappenman 1999; Xie et al. 2004) or by utilizing available information more efficiently.

In this study, we develop generalized mixture distribution models that include spatial covariates at a variety of modeling levels and can be applied to single- or multi-species data. We then demonstrate these methods by application to rockfish data collected during the annual NMFS shelf–slope bottom trawl survey off the US west coast. This application has three primary research objectives: (1) to identify the spatial covariates that contribute to densities of or occurrence probabilities for extreme catch events in single-species survey data for Pacific rockfish (*Sebastes* spp.); (2) to compare the performance of mixture distribution and log-linear models when estimating positive catch rates using simulated data; and (3) to formally test whether and in what manner shoaling behaviors contribute to the occurrence of extreme catch events in multispecies survey data for Pacific rockfish. This application also demonstrates the utility and flexibility of a class of models that is new to fisheries modeling, i.e., mixture distribution models using random effects for multispecies analyses.

Materials and methods

Data

This analysis is based on all NMFS-NWFSC shelf and slope bottom trawl hauls (NOAA Fisheries, 2725 Montlake Boulevard, Seattle, WA 98112, USA) made off the US west coast between 2003 and 2008 (Keller et al. 2008). These data are 3771 hauls, with average duration of 18 min and area swept of 1.8 ha and include tow depth, latitude, and longitude. The data represent 32 species of rockfish that ranged from rare (brown rockfish (*Sebastes auriculatus*), 32 occurrences) to relatively frequent (splitnose rockfish (*Sebastes diploproa*), 826 occurrences) (Table 1). Each of these species was categorized as shoaling or nonshoaling by consulting the life history sections of part 3 of Love et al. (2002): species were classified as schooling if the words "school" or "aggregation" were used to describe either the juvenile or adult life stages. Single-species analyses were limited to 19 species that were present in more than 100 hauls, whereas multispecies and simulation modeling analyses included all 32 species.

Spatial covariates were also calculated at each trawl location to represent habitat associations for ECEs, normal tows, or the relative probability that a given tow was an ECE. We hypothesized that depth and latitude were likely to have explanatory power regarding rockfish catches. Longitude was not used as a covariate in any model because it is strongly correlated with depth along the US west coast and depth is more likely to be biologically significant. We also calculated an index representing untrawlable habitat, i.e., the probability of trawl gear being hung up due to an encounter with untrawlable bottom structures (see Estimating untrawlable habitat section below). This feature was used as a covariate to explore

Table 1. Species' names, the number of positive catches in the NMFS bottom trawl survey, whether this exceeded the threshold for use in single-species analyses (>100 occurrences), and whether individuals of the species shoal either as juveniles or adults.

Common name	Scientific name	No. of tows	Used in single-species analyses?	Shoaling species?
Aurora	*Sebastes aurora*	514	Yes	No
Bank	*Sebastes rufus*	67	No	Yes
Blackgill	*Sebastes melanostomus*	182	Yes	No
Bocaccio	*Sebastes paucispinis*	223	Yes	Yes
Brown	*Sebastes auriculatus*	32	No	No
Calico	*Sebastes dalli*	54	No	No
Canary	*Sebastes pinniger*	263	Yes	Yes
Chilipepper	*Sebastes goodie*	492	Yes	Yes
Copper	*Sebastes caurinus*	41	No	Yes
Cowcod	*Sebastes veils*	83	No	No
Darkblotched	*Sebastes crameri*	678	Yes	No
Flag	*Sebastes rubrivinctus*	54	No	No
Greenblotched	*Sebastes rosenblatti*	67	No	No
Greenspotted	*Sebastes chlorostictus*	225	Yes	No
Greenstriped	*Sebastes elongates*	962	Yes	No
Halfbanded	*Sebastes semicintus*	298	Yes	Yes
Pacific ocean perch	*Sebastes alutus*	246	Yes	Yes
Pygmy	*Sebastes wilsoni*	70	No	Yes
Redbanded	*Sebastes babcocki*	308	Yes	No
Redstripe	*Sebastes proriger*	95	No	Yes
Rosethorn	*Sebastes helvomaculatus*	310	Yes	No
Rougheye	*Sebastes aleutianus*	197	Yes	No
Sharpchin	*Sebastes zacentrus*	227	Yes	Yes
Shortbelly	*Sebastes jordani*	317	Yes	Yes
Silvergray	*Sebastes brevispinis*	35	No	Yes
Splitnose	*Sebastes diploproa*	826	Yes	Yes
Squarespot	*Sebastes hopkinsi*	59	No	Yes
Stripetail	*Sebastes saxicola*	789	Yes	No
Vermilion	*Sebastes miniatus*	49	No	Yes
Widow	*Sebastes entomelas*	126	Yes	Yes
Yelloweye	*Sebastes ruberrimus*	81	No	Yes
Yellowtail	*Sebastes flavidus*	229	Yes	Yes

hypotheses about the effect of untrawlable habitat on rockfish densities and ECEs. For latitude and depth, consideration was given to linear and quadratic effects to allow for the identification of an optimal depth or latitude at which catch rates are maximized. Although future analyses could explore other spatial covariates, we restricted this analysis to variables that are currently assumed to influence rockfish densities.

Estimating untrawlable habitat

To explore hypotheses about the role of untrawlable habitat on rockfish densities and the relative probability of ECEs, we sought to associate each bottom trawl set with a covariate representing untrawlable habitat. We compiled a record of all the NMFS-NWFSC shelf–slope bottom trawl survey locations that were successful, fouled, or deemed to be untrawlable after searching the spatial cell (NOAA Fisheries, 2725 Montlake Boulevard, Seattle, WA 98112, USA) and used this to estimate a spatial field representing the probability of tow failure at each cell in the bottom trawl sampling frame. A trawl record was classified as successful if a bottom trawl was completed there without damage to the net, whereas a trawl record was classified as unsuccessful if the net was damaged or fouled or the captain decided that trawling at that location would be dangerous to the gear or sampling personnel. A regression model was developed to explain these records of trawl success or failure (coded as zero and one, respectively) using latitude and longitude. This model was then used to predict "untrawlability" (ranging continuously from zero to one) at all locations within the depth range of the bottom trawl survey. Specifically, "random forest" (Breiman 2001; Liaw and Wiener 2002) was used for this task because it can account for highly nonlinear interactions among explanatory variables (Hastie et al. 2009) such as could be expected when using location (i.e., latitude and longitude) as a proxy for the specific mechanistic factors that contribute to trawl success or failure. Tenfold crossvalidation (Hastie et al. 2009) was then used to provide a conservative estimate of predictive accuracy and estimated a 58% correlation between the estimated probability of a failed tow and recorded tow failures in each crossvalidation test set. This result corresponds to a Nagelkerke R^2 of 0.33 when random forest predictions were compared against a null binomial model in which every tow has an equal probability of failure. Exploratory analysis also showed that random forest performed better than either logistic regression or generalized additive models. Besides using crossvalidation, we assessed the suitability of this index of untrawlable habitat by looking for patterns when it was used as a predictor for catch rates. We hypothesized that if the index actually represented an important biological effect, it would have a consistent (and probably positive) effect on rockfish catch rates. However, differences between this index and unobserved untrawlability are likely to decrease the statistical significance and attenuate the estimated coefficient for untrawlable habitat in all models. Recorded latitude and longitude of each set were then used to associate each bottom trawl observation with this spatial field. This and all other calculations were conducted using the R statistical platform (R Development Core Team 2009).

Model development

A mixture distribution model was developed to (*i*) differentiate between typical catches and ECEs, (*ii*) evaluate which spatial covariates influenced the density of typical catches or ECEs, and (*iii*) assess the relative probability of encountering a typical catch or ECEs during any given trawl haul by species. This mixture distribution model included three components: (1) the density of catches for normal tows, (2) the density of catches for ECEs, and (3) the relative probability of a given tow resulting in a typical catch or an ECE.

The expected catch rate for "typical" tows was modeled as a log-linear model and included spatial covariates (e.g., depth, depth², latitude, latitude², and untrawlable habitat; eqs. 1 and 2) that were standardized to have mean 0 and standard deviation 1 prior to subsequent analysis:

$$(1) \qquad \lambda_i = \sum_{y=\{Y\}} \beta_{\lambda,y} I_{i,y} + \beta_{\lambda,D} D_i + \beta_{\lambda,D2} D2_i + \beta_{\lambda,L} L_i + \beta_{\lambda,L2} L2_i + \beta_{\lambda,U} U_i$$

where λ is the logarithm of the predicted density of normal tows, $\beta_{\lambda,y}$ is a year-specific intercept for λ, $I_{i,y}$ is 1 if $Y_i = y$ and 0 otherwise, $\hat{\beta}_{\lambda,D}$, $\hat{\beta}_{\lambda,D2}$, $\hat{\beta}_{\lambda,L}$, $\hat{\beta}_{\lambda,L2}$, and $\hat{\beta}_{\lambda,U}$ are the effects of depth, depth², latitude, latitude², and untrawlable habitat on λ, respectively, and D_i, $D2_i$, L_i, $L2_i$, U_i, and Y_i are standardized depth, depth², latitude, latitude², estimated untrawlable habitat, and year for observation *i*.

The expected catch rate for ECEs was modeled as a nonlinear function of predicted "typical" catch rates and was parameterized such that ECEs always had a higher predicted density than typical catches. This parameterization ensured a natural ordering for mixture components (i.e., prevented label switching) and was important for identifying and interpreting the mixture model (Marin et al. 2005). This parameterization also allowed covariates (such as year effects) to influence the catch rate for ECEs by means of changes in expected catch rates:

$$(2) \qquad \xi_i = \lambda_i + \log\left(1 + \exp\left[\beta_\xi + \beta_{\xi,D} D_i + \beta_{\xi,D2} D2_i + \beta_{\xi,L} L_i + \beta_{\xi,L2} L2_i + \beta_{\xi,U} U_i + \sum_{y=\{Y\}} \beta_{\xi,y} I_{i,y}\right]\right)$$

where ξ is the predicted density for ECEs, β_ξ is an intercept for ξ (when a year effect is not present), $\beta_{\xi,D}$, $\beta_{\xi,D2}$, $\beta_{\xi,L}$, $\beta_{\xi,L2}$, and $\beta_{\xi,U}$ are the effects of depth, depth², latitude, latitude², and untrawlable habitat on ξ, $\beta_{\xi,y}$ is a year-specific intercept for ξ, and other symbols are as previously defined.

The component that models the relative probability of normal tows vs. ECEs for an observation *i* was modeled as a logit-transformed linear model and again included spatial covariates (e.g., depth, depth², latitude, latitude², and untrawlable habitat; eq. 3):

$$(3) \qquad \omega_i = \frac{1}{1 + \exp\left[-\left(\beta_\omega + \beta_{\omega,D} D_i + \beta_{\omega,D2} D2_i + \beta_{\omega,L} L_i + \beta_{\omega,L2} L2_i + \beta_{\omega,U} U_i + \sum_{y=\{Y\}} \beta_{\omega,y} I_{i,y}\right)\right]}$$

where β_ω is an intercept for ω (when a year effect is not present), $\beta_{\omega,D}$, $\beta_{\omega,D2}$, $\beta_{\omega,L}$, $\beta_{\omega,L2}$, and $\beta_{\omega,U}$ are the effects of depth, depth², latitude, latitude², and untrawlable habitat on ω, and $\beta_{\omega,y}$ is a year-specific intercept for ω. In this component, a value of ω_i greater than 0.5 implies an increased prior probability of a given tow *i* resulting in a typical catch and not an ECE. ω_i represents the prior probability that tow *i* will result in a typical catch or ECE, but it can also be interpreted as the proportion of tows at the same location as tow *i* that would result in a typical catch, whereas 1 – ω_i represents the proportion that would result in an ECE.

Likelihoods were calculated as a mixture distribution (eq. 4) with previously defined components predicting normal catches and ECEs, as well as the probability of a normal catch for tow *i*, assuming a normal error distribution for log (catches) (eq. 5):

$$(4) \qquad L(\tilde{\beta}|\mathrm{CPE}) = \prod_{i=1}^{n} [\omega_i D(\lambda_i|\mathrm{CPE}_i) + (1 - \omega_i) D(\xi_i|\mathrm{CPE}_i)]$$

$$(5) \qquad D(X_i|\mathrm{CPE}_i) = \frac{1}{\sqrt{2\pi\sigma_j^2}} \exp\left[\frac{-\left(\log(\mathrm{CPE}_i) - \left(X_i - \frac{\sigma_j^2}{2}\right)\right)^2}{2\sigma_j^2}\right]$$

where X_i could represent predicted catch-per-unit-area for either typical (λ_i) or ECE (ξ_i) tows, σ_j is the standard deviation for the normal error distribution for log(catches) in either typical tows ($j = 1$) or ECEs ($j = 2$). Models were fit using a Nelder–Mead optimizer in R.

Equations 4 and 5 are numerically equivalent to a hierarchical model (Royle and Dorazio 2008) in which each observation is assigned a latent class, e.g., has an unobserved state corresponding to a normal tow or ECE. In the hierarchical interpretation, the latent class for each observation is then "integrated out" by computing the likelihood for all fixed effects while summing across the probability of each observation being in one latent class or the other (i.e., by maximum marginal likelihood). We choose to refer to eq. 4 as a mixture distribution rather than a hierarchical model because this emphasizes the marginal sampling distribution rather than the distribution of latent classes, although either interpretation is justified.

This three-component model (eqs. 1–3) contains the conventional log-linear model for positive catches as a nested submodel. In this case, the components for the relative probability of normal tows and ECEs (i.e., eq. 3) and the catch densities for ECEs (i.e., eq. 2) have no coefficients and are excluded from the model. Inclusion of a mixture distribution requires, at a minimum, the estimation of an intercept term that represents the proportional increase in catch for ECEs compared with densities for typical catches (β_η) and the probability that an average tow will encounter an ECE (β_ω). Thus, stepwise model building can begin at the conventional log-linear model (i.e., where $\omega_i = 1$ for all *i*) and then proceed by exploring the addition of the two parameters (i.e., β_ω and β_η) necessary to estimate a mixture component. In this process, the addition of the two parameters representing the mixture distribution can be considered similarly to other possible model coefficients. Once a mixture component has previously been added to the model, the ECE density and relative probability components could also include effects for year, depth, depth^2, latitude, latitude^2, and untrawlable habitat. The component representing densities for normal catches always includes a categorical year effect (allowing for changes in abundance by year) but can also select among effects for depth, depth^2, latitude, latitude^2, and untrawlable habitat.

Annual abundance was estimated from the positive density component of a hurdle model index of abundance and was used to compare the performance of mixture and log-linear models when estimating an annual measure of positive densities (see Comparing performance of mixture and log-linear models section below). This density component involves predicting catch rates at a representative tow location (i.e., where depth, depth^2, latitude, latitude^2, and untrawlable habitat were all set to mean values in the bottom trawl data set) using parameter values from the fitted model but without including predictive errors caused by measurement errors. By doing this predictive calculation (and its 95% confidence interval), the model captures year effects while controlling for the effects of spatial covariates. This calculation was done to explore the impact of mixture distribution models on catch rate predictions.

Objective 1: identifying spatial covariates

Model selection in single-species models was used to identify both (*i*) a model that can parsimoniously predict densities throughout the species range and (*ii*) spatial covariates that contribute to the density of shoaling and solitary individuals or the relative probability of encountering an ECE.

Model selection was conducted for each species using stepwise selection and the Schwartz Bayesian information criterion (BIC; Schwarz 1978). Stepwise (i.e., forward and backwards) model selection was used to select among 131 104 (2^{17} mixture + 2^5 nonmixture) possible sets of covariates while starting at a null model that did not include any mixture component or spatial effects. BIC was used for model selection instead of the Akaike information criterion (AIC; Akaike 1974) based on exploratory simulation modeling work showing that AIC-based stepwise model selection led to selection of consistently more covariates than had been used to simulate data, whereas BIC was relatively accurate in selecting covariates that were used to simulate data.

Model diagnostics were applied to the stepwise-selected models to ensure that they were fitted well. Diagnostics for mixture distribution models include pseudoclass simulations (sensu Wang et al. 2005) and Pearson residuals for predicted classes. Pseudoclass simulations were conducted for each observation by drawing the latent class (i.e., typical catch or ECE) from the relative probability of observing each and then simulating a random catch from the chosen distribution. The predicted distribution of catches for a given fitted model was calculated by repeating this process (i.e., 100 times per observation). This distribution was then compared with the observed distribution. Pearson class residuals were calculated by assuming that each observation belongs to a single, latent class (set to the class that is more likely given the relative probability component; eq. 3). The Pearson residual for each observation was then calculated by subtracting the observed density from the expected density given that class membership. Pearson residuals were plotted against the independent variables to assess lack of fit and were binned by distance to explore spatial correlations. Preliminary analysis showed little evidence for spatial correlation, so spatial variograms were excluded from subsequent analysis.

Objective 2: comparing performance of mixture and log-linear models

The single-species model selection process was validated by simulating survey data using parameters that were selected and estimated in objective 1 and then fitting these simulated data while repeating the model selection process to determine how similar the resulting model was to the model used to simulate the data. In each replicate, this process was conducted using the BIC-selected model and estimated parameter values for all 19 rockfish species. Model selection accuracy was assessed while aggregating results across all of these species. This simulation modeling evaluation was repeated for six configurations formed from all combinations of a three × two cross of two potentially important factors, i.e., sample size and model structure. Three sample sizes were considered: 100 positive catches per species, 2000 positive catches per species, and the number of positive catches that were observed for each species in the bottom trawl data. Two simulation model types were considered. Model type 1 simulated data using a model without any mixture component or spatial covariates (with parameters set to values estimated by applying this model to rockfish data); this is identical to simulating data from a log-linear model that only includes a dummy variable representing year. Model type 2 simulated data using parameter values and the BIC-selected model from objective 1 (including a mixture distribution if this was selected in objective 1). Data were simulated by drawing the desired sample size with replacement from the locations for positive catches for that species, while simulating alternative catches at each selected location using estimated values for included parameters. One-hundred replicates were conducted for each species and configuration (three sample sizes × two model structures), resulting in 19 200 simulated data sets that were fitted using stepwise model selection.

The performance of mixture distribution models was assessed in all configurations by comparison with a conventional log-linear model (i.e., without a mixture component) in which log(catches) were regressed against spatial covariates that were selected using stepwise-BIC selection. The performance of mixture distribution and log-linear models was assessed in two ways. First, the positive catches at a representative location were predicted for the true model used to simulate the data, as well as for the BIC-selected mixture and nonmixture (i.e., log-linear) models. Density predictions at a representative location were used for comparison because this prediction is frequently a component of the hurdle model estimates of an index of stock abundance used in stock assessments (Maunder and Punt 2004). Each model provided predictions of positive catch for each of six years, and this series of six annual predictions was centered to have a mean of one (to reflect its possible use as a relative index of abundance). Relative unsigned error (RUE; eq. 6) was then calculated for mixture and nonmixture models, and average relative unsigned error (ARUE) was estimated as the average of RUE across all 32 species, 100 replicates per species, and 6 years per replicate:

$$(6)\qquad \mathrm{RUE}_{s,y,r} = \frac{\mathrm{abs}(E_{s,y,r} - \widehat{E}_{s,y,r})}{E_{s,y,r}}$$

where abs(X) represents the absolute value of X, $E_{s,y,r}$ and $\widehat{E}_{s,y,r}$ are the true and estimated density for species s in year y and replicate r after standardizing such that $\sum_{y=1}^{6} E_{s,y,r} = 1$ and $\sum_{y=1}^{6} \widehat{E}_{s,y,r} = 1$. Second, the average unsigned error (AUE; eq. 7) between the estimated and true number of parameters was calculated for the mixture distribution and log-linear models:

$$(7)\qquad \mathrm{AUE}_s = \frac{1}{r}\sum_{r=1}^{n_r} \mathrm{abs}(p_s - \widehat{p}_{s,r})$$

where p_s is the number of parameters used to generate data for species s, $\widehat{p}_{s,r}$ is the number of parameters selected by stepwise-BIC model selection for species s in replicate r, and n_r is the number of replicates. The estimated number of parameters demonstrates whether either model was systematically selecting a model that was over- or under-parameterized.

Objective 3: testing shoaling effect on ECEs

Mixed-effects models are seeing increasing use in ecology and fisheries as a method of testing species-level hypotheses (Qian et al. 2010; Thorson and Berkson 2010) and allow effects to be estimated using multispecies data. Multispecies modeling was conducted to formally test for the life history traits that contribute to ECEs. Specifically, we hypothesized that ECEs arise from the encounter between fishing gear and fish shoals, and we tested this hypothesis by exploring whether shoaling and nonshoaling species had systematically different parameters regarding either the relative probability of encountering or catch rates when encountering ECEs. This multispecies modeling framework allowed us to explore whether shoaling species are likely to have a greater probability for fishing gear to encounter a fish shoal (i.e., greater β_ω parameters on average) or whether these encounters are likely to result in larger increases in catch rates (i.e., greater β_ξ parameters on average).

A mixed-effects model was used to test for systematic differences in parameters between shoaling and nonshoaling species and was developed by linking parameters from multiple single-species mixture distribution models within a common, hierarchical structure. Mixed effects are only interpretable when applied to interchangeable parameters (Gelman et al. 2003). In our mixture distribution models, we hypothesized that the ratio of the normal and ECE catch densities (β_ξ; eq. 8) and the relative probabilities between the normal and ECE tows (β_ω; eq. 9) were normally distributed random effects:

$$(1)\qquad \beta_{\xi,j} \sim \mathrm{N}(I_j\mu_{\xi,s} + (1 - I_j)\mu_{\xi,0}, \sigma_\xi^2)$$

$$(2)\qquad \beta_{\omega,j} \sim \mathrm{N}(I_j\mu_{\omega,s} + (1 - I_j)\mu_{\omega,0}, \sigma_\omega^2)$$

where $\mu_{\omega,S}$ and $\mu_{\omega,0}$ are the expected values for β_ω for shoaling species and nonshoaling species, respectively, $\mu_{\xi,S}$ and $\mu_{\xi,0}$ are the expected values for β_ξ for shoaling species and nonshoaling species, respectively, σ_ω and σ_ξ are the standard deviations for among-species variability in β_ω and β_ξ, respectively, and $I_j = 1$ for shoaling species and 0 for nonshoaling species.

Restrictions on different parameters lead to four different possible models in which AIC was used to assess the weight of evidence in favor of one model or another (Burnham and Anderson 2002). We limited analysis to these four models to ensure that all tested models are biologically plausible and interpretable based on prior knowledge of these species. Model 1 ($\mu_{\xi,S} = \mu_{\xi,0}$ and $\mu_{\omega,S} = \mu_{\omega,0}$, i.e., no differences between shoaling and nonshoaling species) represents the null hypothesis that shoaling does not impact bottom trawl survey data. Model 2 ($\mu_{\xi,S} = \mu_{\xi,0}$ and $\mu_{\omega,S} \neq \mu_{\omega,0}$, i.e., differences in relative probability) represents the hypothesis that shoaling behavior changes the encounter rate between survey gear and rockfish aggregations. Model 3 ($\mu_{\xi,S} \neq \mu_{\xi,0}$ and $\mu_{\omega,S} = \mu_{\omega,0}$, i.e., differences in relative density) represents the hypothesis that shoaling behavior impacts the relative density of fishes in rockfish aggregations. Model 4 ($\mu_{\xi,S} \neq \mu_{\xi,0}$ and $\mu_{\omega,S} \neq \mu_{\omega,0}$, i.e., differences in relative probability and density) represents both hypotheses. Although shoaling and nonshoaling species could have a different expected value for the ratio of typical catches and ECEs (models 3 and 4) or the relative probability of encountering an ECE (models 2 and 4), all models assumed that the variances for shoaling and nonshoaling random effects were the same. AIC was used for selection among the four multispecies mixed-effects models because it has been tested in maximum likelihood mixed-effects model selection (Pinheiro and Bates 2009) and because the authors are not aware of studies using other information criteria for mixed-effects model selection.

Each random-effect model was applied to data for all 32 species while including the spatial effects that were selecting in single-species BIC-stepwise model selection (i.e., objective 1). However, all species were then forced to have a mixture distribution component without a year effect for the ECE or relative probability components. All fixed-effect parameters were estimated using maximum likelihood mixed-effects methods, i.e., by integrating across random-effect parameters. The marginal likelihood was calculated for each species using the "cubature" bivariate numerical integration technique (Genz and Malik 1980; Berntsen et al. 1991; Johnson and Narasimhan 2009) to integrate across the β_ξ and β_ω parameters, conditional on the hyperparameters, while taking the

Table 2. Model selection results for best mixture and nonmixture model as selected using BIC.

	Interpretation		Mixture			Nonmixture
	Shoaling	ΔBIC	Density (normal)	Density (ECE)	Weights	Density (normal)
Aurora	No	0	D+D2+L+L2	—	—	D+D2+L+L2
Blackgill	No	0	L2	—	—	L2
Bocaccio	Yes	0	D+D2+L	—	—	D+D2+L
Canary	Yes	81	U+L	D2	D2	L
Chilipepper	Yes	70	D2+L	U+L+L2	D+D2	D+D2+L+L2
Darkblotched	No	14	D+D2+L	—	D2	D+D2+L+L2
Greenspotted	No	0	U+L2	—	—	U+L2
Greenstriped	No	0	D+D2+U+L+L2	—	—	D+D2+U+L+L2
Halfbanded	Yes	14	U+L2	—	—	D+U+L2
Pacific ocean perch	Yes	56	D2	—	L	D2+L
Redbanded	No	0	D2+L2	—	—	D2+L2
Rosethorn	No	0	U+L	—	—	U+L
Rougheye	No	0	D+D2+L	—	—	D+D2+L
Sharpchin	Yes	33	D2	—	D+L	—
Shortbelly	Yes	51	—	D2	U+L+L2	U
Splitnose	Yes	0	D+D2+L+L2	—	—	D+D2+L+L2
Stripetail	No	160	D+D2+L	L2	D+D2+L	D+D2+L+L2
Widow	Yes	36	D2	U	D2	U
Yellowtail	Yes	33	D+D2+L2	U	—	D2+U+L2

Note: ΔBIC, the difference in BIC between the BIC-selected mixture and nonmixture models; ECE, extraordinary catch event; D, depth; D2, depth^2; L, latitude; L2, latitude^2; U, metric of untrawlable habitat.

product across all 32 species. We started the maximization of the mixed-effects likelihood at multiple starting locations for the hyperparameters and used the results that yielded the greatest log-likelihood because likelihood functions for mixture distribution models are frequently multimodal.

Results

Objective 1: identifying spatial covariates

Stepwise-BIC model selection was conducted when fitting the NMFS-NWFSC bottom trawl data both among mixture distribution models and when only allowing nonmixture (i.e., log-linear) models. BIC for the selected model was recorded for both mixture and nonmixture models and was interpreted by calculating the difference in BIC (ΔBIC) between the BIC-selected mixture and nonmixture models (Table 2). ΔBIC was zero when a BIC selection for the mixture model caused the mixture component to be removed; in this case, BIC selection led to a model that is identical to the selected nonmixture model. A mixture distribution structure was selected for 10 of the 19 rockfish species, and ΔBIC for these species ranged between 14 and 160, signaling in those cases a large improvement in fit by including a mixture structure. A year effect was never selected for either the ECE or the relative probability model components for these 19 species; this implies limited evidence in survey data for interannual changes in the proportion of total abundance that is shoaling or the size of shoals relative to nonshoaling densities.

Estimated spatial effects (Table 3) show that depth-squared was always negative for the density of typical catches and ECEs. This implies that catch densities are greatest at an optimal depth and is evidence for depth-specific habitat selection for both solitary individuals and individuals in ECEs. The index of untrawlable habitat is selected for eight of the 19 species for normal and ECE densities where it always has a positive estimated effect: this signifies that densities are estimated to be greater in areas with a high estimated degree of untrawlable habitat. Few systematic effects are present in the relative probability (weighting) component and extreme values for estimated coefficients appear for two species. The low number of selected spatial covariates for ECEs (and the extreme values when selected) implies that survey data are relatively uninformative regarding spatial effects contributing to ECEs.

To visualize predicted catch densities for mixture and nonmixture models, density histograms of catch from the bottom trawl survey after removing all occurrences of zero catch and log-transformation are shown for shoaling (Figs. 1*a*–1*j*) and nonshoaling (Figs. 1*k*–1*s*) species. The densities from the pseudoclass simulations for the BIC-selected mixture and nonmixture models are overlaid on these data. In general, the density plots are indistinguishable between mixture and nonmixture models for those species for which BIC selected a nonmixture model. By contrast, several species can be easily identified visually as having ECEs (i.e., a fat tail to the right of the mode), including canary rockfish, Pacific ocean perch (*S. alutus*), yellowtail (*S. flavidus*), and widow rockfish (*S. entomelas*) both in the observed histogram and in the mixture model prediction of densities. As expected, a difference between mixture and nonmixture density distributions can be seen for most shoaling species (Figs. 1*a*–1*j*) and cannot be seen for most nonshoaling species (Figs. 1*k*–1*s*).

Finally, inspection of stepwise-BIC model selection results (Table 3) shows that DIC selected a mixture component for eight of 10 shoaling species, whereas DIC did not select a mixture component for seven of nine nonshoaling species. The resulting contingency table exhibits a significant (p = 0.023) correspondence between BIC selection of a mixture distribution model and shoaling behaviors when analyzed using a Fisher's exact test. This post hoc analysis is exploratory

Table 3. Estimated spatial effects for the density of typical catches, ECEs, and the likelihood of encountering one or the other from the model selected using BIC.

	$\text{Density}_{\text{normal}}$					$\text{Density}_{\text{ECE}}$					Weights				
	D	D2	U	L	L2	D	D2	U	L	L2	D	D2	U	L	L2
Aurora	−0.6	−0.46			−0.31										
Blackgill					0.35										
Bocaccio	2.76	−3.59													
Canary			0.19				−1.3					−1.34			
Chilipepper		−0.44						0.43	−4.33	−4.32	−23.4	22.0			
Darkblotched	1.02	−2.52										−1.39			
Greenspotted			0.72		−0.49										
Greenstriped	2.36	−2.75	0.43		−0.25										
Halfbanded			0.62		0.48										
Pacific ocean perch		−0.42												−1.23	
Redbanded		−0.63			0.31										
Rosethorn			0.39												
Rougheye	−0.45	−0.34													
Sharpchin		−0.28									−0.61			−0.73	
Shortbelly							−1.44						−1.2	7.01	6.37
Splitnose	1.98	−2.69			−0.27										
Stripetail	1.23	−1.54								−1.67	−13.6	15.2		1.04	
Widow		−0.2						0.46				−1.37			
Yellowtail	3.37	−3.79			0.37			0.67							

Note: See Table 1 for species' scientific names. ECEs, extraordinary catch events; D, depth; D2, depth^2; L, latitude; L2, latitude^2; U, metric of untrawlable habitat.

but provides informal support for the hypothesis that BIC selection of a mixture distribution for single-species data is related to shoaling behaviors.

Objective 2: comparing mixture distribution and log-linear models

Model testing using simulated data (Table 4) showed that stepwise-BIC model selection for mixture distribution models generally selected a model of appropriate complexity (i.e., the number of parameters was similar to the model used to generate the data). In particular, stepwise-BIC model selection usually selected a nonmixture structure when data were simulated from a log-linear model. Mixture distribution models also improved the accuracy of annual predictions of positive catches at a representative location when data were simulated from a mixture distribution but did not greatly increase error when data were simulated from a conventional log-linear model (Fig. 2). Differences between mixture and log-linear models were especially pronounced for the observed sample sizes and model configurations based on the model selected in objective 1 (i.e., Table 2), when the mixture distribution model led to a ~20% ((0.32–0.26)/026) decrease in average relative unsigned error (Table 4, configuration 4).

Objective 3: testing the effect of shoaling on ECEs

AIC model selection among the different mixed-effects model structures (Table 5) demonstrates that shoaling behavior explains a major portion of the increase in densities that occur during ECEs. AIC identifies near equal support between models 3 and 4, both of which estimate an increased density for ECEs shoaling species compared with nonshoaling species. Specifically, model 4 shows that shoaling species have 5.6 times ($e^{3.06-1.34}$) greater densities in ECEs than do nonshoaling species, suggesting that at least part of the observed difference between typical catches and ECEs can be attributed to species-specific shoaling behaviors. Model 4 also includes a difference in the relative probability of each tow being shoaling or nonshoaling, where shoaling species have a lower relative probability of any given tow being an ECE. This effect is unexpected. We speculate that it could arise because, as shoaling causes a greater differentiation in expected catches between ECE and typical tows, more low-catch tows are definitively classified as typical rather than as ECEs for shoaling species.

Discussion

Applications for current work

In this study, we used records of trawl searches and hung tows to estimate a spatial field representing habitat that is untrawlable in the NMFS-NWFSC shelf–slope trawl survey sampling frame. This estimated spatial field had a surprisingly strong crossvalidation accuracy given the small sample sizes involved and could be useful for a variety of future research and management goals, including the stratification of survey areas among multiple sampling gears or the calculation of the effective sampling area for trawl gear. Although the untrawlable habitat covariate was not often selected by stepwise model selection, it had a positive effect on solitary and shoaling densities in all instances where it was selected. This positive impact of untrawlable habitat on rockfish densities supports previous studies showing increased rockfish densities in rocky benthic habitats, despite using data on a drastically enlarged spatial scale (Jagielo et al. 2003). The positive impact of the estimated "untrawlability" also offers some support that the estimated index is correlated with a biologically important effect, although future work is needed to validate this estimated spatial field.

Fig. 1. Histograms showing the log-transformed densities of bottom trawl catch for each of 19 species that had sufficient (>100) observations between 2003 and 2008 in the shell–slope bottom trawl survey, along with predicted density from BIC-selected mixture (broken lines) and nonmixture (solid lines) models, divided between shoaling species (*a*, bocaccio; *b*, canary; *c*, chilipepper; *d*, halfbanded; *e*, Pacific ocean perch; *f*, sharpchin; *g*, shortbelly; *h*, splitnose; *i*, widow; *j*, yellowtail) and nonshoaling species (*k*, aurora; *l*, blackgill; *m*, darkblotched; *n*, greenspotted; *o*, greenstriped; *p*, redbanded; *q*, rosethorn; *r*, rougheye; *s*, stripetail).

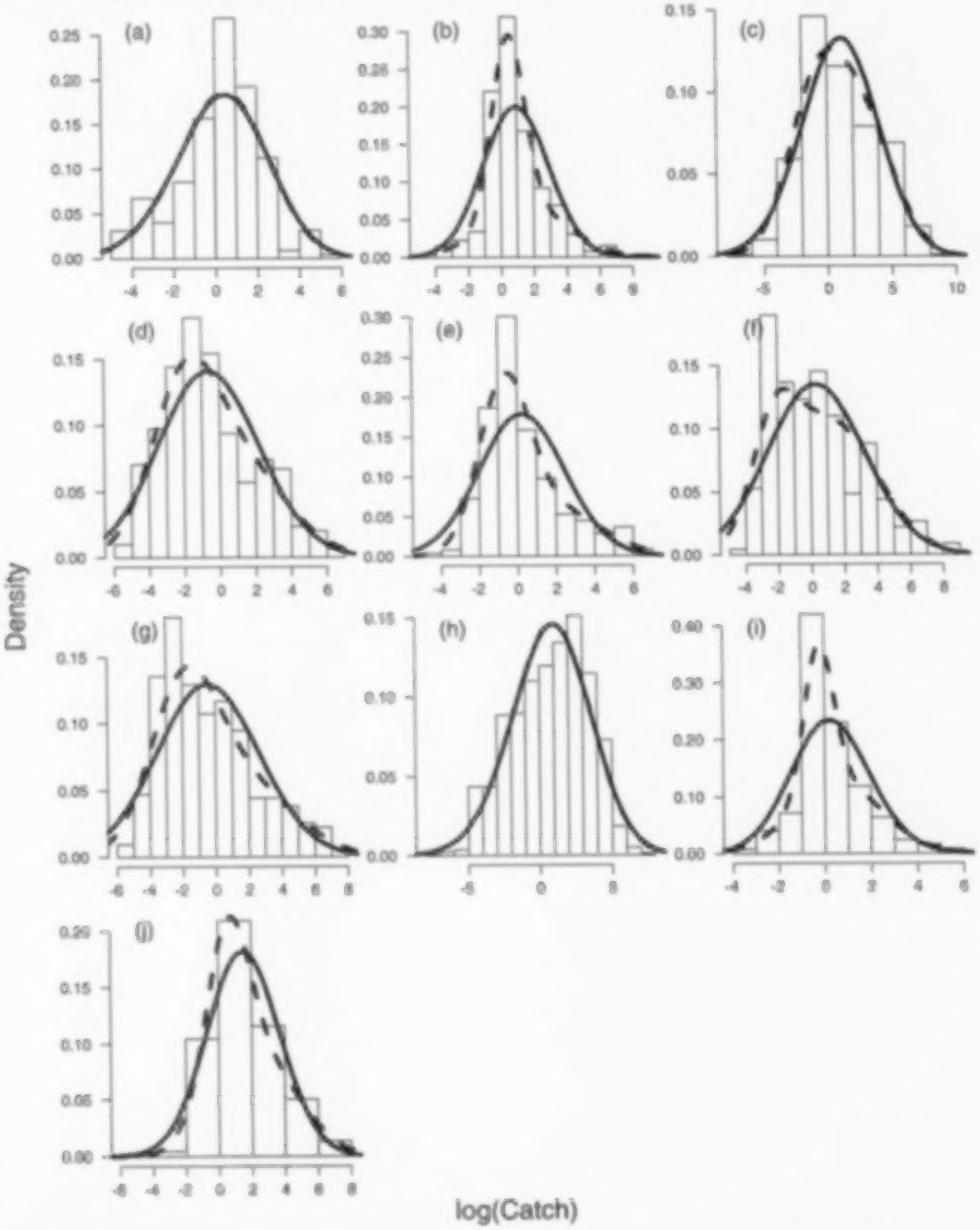

We also developed mixture distribution models that can be applied to either single- or multi-species survey data such as are available for many oceans and fishery management regions. These models can be used for at least three study goals as described below.

Spatial factors for extreme catch events

Given the current research and management interest in habitat impacts on surveys and stock assessments (Copps et al. 2007), the spatial covariates that we have identified could be useful during the planning stages for future resource sam-

Fig. 1 *(concluded).*

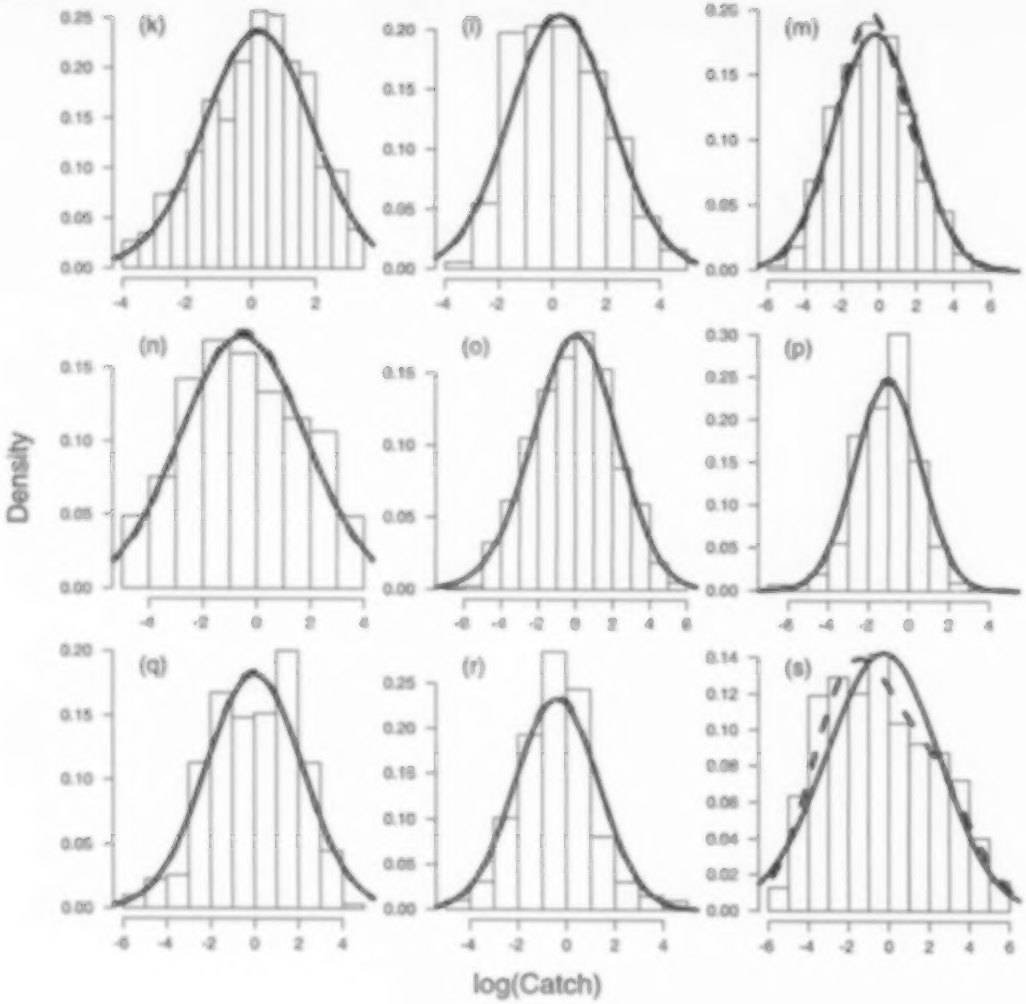

Table 4. Model validation results for six data-generating configurations (with three different sample sizes and two different simulation model types) for positive catch in simulated trawl data, with accuracy for mixture and nonmixture models (as selected by BIC stepwise model selection) as measured by average relative unsigned error (ARUE) estimated catch rates, and average errors in the BIC-selected number of parameters (average absolute value of the difference between estimated and true number of parameters).

Model settings			Estimation type			
			ARUE		Average errors	
Configuration	Sample size	Model used to simulate data	Mixture	Nonmixture	Mixture	Nonmixture
1	100	Nonmixture	0.38	0.35	1.03	0.19
2	100	Estimated	0.30	0.36	1.62	3.03
3	Observed	Nonmixture	0.32	0.30	0.89	0.19
4	Observed	Estimated	0.26	0.32	1.42	2.77
5	2000	Nonmixture	0.08	0.08	0.03	0.03
6	2000	Estimated	0.05	0.08	0.60	2.20

Fig. 2. Density plots showing the distribution of relative unsigned error (RUE) for mixture (broken line) and nonmixture (solid line) models for six configurations of simulation models (*a–f*, configurations 1–6 from Table 4).

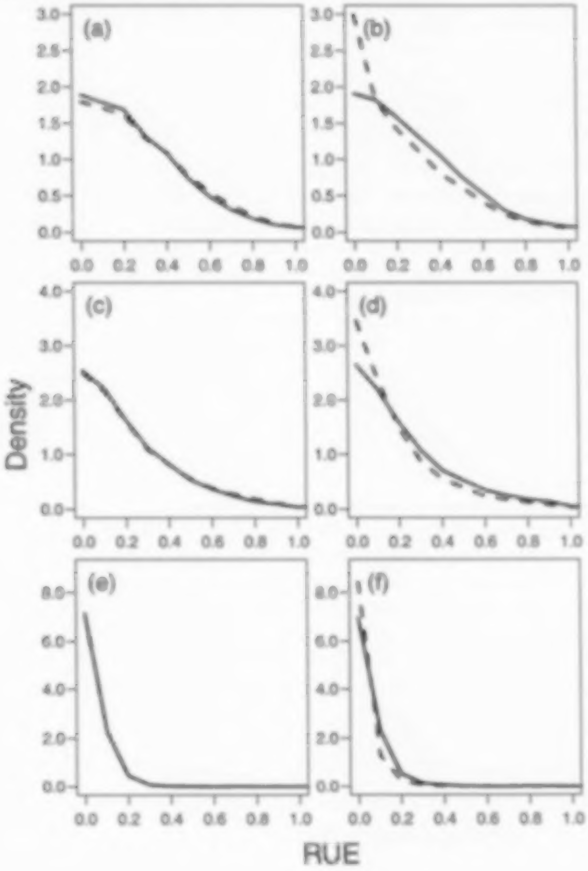

pling methods. Perhaps more importantly, these mixture distribution methods also provide a platform for statistically evaluating hypotheses regarding the spatial covariates that contribute to fish shoals. Catches of rockfish shoals in commercial fisheries can constitute a significant portion of a given year's total allowable catch, so spatial management measures could be designed if spatial covariates can be identified that have strong predictive power for rockfish shoals. Possible management measures include spatial gear and effort restrictions. These methods could also be used to identify spatial covariates contributing to shoal size in pelagic species, with implications for spatial management in these systems.

Improved density prediction for index standardization

Model validation results show that predictions of positive catch rates from mixture distribution models can be more accurate than those from conventional log-linear models using the sample sizes and model configurations that are observed for Pacific rockfish. Stepwise-BIC model selection also appears to correctly select a nonmixture model when appropriate, so concerns about model overfitting should be minimal. However, exploratory analysis showed that, as expected, mixture models slightly increase the width of estimated confidence bounds when estimating an annual index of positive density. This increase could appropriately represent underlying uncertainties due to shoaling behaviors and requires further testing to evaluate.

Species-level traits that contribute to extreme catch events

Mixed-effects mixture distribution results have shown that life history traits such as shoaling behavior can be observed in coast-wide surveys such as the NMFS-NWFSC shelf–slope bottom trawl survey and that shoaling species are likely to exhibit large differences in density for tows that encounter a fish aggregation. We propose that these mixed-effects results could be used as a prior for mixture distribution models that account for shoaling behavior when applied to stocks with few observations in the bottom trawl survey. These priors would be different for shoaling and nonshoaling species and thus can be conditioned on known life history information for any given stock of interest. This improvement can be especially important for data-poor members of the Pacific rockfish complex, given that the revisions to the Magnuson–Stevens Act have mandated that all stocks that are directly targeted or are important for ecosystem considerations be assigned fishery benchmarks.

Comparison with past work

Past work has sought to identify important habitat for rockfish with regard to species hotspots or untrawlable habitat (Zimmermann 2003; Vestfals 2009). Efforts to identify rockfish habitat are likely to continue and intensify as fish monitoring programs are extended to rockfish habitats such as untrawlable areas (Tolimieri et al. 2008). Our results indicate that the identification of rockfish habitat is complicated by differences in the spatial covariates that affect solitary and shoaling rockfish. We also find strong evidence for depth preferences for most analyzed rockfishes and a positive association for untrawlable habitat in several species.

Other methods have previously been proposed to provide an estimate of stock abundance that is robust to extreme catches. Within count models (i.e., numbers per hectare in trawl surveys), the negative binomial distribution is frequently used to explain either unmodeled environmental variability or greater variability than is predicted by the assumption that individuals are randomly distributed; current research seeks to generalize this model class (Royle and Dorazio 2008; Lindén and Mäntyniemi 2011). Within continuous models (i.e., kilograms per hectare as used here), alternative methods include replacing observations with a statistical prediction obtained from nonparametric kernel methods (Kappenman 1999), downweighting the importance of "outliers" by using either robust or quantile regression or a Huber loss function that is less sensitive to extreme values (Huber 1964; Koenker 2005; ADMB Project 2009). These methods treat ECEs as statistical outliers that will erroneously bias any resulting index of abundance. By contrast, we have treated extreme catches as resulting from and informative about an ecological process that is hypothesized a priori to occur for Pacific rockfish and many other fishes. We have also shown that spatial covariates can be distinguished to account for extreme catches in single-species models and that species-level traits such as shoaling can contribute to observed properties of ECEs.

Table 5. ΔAIC values and estimates for all mixed-effects model hyperparameters for all four multispecies models.

Configuration	Name	No. of parameters	ΔAIC	$\mu_{\lambda,S}$	$\mu_{\lambda,O}$	σ_λ	$\mu_{\omega,S}$	$\mu_{\omega,O}$	σ_ω
1	Null model	357	7.04	2.79	—	2.05	–0.42	—	2.97
2	Probability model	358	19.8	2.81	—	2.06	–0.71	–0.02	1.84
3	Density model	358	0.05	3.41	1.46	1.81	–0.39	—	2.47
4	Probability and density model	359	0.00	3.06	1.34	1.92	0.66	–0.08	1.79

Note: $\mu_{\lambda,S}$ and $\mu_{\lambda,O}$, the expected values for β_λ for shoaling species and nonshoaling species, respectively; $\mu_{\omega,S}$ and $\mu_{\omega,O}$, the expected values for β_ω for shoaling species and nonshoaling species, respectively; σ_ω and σ_λ, the standard deviations for among-species variability in β_ω and β_λ, respectively.

Future research

Mixture distribution models remain a subject of active research in the statistics and data analysis communities, and there remain many areas for future research. For our purposes, areas of particular interest include (*i*) model selection tools for single-species and multi-species mixture models, (*ii*) diagnostics for mixture distribution model performance, (*iii*) development of index standardization methods using mixture distribution models, and (*iv*) use of multispecies information as Bayesian priors in mixture distribution models.

Due to the ability of mixture distributions to classify different combinations of observations as extreme or unusual, they will often possess more than one local minimum and will require diagnostics for model convergence. Additionally, the likelihood surface for a mixture distribution model may contain peaks or ridges that correspond to instances in which the relative probability model isolates a few observations and one component has more predictors than this set of observations and consequently can fit them perfectly (Lindsay and Roeder 1992; Celeux et al. 2000; Wang et al. 2005). Likelihood peaks are more likely with multiple covariates for each density component and the relative probability component and thus less likely to occur when starting stepwise model selection at a null model that contains no covariates. Likelihood peaks can also be diagnosed by noticing that a density component has standard deviation approaching zero. Model diagnostics showed no evidence of convergence issues in the 19 200 BIC-stepwise mixture models that were fitted during simulation testing. However, future research could explore additional diagnostics and goodness-of-fit tools for mixture distribution models.

Future research could also integrate mixture distribution models into index standardization methods (Maunder and Punt 2004). Survey data are often transformed into an index of annual abundance using delta-GLM models that model presence–absence and positive catch rate data separately (Pennington 1983; Stefansson 1996). We have demonstrated that mixture distribution models will perform well for predicting positive catches in certain circumstances and that this prediction is similar to the component used for positive catches in delta-GLM models. However, mixture distribution methods will require further development before being used for routine index standardization. Necessary extensions include (*i*) including a model component to account for presence–absence data from research surveys, (*ii*) the capacity to treat research vessel as a random effect (Helser et al. 2004), (*iii*) using spatial strata such as latitude and depth as categorical blocking factors that can incorporate differences is survey sampling intensity, (*iv*) comparing different statistical distributions including lognormal, gamma, and inverse-Gaussian (Dick 2004), and (*v*) summarizing model output as a Bayesian posterior. The movement to Bayesian methods may also require reparameterization to enable the construction of interpretable Bayesian priors, e.g., for spatial covariates. These additions are a topic of current research for the authors and should not pose a hurdle to implementation of mixture distribution models for index standardization.

Finally, future research could evaluate the ability for Bayesian priors or likelihood penalties estimated from the mixed-effects models that we have developed (or a Bayesian treatment of it) to compensate for extreme catch events in data-poor rockfish stocks. With few observations in the NMFS-NWFSC bottom trawl survey, these data-poor stocks may be particularly sensitive to extreme catches such as could be caused by shoals. However, mixture models are unlikely to perform well for stocks that have small sample sizes (as seen in the simulation model) or that have not experienced an ECE. In cases with limited observations, Bayesian priors developed for Pacific rockfish could inform the β_λ and β_ω parameters. As AIC selection in this study has shown, the prior for the β_λ parameter could vary between shoaling and nonshoaling stocks, allowing life history information to inform index standardization for these data-poor stocks. However, this application remains untested and will require further simulation testing before it is feasible for stock assessment purposes.

Acknowledgements

The authors thank J. Brandon, L. Clarke, T. Essington, M. Haltuch, R. Hilborn, J. Wallace, and C. Whitmire, as well as the NOAA Fisheries Northwest Fisheries Science Center, Fishery Resource Analysis and Monitoring Division, NOAA Fisheries, 2725 Montlake Blvd., Seattle, WA 98112, for providing bottom trawl data for successful and unsuccessful tows. We also thank T. Helser for many discussions leading to the ideas for this research. The manuscript was additionally improved by comments from Samu Mäntyniemi and one anonymous reviewer. Support was provided by the University of Washington, the NMFS Sea Grant Population Dynamics Fellowship (NA09OAR4170120), a NMFS groundfish project grant to the University of Washington, and the Joint Institute for the Study of the 353 Atmosphere and Ocean (JISAO) under NOAA Cooperative Agreement No. 354 NA17RJ1232.

References

ADMB Project. 2009. AD model builder: automatic differentiation model builder. Developed by David Fournier. Available from http://www.admb-project.org.

Akaike, H. 1974. New look at statistical-model identification. IEEE Trans. Automat. Contr. **19**(6): 716–723. doi:10.1109/TAC.1974.1100705.

Berntsen, J., Espelid, T.O., and Genz, A. 1991. An adaptive algorithm for the approximate calculation of multiple integrals. ACM Trans. Math. Softw. (TOMS), **17**(4): 437–451. doi:10.1145/210232.210233.

Breiman, L. 2001. Random forests. Mach. Learn. **45**(1): 5–32. doi:10.1023/A:1010933404324.

Burnham, K.P., and Anderson, D. 2002. Model selection and multimodel inference. Springer-Verlag Inc., New York.

Celeux, G., Hurn, M., and Robert, C.P. 2000. Computational and inferential difficulties with mixture posterior distributions. J. Am. Stat. Assoc. **95**(451). doi:10.2307/2669477.

Copps, S.L., Yoklavich, M.M., Parkes, G.B., Wakefield, W.W., Bailey, A., Greene, H.G., Goldfinger, C., and Burns, R.W. 2007. Applying marine habitat data to fishery management on the US West Coast: initiating a policy–science feedback loop. Mapping the seafloor for habitat characterization. Geol. Assoc. Can. Spec. Pap. **47**: 451–462.

Dick, E.J. 2004. Beyond "lognormal versus gamma": discrimination among error distributions for generalized linear models. Fish. Res. **70**(2–3): 351–366. doi:10.1016/j.fishres.2004.08.013.

Gelman, A., Carlin, J.B., Stern, H.S., and Rubin, D.B. 2003. Bayesian data analysis. 2nd ed. Chapman & Hall, Boca Raton, Florida.

Genz, A.C., and Malik, A.A. 1980. An adaptive algorithm for numerical integration over an N-dimensional rectangular region. J. Comput. Appl. Math. **6**(4): 295–302. doi:10.1016/0771-050X(80)90039-X.

Hastie, T., Tibshirani, R., and Friedman, J. 2009. The elements of statistical learning: data mining, inference, and prediction. 2nd edition. Springer-Verlag Inc., New York.

Helser, T.E., Punt, A.E., and Methot, R.D. 2004. A generalized linear mixed model analysis of a multi-vessel fishery resource survey. Fish. Res. **70**(2–3): 251–264. doi:10.1016/j.fishres.2004.08.007.

Huber, P.J. 1964. Robust estimation of a location parameter. Ann. Math. Stat. **35**(1): 73–101. doi:10.1214/aoms/1177703732.

Jagielo, T., Hoffmann, A., Tagart, J., and Zimmermann, M. 2003. Demersal groundfish densities in trawlable and untrawlable habitats off Washington: implications for the estimation of habitat bias in trawl surveys. Fish. Bull. **101**(3): 545–565.

Johnson, S.G., and Narasimhan, B. 2009. Cubature: adaptive multivariate integration over hypercubes. Available from http://cran.r-project.org/web/packages/cubature/.

Kappenman, R.F. 1999. Trawl survey based abundance estimation using data sets with unusually large catches. ICES J. Mar. Sci. **56**(1): 28–35. doi:10.1006/jmsc.1998.0422.

Keller, A.A., Horness, B.H., Fruh, E.L., Simon, V.H., Tuttle, V.J., Bosley, K.L., Buchanan, J.C., Kamikawa, D.J., and Wallace, J.R. 2008. The 2005 U.S. West Coast bottom trawl survey of groundfish resources off Washington, Oregon, and California: estimates of distribution, abundance, and length composition. US Dept. Comm., NOAA Tech. Memo. NMFS-NWFSC-93(July).

Koenker, R. 2005. Quantile regression. Cambridge University Press, Cambridge, UK.

Kyriazidou, E. 1997. Estimation of a panel data sample selection model. Econometrica, **65**(6): 1335–1364. doi:10.2307/2171739.

Liaw, A., and Wiener, M. 2002. Classification and regression by RandomForest. R News, **2**(3): 18–22.

Lindén, A., and Mäntyniemi, S. 2011. Using the negative binomial distribution to model overdispersion in ecological count data. Ecology, **92**(7): 1414–1421. doi:10.1890/10-1831.1.

Lindsay, B.G., and Roeder, K. 1992. Residual diagnostics for mixture models. J. Am. Stat. Assoc. **87**(419): 785–794. doi:10.2307/2290216.

Love, M.S., Yoklavich, M., and Thorsteinson, L. 2002. The rockfishes of the Northeast Pacific. University of California Press, Berkeley, California.

Marin, J.M., Mengersen, K., and Robert, C.P. 2005. Bayesian modelling and inference on mixtures of distributions. Handbook of Statistics, **25**: 459–507. doi:10.1016/S0169-7161(05)25016-2.

Maunder, M.N., and Punt, A.E. 2004. Standardizing catch and effort data: a review of recent approaches. Fish. Res. **70**(2–3): 141–159. doi:10.1016/j.fishres.2004.08.002.

Olsen, M.K., and Schafer, J.L. 2001. A two-part random-effects model for semicontinuous longitudinal data. J. Am. Stat. Assoc. **96**(454): 730–745.

Pennington, M. 1983. Efficient estimators of abundance, for fish and plankton surveys. Biometrics, **39**(1): 281–286. doi:10.2307/2530830.

Pinheiro, J., and Bates, D. 2009. Mixed-effects models in S and S-PLUS. Springer-Verlag Inc., New York.

Qian, S.S., Cuffney, T.F., Alameddine, I., McMahon, G., and Reckhow, K.H. 2010. On the application of multilevel modeling in environmental and ecological studies. Ecology, **91**(2): 355–361. doi:10.1890/09-1043.1. PMID:20392000.

R Development Core Team. 2009. R: a language and environment for statistical computing. Available from http://cran.r-project.org/.

Rose, K.A., Cowan, J.H., Winemiller, K.O., Myers, R.A., and Hilborn, R. 2001. Compensatory density dependence in fish populations: importance, controversy, understanding and prognosis. Fish Fish. **2**(4): 293–327.

Royle, J.A., and Dorazio, R.M. 2008. Hierarchical modeling and inference in ecology: the analysis of data from populations, metapopulations and communities. Academic Press, London, UK.

Schwarz, G. 1978. Estimating the dimension of a model. Ann. Stat. **6**(2): 461–464. doi:10.1214/aos/1176344136.

Stefansson, G. 1996. Analysis of groundfish survey abundance data: combining the GLM and delta approaches. ICES J. Mar. Sci. **53**(3): 577–588. doi:10.1006/jmsc.1996.0079.

Stewart, I.J. 2008. Status of the U.S. canary rockfish resource in 2007. *In* Status of the Pacific coast groundfish fishery through 2008, stock assessment and fishery evaluation: stock assessments, STAR panel reports, and rebuilding analyses. Pacific Fishery Management Council, Portland, Oregon.

Thorson, J.T., and Berkson, J. 2010. Multispecies estimation of Bayesian priors for catchability trends and density dependence in the US Gulf of Mexico. Can. J. Fish. Aquat. Sci. **67**(6): 936–954. doi:10.1139/F10-040.

Tolimieri, N., Clarke, M.E., Singh, H., and Goldfinger, C. 2008. Evaluating the SeaBED AUV for monitoring groundfish in untrawlable habitat. *In* Marine habitat mapping technology for Alaska. Alaska Sea Grant College Program, University of Alaska Fairbanks. pp. 129–141. doi:10.4027/mhmta.2008.09.

Vestfals, C.D. 2009. Identifying habitat factors for canary rockfish (*Sebastes pinniger*) off Washington and Oregon using environmental data and trawl logbooks. Master's thesis, Oregon State University, Corvallis, Oregon.

Wang, C.-P., Hendricks Brown, C., and Bandeen-Roche, K. 2005. Residual diagnostics for growth mixture models. J. Am. Stat. Assoc. **100**(471): 1054–1076. doi:10.1198/016214505000000501.

Xie, H., McHugo, G., Sengupta, A., Clark, R., and Drake, R. 2004. A method for analyzing longitudinal outcomes with many zeros. Ment. Health Serv. Res. **6**(4): 239–246. doi:10.1023/B:MHSR.0000044749.39484.1b. PMID:15588034.

Ye, Y., and Dennis, D. 2009. How reliable are the abundance indices derived from commercial catch-effort standardization? Can. J. Fish. Aquat. Sci. **66**(7): 1169–1178. doi:10.1139/F09-070.

Zimmermann, M. 2003. Calculation of untrawlable areas within the boundaries of a bottom trawl survey. Can. J. Fish. Aquat. Sci. **60**(6): 657–669. doi:10.1139/f03-055.

Zuur, A.F., Ieno, E.N., Walker, N., Saveliev, A.A., and Smith, G.M. 2009. Mixed effects models and extensions in ecology with R. Springer-Verlag Inc., New York.

ERRATUM / ERRATUM

Erratum: Why does egg size of salmonids increase with the mean size of population spawning gravels?

Njal Rollinson and Jeffrey A. Hutchings

Ref.: Can. J. Fish. Aquat. Sci. **68**(8): 1307–1315.

Figure 4 on page 1311 is being reprinted here to correct a conversion error that resulted in a misalignment of the numbers on the *x* axis.

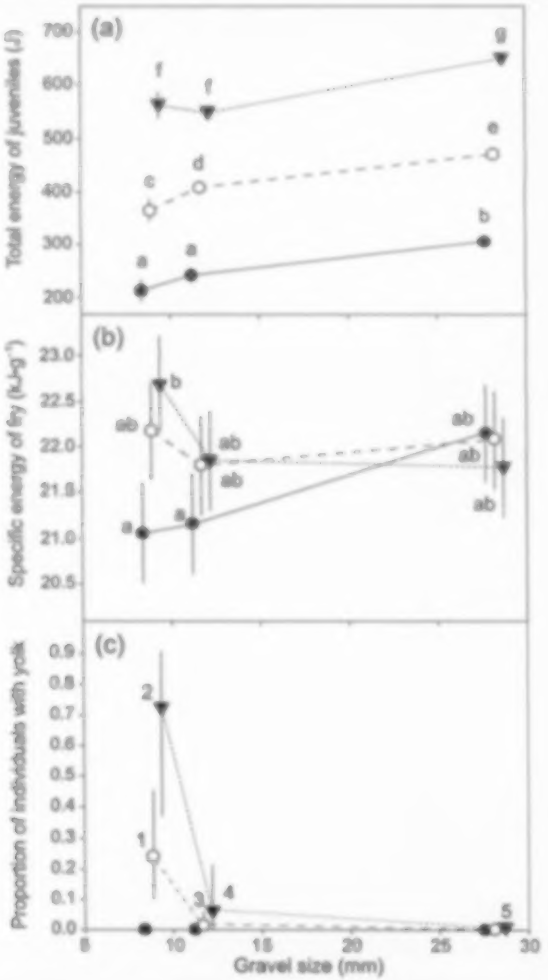

Fig. 4. (*a*) Least squares mean total energy of juveniles. (*b*) Least squares mean specific energy of juveniles. (*c*) Weighted mean proportion of individuals that emerged from the gravel with a visible yolk sac as a function of gravel size and egg size. Data are back-transformed from logits. Values identify one-tailed z tests ($\alpha = 0.01$) performed on logit-transformed data, which evaluated whether nonzero means were significantly greater than zero (1, $z = -2.72$, $P = 0.003$; 2, $z = -3.11$, $P = 0.0009$; 3, $z = -0.57$, $P = 0.28$; 4, $z = -1.09$, $P = 0.14$; 5, $z = -0.56$, $P = 0.28$). Solid circles, small eggs; open circles, medium eggs; solid triangles, large eggs. Letters denote significant differences after a Tukey's honestly significant difference (HSD) test; error bars are 95% confidence intervals.

Received 29 July 2011. Accepted 29 July 2011. Published at www.nrcresearchpress.com/cjfas on 8 September 2011.
J22032

Paper handled by Associate Editor Ian Fleming.

N. Rollinson and J.A. Hutchings. Department of Biology, Dalhousie University, Halifax, NS B3H 4J1, Canada.

Corresponding author: Njal Rollinson (e-mail: njal.rollinson@gmail.com).

doi:10.1139/F2011-121

Contents (concluded) / Table des matières (suite et fin)

George P. Naughton, Matthew L. Keefer, Tami S. Clabough, Michael A. Jepson, Steven R. Lee, Christopher A. Peery, and Christopher C. Caudill	**1615–1624**	Influence of pinniped-caused injuries on the survival of adult Chinook salmon (*Oncorhynchus tshawytscha*) and steelhead trout (*Oncorhynchus mykiss*) in the Columbia River basin
Peter-John F. Hulson, Sara E. Miller, James N. Ianelli, and Terrance J. Quinn II	**1625–1634**	Including mark–recapture data into a spatial age-structured model: walleye pollock (*Theragra chalcogramma*) in the eastern Bering Sea
P. Bradford Hubley and A. Jamie F. Gibson	**1635–1650**	A model for estimating mortality of Atlantic salmon, *Salmo salar*, between spawning events
Fabian Zimmermann, Mikko Heino, and Stein Ivar Steinshamn	**1651–1659**	Does size matter? A bioeconomic perspective on optimal harvesting when price is size-dependent
Omar I. Abdul-Aziz, Nathan J. Mantua, and Katherine W. Myers	**1660–1680**	Potential climate change impacts on thermal habitats of Pacific salmon (*Oncorhynchus* spp.) in the North Pacific Ocean and adjacent seas
James T. Thorson, Ian J. Stewart, and André E. Punt	**1681–1693**	Accounting for fish shoals in single- and multi-species survey data using mixture distribution models

ERRATUM ERRATUM

Njal Rollinson and Jeffrey A. Hutchings	**1694**	Erratum: Why does egg size of salmonids increase with the mean size of population spawning gravels?

Postage paid at Ottawa
Publications mail
Registration No. 40110225

Port payé à Ottawa
Poste-publication
Enregistrement n° 40110225

USPS periodical postage paid at Plattsburgh, NY 12901, US

Canadian Journal of
Fisheries and Aquatic Sciences

Volume 68, Number 9, September 2011

Journal canadien des
# sciences halieutiques et aquatiques

Volume 68, numéro 9, septembre 2011

ARTICLES ARTICLES

Andrew S. Medeiros and Roberto Quinlan 1511–1527 The distribution of the Chironomidae (Insecta: Diptera) along multiple environmental gradients in lakes and ponds of the eastern Canadian Arctic

Zhenhong Li, Daniel L. Villeneuve, Kathleen M. Jensen, Gerald T. Ankley, and Karen H. Watanabe 1528–1538 A computational model for asynchronous oocyte growth dynamics in a batch-spawning fish

Kátya Gisela Abrantes, Jeremy Martin Lyle, Peter D. Nichols, and Jayson Mark Semmens 1539–1551 Do exotic salmonids feed on native fauna after escaping from aquaculture cages in Tasmania, Australia?

Sarah K. Gaichas, Kerim Y. Aydin, and Robert C. Francis 1553–1578 What drives dynamics in the Gulf of Alaska? Integrating hypotheses of species, fishing, and climate relationships using ecosystem modeling

Stephanie Marie Carlson and William Hallowell Satterthwaite 1579–1589 Weakened portfolio effect in a collapsed salmon population complex

L. Godbout, C.C. Wood, R.E. Withler, S. Latham, R.J. Nelson, L. Wetzel, R. Barnett-Johnson, M.J. Grove, A.K. Schmitt, and K.D. McKeegan 1590–1602 Sockeye salmon (*Oncorhynchus nerka*) return after an absence of nearly 90 years: a case of reversion to anadromy

Shijie Zhou, Andre E. Punt, Roy Deng, Marco Kienzle, and Wayne Rochester 1603–1614 Bayesian fishable biomass dynamics models incorporating fished area and relative fish density

Continued on inside back cover / Suite au verso

Front cover: Ihoko Saito/Toshiyuki Tajima/Dex Image/Getty Images.

Page couverture : Ihoko Saito/Toshiyuki Tajima/Dex Image/Getty Images.

NRC Research Press

CANADIAN SCIENCE PUBLISHING | ÉDITIONS SCIENCES CANADA

Printed in Canada by | Imprimé au Canada par
NRC Reprographic Services | Service de reprographie CNRC

Page production by | Mise en page par
NRC Research Press | NRC Research Press

0706-652X(201109)68:9;1-T